

UC Berkeley

UC Berkeley Electronic Theses and Dissertations

Title

The Synthesis of Sustainable Commodity Materials

Permalink

<https://escholarship.org/uc/item/01g698fk>

Author

Shi, Jake

Publication Date

2024

Peer reviewed|Thesis/dissertation

The Synthesis of Sustainable Commodity Materials

By

Jake Xu Shi

A dissertation submitted in partial satisfaction of the
requirements for the degree of

Doctor of Philosophy

in

Chemistry

in the

Graduate Division

of the

University of California Berkeley

Committee in charge:

Professor John F. Hartwig, Chair

Professor Brooks A. Abel

Professor Phillip B. Messersmith

Summer 2024

Abstract

The Synthesis of Sustainable Commodity Chemicals

By

Jake Xu Shi

Doctor of Philosophy in Chemistry

University of California, Berkeley

Professor John F. Hartwig, Chair

The following dissertation discusses the development of reactions that transform polyolefins, selectively cleave polyolefins, and furnish materials with circular economies to address the limitations of commodity plastics. These reactions include the synthesis of circular polymers from renewable natural sources that undergo reversible cleavage of siloxane linkages, derivatization of oxyfunctionalized polyethylenes to furnish materials of higher value with greater reuse, and incorporation of functional groups into the backbone of polyethylene to imbue new properties to the polymer and incorporate cleavable linkages for selective degradation of polyethylene. The development of transition metal-catalyzed C–H acyloxylation reactions of polyolefins will also be discussed.

Chapter 1 is an overview on the synthesis, application, and limitations of polyolefins. Strategies that could potentially overcome the limitations of polyolefins and examples of them in the literature are discussed in detail.

Chapter 2 discusses the synthesis of monomers from the hydrosilylation of plant oils to furnish polyesters, polycarbonates, polyamides, and polyurethanes with in-chain siloxane linkages that enable programmed depolymerization. Acid-catalyzed siloxane metathesis enables the depolymerization and repolymerization of select polymers at the siloxane linkages. Studies on the microbial digestion of isotopically labelled fragments after enzymatic hydrolysis of these polymers suggest that the main chain of the polymer is metabolized to carbon dioxide in soil.

Chapter 3 discusses methods to derivatize pendent ketones and alcohols of oxyfunctionalized polyethylene to incorporate esters and oximes to the backbone to generate monofunctional polyethylenes that can be accessed from waste polymers. Judiciously selected conditions highlight the challenges of performing reactions on polymers. The esters and oximes imbue the monofunctional polyethylenes with enhanced properties when compared to unmodified polyethylene. In addition, these functional groups enable recovery through removal of the functional group or selective dissolution to recover the starting polymers for reuse.

Chapter 4 discusses incorporation of in-chain amide linkages in polyethylene through Beckmann rearrangement. The resulting long-chain polyamides possess similar bulk properties as unmodified polyethylene yet have improved surface properties over unmodified polyethylene. These

polyamides cannot be synthesized through step-growth or ring-opening polymerization. Hydrogenolysis of the amide linkages furnish telechelic alcohols and amines demonstrating a method to selectively cleave materials derived from polyethylene. These amine- and alcohol-terminated fragments were reacted with diisocyanate linkers to furnish polyurea-urethane elastomers with valuable properties.

Chapter 5 discusses the development of nickel-catalyzed C–H acyloxylation of polymers to furnish pendent esters in one chemical step. These ester-containing polymers have enhanced properties from unmodified polyethylene and can be accessed readily from abundant base metals and peroxides.

Table of Contents

Chapter One	1
1.1 Introduction.....	2
1.2 The Synthesis of Polyolefins	2
1.3 The Limitations and Drawbacks of Polyolefins.....	5
1.4 The Synthesis of Polyolefin-Like Polymers with Circular Economies	5
1.5 The Post-Polymerization Functionalization of Polyolefins	12
1.6 Summary.....	18
1.7 References.....	20
Chapter Two.....	37
2.1 Introduction.....	38
2.2 Synthesis of AA-Monomers and Condensation Polymerizations with BB-Monomers.....	39
2.3 Characterization of the Polymers.....	40
2.4 Synthesis of 26-membered Macrolactone Containing Siloxane Bonds.....	42
2.5 Ring-opening Polymerization of Macrolactone.....	43
2.6 Block Copolymer Comprising Ring-Opened Macrolactone 6 and <i>L</i> -lactide	44
2.7 Chemical, Programmed Degradation of Siloxane-Containing Polymers	46
2.8 Repolymerization of Monomers to Assess Circularity	47
2.9 Assessment of the Enzymatic Hydrolysis and Microbial Metabolism of the Polymers and Monomers	48
2.10 Assessment of Microbial Utilization of Monomers in Soil	49
2.11 Conclusion	50
2.12 Experimental Section.....	52
2.12.1 General Information.....	52
2.12.2 Synthesis of monomers	53
2.12.3 Synthesis of Polymers.....	55
2.12.3 Degradation of polymers.....	58
2.12.4 Repolymerization of Ester-Containing Siloxane 9	61
2.12.5 Synthesis of ¹³ C-labeled substrates	62
2.12.6 Biodegradation Studies	68
2.12.7 Catalytic hydrogenation of 1 and 2 with H ₂	71
2.12.8 Optimization of macrocyclization of 5	72
2.12.8 NMR Spectra	73
2.12.9 TGA and DSC (2nd cycle) graph of polymers.....	128
2.12.10 SEC traces of polymers.....	146
2.12.11 Procedure for tensile tests of PU-3.....	154
2.13 References.....	155
Chapter Three.....	156
3.1 Introduction.....	157
3.2 Synthesis of Monofunctional <i>keto</i> -Polyethylene	159
3.3 Synthesis of Monofunctional <i>hydroxy</i> -Polyethylene	160
3.4 Derivatization of Hydroxyl Groups in <i>hydroxy</i> -Polyethylene	161
3.5 Synthesis of Monofunctional Polyethylenes Containing Oximes	163
3.6 Properties of Materials.....	165
3.7 Applications to Waste Plastic	167

3.8 Application to the Separation of Plastic Mixtures	167
3.9 Conclusion	169
3.10 Experimental Section	170
3.10.1 General Information	170
3.10.2 Assessment of the degree of functionalization	171
3.10.3 Calculation of the stoichiometry of catalysts and reagents	171
3.10.4 Calculation of yield	171
3.10.5 Synthesis of polymers	172
3.10.6 Procedure for the reduction polymer 1 with sodium borohydride	180
3.10.7 Procedure for the hydrolysis of polymer 4d	180
3.10.8 Procedure for the hydrolysis of polymer 6a	180
3.10.9 Procedure for the oxidation of and derivatization of waste plastics	181
3.10.10 Procedure for the separation of polymers	183
3.10.11 Characterization of synthesized polymers	184
3.10.12 Characterization of the functionalization of waste plastics	252
3.10.13 Characterization of the hydrolysis of functional groups	262
3.10.14 Characterization for the separation of plastics from a mechanically mixed blend	266
3.10.15 Table of Molecular Weights	269
3.10.16 Differential Scanning Calorimetry (DSC) Data	270
3.10.17 Material testing	290
3.10.18 Thermogravimetric Analysis (TGA)	300
3.11 References	320
Chapter Four	325
4.1 Introduction	326
4.2 Beckmann Rearrangement of Oxime-Polyethylene	327
4.3 Hydrogenolysis of Amide Linkages	329
4.4 Polymerization of Alcohol- and Amine-Terminated Fragments	329
4.5 Materials Testing	330
4.6 Conclusion	332
4.7 Experimental Section	333
4.7.1 General Information	333
4.7.2 Assessment of the Degree of Functionalization	334
4.7.3 Calculation of the Stoichiometry of Catalysts and Reagents	334
4.7.4 Calculation of Yield	334
4.7.5 Synthesis of polymers	335
4.7.6 Hydrogenolysis of Polymers	339
4.7.7 Synthesis of Polyurea-Urethane 4	341
4.7.8 Characterization of Compounds	342
4.7.9 Materials Testing	369
4.8 References	376
Chapter Five	380
5.1 Introduction	381
5.2 Identification of Conditions for the Acyloxylation of C–H bonds	382
5.3 Investigation of the Scope of Peroxides	384
5.4 Material Testing	385
5.5 Conclusions and Future Directions	386

5.6 Experimental Section.....	388
5.6.1 General Information.....	388
5.6.2 Calculation of Yield and Degree of Functionalization.....	389
5.6.3 Synthesis of Nickel Catalysts.....	389
5.6.4 Synthesis of Peroxides.....	390
5.6.5 Synthesis of Functionalized Polyethylenes.....	393
5.6.6 Characterization of Polymers.....	394
5.6.7 Materials Testing.....	396
5.7 References.....	401

Acknowledgement

I am proud to receive a Ph.D. in chemistry from UC Berkeley. First, I am thankful for my parents, Qiaohua Zheng and Yian Shi, for raising me to prioritize academic excellence and diligence. I am thankful for my brother, Dennis Shi, for being dependable, supportive, and inspiring. I am also grateful for my other family members for their support. I want to thank my undergraduate advisor, Prof. Michael P. Marshak, and my mentor, Aaron Crossman, at the University of Colorado Boulder for inspiring me to become a chemist. I also want to thank Prof. Christopher N. Bowman for teaching my undergraduate reactor design course and providing me with valuable information that guided me through graduate school.

I am eternally thankful for my Ph.D. advisor, Prof. John F. Hartwig, for providing me the fruitful opportunity to work in his laboratory. I still vividly remember how excited I was when John called me to let me know that I had been accepted to UC Berkeley. I appreciate John's knowledge, advice, and willingness to trust me to be independent in the laboratory. I have grown so much because of his mentorship. I want to thank the other professors at UC Berkeley who have been instrumental towards my success here: Prof. F. Dean Toste, Prof. Brooks A. Abel, Prof. T. Don Tilley, Prof. Ting Xu, Prof. Phillip B. Messersmith, and Prof. Matt. B. Francis. I want to thank our group assistant, Anneke E. Runtupalit, for managing the group and keeping everything together. I want to thank Dr. Hasan Celik, Dr. Raynald Giovine, Dr. Cooper Citek, and Dr. Eric Dailing for their dedication to managing instruments and facilities that made my work possible.

The most important thing in graduate school for me is the people that I have met. I could not have made it through the tough times without them. I am forever indebted to the people I encountered here, and my achievements mean nothing without them.

To the postdocs: Masha Elkin, Vlad Roytman, Connor Delaney, Kyoungmin Choi, Sean Treacy, Subhjit Pal, Kyan D'Angelo, Carly Schissel, Jacob DeHovtiz, Chin Ho Lee, Akira Tanushi, Molly McFadden, Elias Tanuhadi, Zoha Syed, Alexander Kremismair, Ian Rinehart, and Wei Zhao: thank you for the motivation.

To the older graduate students: Steven Hanna, Trevor Butcher, Jack McCann, Paige Pistono, Eric Kalkman, Kay Xia, Yehao Qiu, Annika Page, Karan Goyal, Reichi Chen, Michael Daugherty, Angel Gonzalez-Valero, Danny Huang, and Jason Ma: thank you for the help.

To Jake Wilson, Isaac Yu, Adrian Huang, Matthew See, RJ Conk, and Suh Hyun Kang: you inspired me to grow not only as a chemist, but also as a person; you have no idea how much I appreciate that.

To Nicodemo Ciccia and John Brunn: those CARA conferences were legendary; thank you for all the wonderful times.

To Christina Pierson (GOAT), Calais Cronin, Josh Roan, Taylor Nuttall, Will Rackear, Andrew Quest, Magan Powell, Isaac Joyner, Yuanzhe Xie, Colin Cooper, Shirley Guo, Connor Filbin, Daniel Chabeda, Thomas Nedungadan, Celine Wang, Paul Sinclair, Chris La, Andrew Smith, Fadi Alsarhan, Trine Quady, Calvin Huffman, Khalid Mahmood, Kincade Stevenson, Alex Solivan, Jeremy Nicolai, Walt Yang, Jenna Manske, Sojung Kim, Miranda Wu, Vanessa Gonzalez, Jaden Lara, Emily Fok, Anna Moeckel, Adam Cahn, Sally Karstens, Colby Kayrouz, Katerina Gorou, Ethan Pezoulas, Conor Boderick, Mike Norinskiy, Sukriyo Chakraborty, Adam Pickett, and Nicole Xu: thank you never failing to make me smile.

To the visiting scholars: Craig Day, Julia Altarejos, Dani Atanes, Tommaso Fantoni, Max Surke, Nils Ansmann, Andrea Brugnetti, Aoibheann O'Connor (the tiny blonde terror), Teresa Horak, Camille Chartier, and Claudius Zimmer: I am so lucky to have met each one of you.

To the undergraduates: Eva Lin, Alex Du, Diane Kim, Nathan Sun, Emily Dai, Jules Stahler, Julia Kim, Melody Tang, Ron Zheng, and Pierre Lahaie-Boivin: thank you for the eagerness to learn.

Lastly, I want to thank my girlfriend and her family. To Abby: Thank you for your never-ending love, support, and encouragement over the last three years. Thank you for never letting me lose sight of the goal and keeping me steady. To Bill, Allison, Paul, Matt, and Remy: thank you making me feel so loved; it feels like I am at home when I am with you.

My four years at UC Berkeley have been one of the most memorable times of my life. I am truly speechless looking back at my time here. It has been a long journey. I wish everyone the best for their future endeavors. Go Bears!

Chapter One

Overview of the synthesis, properties, and limitations of polyolefins and strategies to address their shortcomings

1.1 Introduction

Polymers are molecules with repeating units in their structure. The word *polymer* is derived from the Greek word *polys* meaning “many” and *meros* meaning “part.”¹ Polyolefins are a class of polymers that contain only C–C and C–H σ -bonds that constitute the majority of commodity plastics.² Although polyolefin has “olefin” in its name, these polymers do not contain any olefins because the polymerization of an olefin breaks the C–C π -bond to generate a C–C σ -bond and a propagating species that extends the chain.² Ever since their initial discovery in the 20th century, polyolefins have been integral in everyday life, ranging from enabling convenience, such as single-use packaging, to constructing necessary materials, such as surgical implants.³

1.2 The Synthesis of Polyolefins

Plastics were produced at rate of 380 million tons in 2015, and 150 million tons of total resins produced were polyolefins.⁴ Polyolefins are able to be produced at these substantial rates for three reasons: the thermodynamics of olefin polymerization, the abundance of monomers, and the high activity of polymerization catalysts.^{5, 6} The bond dissociation energy of a C–C π -bond is approximately 60 kcal/mol, and the bond dissociation energy of a C–C σ -bond is approximately 80 kcal/mol resulting in an enthalpy of reaction of about 20 kcal/mol.⁷ Because the polymerization is so thermodynamically favorable, the polymerization of olefins results in polymers with high molecular weight with high ceiling temperatures.⁷ In addition to the favorable polymerization, the monomers for polymerization are easily sourced from abundant petrochemical feedstocks. Typically, crude gasoline from the ground is scrubbed to remove sulfur content and sent to a cracker to cleave the C–C bonds of long alkanes to form a mixture of light olefins.^{8, 9} Cracking crude gasoline also produces light olefins, such as ethylene and propylene, which are the monomers used to produce over half of the plastics in the world.^{4, 8, 9} Finally, the development of transition-metal catalysts that catalyze the polymerization of olefins with high turnover numbers enables the large-scale production of polyolefins.^{5, 6, 10, 11}

Polyethylene, formed from the polymerization of ethylene, is the simplest polyolefin, containing only methylene units in the structure. Approximately 116 million tons of polyethylene were produced in 2015, which accounted for nearly 31% of all plastics produced.⁴ Although polyethylene contains mostly methylene units, the architecture of polyethylene can be diversified depending on the method of polymerization. Low-density polyethylene (LDPE) is a form of polyethylene with high degrees of branching (Figure 1.2.1A). LDPE is typically synthesized by radical-initiated polymerization of ethylene with peroxides but can also be furnished through the transition-metal catalyzed homopolymerization of ethylene; however, LDPE can also be synthesized by transition-metal catalyzed homopolymerization of ethylene using constrained geometry catalysts (CGCs) bearing *ansa*-cyclopentadienyl amido ligands.¹²⁻¹⁵ In free radical polymerization, high degrees of branching are obtained because chain transfer of alkyl radicals formed by cleavage of unsaturated C–C bonds can abstract hydrogen atoms along the same chain or different chain to change the sites of propagation (Figure 1.2.1B).¹² At the same time, constrained geometry catalysts promote β -hydrogen elimination, which introduces sites of branching during the polymerization of ethylene (Figure 1.2.1B).^{13, 14} The mechanism of polymerization of ethylene to form LDPE with CGCs are akin to the insertion mechanisms for the synthesis of HDPE using Ziegler-Natta-type catalysts (Figure 1.2.1C). The high amounts of branching in LDPE makes it difficult for chains to crystallize uniformly, resulting in amorphous regions and lower density materials compared to more crystalline analogues of polyethylene.

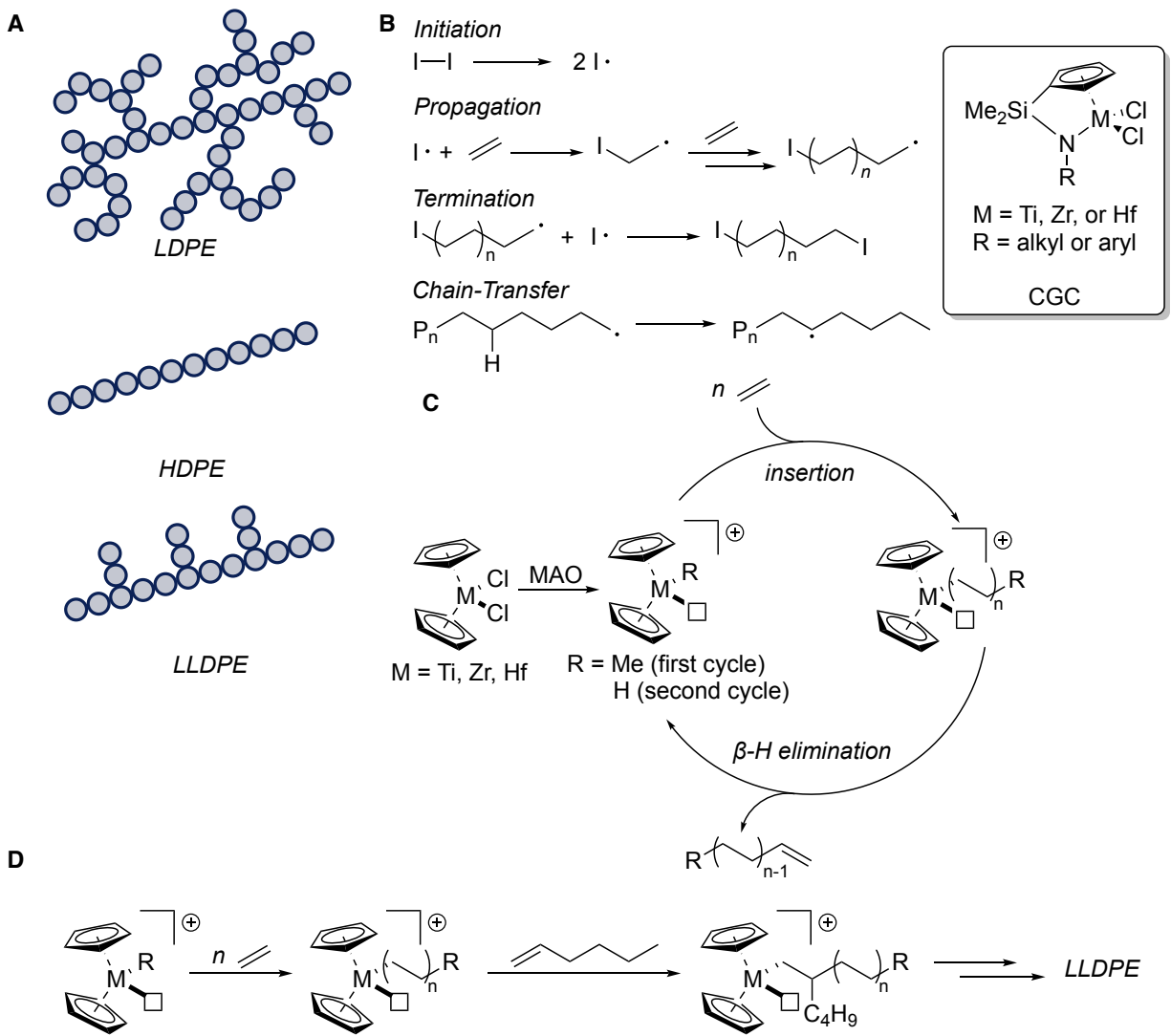


Figure 1.2.1. (A) Different architectures of polyethylene. (B) Mechanism of radical-initiated polymerization of ethylene to form LDPE. (C) Mechanism of ethylene polymerization by Ziegler-Natta catalysts to form HDPE. (D) Mechanism of ethylene and 1-hexene copolymerization to form LLDPE.

High-density polyethylene (HDPE) is another common form of polyethylene that is formed by polymerization of ethylene through insertion polymerization (Figure 1.2.1A). Group IV transition metals (Ti, Zr, Hf) ligated by cyclopentadienyl ligands are often used as catalysts for these polymerizations as well as heterogeneous Cr-based catalysts.^{16, 17} Activation of a metallocene with an initiator such as methyl aluminum oxide (MAO) generates a cationic complex that can undergo iterative coordination of an olefin to the metal center and insertion of the olefin into the propagating polymer chain (Figure 1.2.1C).^{18, 19} The amount of backbiting and chain transfer is suppressed by the insertion mechanism, resulting in more linear polymers formed when compared to polyethylene that is formed by radical polymerization. Because HDPE contains chains that are more linear than LDPE, HDPE is more crystalline than LDPE, thus making it denser than LDPE.

Linear-low density polyethylene (LLDPE) is the last common form of polyethylene (Figure 1.2.1A). The synthesis of LLDPE involves the addition of an α -olefin comonomer, such as 1-

hexene or 1-octene, to copolymerize with ethylene. The resulting copolymerization furnishes a linear polyethylene chain with incorporation of butyl or hexyl chains. LLDPE is furnished by transition-metal catalysts that operate under low pressures of ethylene and low temperatures (Figure 1.2.1D).^{14, 20} The irregularity of the butyl or hexyl chains imbue the polymer with favorable bulk properties and inhibit crystallization of the polymer chains in LLDPE, resulting in a low-density material like LDPE, despite being a linear polymer.

Polypropylene, the second-most produced plastic, is another polyolefin. 68 million tons of polypropylene were produced in 2015, which accounted for 18% of plastics produced globally.⁴ Polypropylene is formed from the polymerization of propylene (Figure 1.2.2). In contrast to ethylene, propylene is prochiral, and the properties of polymers created from propylene polymerization depend greatly on its tacticity. For example, isotactic and syndiotactic polypropylene are much more crystalline than atactic polypropylene because of the regular orientation of the methyl groups that enable efficient packing to create crystalline domains within the polymer matrix. Polypropylene is primarily made with Ziegler-Natta catalysts, and the tacticity of polypropylene can be controlled precisely depending on the catalyst used.^{11, 21} For heterogeneous catalysts, titanium supported catalysts are used in conjunction with trialkyl aluminum or magnesium salts to generate highly isotactic polymers. For homogeneous catalysts, *ansa*-metallocenes are typically used to polymerize propylene through insertion mechanisms similar to ethylene polymerization.^{18, 22} *ansa*-metallocenes with homotopic, enantiotopic, and diastereotopic binding sites produce isotactic, syndiotactic, and atactic polypropylene respectively.^{23, 24} Atactic polypropylene and isotactic polypropylene can be separated by fractionation because of their vastly different solubilities.

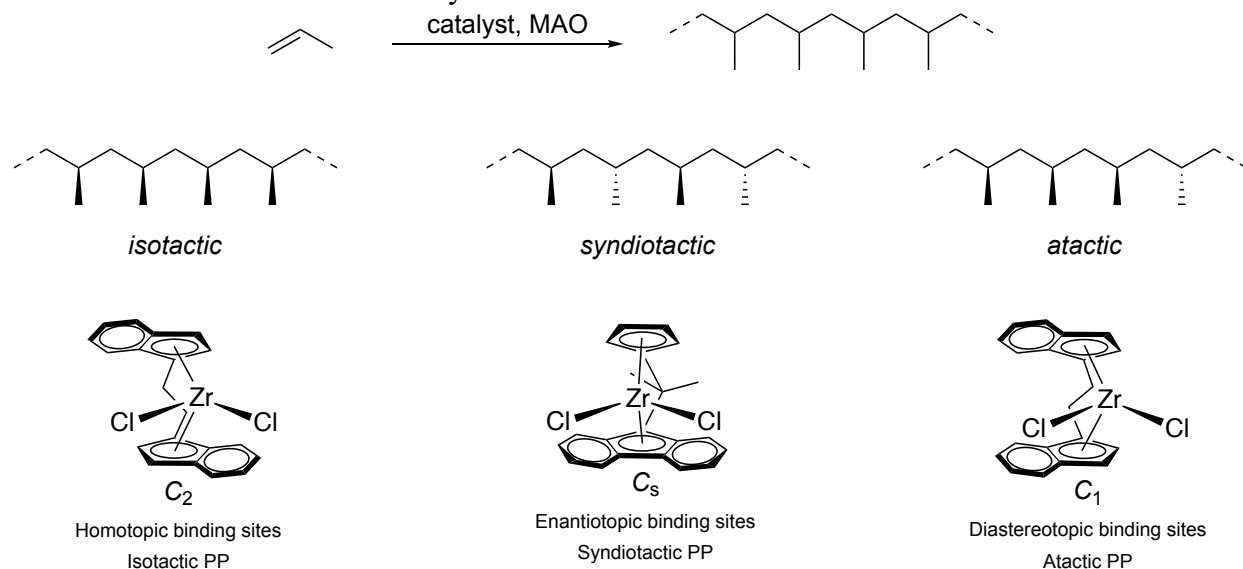


Figure 1.2.2. Propylene polymerization with different *ansa*-metallocene catalysts.

Other prominent polyolefins include polyisobutylene and polymethylpentene. Although these polyolefins are produced at a much lower rate than polyethylene or polypropylene, they are still important materials. Polyisobutylene is formed by cationic polymerization of isobutylene (Figure 1.2.3A).²⁵ The geminal dimethyl groups in the repeat structure of polyisobutylene disfavor crystallization of chains resulting in amorphous materials. Polymethylpentene is synthesized by polymerization of 4-methyl-1-pentene with Ziegler-Natta catalysts. Like the methyl group in PP,

the isobutyl group in polymethylpentene dictates its crystallinity and properties (Figure 1.2.3.B). Typically, polymethylpentene is manufactured in its isotactic form.

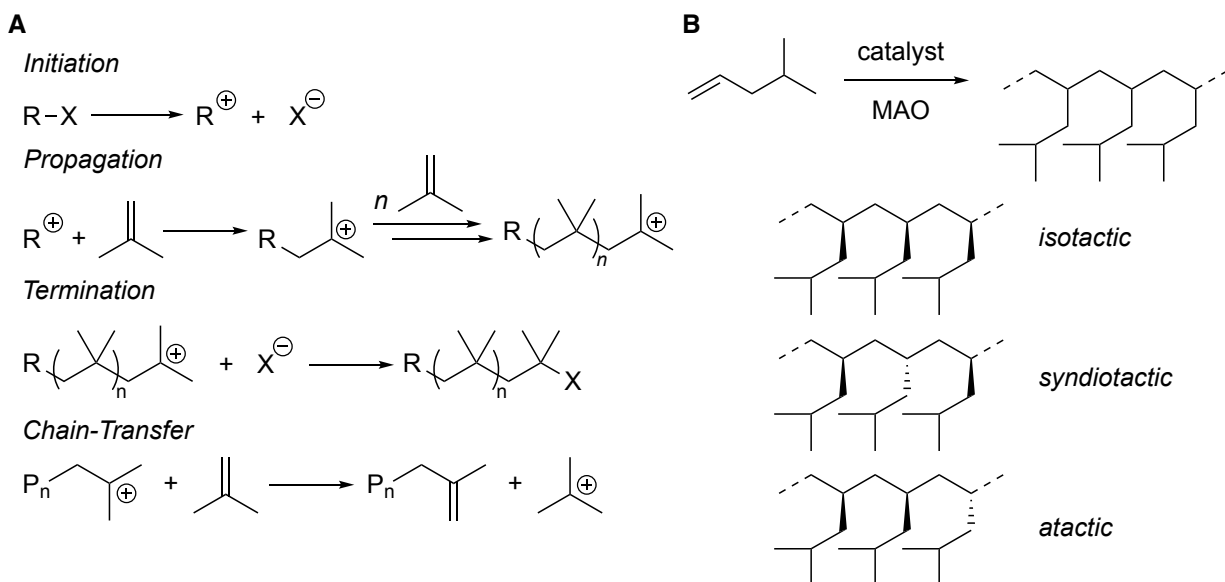


Figure 1.2.3. (A) Mechanism of cationic polymerization of isobutylene. (B) Polymerization of 4-methyl-1-pentene and architectures of polymethylpentene.

1.3 The Limitations and Drawbacks of Polyolefins

Despite their favorable properties, polyolefins have inherent limitations. Because polyolefins are so nonpolar, they are not compatible with materials that are polar or usable in applications requiring polar media. To mitigate this, polyolefins are often blended with additives to generate composites that are rendered suitable for applications in polar media.²⁶⁻³⁰ At the same time, these composites are highly complex materials, and addressing their end-of-life disposal is challenging because of the difficulty to delaminate the layers in the composite or separate the polyolefin from other polymers and small molecules.²⁸⁻³³

In addition, the C–C bonds in polyolefins are difficult to cleave selectively and efficiently, and this difficulty also poses challenges in addressing their end-of-life disposal.^{34, 35} Furthermore, the properties of polyolefins deteriorate upon iterative mechanical recycling because of cleavage or crosslinking of polymer chains and oxidation of the backbone.^{32, 35-37} Consequently, most polyolefins are made as single-use plastics, and their disposal leads to plastic waste accumulation in the environment.³⁸ It is projected that over 25 billion tons of plastic waste will have accumulated in the environment by 2050.⁴ As a result, these factors limiting the degradation and recovery of polyolefins disincentivize their recycling and leads to the accumulation of plastic waste. To this end, methods to create more sustainable plastics are urgently needed.^{38, 39}

1.4 The Synthesis of Polyolefin-Like Polymers with Circular Economies

Polymers that are easily depolymerized have emerged as a promising strategy to supplant traditional polyolefins as commodity plastics because of the ability to recover the starting monomer at their end-of-life treatment.^{34, 40, 41} Furthermore, these polymers would ideally decompose to environmentally benign products in the environment in the event that they are not depolymerized.^{34, 40, 42, 43} In this manner, the accumulation of waste is circumvented, the recovered

monomer can be repolymerized to form virgin polymer without diminished properties, and any lost polymer during collection or processing turns into innocuous chemicals in the environment. To create such polymers, certain criteria should be met: the polymers should be able to be depolymerized and repolymerized cheaply and selectively, the ceiling temperature of the polymers should be low enough to depolymerize the polymer selectively, and the properties of the polymers should be similar to the properties of commercial plastics.^{34, 43, 44} To this end, many groups have reported the synthesis of polymers that mimic or outperform the properties of polyolefins, yet are recyclable.

The installation of carbonyl-based functional groups such as esters or carbonates have been demonstrated to provide handles for depolymerization.^{34, 45} In 2021, Mecking and coworkers reported the synthesis of polyethylene-like polyesters and polycarbonates from monomers derived from renewable plants oils (Figure 1.4.1A).⁴⁶ Olefin-metathesis of oleates and subsequent hydrogenation enabled the synthesis of C₁₈ diester monomers, and the reduction of these diesters furnished C₁₈ diol monomers.

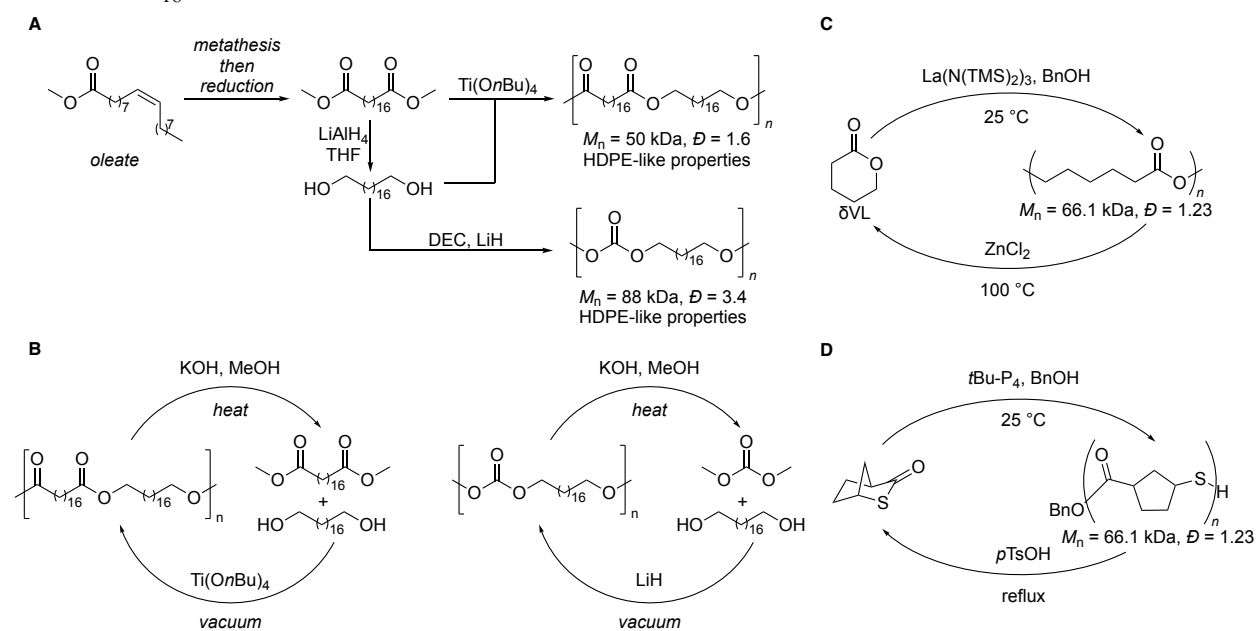


Figure 1.4.1. (A) Synthesis of polyesters and polycarbonates from bio-derived monomers. (B) Depolymerization and repolymerization of polyesters and polycarbonates. (C) Synthesis and depolymerization of poly(δVL). (D) Synthesis and depolymerization of polyolefin-like polythioesters.

Although step-growth in nature, polycondensation of the diesters with diols catalyzed by titanium (IV) butoxide or polymerization of diols with diethyl carbonate (DEC) and lithium hydride afforded polyesters ($M_n = 50$ kDa) and polycarbonates ($M_n = 88$ kDa) of high molecular weights respectively. These polymers were melt processable and possessed comparable bulk properties to HDPE. Analysis of their crystallinity by WAXS revealed that the polyesters and polycarbonates were highly crystalline, owing to the regularity of the repeat units within the polymer.⁴⁷ Most important, methanolysis of the ester or carbonate linkages depolymerized these polymers and provided nearly quantitative recovery of the C₁₈ diester and diol monomers, which underwent repolymerization to afford polymers with undiminished properties, thereby demonstrating recyclability of these polyesters and polycarbonates (Figure 1.4.1B).

In the same year as Mecking, Xu and Chen and coworkers reported the synthesis of chemically recyclable poly(valerolactone)s (PVL) with bulk properties that outperform polyolefins (Figure 1.4.1C).⁴⁸ Polymerization of bio-based δ -valerolactone (δ VL) at room temperature with lanthanum-based catalysts furnished PVLs with polyolefin-like properties and high molecular weight ($M_n = 66$ kDa), and depolymerization of the PVLs with zinc (II) chloride at 100 °C enabled quantitative recovery of the δ VL monomer. The tensile strength, toughness, and resistance to oxygen permeability were all superior to those of unmodified LDPE. In addition to polyesters, Falivene and Chen and coworkers also demonstrated chemically circular polythioesters (Figure 1.4.1D).⁴⁹ By controlling the stereoregularity of the polythioesters with different phosphazene or NHC catalysts, highly crystalline polymers with bulk properties comparable to polyolefins were achieved. The polythioesters were then easily depolymerized in the presence of acid to afford the monomer in quantitative yield.

Hillmyer and coworkers reported the synthesis of chemically recyclable polyesters with mechanical properties similar to HDPE from polycondensation of telechelic polyethylenes derived from isoambrettolide (Figure 1.4.2A).⁵⁰ Methanolysis of isoambrettolide furnished an α,ω -ester alcohol which served as a chain transfer agent (CTA) during the ring-opening metathesis polymerization (ROMP) of *cis*-cyclooctene to furnish unsaturated ester or alcohol terminated polymers. Subsequent addition of ethyl vinyl ether (EVE) to quench the reaction and reduction of the double bonds under high pressures of hydrogen created telechelic polyethylenes (Figure 1.4.2A). Polymerization of these telechelic monomers with each other created linear polyesters, and addition of a branched diester-diol furnished branched polyesters. These polyesters were melt-processable, highly crystalline, and the linear polyesters were depolymerized through methanolysis catalyzed by scandium (III) trifluoromethanesulfonate (Figure 1.4.2B).

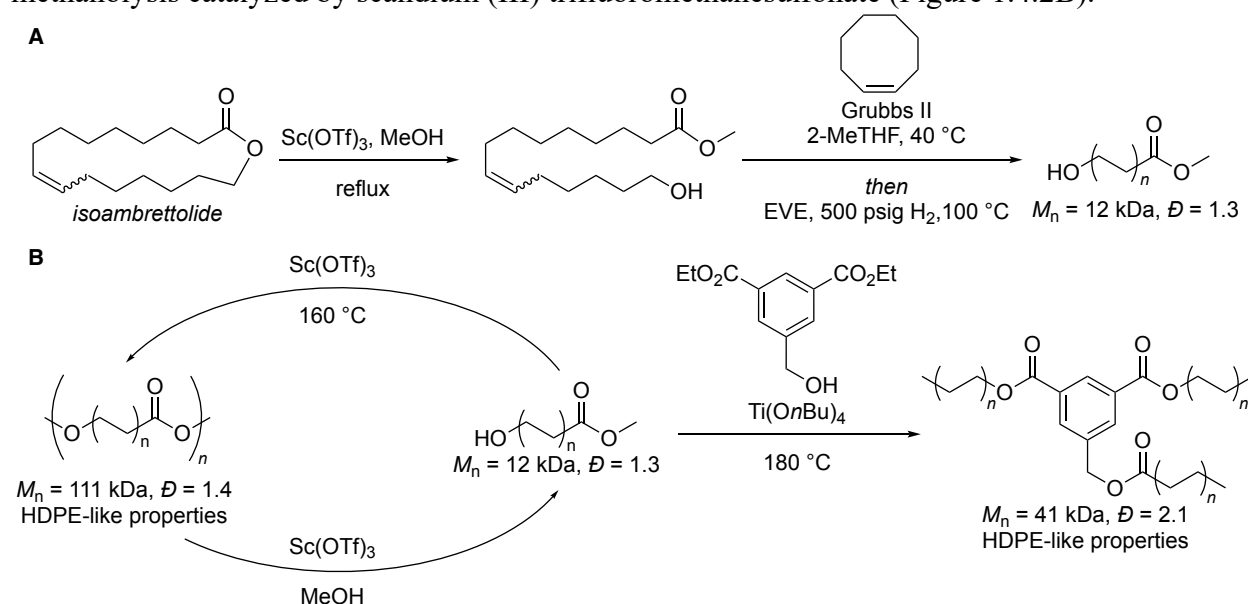


Figure 1.4.2. (A) Synthesis of telechelic polyethylenes. (B) Polycondensation of telechelic polyethylenes to form chemically recyclable linear polyesters or branched polyesters.

Miyake and coworkers also reported the synthesis of chemically recyclable linear and branched polyesters from telechelic fragments derived from ROMP of *cis*-cyclooctene analogs with a diol as a CTA (Figure 1.4.3A).⁵¹ Dehydrogenative step-growth polymerization of these α,ω -diols was catalyzed by a ruthenium-catalyst through liberation of hydrogen gas (Figure 1.4.3B).

Increasing in branching substitution on the backbone enabled precise modulation of the crystallinity and bulk properties of the material. Depolymerization of the polyesters was catalyzed by the same ruthenium-catalyst under high pressures of hydrogen to reductively cleave the ester linkages back to alcohols. The telechelic oligomers were recovered in nearly quantitative yield and repolymerized to form the same polyesters without deterioration in mechanical properties.

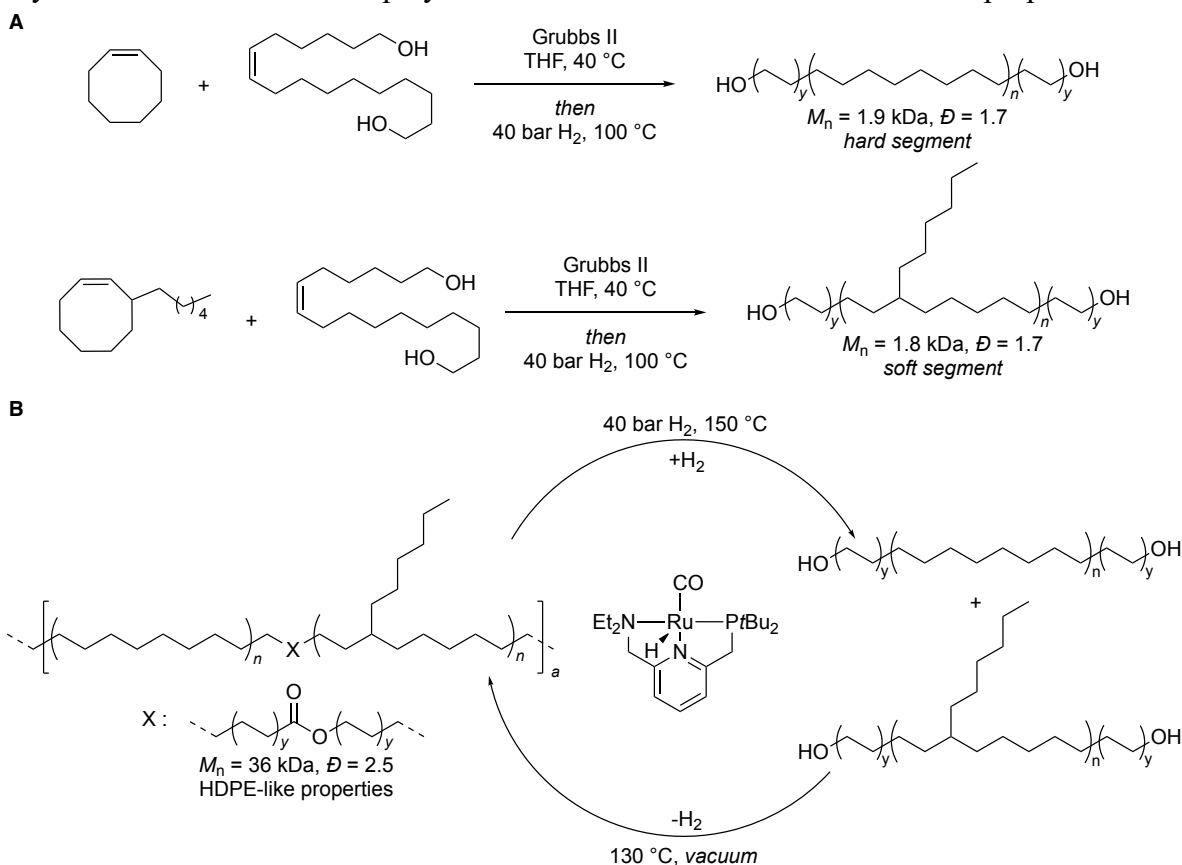


Figure 1.4.3. (A) Synthesis of telechelic polyethylenes. (B) Ruthenium-catalyzed polymerization and depolymerization of telechelic diols to polyesters.

Instead of using ROMP to create the backbone of the polymer, Coates and LaPointe and coworkers performed the copolymerization of propylene with 1,3-butadiene to furnish isotactic PP with sites of unsaturation through hafnium-based catalysts (Figure 1.4.4A).⁵² Subsequent cross metathesis with 2-hydroxyethyl acrylate furnished telechelic fragments containing 2-hydroxyethyl carboxy termini, which were polymerized through polycondensation. These polymers exhibited similar bulk properties as LLDPE and were depolymerized through transesterification of the ester linkages with ethylene glycol catalyzed by 1,5,7-triazabicyclo[4.4.0]dec-5-ene (TBD) to afford the original telechelic fragments containing 2-hydroxyethyl carboxy termini. Coates published a similar strategy to create chemically recyclable polyolefin-like polymers, but instead of copolymerization of propylene and 1,3-butadiene, palladium catalyzed copolymerization of ethylene with dimethyl 7-oxabicyclo[2.2.1]hepta-2,5-diene-2,3-dicarboxylate furnished copolymers that, upon retro Diels-Alder reactions to release dimethyl furan-3,4-dicarboxylate, revealed sites of unsaturation that underwent cross-metathesis (Figure 1.4.4B).⁵³ The remaining C–C π -bonds were reduced prior to polycondensation to improve the bulk properties of the polymer. The installation of esters and carbonates have proven to be viable approaches to creating

chemically circular polymers, and modulation of the branching in the polymer can tune the bulk properties such as mechanical strength or melt processing to mimic polyolefins for specific applications.

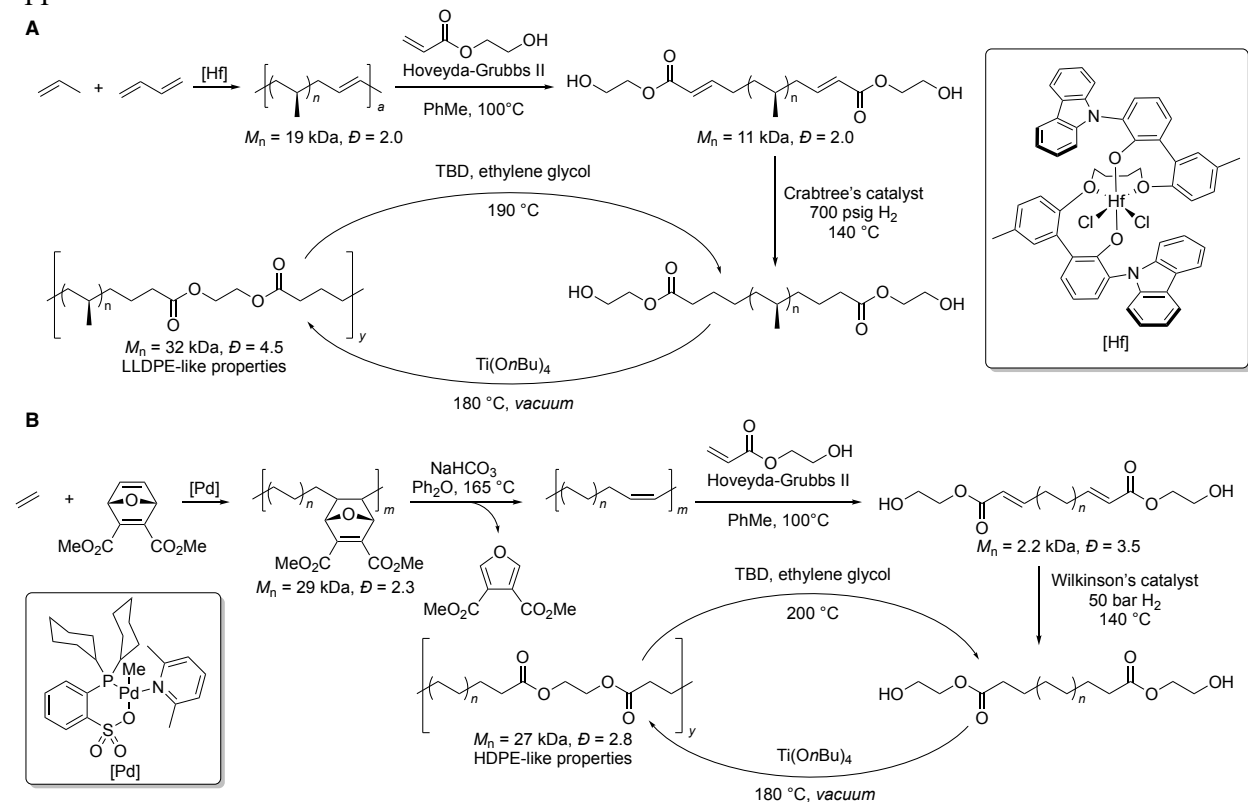


Figure 1.4.4. (A) Synthesis of chemically recyclable ester-linked polypropylene. (B) Synthesis of chemically recyclable ester-linked polyethylene.

Creating chemically circular polymers based on biodegradable polyhydroxyalkanoates (PHAs) has also emerged as an attractive approach to creating alternatives to polyolefins. However, PHAs are highly brittle and have poor bulk properties and are not thermally stable, thus much progress has been made to improve their properties.⁵⁴ In 2023, Coates and coworkers reported the synthesis of methylated polyhydroxybutyrates with polyolefin-like properties (Figure 1.4.5A).⁵⁵ Coates and coworkers developed the polymerization of 2,3-dimethyl- β -propiolactone (DMPL), which is easily synthesized from butene feedstocks, to form poly(3-hydroxy-2-methylbutyrate)s (PHMBs). The methyl group of these PHAs increase the crystallinity of the polymer, enabling the bulk properties of the polymers could be tuned by changing the tacticity of the methyl groups on the backbone with different catalysts. Imbuing bulk and thermal properties comparable to polyethylene and polypropylene to PHMB was achieved by this strategy. In addition, PHMB was depolymerized with MgO as catalyst at 200 °C to afford tiglic acid, which can be repolymerized back to PHMB or used as a precursor for valuable fine chemicals. Rieger and coworkers and Müller and Chen and coworkers also reported a similar strategy starting from *rac*- β -butyrolactone and a chiral yttrium-based catalyst to furnish isotactic poly(3-hydroxybutyrate) with polyolefin-like properties (Figure 1.4.5B).^{56, 57} Lastly, Chen and coworkers demonstrated that installing geminal dimethyl groups in butyrolactone produced monomers that formed monodisperse polyolefin-like PHAs ($M_n > 160 \text{ kDa}$) when polymerized with low amounts (55 ppm) of

phosphazene as catalyst (Figure 1.4.5C).⁵⁸ Simple hydrolysis catalyzed by base enabled recovery of the monomer in quantitative yield. These examples highlight the bioinspired approach in designing monomers that would enable the synthesis of chemically recyclable polyolefin-like polymers.

Chemically circular polymers without carbonyl-based functional groups have also been developed. Coates and coworkers reported the cationic ring-opening polymerization (CROP) of 1,3-dioxolane (DXL) to furnish poly(1,3-dioxolane) PDXL with indium-based catalysts and halide-based initiators in the presence of 2,6-di-*tert*-butyl-pyridine (DTBP) (Figure 1.4.6A).⁵⁹ The indium catalyst enabled reservable chain-end activation to produce polymers with high and precisely tuned molecular weights ($M_n > 220$ kDa) through living polymerization while the DTBP trapped any protons that could promote chain transfer. Analysis of the ceiling temperature revealed the ceiling temperature of PDXL to be 13 °C; however, because the barrier of depolymerization is too high in the absence of a catalyst, PDXL could be melt processed to create common products such as packaging. Differential scanning calorimetry (DSC) showed that the melting temperature (T_m) of PDXL was 58 °C and thermal gravimetric analysis (TGA) revealed a decomposition temperature (T_d) of 337 °C, indicating that the thermal properties of PDXL are similar to those of commodity polyolefins. Tensile tests of PDXL showed that it had similar bulk properties as polyethylene and even isotactic polypropylene. To lower the barrier of depolymerization, Brønsted acid catalysts were used to catalyze the depolymerization of PDXL back to DXL. Reactive distillation of PDXL in the presence of simple acid catalysts such as camphor sulfonic acid (CSA) enabled recovery of DXL in nearly quantitative yield, even amid other plastic additives.

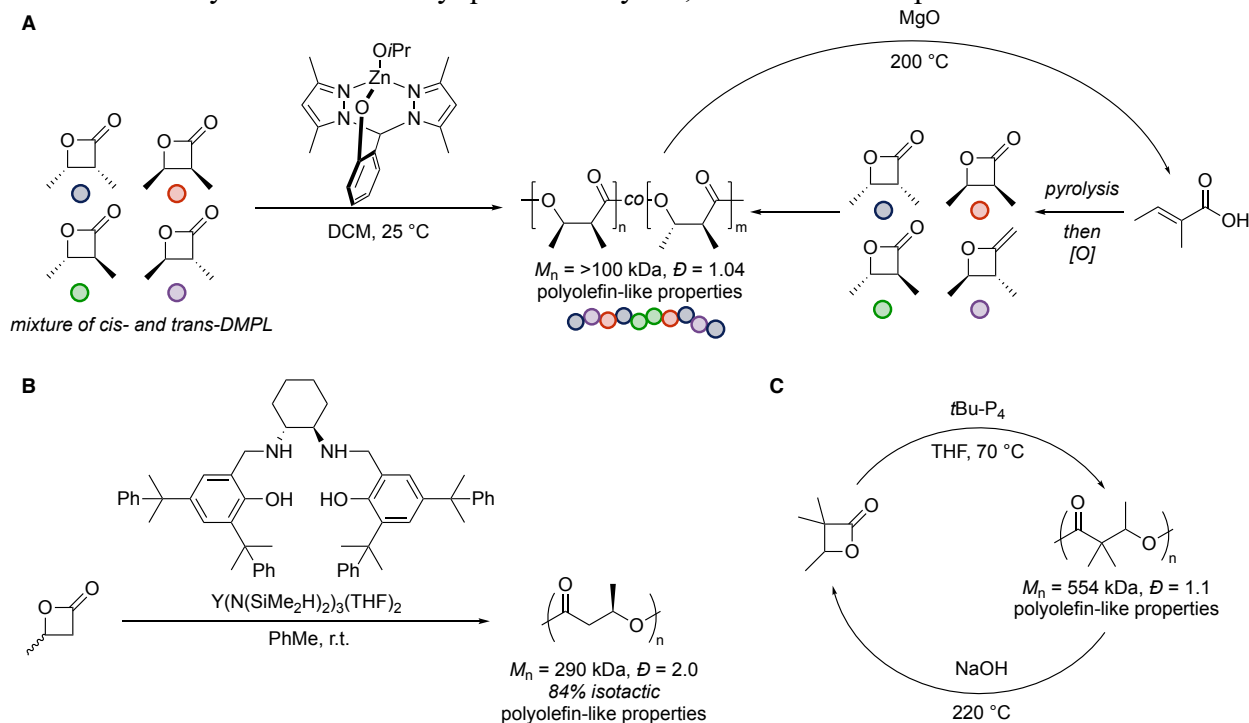


Figure 1.4.5 (A) Synthesis of chemically recyclable polyolefin-like PHAs from monomers derived from butenes. (B) Ring-opening polymerization of butyrolactone. (C) Synthesis of chemically recyclable PHAs.

In 2023, to improve the viability of polyacetals as potential substitutes for polyolefins, Coates and coworkers replaced the indium-based catalyst and halide-based initiator with triethyloxonium

hexafluorophosphate, which served as a cheap, single-component catalyst and initiator (Figure 1.4.6B). Using the oxonium system, DXL was polymerized to PDXL to reach even higher molecular weights ($M_n > 2000$ kDa) than PDXL produced by indium catalysis. The bulk properties of the PDXL produced by this method were able to be modulated depending on the molecular weight of the polymer, reaching mechanical robustness of ultra-high molecular weight polyethylene (UHMWPE) or even crosslinked thermosets such as ionomers.⁶⁰

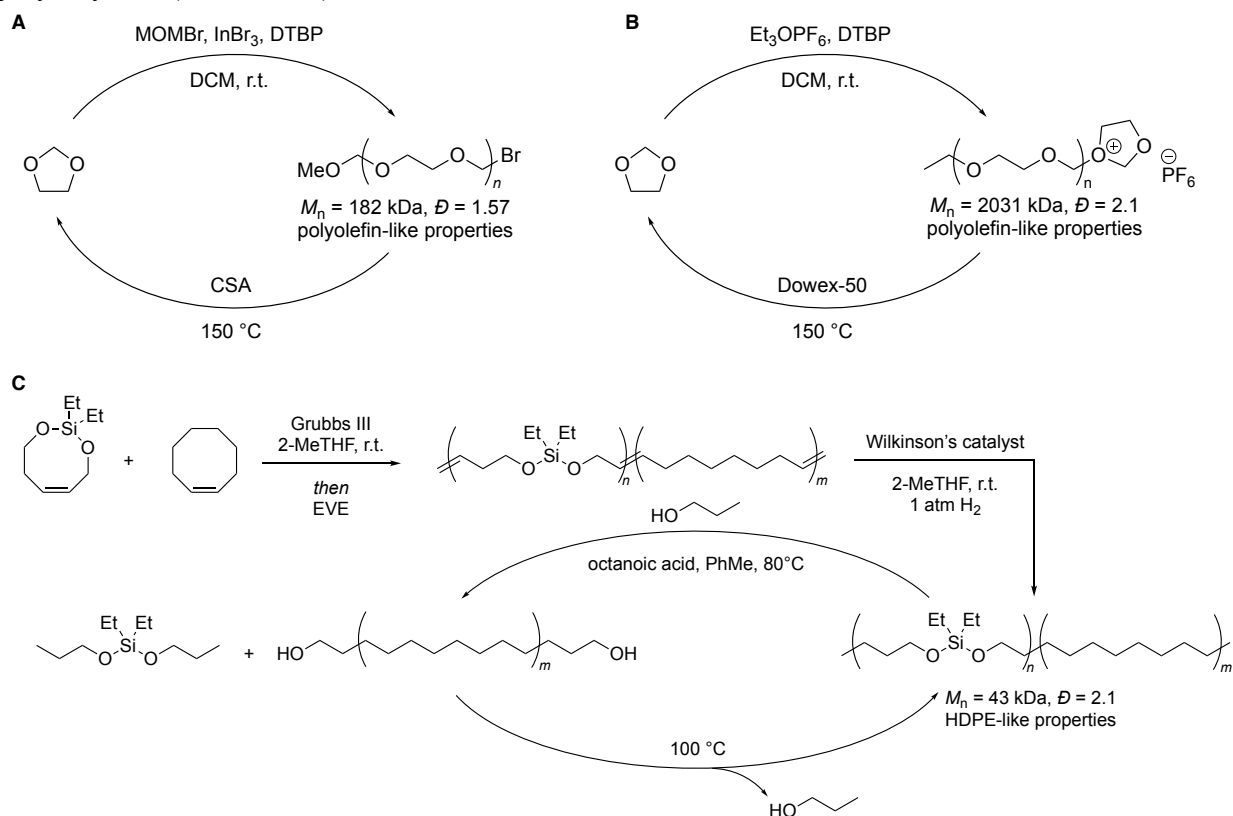


Figure 1.4.6. (A) Polymerization of DXL with indium catalysts. (B) Polymerization of DXL with triethyloxonium hexafluorophosphate. (C) Synthesis of chemically recyclable polyethylenes with siloxane linkages.

Johnson and coworkers utilized siloxane metathesis as a method to generate chemically recyclable polymers (Figure 1.4.6C).⁶¹ Cyclooctene analogs containing a siloxane unit were polymerized with *cis*-cyclooctene through ROMP, and subsequent hydrogenation of the double bonds formed linear polyethylene-like polymers with in chain siloxane linkages. Due to the flexibility of the Si–O bond, the crystallinity, and thereby bulk properties, could be adjusted by controlling the amount of siloxane linkages in the polymer. The polymers possessed identical mechanical properties to HDPE and could be depolymerized by acid-catalyzed alcoholysis of the siloxane moiety to generate α,ω -diols. These diols could be repolymerized with dialkyl siloxanes to regenerate the polymer through step-growth polymerization through extrusion of alcohol from the system.

Overall, many methods have been developed for the synthesis of chemically circular polyolefin-like polymers. These polymers usually contain a labile bond that can be activated for depolymerization back to monomer and have ceiling temperatures that are easily reached, yet these polymers are melt processable at temperatures commodity polyolefins are processed and are

thermally robust like polyolefins. Selective polymerization catalysts and monomer design have allowed the bulk properties to be tuned precisely to access polymers that mimic polyolefins across a wide range of applications. Despite these extensive studies, the scale of which these chemically circular polymers are produced are miniscule compared to the production rate of polyolefins.^{4, 34} Thus, efforts toward the discovery and scaleup of polymers with circularity are being made to increase the feasibility of transitioning from polyolefins to chemically recyclable polymers.

1.5 The Post-Polymerization Functionalization of Polyolefins

The post-polymerization functionalization of polyolefins has also emerged as an attractive method to create sustainable materials.^{41, 62-64} The functionalized polyolefins have small amounts of pendent functional groups that imbue the polymer with enhanced properties over unmodified polyolefins. This enhancement in properties could enable these materials to be used in applications that traditionally require a polyolefin composite, thereby reducing the complexity of commercial plastics that could be more easily recycled than composites.^{33, 63, 65} In addition, the installation of a functional group could enable selective cleavage of the polymer chain at the site of, or in proximity to, the functional group. These smaller fragments can then be repurposed towards the synthesis of more sustainable materials or towards creating more ecologically innocuous segments than unmodified polyolefins.

Functional polyolefins can be synthesized by the copolymerization of α -olefins with vinyl comonomers containing polar functional groups; however, the polar functional group of the comonomer can poison polymerization catalysts, and the radical-mediated strategies to procure these polymers lead to materials with undesired degrees of branching.^{41, 63} In addition, the difference in rates of polymerization of each monomer can lead to unfavorable incorporation and distribution of functional groups in the polymer.⁶³ The combination of these factors requires specific design of catalysts or reagents tailored to furnish specific copolymers; therefore, strategies that can access different polymers from one set of conditions are important. In this regard, because homo-polymerization of olefins is well-studied and demonstrated industrially, a polyolefin with a predefined microstructure can be transformed to yield functional polyolefins with any architecture. Most important, the potential of waste plastics to be used as a feedstock for the synthesis of these polymers could broaden the scope of plastics that can be affected by the post-polymerization functionalization strategy.

Polyolefins are modified industrially by plasma treatment or flame treatment, but these approaches only modify the surface of the polymer. To functionalize polyolefins in bulk, grafting of heterocycles by radical-initiated methodologies to generate polar functional groups is often practiced industrially. However, competing side reactions, such as crosslinking or scission of the polymer, also occur during treatment or grafting, and these changes to the polymer structure can substantially impact the properties.⁶⁶⁻⁶⁹ As a result, methods that selectively functionalize polyolefins in bulk to generate functional polymers with control over chain scission or crosslinking are highly desired.⁶³

Insertion of carbenes or nitrenes into the C–H bonds of polyolefins was initially reported in 1969 by Olsen and Osteraas; however, these carbene or nitrene insertions only modified the surface of polyolefins.^{70, 71} The first strategy to functionalize polyolefins in bulk with carbenes was demonstrated by Aglietto in 1989 with ethyl diazoacetate (EDA) to insert into the C–H bonds of polyethylene at high temperatures (Figure 1.5.1A).⁷² Because the carbene predominately reacts in the singlet state, its radical character is suppressed. This suppression of the triplet state minimizes side reactions such as free-radical mediated chain scission and crosslinking.⁷³ This strategy serves

as a more selective method of installing functional groups to polyolefins over the azidation and nitrene insertion of polyolefins, which are strategies that install nitrogen-based functionalities, accompanied by significant amounts of scission and crosslinking respectively.^{74, 75} The first transition-metal catalyzed carbene insertion into C–H bonds of polyolefins was developed by Pérez and coworkers (Figure 1.5.1B).⁷⁶ They conducted the insertions of EDA into the C–H bonds of model polyolefins, specifically poly(2-butene) and poly(ethylene-1-octene). Recently, carbenes that are generated thermally or photochemically have been used by Wulff and coworkers to crosslink polyolefins (Figure 1.5.1C).⁷⁷ Kumar, Rovis, Chen and coworkers later demonstrated that incorporating exchangeable moieties within the carbene linker enabled dynamic thermosets to be synthesized, thereby bolstering the properties of polyolefin blends (Figure 1.5.1D).⁷⁸

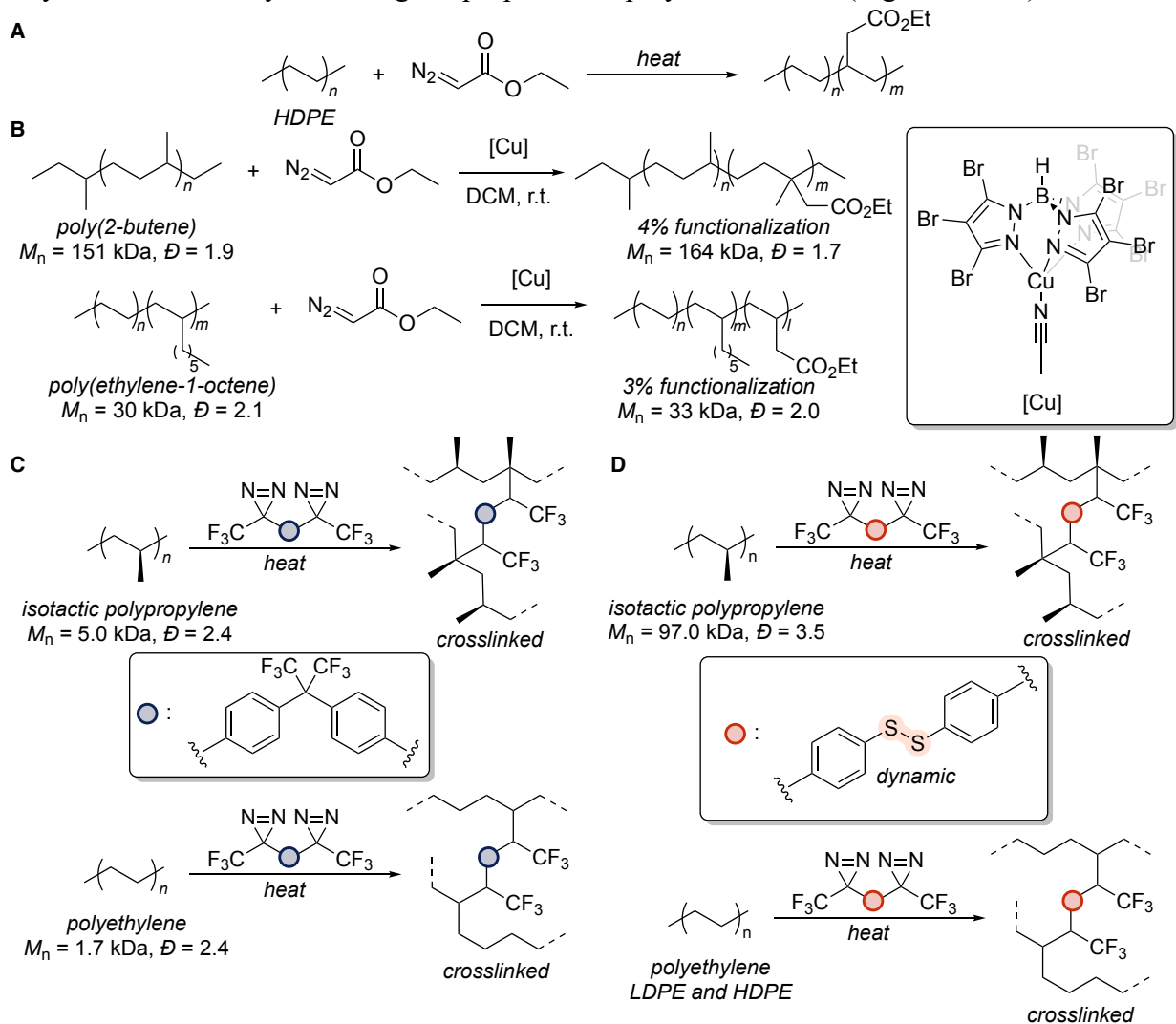


Figure 1.5.1. (A) Functionalization of HDPE by thermal decomposition of EDA. (B) Copper-catalyzed functionalization of model polyolefins with EDA. (C) Crosslinking of polyolefins with carbenes. (D) Crosslinking of polyolefins with dynamic carbenes.

Transition-metal catalyzed strategies other than carbene insertions have been developed to functionalize polyolefins selectively and efficiently.⁴¹ In 2002, Hartwig and Hillmyer reported the rhodium-catalyzed borylation of polyolefins in the melt with bis(pinacolato) diboron (B_2pin_2) as

the diboron reagent (Figure 1.5.2A).⁷⁹ The polymer that underwent borylation was poly(ethylethylene) (PEE). Like the borylation of small alkanes, the borylation of polyolefins occurred selectively at the termini of the side-chains of the polymer. The resulting boronic esters were transformed subsequently to hydroxyl groups by oxidation with hydrogen peroxide. This rhodium-catalyzed borylation was later conducted on polypropylenes to install boronic esters, which were then changed into hydroxyl groups at the end of the side-chains (Figure 1.5.2B).⁸⁰ Ring-opening polymerization (ROP) of ϵ -caprolactone initiated by these alcohols resulted in polypropylene-*graft*-poly(caprolactone) polymers that compatibilized polypropylene and poly(caprolactone) (PCL) blends.

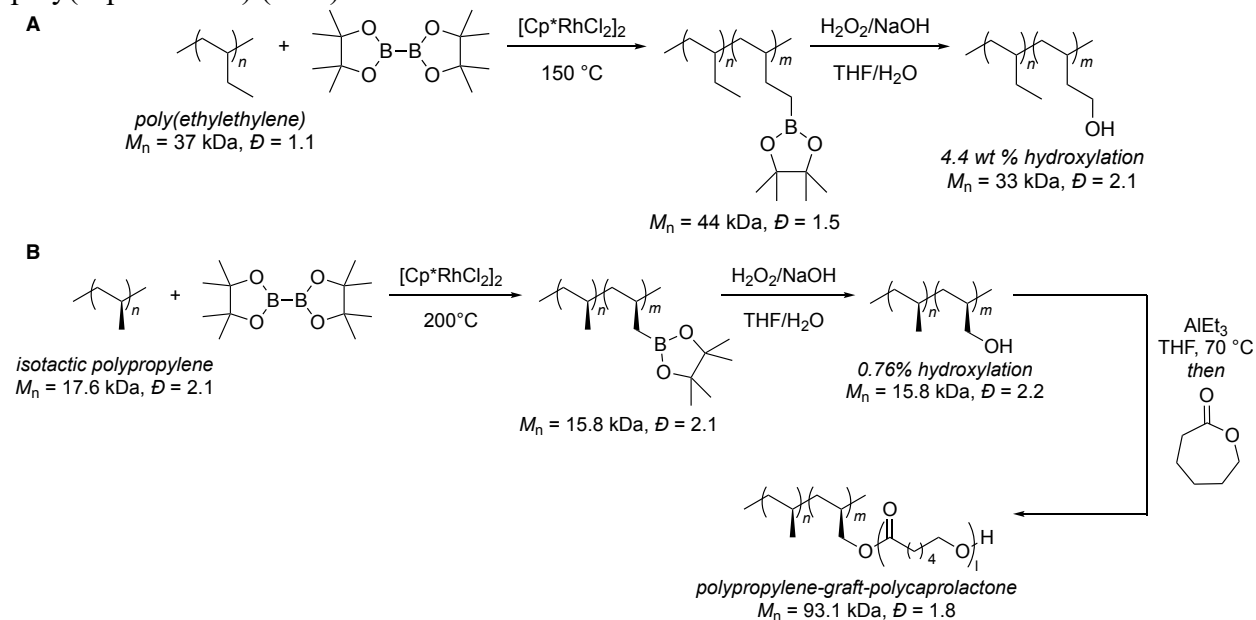


Figure 1.5.2. (A) Rhodium-catalyzed borylation of PEE and subsequent oxidation of boronic esters. (B) Rhodium-catalyzed borylation of *i*PP and synthesis of *i*PP-*graft*-PCL.

Previous examples of the post-polymerization functionalization of polyolefins revealed that installing oxygen-containing functional groups enhances the properties of the polymer. As a result, many groups have developed methods to install oxygen-based functional groups to polyolefins in one step. In 2003, Boen and Hillmyer demonstrated the manganese-porphyrin catalyzed oxidation of model polyolefin, polyethylene-*alt*-polypropylene, with Oxone as the oxidant (Figure 1.5.3A).⁸¹ This reaction functionalized the tertiary C–H bonds of the polymer to pendent tertiary alcohols and the secondary C–H bonds of the polymer to pendent ketones. Hartwig and coworkers reported the oxidation of polyethylenes with nickel catalysts and *meta*-chloroperbenzoic acid (*m*CPBA) as the oxidant (Figure 1.5.3B).⁸² The functional groups installed were ketones, alcohols, esters, and chlorides. The esters and chlorides were installed by Baeyer-Villiger oxidation of the ketones and abstraction of chlorine atom from the solvent respectively. No substantial change in molecular weight was observed after functionalization of LDPE, HDPE, and LLDPE. Functionalization of the hydroxyl groups installed by ROP of ϵ -caprolactone produced PCL oligomers grafted onto the polyethylene backbone that served as compatibilizers between PE and PCL. Hartwig and coworkers later developed the oxyfunctionalization of LDPE, HDPE, and LLDPE with a ruthenium-porphyrin catalyst and 2,6-dichloropyridine *N*-Oxide as oxidant (Figure 1.5.3C).⁸³ Despite the reaction being run in a chlorinated solvent, 1,2-dichloroethane, no chlorination was

observed, and no change in molecular weight of the polymer was observed. The proposed mechanism for this reaction is similar to the mechanism of oxidation catalyzed by cytochrome P-450 monooxygenase enzymes.⁸⁴ A ruthenium(V)-oxo metalloporphyrin abstracts a hydrogen atom from the polymer backbone, generating an alkyl radical that rebounds to the newly formed ruthenium(IV)-hydroxyl metalloporphyrin to install the functional group. The rapid rebound disfavors escape of the alkyl radical from the solvent cage to abstract a chlorine atom from the solvent or undergo β -scission or crosslinking.⁸³ The resulting oxyfunctionalized polyethylenes had similar mechanical properties but enhanced surfaces properties to those of unmodified polyethylene. The same ruthenium catalyst was used to functionalize polyisobutylene to install ketones at the methylene carbons of the polymer backbone (Figure 1.5.3D).⁸⁵ The ketones enabled photodegradation of the polymer, and reduction of the ketones furnished alcohols that underwent crosslinking with bis-silylchlorides.

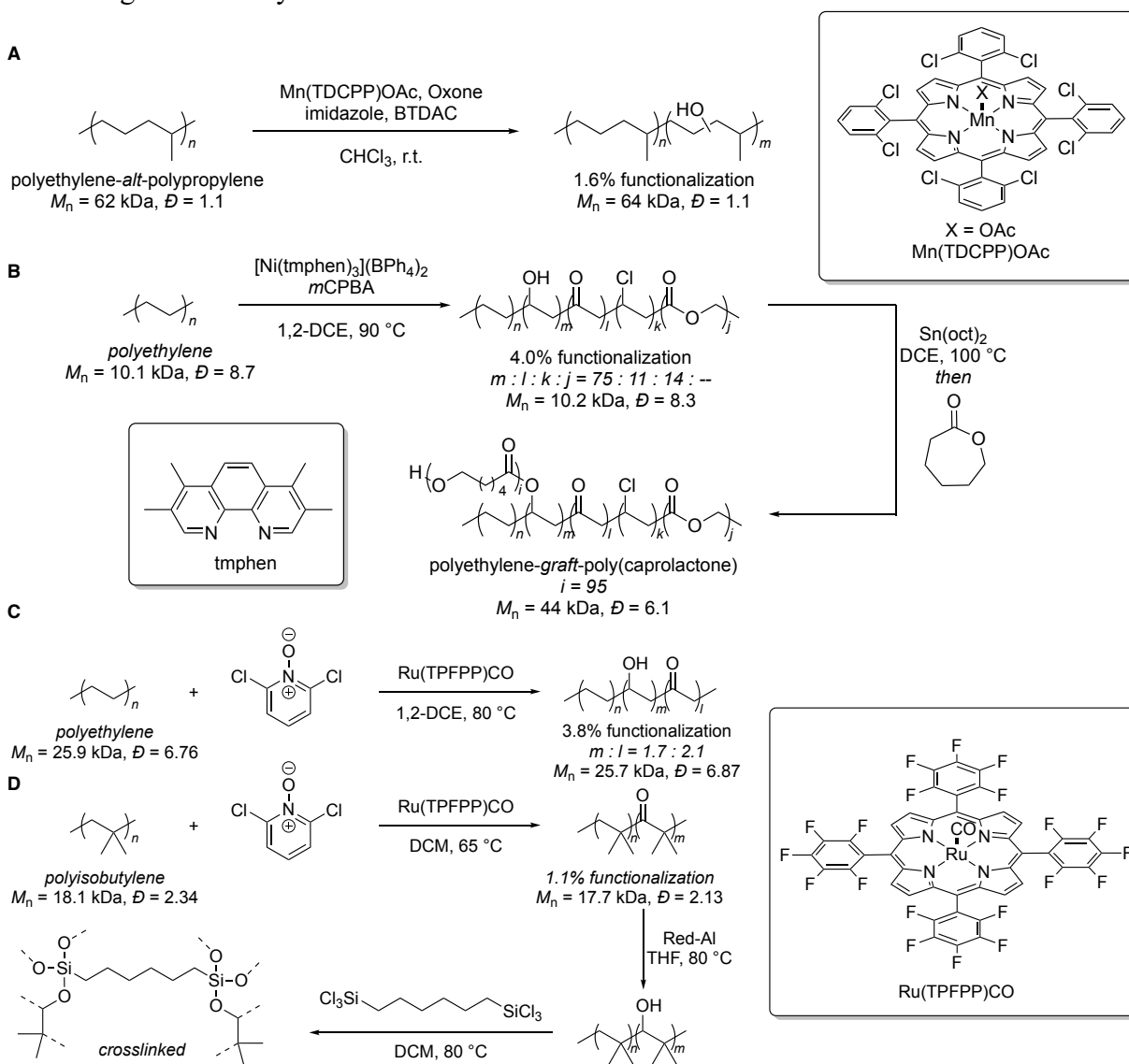


Figure 1.5.3. (A) Manganese-catalyzed oxidation of PEP. (B) Nickel-catalyzed oxidation of polyethylene. (C) Ruthenium-catalyzed oxidation of polyethylene. (D) Ruthenium-catalyzed oxidation of polyisobutylene and subsequent reduction and crosslinking.

Transition-metal free approaches have also been developed to furnish an array of functional groups to the backbone of polyolefins. Leibfarth and Alexanian and coworkers reported a photoinitiated xanthylation of polyolefins to install xanthates along the backbone of PEE and different forms of PE (Figure 1.5.4A).⁸⁶ Using amidyl radicals, the authors functionalized the inert C–H bonds of polyolefins. The installed xanthates were then derivatized to access a series of functional groups. This xanthylation strategy was applied to functionalize the primary C–H bonds of PP (Figure 1.5.4B).⁸⁷ By changing the xanthylamide to an *O*-alkenylhydroxamate, Leibfarth and Alexanian and coworkers induced chain transfer of the formed alkyl radical to an external trap to increase the scope of functional groups that could be installed (Figure 1.5.4C).⁸⁸ Helms and Leibfarth and coworkers also attached triketone-functionalized xanthates to polyolefins that enable reprocessable thermosets to be furnished through dynamic diketoenamine linkages (Figure 1.5.4D).⁸⁹

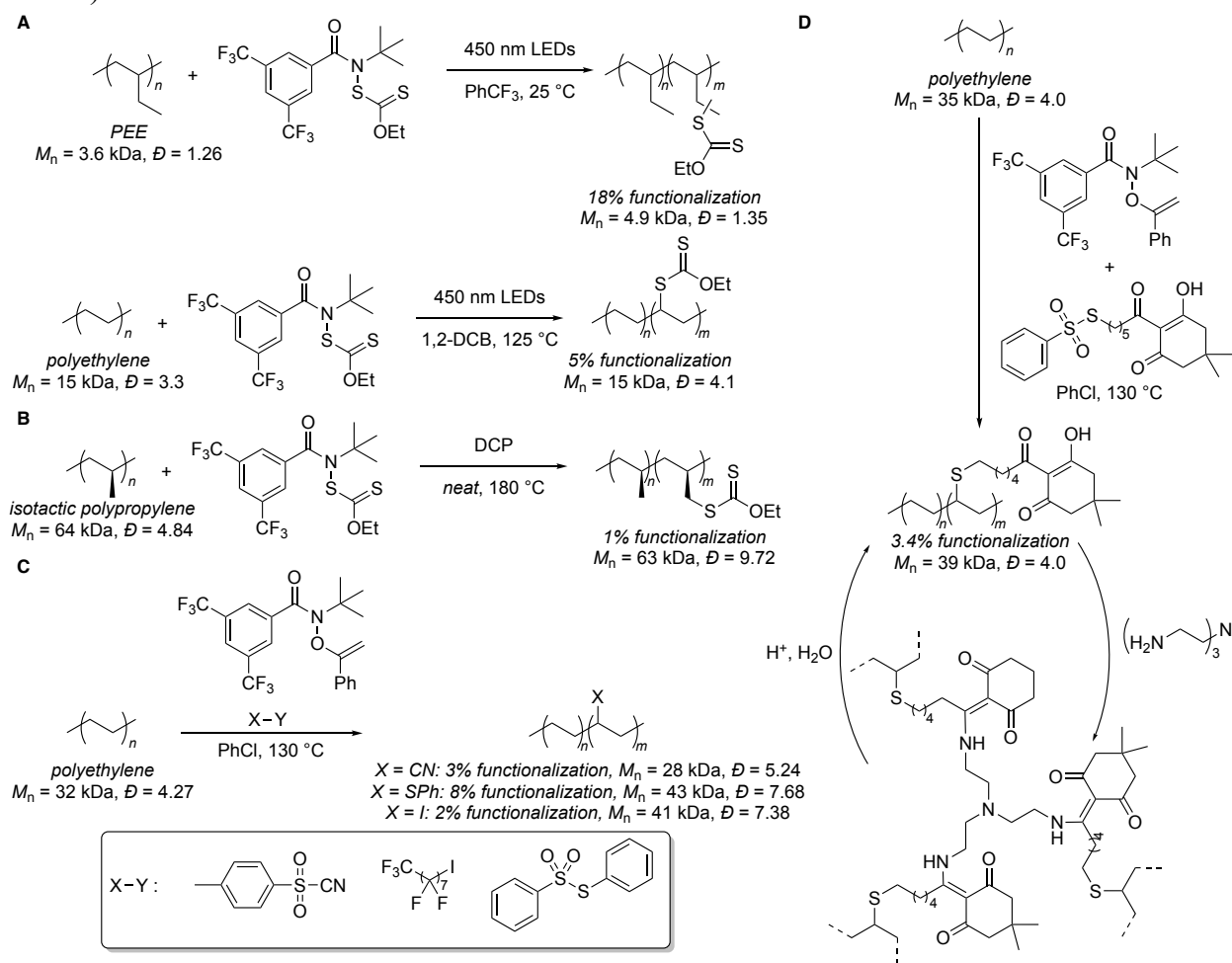


Figure 1.5.4. (A) Photoinitiated xanthylation of PEE. (B) Photoinitiated xanthylation of PE. (C) Xanthylation of PP. (D) Functionalization of PE with various radical traps. (E) Xanthylation of polyethylene to install triketone moieties for condensation with polyamines to form thermosets.

Post-polymerization functionalization also has enabled methods to cleave polyolefins, to generate materials with greener methods of disposal, to create fragments that are precursors for materials with circularity, or to convert polyolefins to value-added products.⁹⁰ One strategy that has emerged is the unsaturation of polyolefins to incorporate olefins into the backbone of the

polymer. The installed olefin can be functionalized further with well preceded reactions. Goldman and Coates and coworkers developed the iridium-catalyzed dehydrogenation of poly(1-hexene) with norbornene as the hydrogen acceptor (Figure 1.5.5A).⁹¹

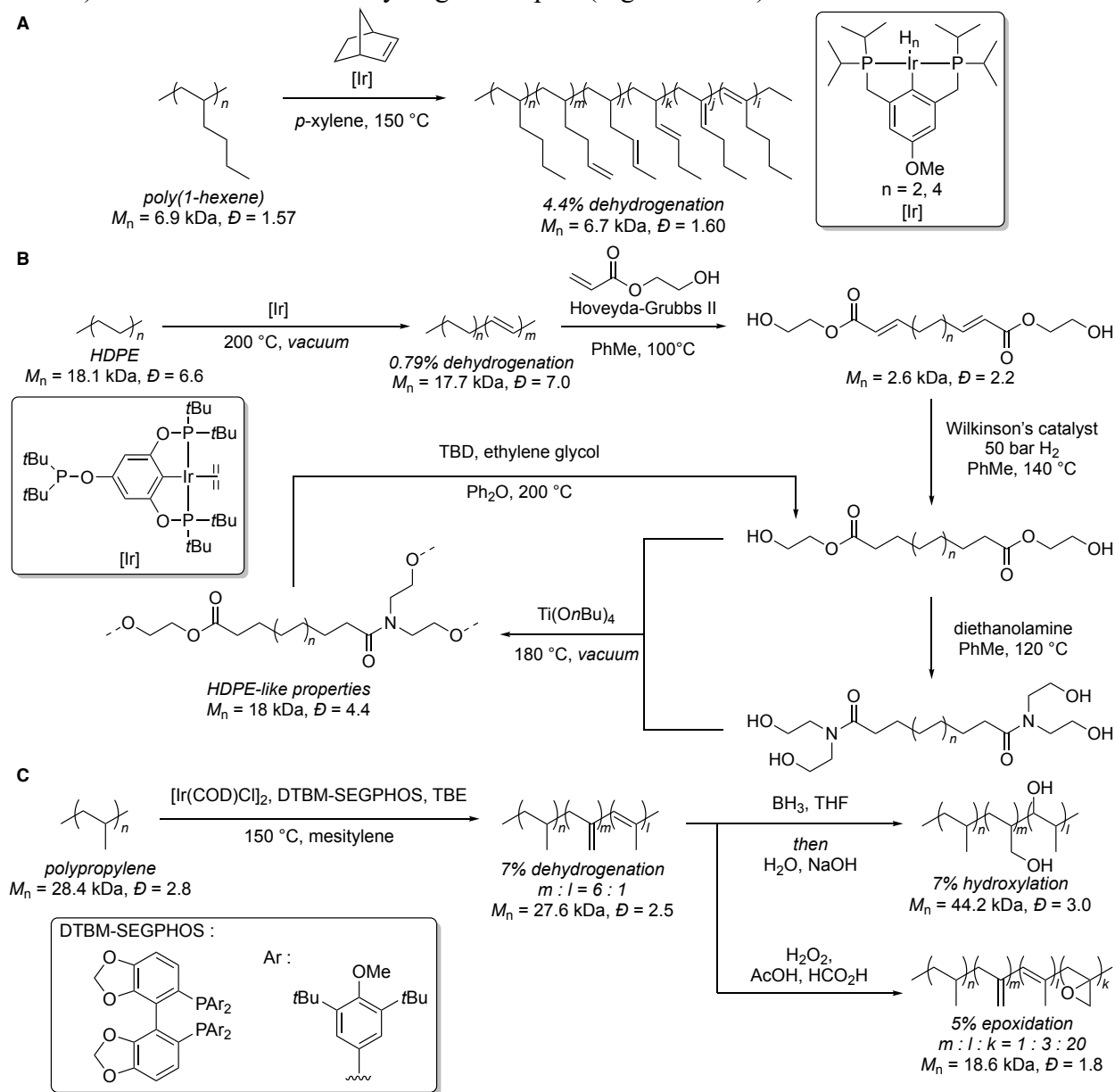


Figure 1.5.5. (A) Dehydrogenation of poly(1-hexene) with norbornene as hydrogen acceptor. (B) Synthesis of chemically recyclable polyethylene from dehydrogenation of HDPE. (C) Dehydrogenation of PP and subsequent functionalization.

Coates utilized iridium-catalyzed dehydrogenation to furnish *dehydro*-PE, which underwent cross metathesis with 2-hydroxyethyl acrylate to furnish telechelic fragments derived from PE (Figure 1.5.5B).⁹² Subsequent hydrogenation of the olefins and polycondensation of the fragments produced polymers with labile ester linkages. However, the bulk properties of the polymer were not comparable to those of polyolefins. To enhance the bulk properties of the polymer, the authors converted some of the telechelic esters to amides with diethanolamine prior to condensation to

increase the dispersity of the polymer. The resultant polymers had similar bulk properties as PE, and the polymers were able to undergo depolymerization and repolymerization by transesterification. Functionalization of the olefins by epoxidation or the sequence of hydroboration and oxidation installed oxygen-based functional groups into PP. These examples highlight the post-polymerization dehydrogenation of polyolefins to increase the sustainability of polyolefins.

Finally, the post-polymerization autoxidation of polyolefins has been demonstrated to cleave and oxidize polyolefins simultaneously to produce a statistical mixture of hydrocarbons equipped with oxygen-based functional groups.⁹⁰ Stahl and Beckham and coworkers reported the autoxidation of polyethylene catalyzed by manganese, cobalt, and *N*-hydroxyphthalimide with oxygen as the oxidant to generate short-chain dicarboxylates (C₄–C₁₇) (Figure 1.5.6A).⁹³ These diacids were then funneled biologically by engineered microbes to produce biodegradable polymers such as PHAs or singular products like β -keto adipate. Mecking and Nelson and coworkers demonstrated that the small-chain diacids that would result from the autoxidation of polyethylene could be repolymerized by polycondensation to generate materials with polyolefin-like properties (Figure 1.5.6B).⁹⁴ These examples highlighted that induced chain cleavage with concomitant post-polymerization functionalization of polyolefins can reduce the barriers to the recycling of polyolefins.

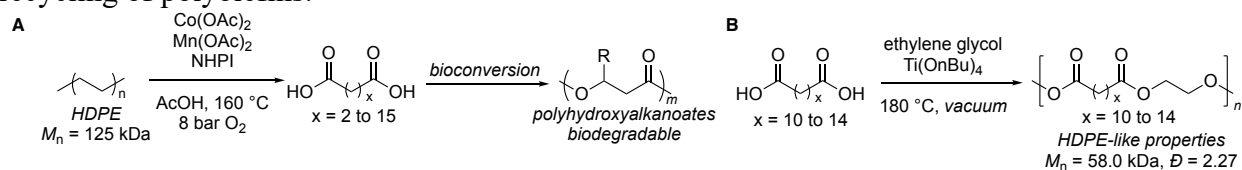


Figure 1.5.6. (A) Autoxidation of HDPE to short-chained diacids for bioconversion to polyhydroxyalkanoates. (B) Polycondensation of a mixture of short-chain diacids to polyesters with HDPE-like properties.

1.6 Summary

Polyolefins, which comprise a plurality of global plastics production, are versatile materials. Their hydrocarbon structure enables them to be thermally and chemically resistant, while providing excellent bulk properties. Since their discovery in the mid-20th century, polyolefins have become the default commodity single-use plastic for convenience as well as necessary materials to improve quality of life. Their synthesis from abundant monomers derived from petrochemical feedstock combined with the development of efficient catalysts for the polymerization of the monomers have culminated in an exponential growth in polyolefin production from the mid-20th century to present day. However, depolymerization of polyolefins back to monomer is extremely challenge because of the high ceiling temperatures of these polymers, and their prolonged existence in the environment has caused severe ecological consequences. In addition, polyolefin composites, which comprise most commercial plastics, are difficult to separate. This difficulty in separating the composites further disincentivizes the recycling of polyolefins used to make them. To mitigate these issues, materials that are “polyolefin-like” and that are circular have emerged as frontrunners to provide a more sustainable alternative to petrochemical-based plastics. In addition, the discovery of new materials with improved properties by post-polymerization functionalization have served as a platform to create more sustainable materials by reducing the complexity of polyolefin composites or creating opportunities to introduce circularity in polyolefins. Many challenges pertaining to treating mixed waste streams with similar levels of efficiency and

selectivity are still present. Still, research towards addressing these problems is progressing rapidly, and promising and practical strategies to tackle the accumulation of plastic are emerging.

1.7 References

- (1) Jensen, W. B. The Origin of the Polymer Concept. *J. Chem. Educ.* **2008**, *85*, 624
- (2) Sailors, H. R.; Hogan, J. P. History of Polyolefins. *Journal of Macromolecular Science, Part A* **1981**, *15*, 1377-1402
- (3) Kim, Y. K. The use of polyolefins in industrial and medical applications. In *Polyolefin Fibres*, Elsevier, 2017; pp 135–155.
- (4) Geyer, R.; Jambeck, J. R.; Law, K. L. Production, use, and fate of all plastics ever made. *Sci. Adv.* **2017**, *3*, e17000782
- (5) Hlatky, G. G. Heterogeneous Single-Site Catalysts for Olefin Polymerization. *Chem. Rev.* **2000**, *100*, 1347–1376
- (6) Soga, K.; Shiono, T. Ziegler-Natta catalysts for olefin polymerizations. *Prog. Polym. Sci.* **1997**, *22*, 1503–1546
- (7) Sawada, H. Thermodynamics of Polymerization. I. *Journal of Macromolecular Science, Part C* **2008**, *3*, 313–338
- (8) Muñoz, I.; Weidema, B. P. Ethylene and propylene production from steam cracking in Europe: a consequential perspective. *Int. J. Life Cycle Assess.* **2024**,
- (9) Chen, J. Q.; Bozzano, A.; Glover, B.; Fuglerud, T.; Kvisle, S. Recent advancements in ethylene and propylene production using the UOP/Hydro MTO process. *Catal. Today* **2005**, *106*, 103–107
- (10) Gibson, V. C.; Spitzmesser, S. K. Advances in Non-Metallocene Olefin Polymerization Catalysts. *Chem. Rev.* **2003**, *103*, 283–316
- (11) Resconi, L.; Cavallo, L.; Fait, A.; Piemontesi, F. Selectivity in Propene Polymerization with Metallocene Catalysts. *Chem. Rev.* **2000**, *100*, 1253–1346
- (12) Luft, G.; Kämpf, R.; Seidl, H. Synthesis conditions and structure of low density polyethylene. I. Short and long chain branching. *Macromol. Mater. Eng.* **1982**, *108*, 203–217
- (13) Wang, W.-J.; Yan, D.; Zhu, S.; Hamielec, A. E. Kinetics of Long Chain Branching in Continuous Solution Polymerization of Ethylene Using Constrained Geometry Metallocene. *Macromolecules* **1998**, *31*, 8677–8683
- (14) Stevens, J. C. Constrained geometry and other single site metallocene polyolefin catalysts: A revolution in olefin polymerization. *Stud. Surf. Sci. Catal.* **1996**, *101*, 11–20
- (15) McKnight, A. L.; Waymouth, R. M. Group 4 *ansa*-Cyclopentadienyl-Amido Catalysts for Olefin Polymerization. *Chem. Rev.* **1998**, *98*, 2587–2598
- (16) Natta, G.; Pino, P.; Corradini, P.; Danusso, F.; Mantica, E.; Mazzanti, G.; Moraglio, G. Crystalline High Polymer of α -Olefins. *J. Am. Chem. Soc.* **1955**, *77*, 1708–1710
- (17) Hogan, J. P. Ethylene polymerization catalysis over chromium oxide. *J. Polym. Sci. A Polym. Chem.* **1970**, *8*, 2637-2652
- (18) Cossee, P. Ziegler-Natta catalysis I. Mechanism of polymerization of α -olefins with Ziegler-Natta catalysts. *J. Catal.* **1964**, *3*, 80–88
- (19) Chen, E. Y.-X.; Marks, T. J. Cocatalysts for Metal-Catalyzed Olefin Polymerization: Activators, Activation Processes, and Structure-Activity Relationships. *Chem. Rev.* **2000**, *100*, 1391–1434
- (20) Shapiro, P. J.; Cotter, D. W.; Schaefer, W. P.; Labinger, J. A.; Bercaw, J. E. Model Ziegler-Natta α -Olefin Polymerization Catalysts Derived from $[\{(\eta^5\text{-C}_5\text{Me}_4)\text{SiMe}_2(\eta^1\text{-NCMe}_3)\}(\text{PMe}_3)\text{Sc}(\mu_2\text{-H})]_2$ and $[\{(\eta^5\text{-C}_5\text{Me}_4)\text{SiMe}_2(\eta^1\text{-NCMe}_3)\}(\mu_2\text{-CH}_2\text{CH}_2\text{CH}_3)]_2$. Synthesis, Structures, and Kinetic and Equilibrium Investigations of the Catalytically Active Species in Solution. *J. Am. Chem. Soc.* **1994**, *116*, 4623–4640

- (21) Fisch, A. G. Ziegler-Natta Catalysts. In *Kirk-Othmer Encyclopedia of Chemical Technology*, Wiley, 2019; pp 1–22.
- (22) Cossee, P. On the reaction mechanism of the ethylene polymerization with heterogeneous ziegler-natta catalysts. *Tetrahedron Lett.* **1960**, *1*, 12–16
- (23) Collins, S.; Kelly, W. M.; Holden, D. A. Polymerization of Propylene Using Supported, Chiral, *ansa*-Metallocene Catalysts: Production of Polypropylene with Narrow Molecular Weight Distribution. *Macromolecules* **1991**, *25*, 1780–1785
- (24) Kim, I.; Jordan, R. F. Propylene Polymerization with *ansa*-Metallocene Amide Complexes. *Macromolecules* **1996**, *29*, 489–491
- (25) Shiman, D. I.; Vasilenko, I. V.; Kostjuk, S. V. Cationic polymerization of isobutylene by AlCl₃/ether complexes in non-polar solvents: Effect of ether structure on the selectivity of β -H elimination. *Polymer* **2013**, *54*, 2235–2242
- (26) Popelka, E.; Khanam, P. N.; AlMaadeed, M. A. Surface modification of polyethylene/graphene composite using corona discharge. *J. Phys. D: Appl. Phys.* **2018**, *51*, 105302
- (27) Vocke, C.; Anttila, U.; Heino, M.; Hietaoja, P.; Seppälä, J. Use of oxazoline functionalized polyolefins and elastomers as compatibilizers for thermoplastic blends. *J. Appl. Polym. Sci.* **1998**, *70*, 1923–1930
- (28) Wiesinger, H.; Wang, Z.; Hellweg, S. Deep Dive into Plastic Monomers, Additives, and Processing Aids. *Environ. Sci. Technol.* **2021**, *55*, 9339–9351
- (29) Chen, W.; Gong, Y.; Mckie, M.; Almuhtaram, H.; Sun, J.; Barrett, H.; Yang, D.; Wu, M.; Andrews, R. C.; Peng, H. Defining the Chemical Additives Driving *In Vitro* Toxicities of Plastics. *Environ. Sci. Technol.* **2022**, *56*, 14627–14639
- (30) Hahladakis, J. N.; Velis, C. A.; Weber, R.; Iacovidou, E.; Purnell, P. An overview of chemical additives present in plastics: Migration, release, fate and environmental impact during their use, disposal and recycling. *J. Hazard. Mater.* **2018**, *344*, 179–199
- (31) Spell, H. L.; Eddy, R. D. Determination of additives in polyethylene by absorption spectroscopy. *Anal. Chem.* **1960**, *32*, 1811–1814
- (32) Ragaert, K.; Delva, L.; Van Greem, K. Mechanical and chemical recycling of solid plastic waste. *Waste Manag.* **2017**, *69*, 24–58
- (33) Zhao, Y.-B.; Lv, X.-D.; Ni, H.-G. Solvent-based separation and recycling of waste plastics: A review. *Chemosphere* **2018**, *209*, 707–720
- (34) Coates, G. W.; Getzler, Y. D. Y. L. Chemical recycling to monomer for an ideal, circular polymer economy. *Nat. Rev. Mater.* **2020**, *5*, 501–516
- (35) Ignatyev, I. A.; Thielemans, W.; Vander Beke, B. Recycling of Polymers: A Review. *ChemSusChem* **2014**, *7*, 1579–1593
- (36) Vollmer, I.; Jenks, M. J. F.; Roelands, M. C. P.; White, R. J.; Harmelen, T.; Wild, P.; Laan, G. P.; Meirer, F.; Keurentjes, J. T. F.; Weckhuysen, B. M. Beyond Mechanical Recycling: Giving New Life to Plastic Waste. *Angew. Chem. Int. Ed.* **2020**, *59*, 15402–15423
- (37) Pinheiro, L. A.; Chinelatto, M. A.; Canevarolo, S. V. The role of chain scission and chain branching in high density polyethylene during thermo-mechanical degradation. *Polym. Degrad. Stab.* **2004**, *86*, 445–453
- (38) Ellen MacArthur Foundation and McKinsey & Company. <http://www.ellenmacarthurfoundation.org/publications>. (accessed 2021-08-15). The New Plastics Economy — Rethinking the future of plastics

- (39) Geyer, R.; Jambeck, J. R.; Law, K. L. Production, use, and fate of all plastics ever made. *Sci. Adv.* **2017**, *3*, e1700782
- (40) Von Vacano, B.; Mangold, H.; Vandermeulen, G. W. M.; Battagliarin, G.; Hofmann, M.; Bean, J.; Künkel, A. Sustainable Design of Structural and Functional Polymers for a Circular Economy. *Angew. Chem. Int. Ed.* **2023**, *62*,
- (41) Plummer, C. M.; Li, L.; Chen, Y. The post-modification of polyolefins with emerging synthetic methods. *Polym. Chem.* **2020**, *11*, 6862–6872
- (42) Zuin, V. G.; Kümmerer, K. Chemistry and materials science for a sustainable circular polymeric economy. *Nat. Rev. Mater.* **2022**, *7*, 76-78
- (43) Shi, C.; Reilly, L. T.; Phani Kumar, V. S.; Coile, M. W.; Nicholson, S. R.; Broadbelt, L. J.; Beckham, G. T.; Chen, E. Y.-X. Design principles for intrinsically circular polymers with tunable properties. *Chem* **2021**, *7*, 2896-2912
- (44) Shi, C.; Reilly, L. T.; Chen, E. Y. X. Hybrid Monomer Design Synergizing Property Trade-offs in Developing Polymers for Circularity and Performance. *Angew. Chem. Int. Ed.* **2023**, *62*,
- (45) Arrington, A. S.; Brown, J. R.; Win, M. S.; Winey, K. I.; Long, T. E. Melt polycondensation of carboxytelechelic polyethylene for the design of degradable segmented copolyester polyolefins. *Polym. Chem.* **2022**, *13*, 3116–3125
- (46) Häußler, M.; Eck, M.; Rothauer, D.; Mecking, S. Closed-loop recycling of polyethylene-like materials. *Nature* **2021**, *590*, 423–427
- (47) Arrington, A. S.; Long, T. E. Influence of carboxytelechelic oligomer molecular weight on the properties of chian extended polyethylenes. *Polymer* **2022**, *259*, 125319
- (48) Li, X. L.; Clarke, R. W.; An, H. Y.; Gowda, R. R.; Jiang, J. Y.; Xu, T. Q.; Chen, E. Y. X. Dual Recycling of Depolymerization Catalyst and Biodegradable Polyester that Markedly Outperforms Polyolefins. *Angew. Chem. Int. Ed.* **2023**, *62*, e202303791
- (49) Shi, C.; McGraw, M. L.; Li, Z.-C.; Cavallo, L.; Falivene, L.; Chen, E. Y.-X. High-performance pan-tactic polythioesters with intrinsic crystallinity and chemical recyclability. *Sci. Adv.* **2020**, *6*, 10.1126/sciadv.abc0495
- (50) Jang, Y.-J.; Nguyen, S.; Hillmyer, M. A. Chemically Recyclable Linear and Branched Polyethylenes Synthesized from Stoichiometrically Self Balanced Telechelic Polyethylenes. *J. Am. Chem. Soc.* **2024**, *146*, 4771–4782
- (51) Zhao, Y.; Rettner, E. M.; Harry, K. L.; Hu, Z.; Miscall, J.; Rorrer, N. A.; Miyake, G. M. Chemically recyclable polyolefin-like multiblock polymers. *Science* **2023**, *382*, 310–314
- (52) Kocen, A. L.; Cui, S.; Lin, T.-W.; LaPointe, A. M.; Coates, G. W. Chemically Recyclable Ester-Linked Polypropylene. *J. Am. Chem. Soc.* **2022**, *144*, 12613–12618
- (53) Parke, S. M.; Lopez, J. C.; Cui, S.; LaPointe, A. M.; Coates, G. W. Polyethylene Incorporating Diels–Alder Comonomers: A “Trojan Horse” Strategy for Chemically Recyclable Polyolefins. *Angew. Chem. Int. Ed.* **2023**, *62*, e202301927
- (54) Sudesh, K.; Abe, H.; Doi, Y. Synthesis, structure and properties of polyhydroxyalkanoates: biological polyesters. *Prog. Polym. Sci.* **2000**, *25*, 1503–1555
- (55) Zhou, Z.; Lapointe, A. M.; Shaffer, T. D.; Coates, G. W. Nature-inspired methylated polyhydroxybutyrates from C1 and C4 feedstocks. *Nat. Chem.* **2023**, *15*, 856–861
- (56) Bruckmoser, J.; Pongratz, S.; Stieglitz, L.; Rieger, B. Highly Ioselective Ring-Opening Polymerization of *rac*- β -Butyrolactone: Access to Synthetic Poly(3-hydroxybutyrate) with Polyolefin-like Material Properties. *J. Am. Chem. Soc.* **2023**, *145*, 11494–11498

- (57) Zhang, Z.; Quinn, E. C.; Olmedo-Martínez, J. L.; Caputo, M. R.; Franklin, K. A.; Müller, A. J.; Chen, E. Y. X. Toughening Brittle Bio-P3HB with Synthetic P3HB of Engineered Stereomicrostructures. *Angew. Chem. Int. Ed.* **2023**, *62*,
- (58) Zhou, L.; Zhang, Z.; Shi, C.; Scoti, M.; Barange, D. K.; Gowda, R. R.; Chen, E. Y.-X. Chemically circular, mechanically tough, and melt-processable polyhydroxyalkanoates. *Science* **2023**, *380*, 64–69
- (59) Abel, B. A.; Snyder, R. L.; Coates, G. W. Chemically recyclable thermoplastics from reversible-deactivation polymerization of cyclic acetals. *Science* **2021**, *373*, 783–789
- (60) Hester, H. G.; Abel, B. A.; Coates, G. W. Ultra-High-Molecular-Weight Poly(Dioxolane): Enhancing the Mechanical Performance of a Chemically Recyclable Polymer. *J. Am. Chem. Soc.* **2023**, *145*, 8800–8804
- (61) Johnson, A. M.; Johnson, J. A. Thermally Robust yet Deconstructable and Chemically Recyclable High-Density Polyethylene (HDPE)-Like Materials Based on Si–O Bonds. *Angew. Chem. Int. Ed.* **2023**, *135*,
- (62) Jehanno, C.; Alty, J. W.; Roosen, M.; De Meester, S.; Dove, A. P.; Chen, E. Y.-X.; Leibfarth, F. A.; Sardon, H. Critical advances and future opportunities in upcycling commodity polymers. *Nature* **2022**, *603*, 803–814
- (63) Boaen, N. K.; Hillmyer, M. A. Post-polymerization functionalization of polyolefins. *Chem. Soc. Rev.* **2005**, *34*, 267
- (64) Menendez Rodriguez, G.; Díaz-Requejo, M. M.; Pérez, P. J. Metal-Catalyzed Postpolymerization Strategies for Polar Group Incorporation into Polyolefins Containing C–C, C=C, and Aromatic Rings. *Macromolecules* **2021**, *54*, 4971–4985
- (65) Walker, T. W.; Frelka, N.; Shen, Z.; Chew, A. K.; Banick, J.; Grey, S.; Kim, M. S.; Dumesic, J. A.; Van Lehn, R. C.; Huber, G. W. Recycling of multilayer plastic packaging materials by solvent-targeted recovery and precipitation. *Sci. Adv.* **2020**, *6*, aba7599
- (66) Wu, D. Y.; Gutowski, W. S.; Li, S.; Griesser, H. J. Ammonia plasma treatment of polyolefins for adhesive bonding with a cyanoacrylate adhesive. *J. Adhes. Sci. Technol.* **2012**, *9*, 501–525
- (67) Sanchis, M. R.; Blanes, V.; Blanes, M.; Garcia, D.; Balart, R. Surface modification of low density polyethylene (LDPE) film by low pressure O₂ plasma treatment. *Eur. Polym. J.* **2006**, *42*, 1558–1568
- (68) Seko, N.; Ninh, N. T. Y.; Tamada, M. Emulsion grafting of glycidyl methacrylate onto polyethylene fiber. *Radiat. Phys. Chem.* **2010**, *79*, 22–26
- (69) Samay, G.; Nagy, T.; White, J. L. Grafting maleic anhydride and comonomers onto polyethylene. *J. Appl. Polym. Sci.* **1995**, *56*, 1423–1433
- (70) Olsen, D. A.; Osteraas, A. J. Difluorocarbene modification of polymer and fiber surfaces. *J. Appl. Polym. Sci.* **1969**, *13*, 1523–1535
- (71) Osteraas, A. J.; Olsen, D. A. Incorporation of Functional Groups onto the Surface of Polyethylene. *Nature* **1969**, *221*, 1140–1141
- (72) Aglietto, M.; Bertani, R.; Ruggeri, G.; Fiordiponti, P.; Segre, A. L. Functionalization of polyolefins: structure of functional groups in polyethylene reacted with ethyl diazoacetate. *Macromolecules* **1989**, *22*, 1492–1493
- (73) Aglietto, M.; Alterio, R.; Bertani, R.; Galleschi, F.; Ruggeri, G. Polyolefin functionalization by carbene insertion for polymer blends. *Polymer* **1989**, *30*, 1133–1136
- (74) Bateman, S. A.; Wu, D. Y. Sulfonyl azides—an alternative route to polyolefin modification. *J. Appl. Polym. Sci.* **2002**, *84*, 1395–1402

- (75) Liu, D.; Bielawski, C. W. Direct azidation of isotactic polypropylene and synthesis of ‘grafted to’ derivatives thereof using azide–alkyne cycloaddition chemistry. *Polym. Int.* **2016**, *66*, 70–76
- (76) D’íaz-Requejo, M. M.; Wehrmann, P.; Leatherman, M. D.; Trofimenko, S.; Mecking, S.; Brookhart, M.; Pérez, P. J. Controlled, Copper-Catalyzed Functionalization of Polyolefins. *Macromolecules* **2005**, *38*, 4966–4969
- (77) Lepage, M. L.; Simhadri, C.; Liu, C.; Takaffoli, M.; Bi, L.; Crawford, B.; Milani, A. S.; Wulff, J. E. A broadly applicable cross-linker for aliphatic polymers containing C–H bonds. *Science* **2019**, *366*, 875–878
- (78) Clarke, R. W.; Sandmeier, T.; Franklin, K. A.; Reich, D.; Zhang, X.; Vengallur, N.; Patra, T. K.; Tannenbaum, R. J.; Adhikari, S.; Kumar, S. K.; Rovis, T.; Chen, E. Y.-X. Dynamic crosslinking compatibilizes immiscible mixed plastics. *Nature* **2023**, *616*, 731–739
- (79) Kondo, Y.; García-Cuadrado, D.; Hartwig, J. F.; Boen, N. K.; Wagner, N. L.; Hillmyer, M. A. Rhodium-Catalyzed, Regiospecific Functionalization of Polyolefins in the Melt. *J. Am. Chem. Soc.* **2002**, *124*, 1164–1165
- (80) Bae, C.; Hartwig, J. F.; Boen Harris, N. K.; Long, R. O.; Anderson, K. S.; Hillmyer, M. A. Catalytic Hydroxylation of Polypropylenes. *J. Am. Chem. Soc.* **2005**, *127*, 767–776
- (81) Boen, N. K.; Hillmyer, M. A. Selective and Mild Oxyfunctionalization of Model Polyolefins. *Macromolecules* **2003**, *36*, 7027–7034
- (82) Bunescu, A.; Lee, S.; Li, Q.; Hartwig, J. F. Catalytic Hydroxylation of Polyethylenes. *ACS Cent. Sci.* **2017**, *3*, 895–903
- (83) Chen, L.; Malollari, K. G.; Uliana, A.; Sanchez, D.; Messersmith, P. B.; Hartwig, J. F. Selective, Catalytic Oxidations of C–H Bonds in Polyethylenes Produce Functional Materials with Enhanced Adhesion. *Chem* **2021**, *7*, 137–145
- (84) Huang, X.; Groves, J. T. Beyond ferryl-mediated hydroxylation: 40 years of the rebound mechanism and C–H activation. *J. Biol. Inorg. Chem.* **2017**, *22*, 185–207
- (85) Chen, L.; Malollari, K. G.; Uliana, A.; Hartwig, J. F. Ruthenium-Catalyzed, Chemoselective and Regioselective Oxidation of Polyisobutene. *J. Am. Chem. Soc.* **2021**, *143*, 4531–4535
- (86) Williamson, J. B.; Czaplowski, W. L.; Alexanian, E. J.; Leibfarth, F. A. Regioselective C–H Xanthylation as a Platform for Polyolefin Functionalization. *Angew. Chem. Int. Ed.* **2018**, *57*, 6261–6265
- (87) Williamson, J. B.; Na, C. G.; Johnson III, R. R.; William, D. F. M.; Alexanian, E. J.; Leibfarth, F. A. Chemo- and Regioselective Functionalization of Isotactic Polypropylene: A Mechanistic and Structure–Property Study. *J. Am. Chem. Soc.* **2019**, *141*, 12815–12823
- (88) Fazekas, T. J.; Alty, J. W.; Neidhart, E. K.; Miller, A. S.; Leibfarth, F. A.; Alexanian, E. J. Diversification of aliphatic C–H bonds in small molecules and polyolefins through radical chain transfer. *Science* **2022**, *375*, 545–550
- (89) Neidhart, E. K.; Hua, M.; Peng, Z.; Kearney, L. T.; Bhat, V.; Vashahi, F.; Alexanian, E. J.; Sheiko, S. S.; Wang, C.; Helms, B. A.; Leibfarth, F. A. C–H Functionalization of Polyolefins to Access Reprocessable Polyolefin Thermosets. *J. Am. Chem. Soc.* **2023**, *145*, 27450–27458
- (90) Schwab, S. T.; Baur, M.; Nelson, T. F.; Mecking, S. Synthesis and Deconstruction of Polyethylene-type Materials. *Chem. Rev.* **2024**, *124*, 2327–2351
- (91) Ray, A.; Zhu, K.; Kissin, Y. V.; Cherian, A. E.; Coates, G. W.; Goldman, A. S. Dehydrogenation of aliphatic polyolefins catalyzed by pincer-ligated iridium complexes. *Chem. Commun.* **2005**, 3388–3390

- (92) Arroyave, A.; Cui, S.; Lopez, J. C.; Kocen, A. L.; LaPointe, A. M.; Delferro, M.; Coates, G. W. Catalytic Chemical Recycling of Post-Consumer Polyethylene. *J. Am. Chem. Soc.* **2022**, *144*, 23280–23285
- (93) Sullivan, K. P.; Werner, A. Z.; Ramirez, K. J.; Ellis, L. D.; Bussard, J. R.; Black, B. A.; Brandner, D. G.; Bratti, F.; Buss, B. L.; Dong, X.; Haugen, S. J.; Ingraham, M. A.; Konev, M. O.; Michener, W. E.; Miscall, J.; Pardo, I.; Woodworth, S. P.; Guss, A. M.; Román-Leshkov, Y.; Stahl, S. S.; Beckham, G. T. Mixed plastics waste valorization through tandem chemical oxidation and biological funneling. *Science* **2022**, *378*, 207–211
- (94) Nelson, T. F.; Rothauer, D.; Sander, M.; Mecking, S. Degradable and Recyclable Polyesters from Multiple Chain Length Bio- and Waste-Sourceable Monomers. *Angew. Chem. Int. Ed.* **2023**, *62*, e202310729
- (95) Tsarevsky, N. V. Degradable and biodegradable polymers by controlled/living radical polymerization: from synthesis to application. In *Green Polymerization Methods: Renewable Starting Materials, Catalysis and Waste Reduction*, Mathers, R. T., Meier, M. A. R. Eds.; WILEY-VCH Verlag GmbH & Co. KGaA, 2011; pp 235–261.
- (96) Biermann, U.; Bornscheuer, U.; Meier, M. A.; Metzger, J. O.; Schafer, H. J. Oils and fats as renewable raw materials in chemistry. *Angew. Chem. Int. Ed.* **2011**, *50*, 3854–3871
- (97) Jain, J. P.; Sokolsky, M.; Kumar, N.; Domb, A. J. Fatty Acid Based Biodegradable Polymer. *Polym. Rev.* **2008**, *48*, 156–191
- (98) Montero de Espinosa, L.; Meier, M. A. R. Plant oils: The perfect renewable resource for polymer science?! *Eur. Polym. J.* **2011**, *47*, 837–852
- (99) Meier, M. A. R.; Metzger, J. O.; Schubert, U. S. Plant oil renewable resources as green alternatives in polymer science. *Chem. Soc. Rev.* **2007**, *36*, 1788–1802
- (100) Desroches, M.; Escouvois, M.; Auvergne, R.; Caillol, S.; Boutevin, B. From Vegetable Oils to Polyurethanes: Synthetic Routes to Polyols and Main Industrial Products. *Polym. Rev.* **2012**, *52*, 38–79
- (101) Kunduru, K. R.; Basu, A.; Haim Zada, M.; Domb, A. J. Castor Oil-Based Biodegradable Polyesters. *Biomacromolecules* **2015**, *16*, 2572–2587
- (102) Enferadi Kerenkan, A.; Béland, F.; Do, T.-O. Chemically catalyzed oxidative cleavage of unsaturated fatty acids and their derivatives into valuable products for industrial applications: a review and perspective. *Catal. Sci. Technol.* **2016**, *6*, 971–987
- (103) Rybak, A.; Fokou, P. A.; Meier, M. A. R. Metathesis as a versatile tool in oleochemistry. *Eur. J. Lipid Sci. Technol.* **2008**, *110*, 797–804
- (104) Goldbach, V.; Roesle, P.; Mecking, S. Catalytic Isomerizing ω -Functionalization of Fatty Acids. *ACS Catal.* **2015**, *5*, 5951–5972
- (105) Sahmetlioglu, E.; Nguyen, H. T. H.; Nsengiyumva, O.; Göktürk, E.; Miller, S. A. Silicon Acetal Metathesis Polymerization. *ACS Macro Lett.* **2016**, *5*, 466–470
- (106) Cheng, C.; Watts, A.; Hillmyer, M. A.; Hartwig, J. F. Polysilylether: A Degradable Polymer from Biorenewable Feedstocks. *Angew. Chem. Int. Ed.* **2016**, *55*, 11872–11876
- (107) Lohmeijer, B. G. G.; Dubois, G.; Liebfarth, F.; Pratt, R. C.; Nederberg, F.; Nelson, A.; Waymouth, R. M.; Wade, C.; Hedrick, J. L. Organocatalytic Living Ring-Opening Polymerization of Cyclic Carbosiloxanes. *Org. Lett.* **2006**, *8*, 4683–4686
- (108) Kazmierski, K.; Chojnowski, J.; Mcvie, J. The Acid-Catalyzed Condensation of Methyl-Substituted Model Oligosiloxanes Bearing Silanol and Ethoxysilane Functions. *Eur. Polym. J.* **1994**, *30*, 515–527

- (109) Cypryk, M.; Apeloig, Y. Mechanism of the acid-catalyzed Si-O bond cleavage in siloxanes and siloxanols. A theoretical study. *Organometallics* **2002**, *21*, 2165–2175
- (110) Shanks, R.; Kong, I. Thermoplastic Elastomers. In *Thermoplastic Elastomers*, El-Sonbati, A. Ed.; InTech, 2012; pp 137–154.
- (111) Dechy-Cabaret, O.; Martin-Vaca, B.; Bourissou, D. Controlled ring-opening polymerization of lactide and glycolide. *Chem. Rev.* **2004**, *104*, 6147–6176
- (112) Yao, K.; Tang, C. Controlled Polymerization of Next-Generation Renewable Monomers and Beyond. *Macromolecules* **2013**, *46*, 1689–1712
- (113) Lecomte, P.; Jérôme, C. Recent Developments in Ring-Opening Polymerization of Lactones. In *Synthetic Biodegradable Polymers*, Rieger, B., Künkel, A., Coates, G. W., Reichardt, R., Dinjus, E., Zevaco, T. A. Eds.; Springer Berlin Heidelberg, 2012; pp 173–217.
- (114) Tschan, M. J. L.; Brulé, E.; Haquette, P.; Thomas, C. M. Synthesis of biodegradable polymers from renewable resources. *Polym. Chem.* **2012**, *3*, 836–851
- (115) Slivniak, R.; Domb, A. J. Macrolactones and polyesters from ricinoleic acid. *Biomacromolecules* **2005**, *6*, 1679–1688
- (116) Liu, G.; Kong, X.; Wan, H.; Narine, S. Production of 9-hydroxynonanoic acid from methyl oleate and conversion into lactone monomers for the synthesis of biodegradable polylactones. *Biomacromolecules* **2008**, *9*, 949–953
- (117) Abraham, S.; Narine, S. S. Polynonanolactone synthesized from vegetable oil: Evaluation of physical properties, biodegradation, and drug release behavior. *J. Polym. Sci., Part A: Polym. Chem.* **2009**, *47*, 6373–6387
- (118) Witt, T.; Mecking, S. Large-ring lactones from plant oils. *Green Chem.* **2013**, *15*, 2361–2364
- (119) Witt, T.; Haussler, M.; Mecking, S. No Strain, No Gain? Enzymatic Ring-Opening Polymerization of Strainless Aliphatic Macrolactones. *Macromol. Rapid Commun.* **2017**, *38*,
- (120) Myers, D.; Witt, T.; Cyriac, A.; Bown, M.; Mecking, S.; Williams, C. K. Ring opening polymerization of macrolactones: high conversions and activities using an yttrium catalyst. *Polym. Chem.* **2017**, *8*, 5780–5785
- (121) van der Meulen, I.; Gubbels, E.; Huijser, S.; Sablong, R.; Koning, C. E.; Heise, A.; Duchateau, R. Catalytic Ring-Opening Polymerization of Renewable Macrolactones to High Molecular Weight Polyethylene-like Polymers. *Macromolecules* **2011**, *44*, 4301–4305
- (122) Katir, N.; El Kadib, A.; Dahrouch, M.; Castel, A.; Gatica, N.; Benmaarouf, Z.; Riviere, P. Amphiphilic polyesters derived from silylated and germylated fatty compounds. *Biomacromolecules* **2009**, *10*, 850–857
- (123) Frampton, M. B.; Subczynska, I.; Zelisko, P. M. Biocatalytic Synthesis of Silicone Polyesters. *Biomacromolecules* **2010**, *11*, 1818–1825
- (124) El Kadib, A.; Katir, N.; Marcotte, N.; Molvinger, K.; Castel, A.; Rivière, P.; Brunel, D. Nanocomposites from natural templates based on fatty compound-functionalised siloxanes. *J. Mater. Chem.* **2009**, *19*, 6004–6014
- (125) Spasyuk, D.; Smith, S.; Gusev, D. G. Replacing phosphorus with sulfur for the efficient hydrogenation of esters. *Angew. Chem. Int. Ed.* **2013**, *52*, 2538–2542
- (126) Saudan, L. A.; Saudan, C. M.; Debieux, C.; Wyss, P. Dihydrogen reduction of carboxylic esters to alcohols under the catalysis of homogeneous ruthenium complexes: high efficiency and unprecedented chemoselectivity. *Angew. Chem. Int. Ed.* **2007**, *46*, 7473–7476
- (127) Kuriyama, W.; Matsumoto, T.; Ogata, O.; Ino, Y.; Aoki, K.; Tanaka, S.; Ishida, K.; Kobayashi, T.; Sayo, N.; Saito, T. Catalytic Hydrogenation of Esters. Development of an Efficient Catalyst

and Processes for Synthesising (R)-1,2-Propanediol and 2-(1-Menthoxy)ethanol. *Org. Process Res. Dev.* **2012**, *16*, 166–171

(128) Xu, J.; Feng, E.; Song, J. Renaissance of Aliphatic Polycarbonates: New Techniques and Biomedical Applications. *J. Appl. Polym. Sci.* **2014**, *131*, DOI: 10.1002/app.39822

(129) Sun, J.; Kuckling, D. Synthesis of high-molecular-weight aliphatic polycarbonates by organo-catalysis. *Polym. Chem.* **2016**, *7*, 1642–1649

(130) Andriot, M.; Chao, S. H.; Colas, A.; Cray, S.; de Buyl, F.; DeGroot, J. V. J.; Dupont, A.; Easton, T.; Garaud, J. L.; E., G.; Gubbels, F.; Jungk, M.; Leadley, S.; Lecomte, J. P.; Lenoble, B.; Meeks, R.; Mountney, A.; Shearer, G.; Stassen, S.; Stevens, C.; Thomas, X.; Wolf, A. T. Silicones in industrial applications. In *Inorganic Polymers*, Jaeger, R. D., Gleria, M. Eds.; Nova Science Publishers, 2007; pp 61–161.

(131) Reding, M. T.; Buchald, S. L. An Inexpensive Air-Stable Titanium-Based System for the Conversion of Esters to Primary Alcohols. *J. Org. Chem.* **1995**, *60*, 7884–7890

(132) Duda, A.; Kowalski, A.; Penczek, S.; Uyama, H.; Kobayashi, S. Kinetics of the ring-opening polymerization of 6-, 7-, 9-, 12-, 13-, 16-, and 17-membered lactones. Comparison of chemical and enzymatic polymerizations. *Macromolecules* **2002**, *35*, 4266–4270

(133) Focarete, M. L.; Scandola, M.; Kumar, A.; Gross, R. A. Physical Characterization of Poly(ω -pentadecalactone) Synthesized by Lipase-Catalyzed Ring-Opening Polymerization. *J. Polym. Sci., Part B: Polym. Phys.* **2001**, *39*, 1721–1729

(134) van der Meulen, I.; de Geus, M.; Antheunis, H.; Deumens, R.; Joosten, E. A. J.; Koning, C. E.; Heise, A. Polymers from Functional Macrolactones as Potential Biomaterials: Enzymatic Ring Opening Polymerization, Biodegradation, and Biocompatibility. *Biomacromolecules* **2008**, *9*, 3404–3410

(135) de Geus, M.; van der Meulen, I.; Goderis, B.; van Hecke, K.; Dorschu, M.; van der Werff, H.; Koning, C. E.; Heise, A. Performance polymers from renewable monomers: high molecular weight poly(pentadecalactone) for fiber applications. *Polym. Chem.* **2010**, *1*, 525–533

(136) Bisht, K. S.; Henderson, L. A.; Gross, R. A. Enzyme-Catalyzed Ring-Opening Polymerization of ω -Pentadecalactone. *Macromolecules* **1997**, *30*, 2705–2711

(137) Nakayama, Y.; Watanabe, N.; Kusaba, K.; Sasaki, K.; Cai, Z.; Shiono, T.; Tsutsumi, C. High activity of rare earth tetrahydroborates for ring-opening polymerization of ω -pentadecalactone. *J. Appl. Polym. Sci.* **2011**, *121*, 2098–2103

(138) Fernández, J.; Etxeberria, A.; Sarasua, J.-R. Synthesis and properties of ω -pentadecalactone-co- δ -hexalactone copolymers: a biodegradable thermoplastic elastomer as an alternative to poly(ϵ -caprolactone). *RSC Adv.* **2016**, *6*, 3137–3149

(139) Bouyahyi, M.; Duchateau, R. Metal-Based Catalysts for Controlled Ring-Opening Polymerization of Macrolactones: High Molecular Weight and Well-Defined Copolymer Architectures. *Macromolecules* **2014**, *47*, 517–524

(140) Amador, A. G.; Watts, A.; Neitzel, A. E.; Hillmyer, M. A. Entropically Driven Macrolide Polymerizations for the Synthesis of Aliphatic Polyester Copolymers Using Titanium Isopropoxide. *Macromolecules* **2019**, *52*, 2371–2383

(141) Bouyahyi, M.; Pepels, M. P. F.; Heise, A.; Duchateau, R. ω -Pentadecalactone Polymerization and ω -Pentadecalactone/ ϵ -Caprolactone Copolymerization Reactions Using Organic Catalysts. *Macromolecules* **2012**, *45*, 3356–3366

(142) Pascual, A.; Sardon, H.; Veloso, A.; Ruipérez, F.; Mecerreyes, D. Organocatalyzed Synthesis of Aliphatic Polyesters from Ethylene Brassylate: A Cheap and Renewable Macrolactone. *ACS Macro Lett.* **2014**, *3*, 849–853

- (143) Walther, P.; Naumann, S. N-Heterocyclic Olefin-Based (Co)polymerization of a Challenging Monomer: Homopolymerization of ω -Pentadecalactone and Its Copolymers with γ -Butyrolactone, δ -Valerolactone, and ϵ -Caprolactone. *Macromolecules* **2017**, *50*, 8406–8416
- (144) Pepels, M. P. F.; Hofman, W. P.; Kleijnen, R.; Spoelstra, A. B.; Koning, C. E.; Goossens, H.; Duchateau, R. Block Copolymers of “PE-Like” Poly(pentadecalactone) and Poly(l-lactide): Synthesis, Properties, and Compatibilization of Polyethylene/Poly(l-lactide) Blends. *Macromolecules* **2015**, *48*, 6909–6921
- (145) Todd, R.; Tempelaar, S.; Lo Re, G.; Spinella, S.; McCallum, S. A.; Gross, R. A.; Raquez, J.-M.; Dubois, P. Poly(ω -pentadecalactone)-b-poly(l-lactide) Block Copolymers via Organic-Catalyzed Ring Opening Polymerization and Potential Applications. *ACS Macro Lett.* **2015**, *4*, 408–411
- (146) Coles, Martyn P.; Hitchcock, Peter B. Zinc Guanidinate Complexes and Their Application in Ring-Opening Polymerisation Catalysis. *Eur. J. Inorg. Chem.* **2004**, *2004*, 2662–2672
- (147) van der Meulen, I.; Gubbels, E.; Huijser, S.; Sablong, R. I.; Koning, C. E.; Heise, A.; Duchateau, R. Catalytic Ring-Opening Polymerization of Renewable Macrolactones to High Molecular Weight Polyethylene-like Polymers. *Macromolecules* **2011**, *44*, 4301–4305
- (148) Brook, M. A. *Silicon in organic, organometallic, and polymer chemistry*; Wiley, 2000.
- (149) Swint, S. A.; Buese, M. A. A disiloxane equilibration approach to the preparation and characterization of 5,5'-(1,1,3,3-tetramethyldisiloxane-1,3-diyl)bisbicyclo[2.2.1]heptane-2,3-dicarboxylic anhydride. *J. Organomet. Chem.* **1991**, *402*, 145–153
- (150) Zumstein, M. T.; Kohler, H.-P. E.; McNeill, K.; Sander, M. High-Throughput Analysis of Enzymatic Hydrolysis of Biodegradable Polyesters by Monitoring Cohydrolysis of a Polyester-Embedded Fluorogenic Probe. *Environ. Sci. Technol.* **2017**, *51*, 4358–4367
- (151) De Hoe, G. X.; Zumstein, M. T.; Tiegs, B. J.; Brutman, J. P.; McNeill, K.; Sander, M.; Coates, G. W.; Hillmyer, M. A. Sustainable Polyester Elastomers from Lactones: Synthesis, Properties, and Enzymatic Hydrolyzability. *J. Am. Chem. Soc.* **2018**, *140*, 963–973
- (152) Zumstein, M. T.; Schintlmeister, A.; Nelson, T. F.; Baumgartner, R.; Wobken, D.; Wagner, M.; Kohler, H.-P. E.; McNeill, K.; Sander, M. Biodegradation of synthetic polymers in soils: Tracking carbon into CO₂ and microbial biomass. *Sci. Adv.* **2018**, *4*, eaas9024
- (153) Nelson, T. F.; Baumgartner, R.; Jaggi, M.; Bernasconi, S. M.; Battagliarin, G.; Sinkel, C.; Künkel, A.; Kohler, H.-P. E.; McNeill, K.; Sander, M. Biodegradation of poly(butylene succinate) in soil laboratory incubations assessed by stable carbon isotope labelling. *Nat. Commun.* **2022**, *13*, 5691
- (154) Batiste, D. C.; De Hoe, G. X.; Nelson, T. F.; Sodnikar, K.; McNeill, K.; Sander, M.; Hillmyer, M. A. Site-Specific Mineralization of a Polyester Hydrolysis Product in Natural Soil. *ACS Sustain. Chem. Eng.* **2022**, *10*, 1373–1378
- (155) Kaihara, S.; Matsumura, S.; Mikos, A. G.; Fisher, J. P. Synthesis of poly(L-lactide) and polyglycolide by ring-opening polymerization. *Nat. Protoc.* **2007**, *2*, 2767–2771
- (156) Tan, C.; Zou, C.; Chen, C. Material Properties of Functional Polyethylenes from Transition-Metal-Catalyzed Ethylene–Polar Monomer Copolymerization. *Macromolecules* **2022**, *55*, 1910–1922
- (157) Balzade, Z.; Sharif, F.; Reza Ghaffarian Anbaran, S. Tailor-Made Functional Polyolefins of Complex Architectures: Recent Advances, Applications, and Prospects. *Macromolecules* **2022**, *55*, 1910–1922
- (158) Franssen, N. M. G.; Reek, J. N. H.; De Bruin, B. Synthesis of functional ‘polyolefins’: state of the art and remaining challenges. *Chem. Soc. Rev.* **2013**, *42*, 5809

- (159) Boffa, L. S.; Novak, B. M. Copolymerization of Polar Monomers with Olefins Using Transition-Metal Complexes. *Chem. Rev.* **2000**, *100*, 1479–1494
- (160) Williamson, J. B.; Lewis, S. E.; Johnson, R. R.; Manning, I. M.; Leibfarth, F. A. C–H Functionalization of Commodity Polymers. *Angew. Chem. Int. Ed.* **2019**, *58*, 8654–8668
- (161) Zhang, Y.; Wang, T.; Bai, J.; You, W. Repurposing Mitsunobu Reactions as a Generic Approach toward Polyethylene Derivatives. *ACS Macro Lett.* **2022**, *11*, 33–38
- (162) Hirashita, T.; Sugihara, Y.; Ishikawa, S.; Naito, Y.; Matsukawa, Y.; Araki, S. Revisiting Sodium Hypochlorite Pentahydrate (NaOCl·5H₂O) for the Oxidation of Alcohols in Acetonitrile without Nitroxyl Radicals. *Synlett* **2018**, *29*, 2404–2407
- (163) Kimura, Y.; Okada, T.; Asawa, T.; Sugiyama, Y.; Kirihara, M.; Iwai, T. Sodium Hypochlorite Pentahydrate (NaOCl·5H₂O) Crystals as an Extra-ordinary Oxidant for Primary and Secondary Alcohols. *Synlett* **2014**, *25*, 596–598
- (164) Almeida, M. L. S.; Beller, M.; Wang, G.-Z.; Bäckvall, J.-E. Ruthenium(II)-Catalyzed Oppenauer-Type Oxidation of Secondary Alcohols. *Chem. Eur. J.* **1996**, *2*, 1533–1536
- (165) Fujita, K.-I.; Yoshida, T.; Imori, Y.; Yamaguchi, R. Dehydrogenative Oxidation of Primary and Secondary Alcohols Catalyzed by a Cp*Ir Complex Having a Functional C,N-Chelate Ligand. *Org. Lett.* **2011**, *13*, 2278–2281
- (166) Fujita, K.-I.; Tanino, N.; Yamaguchi, R. Ligand-Promoted Dehydrogenation of Alcohols Catalyzed by Cp*Ir Complexes. A New Catalytic System for Oxidant-Free Oxidation of Alcohols. *Org. Lett.* **2007**, *9*, 109–111
- (167) Murahashi, S.-I.; Naota, T.; Oda, Y.; Hirai, N. Ruthenium-Catalyzed Oxidation of Alcohols with Peracids. *Synlett* **1995**, *1995*, 733–734
- (168) Ikariya, T.; Blacker, A. J. Asymmetric Transfer Hydrogenation of Ketones with Bifunctional Transition Metal-Based Molecular Catalysts†. *Acc. Chem. Res.* **2007**, *40*, 1300–1308
- (169) Ohkuma, T.; Ooka, H.; Yamakawa, M.; Ikariya, T.; Noyori, R. Stereoselective Hydrogenation of Simple Ketones Catalyzed by Ruthenium(II) Complexes. *J. Org. Chem.* **1996**, *61*, 4872–4873
- (170) Burdurlu, E.; Kiliç, Y.; Eli'Bol, G. C.; Kiliç, M. Shear strength of calabrian pine (*Pinus brutia* Ten.) bonded with polyurethane and polyvinyl acetate adhesives. *J. Appl. Polym. Sci.* **2006**, *100*, 4856–4867
- (171) Hagenmaier, R. D.; Grohmann, K. Polyvinyl Acetate as a High-gloss Edible Coating. *Journal of Food Science* **1999**, *64*, 1064–1067
- (172) Kramár, S.; Trcala, M.; Chitbanyong, K.; Král, P.; Puangsin, B. Basalt-Fiber-Reinforced Polyvinyl Acetate Resin: A Coating for Ductile Plywood Panels. *Materials* **2019**, *13*, 49
- (173) Kamiya, Y.; Mizoguchi, K.; Naito, Y.; Hirose, T. Gas sorption in poly(vinyl benzoate). *J. Polym. Sci., Part B: Polym. Phys.* **1986**, *24*, 535–547
- (174) Hirose, T.; Mizoguchi, K.; Kamiya, Y. Gas transport in poly(vinyl benzoate). *J. Appl. Polym. Sci.* **1985**, *30*, 401–410
- (175) Dezern, J. F. Synthesis and characterization of BTDA-based polyamide-imides. *J. Polym. Sci., Part A: Polym. Chem.* **1988**, *26*, 2157–2169
- (176) Naumoska, K.; Jug, U.; Metličar, V.; Vovk, I. Oleamide, a Bioactive Compound, Unwittingly Introduced into the Human Body through Some Plastic Food/Beverages and Medicine Containers. *Foods* **2020**, *9*, 549
- (177) Saillenfait, A.-M.; Ndaw, S.; Robert, A.; Sabaté, J.-P. Recent biomonitoring reports on phosphate ester flame retardants: a short review. *Archives of Toxicology* **2018**, *92*, 2749–2778

- (178) Till, D. E.; Ehntholt, D. J.; Reid, R. C.; Schwartz, P. S.; Sidman, K. R.; Schwope, A. D.; Whelan, R. H. Migration of BHT antioxidant from high density polyethylene to foods and food simulants. *Industrial & Engineering Chemistry Product Research and Development* **1982**, *21*, 106–113
- (179) Su, J.; Chen, F.; Cryns, V. L.; Messersmith, P. B. Catechol Polymers for pH-Responsive, Targeted Drug Delivery to Cancer Cells. *J. Am. Chem. Soc.* **2011**, *133*, 11850–11853
- (180) Putnam, A. A.; Wilker, J. J. Changing polymer catechol content to generate adhesives for high versus low energy surfaces. *Soft Matter* **2021**, *17*, 1999–2009
- (181) Zhang, Q.; Nurumbetov, G.; Simula, A.; Zhu, C.; Li, M.; Wilson, P.; Kempe, K.; Yang, B.; Tao, L.; Haddleton, D. M. Synthesis of well-defined catechol polymers for surface functionalization of magnetic nanoparticles. *Polym. Chem.* **2016**, *7*, 7002–7010
- (182) Hill, M. R.; Mukherjee, S.; Costanzo, P. J.; Sumerlin, B. S. Modular oxime functionalization of well-defined alkoxyamine-containing polymers. *Polym. Chem.* **2012**, *3*, 1758–1762
- (183) Binder, W. H.; Sachsenhofer, R. ‘Click’ Chemistry in Polymer and Material Science: An Update. *Macromolecular Rapid Communications* **2008**, *29*, 952–981
- (184) Collins, J.; Nadgorny, M.; Xiao, Z.; Connal, L. A. Doubly Dynamic Self-Healing Materials Based on Oxime Click Chemistry and Boronic Acids. *Macromolecular Rapid Communications* **2017**, *38*, 1600760
- (185) Calatayud, M.; Ruppert, A. M.; Weckhuysen, B. M. Theoretical Study on the Role of Surface Basicity and Lewis Acidity on the Etherification of Glycerol over Alkaline Earth Metal Oxides. *Chem. Eur. J.* **2009**, *15*, 10864–10870
- (186) Andrade, J. T.; Alves, S. L. G.; Lima, W. G.; Sousa, C. D. F.; Carmo, L. F.; De Sá, N. P.; Morais, F. B.; Johann, S.; Villar, J. A. F. P.; Ferreira, J. M. S. Pharmacologic potential of new nitro-compounds as antimicrobial agents against nosocomial pathogens: design, synthesis, and in vitro effectiveness. *Folia Microbiologica* **2020**, *65*, 393–405
- (187) Clark, N. G.; Croshaw, B.; Leggetter, B. E.; Spooner, D. F. Synthesis and antimicrobial activity of aliphatic nitro compounds. *Journal of Medicinal Chemistry* **1974**, *17*, 977–981
- (188) Yan, Z.; Liu, J.; Miao, C.; Su, P.; Zheng, G.; Cui, B.; Geng, T.; Fan, J.; Yu, Z.; Bu, N.; Yuan, Y.; Xia, L. Pyrene-Based Fluorescent Porous Organic Polymers for Recognition and Detection of Pesticides. *Molecules* **2021**, *27*, 126
- (189) Zhao, Y.; Long, J.; Zhuang, P.; Ji, Y.; He, C.; Wang, H. Transforming polyethylene and polypropylene into nontraditional fluorescent polymers by thermal oxidation. *Journal of Materials Chemistry C* **2022**, *10*, 1010–1016
- (190) Yin, S.; Duvigneau, J.; Vancso, G. J. Fluorescent Polyethylene by In Situ Facile Synthesis of Carbon Quantum Dots Facilitated by Silica Nanoparticle Agglomerates. *ACS Applied Polymer Materials* **2021**, *3*, 5517–5526
- (191) Rahman, M. A.; Bowland, C.; Ge, S.; Acharya, S. R.; Kim, S.; Cooper, V. R.; Chen, X. C.; Irle, S.; Sokolov, A. P.; Savara, A.; Saito, T. Design of tough adhesive from commodity thermoplastics through dynamic crosslinking. *Sci. Adv.* **2021**, *7*, eabk2451
- (192) Lallemand, M.; Yu, L.; Cai, W.; Rischka, K.; Hartwig, A.; Haag, R.; Hugel, T.; Balzer, B. N. Multivalent non-covalent interactions lead to strongest polymer adhesion. *Nanoscale* **2022**, *14*, 3768–3776
- (193) Buaksuntear, K.; Limarun, P.; Suethao, S.; Smitthipong, W. Non-Covalent Interaction on the Self-Healing of Mechanical Properties in Supramolecular Polymers. *International Journal of Molecular Sciences* **2022**, *23*, 6902

- (194) Yang, J.; Bos, I.; Pranger, W.; Stuiver, A.; Velders, A. H.; Cohen Stuart, M. A.; Kamperman, M. A clear coat from a water soluble precursor: a bioinspired paint concept. *Journal of Materials Chemistry A* **2016**, *4*, 6868–6877
- (195) Anouar, B. S.; Guinot, C.; Ruiz, J.-C.; Carton, F.; Dole, P.; Joly, C.; Yvan, C. Purification of post-consumer polyolefins via supercritical CO₂ extraction for the recycling in food contact applications. *The Journal of Supercritical Fluids* **2015**, *98*, 25–32
- (196) Knez, Ž.; Markočič, E.; Leitgeb, M.; Primožič, M.; Hrnčič, M. K.; Škerget, M. Industrial applications of supercritical fluids: A review. *Energy* **2014**, *77*, 235–243
- (197) Tian, H.-Z.; Wu, S.-F.; Lin, G.-Q.; Sun, X.-W. Asymmetric synthesis of pyrrolo[2,3-b]indole scaffolds by organocatalytic [3 + 2] dearomative annulation. *Tetrahedron Lett.* **2022**, *103*, 153969
- (198) Han, L.; Geng, J.; Wang, Z.; Hua, J. Balancing anti-migration and anti-aging behavior of binary antioxidants for high-performance 1,2-polybutadiene rubber. *Polymers for Advanced Technologies* **2022**, *33*, 3619–3627
- (199) Ruiz-Avila, L. B.; Huecas, S.; Artola, M.; Vergoñós, A.; Ramírez-Aportela, E.; Cercenado, E.; Barasoain, I.; Vázquez-Villa, H.; Martín-Fontecha, M.; Chacón, P.; López-Rodríguez, M. L.; Andreu, J. M. Synthetic Inhibitors of Bacterial Cell Division Targeting the GTP-Binding Site of FtsZ. *ACS. Chem. Bio.* **2013**, *8*, 2072–2083
- (200) Li, D.; Zhou, L.; Wang, X.; He, L.; Yang, X. Effect of Crystallinity of Polyethylene with Different Densities on Breakdown Strength and Conductance Property. *Materials* **2019**, *12*, 1746
- (1) Jensen, W. B. The Origin of the Polymer Concept. *J. Chem. Educ.* **2008**, *85*, 624
- (2) Sailors, H. R.; Hogan, J. P. History of Polyolefins. *Journal of Macromolecular Science, Part A* **1981**, *15*, 1377-1402
- (3) Kim, Y. K. The use of polyolefins in industrial and medical applications. In *Polyolefin Fibres*, Elsevier, 2017; pp 135–155.
- (4) Geyer, R.; Jambeck, J. R.; Law, K. L. Production, use, and fate of all plastics ever made. *Sci. Adv.* **2017**, *3*, e17000782
- (5) Hlatky, G. G. Heterogeneous Single-Site Catalysts for Olefin Polymerization. *Chem. Rev.* **2000**, *100*, 1347–1376
- (6) Soga, K.; Shiono, T. Ziegler-Natta catalysts for olefin polymerizations. *Prog. Polym. Sci.* **1997**, *22*, 1503–1546
- (7) Sawada, H. Thermodynamics of Polymerization. I. *Journal of Macromolecular Science, Part C* **2008**, *3*, 313–338
- (8) Muñoz, I.; Weidema, B. P. Ethylene and propylene production from steam cracking in Europe: a consequential perspective. *Int. J. Life Cycle Assess.* **2024**,
- (9) Chen, J. Q.; Bozzano, A.; Glover, B.; Fuglerud, T.; Kvisle, S. Recent advancements in ethylene and propylene production using the UOP/Hydro MTO process. *Catal. Today* **2005**, *106*, 103–107
- (10) Gibson, V. C.; Spitzmesser, S. K. Advances in Non-Metallocene Olefin Polymerization Catalysts. *Chem. Rev.* **2003**, *103*, 283–316
- (11) Resconi, L.; Cavallo, L.; Fait, A.; Piemontesi, F. Selectivity in Propene Polymerization with Metallocene Catalysts. *Chem. Rev.* **2000**, *100*, 1253–1346
- (12) Luft, G.; Kämpf, R.; Seidl, H. Synthesis conditions and structure of low density polyethylene. I. Short and long chain branching. *Macromol. Mater. Eng.* **1982**, *108*, 203–217
- (13) Wang, W.-J.; Yan, D.; Zhu, S.; Hamielec, A. E. Kinetics of Long Chain Branching in Continuous Solution Polymerization of Ethylene Using Constrained Geometry Metallocene. *Macromolecules* **1998**, *31*, 8677–8683

- (14) Stevens, J. C. Constrained geometry and other single site metallocene polyolefin catalysts: A revolution in olefin polymerization. *Stud. Surf. Sci. Catal.* **1996**, *101*, 11–20
- (15) McKnight, A. L.; Waymouth, R. M. Group 4 *ansa*-Cyclopentadienyl-Amido Catalysts for Olefin Polymerization. *Chem. Rev.* **1998**, *98*, 2587–2598
- (16) Natta, G.; Pino, P.; Corradini, P.; Danusso, F.; Mantica, E.; Mazzanti, G.; Moraglio, G. Crystalline High Polymer of α -Olefins. *J. Am. Chem. Soc.* **1955**, *77*, 1708–1710
- (17) Hogan, J. P. Ethylene polymerization catalysis over chromium oxide. *J. Polym. Sci. A Polym. Chem.* **1970**, *8*, 2637–2652
- (18) Cossee, P. Ziegler-Natta catalysis I. Mechanism of polymerization of α -olefins with Ziegler-Natta catalysts. *J. Catal.* **1964**, *3*, 80–88
- (19) Chen, E. Y.-X.; Marks, T. J. Cocatalysts for Metal-Catalyzed Olefin Polymerization: Activators, Activation Processes, and Structure-Activity Relationships. *Chem. Rev.* **2000**, *100*, 1391–1434
- (20) Shapiro, P. J.; Cotter, D. W.; Schaefer, W. P.; Labinger, J. A.; Bercaw, J. E. Model Ziegler-Natta α -Olefin Polymerization Catalysts Derived from $[\{(\eta^5\text{-C}_5\text{Me}_4)\text{SiMe}_2(\eta^1\text{-NCMe}_3)\}(\text{PMe}_3)\text{Sc}(\mu_2\text{-H})]_2$ and $[\{(\eta^5\text{-C}_5\text{Me}_4)\text{SiMe}_2(\eta^1\text{-NCMe}_3)\}(\mu_2\text{-CH}_2\text{CH}_2\text{CH}_3)\text{Sc}]_2$. Synthesis, Structures, and Kinetic and Equilibrium Investigations of the Catalytically Active Species in Solution. *J. Am. Chem. Soc.* **1994**, *116*, 4623–4640
- (21) Fisch, A. G. Ziegler-Natta Catalysts. In *Kirk-Othmer Encyclopedia of Chemical Technology*, Wiley, 2019; pp 1–22.
- (22) Cossee, P. On the reaction mechanism of the ethylene polymerization with heterogeneous ziegler-natta catalysts. *Tetrahedron Lett.* **1960**, *1*, 12–16
- (23) Collins, S.; Kelly, W. M.; Holden, D. A. Polymerization of Propylene Using Supported, Chiral, *ansa*-Metallocene Catalysts: Production of Polypropylene with Narrow Molecular Weight Distribution. *Macromolecules* **1991**, *25*, 1780–1785
- (24) Kim, I.; Jordan, R. F. Propylene Polymerization with *ansa*-Metallocene Amide Complexes. *Macromolecules* **1996**, *29*, 489–491
- (25) Shiman, D. I.; Vasilenko, I. V.; Kostjuk, S. V. Cationic polymerization of isobutylene by AlCl_3 /ether complexes in non-polar solvents: Effect of ether structure on the selectivity of β -H elimination. *Polymer* **2013**, *54*, 2235–2242
- (26) Popelka, E.; Khanam, P. N.; AlMaadeed, M. A. Surface modification of polyethylene/graphene composite using corona discharge. *J. Phys. D: Appl. Phys.* **2018**, *51*, 105302
- (27) Vocke, C.; Anttila, U.; Heino, M.; Hietaoja, P.; Seppälä, J. Use of oxazoline functionalized polyolefins and elastomers as compatibilizers for thermoplastic blends. *J. Appl. Polym. Sci.* **1998**, *70*, 1923–1930
- (28) Wiesinger, H.; Wang, Z.; Hellweg, S. Deep Dive into Plastic Monomers, Additives, and Processing Aids. *Environ. Sci. Technol.* **2021**, *55*, 9339–9351
- (29) Chen, W.; Gong, Y.; Mckie, M.; Almuhtaram, H.; Sun, J.; Barrett, H.; Yang, D.; Wu, M.; Andrews, R. C.; Peng, H. Defining the Chemical Additives Driving *In Vitro* Toxicities of Plastics. *Environ. Sci. Technol.* **2022**, *56*, 14627–14639
- (30) Hahladakis, J. N.; Velis, C. A.; Weber, R.; Iacovidou, E.; Purnell, P. An overview of chemical additives present in plastics: Migration, release, fate and environmental impact during their use, disposal and recycling. *J. Hazard. Mater.* **2018**, *344*, 179–199
- (31) Spell, H. L.; Eddy, R. D. Determination of additives in polyethylene by absorption spectroscopy. *Anal. Chem.* **1960**, *32*, 1811–1814

- (32) Ragaert, K.; Delva, L.; Van Greem, K. Mechanical and chemical recycling of solid plastic waste. *Waste Manag.* **2017**, *69*, 24–58
- (33) Zhao, Y.-B.; Lv, X.-D.; Ni, H.-G. Solvent-based separation and recycling of waste plastics: A review. *Chemosphere* **2018**, *209*, 707–720
- (34) Coates, G. W.; Getzler, Y. D. Y. L. Chemical recycling to monomer for an ideal, circular polymer economy. *Nat. Rev. Mater.* **2020**, *5*, 501–516
- (35) Ignatyev, I. A.; Thielemans, W.; Vander Beke, B. Recycling of Polymers: A Review. *ChemSusChem* **2014**, *7*, 1579-1593
- (36) Vollmer, I.; Jenks, M. J. F.; Roelands, M. C. P.; White, R. J.; Harmelen, T.; Wild, P.; Laan, G. P.; Meirer, F.; Keurentjes, J. T. F.; Weckhuysen, B. M. Beyond Mechanical Recycling: Giving New Life to Plastic Waste. *Angew. Chem. Int. Ed.* **2020**, *59*, 15402–15423
- (37) Pinheiro, L. A.; Chinelatto, M. A.; Canevarolo, S. V. The role of chain scission and chain branching in high density polyethylene during thermo-mechanical degradation. *Polym. Degrad. Stab.* **2004**, *86*, 445–453
- (38) Ellen MacArthur Foundation and McKinsey & Company. <http://www.ellenmacarthurfoundation.org/publications>. (accessed 2021-08-15). The New Plastics Economy — Rethinking the future of plastics
- (39) Geyer, R.; Jambeck, J. R.; Law, K. L. Production, use, and fate of all plastics ever made. *Sci. Adv.* **2017**, *3*, e1700782
- (40) Von Vacano, B.; Mangold, H.; Vandermeulen, G. W. M.; Battagliarin, G.; Hofmann, M.; Bean, J.; Künkel, A. Sustainable Design of Structural and Functional Polymers for a Circular Economy. *Angew. Chem. Int. Ed.* **2023**, *62*,
- (41) Plummer, C. M.; Li, L.; Chen, Y. The post-modification of polyolefins with emerging synthetic methods. *Polym. Chem.* **2020**, *11*, 6862–6872
- (42) Zuin, V. G.; Kümmerer, K. Chemistry and materials science for a sustainable circular polymeric economy. *Nat. Rev. Mater.* **2022**, *7*, 76-78
- (43) Shi, C.; Reilly, L. T.; Phani Kumar, V. S.; Coile, M. W.; Nicholson, S. R.; Broadbelt, L. J.; Beckham, G. T.; Chen, E. Y.-X. Design principles for intrinsically circular polymers with tunable properties. *Chem* **2021**, *7*, 2896-2912
- (44) Shi, C.; Reilly, L. T.; Chen, E. Y. X. Hybrid Monomer Design Synergizing Property Trade-offs in Developing Polymers for Circularity and Performance. *Angew. Chem. Int. Ed.* **2023**, *62*,
- (45) Arrington, A. S.; Brown, J. R.; Win, M. S.; Winey, K. I.; Long, T. E. Melt polycondensation of carboxytelechelic polyethylene for the design of degradable segmented copolyester polyolefins. *Polym. Chem.* **2022**, *13*, 3116–3125
- (46) Häußler, M.; Eck, M.; Rothauer, D.; Mecking, S. Closed-loop recycling of polyethylene-like materials. *Nature* **2021**, *590*, 423–427
- (47) Arrington, A. S.; Long, T. E. Influence of carboxytelechelic oligomer molecular weight on the properties of chain extended polyethylenes. *Polymer* **2022**, *259*, 125319
- (48) Li, X. L.; Clarke, R. W.; An, H. Y.; Gowda, R. R.; Jiang, J. Y.; Xu, T. Q.; Chen, E. Y. X. Dual Recycling of Depolymerization Catalyst and Biodegradable Polyester that Markedly Outperforms Polyolefins. *Angew. Chem. Int. Ed.* **2023**, *62*, e202303791
- (49) Shi, C.; McGraw, M. L.; Li, Z.-C.; Cavallo, L.; Falivene, L.; Chen, E. Y.-X. High-performance pan-tactic polythioesters with intrinsic crystallinity and chemical recyclability. *Sci. Adv.* **2020**, *6*, 10.1126/sciadv.abc0495

- (50) Jang, Y.-J.; Nguyen, S.; Hillmyer, M. A. Chemically Recyclable Linear and Branched Polyethylenes Synthesized from Stoichiometrically Self-Balanced Telechelic Polyethylenes. *J. Am. Chem. Soc.* **2024**, *146*, 4771–4782
- (51) Zhao, Y.; Rettner, E. M.; Harry, K. L.; Hu, Z.; Miscall, J.; Rorrer, N. A.; Miyake, G. M. Chemically recyclable polyolefin-like multiblock polymers. *Science* **2023**, *382*, 310–314
- (52) Kocen, A. L.; Cui, S.; Lin, T.-W.; LaPointe, A. M.; Coates, G. W. Chemically Recyclable Ester-Linked Polypropylene. *J. Am. Chem. Soc.* **2022**, *144*, 12613–12618
- (53) Parke, S. M.; Lopez, J. C.; Cui, S.; LaPointe, A. M.; Coates, G. W. Polyethylene Incorporating Diels–Alder Comonomers: A “Trojan Horse” Strategy for Chemically Recyclable Polyolefins. *Angew. Chem. Int. Ed.* **2023**, *62*, e202301927
- (54) Sudesh, K.; Abe, H.; Doi, Y. Synthesis, structure and properties of polyhydroxyalkanoates: biological polyesters. *Prog. Polym. Sci.* **2000**, *25*, 1503–1555
- (55) Zhou, Z.; Lapointe, A. M.; Shaffer, T. D.; Coates, G. W. Nature-inspired methylated polyhydroxybutyrates from C1 and C4 feedstocks. *Nat. Chem.* **2023**, *15*, 856–861
- (56) Bruckmoser, J.; Pongratz, S.; Stieglitz, L.; Rieger, B. Highly Iselective Ring-Opening Polymerization of *rac*- β -Butyrolactone: Access to Synthetic Poly(3-hydroxybutyrate) with Polyolefin-like Material Properties. *J. Am. Chem. Soc.* **2023**, *145*, 11494–11498
- (57) Zhang, Z.; Quinn, E. C.; Olmedo-Martínez, J. L.; Caputo, M. R.; Franklin, K. A.; Müller, A. J.; Chen, E. Y. X. Toughening Brittle Bio-P3HB with Synthetic P3HB of Engineered Stereomicrostructures. *Angew. Chem. Int. Ed.* **2023**, *62*,
- (58) Zhou, L.; Zhang, Z.; Shi, C.; Scoti, M.; Barange, D. K.; Gowda, R. R.; Chen, E. Y.-X. Chemically circular, mechanically tough, and melt-processable polyhydroxyalkanoates. *Science* **2023**, *380*, 64–69
- (59) Abel, B. A.; Snyder, R. L.; Coates, G. W. Chemically recyclable thermoplastics from reversible-deactivation polymerization of cyclic acetals. *Science* **2021**, *373*, 783–789
- (60) Hester, H. G.; Abel, B. A.; Coates, G. W. Ultra-High-Molecular-Weight Poly(Dioxolane): Enhancing the Mechanical Performance of a Chemically Recyclable Polymer. *J. Am. Chem. Soc.* **2023**, *145*, 8800–8804
- (61) Johnson, A. M.; Johnson, J. A. Thermally Robust yet Deconstructable and Chemically Recyclable High-Density Polyethylene (HDPE)-Like Materials Based on Si–O Bonds. *Angew. Chem. Int. Ed.* **2023**, *135*,
- (62) Jehanno, C.; Alty, J. W.; Roosen, M.; De Meester, S.; Dove, A. P.; Chen, E. Y.-X.; Leibfarth, F. A.; Sardon, H. Critical advances and future opportunities in upcycling commodity polymers. *Nature* **2022**, *603*, 803–814
- (63) Boasen, N. K.; Hillmyer, M. A. Post-polymerization functionalization of polyolefins. *Chem. Soc. Rev.* **2005**, *34*, 267
- (64) Menendez Rodriguez, G.; Díaz-Requejo, M. M.; Pérez, P. J. Metal-Catalyzed Postpolymerization Strategies for Polar Group Incorporation into Polyolefins Containing C–C, C=C, and Aromatic Rings. *Macromolecules* **2021**, *54*, 4971–4985
- (65) Walker, T. W.; Frelka, N.; Shen, Z.; Chew, A. K.; Banick, J.; Grey, S.; Kim, M. S.; Dumesic, J. A.; Van Lehn, R. C.; Huber, G. W. Recycling of multilayer plastic packaging materials by solvent-targeted recovery and precipitation. *Sci. Adv.* **2020**, *6*, aba7599
- (66) Wu, D. Y.; Gutowski, W. S.; Li, S.; Griesser, H. J. Ammonia plasma treatment of polyolefins for adhesive bonding with a cyanoacrylate adhesive. *J. Adhes. Sci. Technol.* **2012**, *9*, 501–525

- (67) Sanchis, M. R.; Blanes, V.; Blanes, M.; Garcia, D.; Balart, R. Surface modification of low density polyethylene (LDPE) film by low pressure O₂ plasma treatment. *Eur. Polym. J.* **2006**, *42*, 1558–1568
- (68) Seko, N.; Ninh, N. T. Y.; Tamada, M. Emulsion grafting of glycidyl methacrylate onto polyethylene fiber. *Radiat. Phys. Chem.* **2010**, *79*, 22–26
- (69) Samay, G.; Nagy, T.; White, J. L. Grafting maleic anhydride and comonomers onto polyethylene. *J. Appl. Polym. Sci.* **1995**, *56*, 1423–1433
- (70) Olsen, D. A.; Osteraas, A. J. Difluorocarbene modification of polymer and fiber surfaces. *J. Appl. Polym. Sci.* **1969**, *13*, 1523–1535
- (71) Osteraas, A. J.; Olsen, D. A. Incorporation of Functional Groups onto the Surface of Polyethylene. *Nature* **1969**, *221*, 1140–1141
- (72) Aglietto, M.; Bertani, R.; Ruggeri, G.; Fiordiponti, P.; Segre, A. L. Functionalization of polyolefins: structure of functional groups in polyethylene reacted with ethyl diazoacetate. *Macromolecules* **1989**, *22*, 1492–1493
- (73) Aglietto, M.; Alterio, R.; Bertani, R.; Galleschi, F.; Ruggeri, G. Polyolefin functionalization by carbene insertion for polymer blends. *Polymer* **1989**, *30*, 1133–1136
- (74) Bateman, S. A.; Wu, D. Y. Sulfonyl azides—an alternative route to polyolefin modification. *J. Appl. Polym. Sci.* **2002**, *84*, 1395–1402
- (75) Liu, D.; Bielawski, C. W. Direct azidation of isotactic polypropylene and synthesis of ‘grafted to’ derivatives thereof using azide–alkyne cycloaddition chemistry. *Polym. Int.* **2016**, *66*, 70–76
- (76) D’íaz-Requejo, M. M.; Wehrmann, P.; Leatherman, M. D.; Trofimenko, S.; Mecking, S.; Brookhart, M.; Pérez, P. J. Controlled, Copper-Catalyzed Functionalization of Polyolefins. *Macromolecules* **2005**, *38*, 4966–4969
- (77) Lepage, M. L.; Simhadri, C.; Liu, C.; Takaffoli, M.; Bi, L.; Crawford, B.; Milani, A. S.; Wulff, J. E. A broadly applicable cross-linker for aliphatic polymers containing C–H bonds. *Science* **2019**, *366*, 875–878
- (78) Clarke, R. W.; Sandmeier, T.; Franklin, K. A.; Reich, D.; Zhang, X.; Vengallur, N.; Patra, T. K.; Tannenbaum, R. J.; Adhikari, S.; Kumar, S. K.; Rovis, T.; Chen, E. Y.-X. Dynamic crosslinking compatibilizes immiscible mixed plastics. *Nature* **2023**, *616*, 731–739
- (79) Kondo, Y.; García-Cuadrado, D.; Hartwig, J. F.; Boen, N. K.; Wagner, N. L.; Hillmyer, M. A. Rhodium-Catalyzed, Regiospecific Functionalization of Polyolefins in the Melt. *J. Am. Chem. Soc.* **2002**, *124*, 1164–1165
- (80) Bae, C.; Hartwig, J. F.; Boen Harris, N. K.; Long, R. O.; Anderson, K. S.; Hillmyer, M. A. Catalytic Hydroxylation of Polypropylenes. *J. Am. Chem. Soc.* **2005**, *127*, 767–776
- (81) Boen, N. K.; Hillmyer, M. A. Selective and Mild Oxyfunctionalization of Model Polyolefins. *Macromolecules* **2003**, *36*, 7027–7034
- (82) Bunescu, A.; Lee, S.; Li, Q.; Hartwig, J. F. Catalytic Hydroxylation of Polyethylenes. *ACS Cent. Sci.* **2017**, *3*, 895–903
- (83) Chen, L.; Malollari, K. G.; Uliana, A.; Sanchez, D.; Messersmith, P. B.; Hartwig, J. F. Selective, Catalytic Oxidations of C–H Bonds in Polyethylenes Produce Functional Materials with Enhanced Adhesion. *Chem* **2021**, *7*, 137–145
- (84) Huang, X.; Groves, J. T. Beyond ferryl-mediated hydroxylation: 40 years of the rebound mechanism and C–H activation. *J. Biol. Inorg. Chem.* **2017**, *22*, 185–207
- (85) Chen, L.; Malollari, K. G.; Uliana, A.; Hartwig, J. F. Ruthenium-Catalyzed, Chemoselective and Regioselective Oxidation of Polyisobutene. *J. Am. Chem. Soc.* **2021**, *143*, 4531–4535

- (86) Williamson, J. B.; Czaplyski, W. L.; Alexanian, E. J.; Leibfarth, F. A. Regioselective C–H Xanthylation as a Platform for Polyolefin Functionalization. *Angew. Chem. Int. Ed.* **2018**, *57*, 6261–6265
- (87) Williamson, J. B.; Na, C. G.; Johnson III, R. R.; William, D. F. M.; Alexanian, E. J.; Leibfarth, F. A. Chemo- and Regioselective Functionalization of Isotactic Polypropylene: A Mechanistic and Structure–Property Study. *J. Am. Chem. Soc.* **2019**, *141*, 12815–12823
- (88) Fazekas, T. J.; Alty, J. W.; Neidhart, E. K.; Miller, A. S.; Leibfarth, F. A.; Alexanian, E. J. Diversification of aliphatic C–H bonds in small molecules and polyolefins through radical chain transfer. *Science* **2022**, *375*, 545–550
- (89) Neidhart, E. K.; Hua, M.; Peng, Z.; Kearney, L. T.; Bhat, V.; Vashahi, F.; Alexanian, E. J.; Sheiko, S. S.; Wang, C.; Helms, B. A.; Leibfarth, F. A. C–H Functionalization of Polyolefins to Access Reprocessable Polyolefin Thermosets. *J. Am. Chem. Soc.* **2023**, *145*, 27450–27458
- (90) Schwab, S. T.; Baur, M.; Nelson, T. F.; Mecking, S. Synthesis and Deconstruction of Polyethylene-type Materials. *Chem. Rev.* **2024**, *124*, 2327–2351
- (91) Ray, A.; Zhu, K.; Kissin, Y. V.; Cherian, A. E.; Coates, G. W.; Goldman, A. S. Dehydrogenation of aliphatic polyolefins catalyzed by pincer-ligated iridium complexes. *Chem. Commun.* **2005**, 3388–3390
- (92) Arroyave, A.; Cui, S.; Lopez, J. C.; Kocen, A. L.; LaPointe, A. M.; Delferro, M.; Coates, G. W. Catalytic Chemical Recycling of Post-Consumer Polyethylene. *J. Am. Chem. Soc.* **2022**, *144*, 23280–23285
- (93) Sullivan, K. P.; Werner, A. Z.; Ramirez, K. J.; Ellis, L. D.; Bussard, J. R.; Black, B. A.; Brandner, D. G.; Bratti, F.; Buss, B. L.; Dong, X.; Haugen, S. J.; Ingraham, M. A.; Konev, M. O.; Michener, W. E.; Miscall, J.; Pardo, I.; Woodworth, S. P.; Guss, A. M.; Román-Leshkov, Y.; Stahl, S. S.; Beckham, G. T. Mixed plastics waste valorization through tandem chemical oxidation and biological funneling. *Science* **2022**, *378*, 207–211
- (94) Nelson, T. F.; Rothauer, D.; Sander, M.; Mecking, S. Degradable and Recyclable Polyesters from Multiple Chain Length Bio- and Waste-Sourceable Monomers. *Angew. Chem. Int. Ed.* **2023**, *62*, e202310729

Chapter Two

Polymers from Plant Oils Linked by Siloxane Bonds for Programmed Depolymerization

2.1 Introduction

The annual global production of plastic materials in 2015 reached 400 Mt, and the total amount of plastics produced since 1950 is 8300 Mt.⁴ The concomitant waste generation from the use of plastics is a major issue facing their continued use. Most plastics are used to produce short-lived products, such as packaging materials, which are typically discarded within a year of being produced. Such single, short-term use has generated an interest in preparing polymers that can undergo programmed degradation chemically or enzymatically, in some cases by incorporating functional groups that can be the point for depolymerization.⁹⁵ Such programmed degradation to form specific monomers can be envisioned to enable chemical circularity of the materials.

To create plastics with greater potential for triggered depolymerization, new monomers should be investigated, and, to further minimize the use of limited resources, these new monomers should be derived from natural sources. Plant oils are among the most prevalent of such sources,⁹⁶ particularly those containing linear, carbon-rich chains suitable for the synthesis of polymers.⁹⁷⁻¹⁰¹ Various synthetic strategies, such as ozonolysis, catalytic oxidative cleavage,¹⁰² cross metathesis,^{46, 103} and tandem isomerization and functionalization of internal olefins,¹⁰⁴ have been reported for the preparation of α,ω -difunctionalized-monomers from fatty acid derivatives to produce α,ω -diacids, α,ω -hydroxy carboxylic acids, α,ω -dienes, and derivatives thereof.

Strategies to construct degradable polymers by Si–O bond formation and to depolymerize polymers by Si–O bond cleavage have begun to be followed.^{61, 105-107} We reported the functionalization of fatty acids with silicon reagents as a strategy to prepare α,ω -difunctionalized monomers and the corresponding polymers that can be degraded at Si–O bonds. 10-Undecenoic acid or its methyl ester derived from castor oil was converted to an AB monomer terminated by an alcohol and a silane by hydrosilylation of the alkene and reduction of the carboxylate function. Polymerization generated a polymer that would undergo degradation of the poly(silyl ether) to produce a diol containing a siloxane (Figure 2.1.1).¹⁰⁶ However, the polymer was metastable and underwent spontaneous hydrolysis during processing and the diol produced from this cleavage is distinct from the monomer used to make the original material. Because the hydrolysis of the siloxane bond is slower than that of the silyl ether and can be recreated by condensation,^{108, 109} we anticipated that the stability and circularity of the polymers generated from silicon-linked monomers derived from fatty acids would simultaneously increase by replacing the silyl ether linkage with the siloxane linkage.

In many cases, cyclic monomers are attractive for preparing advanced materials because controlled ring-opening polymerization allow molar masses to be precisely controlled and block copolymers to be constructed.¹¹⁰ Controlled ring-opening polymerization (ROP) of sugar-derived lactide and small lactones is well-established to prepare renewable polymers.^{55, 56, 58, 111-114} The ROP of fatty-acid derived cyclic monomers, which are usually macrolactones, is less established but could lead to segments with properties that complement those from lactide.¹¹⁵⁻¹¹⁷ Recently, 19- and 23-membered lactones from fatty acids and their semi-crystalline polymers have been developed as alternatives to polyethylene.¹¹⁸⁻¹²¹ Because of the flexibility of the Si–O bond, these macrocyclic monomers containing a siloxane unit would produce polymers that have low glass transition temperatures (T_g) and that could, thereby, serve as a soft block of renewable and degradable thermoplastic elastomers (TPEs).

We report the synthesis of siloxane-containing AA-monomers and a cyclic monomer derived from castor oil, the conversion of these monomers to degradable polymers, along with methods for programmed cleavage of the polymer to monomers and repolymerization of those monomers back to the original polymer. Hydrolysis or exchange of the siloxane linkage efficiently cleaves

the siloxane-containing polymers into monomers. Assessment of the biodegradability of the cleavage products showed differential use of the carbon sites within these monomers by microorganisms, illustrating the potential for biodegradability of material that could escape the intended circularity of use, depolymerization, and reuse.

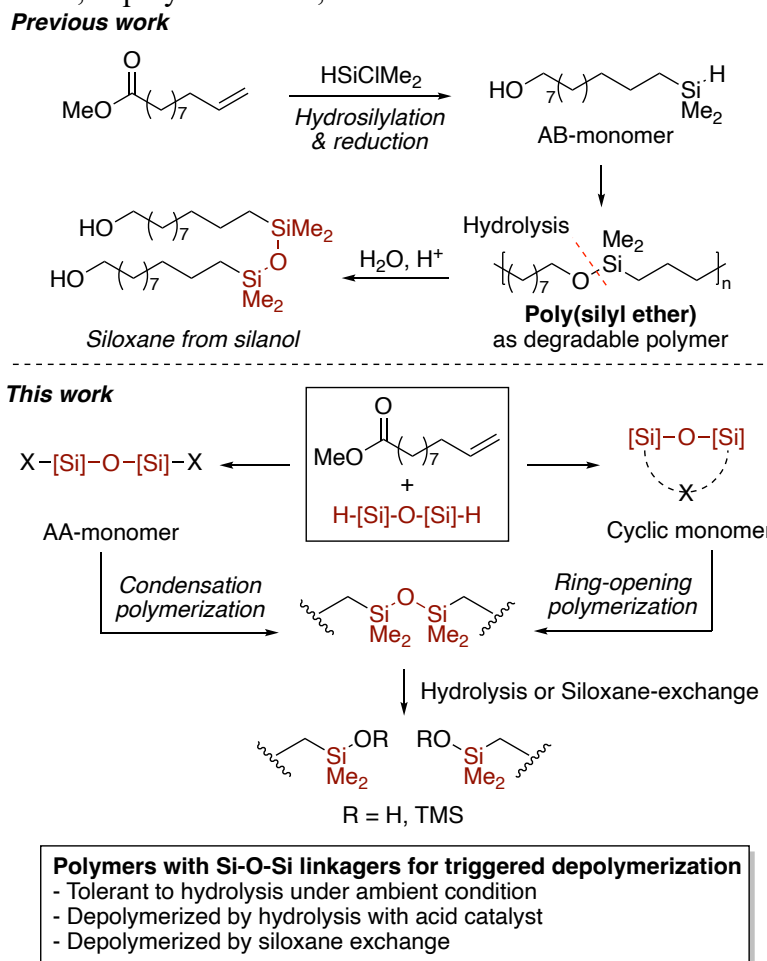


Figure 2.1.1. Synthesis and degradation of poly(silyl ether)s in previous work and a new design of polymers that would be more stable and would contain siloxane units linking a fatty acid derivative.

2.2 Synthesis of AA-Monomers and Condensation Polymerizations with BB-Monomers

To begin our studies on the synthesis of chemically degradable polymers from renewable sources linked by siloxane units, we designed a two-step synthesis of the siloxane-containing diol **3** from methyl 10-undecenoate **1** and the commodity siloxane 1,1,3,3-tetramethyldisiloxane (TMDSO) (Figure 2.2.1). The hydrosilylation of ester **1** with TMDSO catalyzed by Karstedt's catalyst (10 ppm) afforded diester **2**.¹²²⁻¹²⁴ For environmental and practical reasons, diester **2** was converted to diol **3** by catalytic hydrogenation, rather than reduction with stoichiometric metal hydride reagents. Among reported Ru-catalysts for the hydrogenation of esters, Gusev's catalyst (Ru-SNS)¹²⁵ and the Firmenich catalyst (Ru-PNNP)¹²⁶ were not active for the hydrogenation of the esters in compound **2** (as a crude mixture from the hydrosilylation of **1**), but hydrogenation of

these units in crude diester **2** with the Ru-MACHO catalyst¹²⁷ afforded diol **3** in 62% yield on gram-scale (see Table 2.17.2.1).

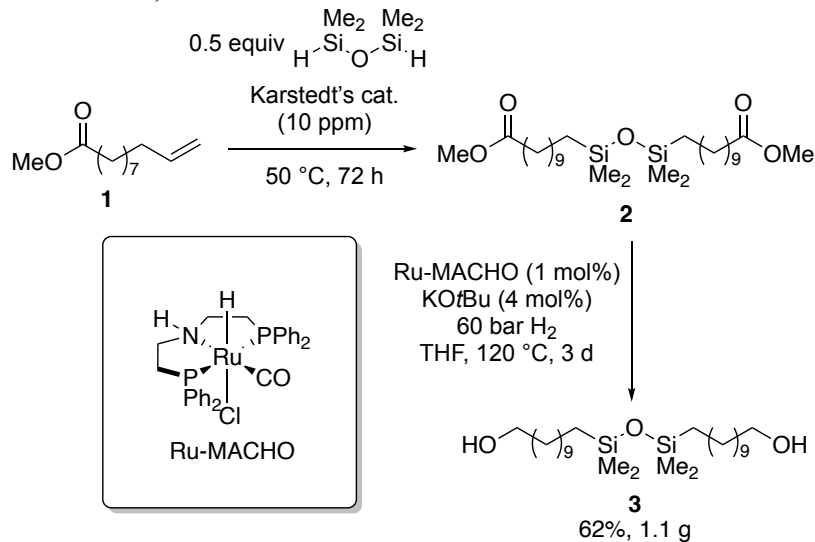


Figure 2.2.1. Synthesis of diester **2** and diol **3** from methyl 10-undecenoate **1**

The step-growth polymerization of the AA monomer diol **3** with various BB-monomers was conducted, and the data for these reactions are summarized in Table 2.1.1. Diol **3** was subjected to polymerization with methylenediphenyldiisocyanate (MDI) to construct polyurethane **PU-3** (Table 2.1.1, entry 1) with 1 mol % $\text{Sn}(\text{2-ethylhexanoate})_2$ ($\text{Sn}(\text{Oct})_2$) as the catalyst. Monomer **3** was also converted to an aliphatic polycarbonate, which is a potential material for biomedical applications.¹²⁸ The reaction of **3** with 33 mol % of triphosgene led to a mixture of low-molecular weight products, presumably due to the hydrolysis of the siloxane linkage by the HCl by-product, but the reaction of **3** with dimethyl carbonate catalyzed by $\text{Sn}(\text{Oct})_2$ led to the high-molecular-weight polycarbonate **PC-3**¹²⁹ (Table 2.1.1, entry 2). The reaction of monomer **3** with the siloxane-linked diester **2** catalyzed by $\text{Ti}(\text{O}i\text{Bu})_4$ afforded the polyester, **PE-2-3** (Table 2.1.1, entry 3).

The siloxane-linked diester **2** also underwent polymerization with diols and diamines to form high molar mass polyesters and polyamides. The reaction of **2** with aliphatic diols (1,10-decanediol and 1,12-dodecanediol) and diamines (1,5-diaminopentane and 1,12-diaminododecane) with $\text{Sn}(\text{Oct})_2$ as catalyst produced the linear polyesters **PE-2-C10** and **PE-2-C12** and the linear polyamides **PA-2-C5** and **PA-2-C12** (Table 2.1.1, entries 4–7). For the synthesis of the polyesters, the transesterification was conducted first between 130 $^\circ\text{C}$ and 150 $^\circ\text{C}$ under a flow of N_2 to remove the methanol byproduct. The final condensation was conducted at low pressures (< 50 mTorr) to give high molecular weight polymers. The apparent molecular weights of all polymers were determined by SEC in THF using PS standards, except those of polyamides due to their low solubility (Table 2.1.1).

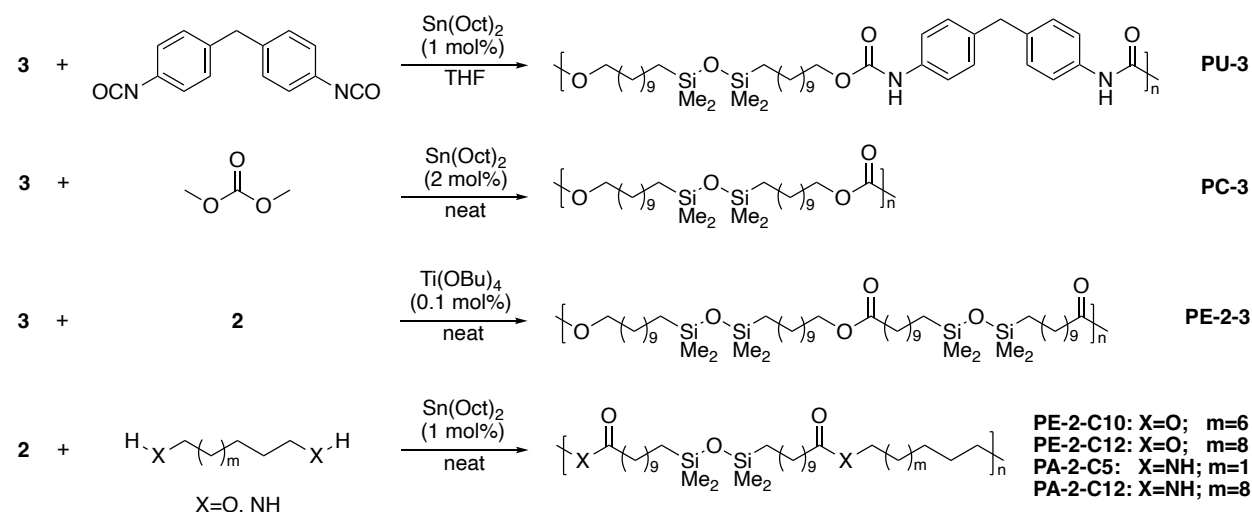
2.3 Characterization of the Polymers

NMR spectroscopic analysis revealed that the resulting polymers possess the characteristic signals for the siloxane units and the corresponding polymerization partners. For example, the ^1H NMR spectrum of **PU-3** contains a singlet at 0.02 ppm for the $\text{Si}(\text{CH}_3)_2$, a triplet at 4.13 ppm ($J = 6.7$ Hz) for the CH_2 adjacent to the carbamate, and a singlet at 3.87 ppm for the CH_2 from MDI (see Figure 2.12.8.11). The molecular weight of **PU-3** determined by NMR spectroscopy was 38

kg·mol⁻¹, which is consistent with the molecular weight of this sample determined by SEC in THF (PS standard, $M_n/M_w/D = 35 \text{ kg}\cdot\text{mol}^{-1}/69 \text{ kg}\cdot\text{mol}^{-1}/1.98$).

The thermal stability of the polymers was determined by thermogravimetric analysis (TGA). The thermal profile of **PU-3** (Table 2.1, entry 1) exhibited a two-stage decomposition. The first stage occurred with an onset temperature at 250 °C, and the second stage with an onset temperature at 400 °C. (see Figure 2.12.9.1) The ratio of the mass loss of each step corresponds to the decomposition of the alkyl chains in the first stage (~ 65% of mass loss) and the aryl moieties in the second stage (~35 % of mass loss). The thermal stability of polyesters and polyamides (Table 2.2.1, entries 3–7) was high, with $T_{d,5\%}$ (temperature at 5% weight-loss) over 340 °C under nitrogen.

Table 2.1.1. Polymers from diester **2** and diol **3**



entry	polymer	M_n^a (kg mol ⁻¹)	M_w^a (kg mol ⁻¹)	D^a	yield (%)	T_m (°C) ^b	$T_{d,5\%}$ (°C) ^c
1	PU-3	35	69	1.98	79	99	279
2	PC-3	18	36	1.96	54	-23 ^d	306 ^d
3	PE-2-3	58	144	2.48	72	-10	386
4	PE-2-C10	22	57	2.54	56	23	348
5	PE-2-C12	21	45	2.18	56	17	352
6	PA-2-C5	n.a ^e	n.a ^e	n.a ^e	54	92	388
7	PA-2-C12	n.a ^e	n.a ^e	n.a ^e	86	99	381

^aDetermined by SEC in THF versus polystyrene standard. ^bDetermined from the second cycle of DSC with a heating rate of 10 °C min⁻¹. ^cDetermined by TGA. ^dThermal data obtained from a high MW **PC-3** (that did not fully dissolve in THF, DMF, 1,2,4-trichlorobenzene, and chloroform and lacks MW data). ^eNot available due to the low solubility in THF and CHCl₃.

Differential scanning calorimetry (DSC) revealed the melting temperature (T_m) of the polymers in Table 1. All polymers were found to be semi-crystalline, with T_m values that depend on the polymer backbone, but without an apparent glass-transition temperature (T_g), even down to -85 °C. The T_m values of the polyesters are near or below room temperature (Table 2.2.1, entries 3–5),

whereas those of the polyurethane (Table 2.2.1, entry 1) and of the polyamides (Table 2.2.1, entries 6–7) were higher (92 – 99 °C) because of the hydrogen bonding in the solid material. The T_m of polyester **PE-2-3**, for which the ratio of siloxane was higher than that of the other polymers because both monomers contained a siloxane, was lower ($T_m = -10$ °C; Table 2.2.1, entry 3) than that of the polyester prepared from the siloxane-containing diester and a conventional alkyl diol. This low value, presumably, arises from the flexibility and low intermolecular interactions of the silicone unit.¹³⁰

We also performed tensile tests of **PU-3** to measure the mechanical properties of the polyurethane containing siloxane linkages (Figure 2.3.1). **PU-3** was able to be processed at 120 °C under 2000 psig, which are conditions similar to those for processing commodity thermoplastics (see Section 2.12.11). Tensile tests revealed that the elongation at break, tensile strength, toughness, and yield stress were $522.1 \pm 35.4\%$, 7.6 ± 0.5 MPa, 33.8 ± 2.9 MJ/m³, and 6.8 ± 0.4 MPa respectively. These mechanical properties of **PU-3** are adequate to be used as a thermoplastic in a broad range of applications and demonstrate the potential of siloxane-containing polymers to be used as materials.

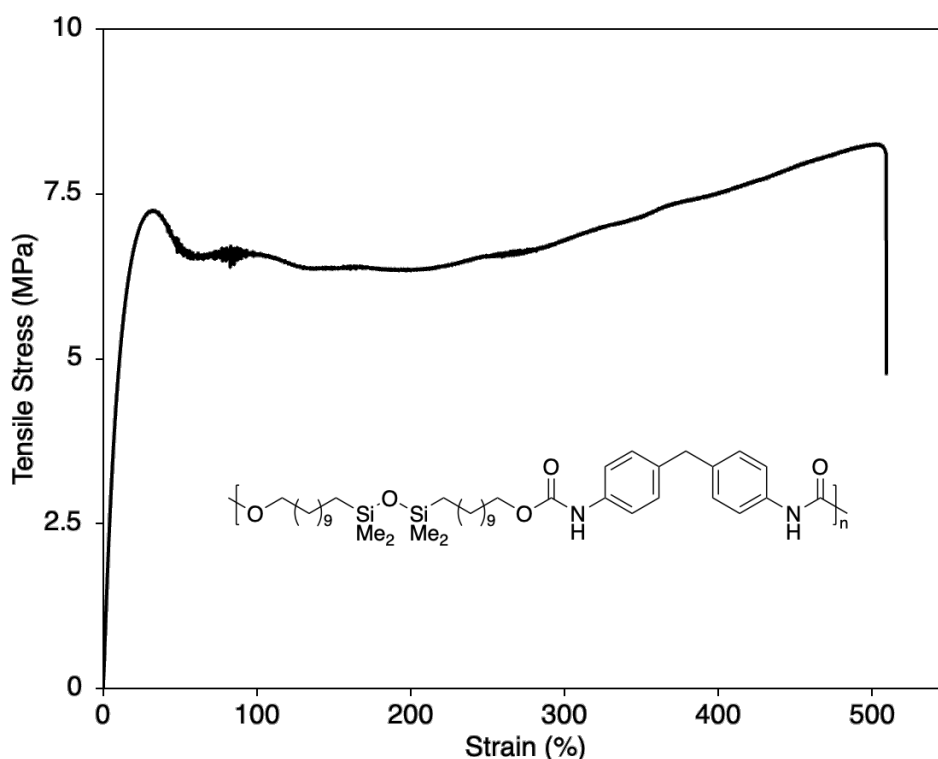


Figure 2.3.1. Stress-strain curve of PU-3

2.4 Synthesis of 26-membered Macrolactone Containing Siloxane Bonds

In addition to the linear siloxane-containing monomers and polymers derived from them, cyclic monomers amenable to ROP were prepared. The siloxane-containing macrolactone **6** was envisioned to be accessible from undecenoate **1** and the corresponding undecenol **7** by a combination of condensation and hydrosilylation (Figure 2.4.1A). We conducted this synthesis by intramolecular hydrosilylation to form the macrocycle, rather than a typical esterification of an α -hydroxy carboxylic acid or ester because the hydrosilylation is irreversible. Cyclization by an irreversible reaction suppresses potential equilibration and oligomerization under the cyclization

conditions. Given that hydrosilylation has not been shown previously to form macrolactones, our studies would assess the feasibility and practicality of using this reaction for this purpose.

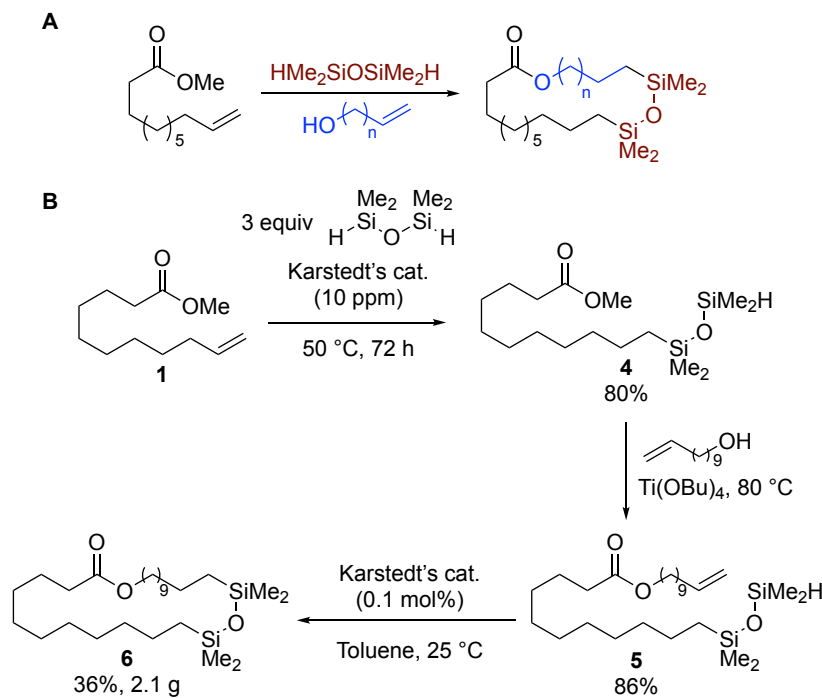


Figure 2.4.1. (A) Strategy to produce cyclic monomer with siloxane from **1**. (B) Synthesis of macrolactone **6**.

The route to prepare the lactone containing the siloxane unit is shown in Scheme 2B. Mono-hydrosilylation of TMDSO with **1** was conducted first. This reaction with excess TMDSO (3 equiv) minimized the formation of the double hydrosilylation product (diester, **2**) and formed the mono-hydrosilylation product **4** in 80% yield after distillation. 10-Undecenol, a reduced form of **1**,¹³¹ was selected as the bio-based α -alkenyl alcohol partner for transesterification. The transesterification catalyzed by $Ti(OBu)_4$ (0.2 mol %) under a constant stream of nitrogen to remove the methanol byproduct formed ester **5** in 86% yield after column chromatography. A series of concentrations and solvents were tested for the final cyclization step (see Table 2.12.8.1). The yield of the monocyclic product was slightly higher from reactions run in toluene than from those run in other solvents, such as THF, CH_2Cl_2 , or heptane. Slow addition of **5** into a dilute toluene solution of Karstedt's catalyst conducted on a gram scale gave mono-, di-, and tricyclic products, as well as linear and cyclic oligomers and compounds that contain internal alkenes resulting from alkene isomerization. The purification of the desired product was achieved by pre-treating the silica with $AgNO_3$, presumably causing alkene-containing products to bind to Ag^+ . By this method of purification, 26-membered macrolactone **6** was obtained in 36% yield on a multigram scale and subjected to studies on its polymerization (Figure 2.4.1B).

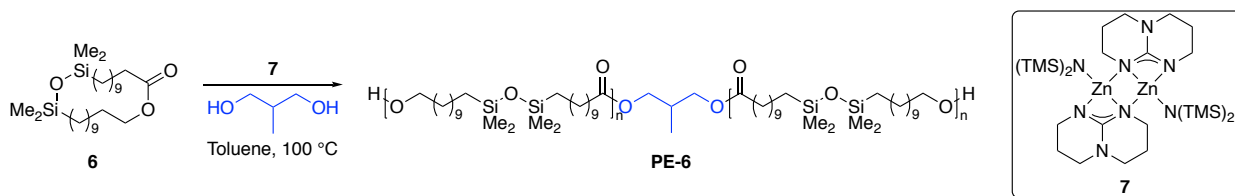
2.5 Ring-opening Polymerization of Macrolactone

The polymerization of macrolactones is usually slower than the polymerization of lactide or ϵ -caprolactone because of the lack of ring strain.¹³² The ROP of macrolactones have been reported with enzymes,¹³³⁻¹³⁶ organometallic species,^{121, 137-140} and organocatalysts¹⁴¹⁻¹⁴³ to form high molecular-weight material. However, in most cases, transesterification competes with propagation,

thereby reducing control over the molecular weight of the polymerization and the ability to synthesize block copolymers.^{139, 144, 145}

Thus, we sought to identify a catalyst for the ROP of **6** that would maximize the rate of ring opening and minimize the rates of transesterification. The ROP of **6**, followed by initiation of the ROP of lactide with the resulting polymer would lead to ABA block copolymers with the properties of thermoplastic elastomers. Duchateau and co-workers recently reported the ROP of pentadecalactone (PDL) with Zn-based catalysts to prepare block copolymers of PDL and ϵ -caprolactone, suggesting that competitive transesterification was less prevalent when the reaction is conducted with this catalyst.¹³⁹ Based on this report and relevant previous work, we found that TBD-based Zn-guanidinate **7**¹⁴⁶ catalyzed the ROP of **6** to form polyester **PE-6** with molecular weights on the order of tens of kg·mol⁻¹ and \bar{D} values between 1.4 and 1.6 (Table 2.5.1).

Table 2.5.1. Ring-opening polymerization (ROP) of macrolactone **6** catalyzed by [Zn]-catalyst **7**.



entry	polymer	$M_{n,NM}$ R (kg mol ⁻¹)	$M_{n,SEC}^b$ mol ⁻¹) ^c	(kg	\bar{D}^c	T_m (°C) ^d	$T_{d,5\%}$ (°C) ^e
1 ^a	PE-6	20.7	24.5	1.68	10	359	
2 ^b	PLLA-PE-6-PLLA	26.2	31.4	1.54	-13	228	

^aPolymerization was conducted in concentrated toluene solution (> 1.5 g/mL) at 100 °C for 1 d.

^bPolymerization was conducted in dichloromethane solution at room temperature for 2 h.

^cDetermined by SEC in THF versus polystyrene standard. ^dDetermined from the second cycle of DSC with a heating rate of 10 °C min⁻¹. ^eDetermined by TGA.

2.6 Block Copolymer Comprising Ring-Opened Macrolactone **6** and *L*-lactide

An ABA triblock copolymer from bio-based monomers was synthesized by the addition of *L*-lactide (**PLLA**, A-block) to **PE-6**. Addition of *L*-lactide ([*L*-lactide]/[diol]=36; 22 wt % relative to **6**; DP of each A-block = 18) to the diluted reaction mixture in CH₂Cl₂ at 25 °C led to the triblock copolymer **PLLA₁₈-PE-6₄₄-PLLA₁₈**. Monitoring the reaction by ¹H NMR spectroscopy indicated that the lactide had fully converted after 2 h, while the unreacted monomer **6** was not consumed. This result reflects the large rate difference in the ROP of lactide vs **6** and ensures the uniformity of the A-blocks.

The ¹H NMR spectrum of the resulting polymer was consistent with the proposed structure. Notable features in the ¹H NMR spectrum of the triblock copolymer include a doublet at 0.99 ppm ($J = 6.9$ Hz) and two doublets at 4.01 ppm ($J = 2.4$ Hz) and 4.00 ppm ($J = 2.0$ Hz), corresponding to the chain initiator derived from 2-methyl-1,3-propanediol, a multiplet at 4.11 ppm, corresponding to the methylene protons at the junctions between **PLLA** and **PE-6**, and a multiplet at 4.36 ppm corresponding to the methine protons at the end of the **PLLA** chains (Figure 2.6.1.C). $M_{n,NMR}$ was determined by comparing the integration of the CH₂ group of **PE-6** at 4.05 ppm and the CH group of **PLLA** at 5.16 ppm to that of the CH₃ group of the initiator at 0.99 ppm. In

addition, SEC analysis revealed an increase in the molecular weight from the pre-polymer **PE-644** to the block copolymer **PLLA₁₈-PE-644-PLLA₁₈** (Table 2.5.1, entries 1–2). TGA of the copolymer showed a 5% weight loss at 228 °C (see Figure 2.12.9.17). Similar to **PE-6**, the triblock **PLLA₁₈-PE-644-PLLA₁₈** exhibited a melting temperature of -13 °C. (see Figure 2.12.9.18). Finally, no melting transition for the **PLLA** segments was observed up to 200 °C.

To construct a polyester that contains chain-ends that are alcohols and that can, thereby, initiate chain extension by lactide, the polymerization of **6** was initiated with 2-methyl-1,3-propanediol. Polymerization of **6** with monomer-to-initiator ratio ($= [\mathbf{6}]/[\text{diol}]$) of 50 was conducted with 1 mol % of **7** to the monomer at 100 °C. The monomer conversion reached 88% after 1 d ($DP = 44$). After purification of the polymers, SEC analysis with polystyrene standards and ¹H NMR spectroscopy were used to reveal the molecular weight of the isolated polymer (**PE-6**). The M_n from the ¹H NMR spectrum ($M_{n,NMR}$) was determined by comparing the integration of the CH₂ group of **PE-6** at 4.05 ppm to that of the CH₃ group of the initiator at 0.99 ppm (Table 2.5.1, entry 1).

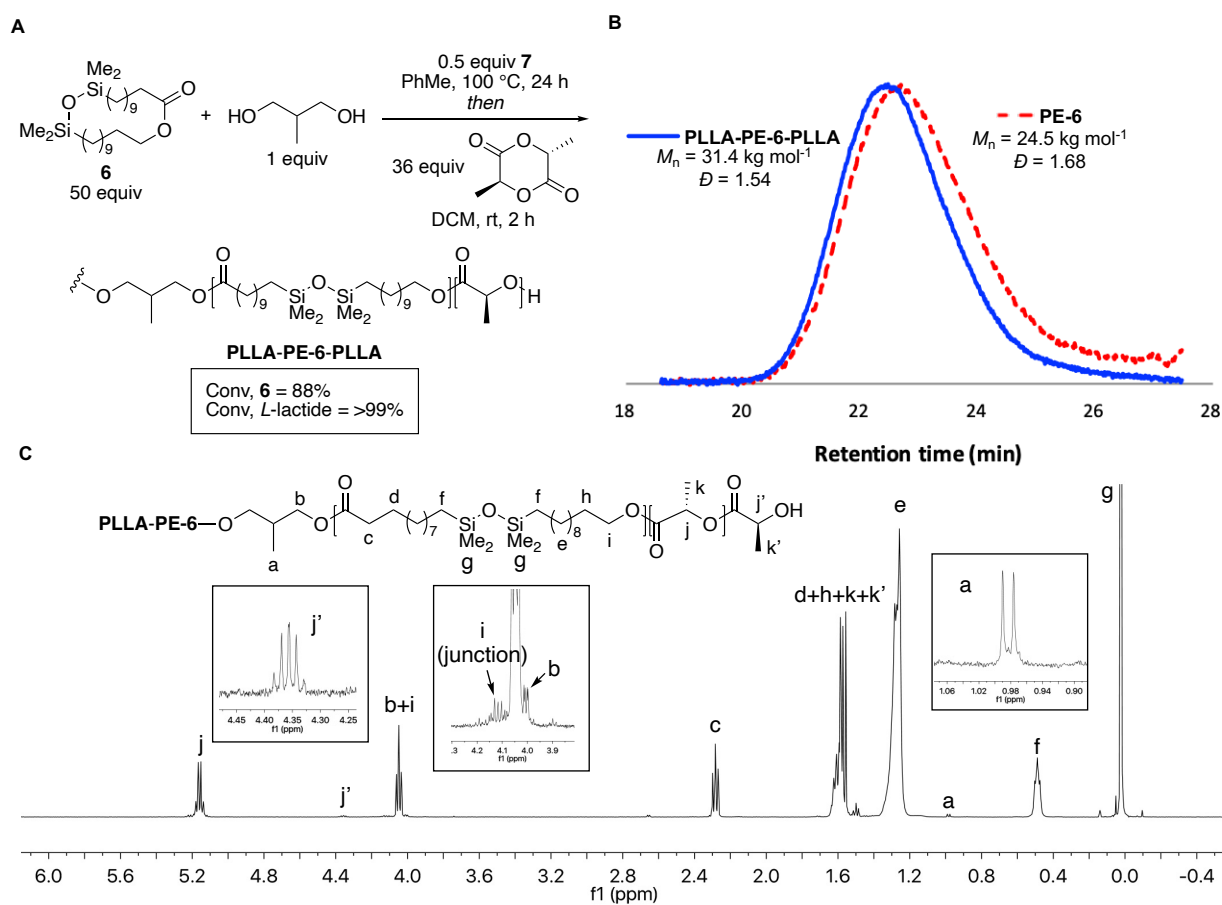


Figure 2.5.1. (A) Block copolymerization of macrolactone and *L*-lactide. (B) SEC traces before (**PE-644**, red; $M_n = 24.5 \text{ kg mol}^{-1}$, $D = 1.68$) and after (**PLLA₁₈-PE-644-PLLA₁₈**, blue; $M_n = 31.4 \text{ kg mol}^{-1}$, $D = 1.54$) the addition of *L*-lactide. (C) ¹H NMR spectrum of PLLA-PE-6-PLLA.

The thermal stability of **PE-6** was high, with $T_{d,5\%}$ occurring at 359 °C (see Figure 2.12.9.15). The T_m of **PE-6** was -10 °C, as determined by DSC analysis, and no T_g was observed down to -85 °C (see Figure 2.12.9.16). This low T_m value differs from that of poly(PDL) (~ 100 °C),¹⁴⁷ despite

the absence of branching in the polymer chain, suggesting that the incorporation of the siloxane units dramatically changes the flexibility of polymer.

2.7 Chemical, Programmed Degradation of Siloxane-Containing Polymers

Programmed depolymerization of the polymers containing siloxane linkages at the Si–O bonds was affected by alcoholysis, hydrolysis and siloxane exchange. Reversible equilibrium between siloxanes catalyzed by acid or base is known to be an important means to control the molecular weights of silicone polymers.¹⁴⁸ The hydrolysis with water reduces the molecular weight of polysiloxanes, producing silanols and disiloxanes (Figure 2.7.1A). Thus, we evaluated depolymerization of the materials by reaction with the combination of an excess of water or hexamethyldisiloxane (HMDSO) and an acid catalyst.

To assess the potential hydrolysis of the siloxane groups, we subjected **PU-3** to various acidic and basic conditions, either in water or a mixture of water and organic solvents. The reaction of **PU-3** in a mixture of THF and MeOH with a catalytic amount of *p*-toluenesulfonic acid (TsOH) readily afforded the corresponding silyl methyl ether after 1 d at 20 °C, and subsequent addition of H₂O led to the silanol **8** (Figure 2.7.1B). Silanol **8** underwent self-condensation to form oligomers during the workup (12% conversion of **8**, see Figure 2.12.8.20).

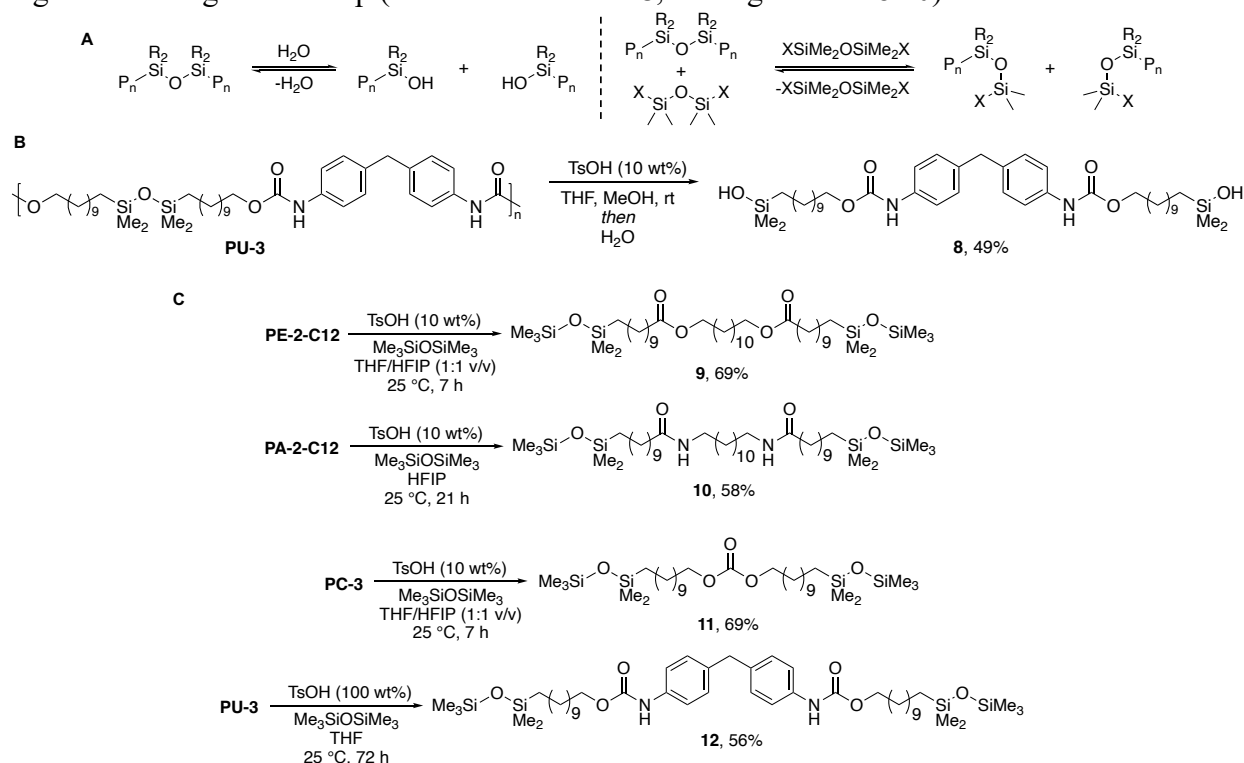


Figure 2.7.1. (A) Equilibria from reaction of polysiloxanes with water or disiloxane. (B) Degradation of siloxane-containing polyurethane **PU-3** with methanol and water. (C) Degradation of siloxane-containing polycarbonate **PC-3**, polyester **PE-2-C12**, polyamide **PA-2-C12**, and polyurethane **PU-3** with hexamethyldisiloxane.

Siloxane exchange would be a second method for depolymerization of these materials, in this case to provide monomers with stable end caps. These end caps, however, would enable repolymerization by the reverse of the cleavage process. To test depolymerization by siloxane

exchange, we conducted reactions of the polymer with HMDSO with an acid catalyst (Figure 2.7.1C). Indeed, TsOH initiated the exchange of the siloxane bond of polyester (**PE-2-C12**) with that of HMDSO, affording the cleavage product **9** that contains disiloxanes as termini. The mixed solvent of THF and hexafluoroisopropanol (HFIP) promoted the conversion of **PE-2-C12** to **9** at room temperature after 7 h, whereas the reaction of **PE-2-C12** with HMDSO in THF alone afforded only 18% of the product of siloxane exchange after 1 d. No self-condensation of **9** was observed during workup, and pure **9** was obtained in 69% isolated yield. This exchange strategy also led to depolymerization of polyamide **PA-2-C12** to **10** (58% isolated yield) and polycarbonate **PC-3** to **11** (69% isolated yield). Depolymerization of polyurethane (**PU-3**) to **12** required higher loading of acid catalyst in solely THF, and pure **12** was obtained in 56% yield after 3 d.

To further investigate the robustness of depolymerization of the siloxane-linkages, polyester **PE-2-C12** was subjected to depolymerization conditions in the presence of other common plastics such as polyethylene terephthalate (PET) from a plastic bottle, polyethylene (PE) from a coffee container, and polypropylene (PP) from a centrifuge tube (Figure 2.7.2). Depolymerization product **9** was obtained in 79% isolated yield after 40 h. The ability of these siloxane-linkages to be cleaved in the presence of mixed waste plastics highlights the advantage of installing programmed units for depolymerization in these materials.

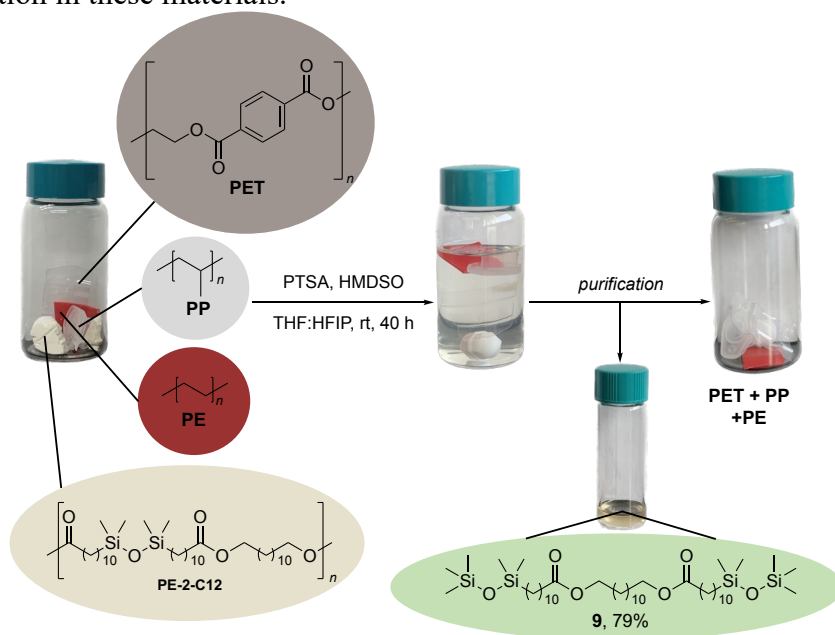


Figure 2.7.2. Degradation of polyester **PE-2-C12** in the presence of polyethylene, polypropylene, and polyethylene terephthalate

2.8 Repolymerization of Monomers to Assess Circularity

Because this process is thermoneutral and HMDSO is volatile, this exchange process should enable reversibility between monomer and polymer (Figure 2.8.1).¹⁴⁹ To examine this reversibility, repolymerization of monomer **9** obtained from siloxane cleavage of polymer **PE-2-C12** ($M_n = 10.5 \text{ kg mol}^{-1}$, $D = 1.6$) was investigated with various catalysts under vacuum (Table 2.12.4.1). When strong Brønsted acid catalysts such as triflic acid (TfOH) or perfluorobutane-1-sulfonic acid (PFBS) were used as catalyst, oligomers of high molecular weight were obtained as determined by SEC (Table 2.12.4.1). The molecular weight of polymer **PE-2-C12** derived from polymerization of **9** ($M_n = 10.5 \text{ kg mol}^{-1}$, $D = 1.7$) was similar to the molecular weight of polymer

PE-2-C12 synthesized by polymerization of α,ω -diester **2** with 1,12-dodecanediol catalyzed by $\text{Sn}(\text{Oct})_2$ as assessed by SEC. Although the original polymerization and the repolymerization occur by extrusion of different molecules, MeOH and HMDSO respectively, they lead to polymers with similar molecular weights. The ability of these siloxane containing polymers to undergo depolymerization and repolymerization enables a circular economy for these materials.

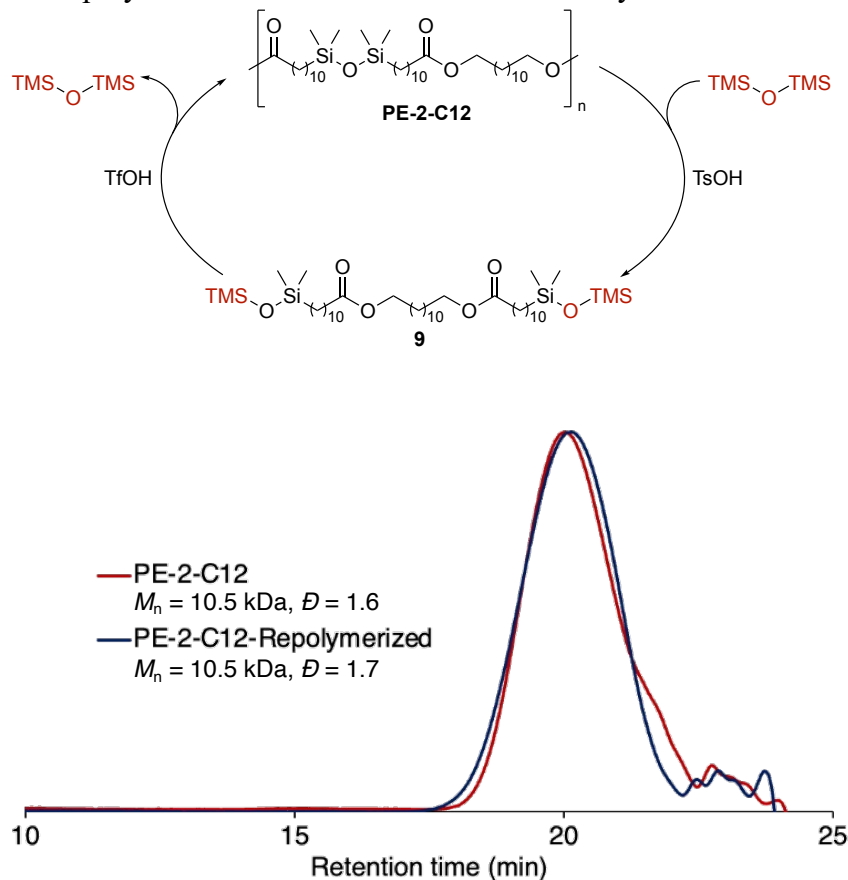


Figure 2.8.1. Repolymerization of monomer **9** to polymer PE-2-C12

2.9 Assessment of the Enzymatic Hydrolysis and Microbial Metabolism of the Polymers and Monomers

Finally, we assessed the propensity of a selection of the synthesized polymers to undergo enzymatic hydrolysis. To do so, we exposed films of **PE-2-C10**, **PE-2-C12**, and **PU-3** cast on glass slides to aqueous solutions containing *Fusarium solani* cutinase (FsC; $82.7 \mu\text{g mL}^{-1}$; pH 7, 30°C) (Figure 2.9.1). The progress of ester and carbamate hydrolysis was monitored by the production of acidic groups quantified by pH-stat titration, as described previously.^{150, 151} All three polymers underwent significant enzymatic hydrolysis on the timescale of hours to days. For reasons that are difficult to pinpoint, the degree of hydrolysis plateaued after approximately two to three days in each case. The extent of hydrolysis of ester and carbamate units was determined to be 45–50 % for **PE-2-C10**, 31–49 % for **PE-2-C12**, and 34–42% for **PU-3**, assuming one equivalent of hydroxide is consumed per hydrolysis of an ester and two equivalents of hydroxide are consumed per hydrolysis of a carbamate unit.

The degrees of enzymatic polymer hydrolysis reported here represent lower limits because the mass of polymer added was determined by the mass of the air-dried, solvent-cast films. If these films contained residual CHCl_3 solvent from the casting procedure, less polymer would have been present, and the calculated degrees of hydrolysis would be higher. Further studies will be needed to determine the activity of different classes of enzymes on these polymers, the factors controlling their enzymatic hydrolysis, and identification of the products from this hydrolysis. Nevertheless, exposure of the films to the tested cutinase produced by soil filamentous fungi resulted in partial enzymatic hydrolysis and the formation of oligomers, thereby demonstrating the potential of each of the tested polymers to undergo enzymatic hydrolysis.

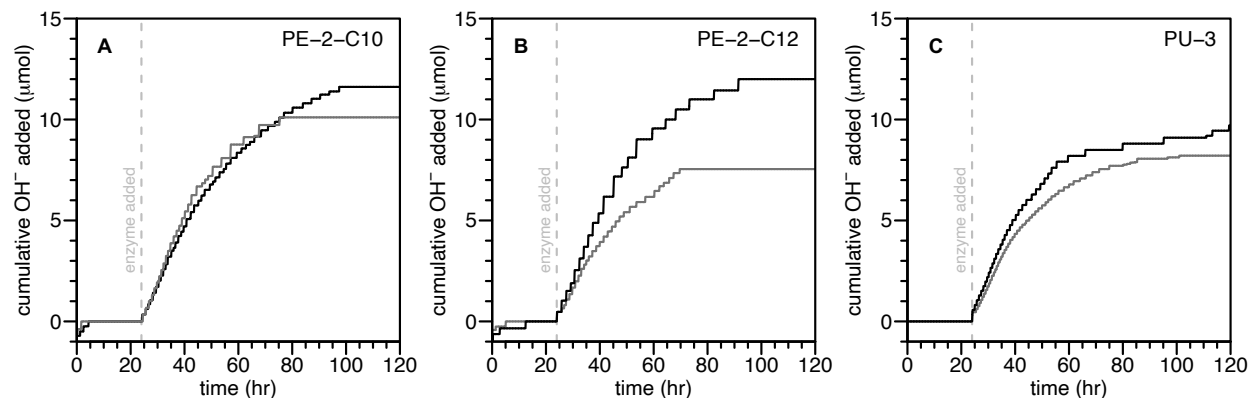


Figure 2.9.1. Enzymatic hydrolysis of polymers PE-2-C10 (A), PE-2-C12 (B), and PU-3 (C) by cutinase from *Fusarium solani* (FsC; concentration= $82.7 \mu\text{g FsC mL}^{-1}$) at 30°C and pH 7.0, as determined by cumulative amounts of base (5 mM KOH) needed to maintain a constant pH during hydrolysis using an automated pH-stat titration setup. Polymers were added to beakers containing FsC-free solutions at a time of 0 h, and FsC was added to beakers at a time of 24 h. Black and grey curves show data for duplicate incubations of each polymer.

2.10 Assessment of Microbial Utilization of Monomers in Soil

To assess the microbial metabolism of the central siloxane component shared by these materials, we prepared two ^{13}C -labelled variants of diester **2** and monitored the production of $^{13}\text{CO}_2$ resulting from incubation of these compounds in soil, following previously established methods (Figure 2.10.1).^{152, 153} The two variants of diester **2** carried ^{13}C -labels in different positions—diester **2- $^{13}\text{C-a}$** on C-10 (C-1 = carboxylate) of the undecanoate chain and diester **2- $^{13}\text{C-b}$** on one of the methylsiloxane carbons. These two variants, which would presumably be formed upon enzymatic hydrolysis of the polymers, were chosen to assess the overall biodegradability of the entire molecule.¹⁵⁴ From the soil incubation of **2- $^{13}\text{C-a}$** , with the ^{13}C label in the undecanoate chain, clear production of $^{13}\text{CO}_2$ was observed during the 126 d testing period, reaching $64 \pm 10\%$ ($n = 3$) of the $^{13}\text{CO}_2$ level resulting from incubations of the biodegradable reference compound ^{13}C -glucose in the same soil (note that the non-mineralized fraction of glucose ^{13}C is ascribed to incorporation of that carbon into microbial biomass). Furthermore, based on the continuous mineralization of this position throughout the incubation period, we expect that metabolism would continue to higher extents if the incubation times extended beyond 126 d. As expected from the abiotic character of a dimethylsilyl unit, soil incubations of **2- $^{13}\text{C-b}$** with the label on the methylsilane carbon resulted in little production of $^{13}\text{CO}_2$ ($1 \pm 3\%$, $n = 3$). The fate of the methylsiloxane moiety under environmental degradation conditions, therefore, remains

unknown, but carbons in the polymer backbone, as suggested by those evaluated, are expected to be susceptible to microbial metabolism.

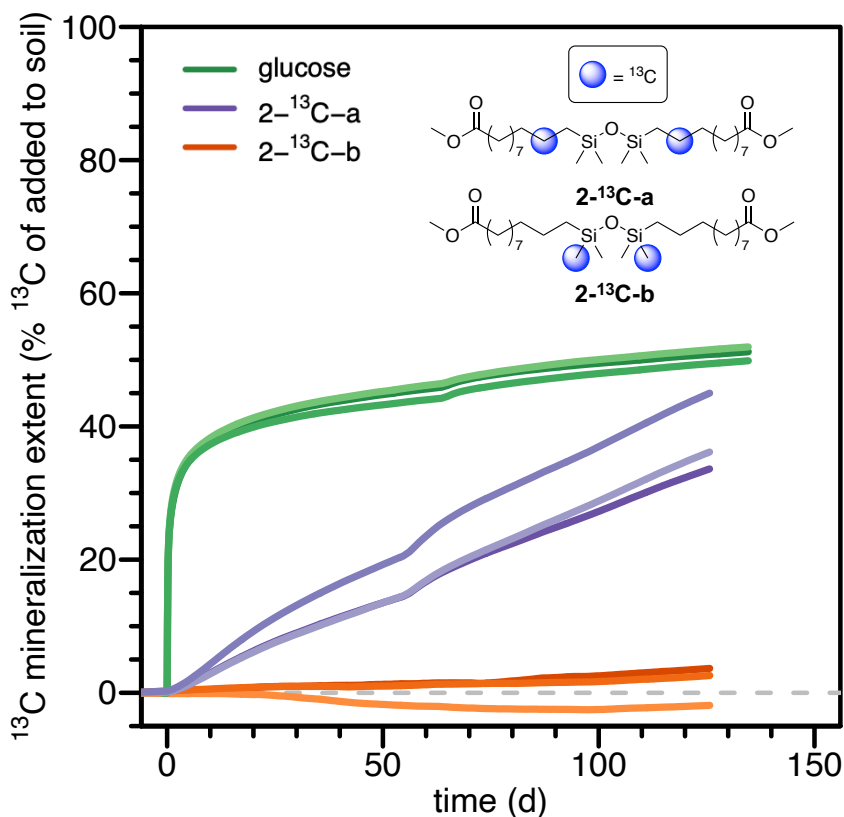


Figure 2.10.1. Cumulative mineralization extents of uniformly ¹³C-labelled glucose (green traces) and position-specifically ¹³C-labelled variants of the siloxane-containing diester 2, containing a ¹³C-label in the undecenoate chain (i.e., 2-¹³C-a; purple traces) or in the siloxane-methyl (i.e., 2-¹³C-b; orange traces) in a soil at 25°C. Mineralization extents were calculated as the integral of measured mineralization rate curves, followed by normalizing the mineralized amount of ¹³C-carbon by the amount of substrate-¹³C added to each soil. Substrates were added to three separate soil incubation bottles, resulting in triplicates for each substrate; the mineralization curves are shown for each individual incubation.

2.11 Conclusion

Degradable polymers have been synthesized by linking monomers from renewable seed oils with a siloxane unit. A diol, a diester, and a 26-membered macrolactone were prepared from 10-undecenoate and 1,1,3,3-tetramethyldisiloxane. The siloxane moieties were incorporated into the monomers by hydrosilylation of the alkenes. Polycondensation of AA-monomers comprising the siloxane with alcohol or ester chain ends with a set of BB-monomers provided a broad range of siloxane-containing polymers possessing varied thermal properties. The ring-opening polymerization of the macrolactone-containing siloxane produced a flexible polyester, which served as the soft midblock of ABA triblock copolymers. The siloxane-containing polymers degraded into silanols or disiloxanes under mild conditions without the hydrolysis of carbonyl functionalities. Polymerization of the monomers formed by degradation was successful to reform polyesters, demonstrating circularity of these polymers. Studies to gain information on the

enzymatic hydrolyzability of these siloxane-containing polymers provided clear evidence that the polyester and polyurethane materials undergo hydrolysis upon exposure to a fungal cutinase. Furthermore, studies on carbon utilization of position-specific ^{13}C -labeled siloxane-diester monomers, that are expected to be released upon enzymatic hydrolysis of the respective polymer, by soil microorganisms showed that the alkyl main chain carbons were metabolized over the methyl carbons of the siloxane units by soil microbes to CO_2 .

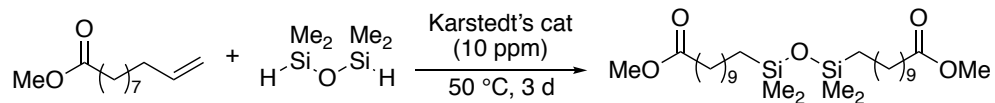
2.12 Experimental Section

2.12.1 General Information

All chemicals were purchased from commercial sources unless otherwise stated. Compound **7** was prepared according to the literature procedure.¹⁴⁶ (*L*)-Lactide was purchased from commercial sources and purified by recrystallization from toluene according to the literature procedure.¹⁵⁵ Dry solvents (THF, DCM, diethyl ether) were dried by an Innovative Technology Pure-Solv solvent purification system and stored over molecular sieves. Analytical thin-layer chromatography (TLC) was performed on pre-coated, glass-backed silica gel plates. NMR spectra were acquired on Bruker AVQ-400, AVB-400, DRX 500, and AV-600 spectrometers. Chemical shifts were reported in ppm relative to residual solvent peaks ($\text{CDCl}_3 = 7.26$ ppm for ^1H and 77.16 ppm for ^{13}C or $\text{C}_2\text{D}_2\text{Cl}_4 = 6.00$ ppm for ^1H and 73.78 ppm for ^{13}C). Coupling constants were reported in Hz. SEC was performed on all polymers synthesized except through repolymerization with a Malvern Viscotek TDA Max chromatography system equipped with PLgel MIXED-C columns using THF as the eluent (30 °C, 1 mL/min) calibrated with polystyrene standards. SEC was performed on polymers synthesized by repolymerization with a Malvern OMNISEC equipped with two Malvern T6000M mixed bed columns in series using THF as the eluent (35 °C, 1 mL/min) with refractive index, light scattering, and intrinsic viscosity detectors calibrated with a single poly(styrene) standard. Molecular weight ($M_{n,\text{NMR}}$) was calculated by ^1H NMR spectroscopy by comparing the integration of the resonance that is characteristic of the chain-end or initiator of the polymer to the integration of the resonances that are characteristic of the backbone of the polymer. DSC was performed on a TA Instruments Q200 calorimeter (purge gas: He, flow rate: 25 mL/min, ramp rate: 10 °C/min, temperature range: -90 - 200 °C). TGA was performed on a TA instrument Q500 thermogravimetric analyzer under nitrogen from 25 to 500 °C at a ramp rate of 10 °C/min. High-resolution mass spectral data were obtained from the QB3/Chemistry Mass Spectrometry Facility at the University of California, Berkeley and the Lawrence-Berkeley National Laboratory Catalysis Center using PerkinElmer AxION 2 UHPLC-TOF system. Compression molding was conducted on a Grizzly Industrial 10-ton benchtop shop press with heated plates (model H6231Z) or a Carver benchtop lab press with heated plates (model 4386). Tensile testing was conducted according to ASTM D638 on an Instron universal materials tester. Tensile stress and strain were measured at room temperature using an extension rate of 50 mm/min.

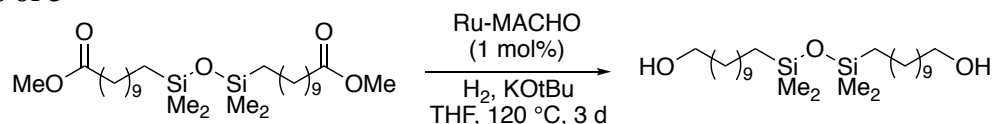
2.12.2 Synthesis of monomers

Synthesis of 2



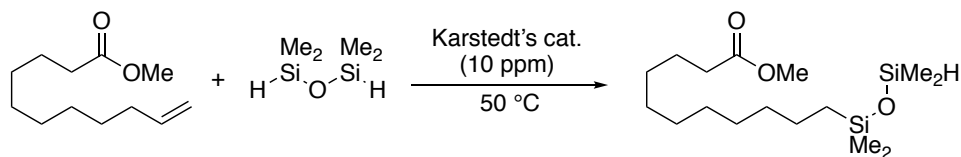
To a mixture of methyl 10-undecenoate (2.0 g, 10 mmol) and 1,1,3,3-tetramethyldisiloxane (0.67 g, 5.0 mmol) in a 4-mL vial was added Karstedt's catalyst (1 μ L of 2% xylene solution, 10 ppm relative to the alkene) under N_2 , and the vial was capped with a Teflon-lined cap and heated at 50 °C (stirring is optional) for 72 h to obtain **2** as a colorless liquid. The crude mixture was used directly for the synthesis of **3** and the polymerization. 1H NMR (500 MHz, $CDCl_3$) δ 3.66 (s, 6H), 2.30 (t, $J = 7.6$ Hz, 4H), 1.66 – 1.56 (m, 4H), 1.34 – 1.20 (m, 28H), 0.49 (t, $J = 7.4$ Hz, 4H), 0.02 (s, 12H). ^{13}C NMR (151 MHz, $CDCl_3$) δ 174.45 (s), 51.55 (s), 34.27 (s), 33.57 (s), 29.68 (s), 29.64 (s), 29.52 (s), 29.42 (s), 29.32 (s), 25.12 (s), 23.43 (s), 18.57 (s), 0.54 (s). HRMS (APCI+) calcd for $C_{28}H_{59}O_5Si_2^+$ [$M+H^+$]: 531.3896, found: 531.3900.

Synthesis of 3



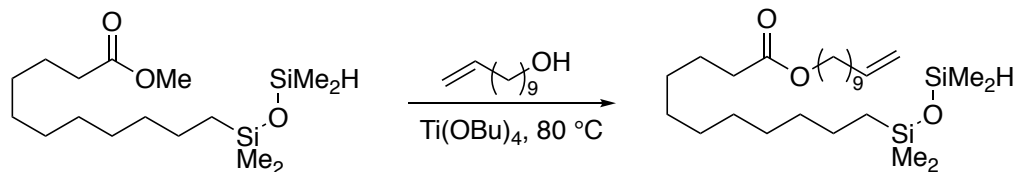
To a Parr reactor (internal volume \sim 10 mL) were added Ru-MACHO (24 mg, 0.040 mmol), KOtBu (16 mg, 0.14 mmol), THF (6 mL), and diester **2** (2.00 g, 3.77 mmol), in that order, under N_2 , and the reactor was pressurized to 60 bar with H_2 and heated in an Al-heating block set at 120 °C for 3 days. The reactor was then cooled to 23 °C and depressurized, and the reaction mixture was purified by silica gel column chromatography (0:10 to 3:7 ethyl acetate:hexanes) to afford **3** as a colorless liquid (1.1 g, 62% yield). 1H NMR (500 MHz, $CDCl_3$) δ 3.64 (t, $J = 6.2$ Hz, 4H), 1.57 (p, $J = 6.9$ Hz, 4H), 1.39 – 1.21 (m, 32H), 0.49 (t, $J = 7.6$ Hz, 4H), 0.03 (s, 12H). ^{13}C NMR (151 MHz, $CDCl_3$) δ 63.19 (s), 33.58 (s), 32.95 (s), 29.79 (s), 29.78 (s), 29.74 (s), 29.60 (s), 29.55 (s), 25.90 (s), 23.43 (s), 18.56 (s), 0.54 (s). HRMS (APCI+) calcd for $C_{26}H_{59}O_3Si_2^+$ [$M+H^+$]: 475.3997, found: 475.3995.

Synthesis of 4



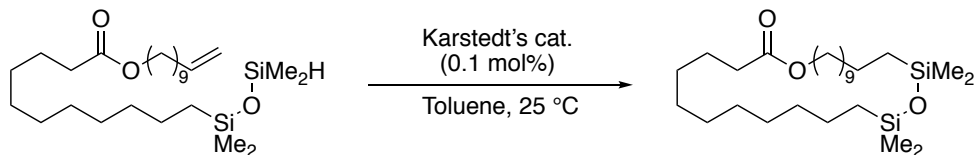
To a mixture of methyl 10-undecenoate (10.3 g, 52.0 mmol) and 1,1,3,3-tetramethyldisiloxane (21.0 g, 156 mmol) under N_2 was added Karstedt's catalyst (10 μ L of 2 wt% xylene solution), and the mixture was heated under N_2 at 50 °C for 2 d. The conversion was 85% at this point (monitored by NMR spectroscopy). Then another batch of Karstedt's catalyst (2 μ L of 2 wt% xylene solution) was added, and the mixture was heated for another 2 d until all **1** had been converted (monitored by NMR spectroscopy). **4** was obtained by vacuum distillation (20 mTorr, 130 °C) as a colorless liquid (13.9 g, 80.6% yield). 1H NMR (600 MHz, $CDCl_3$) δ 4.67 (p, $J = 2.6$ Hz, 1H), 3.66 (s, 3H), 2.30 (t, $J = 7.6$ Hz, 2H), 1.70 – 1.53 (m, 2H), 1.34 – 1.21 (m, 14H), 0.56 – 0.43 (m, 2H), 0.16 (d, $J = 2.5$ Hz, 6H), 0.05 (s, 6H). ^{13}C NMR (151 MHz, $CDCl_3$) δ 174.49 (s), 51.57 (s), 34.27 (s), 33.52 (s), 29.65 (s), 29.62 (s), 29.47 (s), 29.40 (s), 29.31 (s), 25.11 (s), 23.32 (s), 18.27 (s), 1.05 (s), 0.19 (s). HRMS (EI+) calcd for $C_{16}H_{35}O_3Si_2^+$: 331.2119, found: 331.2126.

Synthesis of 5



To a mixture of **4** (4.0 g, 12 mmol) and 10-undecenol (3.1 g, 18 mmol) in a 20-mL vial under N_2 was added $\text{Ti}(\text{OBu})_4$ (8.1 mg, 0.024 mmol), and the mixture was heated at $80\text{ }^\circ\text{C}$ while being purged by a constant stream of N_2 for 3 d. The conversion of **4** was monitored by NMR spectroscopy. After full conversion of **4**, the vial was opened under air, triethylamine (15 μL) was added to the mixture, and the mixture was stirred at $25\text{ }^\circ\text{C}$ for 1 h. The mixture was then purified by column chromatography (0% to 5% diethyl ether in hexanes) to afford **5** as a colorless liquid (4.9 g, 86% yield). ^1H NMR (300 MHz, CDCl_3) δ 5.81 (ddt, $J = 16.9, 10.2, 6.7$ Hz, 1H), 5.06 – 4.87 (m, 2H), 4.67 (hept, $J = 2.8$ Hz, 1H), 4.05 (t, $J = 6.7$ Hz, 2H), 2.29 (t, $J = 7.5$ Hz, 2H), 2.04 (q, $J = 6.9$ Hz, 2H), 1.65 – 1.58 (m, 4H), 1.44 – 1.17 (m, 26H), 0.52 (t, $J = 7.5$ Hz, 2H), 0.16 (d, $J = 2.8$ Hz, 6H), 0.05 (s, 6H). ^{13}C NMR (151 MHz, CDCl_3) δ 174.15 (s), 139.33 (s), 114.28 (s), 64.53 (s), 34.57 (s), 33.95 (s), 33.53 (s), 29.67 (s), 29.65 (s), 29.61 (s), 29.54 (s), 29.49 (s), 29.43 (s), 29.38 (s), 29.33 (s), 29.25 (s), 29.07 (s), 28.81 (s), 26.08 (s), 25.19 (s), 23.33 (s), 18.29 (s), 1.05 (s), 0.19 (s). HRMS (EI+) calcd for $\text{C}_{26}\text{H}_{53}\text{O}_3\text{Si}_2^+$: 469.3528, found: 469.3517.

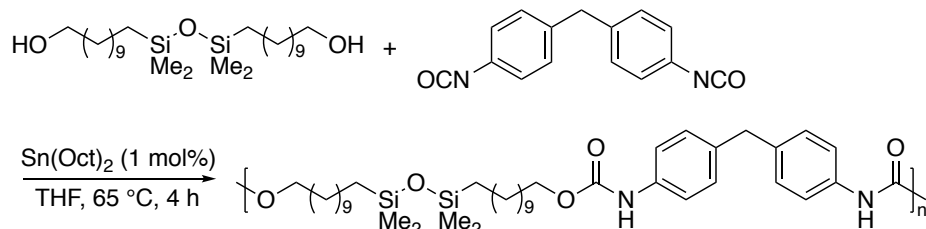
Synthesis of 6



To a solution of Karstedt's catalyst (80 μL of 2 wt% xylene solution) in toluene (140 mL) under N_2 at $25\text{ }^\circ\text{C}$ was added dropwise a solution of **5** (5.90 g, 12.5 mmol) in toluene (140 mL) over 24 h. After the addition has finished, the solution was stirred for 2 h at $25\text{ }^\circ\text{C}$, and the volatiles were evaporated. The crude mixture was purified by column chromatography (0% to 5% Et_2O in hexanes over silica treated with 3 wt% AgNO_3) to afford **6** as a colorless liquid that spontaneously solidified after several days of storage at $25\text{ }^\circ\text{C}$ (2.09 g, 36% yield). ^1H NMR (600 MHz, CDCl_3) δ 4.10 (t, $J = 5.7$ Hz, 2H), 2.31 (t, $J = 7.0$ Hz, 2H), 1.67 – 1.58 (m, 4H), 1.42 – 1.21 (m, 30H), 0.53 – 0.45 (m, 4H), 0.02 (s, 12H). ^{13}C NMR (151 MHz, CDCl_3) δ 174.19 (s), 64.39 (s), 34.93 (s), 33.62 (s), 33.60 (s), 29.85 (s), 29.77 (s, three peaks overlapping), 29.74 (s), 29.66 (s), 29.63 (s), 29.43 (s), 29.40 (s), 29.16 (s), 28.78 (s), 26.36 (s), 25.48 (s), 23.47 (s), 23.43 (s), 18.60 (s), 18.58 (s), 0.64 (s), 0.60 (s). HRMS (EI+) calcd for $\text{C}_{26}\text{H}_{54}\text{O}_3\text{Si}_2^+$: 470.3611, found: 470.3615.

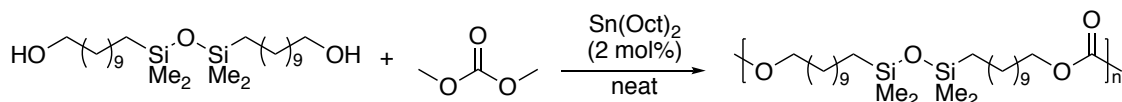
2.12.3 Synthesis of Polymers

Synthesis of PU-3



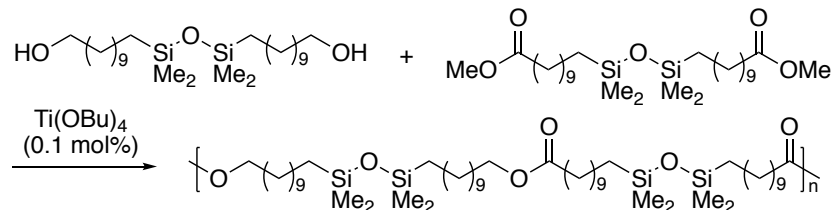
To a mixture of **3** (241 mg, 0.507 mmol) and methylene diphenyl diisocyanate (127 mg, 0.507 mmol) dissolved in dry THF (5 mL) in a 20-mL vial under N₂ was added Sn(Oct)₂ (1.7 μL, 0.010 mmol), and the vial was capped with a PTFE-lined cap and heated to 65 °C for 4 h with stirring. The content was cooled to 23 °C and added dropwise to MeCN (250 mL) under vigorous stirring. The precipitated polymer was collected by filtration, washed with a small portion of MeCN, and dried under vacuum. The resulting polymer was a colorless solid (291 mg, 79% yield). ¹H NMR (500 MHz, C₆D₆) δ 7.28 (d, *J* = 7.3 Hz, 4H), 7.08 (d, *J* = 8.3 Hz, 4H), 6.60 (s, 2H), 4.13 (t, *J* = 6.7 Hz, 4H), 3.87 (s, 2H), 1.70 – 1.61 (m, 4H), 1.40 - 1.20 (m, 28H), 0.49 (t, *J* = 7.4 Hz, 4H), 0.02 (s, 12H).

Synthesis of PC-3



To a mixture of **3** (286 mg, 0.602 mmol) and Sn(Oct)₂ (5.0 mg, 0.012 mmol) in a 20-mL vial under N₂ was added dimethyl carbonate (0.1 mL, 1.2 mmol), and the vial was capped with a PTFE-lined cap. The mixture was stirred at 130 °C under the N₂-filled closed system until achieving the equilibrium determined by ¹H NMR spectroscopy, then at 130 °C under high vacuum, then finally at 160 °C under high vacuum overnight. The mixture was diluted with CHCl₃ (0.5 - 1 mL) and added dropwise to MeOH (100 mL) under vigorous stirring. The product was obtained after decanting the solvents and drying under high vacuum (163 mg, 54% yield). ¹H NMR (400 MHz, CDCl₃) δ 4.11 (t, *J* = 6.8 Hz, 4H), 1.70 – 1.61 (m, 4H), 1.40 – 1.20 (m, 32H), 0.49 (t, *J* = 7.1 Hz, 4H), 0.02 (s, 12H).

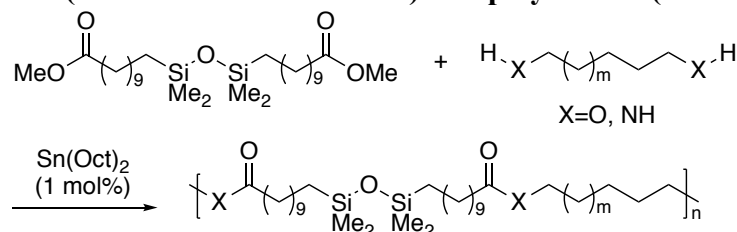
Synthesis of PE-2-3



To a mixture of **2** (107 mg, 0.202 mmol) and **3** (96.6 mg, 0.203 mmol) was added Ti(OBu)₄ (0.10 μL, ~0.13 mol%) under N₂, and the mixture was stirred at 100 °C for 20 h while being purged by a stream of N₂, then at 130 °C under high vacuum (~50 mTorr) for 5 h, and finally at 140 °C under high vacuum for 24 h. The mixture was diluted in CH₂Cl₂ (0.5 mL) and added dropwise to acetone (20 mL) under vigorous stirring. The product was obtained as a colorless gum after decanting the solvents and drying under high vacuum (135 mg, 71.7% yield). ¹H NMR (500 MHz, CDCl₃) δ

4.05 (t, $J = 6.8$ Hz, 4H), 2.28 (t, $J = 7.6$ Hz, 4H), 1.66 – 1.57 (m, 8H), 1.30 – 1.24 (m, 60H), 0.49 (t, $J = 7.3$ Hz, 8H), 0.02 (s, 24 H).

Synthesis of polyesters (PE-2-C10 and PE-2-C12) and polyamides (PA-2-C5 and PA-2-C12)



To a mixture of **2** (0.30 mmol) and diol or diamine (0.36 mmol, 20% excess) was added Sn(Oct)₂ (1.0 μL, 1.0 mol%) under N₂, and the mixture was stirred at 130 °C for 2 h while being purged by a stream of N₂, then at 150 °C for 2 h while being purged by a stream of N₂, then finally at 150 °C under high vacuum (~50 mTorr) for 3 h. Then the mixtures were diluted with CHCl₃ (0.5 - 1 mL) and added dropwise to MeOH (20 mL, for polyesters) or acetone (20 mL, for polyamides) under vigorous stirring. The products were obtained after decanting the solvents and drying under high vacuum.

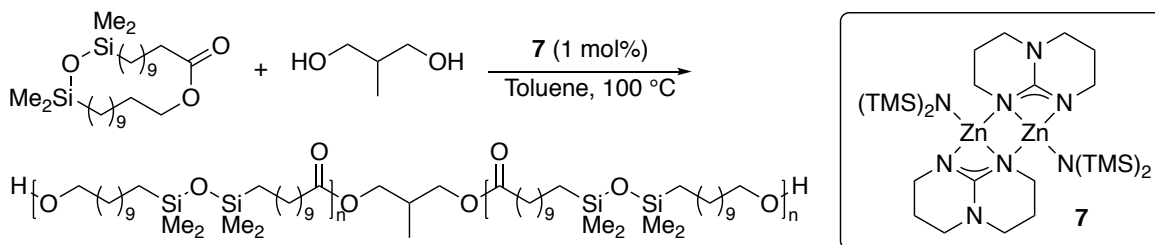
PE-2-C10 (X=O, m=6): ¹H NMR (500 MHz, CDCl₃) δ 4.05 (t, $J = 6.8$ Hz, 4H), 2.28 (t, $J = 7.6$ Hz, 4H), 1.61 (p, $J = 7.0$ Hz, 8H), 1.28 (m, 40H), 0.49 (t, $J = 7.5$ Hz, 4H), 0.02 (s, 12H).

PE-2-C12 (X=O, m=8): ¹H NMR (400 MHz, CDCl₃) δ 4.05 (t, $J = 6.7$ Hz, 4H), 2.28 (t, $J = 7.6$ Hz, 4H), 1.61 (p, $J = 6.8$ Hz, 8H), 1.37 – 1.24 (m, 44H), 0.48 (t, $J = 7.4$ Hz, 4H), 0.02 (s, 12H).

PA-2-C5 (X=N, m=1): ¹H NMR (500 MHz, CDCl₃) δ 6.05 (br, 2H), 3.22 (d, $J = 6.9$ Hz, 4H), 2.16 (t, $J = 7.6$ Hz, 4H), 1.62 (m, 4H), 1.52 (m, 4H), 1.26 (m, 30H), 0.48 (t, $J = 7.6$ Hz, 4H), 0.02 (s, 12H).

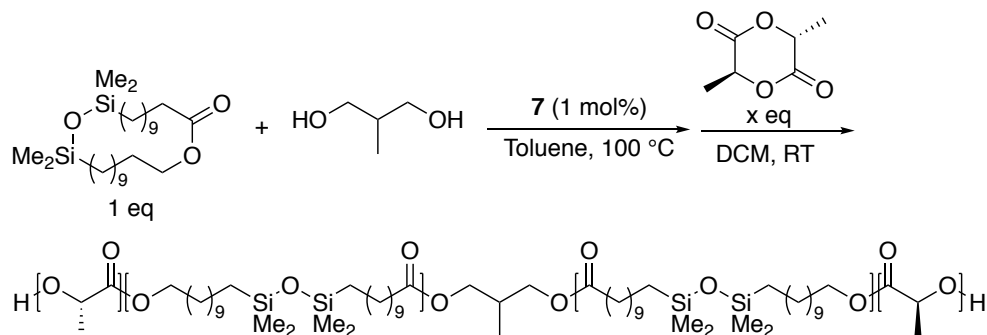
PA-2-C12 (X=N, m=8): ¹H NMR (500 MHz, CDCl₃) δ 5.67 (br, 2H), 3.22 (q, $J = 6.7$ Hz, 4H), 2.15 (t, $J = 7.6$ Hz, 4H), 1.61 (m, 4H), 1.47 (m, 4H), 1.38 – 1.17 (m, 44H), 0.49 (t, $J = 7.6$ Hz, 4H), 0.02 (s, 12H).

Synthesis of PE-6



To a 4-mL vial under N₂ was charged **7** (0.7 mg, 0.002 mmol), 2-methyl-1,3-propanediol (0.18 mg, 0.0020 mmol) in toluene (60 μL), and **6** (94 mg, 0.20 mmol), and the mixture was stirred under N₂ at 100 °C for 21 h. The conversion of **6** was monitored by NMR spectroscopy. At 21 h, the conversion was ~85%. The vial was opened under air, and the sample was diluted with CHCl₃ (0.4 mL) and iPrOH (0.1 mL) before being added dropwise to a stirring mixture of iPrOH and acetone (20:1). The precipitated polymer was washed with iPrOH and dried at 40 °C under vacuum. A colorless viscous liquid was obtained (60 mg, 64% yield). ¹H NMR (500 MHz, CDCl₃) δ 4.05 (t, $J = 6.8$ Hz, 2H), 2.28 (t, $J = 7.6$ Hz, 2H), 1.61 (p, $J = 6.8$ Hz, 4H), 1.27 (d, $J = 14.1$ Hz, 30H), 0.49 (t, $J = 7.5$ Hz, 4H), 0.02 (s, 12H).

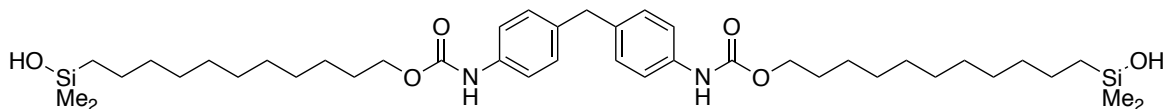
Synthesis of PLLA-PE-6-PLLA



To a 4-mL vial under N_2 were charged **7** (2.3 mg, 0.0063 mmol), 2-methyl-1,3-propanediol (1.2 mg, 0.013 mmol) in toluene (380 μ L), and **6** (300 mg, 0.638 mmol), and the mixture was stirred under N_2 at 100 $^\circ$ C for 30 h. The conversion of **6** at this point was 88%, as determined by NMR spectroscopy. The mixture was diluted with CH_2Cl_2 (1 mL), and to the mixture was added L-lactide (80 mg, 0.56 mmol), and the mixture was stirred at 25 $^\circ$ C for 2 h. All lactide had been converted at this point, as determined by NMR spectroscopy. The vial was opened under air, and to it was added iPrOH (0.3 mL). The mixture was stirred at 25 $^\circ$ C for 1 h before being added dropwise to a stirring mixture of MeOH (100 mL), iPrOH (100 mL), and acetone (20 mL). A white fiber solid was obtained after decanting the solvents and was rinsed with iPrOH and dried under vacuum at 40 $^\circ$ C (237 mg, 62% yield). 1H NMR (500 MHz, $CDCl_3$) δ 5.16 (q, $J = 7.1$ Hz, 1H*x), 4.05 (t, $J = 6.8$ Hz, 2H), 2.28 (t, $J = 7.6$ Hz, 2H), 1.64 – 1.56 (m, 4H and 3H*x), 1.35 – 1.22 (m, 30H), 0.49 (t, $J = 7.5$ Hz, 4H), 0.02 (s, 12H).

2.12.3 Degradation of polymers

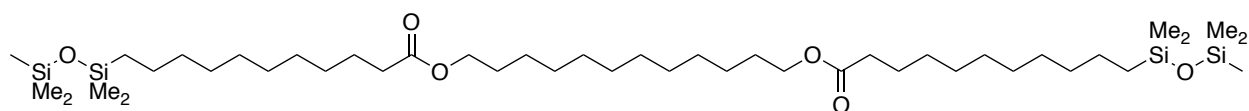
8 from PU-3



To a solution of **PU-3** (30 mg) in THF (3 mL) and MeOH (2 mL) was added TsOH·H₂O (3 mg). The mixture was stirred at 20 °C for 16 h until all the starting material had converted, based on monitoring by TLC. Then, H₂O (15 mL) was added, and the mixture was stirred vigorously for 1 h until all of the silyl methyl ether was converted, as determined by TLC. Then, H₂O (10 mL) was added, and the organic products were extracted with Et₂O (20 mL). The organic fraction was washed with NaHCO₃ (saturated aqueous, 20 mL) and brine (20 mL), dried over Na₂SO₄, and the solvents were evaporated. The crude material was purified by flash silica gel chromatography to afford the product as colorless solid (15 mg, 49% yield). NMR analysis indicates that 12% of the silanol groups underwent self-condensation to form siloxane linkages during the removal of the solvents from pure column fractions.

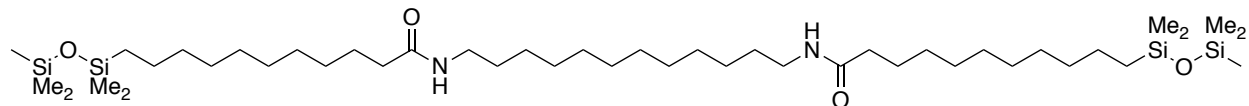
¹H NMR (600 MHz, CDCl₃) δ 7.28 (m, 4H), 7.09 (d, *J* = 8.3 Hz, 4H), 6.58 (br, 2H), 4.14 (t, *J* = 6.7 Hz, 4H), 3.88 (s, 2H), 1.69 – 1.60 (m, 4H), 1.39 – 1.23 (m, 32H), 0.59 (m, 4H); δ 0.49 (oligomer from self-condensation), 0.12 (s, 12H; δ 0.03 (oligomer from self-condensation)). ¹³C NMR (151 MHz, CDCl₃) δ 153.94 (bs), 136.38 (bs), 136.17 (bs), 129.55 (s), 118.95 (bs), 65.54 (s), 40.67 (s), 33.52 (s), 29.68 (s), 29.62 (s, two peaks overlapping), 29.45 (s), 29.37 (s), 29.07 (s), 25.98 (s), 23.28 (s), 17.96 (s), -0.10 (s). HRMS (APCI+) calcd for C₄₁H₇₁N₂O₆Si₂⁺ [*M*+H⁺]: 743.4845, found: 743.4845.

9 from PE-2-C12



To a solution of **PE-2-C12** (30 mg, 0.045 mmol) in THF (1.5 mL) and hexafluoroisopropanol (1.5 mL) were added hexamethyl disiloxane (0.3 mL, 1.4 mmol) and TsOH·H₂O (3.0 mg). The mixture was stirred at 25 °C for 7 h until all the starting material had converted, based on monitoring by TLC. The reaction mixture was poured into 20 mL of saturated aqueous NaHCO₃. The organic fraction was extracted with Et₂O (20 mL x 3 times), dried over Na₂SO₄, and the solvents were evaporated. The crude material was purified by flash silica gel chromatography to afford the product as colorless liquid (25.7 mg, 69% yield). ¹H NMR (500 MHz, CDCl₃) δ 4.05 (t, *J* = 6.7 Hz, 4H), 2.29 (t, *J* = 7.6 Hz, 4H), 1.61 (t, *J* = 7.1 Hz, 8H), 1.36 – 1.21 (m, 44H), 0.50 (t, *J* = 7.6 Hz, 4H), 0.06 (s, 18H), 0.03 (s, 12H). ¹³C NMR (101 MHz, CDCl₃) δ 174.02 (s), 64.40 (s), 34.44 (s), 33.44 (s), 29.55 (s, four peaks overlapping), 29.38 (s), 29.31 (s), 29.29 (s), 29.20 (s), 28.69 (s), 25.96 (s), 25.06 (s), 23.29 (s), 18.40 (s), 2.00 (s), 0.37 (s). HRMS (EI+) calcd for C₄₄H₉₄O₆Si₄⁺: 830.6128, found: 830.6128.

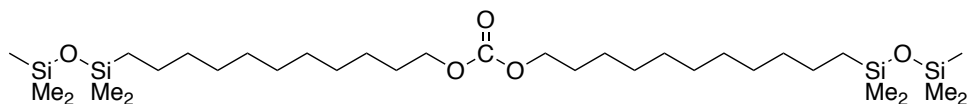
10 from PA-2-C12



To a solution of **PA-2-C12** (30 mg, 0.045 mmol) in hexafluoroisopropanol (1.5 mL) were added hexamethyl disiloxane (0.75 mL, 3.5 mmol) and TsOH·H₂O (3.0 mg). The mixture was stirred at 25 °C for 2 d until all the starting material had converted, based on monitoring by TLC. 2 mL of saturated aqueous NaHCO₃ was added to the mixture to quench the acid catalyst. The organic fraction was washed with brine (30 mL), extracted with ethyl acetate (50 mL x 3 times), dried over Na₂SO₄, and the solvents were evaporated. The crude material was purified by flash silica gel chromatography to afford the product as white sticky solid (22 mg, 58% yield).

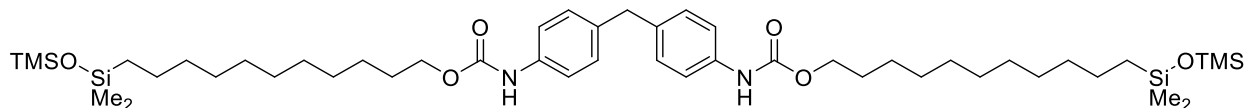
¹H NMR (500 MHz, CDCl₃) δ 5.39 (s, 2H), 3.23 (q, *J* = 6.9 Hz, 4H), 2.19 – 2.10 (m, 4H), 1.62 (m, 4H), 1.48 (m, 4H), 1.35 – 1.18 (m, 44H), 0.49 (t, *J* = 7.3 Hz, 4H), 0.06 (s, 18H), 0.03 (s, 12H). ¹³C NMR (151 MHz, CDCl₃) δ 173.17 (s), 39.63 (s), 37.10 (s), 33.56 (s), 29.83 (s), 29.69 (s, two peaks overlapping), 29.61 (s, two peaks overlapping), 29.53 (s), 29.51 (s), 29.49 (s), 29.39 (s), 27.04 (s), 26.01 (s), 23.41 (s), 18.52 (s), 2.12 (s), 0.50 (s). HRMS (APCI+) calcd for C₄₄H₉₇N₂O₄Si₄⁺ [*M*+H⁺]: 829.6525, found: 829.6522.

11 from PC-3



To a solution of **PC-3** (26 mg, 0.068 mmol) in THF (1.5 mL) and hexafluoroisopropanol (1.5 mL) were added hexamethyl disiloxane (0.3 mL, 1.4 mmol) and TsOH·H₂O (2.8 mg). The mixture was stirred at 25 °C for 7 h until all the starting material had converted based on monitoring by TLC. The reaction mixture was poured into 20 mL of saturated aqueous NaHCO₃. The organic fraction was extracted with Et₂O (20 mL x 3 times), dried over Na₂SO₄, and the solvents were evaporated. The crude material was purified by flash silica gel chromatography to afford the product as colorless liquid (23.6 mg, 69% yield). ¹H NMR (600 MHz, Chloroform-*d*) δ 4.12 (t, *J* = 6.8 Hz, 4H), 1.70 – 1.61 (m, 4H), 1.39 – 1.22 (m, 32H), 0.53 – 0.45 (m, 4H), 0.06 (s, 18H), 0.03 (s, 12H). ¹³C NMR (151 MHz, CDCl₃) δ 155.60 (s), 68.19 (s), 33.57 (s), 29.75 (s), 29.71 (s), 29.66 (s), 29.53 (s), 29.40 (s), 28.86 (s), 25.87 (s), 23.43 (s), 18.53 (s), 2.13 (s), 0.51 (s). HRMS (APCI+) calcd for C₄₄H₉₇N₂O₄Si₄⁺ [*M*+H⁺]: 663.4686, found: 663.4678.

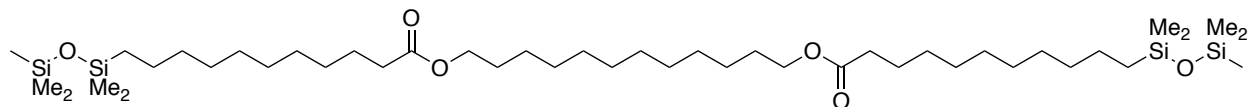
12 from PU-3



To a solution of **PU-3** (30 mg, 0.041 mmol) in THF (1.5 mL) and hexamethyl disiloxane (1.5 mL, 7.1 mmol) was added TsOH·H₂O (30 mg). The mixture was stirred at 23 °C for 72 h until all the starting material had converted, based on monitoring by TLC. Then, H₂O (10 mL) was added, and the organic products were extracted with Et₂O (10 mL). The organic fraction was washed with

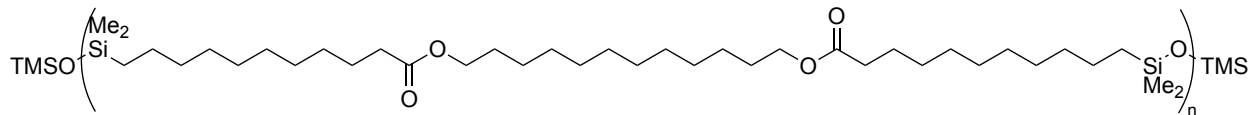
NaHCO₃ (saturated aqueous, 10 mL) and brine (10 mL), dried over Na₂SO₄, and the solvents were evaporated. The crude material was purified by flash silica gel chromatography (0:10 hexanes to 3:7 ethyl acetate:hexanes) to afford the product as a sticky colorless solid (17 mg, 56% yield). ¹H NMR (600 MHz, C₂D₂Cl₄) δ 7.32 (d, *J* = 8.4 Hz, 4H), 7.15 (d, *J* = 8.3 Hz, 4H), 6.49 (s, 2H), 4.20 (t, *J* = 6.7 Hz, 4H), 3.94 (s, 2H), 1.73 (s, 4H), 1.35 (s, 36H), 0.59 (t, *J* = 7.5 Hz, 4H), 0.13 (s, 18H), 0.11 (s, 12H). ¹³C NMR (151 MHz, CD₂Cl₂) δ 153.6 (s), 136.2 (s), 136.0 (s), 129.2 (s), 119.1 (s), 65.4 (s), 40.4 (s), 33.0 (s), 29.3 (s), 29.3 (s), 29.3 (s), 29.1 (s), 29.0 (s), 28.8 (s), 25.7 (s), 23.0 (s), 18.3 (s), 1.8 (s), 0.2 (s). HRMS (ESI+) calcd for C₄₇H₈₆N₂O₆Si₄Na⁺: 909.5456, found: 909.5435.

9 from PE-2-C12 in the presence of waste PET, PP, and PE



To a solution of **PE-2-C12** (314 mg, 0.47 mmol) in THF (5.0 mL) and hexafluoroisopropanol (5.0 mL) were added hexamethyl disiloxane (5.0 mL, 24 mmol), TsOH·H₂O (40 mg), PET (54 mg), PE (150 mg), and PP (260 mg). The mixture was stirred at 25 °C for 40 h until all the starting material had converted, based on monitoring by TLC. The reaction mixture was poured into 50 mL of saturated aqueous NaHCO₃. The organic fraction was extracted with Et₂O (50 mL x 3 times), dried over Na₂SO₄, and the solvents were evaporated. The crude material was purified by flash silica gel chromatography to afford the product as a light-yellow liquid (303 mg, 79% yield). ¹H NMR (500 MHz, CDCl₃) δ 4.05 (t, *J* = 6.7 Hz, 4H), 2.29 (t, *J* = 7.6 Hz, 4H), 1.61 (t, *J* = 7.1 Hz, 8H), 1.36 – 1.21 (m, 44H), 0.50 (t, *J* = 7.6 Hz, 4H), 0.06 (s, 18H), 0.03 (s, 12H).

2.12.4 Repolymerization of Ester-Containing Siloxane **9** PE-2-C12 from **9**



To a flame-dried 4 mL vial with a stir bar were added **9** (230 mg, 0.28 mmol). The contents of the vial were sparged with nitrogen for 5 min and TfOH (10 μ L, 0.12 mmol) was added under nitrogen. The vial was then heated at 120 $^{\circ}$ C under vacuum (400 mbar) for 24 h. Then triethylamine (100 μ L, 0.72 mmol) was added to the vial to quench any remaining acid. The residue was dissolved in 2 mL CHCl_3 , and the solution was added dropwise to MeOH (20 mL) under vigorous stirring to precipitate the polymer. The slurry was filtered and washed with copious amounts of MeOH and dried under vacuum to afford **PE-2-C12** as a white solid (150 mg). ^1H NMR (400 MHz, CDCl_3) δ 4.05 (t, J = 6.7 Hz, 4H), 2.28 (t, J = 7.6 Hz, 4H), 1.61 (p, J = 6.8 Hz, 8H), 1.37 – 1.24 (m, 44H), 0.49 (t, J = 7.4 Hz, 4H), 0.03 (s, 12H).

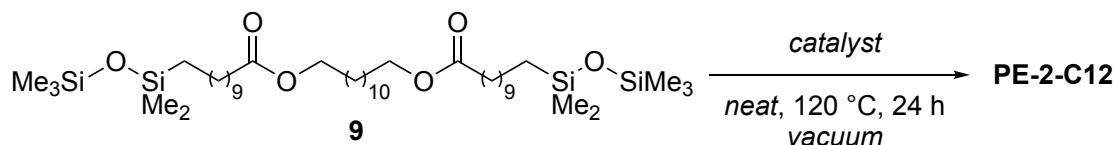


Table 2.12.4.1. Effect of catalyst on the repolymerization of **9** to PE-2-C12

Entry	Catalyst	Vacuum (mbar)	M_n (kDa)	\bar{D}
1	10 wt% <i>p</i> -TsOH	100	n.d. ^a	n.d. ^a
2	20 wt% Sn(Oct) ₂	160	n.d. ^a	n.d. ^a
3	10 wt% 18-DB-C-6•KF	170	n.d. ^a	n.d. ^a
4	5 wt% P ₄ - <i>t</i> -Bu	300	5.3	1.7
5	7 wt% TfOH	400	10.5	1.7
7	7 wt% PFBS	400	10.7	2.2

^aIndicates that no oligomerization was observed by SEC.

2.12.5 Synthesis of ^{13}C -labeled substrates

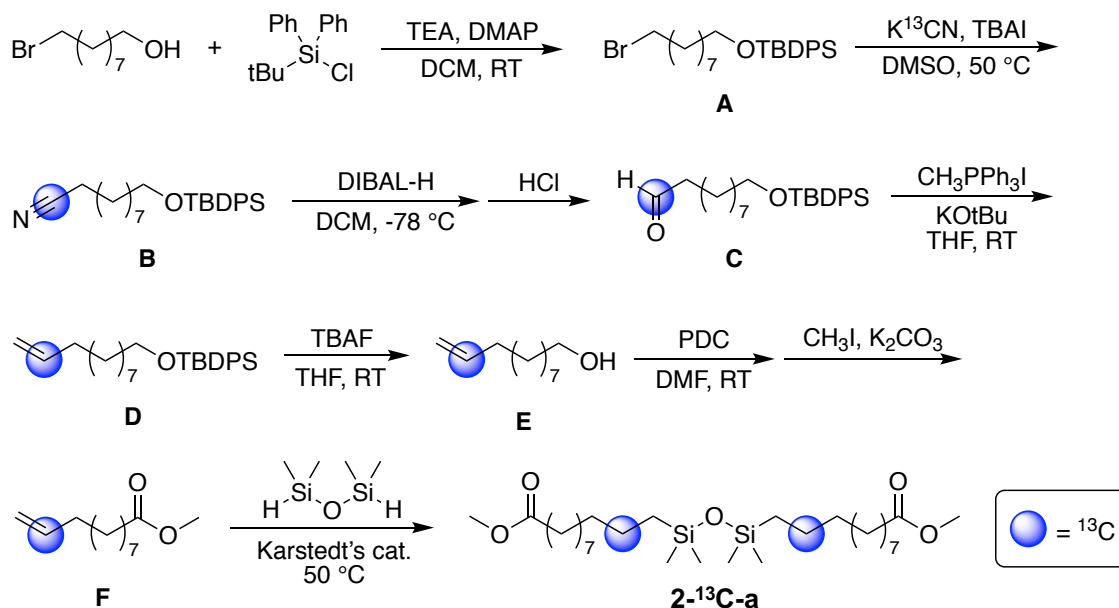


Figure 2.12.5.1. Overall scheme for the synthesis of 2- ^{13}C -a

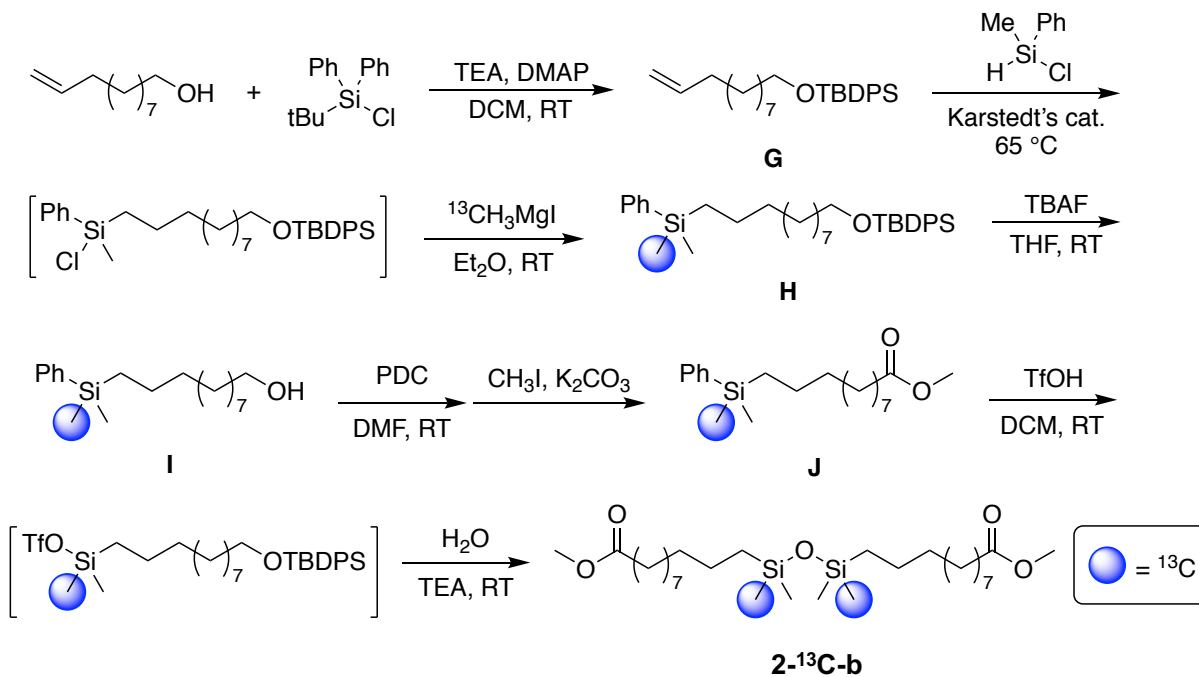
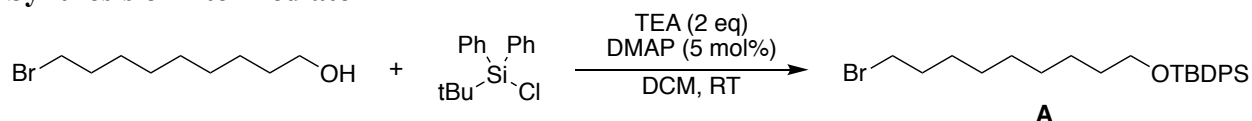


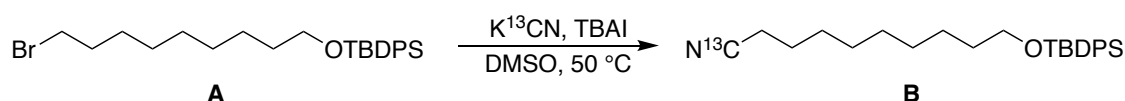
Figure 2.12.5.2. Overall scheme for the synthesis of 2- ^{13}C -b

Synthesis of intermediate A



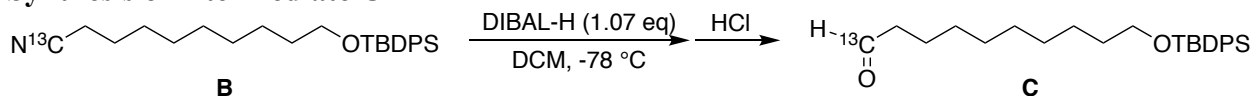
To a solution of 9-bromo-1-nonanol (1.42 g, 6.36 mmol) in dry DCM (20 mL) were added tert-butyl(chloro)diphenylsilane (2.0 mL, 7.6 mmol), 4-dimethylaminopyridine (DMAP) (36 mg, 0.32 mmol) and triethylamine (1.8 mL, 13 mmol). The mixture was stirred at 25 °C overnight. The reaction mixture was quenched with saturated aqueous NaHCO₃ and extracted with ethyl acetate. The combined organic layers were dried over Na₂SO₄ and filtered, and the filtrate was evaporated in vacuo. The residue was purified by column chromatography (hexane) on silica gel to afford **A** as a colorless oil (2.07 g, 70.4% yield). ¹H NMR (600 MHz, CDCl₃) δ 7.67 (d, *J* = 6.5 Hz, 4H), 7.43 – 7.36 (m, 6H), 3.65 (t, *J* = 6.5 Hz, 2H), 3.40 (t, *J* = 6.9 Hz, 2H), 1.84 (p, *J* = 7.0 Hz, 2H), 1.55 (m, 2H), 1.41 (m, 2H), 1.36 – 1.21 (m, 8H), 1.04 (s, 9H). ¹³C NMR (151 MHz, CDCl₃) δ 135.71 (s), 134.31 (s), 129.61 (s), 127.70 (s), 64.11 (s), 34.15 (s), 32.98 (s), 32.68 (s), 29.52 (s), 29.38 (s), 28.84 (s), 28.30 (s), 27.03 (s), 25.86 (s), 19.37 (s). HRMS (ESI⁺) calcd for C₂₅H₃₈BrOSi⁺ [M+H⁺]: 461.1870, found: 461.1876.

Synthesis of intermediate B



To a solution of **A** (1.40 g, 3.03 mmol) in DMSO (8 mL) were added potassium cyanide-¹³C (231 mg, 3.49 mmol) and tetrabutylammonium iodide (56 mg, 0.15 mmol). The mixture was heated at 50 °C for 2 days. The reaction mixture was poured into excess of deionized water, and the organic layer was extracted with diethyl ether. The combined organic layers were dried over Na₂SO₄ and filtered, and the filtrate was evaporated in vacuo. The residue was purified by column chromatography (5% ethyl acetate in hexane) on silica gel to afford **B** as a colorless oil (1.03 g, 83% yield). ¹H NMR (400 MHz, CDCl₃) δ 7.71 – 7.63 (m, 4H), 7.47 – 7.33 (m, 6H), 3.65 (t, *J* = 6.5 Hz, 2H), 2.33 (dt, *J* = 9.6, 7.1 Hz, 2H), 1.65 (m, 2H), 1.55 (m, 2H), 1.42 (m, 2H), 1.38 – 1.22 (m, 8H), 1.04 (s, 9H). ¹³C NMR (151 MHz, CDCl₃) δ 135.71 (s), 134.31 (s), 129.62 (s), 127.70 (s), 119.97 (s), 64.09 (s), 32.66 (s), 29.36 (d, *J* = 5.5 Hz), 28.84 (s), 28.79 (d, *J* = 3.3 Hz), 27.02 (s), 25.84 (s), 25.52 (d, *J* = 2.8 Hz), 19.38 (s), 17.43 (s), 17.06 (s). HRMS (ESI⁺) calcd for C₂₅¹³CH₃₈NOSi⁺ [M+H⁺]: 409.2751, found: 409.2753.

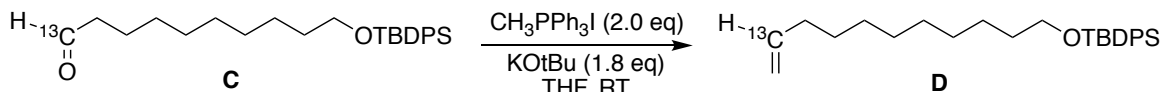
Synthesis of intermediate C



To a solution of **B** (500 mg, 1.22 mmol) in dry DCM (3 mL) was added a solution of diisobutylaluminum hydride (25 wt% in toluene, 0.73 g, 1.3 mmol) dropwise at -78 °C under N₂. The mixture was stirred at the same temperature for 2 h, and then HCl solution in dry diethyl ether was added. After the temperature was elevated to 0 °C, the reaction mixture was quenched by addition of saturated aqueous NaHCO₃, and the organic layer was extracted with ethyl acetate. The combined organic layers were dried over Na₂SO₄ and filtered, and the filtrate was evaporated in vacuo. The residue was purified by column chromatography (5% ethyl acetate in hexane) on silica gel to afford **C** as a colorless oil (394 mg, 78% yield). ¹H NMR (600 MHz, CDCl₃) δ 9.76 (dt, *J* = 169.8, 1.9 Hz, 1H), 7.68 (d, *J* = 8.0 Hz, 4H), 7.45 – 7.35 (m, 6H), 3.66 (t, *J* = 6.3 Hz, 2H), 2.42

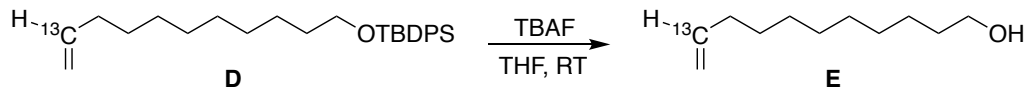
(qd, $J = 7.6, 1.9$ Hz, 2H), 1.66 – 1.52 (m, 4H), 1.40 – 1.21 (m, 10H), 1.06 (d, $J = 1.2$ Hz, 9H). ^{13}C NMR (151 MHz, CDCl_3) δ 203.03 (s), 135.71 (s), 134.32 (s), 129.61 (s), 127.70 (s), 64.11 (s), 44.04 (d, $J = 39.0$ Hz), 32.69 (s), 29.50 (s), 29.42 (s, two peaks overlapping), 29.28 (d, $J = 3.4$ Hz), 27.02 (s), 25.87 (s), 22.22 (s), 19.37 (s). HRMS (ESI+) calcd for $\text{C}_{25}^{13}\text{CH}_{39}\text{O}_2\text{Si}$ [$\text{M}+\text{H}^+$]: 412.2747, found: 412.2745.

Synthesis of intermediate D



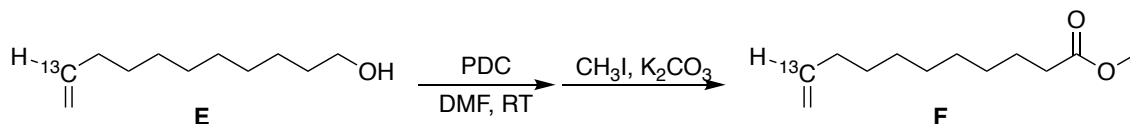
To a solution of **C** (343 mg, 0.832 mmol) in dry THF (8 mL) was added the suspension of methyltriphenylphosphonium iodide (676 mg, 1.66 mmol) and potassium tert-butoxide (168 mg, 1.50 mmol) in dry THF (4 mL) at 0 °C under N_2 . The reaction mixture was stirred for 6 h at room temperature and quenched by addition of excess of saturated aqueous NH_4Cl . The organic layer was extracted with ethyl acetate and dried over Na_2SO_4 and filtered. The filtrate was evaporated in vacuo, and the residue was purified by column chromatography (hexane) on silica gel to afford **D** as a colorless oil (236 mg, 69% yield). ^1H NMR (600 MHz, CDCl_3) δ 7.68 (d, $J = 7.1$ Hz, 4H), 7.45 – 7.36 (m, 6H), 5.82 (dddt, $J = 150.6, 17.0, 10.2, 6.7$ Hz, 1H), 5.00 (dq, $J = 17.1, 2.0$ Hz, 1H), 4.94 (ddd, $J = 10.2, 2.3, 1.2$ Hz, 1H), 3.66 (t, $J = 6.5$ Hz, 2H), 2.05 (p, $J = 6.7$ Hz, 2H), 1.60 – 1.53 (m, 2H), 1.42 – 1.23 (m, 12H), 1.06 (s, 9H). ^{13}C NMR (151 MHz, CDCl_3) δ 139.40 (s), 135.73 (s), 134.36 (s), 129.61 (s), 127.70 (s), 114.21 (d, $J = 68.9$ Hz), 64.17 (s), 33.97 (d, $J = 41.9$ Hz), 32.74 (s), 29.71 (s), 29.59 (s), 29.52 (s), 29.29 (d, $J = 3.4$ Hz), 29.11 (d, $J = 2.2$ Hz), 27.04 (s), 25.92 (s), 19.39 (s). HRMS (APCI+) calcd for $\text{C}_{26}^{13}\text{CH}_{41}\text{OSi}^+$: 410.2955, found: 410.2958.

Synthesis of intermediate E



To a solution of **D** (218 mg, 0.533 mmol) in dry THF (1 mL) was added the solution of tetrabutylammonium fluoride in THF (1.0 M, 0.6 mL), and the mixture was stirred at room temperature for 2 h. The crude material was purified by column chromatography (10% ethyl acetate in hexane) on silica gel to afford **E** as a colorless oil (56 mg, 61% yield). ^1H NMR (600 MHz, CDCl_3) δ 5.79 (dddt, $J = 150.6, 16.9, 10.2, 6.7$ Hz, 1H), 4.97 (dt, $J = 17.1, 2.0$ Hz, 1H), 4.91 (d, $J = 10.2$ Hz, 1H), 3.60 (t, $J = 6.7$ Hz, 2H), 2.02 (p, $J = 6.9$ Hz, 2H), 1.85 (s, 1H), 1.54 (p, $J = 6.8$ Hz, 2H), 1.44 – 1.20 (m, 12H). ^{13}C NMR (151 MHz, CDCl_3) δ 139.28 (s), 114.17 (d, $J = 69.3$ Hz), 63.05 (s), 33.89 (d, $J = 41.8$ Hz), 32.88 (s), 29.66 (s), 29.53 (s, two peaks overlapping), 29.22 (d, $J = 3.7$ Hz), 29.03 (d, $J = 2.2$ Hz), 25.85 (s). We were unable to obtain satisfactory HRMS data for this complex by EI, ESI or APCI, but suitable data were obtained from further products in the synthetic sequence.

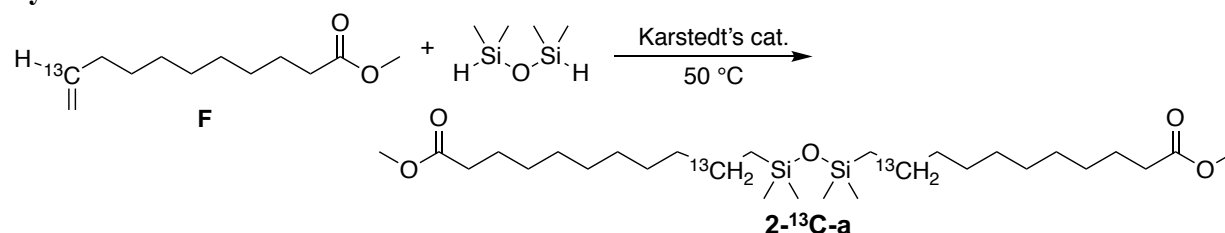
Synthesis of intermediate F



To a solution of **E** (71.8 mg, 0.419 mmol) in anhydrous DMF (1.5 mL) was added pyridinium dichromate (473 mg, 1.26 mmol). The mixture was stirred at room temperature for 2 days. The crude material was filtered on Celite, and the filtrate was poured into deionized water. The organic

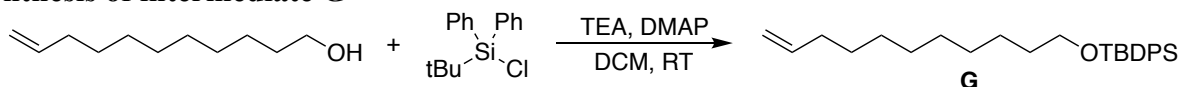
layer was extracted with ethyl acetate and hexane, and volatile solvents were evaporated in vacuo. To the concentrated crude mixture were added methyl iodide (78 μ L, 1.3 mmol) and potassium carbonate (290 mg, 2.10 mmol), and the reaction mixture was stirred overnight. The crude material was purified by column chromatography (hexane) on silica gel to afford **F** as a colorless oil (36.5 mg, 44% yield). ^1H NMR (600 MHz, CDCl_3) δ 5.79 (dddt, $J = 150.6, 16.9, 10.2, 6.6$ Hz, 1H), 4.97 (dt, $J = 17.1, 2.0$ Hz, 1H), 4.91 (d, $J = 10.4$ Hz, 1H), 3.65 (s, 3H), 2.29 (t, $J = 7.5$ Hz, 2H), 2.02 (p, $J = 6.8$ Hz, 2H), 1.60 (p, $J = 7.3$ Hz, 2H), 1.40 – 1.26 (m, 10H). ^{13}C NMR (151 MHz, CDCl_3) δ 174.21 (s), 139.08 (s), 114.04 (d, $J = 69.3$ Hz), 51.34 (s), 34.04 (s), 33.71 (d, $J = 41.9$ Hz), 29.21 (s), 29.13 (s), 29.07 (s), 28.98 (d, $J = 3.6$ Hz), 28.83 (d, $J = 2.1$ Hz), 24.89 (s). HRMS (APCI+) calcd for $\text{C}_{11}^{13}\text{CH}_2\text{O}_2^+$: 200.1726, found: 200.1728.

Synthesis of 2- ^{13}C -a



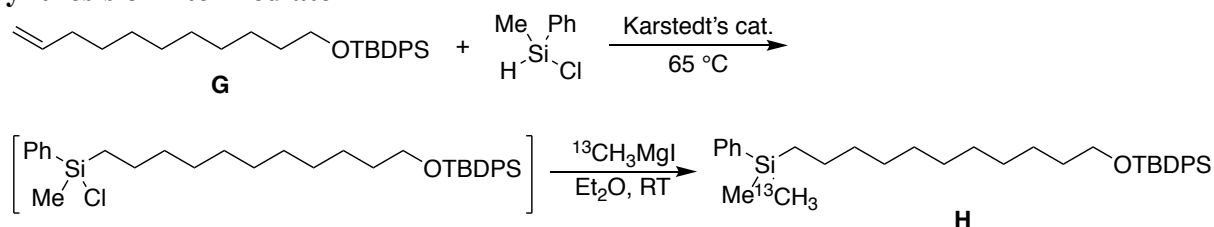
To a mixture of **F** (22.1 mg, 0.111 mmol) and 1,1,3,3-tetramethyldisiloxane (7.4 mg, 0.055 mmol) under N_2 was added Karstedt's catalyst (90 μ L of 0.02 wt% toluene solution). The mixture was heated under N_2 at 50 $^\circ\text{C}$ until most of **F** had been converted (monitored by NMR spectroscopy). The crude mixture was purified by column chromatography (2% ethyl acetate in hexanes) to afford **2- ^{13}C -a** as a colorless liquid (19.6 mg, 66% yield). ^1H NMR (600 MHz, CDCl_3) δ 3.66 (s, 6H), 2.30 (t, $J = 7.6$ Hz, 4H), 1.66 – 1.56 (m, 4H), 1.34 – 1.21 (m, 28H), 0.52 – 0.46 (m, 4H), 0.02 (s, 12H). ^{13}C NMR (151 MHz, CDCl_3) δ 174.45 (s), 51.55 (s), 34.28 (s), 33.58 (d, $J = 34.6$ Hz), 29.69 (d, $J = 4.1$ Hz), 29.65 (s), 29.52 (s), 29.42 (s), 29.33 (s), 25.13 (s), 23.44 (s), 18.57 (d, $J = 31.4$ Hz), 0.54 (s). HRMS (APCI+) calcd for $\text{C}_{26}^{13}\text{C}_2\text{H}_{58}\text{O}_5\text{Si}_2^+$ [$\text{M}+\text{H}^+$]: 533.3963, found: 533.3967.

Synthesis of intermediate **G**



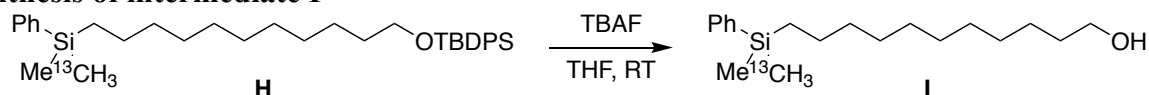
To a mixture of 10-undecen-1-ol (850 mg, 4.99 mmol), 4-dimethylaminopyridine (DMAP) (28 mg, 0.25 mmol) and triethylamine (1.0 mL, 7.2 mmol) in dry DCM (15 mL) was added tert-butyl(chloro)diphenylsilane (1.65 g, 5.99 mmol). The mixture was stirred at 25 $^\circ\text{C}$ overnight. The reaction mixture was quenched with saturated aqueous NaHCO_3 , and the organic layer was extracted with ethyl acetate. The combined organic layers were dried over Na_2SO_4 and filtered, and the filtrate was evaporated in vacuo. The residue was purified by column chromatography (2.5% ethyl acetate in hexane) on silica gel to afford **G** as a colorless oil (1.92 g, 94% yield). ^1H NMR (500 MHz, CDCl_3) δ 7.70 – 7.64 (m, 4H), 7.46 – 7.34 (m, 6H), 5.82 (ddt, $J = 16.9, 10.2, 6.7$ Hz, 1H), 5.04 – 4.90 (m, 2H), 3.65 (t, $J = 6.5$ Hz, 2H), 2.04 (q, $J = 7.1$ Hz, 2H), 1.55 (m, 2H), 1.42 – 1.21 (m, 12H), 1.04 (s, 9H). ^{13}C NMR (151 MHz, CDCl_3) δ 139.39 (s), 135.73 (s), 134.36 (s), 129.61 (s), 127.70 (s), 114.25 (s), 64.17 (s), 33.98 (s), 32.75 (s), 29.72 (s), 29.59 (s), 29.52 (s), 29.30 (s), 29.11 (s), 27.04 (s), 25.93 (s), 19.39 (s). HRMS (APCI+) calcd for $\text{C}_{27}\text{H}_{41}\text{OSi}^+$ [$\text{M}+\text{H}^+$]: 409.2921, found: 409.2920.

Synthesis of intermediate H



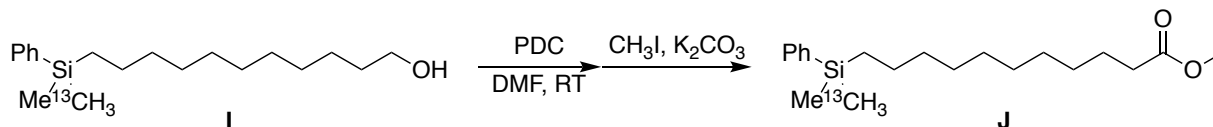
Methyl iodide- ^{13}C (923 mg, 6.46 mmol) and Mg (664 mg, 27.3 mmol) were mixed in dry diethyl ether (15 mL) under N_2 , and the mixture was cannula-filtered to afford 0.45 M of methylmagnesium iodide- ^{13}C solution (titrated with the mixture of phenanthroline and isopropyl alcohol in dry DCM). To a mixture of **G** (551 mg, 1.35 mmol) and methylphenylchlorosilane (276 mg, 1.76 mmol) in a 20-mL vial was added Karstedt's catalyst (108 μL of 0.02% toluene solution, 100 ppm relative to the alkene) under N_2 . The vial was capped with a Teflon-lined cap and stirred at $65\text{ }^\circ\text{C}$ for 3 h (monitored by NMR spectroscopy). To the reaction mixture was added the methylmagnesium iodide- ^{13}C solution (5.6 mL, 2.5 mmol) and stirred until all silyl chloride had been converted (as determined by ^1H NMR spectroscopy). The reaction mixture was quenched by addition of excess ethyl acetate, and the organic layer was washed with aqueous NH_4Cl . The organic layers were dried over Na_2SO_4 and filtered, and the filtrate was evaporated in vacuo. The residue was purified by column chromatography (hexane) on silica gel to afford **H** as a colorless oil (584 mg, 79% yield). ^1H NMR (500 MHz, CDCl_3) δ 7.69 (m, 4H), 7.52 (m, 2H), 7.47 – 7.35 (m, 9H), 3.67 (t, $J = 6.5$, 2H), 1.56 (m, 2H), 1.37 – 1.19 (m, 16H), 1.07 (s, 9H), 0.76 (t, $J = 7.0$ Hz, 2H), 0.27 (d, $J = 119.2$ Hz, 3H), 0.27 (s, 3H). ^{13}C NMR (126 MHz, CDCl_3) δ 139.91 (d, $J = 3.7$ Hz), 135.72 (s), 134.33 (s), 133.69 (s), 129.61 (s), 128.85 (s), 127.82 (s), 127.70 (s), 64.16 (s), 33.78 (s), 32.74 (s), 29.78 (s), 29.77 (s), 29.74 (s), 29.54 (s), 29.47 (s), 27.02 (s), 25.92 (s), 24.02 (s), 19.38 (s), 15.84 (d, $J = 3.6$ Hz), -2.85 (s). HRMS (CI^+) calcd for $\text{C}_{34}^{13}\text{CH}_{53}\text{OSi}_2^+$ [$\text{M}+\text{H}^+$]: 546.3669, found: 546.3665.

Synthesis of intermediate I



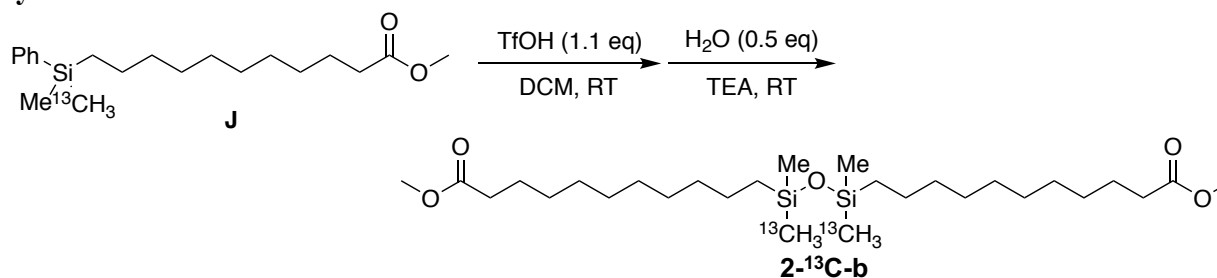
To a solution of **H** (54.7 mg, 1.00 mmol) in dry THF (3 mL) was added the solution of tetrabutylammonium fluoride in THF (1.0 M, 1.5 mL), and the mixture was stirred at room temperature for 2 h. The reaction mixture was diluted with diethyl ether and washed with saturated aqueous NaHCO_3 . The organic layers were dried over Na_2SO_4 and filtered, and the filtrate was evaporated in vacuo. The residue was purified by column chromatography (5% to 10% ethyl acetate in hexane) on silica gel to afford **I** as a colorless oil (295 mg, 96% yield). ^1H NMR (500 MHz, CDCl_3) δ 7.54 – 7.49 (m, 2H), 7.36 (m, 3H), 3.64 (t, $J = 6.6$ Hz, 2H), 1.64 – 1.52 (m, 2H), 1.39 – 1.20 (m, 16H), 0.74 (m, 2H), 0.25 (d, $J = 2.0$ Hz, 3H), 0.25 (d, $J = 119.2$ Hz, 3H). ^{13}C NMR (126 MHz, CDCl_3) δ 139.90 (d, $J = 3.4$ Hz), 133.68 (s), 128.84 (s), 127.81 (s), 63.22 (s), 33.74 (s), 32.94 (s), 29.73 (s, two peaks overlapping), 29.69 (s), 29.56 (s), 29.43 (s), 25.87 (s), 23.99 (s), 15.82 (d, $J = 3.4$ Hz), -2.87 (s). HRMS (EI^+) calcd for $\text{C}_{18}^{13}\text{CH}_{34}\text{OSi}^+$: 307.2412, found: 307.2416.

Synthesis of intermediate J



To a solution of **I** (263 mg, 0.855 mmol) in anhydrous DMF (8.5 mL) was added pyridinium dichromate (1.20g, 3.19 mmol), and the mixture was stirred at room temperature for 24 h. To the crude material was added excess silica gel, and the black slurry was filtered on Celite. The filtrate was evaporated in vacuo, and to the residue were added methyl iodide (160 μ L, 2.57 mmol) and potassium carbonate (592 mg, 4.29 mmol). The mixture was stirred at room temperature overnight, and the crude material was purified by column chromatography (0.5 to 2% ethyl acetate in hexane) on silica gel to afford **F** as a colorless oil (114.2 mg, 40% yield). ^1H NMR (500 MHz, CDCl_3) δ 7.54 – 7.47 (m, 2H), 7.38 – 7.31 (m, 3H), 3.66 (s, 3H), 2.30 (t, $J = 7.6$ Hz, 2H), 1.60 (m, 2H), 1.34 – 1.20 (m, 14H), 0.73 (t, $J = 7.1$ Hz, 2H), 0.25 (d, $J = 2.1$ Hz, 3H), 0.24 (d, $J = 119.2$ Hz, 3H). ^{13}C NMR (151 MHz, CDCl_3) δ 174.44 (s), 139.90 (d, $J = 3.6$ Hz), 133.69 (s), 128.84 (s), 127.81 (s), 51.55 (s), 34.27 (s), 33.71 (s), 29.63 (s), 29.60 (s), 29.40 (s), 29.38 (s), 29.30 (s), 25.11 (s), 24.00 (s), 15.84 (d, $J = 3.8$ Hz), -2.86 (s). HRMS (EI+) calcd for $\text{C}_{19}^{13}\text{CH}_{34}\text{O}_2\text{Si}^+$: 335.2362, found: 335.2363.

Synthesis of 2- ^{13}C -b



To a solution of **J** (92.7 mg, 0.276 mmol) in dry DCM (1 mL) was added trifluoromethanesulfonic acid (27 μ L, 0.30 mmol) under N_2 at room temperature over 30 min. To the reaction mixture were added 55 μ L of H_2O solution in triethylamine (2.5 M, prepared by addition of 45.2 mg of H_2O in 1-mL volumetric flask and filling the rest of the flask with triethylamine) and dry DCM (1 mL) at 0°C . The resulting mixture was stirred at room temperature for 3 h. The crude material was filtered on Celite and washed with diethyl ether. The filtrate was evaporated in vacuo, and the residue was purified by column chromatography (5% ethyl acetate in hexane) on silica gel to afford **2- ^{13}C -b** as a colorless oil (68.4 mg, 93% yield). ^1H NMR (500 MHz, CDCl_3) δ 3.66 (s, 6H), 2.30 (t, $J = 7.6$ Hz, 4H), 1.62 (m, 4H), 1.34 – 1.22 (m, 28H), 0.02 (d, $J = 1.6$ Hz, 6H), 0.02 (d, $J = 117.9$ Hz, 6H). ^{13}C NMR (126 MHz, CDCl_3) δ 174.46 (s), 51.57 (s), 34.25 (s), 33.58 (s), 29.67 (s), 29.64 (s), 29.51 (s), 29.41 (s), 29.31 (s), 25.11 (s), 23.42 (s), 18.55 (d, $J = 5.9$ Hz), 0.53 (s). HRMS (APCI+) calcd for $\text{C}_{26}^{13}\text{CH}_{59}\text{O}_5\text{Si}_2^+$ [$\text{M}+\text{H}^+$]: 533.3963, found: 533.3968.

2.12.6 Biodegradation Studies

2.12.6.1 Mineralization of position-specifically ^{13}C -labelled compound 2

Soil. Soil biodegradation studies were conducted in a standard test soil (soil “6S”) obtained from LUFA Speyer (Germany). The soil was sampled from the topsoil (0–20 cm) of an agricultural field and subsequently air-dried, sieved through 2 mm, and stored at 4 °C until use. Based on the soil particle size distribution, it is classified as a “clay” soil according to the USDA soil type classification. The soil contained 1.77 wt% organic carbon and 0.18 wt% total nitrogen and had a pH of 7.2 as measured in 0.01 M CaCl_2 . The soil was prepared for incubations by adjusting the water content to 45% of its maximum water holding capacity (max. = 40.8 g H_2O 100 g^{-1} soil). The incubations were set up by adding 100 g (dry weight equivalents) of wetted soil to twelve 250 mL glass bottles, followed by attaching these incubation bottles to a flow-through incubation system with automated $^{13}\text{CO}_2$ measurement in the bottle outflow air. The bottles were left with soil attached for two weeks prior to adding substrates to allow for the soil respiration to reach a steady state after adjusting to new moisture and temperature conditions.

Incubation system. Soil biodegradation studies were conducted with a flow-through soil incubation system described previously.¹⁵³ In brief, the incubation bottles were housed in a temperature-controlled dark incubation chamber set to 25.0 (\pm 0.2) °C, and well-mixed humidified ambient air was continuously pulled through the bottle headspaces via PVC tubing fitted through custom-made air tight lids. The outflow from each bottle ran through a 3-way solenoid valve, which directed the flow to flush into the open air using a diaphragm pump. At selected times, the flow from one bottle was directed instead to the measuring instrument, an isotope-sensitive cavity ring-down spectroscopy analyzer (CRDS; model G2201i; Picarro, USA), for the real-time quantification of the concentrations of $^{13}\text{CO}_2$ and $^{12}\text{CO}_2$. The flow rate of the diaphragm pumps in both the flushing and instrument flow directions was set to 24 mL min^{-1} . Periodically, instead of an incubation bottle, one of two calibration gases containing CO_2 in synthetic air at known CO_2 concentrations and isotopic compositions (420 ± 8 ppm CO_2 , $\delta^{13}\text{C} = -36.2 \pm 0.2$ ‰; 721 ± 14 ppm CO_2 , $\delta^{13}\text{C} = -2.8 \pm 0.2$ ‰) was measured with the CRDS to correct for very minor instrument drifts in CO_2 analysis. The incubation system was programmed to measure continuously, switching between samples every 15 min. The data from the last 5 minutes of each of these periods was used. This measurement data was time averaged to result in single values for each concentration per measurement period.

Substrate mineralization. After the soils equilibrated in the flow-through system, the ^{13}C -labelled substrates were added to the soils as follows. The two position-specifically, ^{13}C -labelled variants of the siloxane-containing diester **2** (i.e., **2- ^{13}C -a** carrying a ^{13}C -label on C-10 (C-1 = carboxylate) of the undecanoate chain and **2- ^{13}C -b** carrying a ^{13}C -label on the siloxane-methyl carbon) were dissolved separately in two dichloromethane solutions and these solutions were added to fine silica powder (0.5–10 μm diameter particles, Sigma-Aldrich). The dichloromethane was evaporated in a fume hood, and the powder was homogenized by hand. Aliquots of the powder with adsorbed compound were then added to the soils (50 mg silica 100 g^{-1} soil dry weight, equivalent to 2 mg diester 100 g^{-1} soil dry weight). This procedure was chosen to ensure that the test compound was added to soil in a dispersed manner. We did not attempt to dissolve the compounds in water and subsequently add it in dissolved states as we expect limited water solubility of the tested compounds. Glucose served as a reference compound for the mineralization measurements. To this end, ^{13}C -labelled glucose (Cambridge Isotope Laboratories, USA) was dissolved in Milli-Q H_2O (resistivity of ≥ 18.2 $\text{M}\Omega$ cm) to a concentration of 1 mg mL^{-1} . 1 mL of this solution was added to triplicate soil incubation bottles, resulting in the addition of 1 mg glucose

per 100 g soil (dry weight). $^{13}\text{CO}_2$ and $^{12}\text{CO}_2$ concentrations of the soil efflux gasses were measured over a total of 135 days after addition of glucose or 126 days after addition of **2- ^{13}C -a** and **2- ^{13}C -b**. The amounts of substrate- ^{13}C that mineralized over time were determined by first calculating the fractional contributions of substrate mineralization to the total measured CO_2 , $f_{\text{substrate}}$, according to:²

$$f_{\text{substrate}} = \frac{(\delta^{13}\text{C}_{\text{soil+substrate}} - \delta^{13}\text{C}_{\text{soil}})}{(\delta^{13}\text{C}_{\text{substrate}} - \delta^{13}\text{C}_{\text{soil}})} \quad (\text{Eq. 1})$$

in which $\delta^{13}\text{C}_{\text{soil+substrate}}$ and $\delta^{13}\text{C}_{\text{soil}}$ are the $\delta^{13}\text{C}$ values of the CO_2 from incubation bottles containing soil with added substrate or no substrate, respectively, and $\delta^{13}\text{C}_{\text{substrate}}$ is the theoretical value of the CO_2 resulting from complete mineralization of the ^{13}C -labelled substrate. These fractions were then used to calculate the amount of the measured CO_2 , $[\text{CO}_2]_{\text{soil+substrate}}$ (ppm CO_2), that was derived from mineralization of substrate- ^{13}C , $[\text{CO}_2]_{\text{substrate}}$ (ppm $^{13}\text{CO}_2$), according to:

$$[\text{CO}_2]_{\text{substrate}} = f_{\text{substrate}} \cdot [\text{CO}_2]_{\text{soil+substrate}} \cdot \%^{13}\text{C}_{\text{substrate}} \quad (\text{Eq. 2})$$

In which $\%^{13}\text{C}_{\text{substrate}}$ is the atom% ^{13}C of the added substrate. Finally, the rate of substrate- ^{13}C mineralization, $r(^{13}\text{C}_{\text{mineralized}})$ ($\mu\text{g } ^{13}\text{C hr}^{-1}$), was measured according to:

$$r(^{13}\text{C}_{\text{mineralized}}) = \quad (\text{Eq. 3})$$

In which Q is the flow rate of the gas through the CRDS ($= 1.44 \text{ L h}^{-1}$), M is the molar mass of ^{13}C ($= 13.003 \text{ g mol}^{-1}$), and V is the molar volume of air at $25 \text{ }^\circ\text{C}$ and 1 atm ($= 24.465 \text{ L mol}^{-1}$). The amount of substrate- ^{13}C mineralized was expressed as a percent of the total amount of added substrate- ^{13}C , $^{13}\text{C}_{\text{mineralized}}$ (%), by integrating the mineralization rates over the incubation time, t (hr), and normalizing by the amounts of added substrate- ^{13}C , $n(^{13}\text{C}_{\text{added}})$ ($\mu\text{g } ^{13}\text{C}$), according to:

$$^{13}\text{C}_{\text{mineralized}} = \frac{\int_0^t r(^{13}\text{C}_{\text{mineralized}}) dt}{n(^{13}\text{C}_{\text{added}})} \cdot 100 \quad (\text{Eq. 4})$$

The amounts of added substrate- ^{13}C , $n(^{13}\text{C}_{\text{added}})$, were calculated as the sum of the amounts of substrate-derived ^{13}C that was mineralized over the course of the incubation and that remained in the soil at the end of the incubation (see below).

Substrate-derived ^{13}C remaining in soil. The total $^{12}\text{CO}_2$ and $^{13}\text{CO}_2$ that resulted from combusting the soils after incubation were quantified in order to calculate to substrate-added ^{13}C remaining in the soil, $^{13}\text{C}_{\text{non-mineralized}}$. To do so, after collecting the final mineralization measurement time points, the soils were frozen at $-20 \text{ }^\circ\text{C}$ and subsequently freeze-dried. The freeze-dried soils were milled using a vibratory disk mill (model RS1, Retsch), and 10 mg aliquots of the milled soils were weighed into tin capsules. The crimped capsules were introduced into an elemental analyzer (EA; Thermo Fisher FlashEA 1112) coupled to a continuous flow interface (Thermo Fisher ConFlo IV) and isotope-ratio mass spectrometer (IRMS; Thermo Fisher Delta V Plus) (EA-IRMS). The EA-IRMS was operated with the same columns and conditions as previously described.¹⁵³ The carbon contents (%mass) and isotopic signatures ($\delta^{13}\text{C}$) of each soil sample were measured using a calibration curve determined by measuring different organic compounds with known carbon contents and isotopic signatures (nicotinamide (Thermo) with 59.0% C and $\delta^{13}\text{C} = -31.2\text{‰}$; peptone (Sigma) with 43.4% C and $\delta^{13}\text{C} = -15.6\text{‰}$; glucose (custom mixture) with 40.0% C and $\delta^{13}\text{C} = 61.5\text{‰}$).

The total substrate- ^{13}C mass balance (i.e., sum of $^{13}\text{C}_{\text{mineralized}}$, final extents shown in Figure 5 of main text, and $^{13}\text{C}_{\text{non-mineralized}}$) was smaller than the expected amount of ^{13}C added in form of **2- ^{13}C -a** and **2- ^{13}C -b** (i.e., ^{13}C mass balances of different added substrates: glucose, $101 (\pm 7)\%$; **2- ^{13}C -a**, $86 (\pm 6)\%$; **2- ^{13}C -b**, $75 (\pm 8)\%$; $n = 3$ corresponding to triplicate incubations for each substrate). The smaller measured than nominal ^{13}C amounts for the diesters likely resulted from less ^{13}C esters being transferred to the soil given the procedure for preparing and adding them (i.e.,

by coating onto fine silica particles, see above for more details). Therefore, the measured mineralization extents over time in Figure 2.10.1 in the text are normalized to the actual measured ^{13}C mass balances (sum of $^{13}\text{C}_{\text{mineralized}}$ and $^{13}\text{C}_{\text{non-mineralized}}$).

2.12.6.2 Enzymatic hydrolysis of siloxane-containing polymers

To determine the enzymatic hydrolyzability of the polymers **PE-2-C10**, **PE-2-C12**, and **PU-3**, we used a pH-stat titration setup that has been previously described.¹⁵¹ In brief, we incubated the polymers in thermo-jacketed beakers (temperature set to 30 °C) containing 10 mM KCl to which we later added cutinase isolated from the fungi *Fusarium solani* (FsC) in a final concentration of 82.7 μg FsC mL^{-1} . For the addition of the polymers to these beakers, we first dissolved each polymer in chloroform, and added the solutions dropwise onto glass microscopy slides (diameter 22 mm). We then allowed the chloroform to evaporate, leaving films of polymer coated onto the glass slides. We allowed the polymer-coated glass slides to equilibrate in the KCl solutions 24 hours before the addition of FsC. Using a Titrand 907 system (Metrohm, Switzerland), the pH in each beaker was constantly held at 7.0 by the addition of 5 mM KOH. We recorded the amount of base added into each beaker over time to titrate the free protons released into solution upon hydrolysis of ester and carbamate bonds of each polymer.

2.12.7 Catalytic hydrogenation of **1** and **2** with H₂

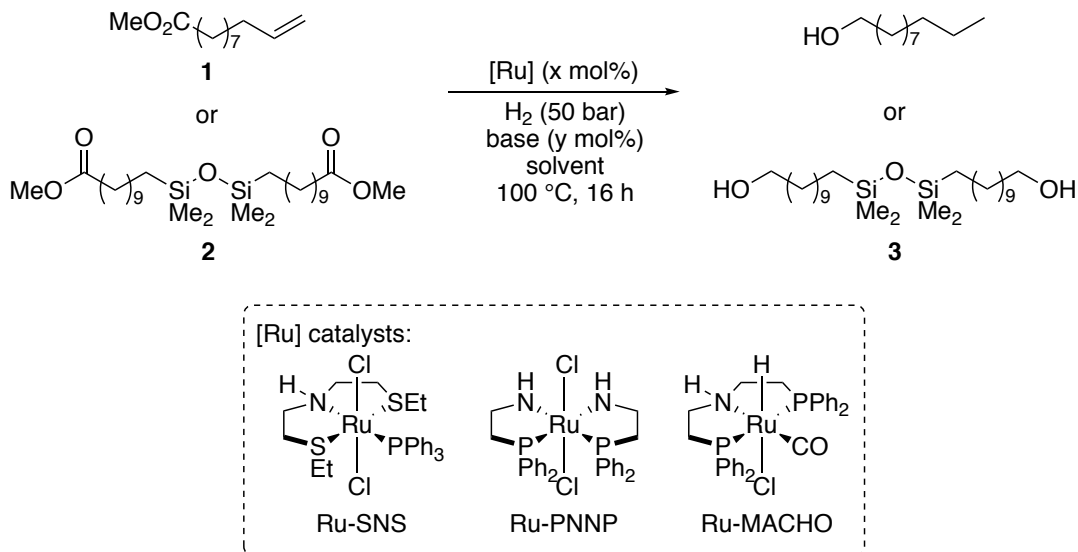


Table 2.12.7.1. Effect of catalyst on the hydrogenation of siloxane-containing diester **1**

entry	substrate	[Ru]	base	x	y	solvent	time (h)	conv (%)
1	1	Ru-SNS	KOMe	0.1	1	THF	2	0
2	1	Ru-PNNP	NaOMe	0.1	1	THF	3	0
3	1	Ru-MACHO	NaOMe	0.1	10	MeOH	16	60
4	1	Ru-MACHO	NaOMe	1	1	THF	16	60
5	2	Ru-MACHO	NaOMe	1	10	MeOH	16	<5
6	2	Ru-MACHO	KOtBu	1	4	THF	16	>95

2.12.8 Optimization of macrocyclization of 5

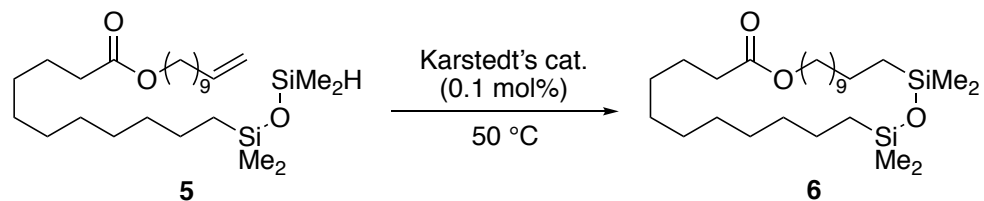


Table 2.12.8.1. Investigation of conditions for the synthesis of macrolactone **6**

solvent	conc (mM)	yield (%)
THF	10	25
THF	2.5	27
THF	1	28
THF	0.7	30
Toluene	1	34
Heptane	1	31
CH ₂ Cl ₂	1	30
Et ₂ O	1	29
1,4-Dioxane	1	30

2.12.8 NMR Spectra

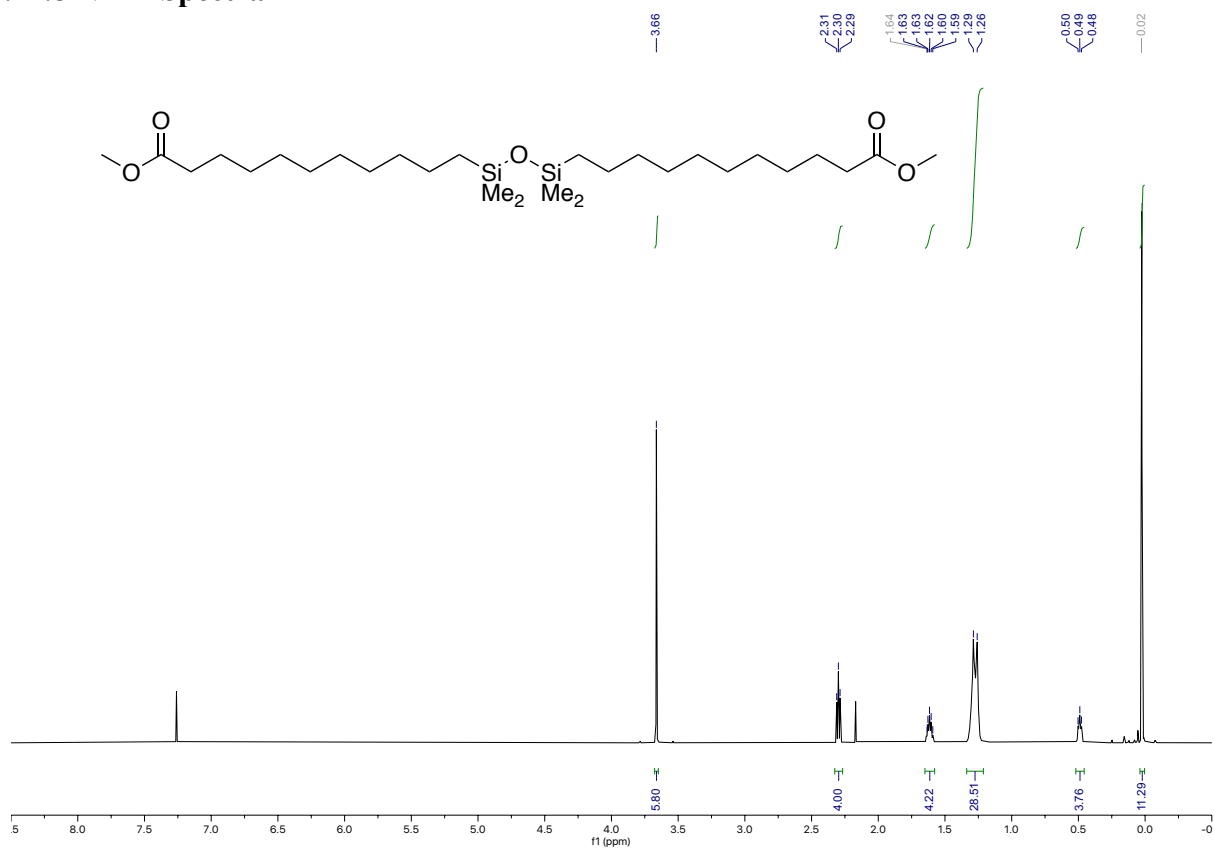


Figure 2.12.8.1. ¹H NMR spectra of compound 2

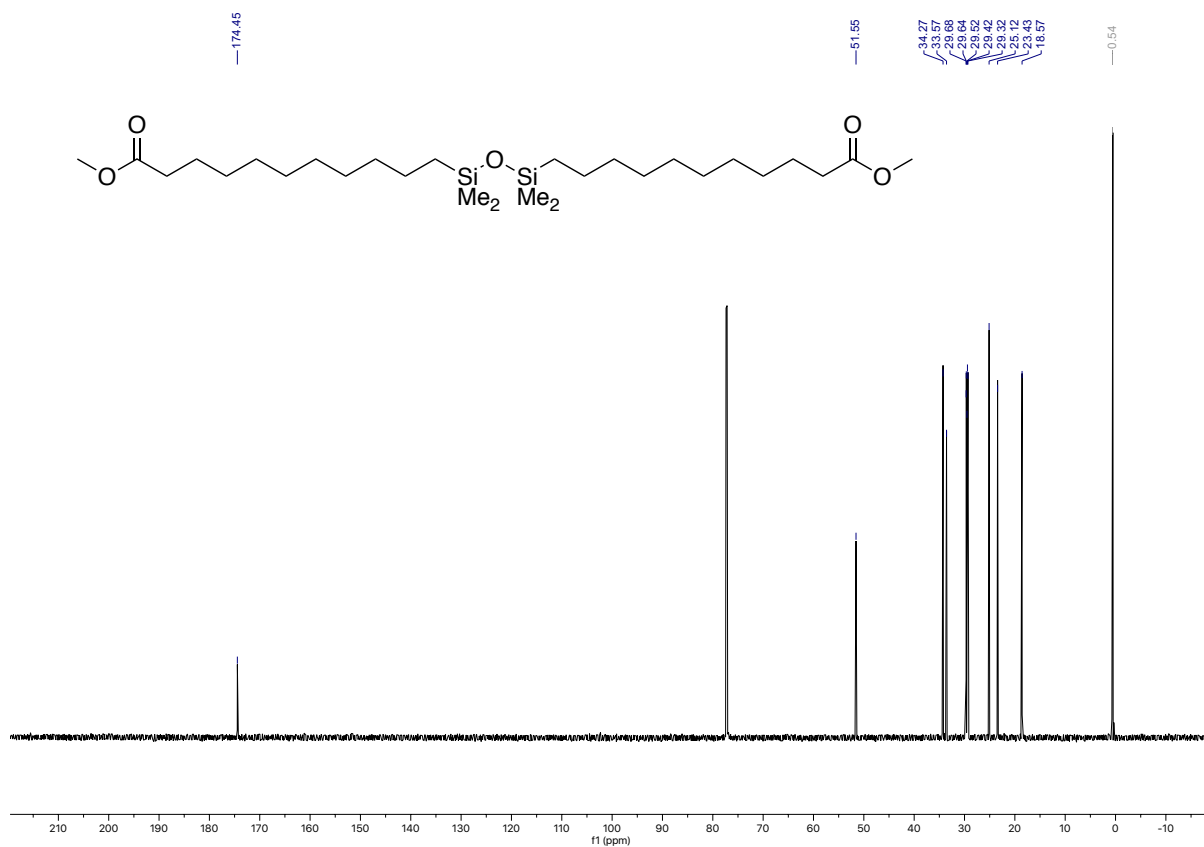


Figure 2.12.8.2. ¹³C NMR spectra of compound 2

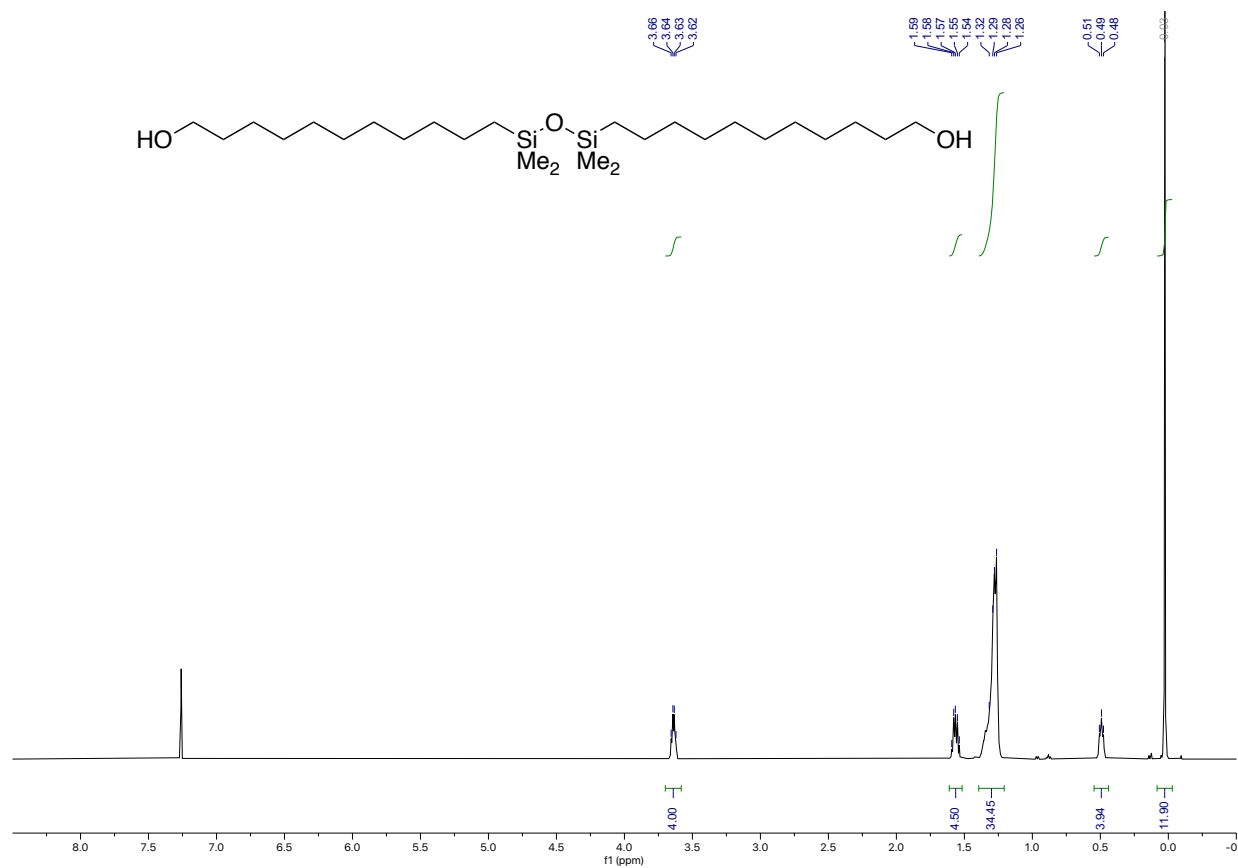


Figure 2.12.8.3. ¹H NMR spectra of compound **3**

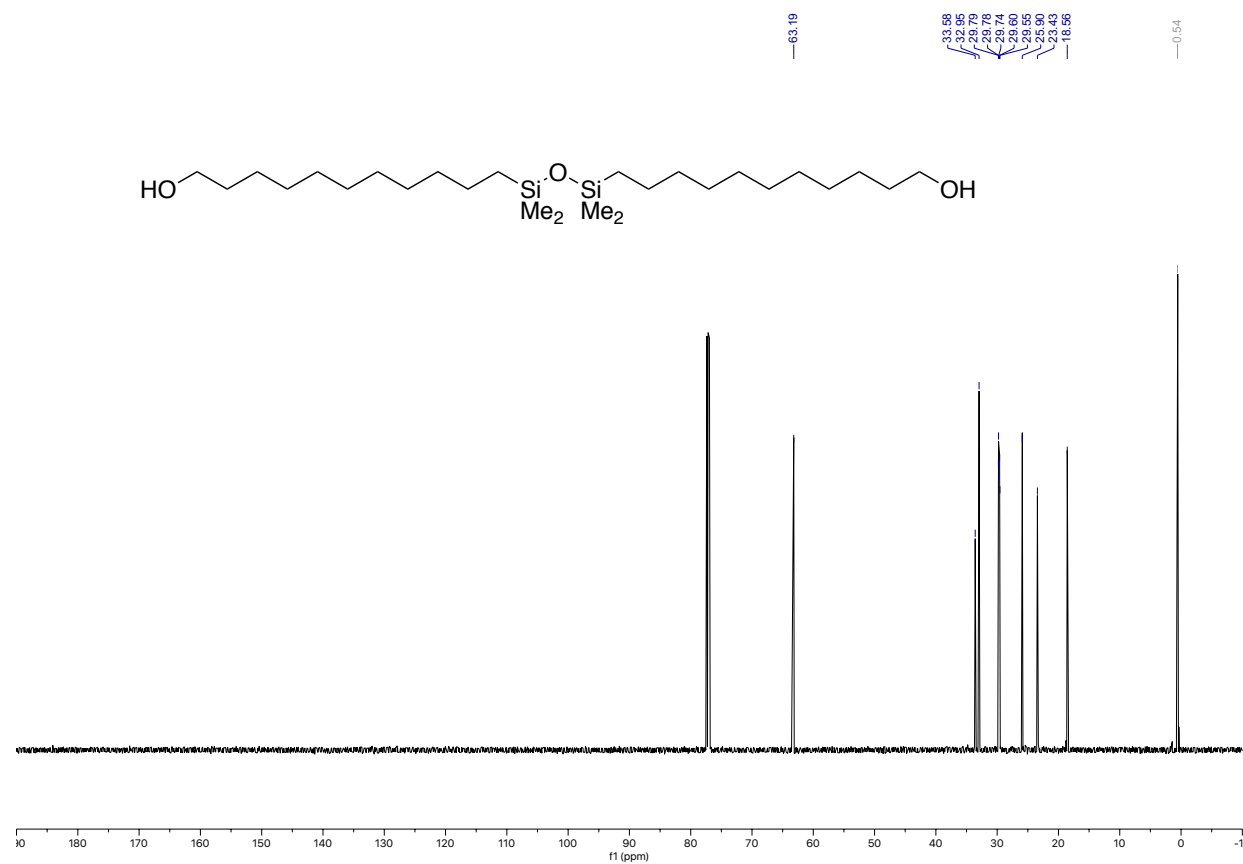


Figure 2.12.8.4. ¹³C NMR spectra of compound 3

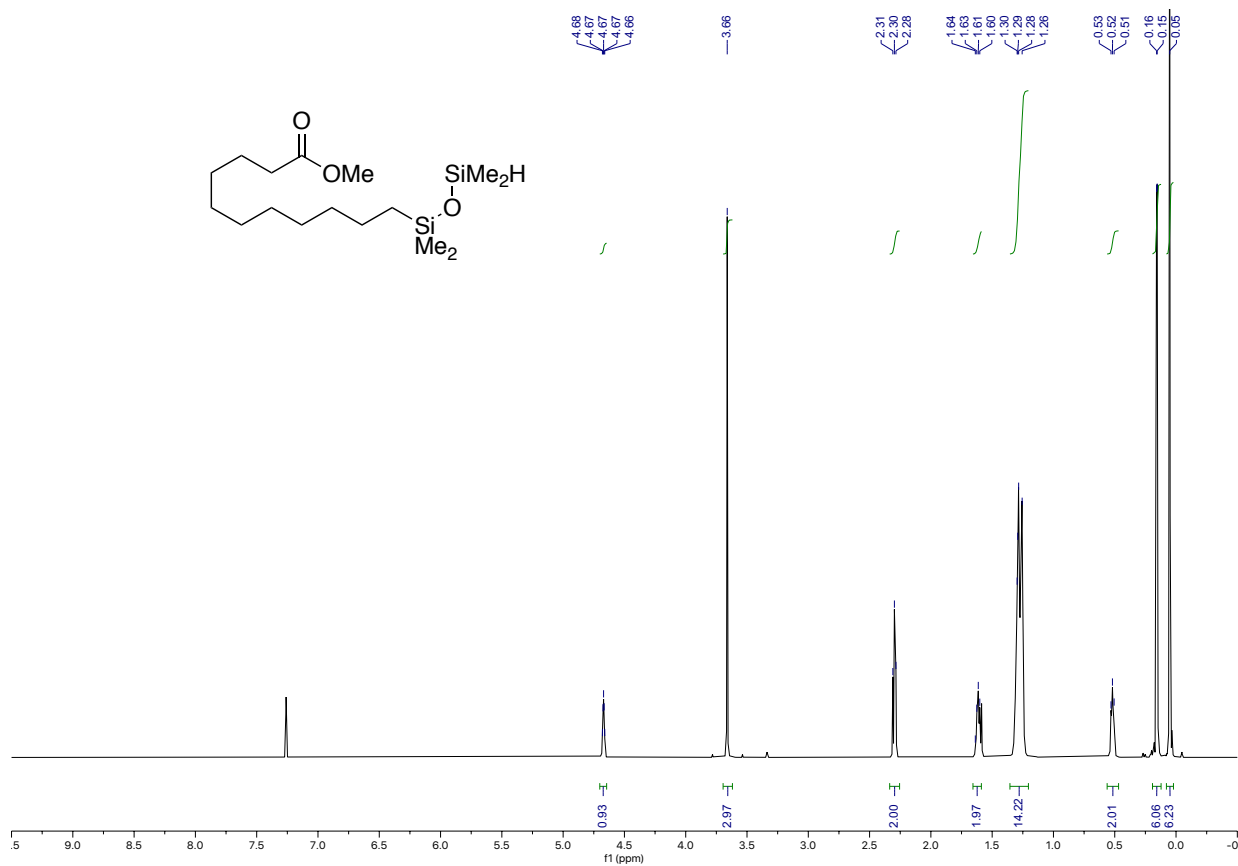


Figure 2.12.8.5. ¹H NMR spectra of compound 4

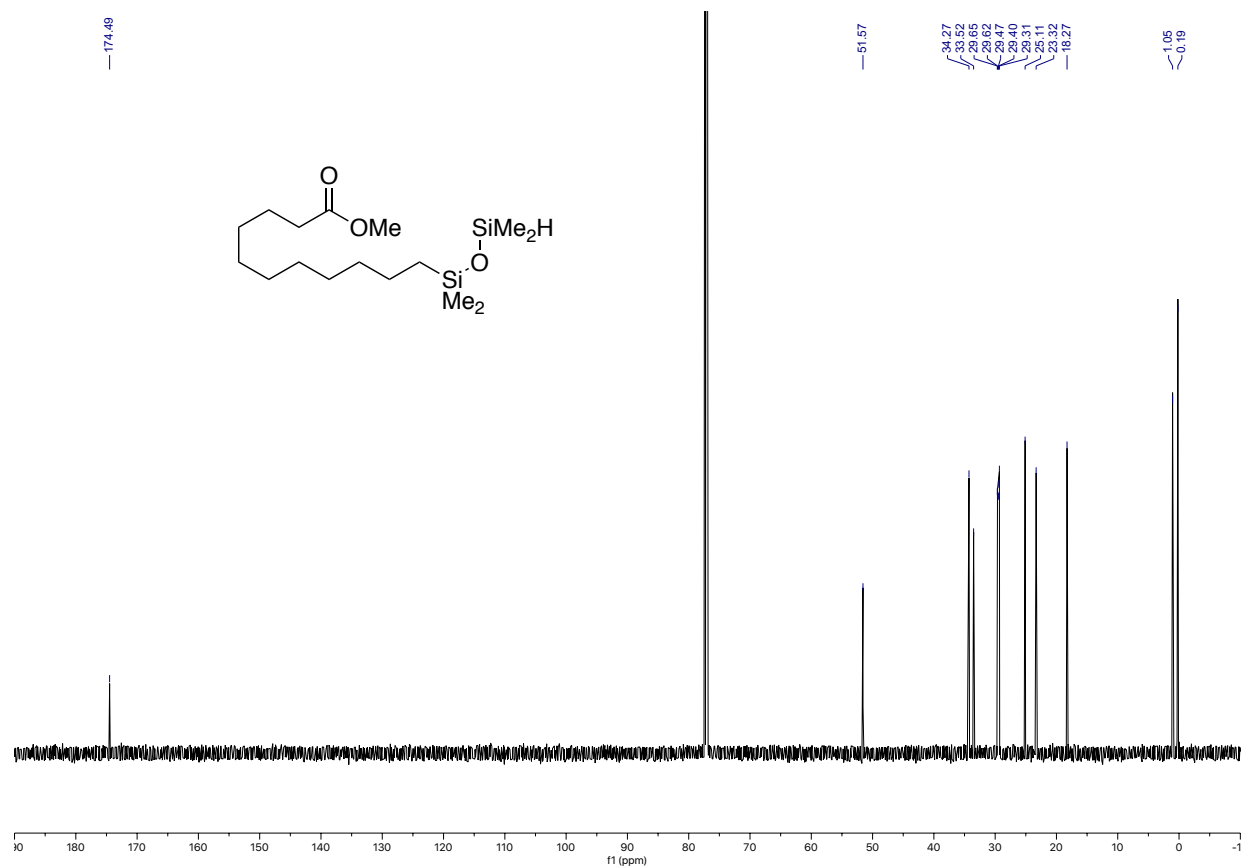


Figure 2.12.8.6. ^{13}C NMR spectra of compound 4

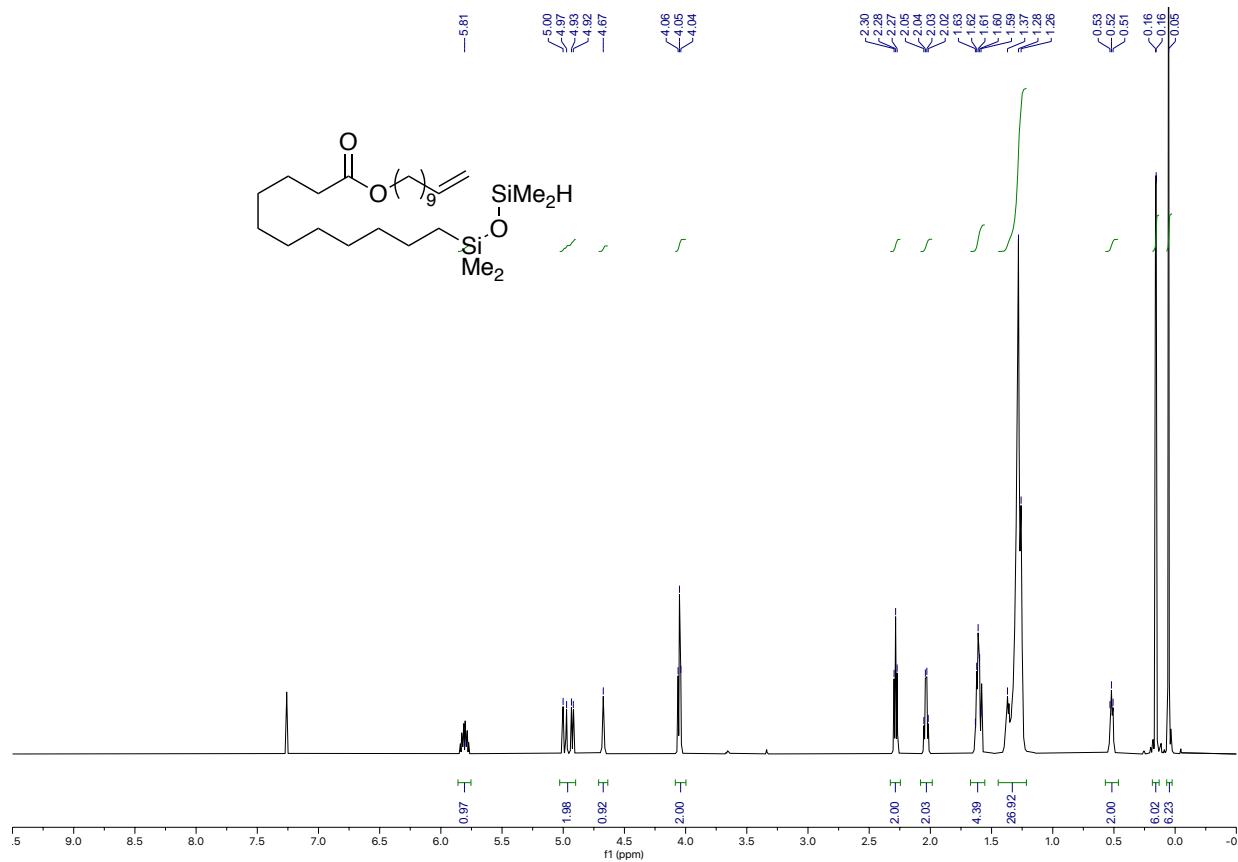


Figure 2.12.8.7. ¹H NMR spectra of compound 5

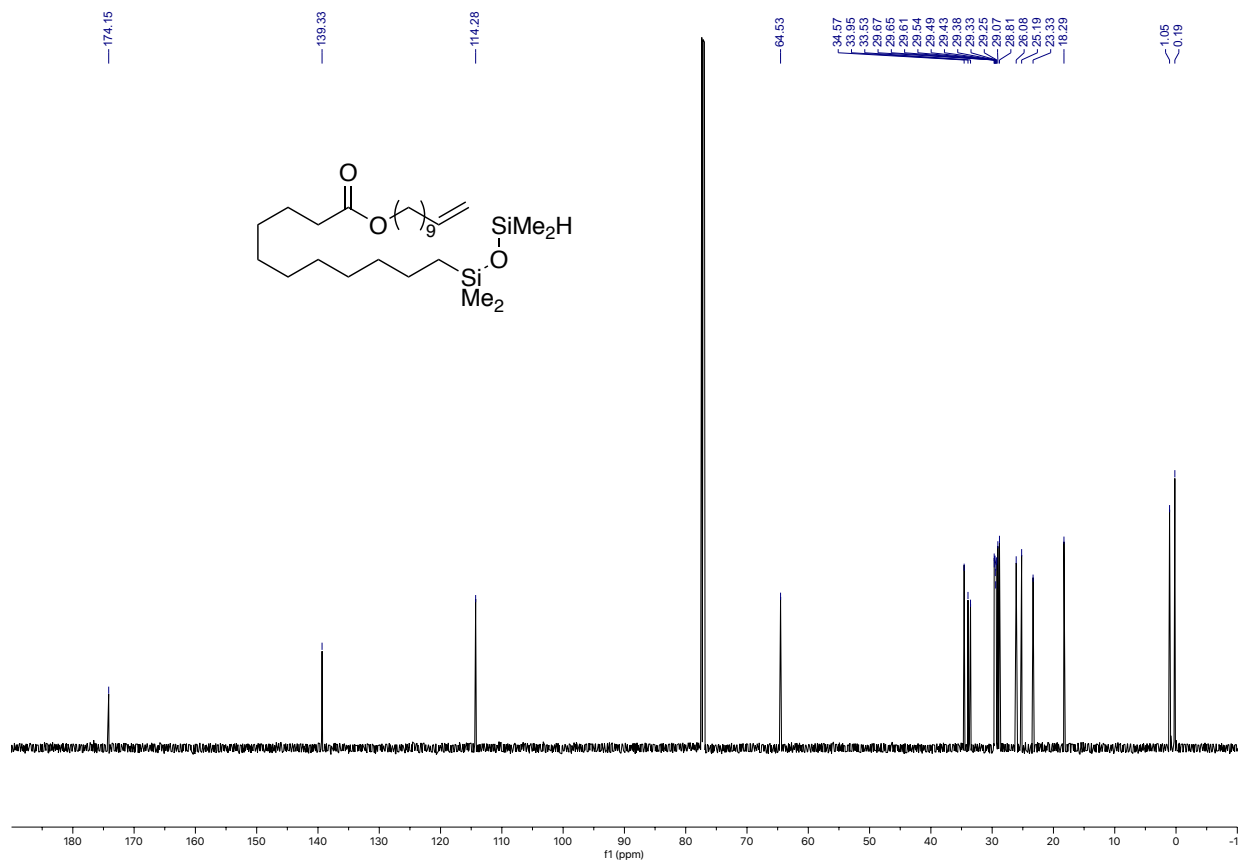


Figure 2.12.8.8. ^{13}C NMR spectra of compound 5

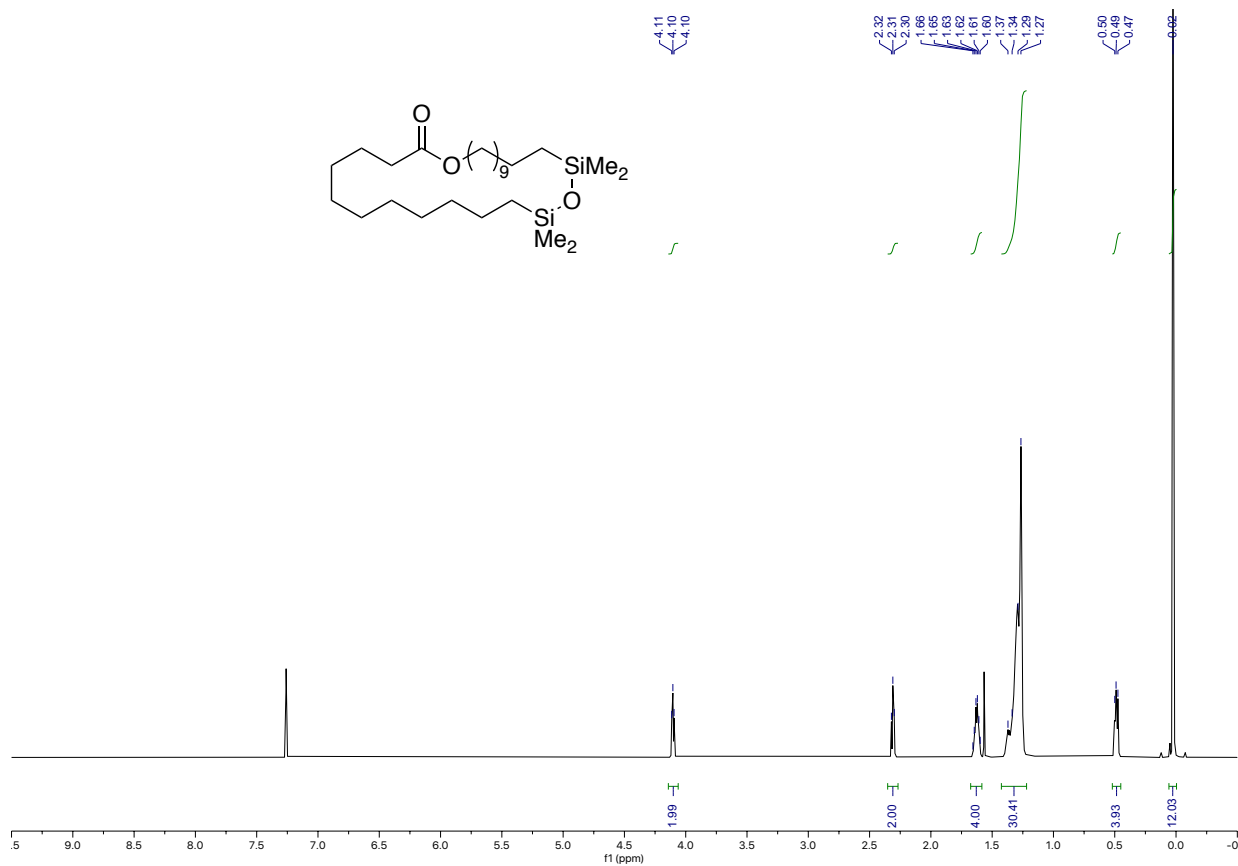


Figure 2.12.8.9. ¹H NMR spectra of compound 6

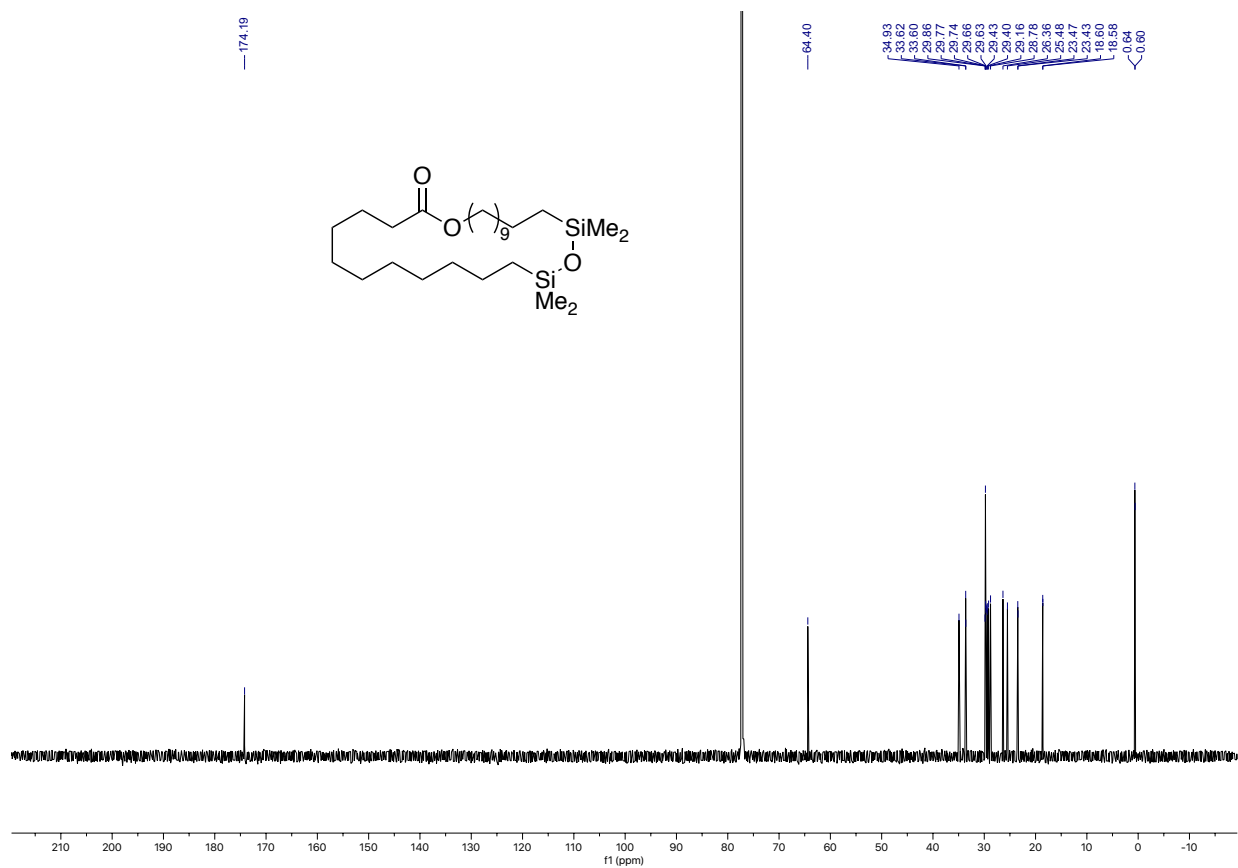


Figure 2.12.8.10. ^{13}C NMR spectra of compound 6

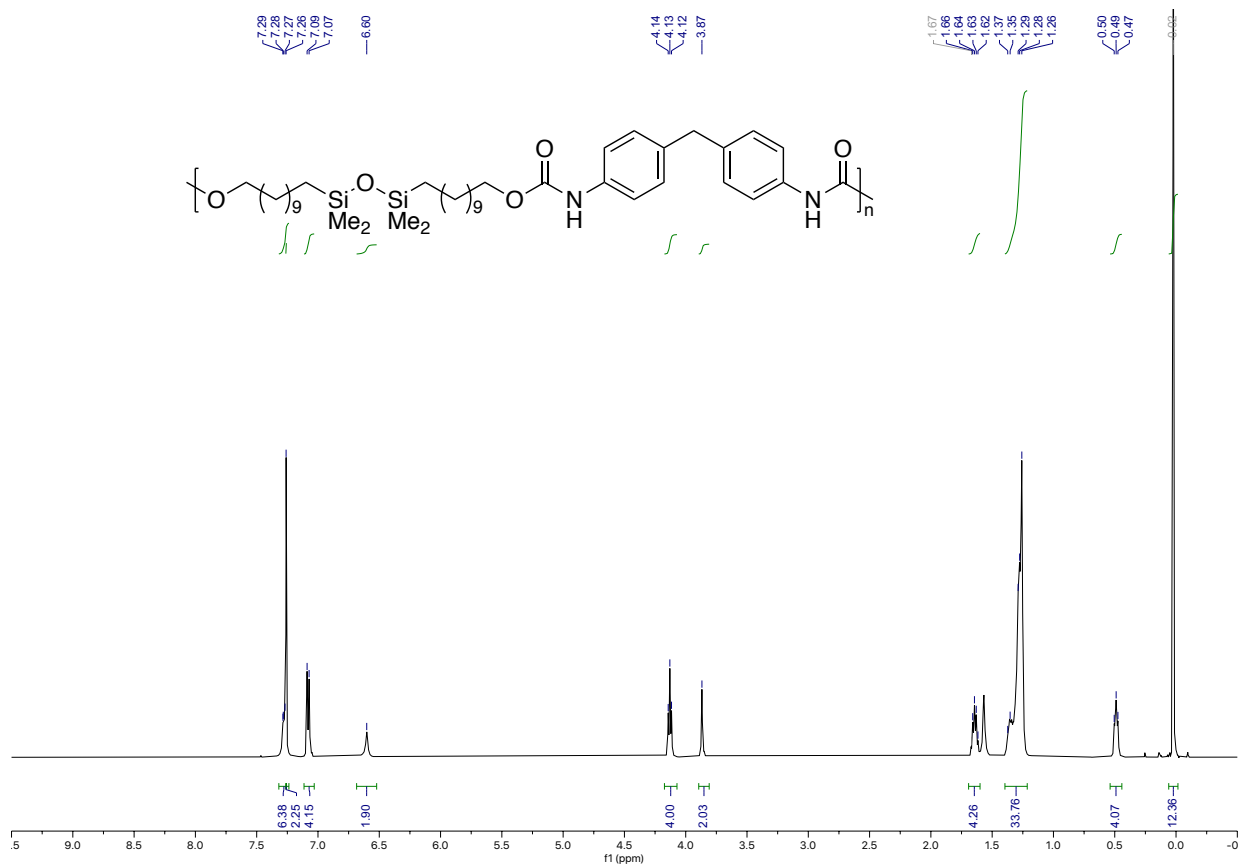


Figure 2.12.8.11. ¹H NMR spectra of polymer **PU-3**

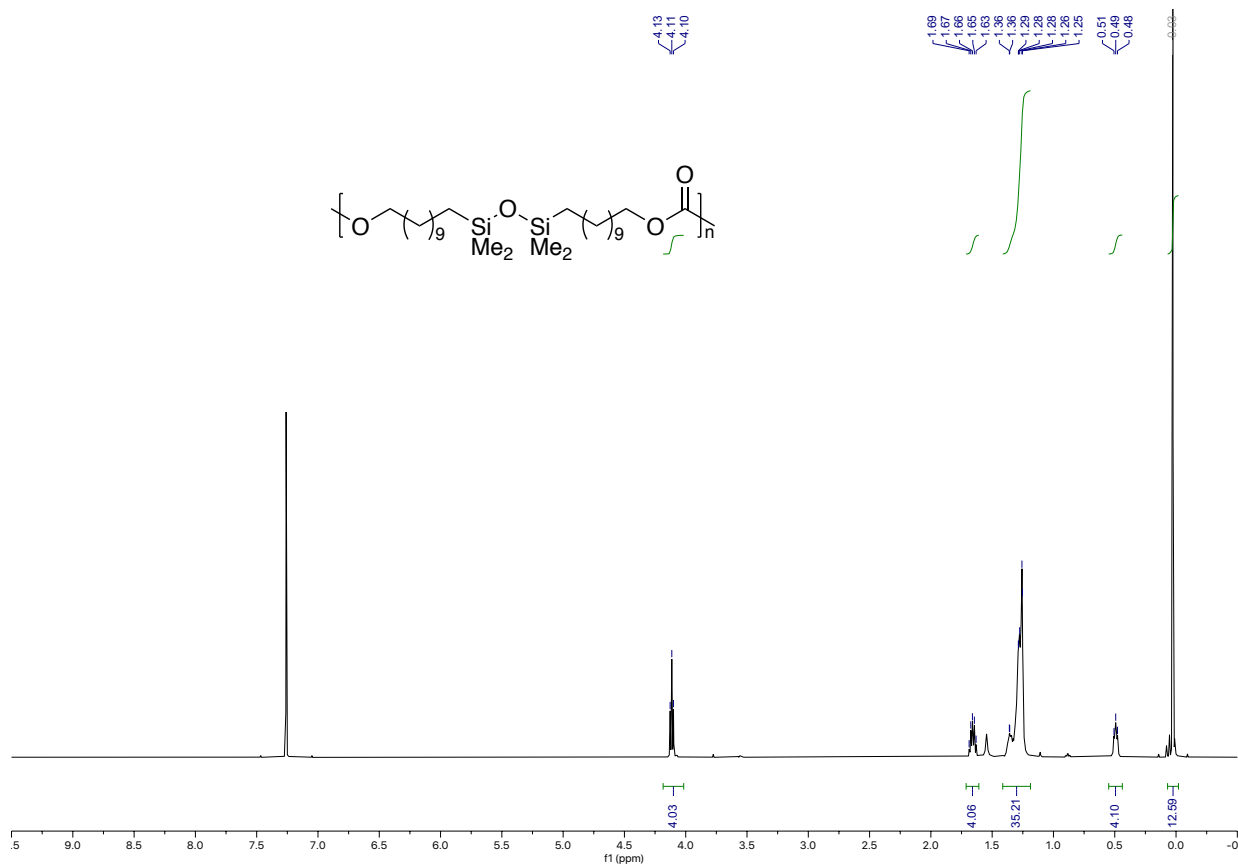


Figure 2.12.8.12. ^1H NMR spectra of polymer PC-3

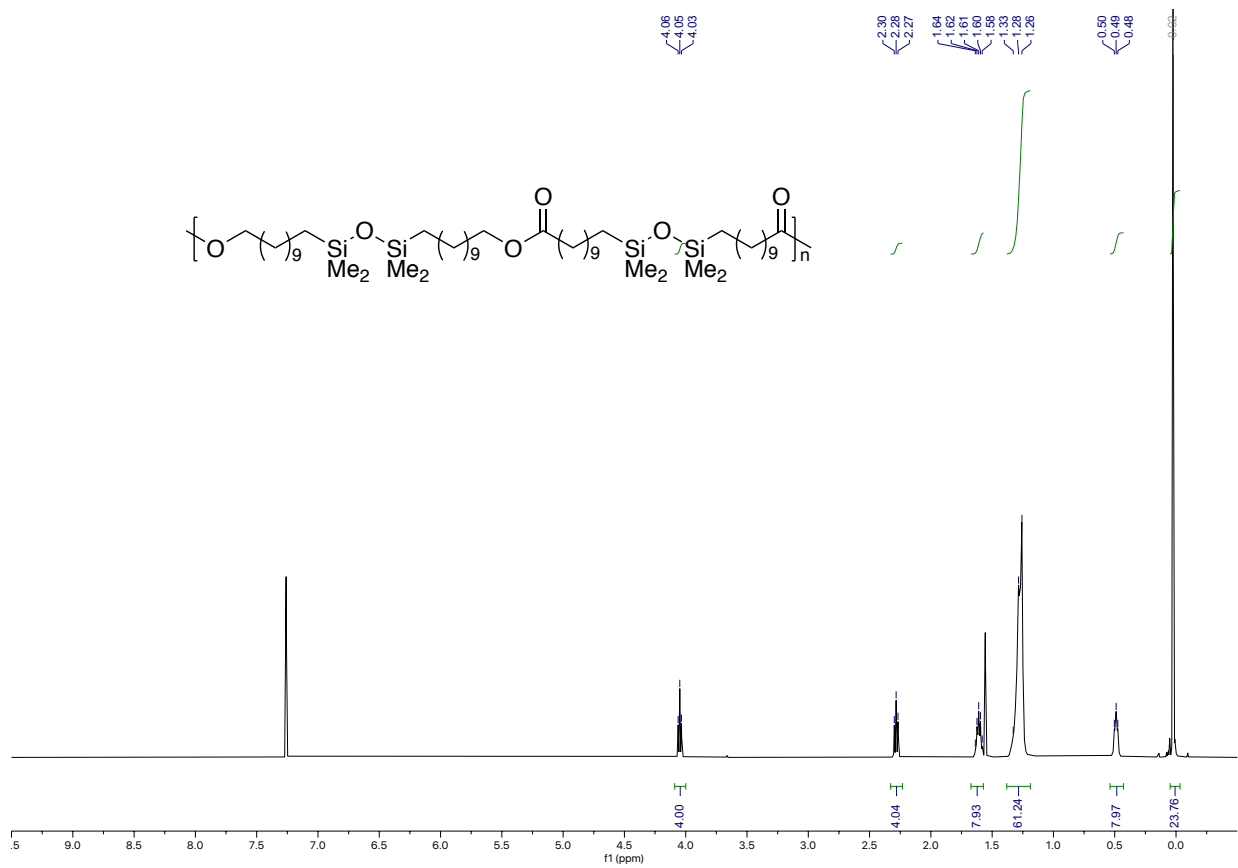


Figure 2.12.8.13. ¹H NMR spectra of polymer **PE-2-3**

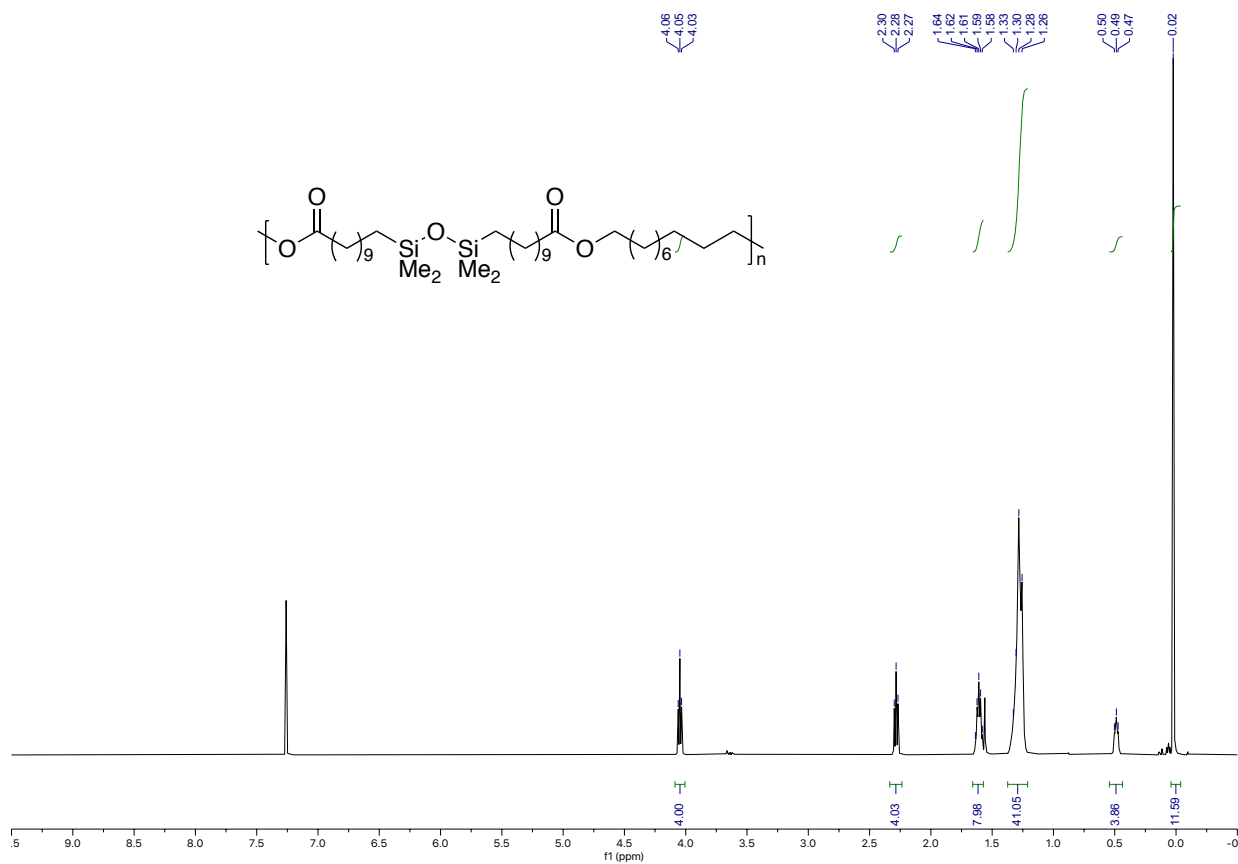


Figure 2.12.8.14. ¹H NMR spectra of polymer PE-2-C10

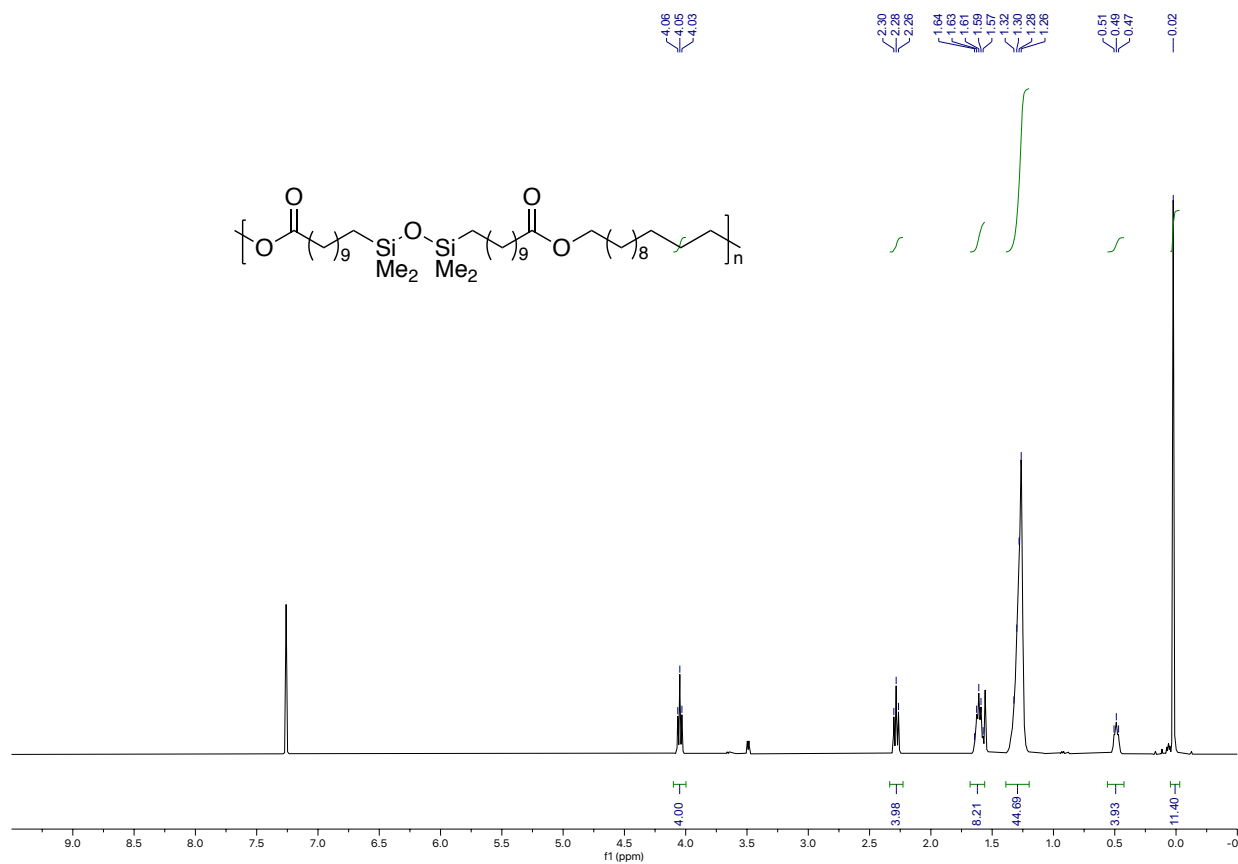


Figure 2.12.8.15. ¹H NMR spectra of polymer PE-2-C12

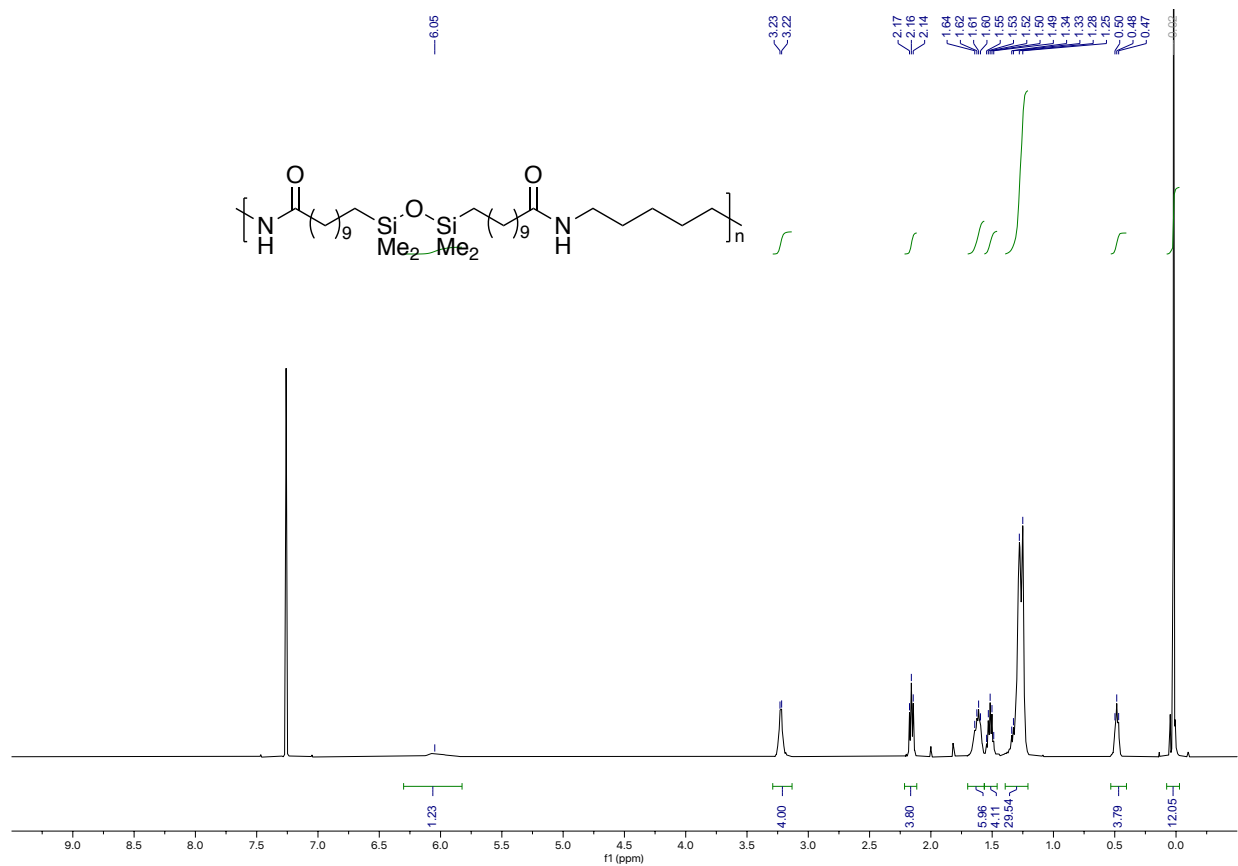


Figure 2.12.8.16. ^1H NMR spectra of polymer PA-2-C5

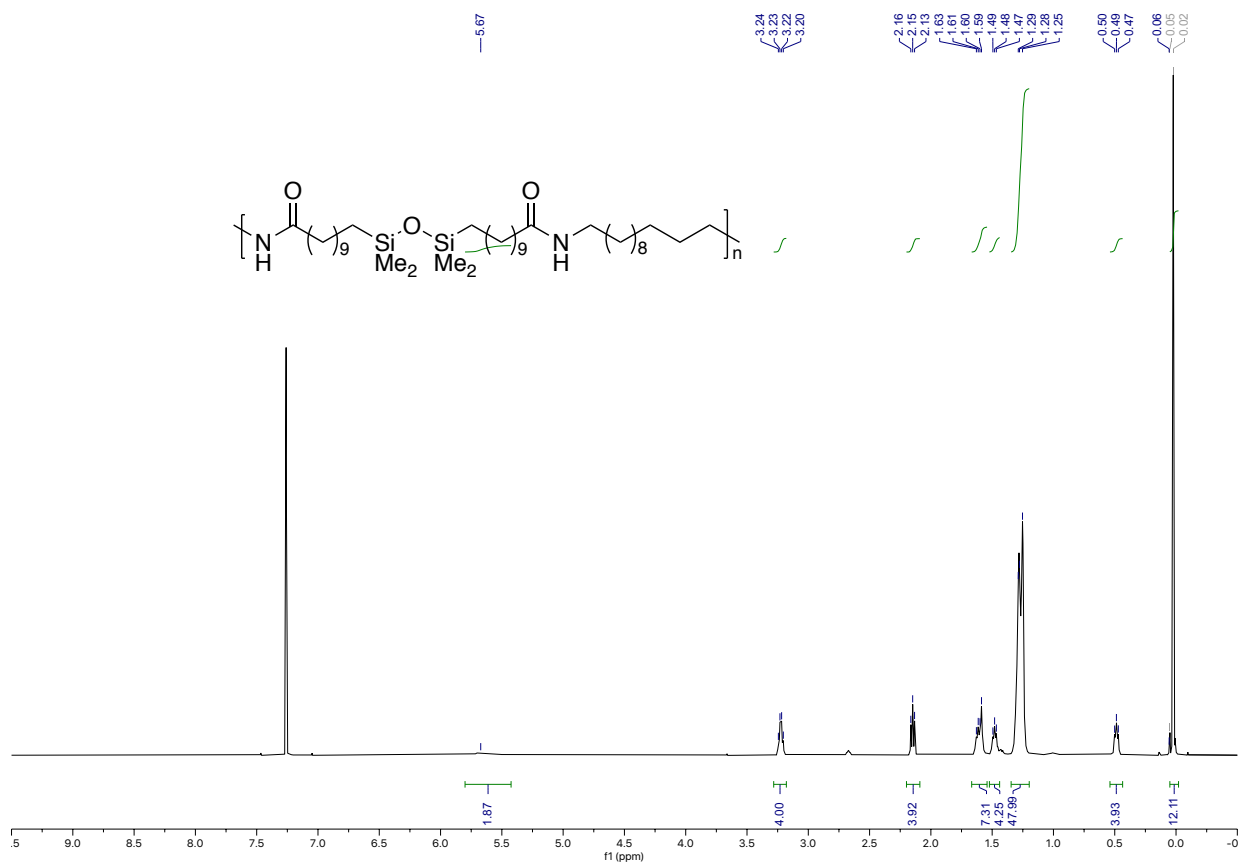


Figure 2.12.8.17. ¹H NMR spectra of polymer PA-2-C12



Figure 2.12.8.18. ¹H NMR spectra of polymer PE-6

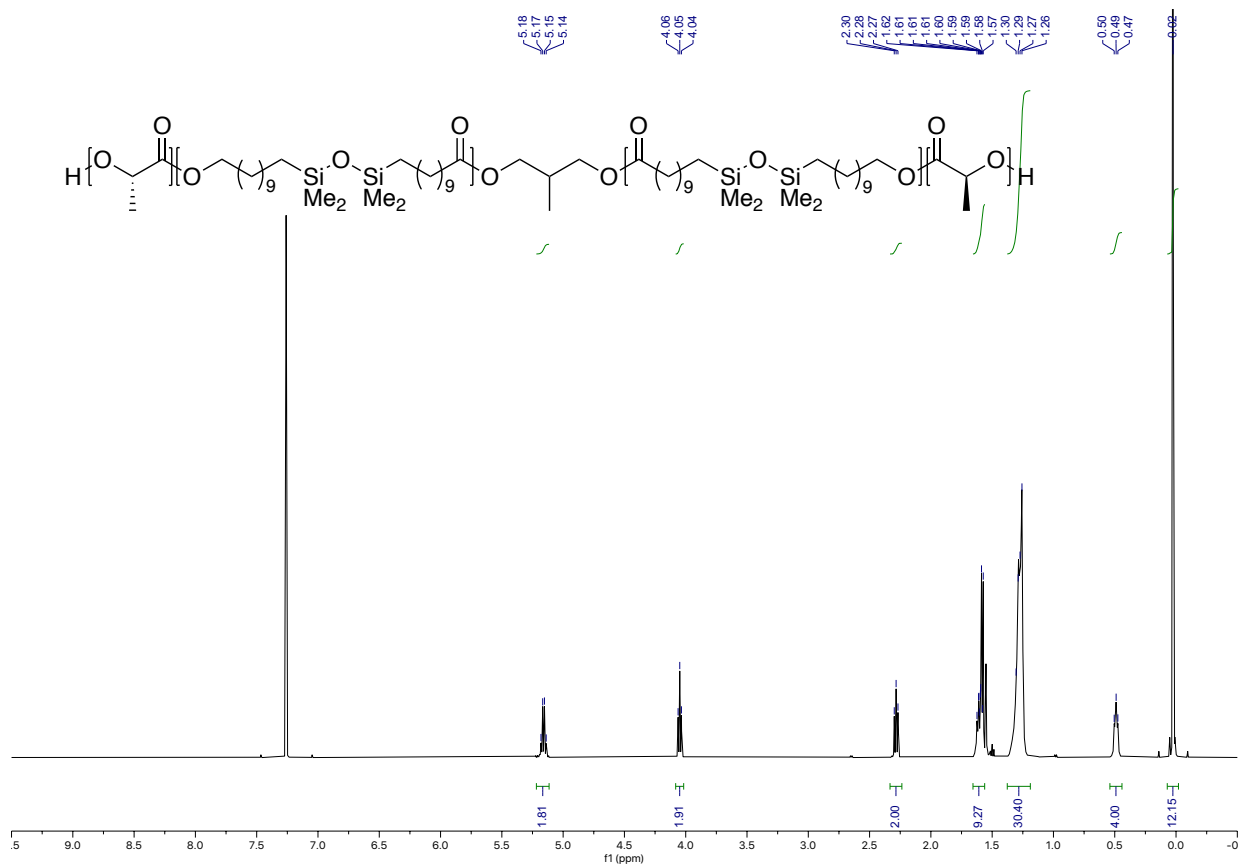


Figure 2.12.8.19. ¹H NMR spectra of polymer PLLA-PE-6-PLLA

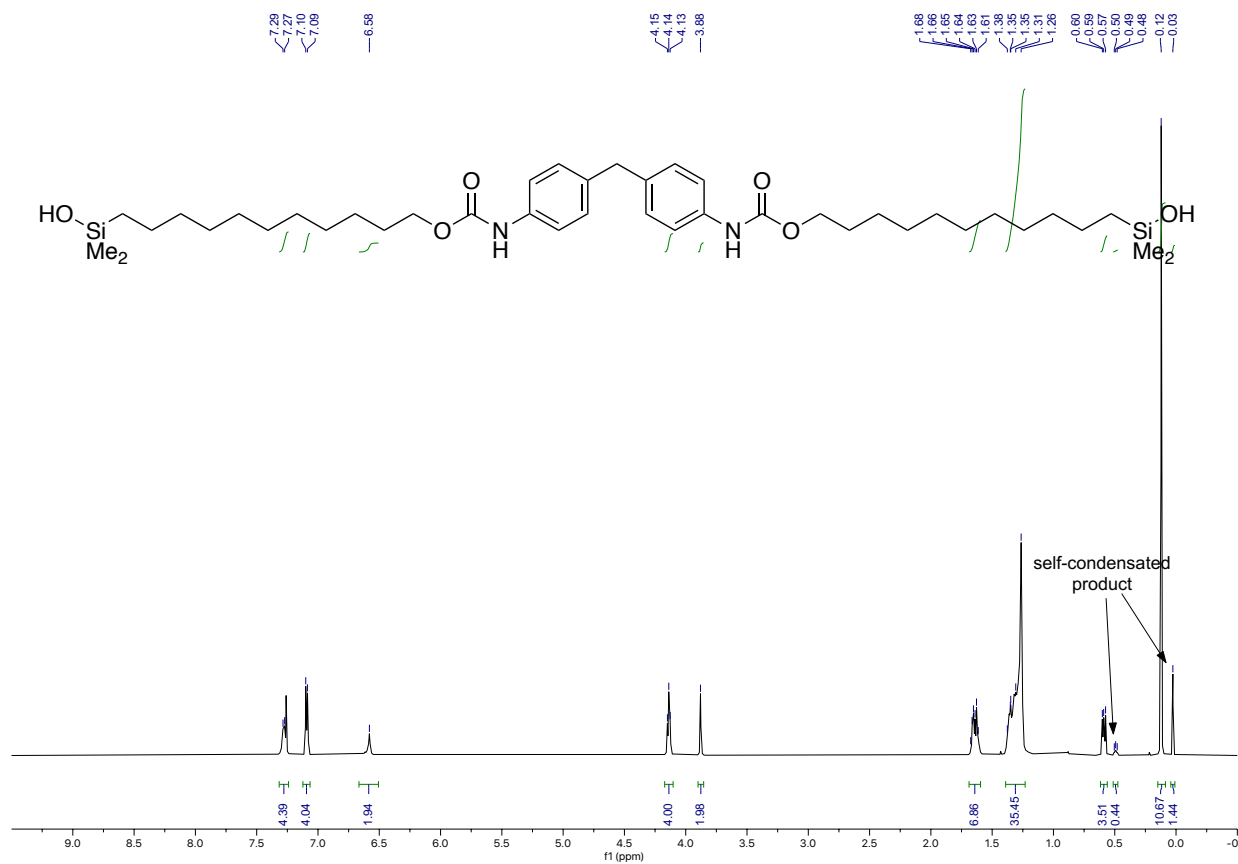


Figure 2.12.8.20. ¹H NMR spectra of compound 8

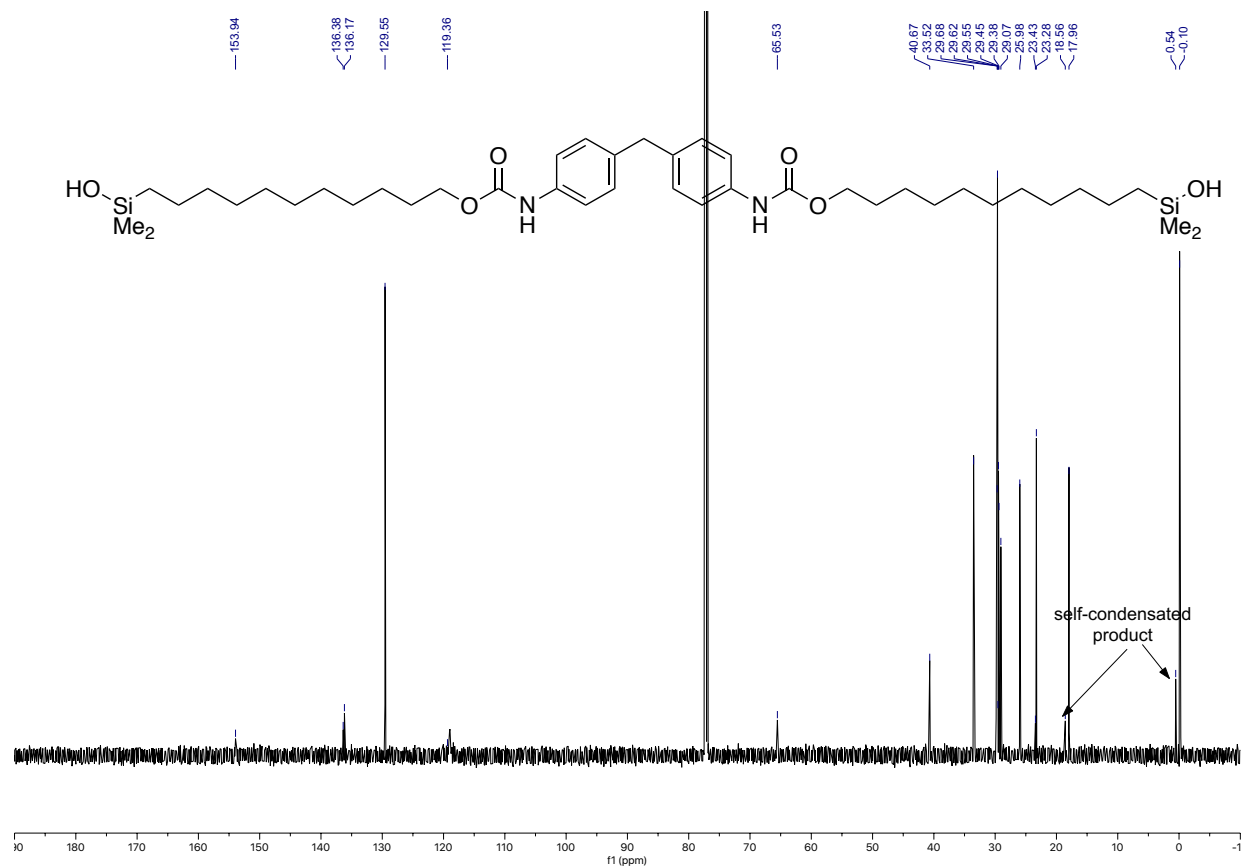


Figure 2.12.8.21. ^{13}C NMR spectra of compound 8

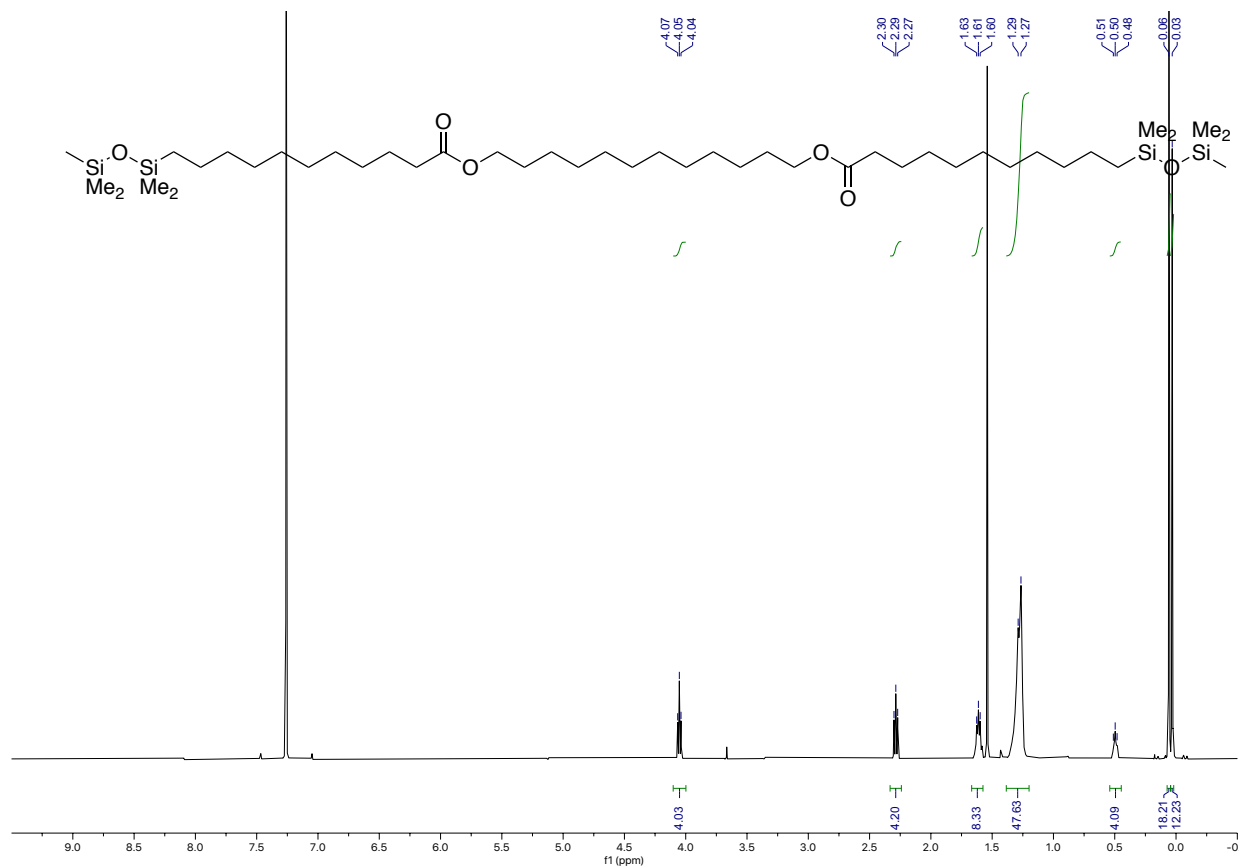


Figure 2.12.8.22. ¹H NMR spectra of compound 9

EK-03-253_13C.2.fid
AVB-400 ZBO Carbon Starting parameters 6/11/03 RN

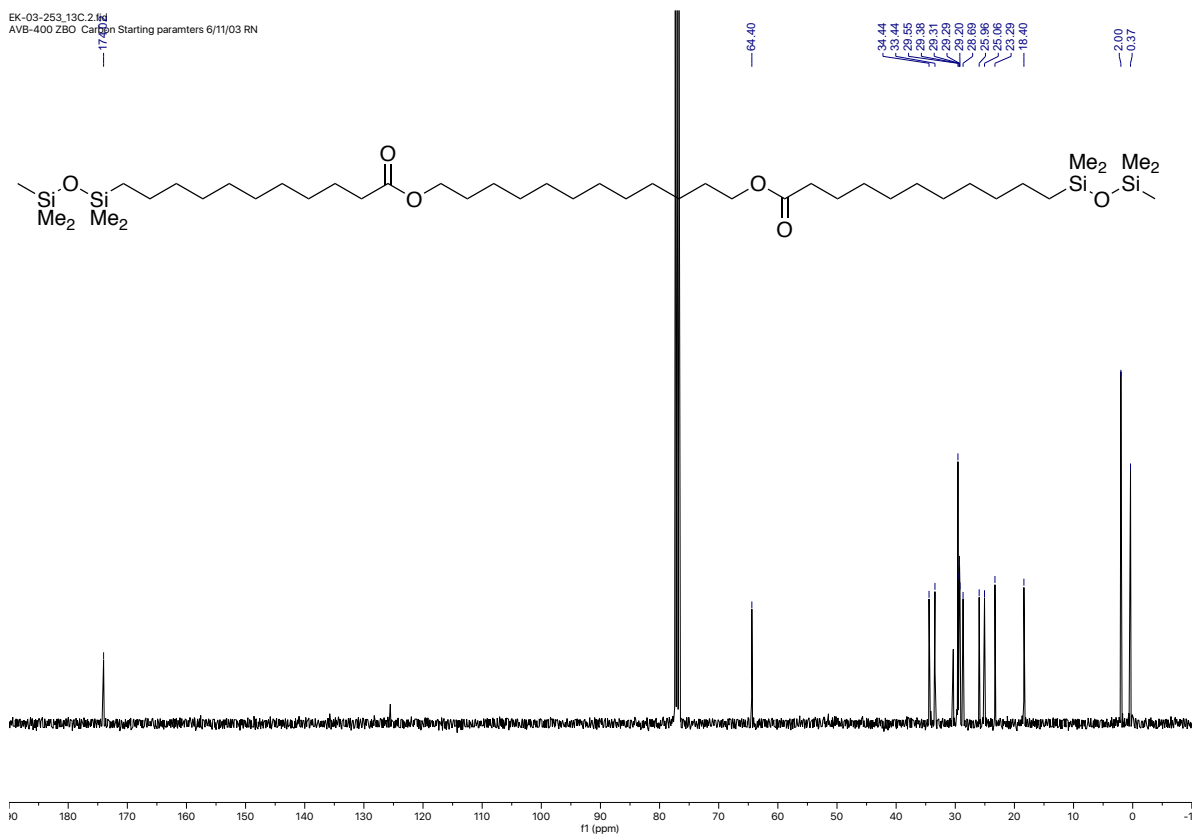


Figure 2.12.8.23. ¹³C NMR spectra of compound 9

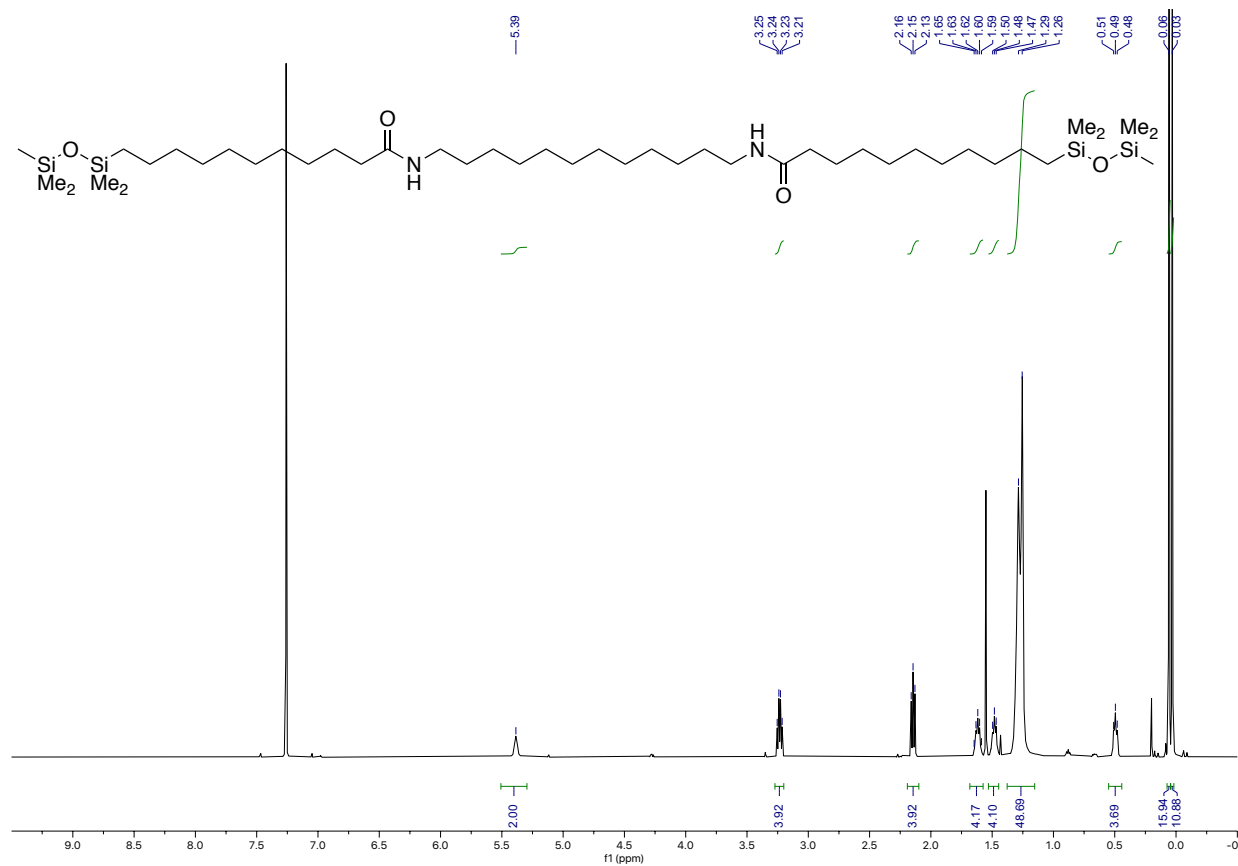


Figure 2.12.8.24. ¹H NMR spectra of compound 10

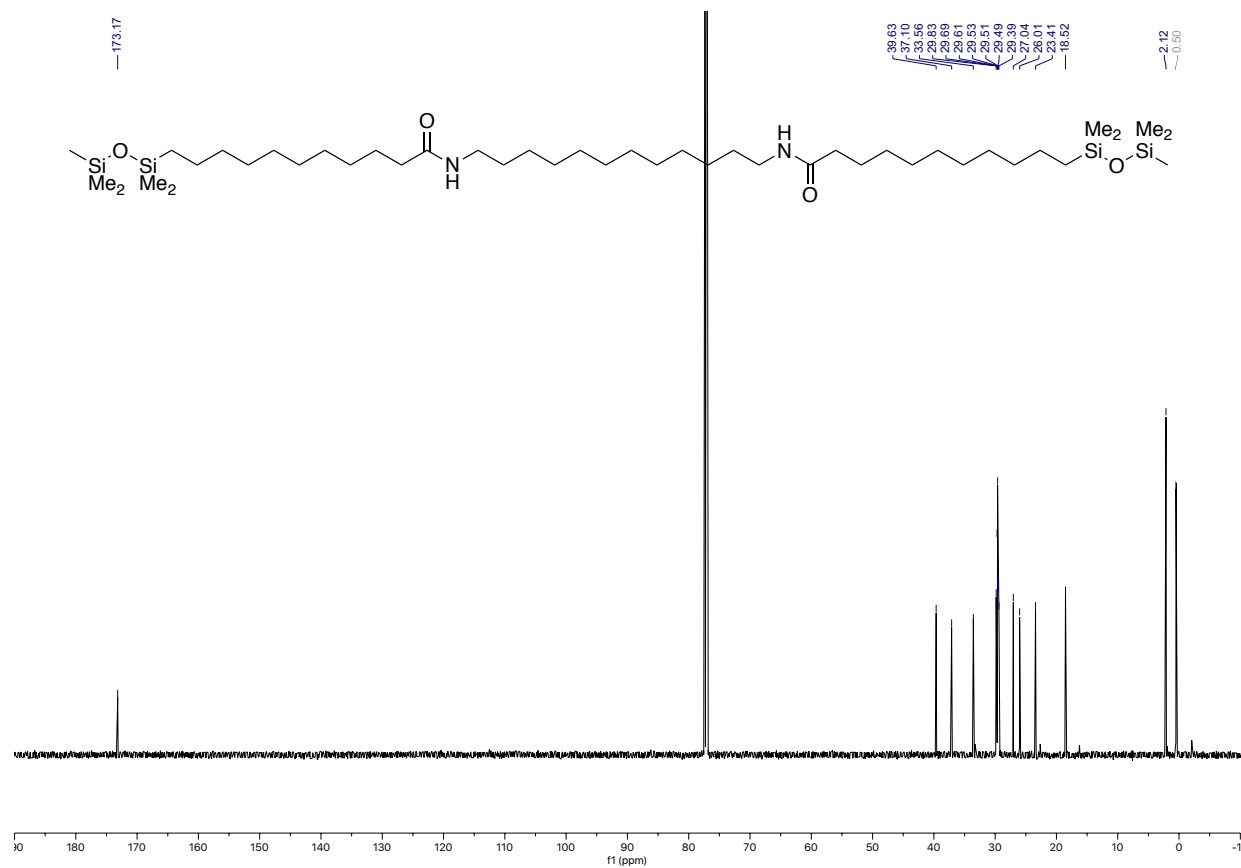


Figure 2.12.8.25. ^{13}C NMR spectra of compound 10

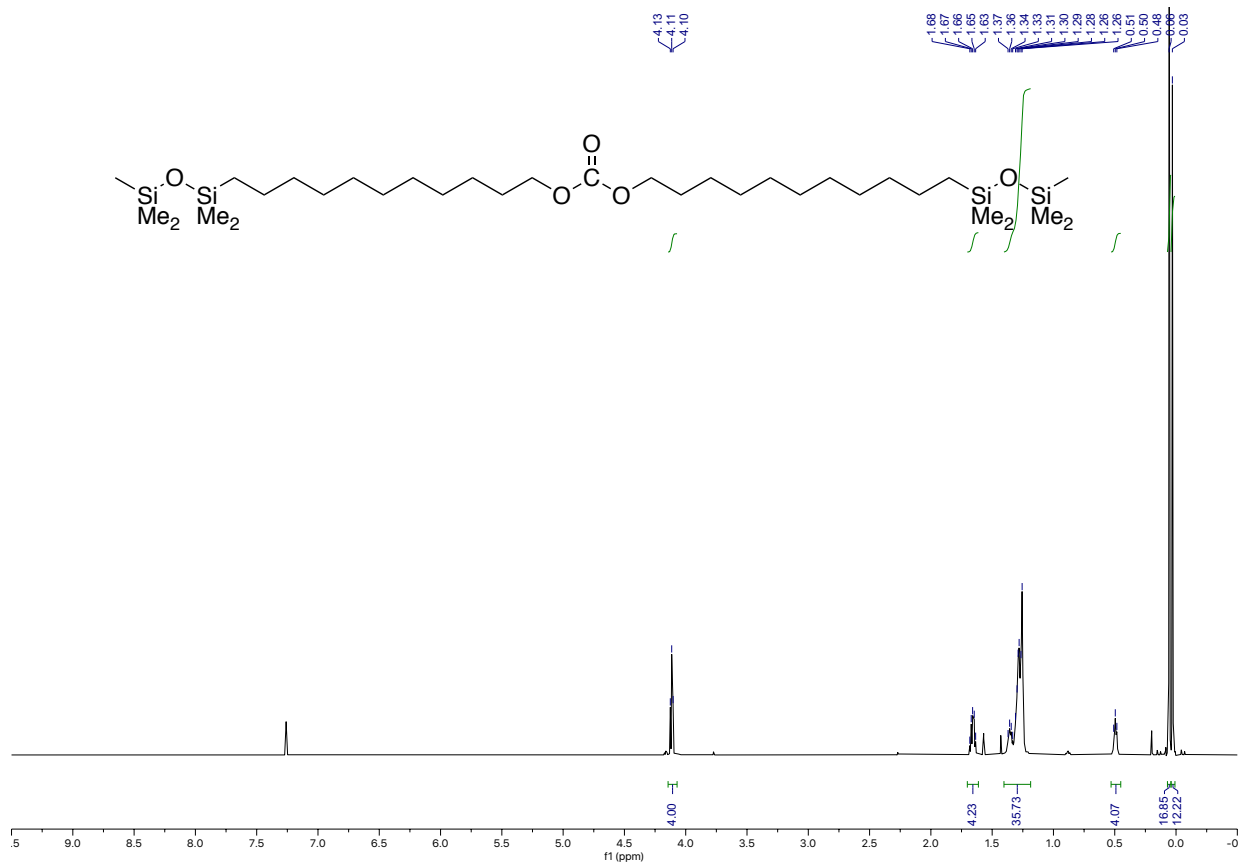


Figure 2.12.8.26. ¹H NMR spectra of compound 11

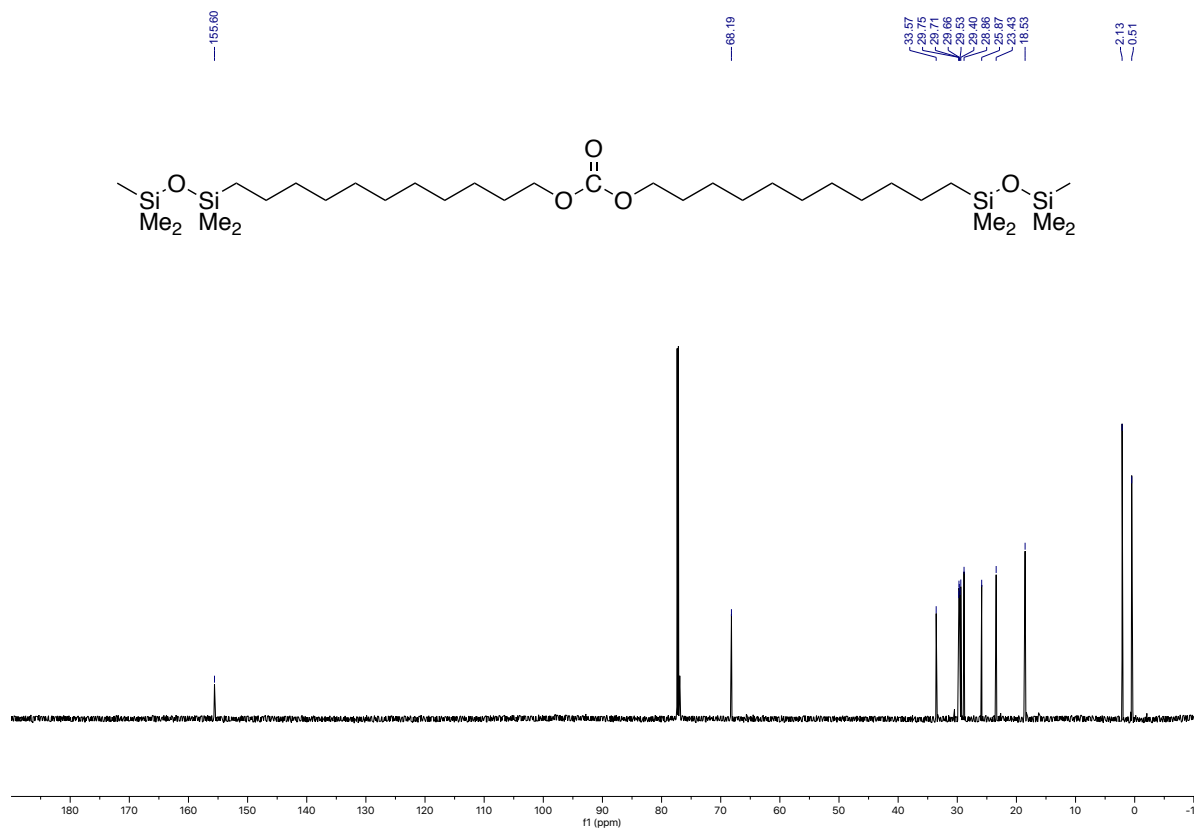


Figure 2.12.8.27. ^{13}C NMR spectra of compound 11

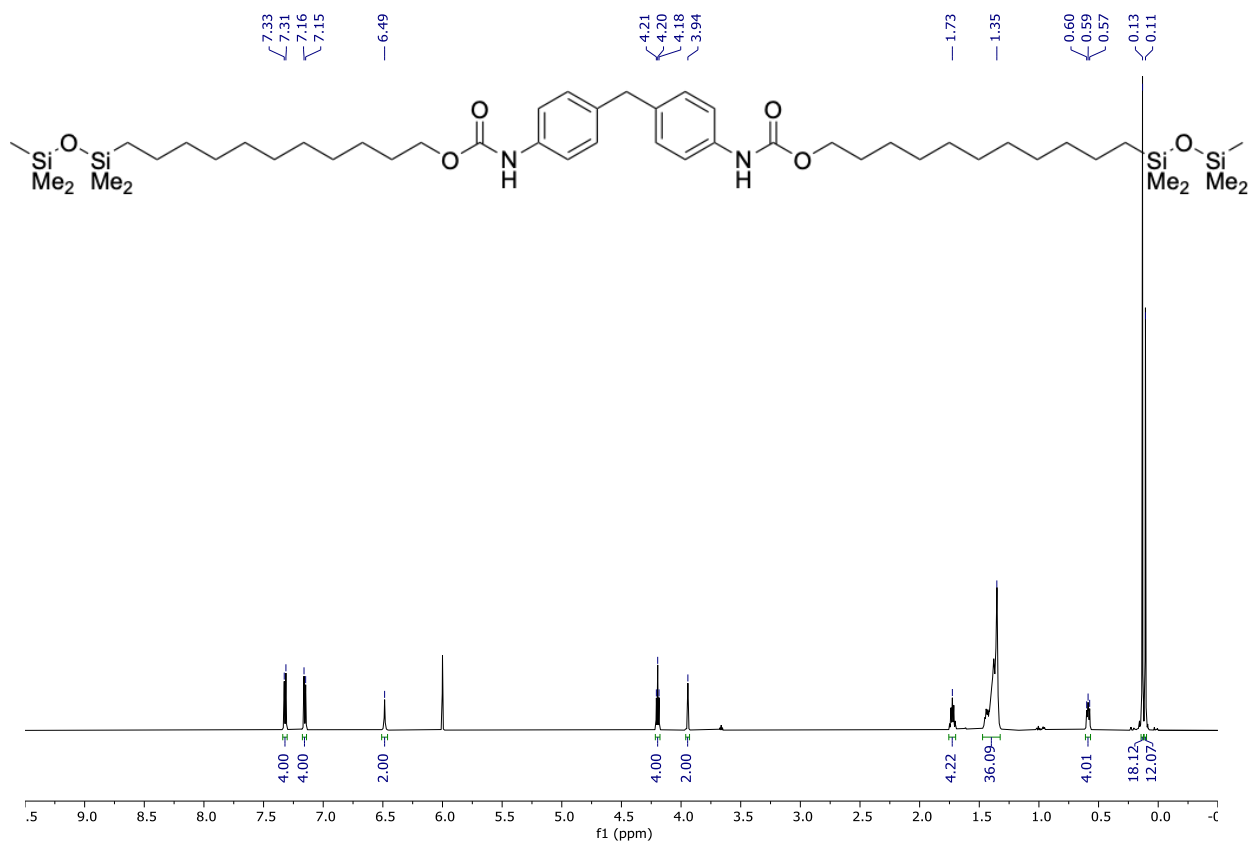


Figure 2.12.8.28. ¹H NMR spectra of compound 12

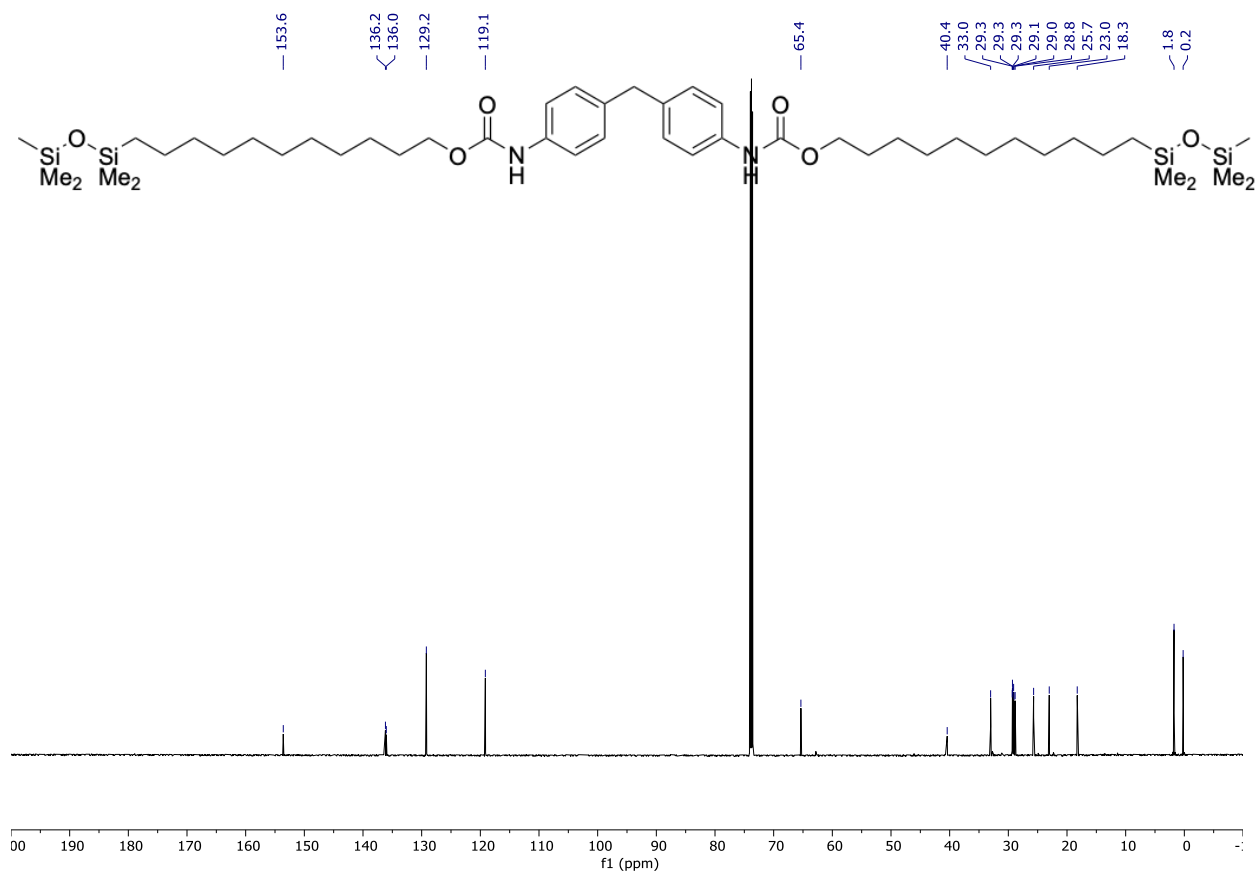


Figure 2.12.8.29. ¹³C NMR spectra of compound 12



Figure 2.12.8.30. ¹H NMR spectra of compound **9** after depolymerization in the presence of PET, PP, and PE

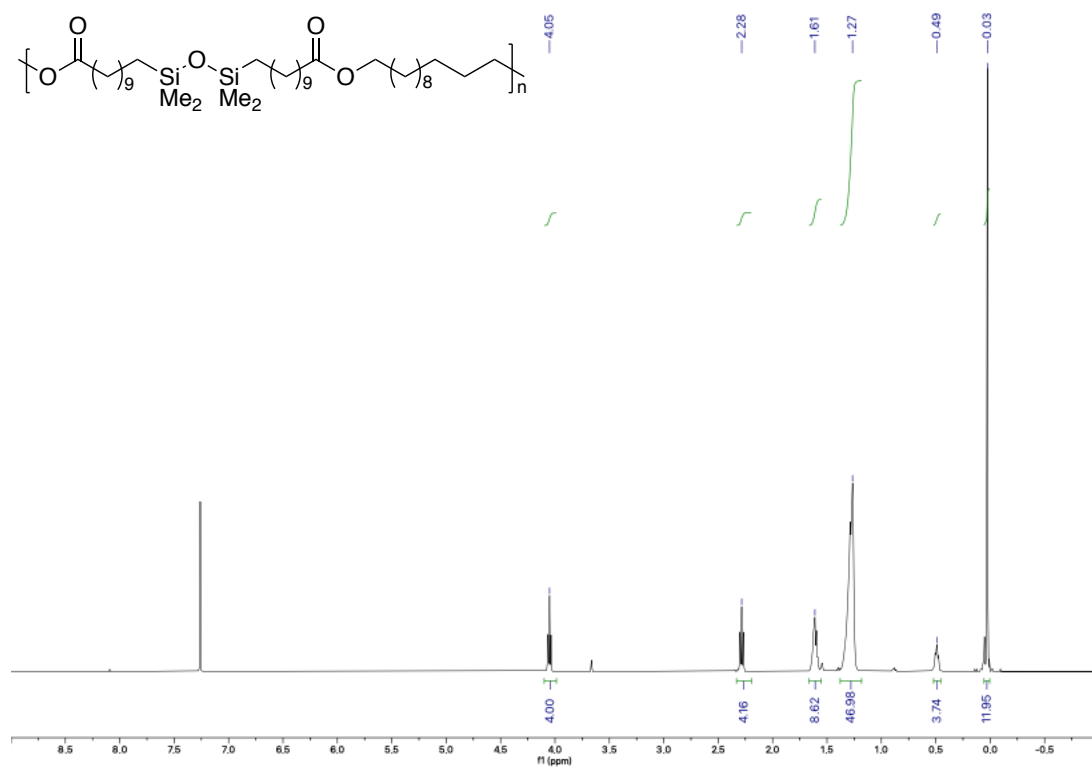


Figure 2.12.8.31. ^1H NMR spectra of repolymerized PE-2-C12

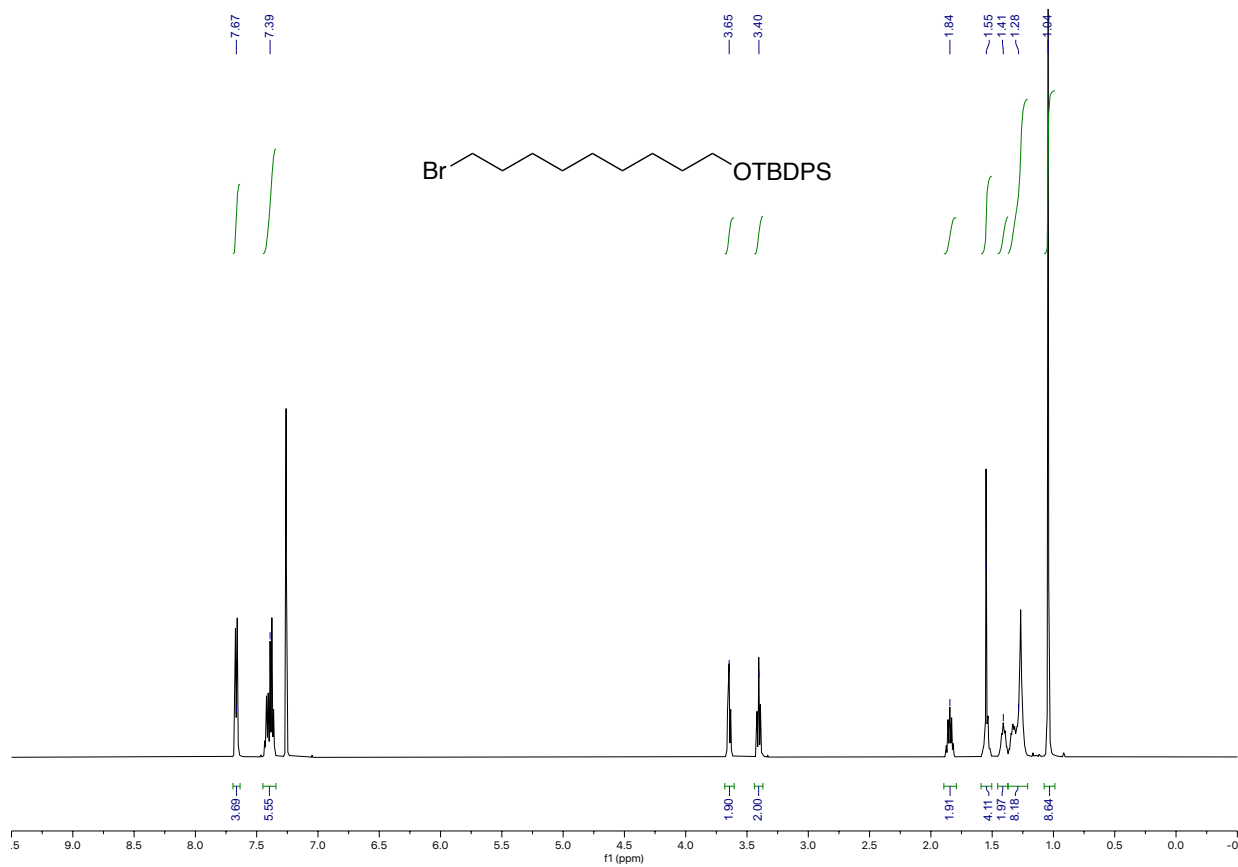


Figure 2.12.8.32. ¹H NMR spectra of intermediate A

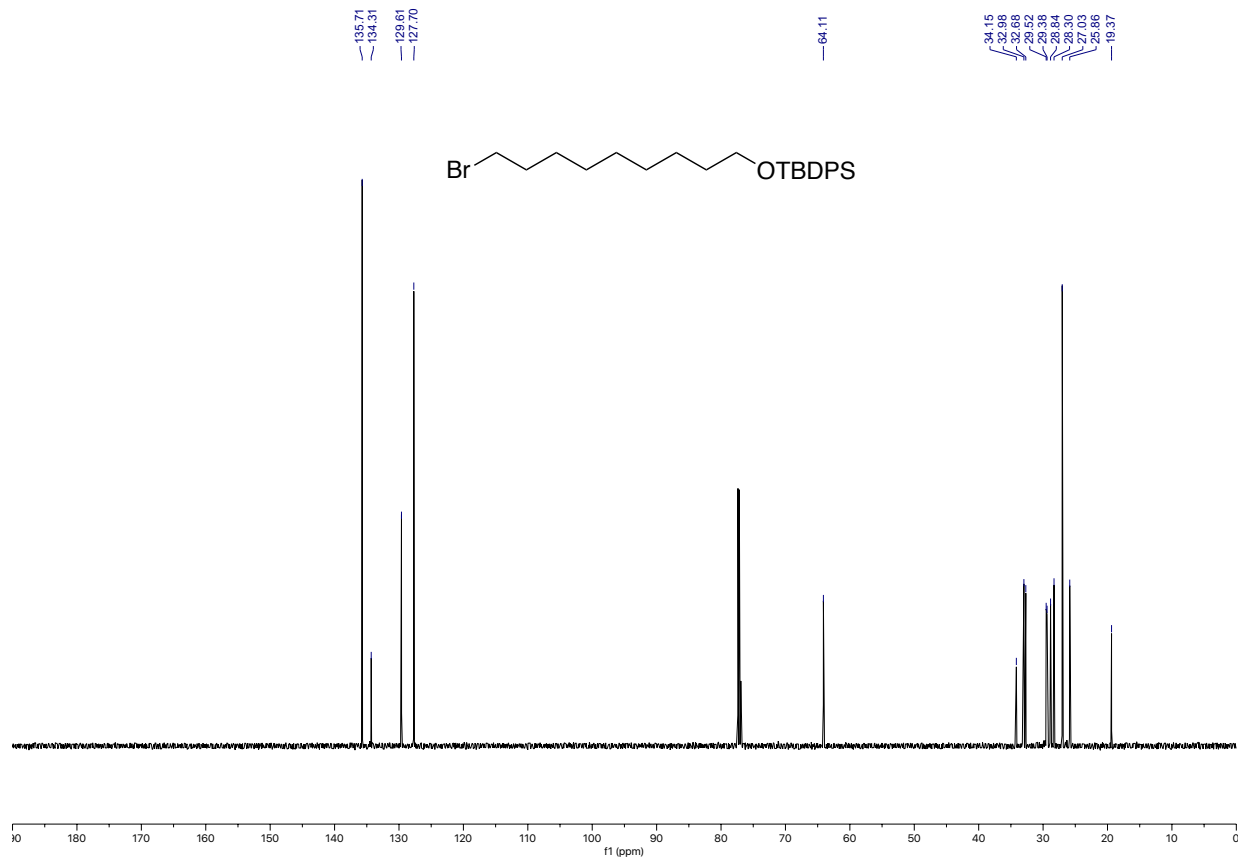


Figure 2.12.8.33. ^{13}C NMR spectra of intermediate A

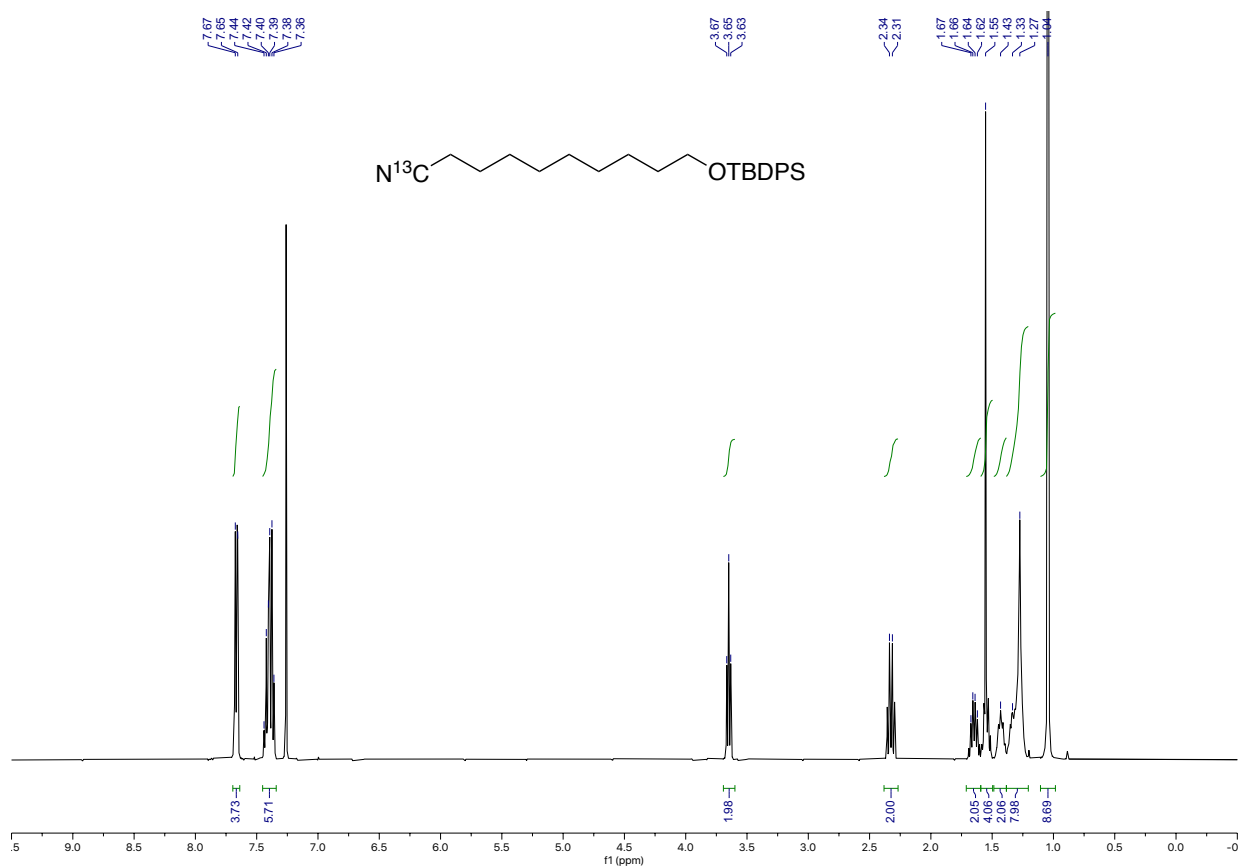


Figure 2.12.8.34. 1H NMR spectra of intermediate **B**

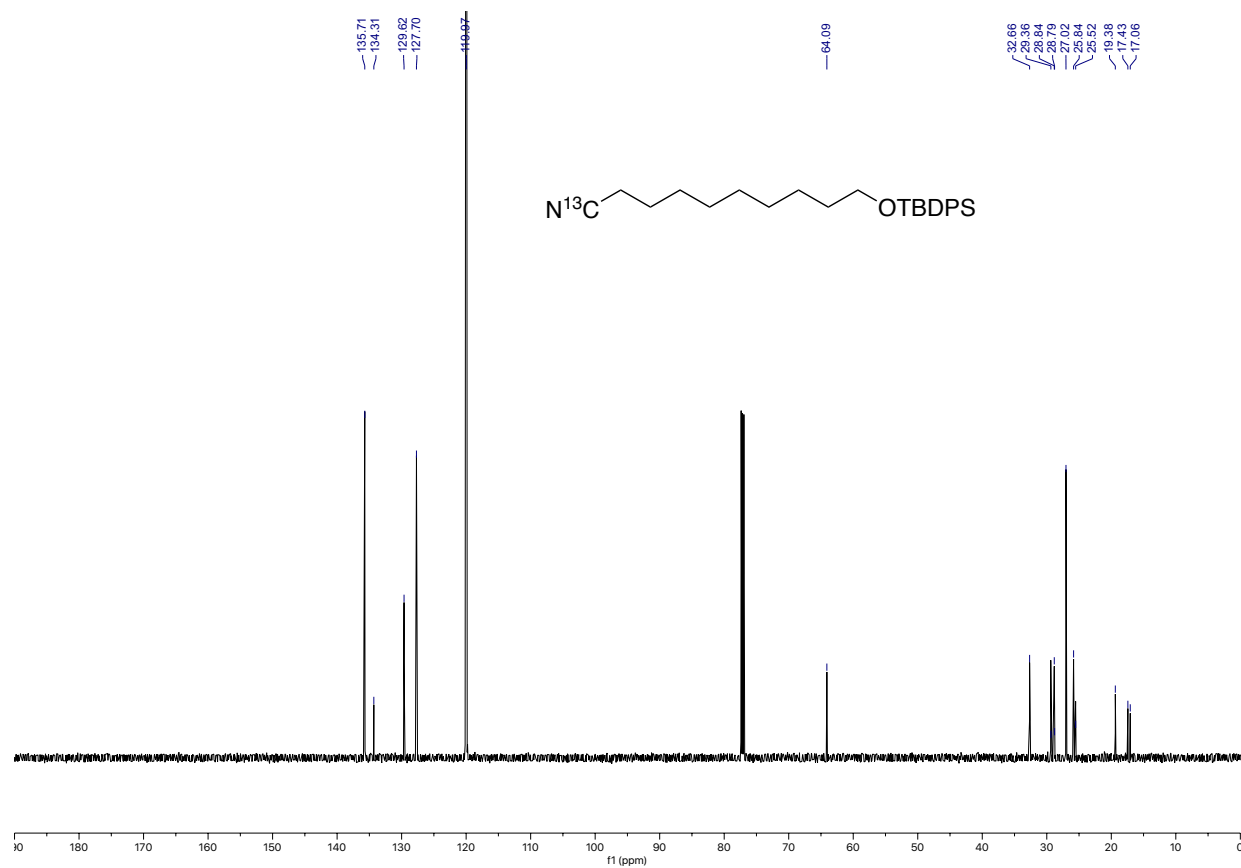


Figure 2.12.8.35. ^{13}C NMR spectra of intermediate B

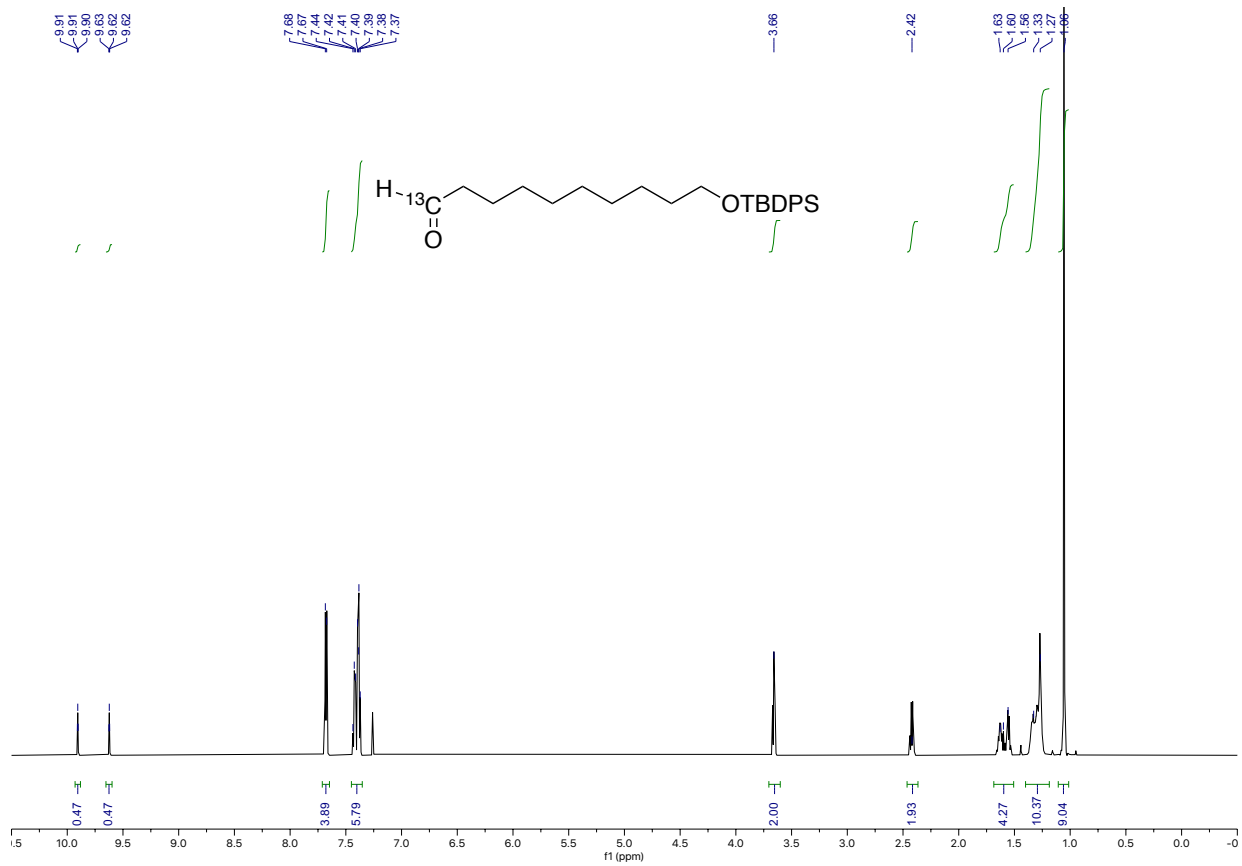


Figure 2.12.8.36. ¹H NMR spectra of intermediate C

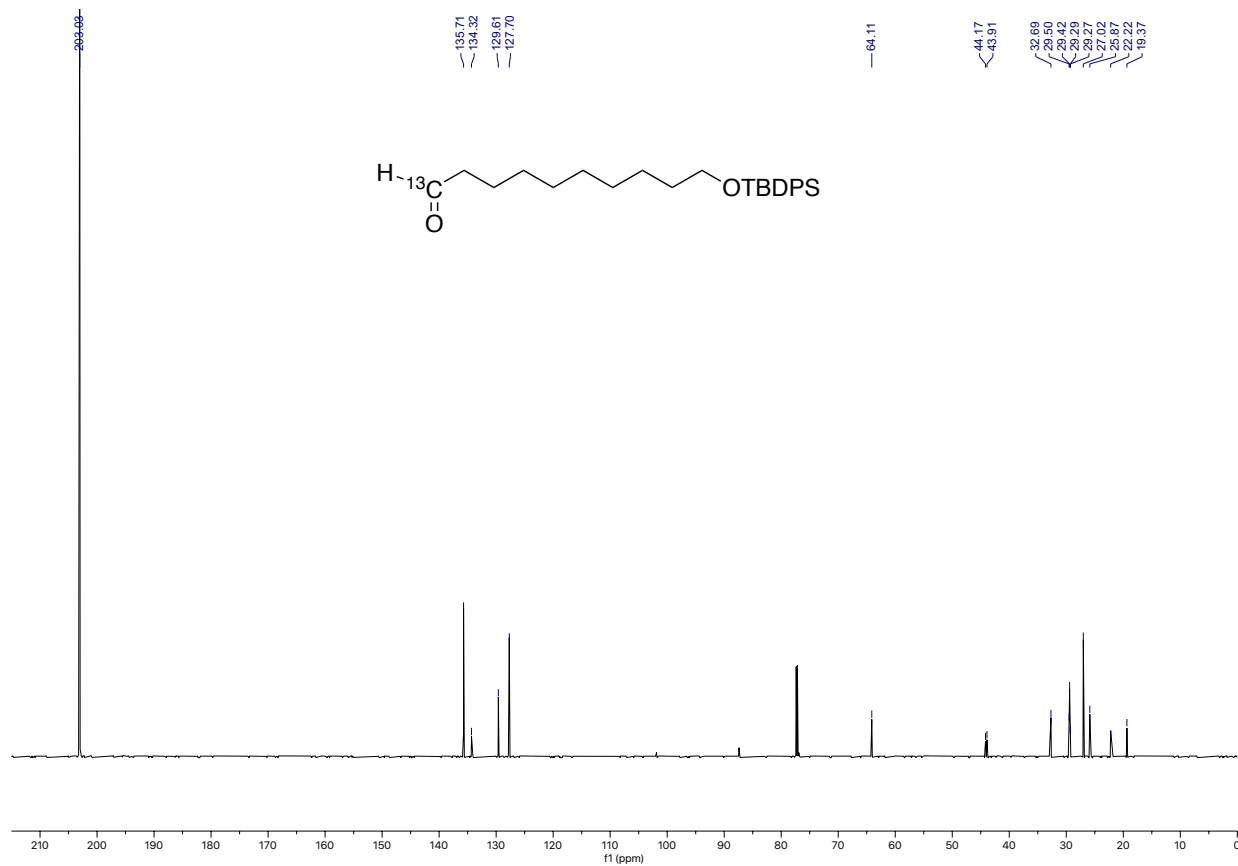


Figure 2.12.8.37. ^{13}C NMR spectra of intermediate C

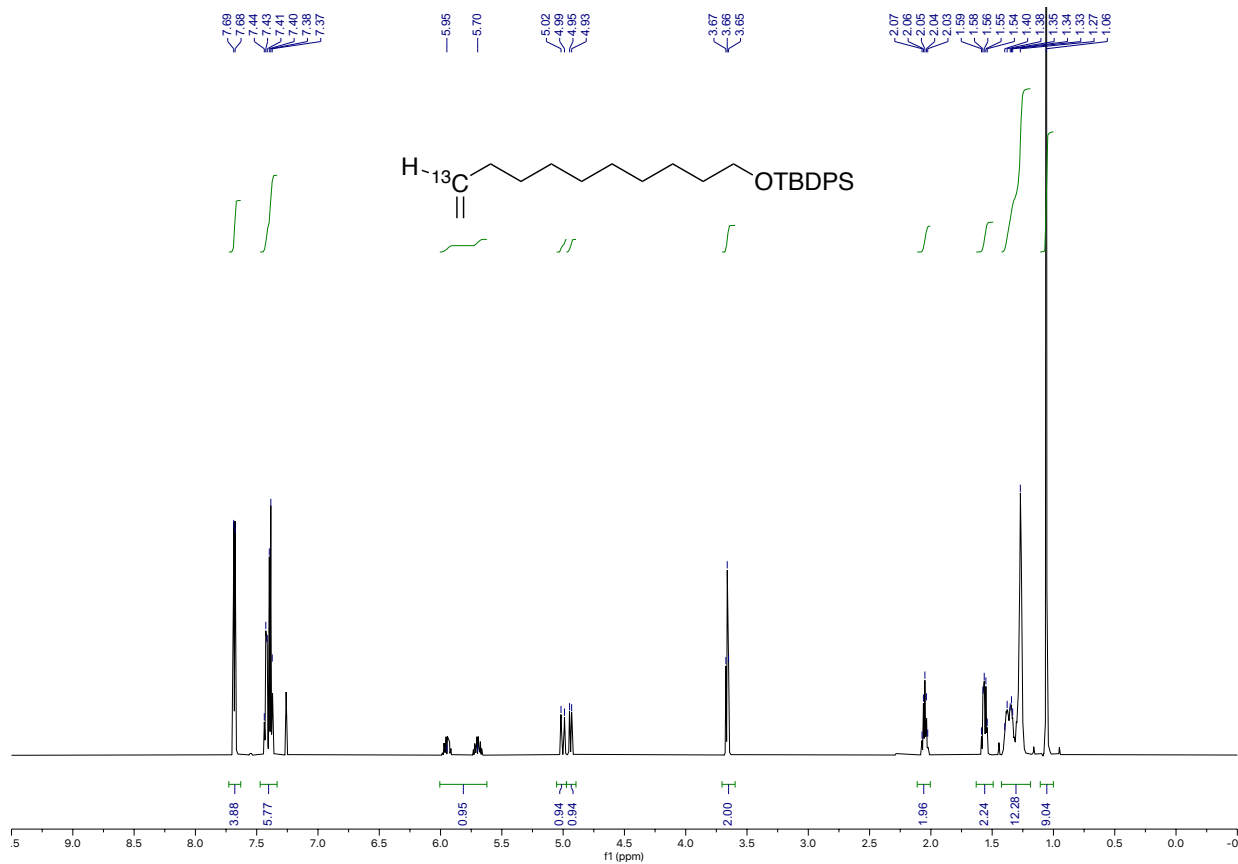


Figure 2.12.8.38. ^1H NMR spectra of intermediate **D**

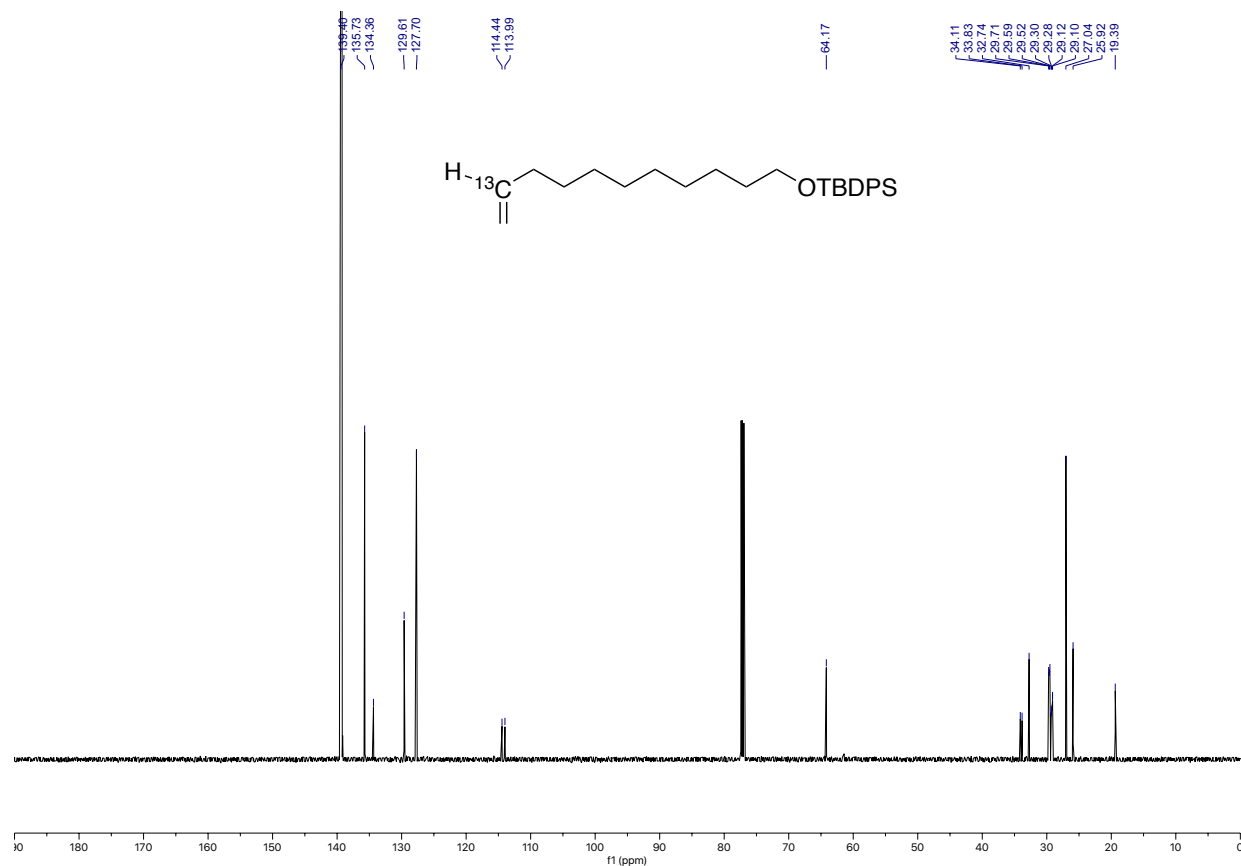


Figure 2.12.8.39. ^{13}C NMR spectra of intermediate **D**

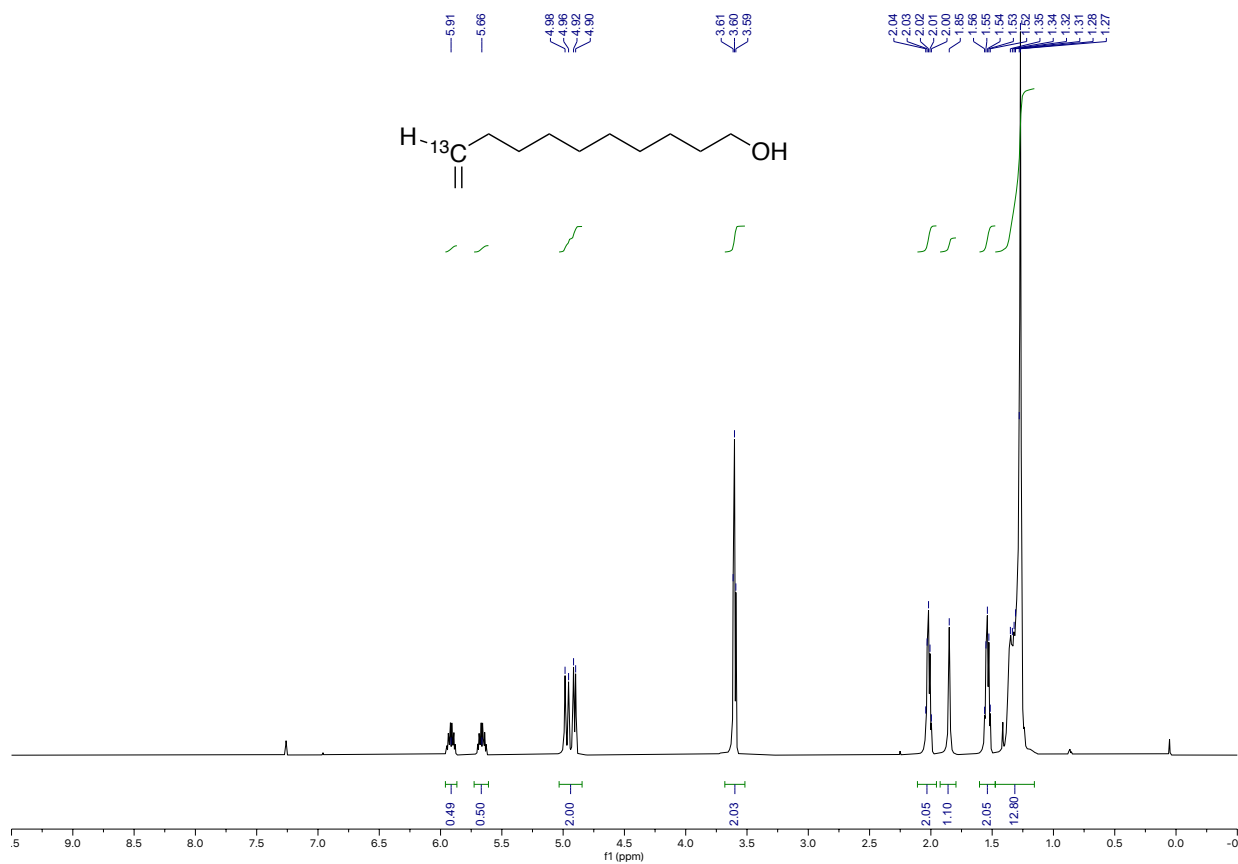


Figure 2.12.8.40. ^1H NMR spectra of intermediate E

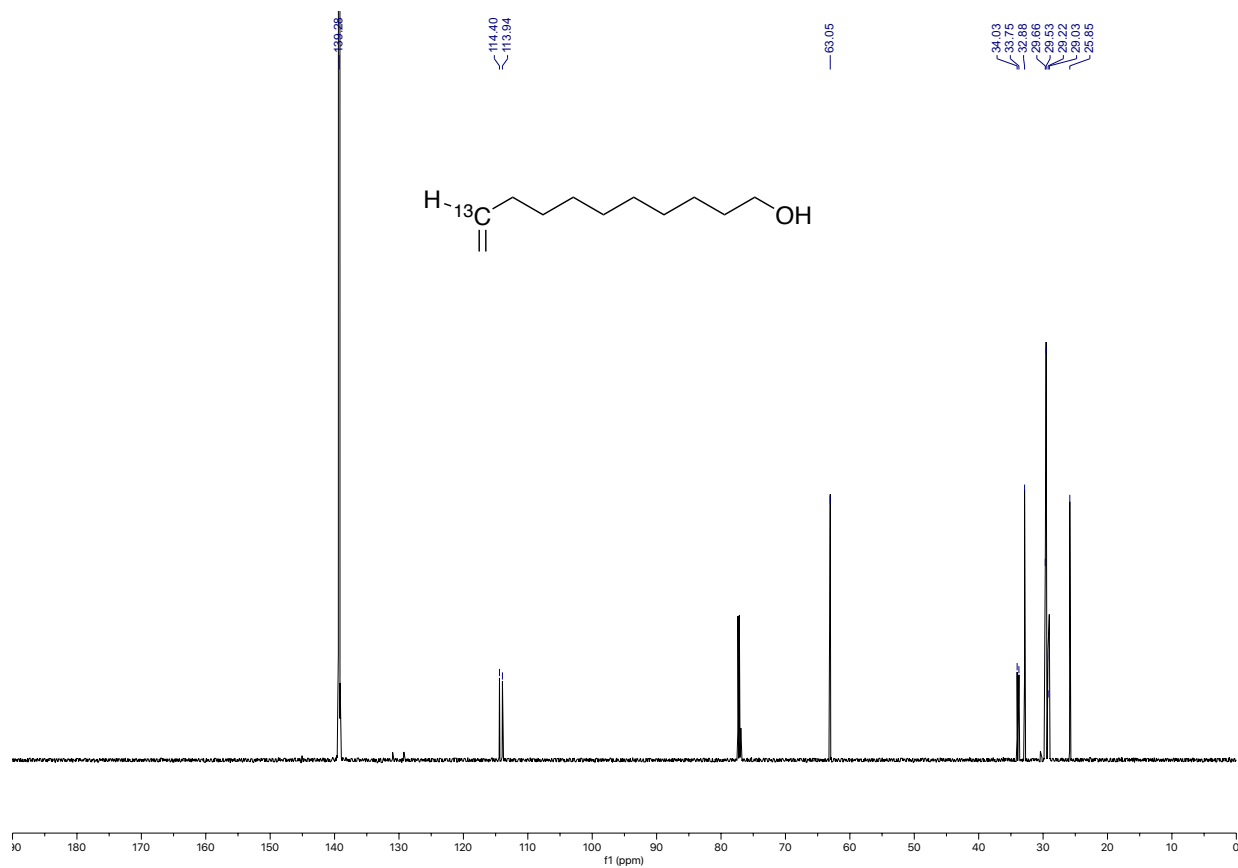


Figure 2.12.8.41. ^{13}C NMR spectra of intermediate E

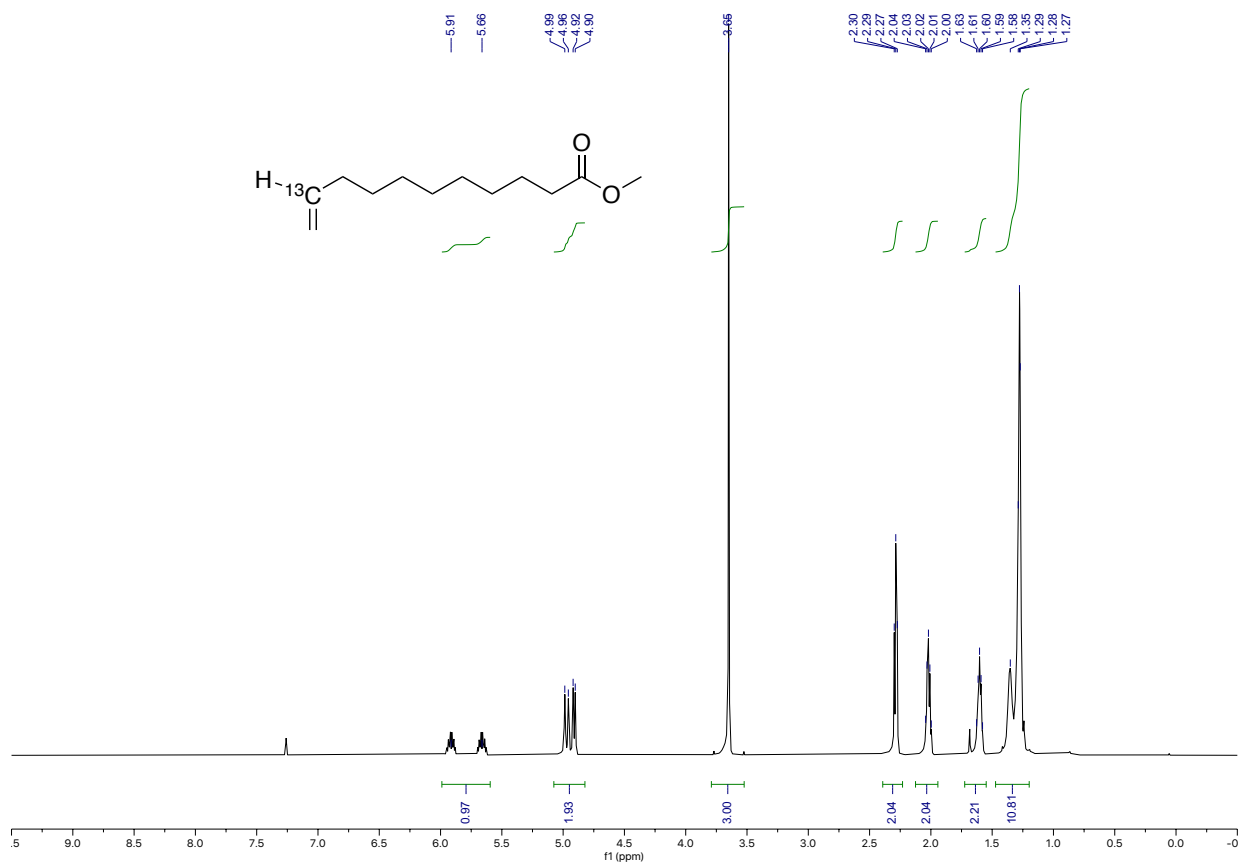


Figure 2.12.8.42. ¹H NMR spectra of intermediate **F**

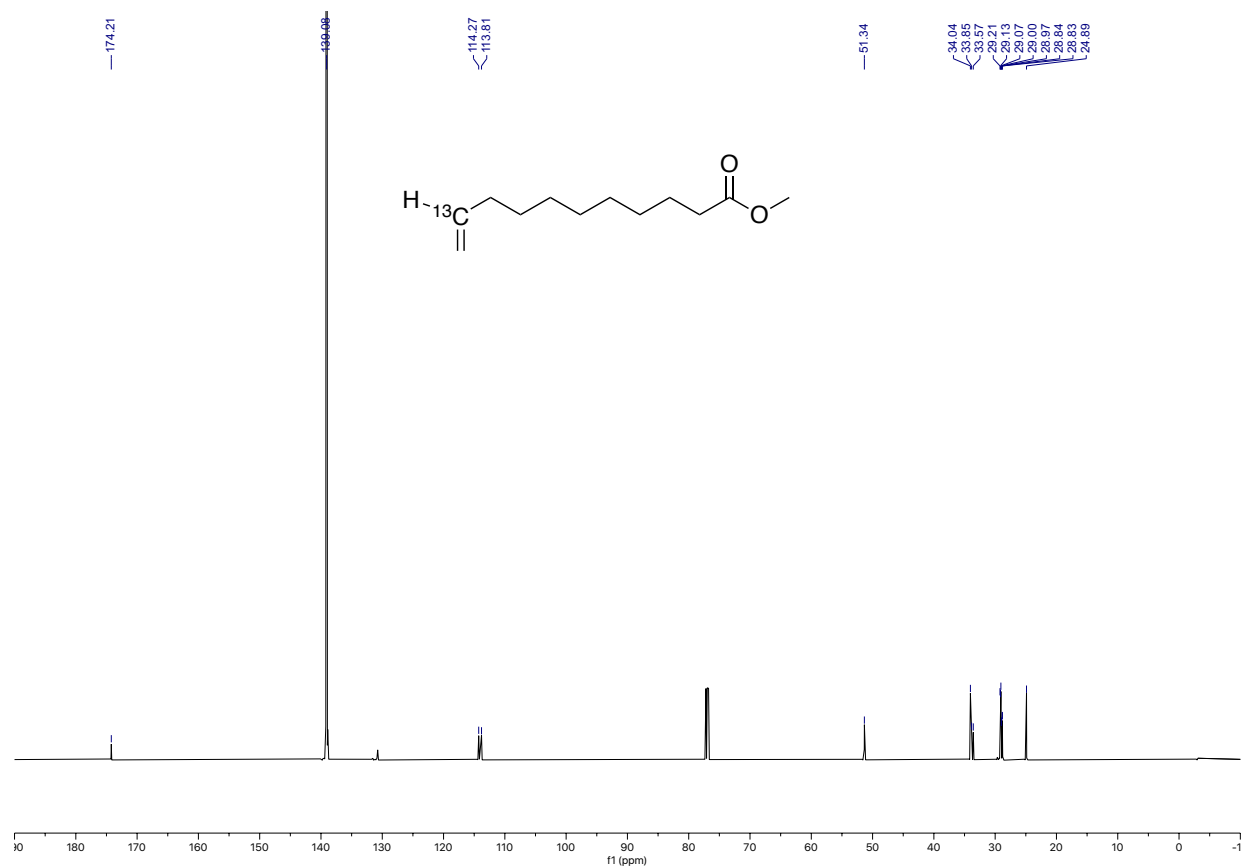


Figure 2.12.8.43. ^{13}C NMR spectra of intermediate F

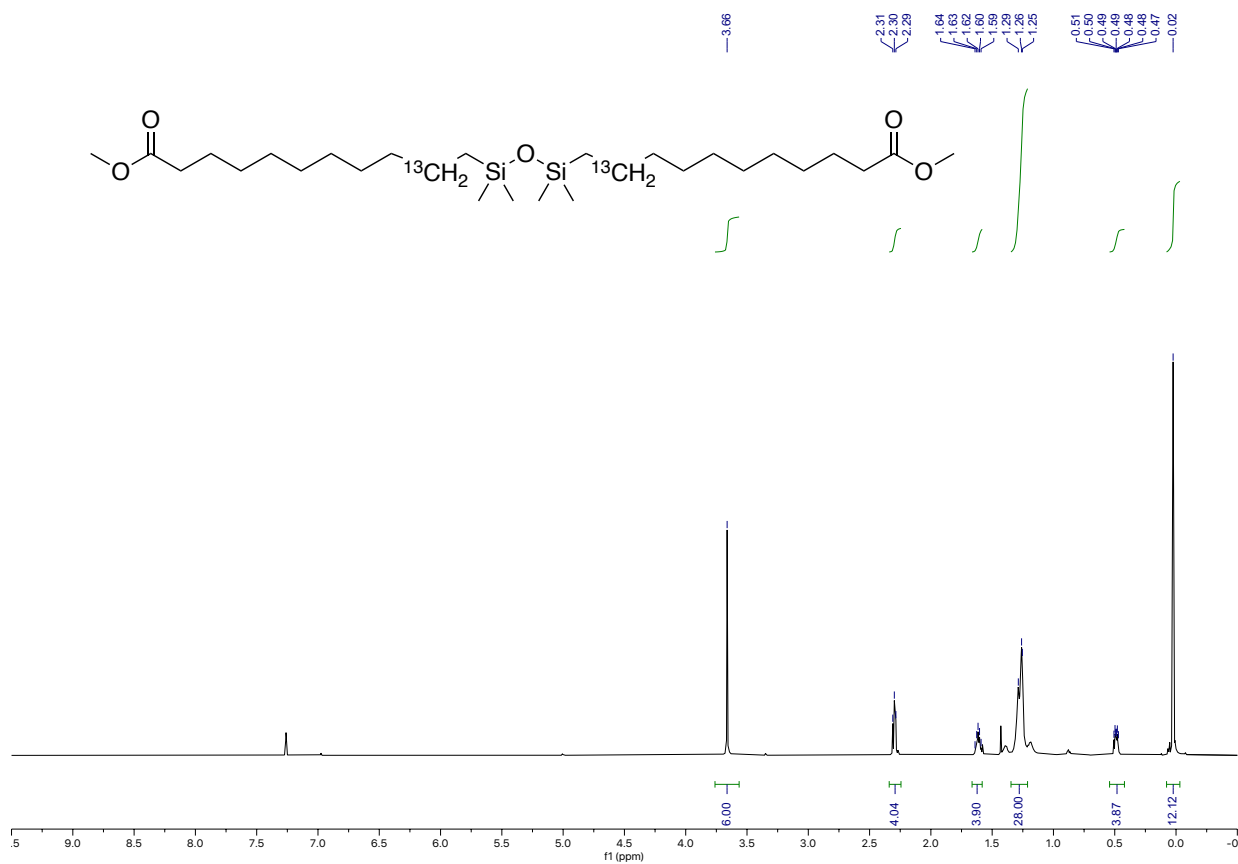


Figure 2.12.8.44. ¹H NMR spectra of compound 12

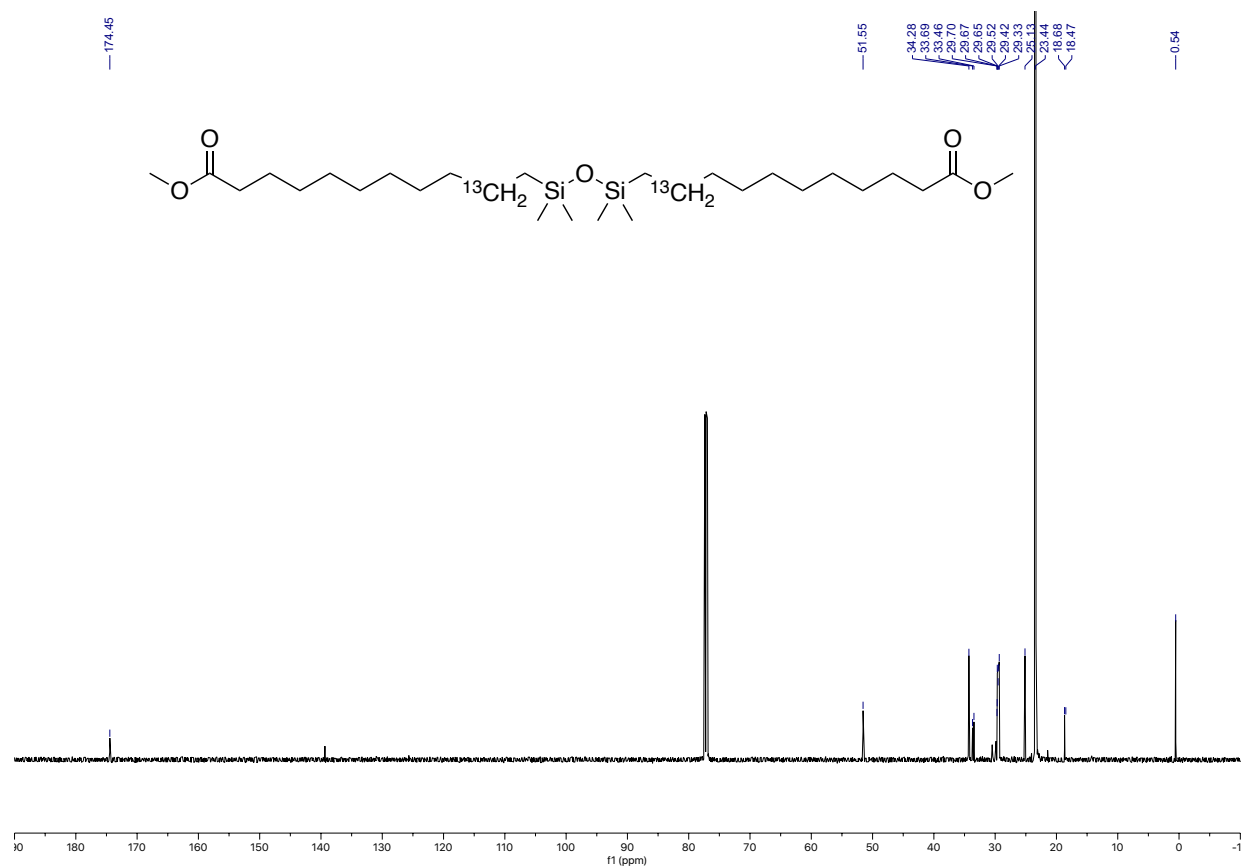


Figure 2.12.8.45. ^{13}C NMR spectra of compound 12

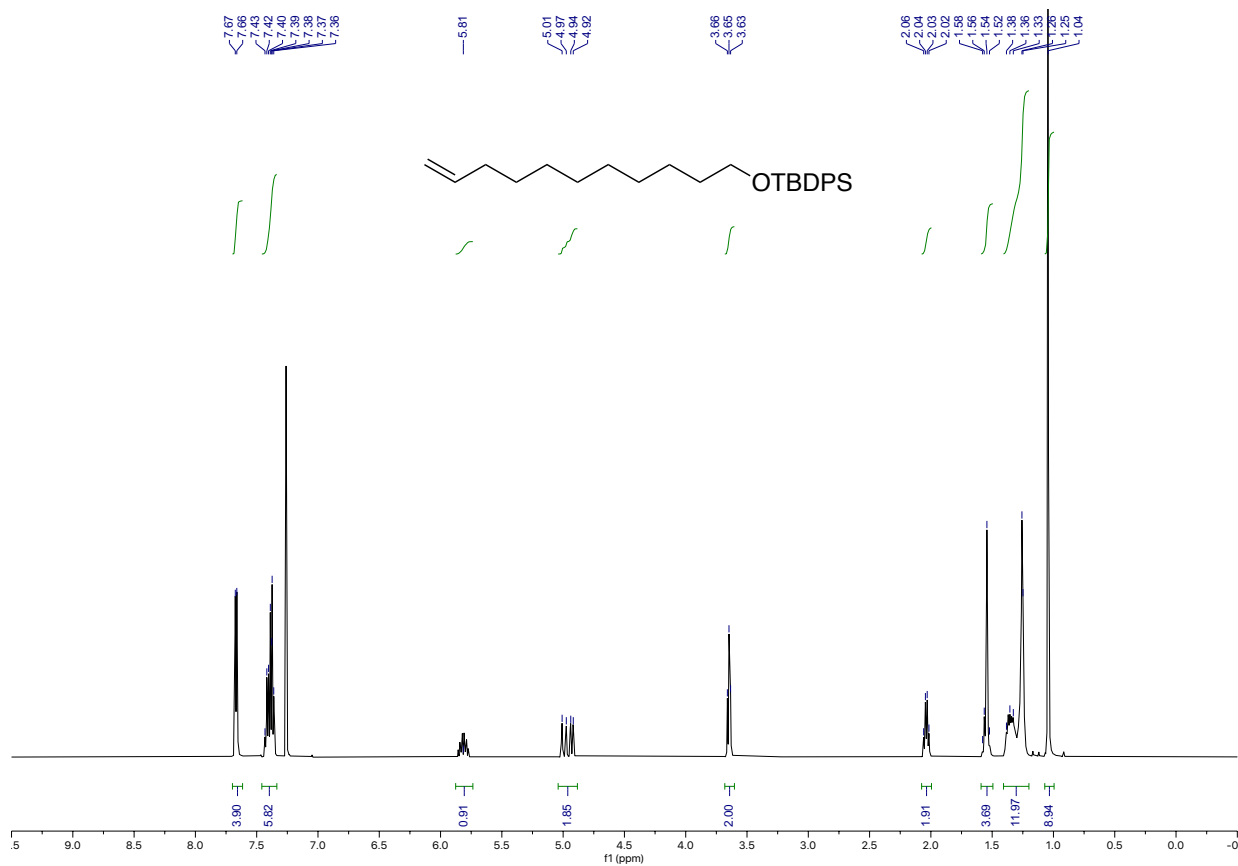


Figure 2.12.8.46. ¹H NMR spectra of intermediate G

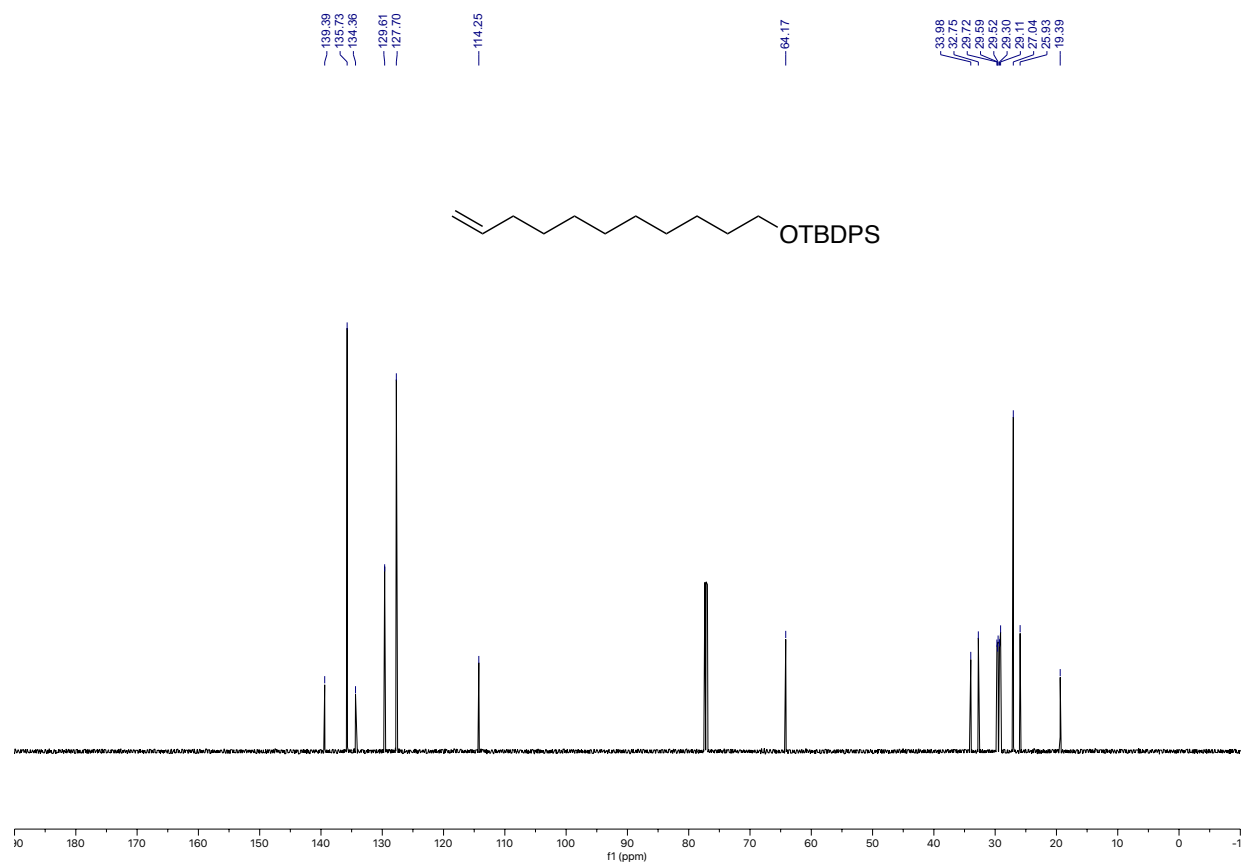


Figure 2.12.8.47. ^{13}C NMR spectra of intermediate **G**

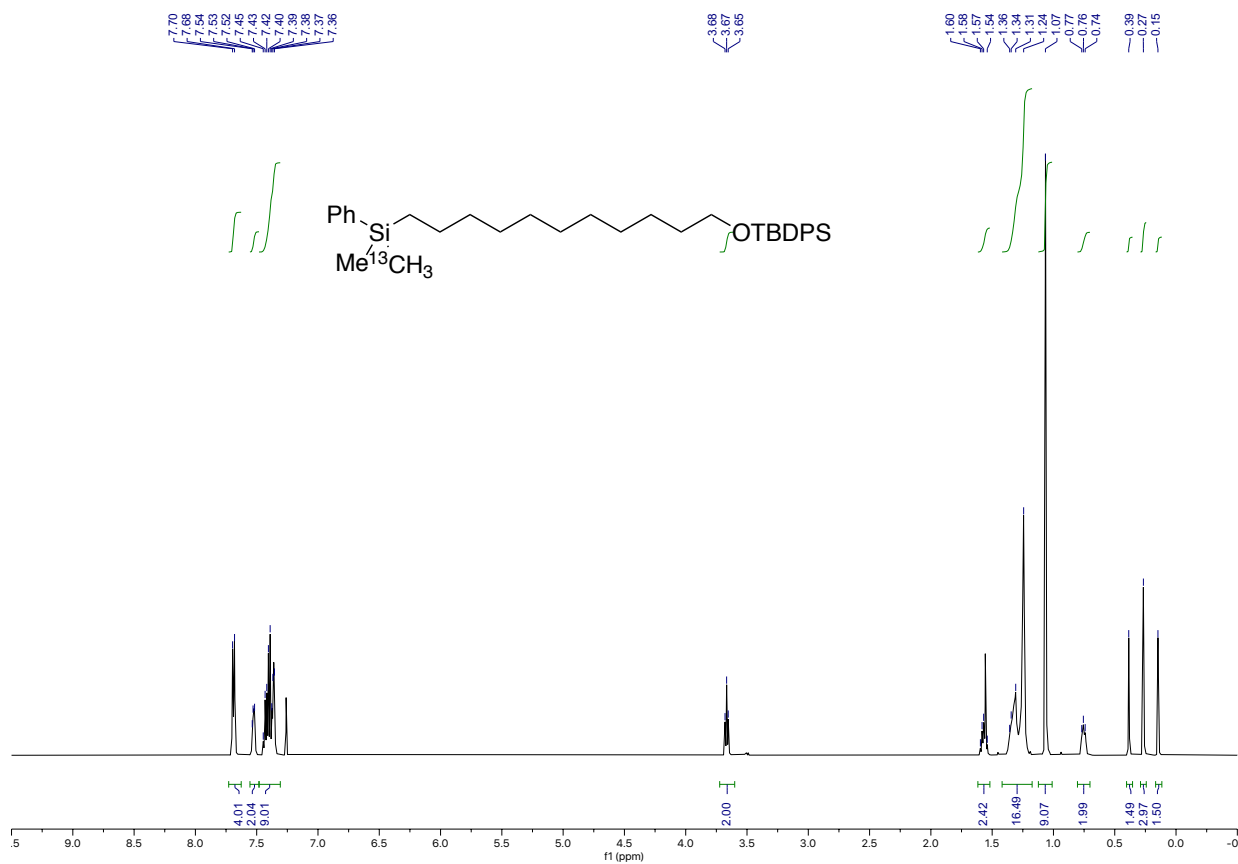


Figure 2.12.8.48. ^1H NMR spectra of intermediate **H**

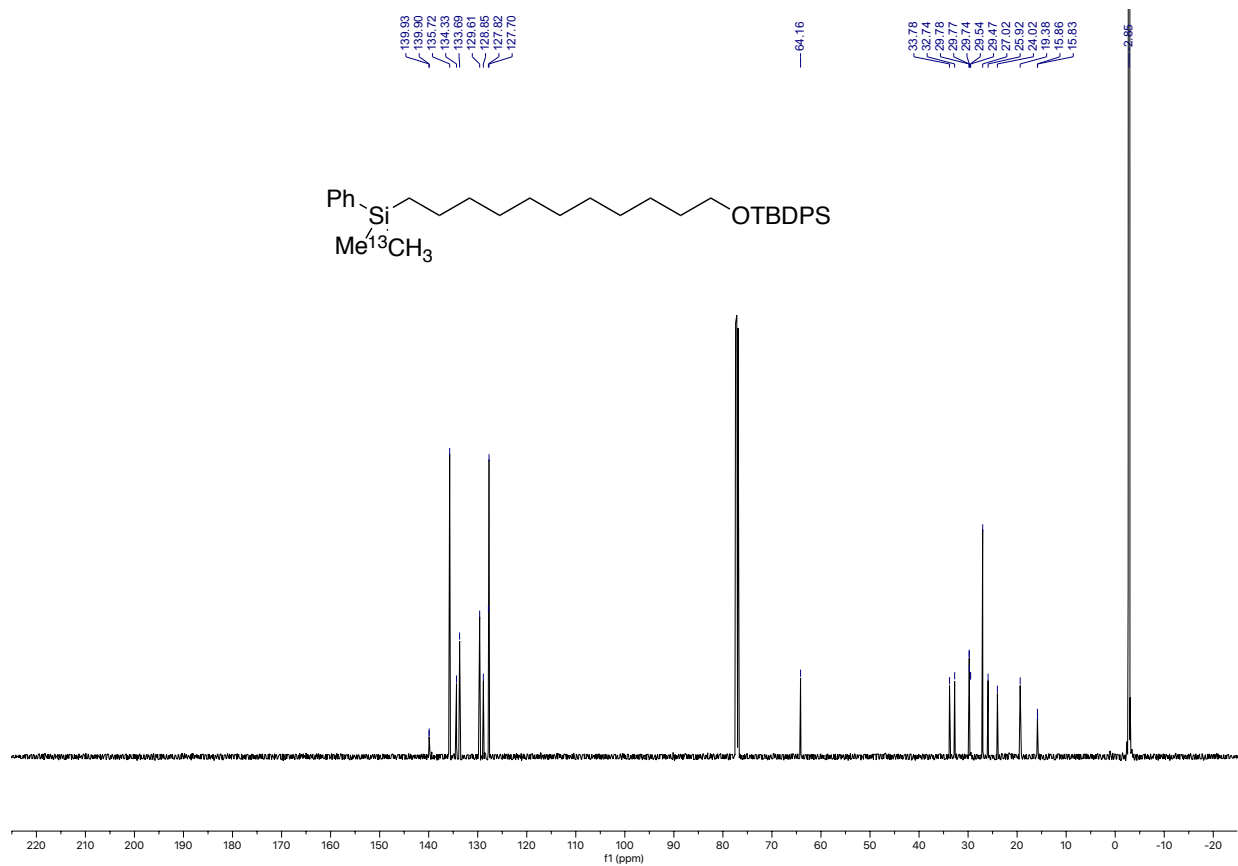


Figure 2.12.8.49. ^{13}C NMR spectra of intermediate H

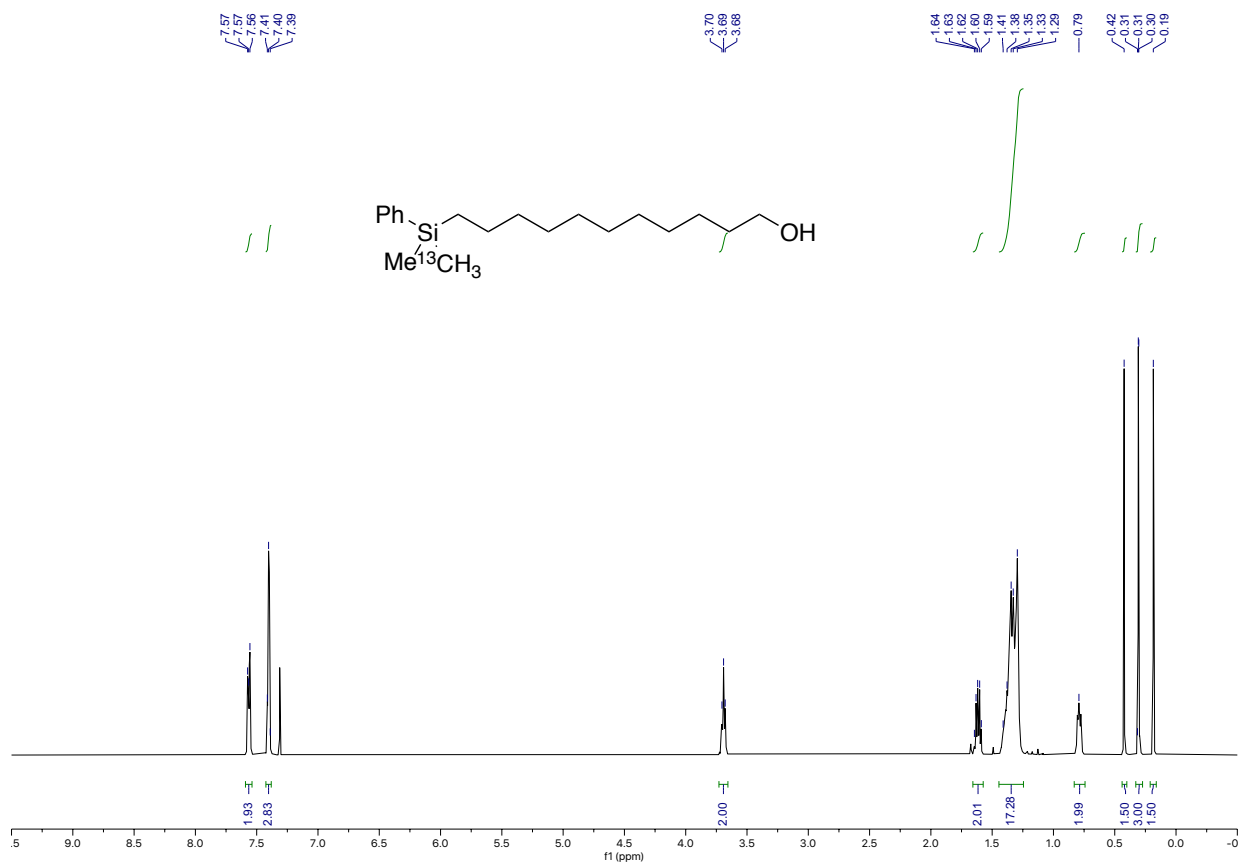


Figure 2.12.8.50. ¹H NMR spectra of intermediate I

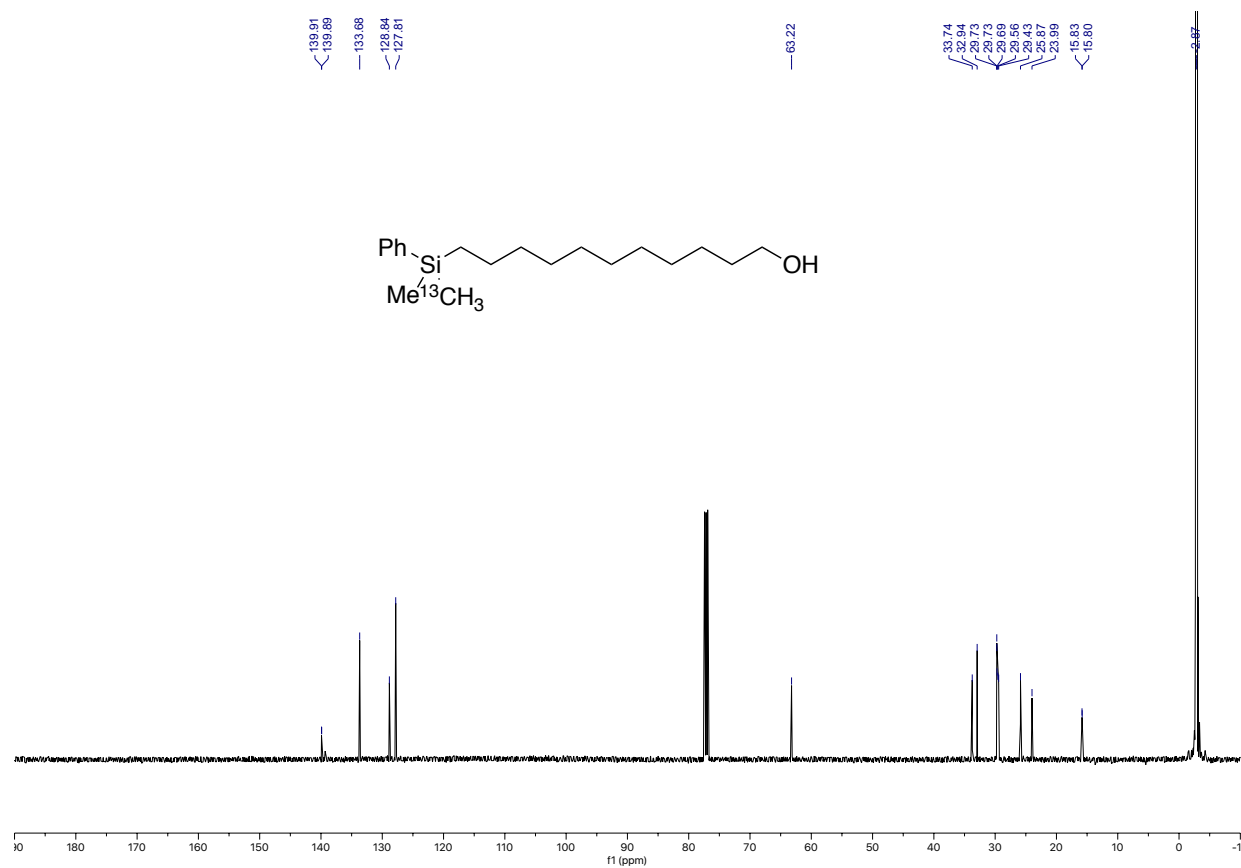


Figure 2.12.8.51. ^{13}C NMR spectra of intermediate I

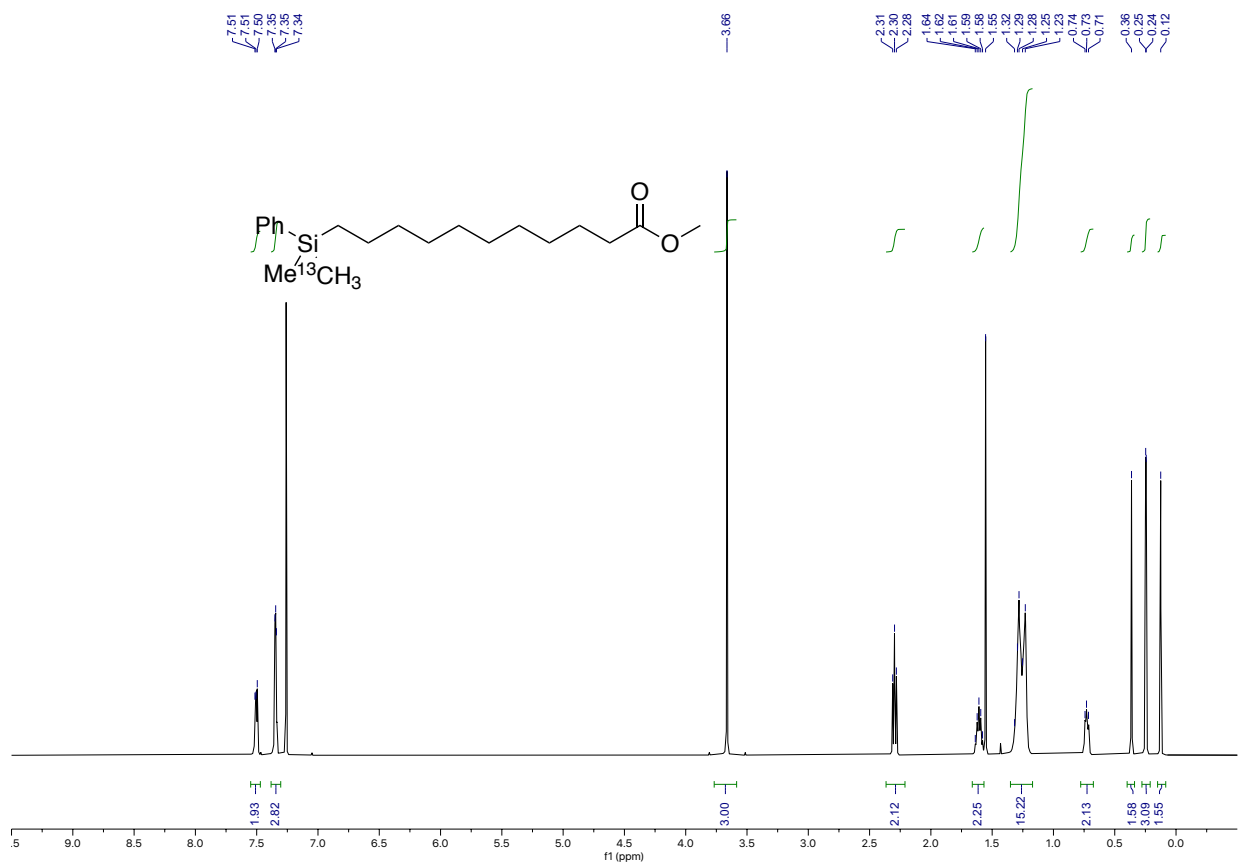


Figure 2.12.8.52. ^1H NMR spectra of intermediate J

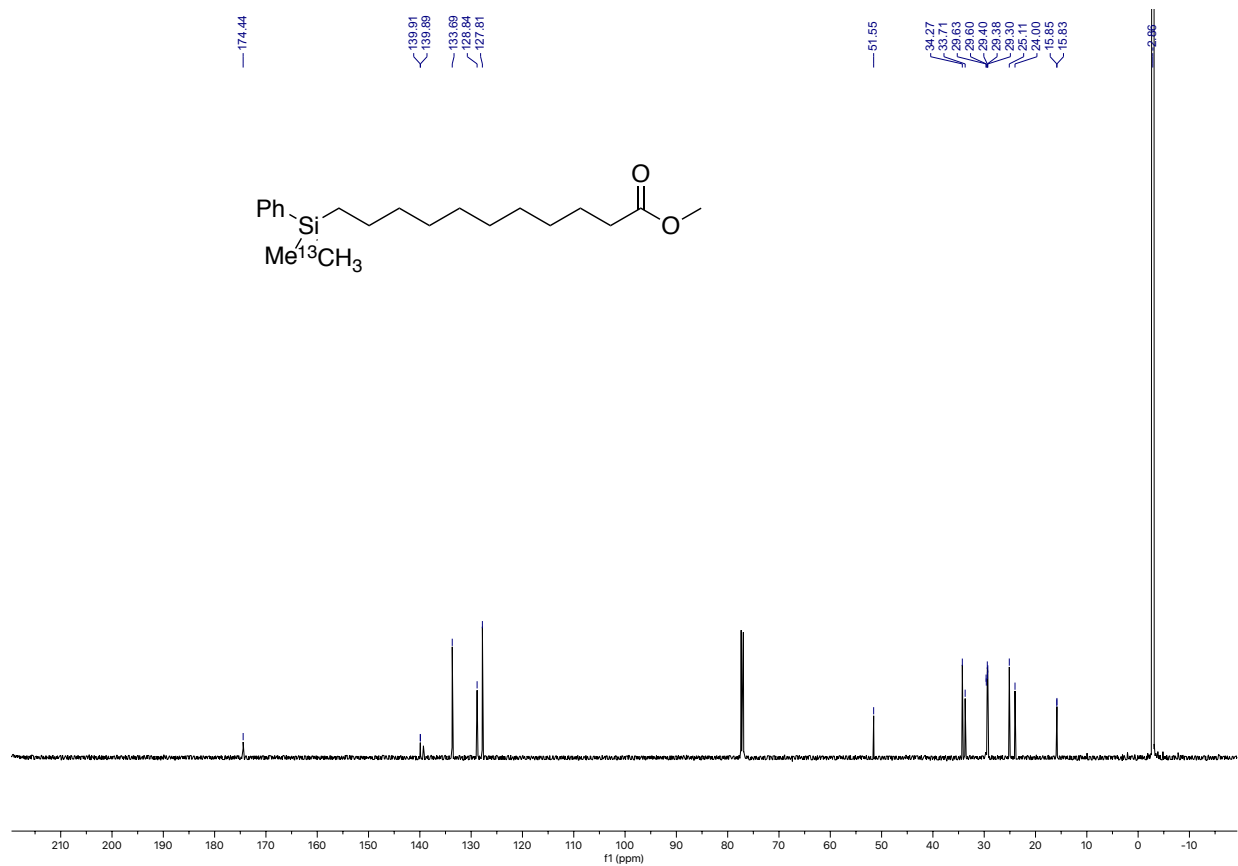


Figure 2.12.8.53. ^{13}C NMR spectra of intermediate J

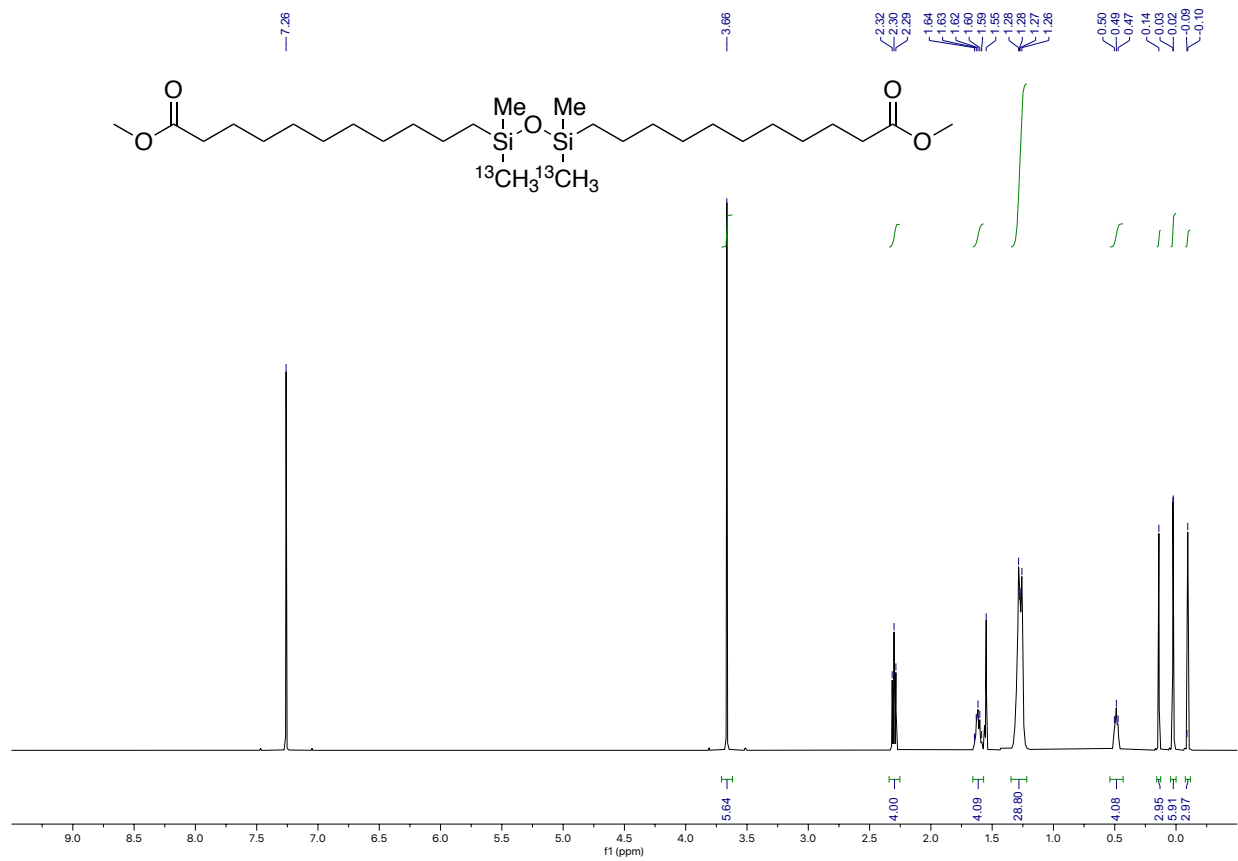


Figure 2.12.8.54. ^1H NMR spectra of compound 13

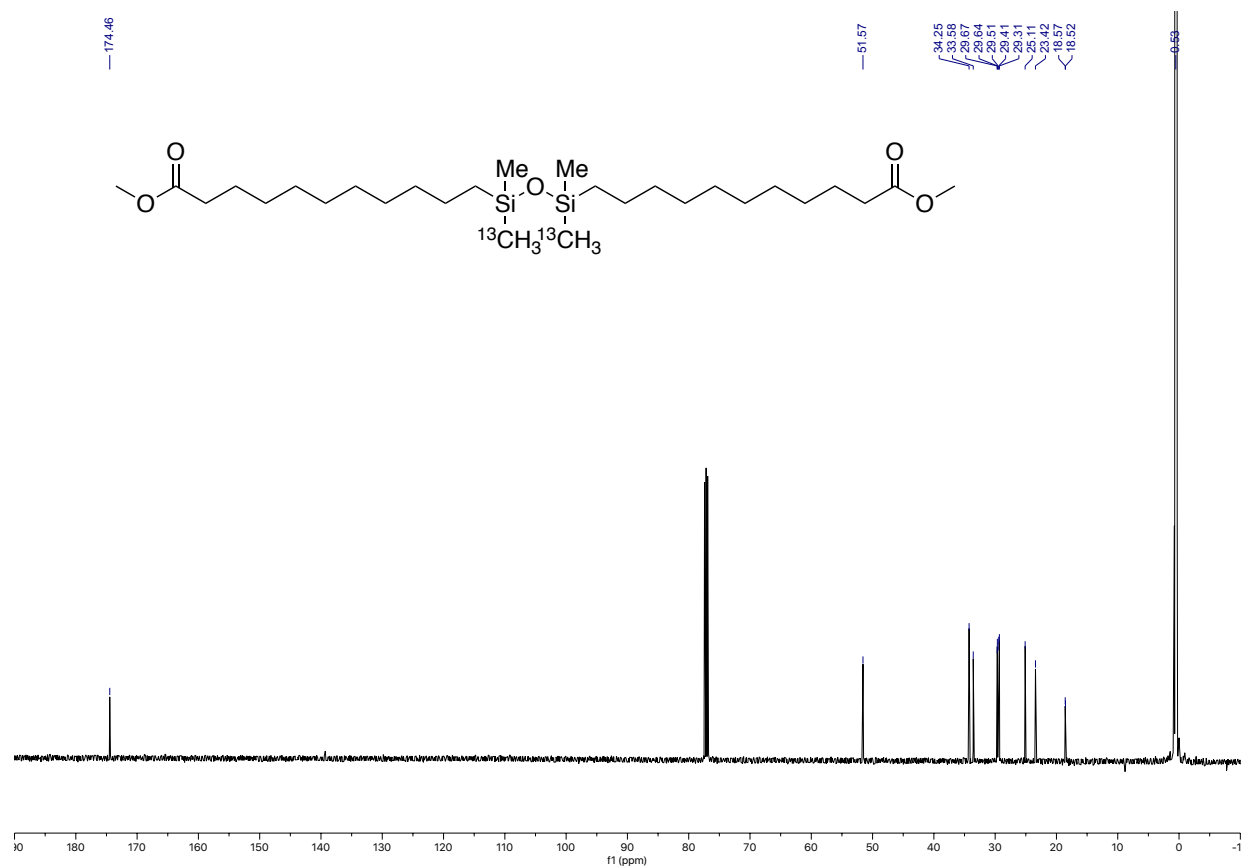


Figure 2.12.8.55. ^{13}C NMR spectra of compound 13

2.12.9 TGA and DSC (2nd cycle) graph of polymers

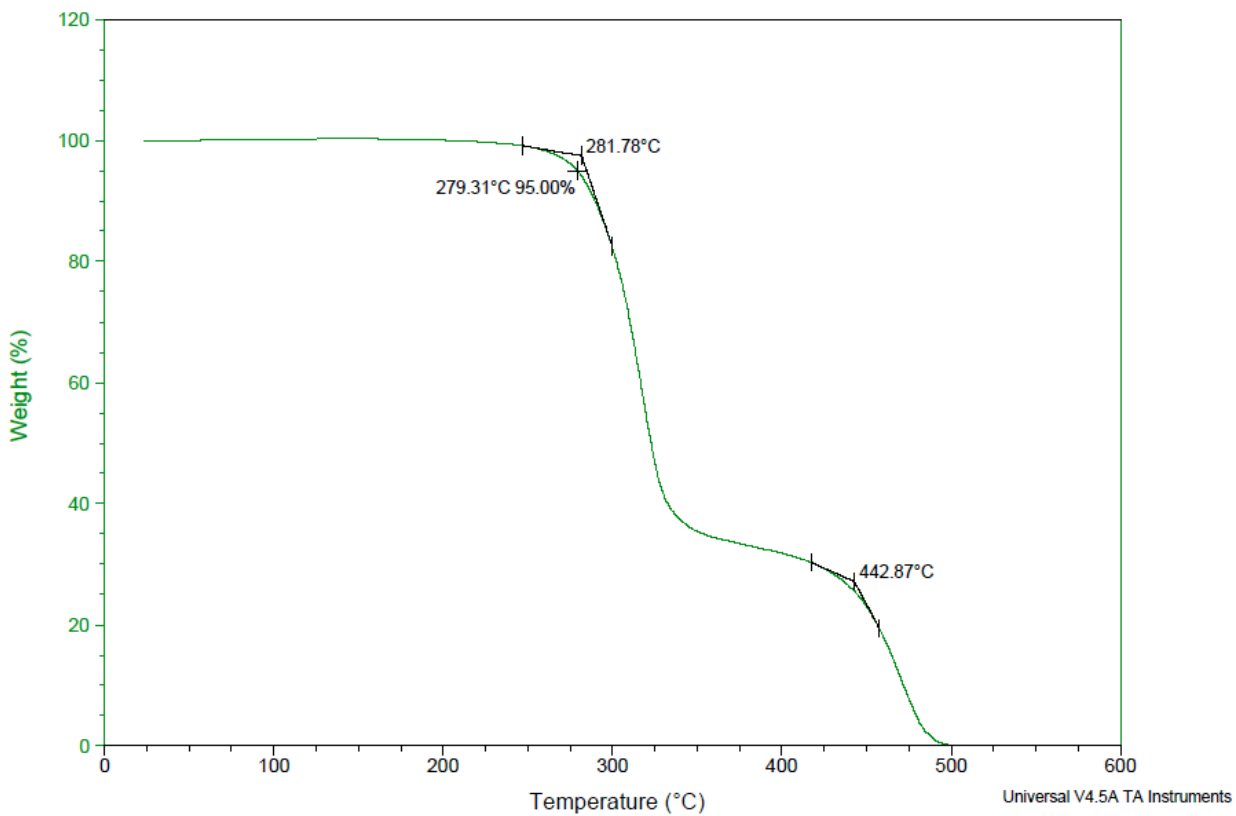


Figure 2.12.9.1. TGA curve of polymer PU-3

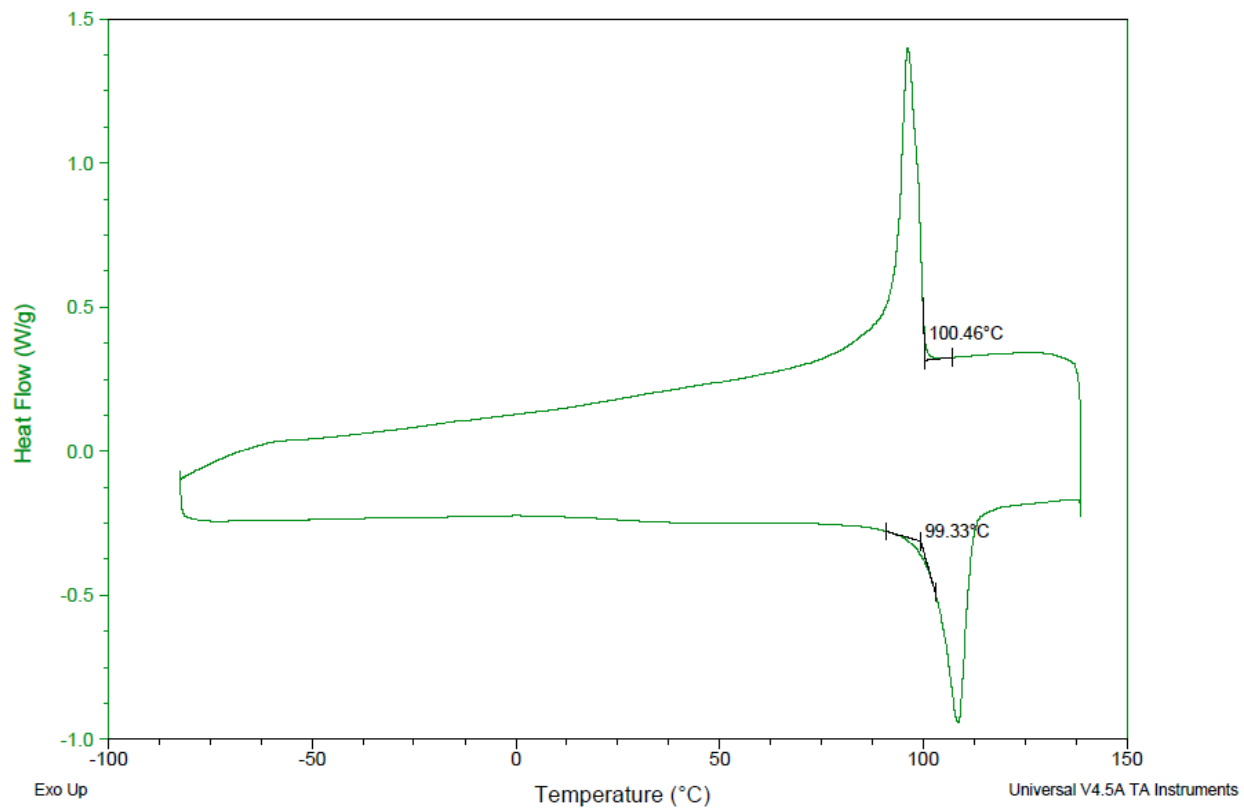


Figure 2.12.9.2. DSC curve of polymer **PU-3**

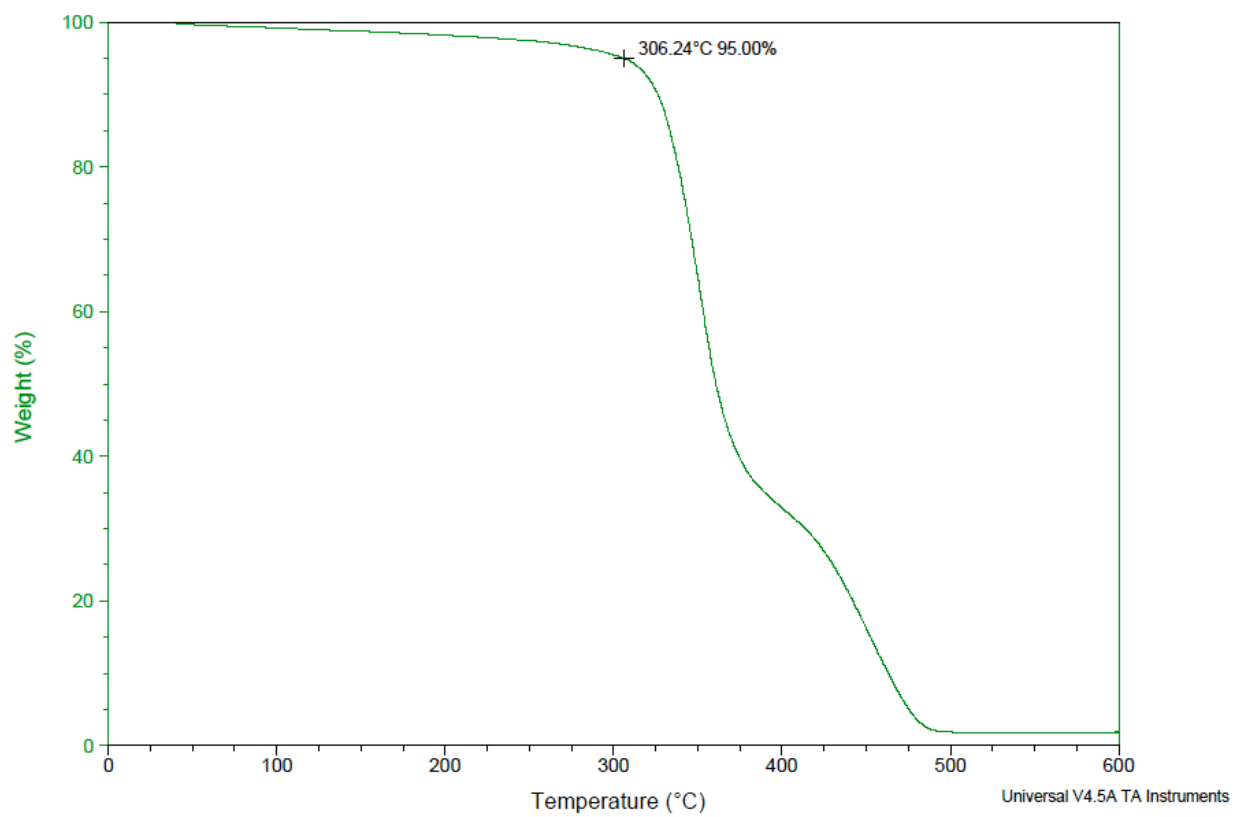


Figure 2.12.9.3. TGA curve of polymer **PC-3**

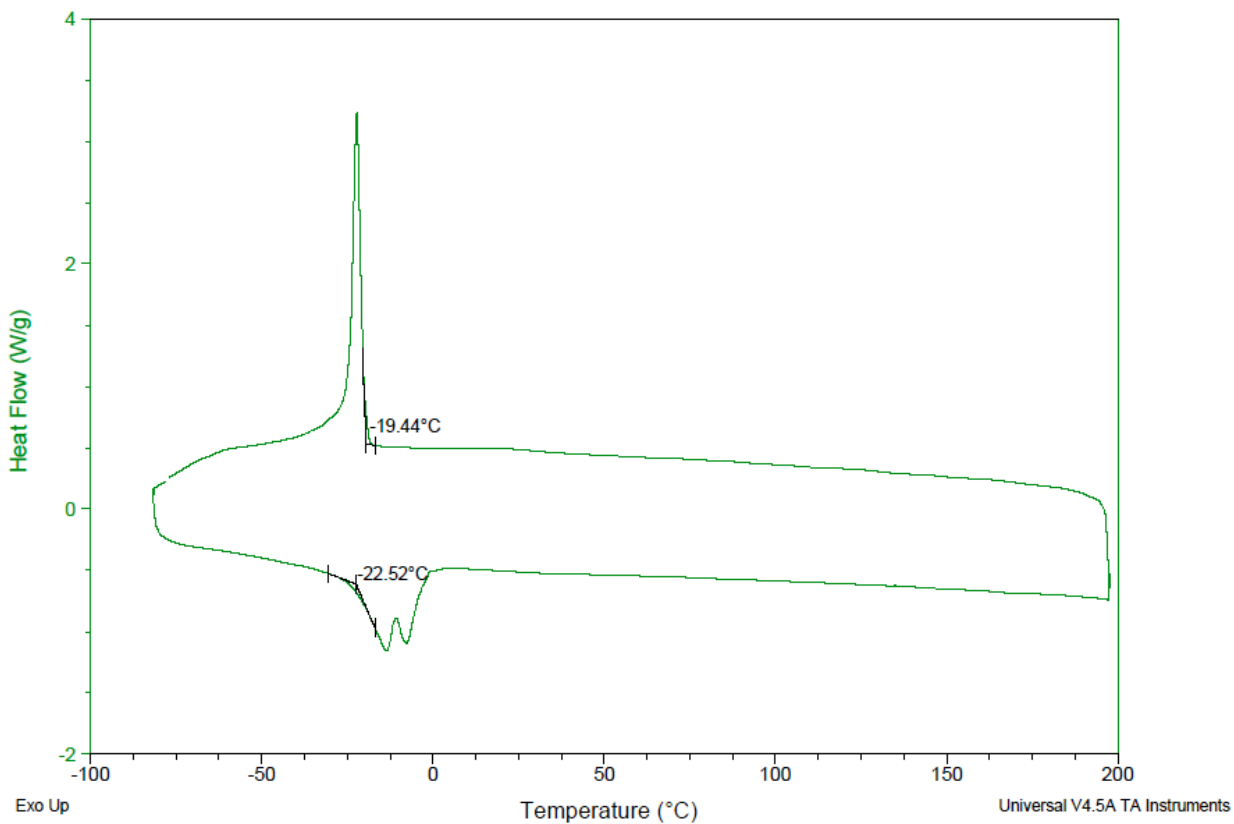


Figure 2.12.9.4. DSC curve of polymer **PC-3**

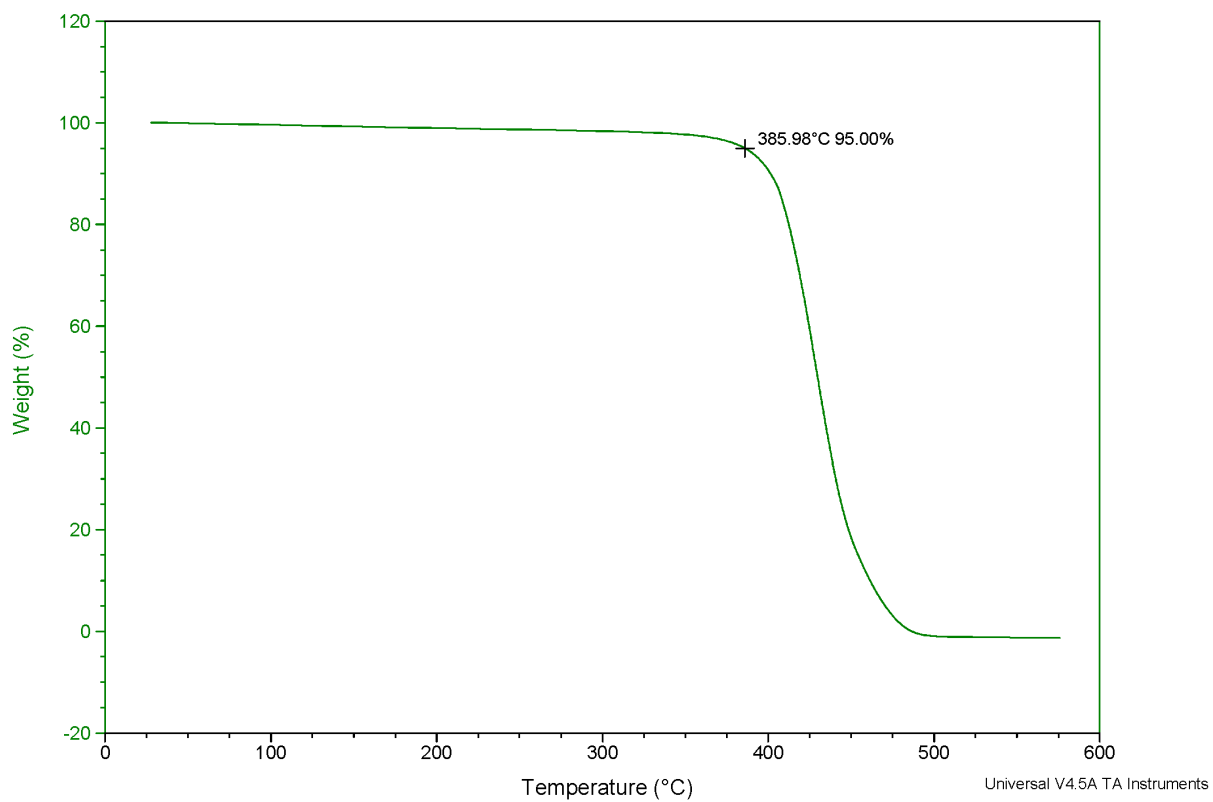


Figure 2.12.9.5. TGA curve of polymer **PE-2-3**

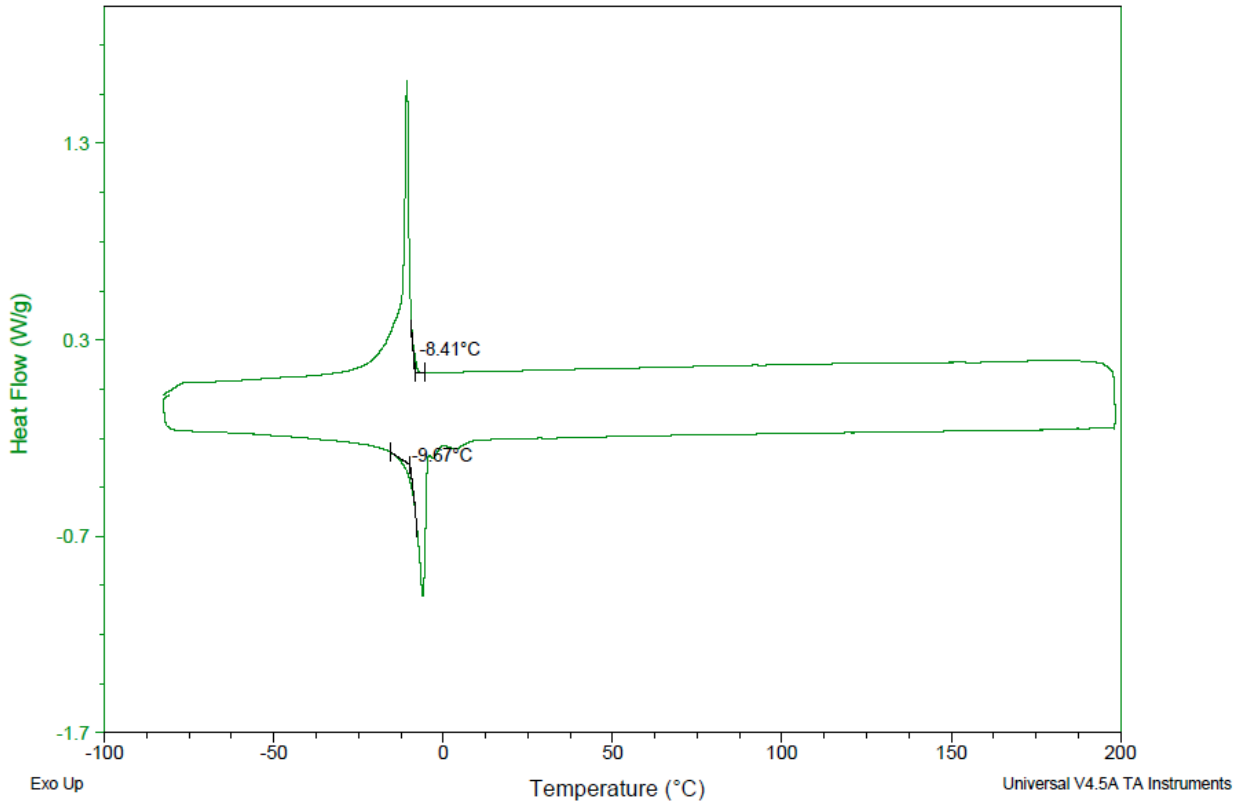


Figure 2.12.9.6. DSC curve of polymer **PE-2-3**

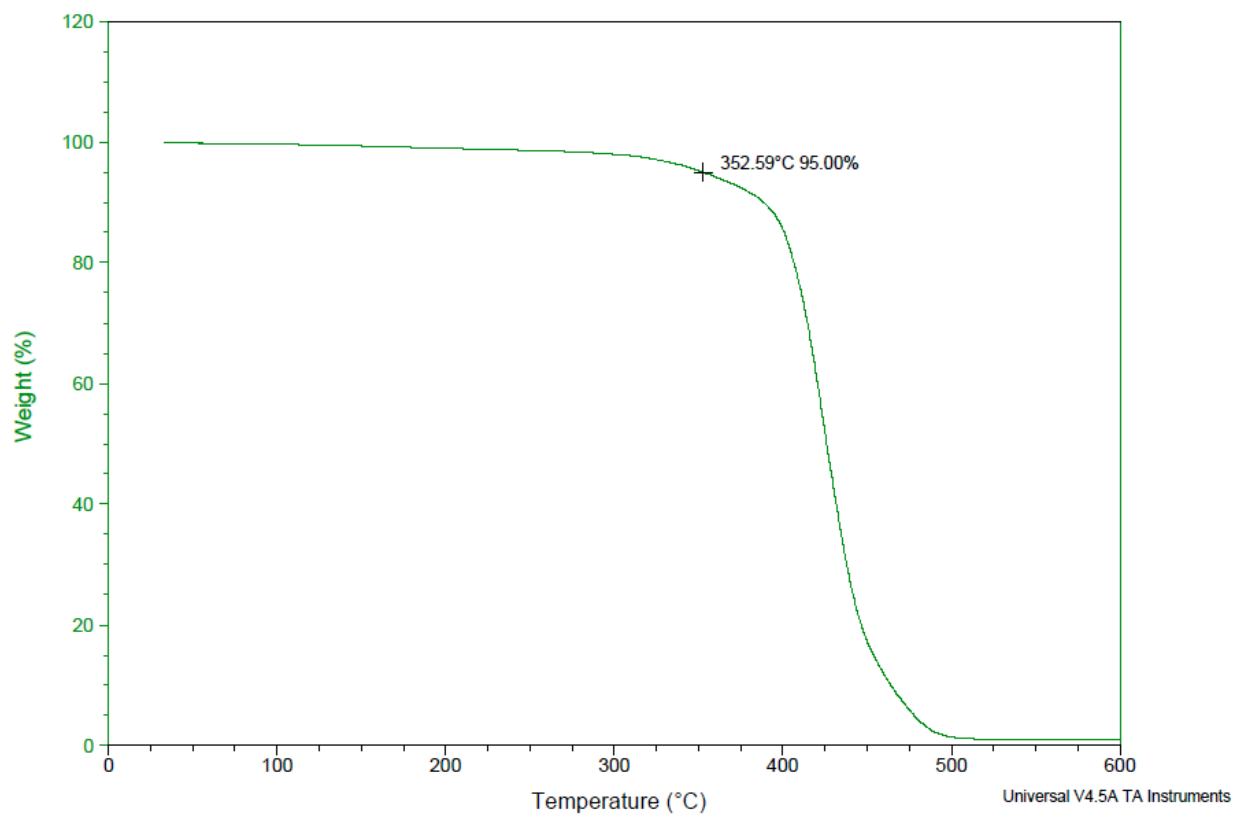


Figure 2.12.9.7. TGA curve of polymer **PE-2-C10**

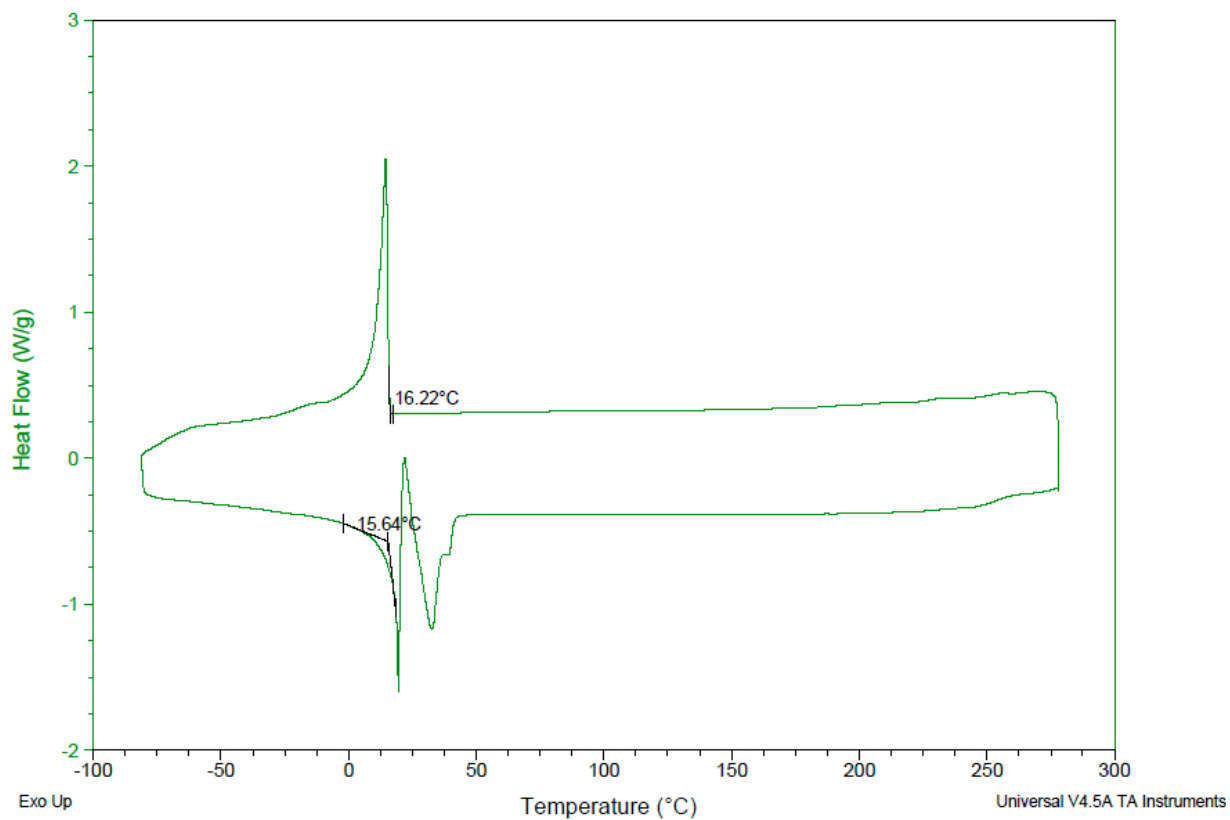


Figure 2.12.9.8. DSC curve of polymer **PE-2-C10**

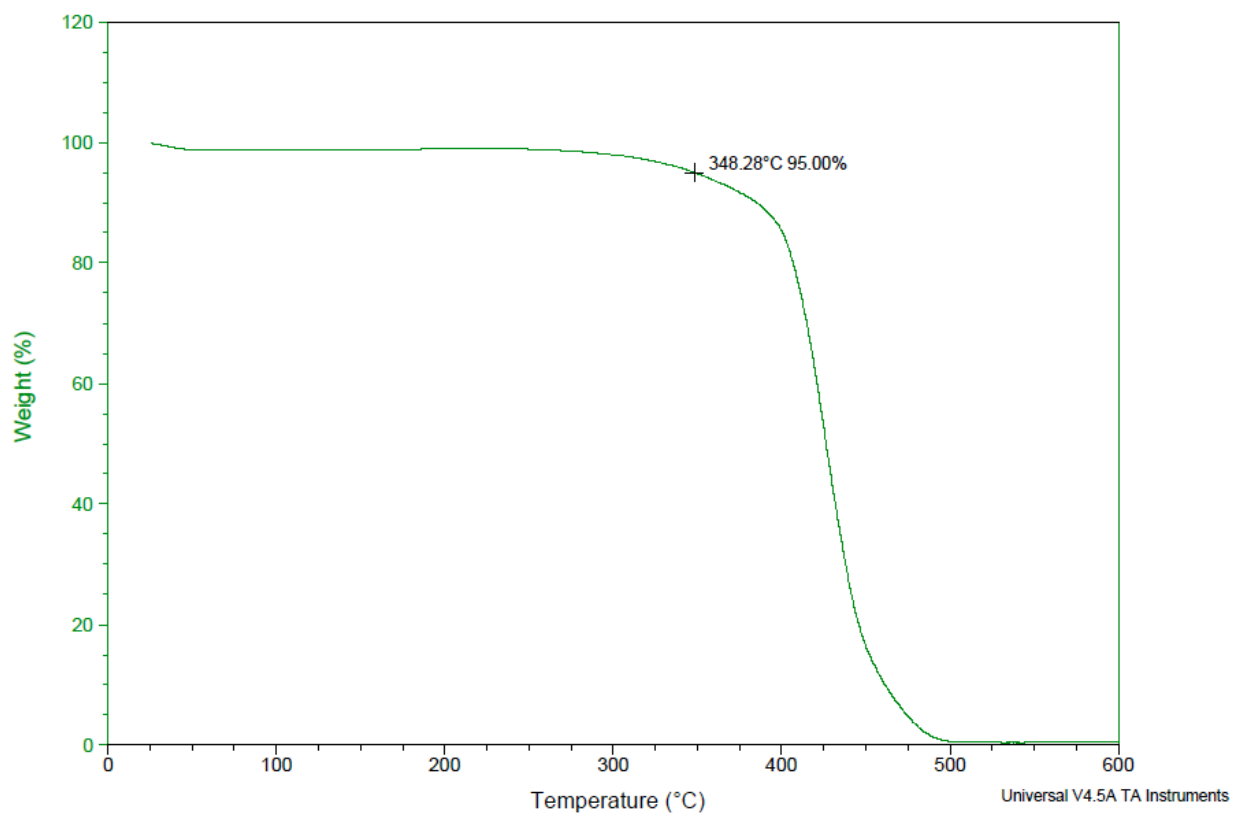


Figure 2.12.9.9. TGA curve of polymer **PE-2-C12**

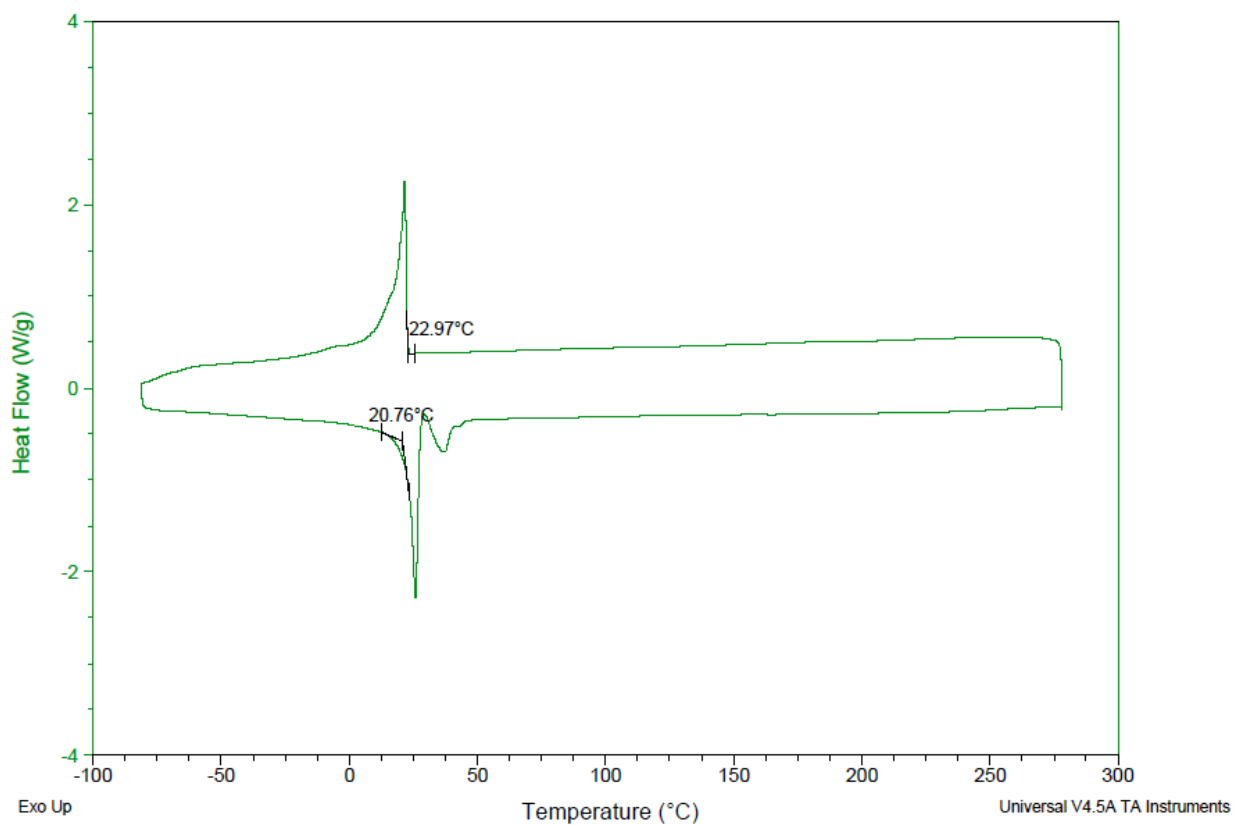


Figure 2.12.9.10. DSC curve of polymer PE-2-C12

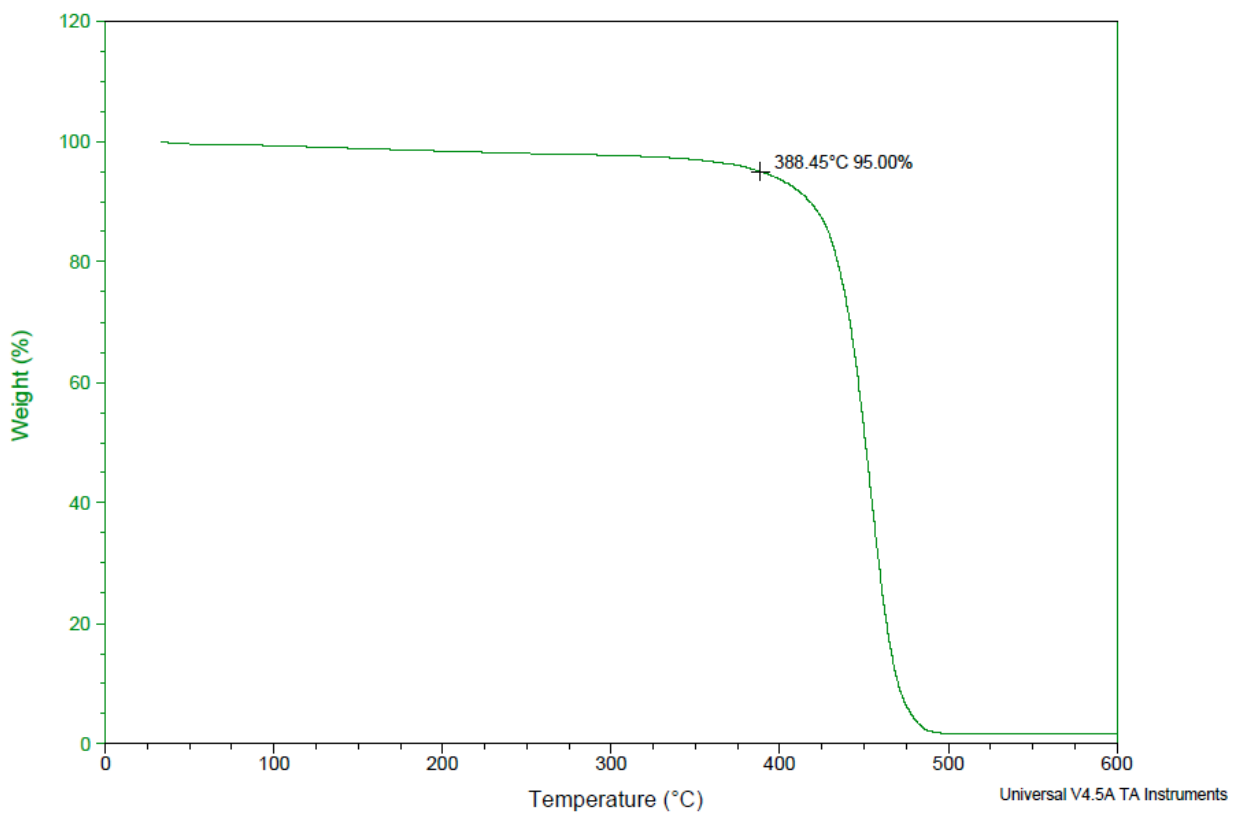


Figure 2.12.9.11. TGA curve of polymer **PA-2-C5**

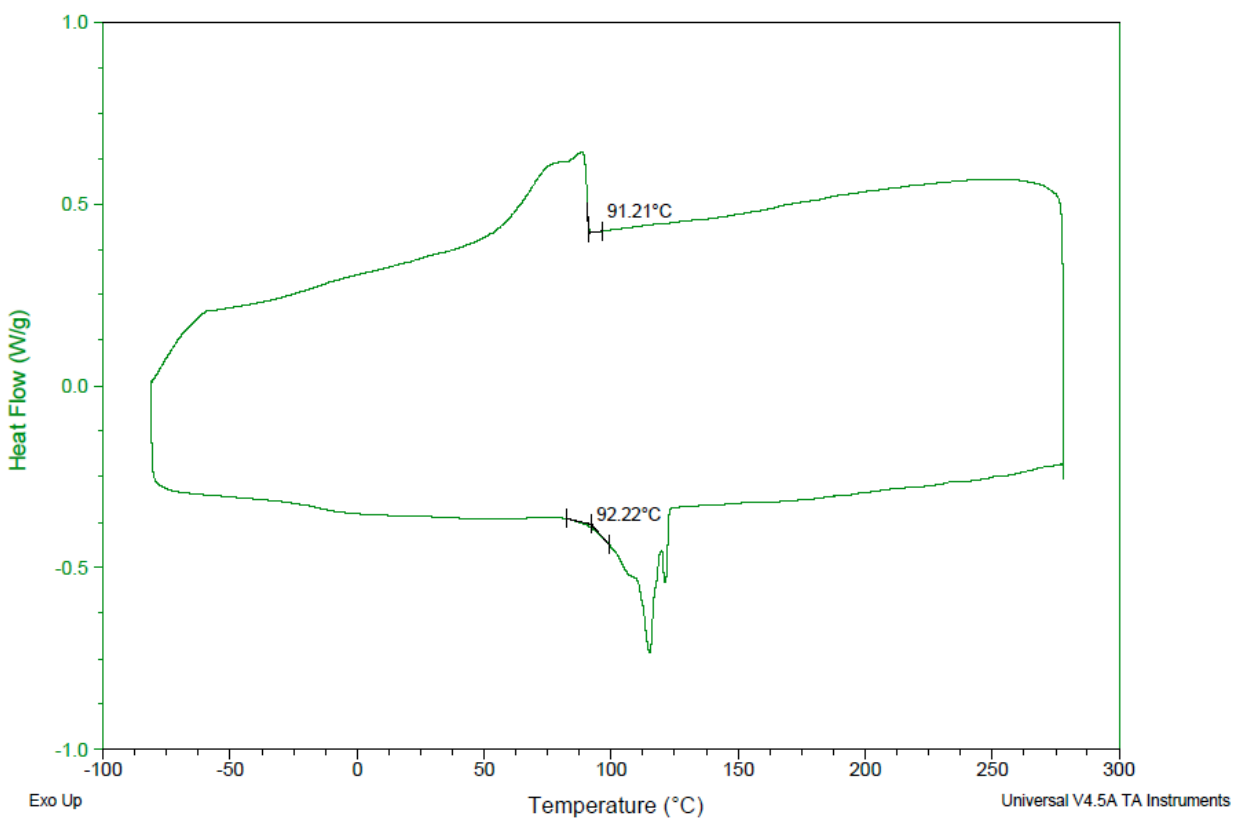


Figure 2.12.9.12. TGA curve of polymer PA-2-C5

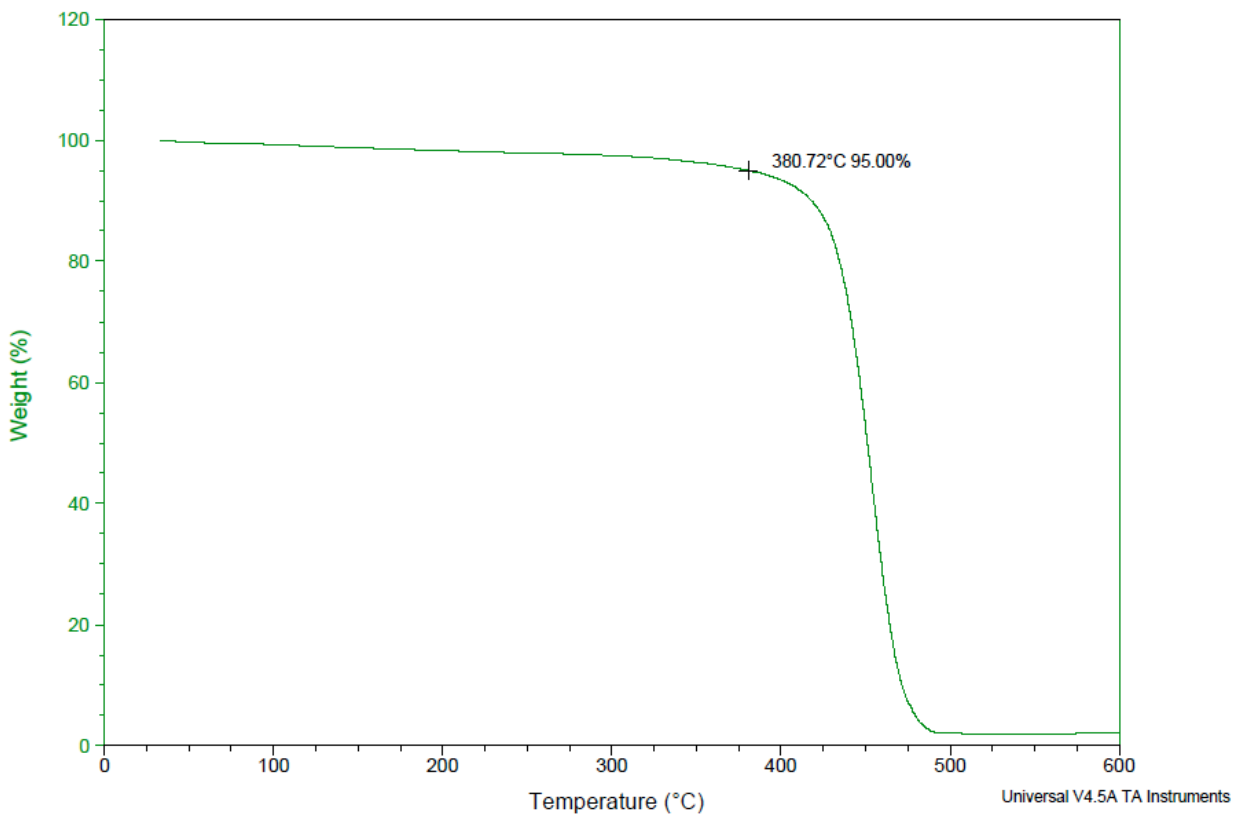


Figure 2.12.9.13. TGA curve of polymer PA-2-C12

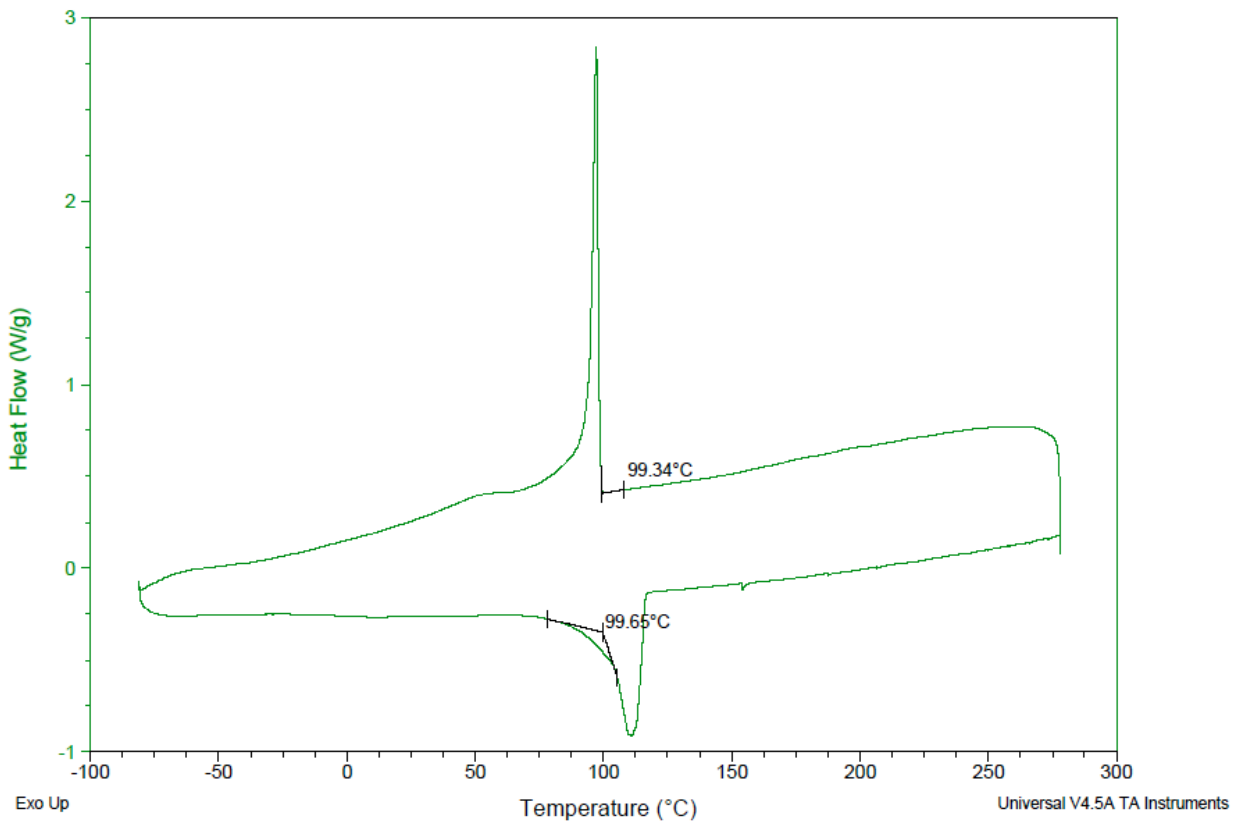


Figure 2.12.9.14. DSC curve of polymer PA-2-C12

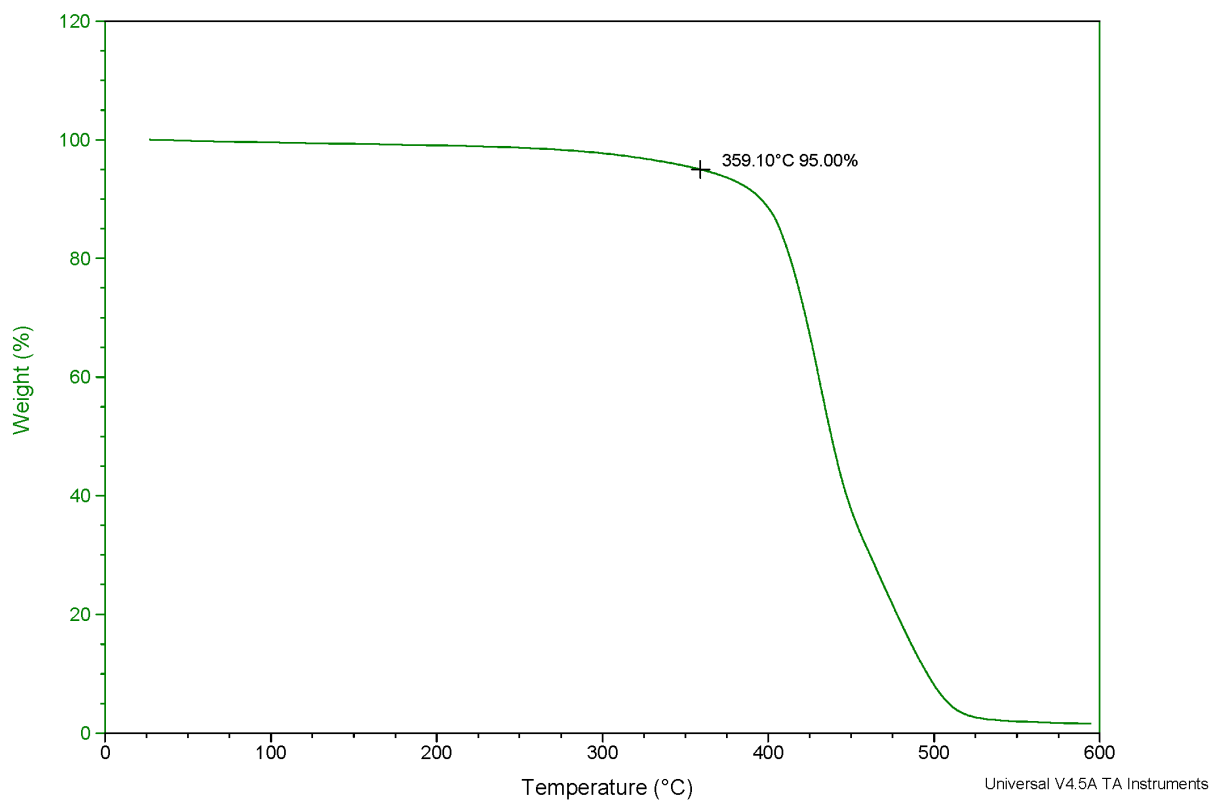


Figure 2.12.9.15. TGA curve of polymer **PE-6**

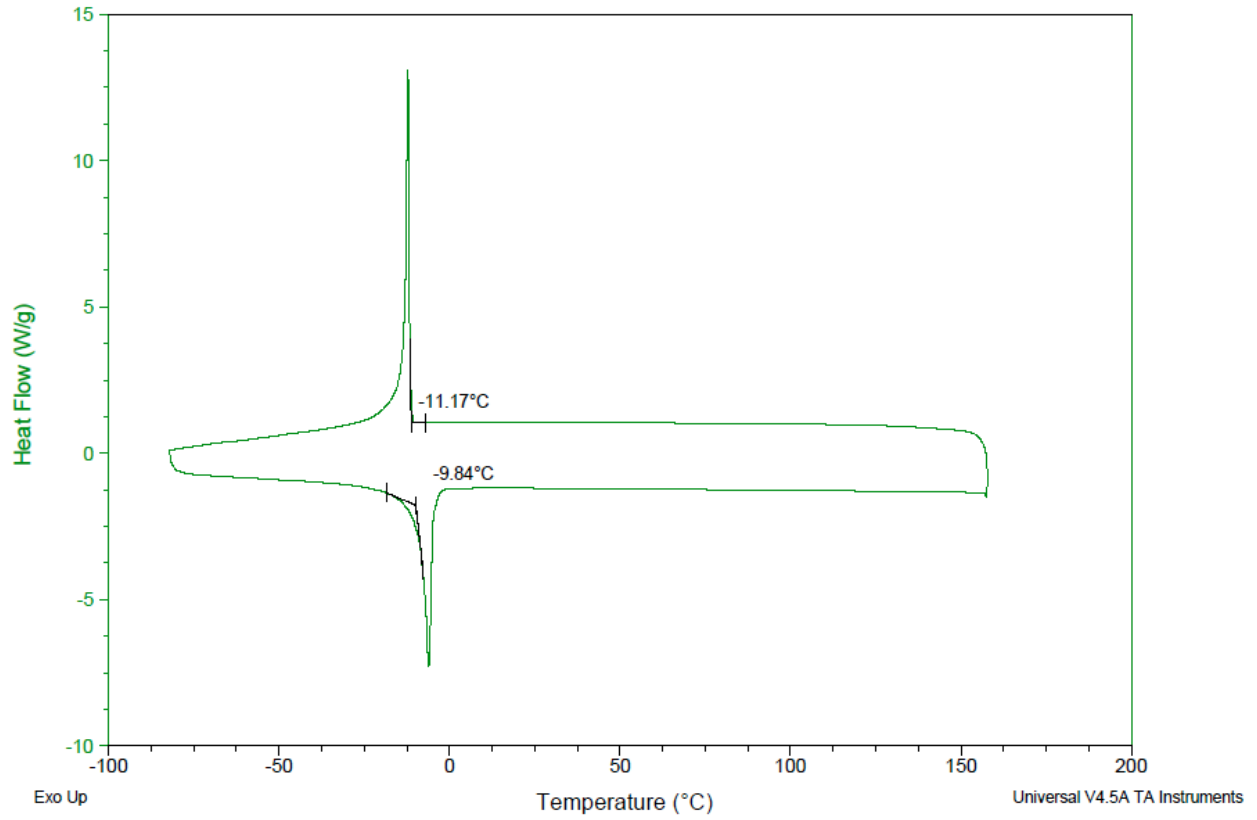


Figure 2.12.9.16. DSC curve of polymer **PE-6**

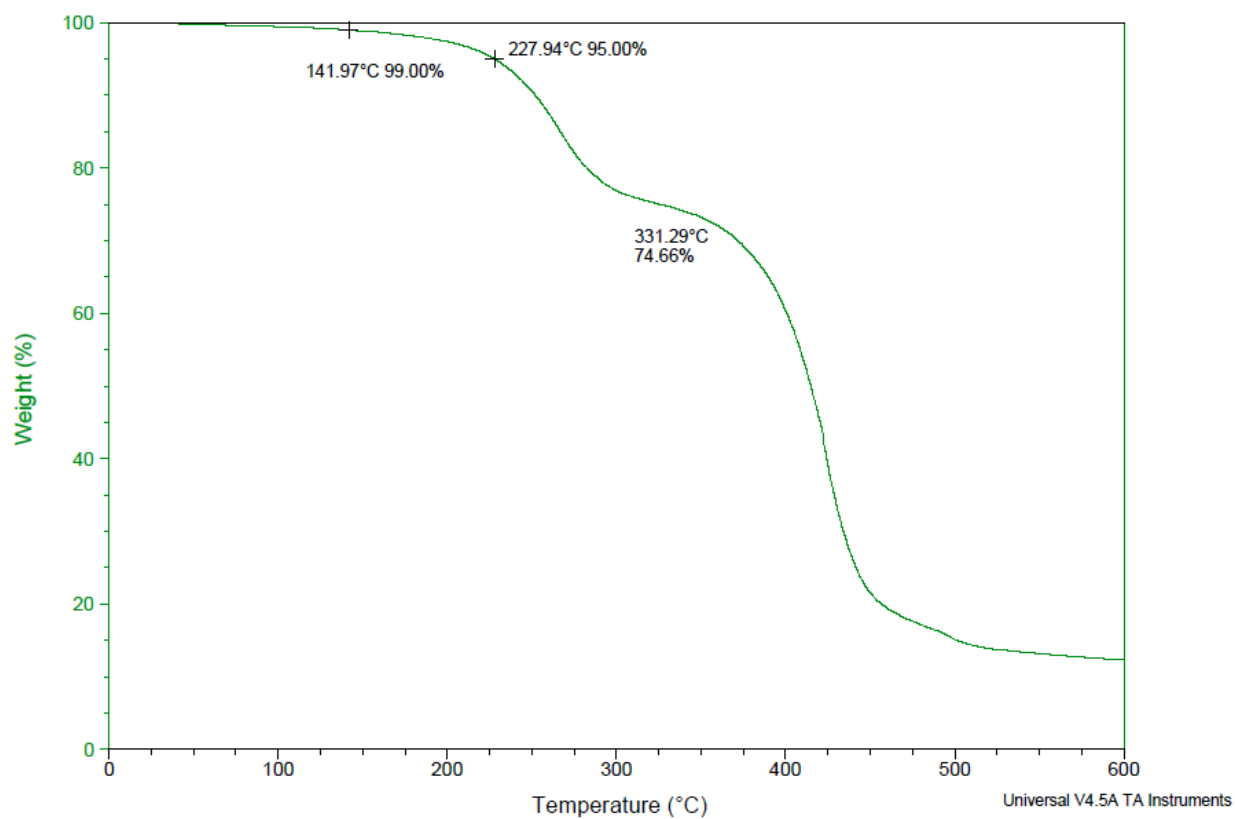


Figure 2.12.9.17. TGA curve of polymer PLLA₁₈-PE-644-PLLA₁₈

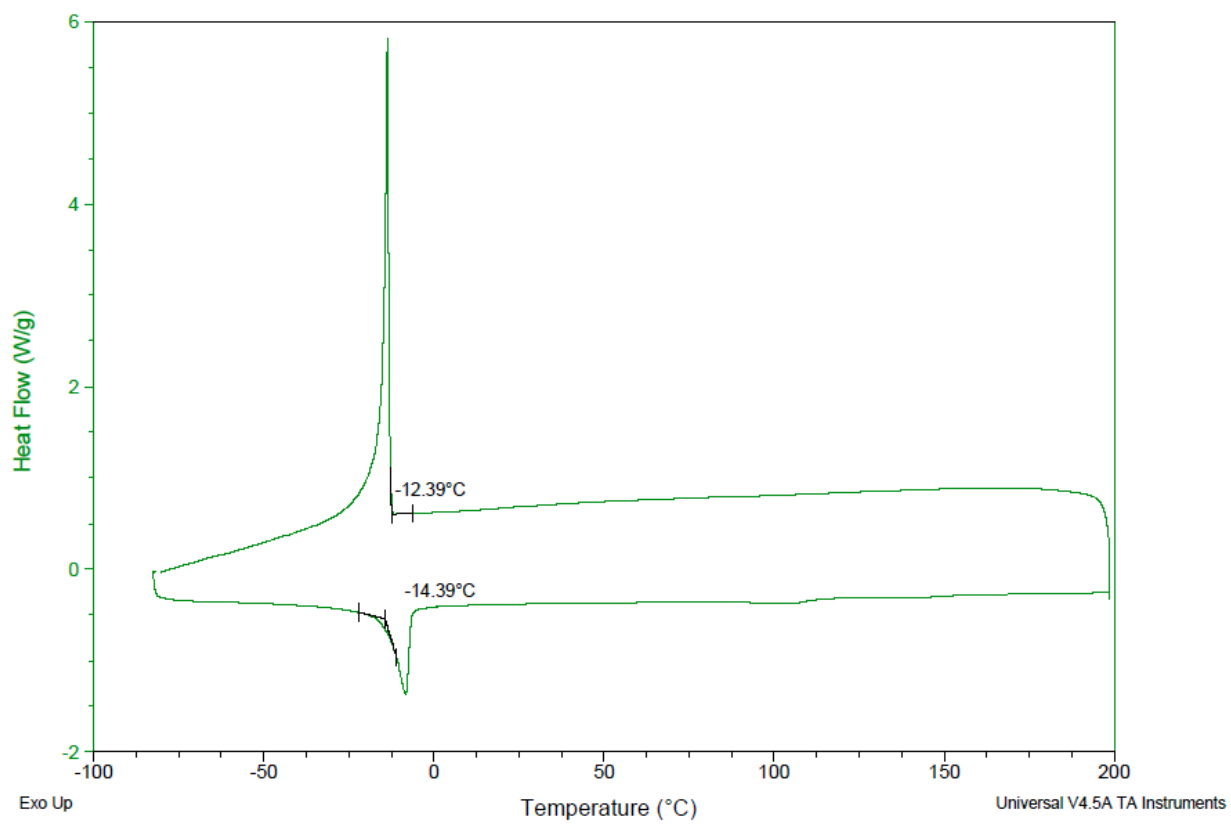


Figure 2.12.9.18. DSC curve of polymer **PLLA₁₈-PE-644-PLLA₁₈**

2.12.10 SEC traces of polymers

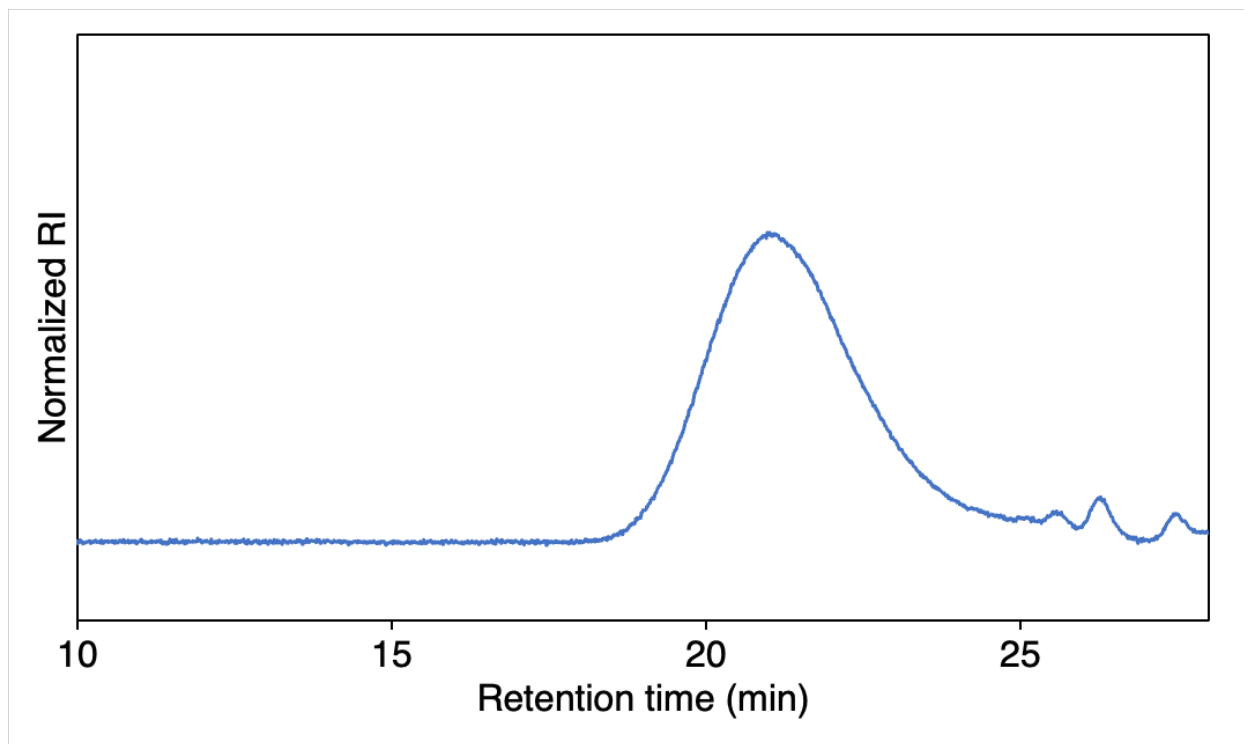


Figure 2.12.10.1. SEC trace of PU-3

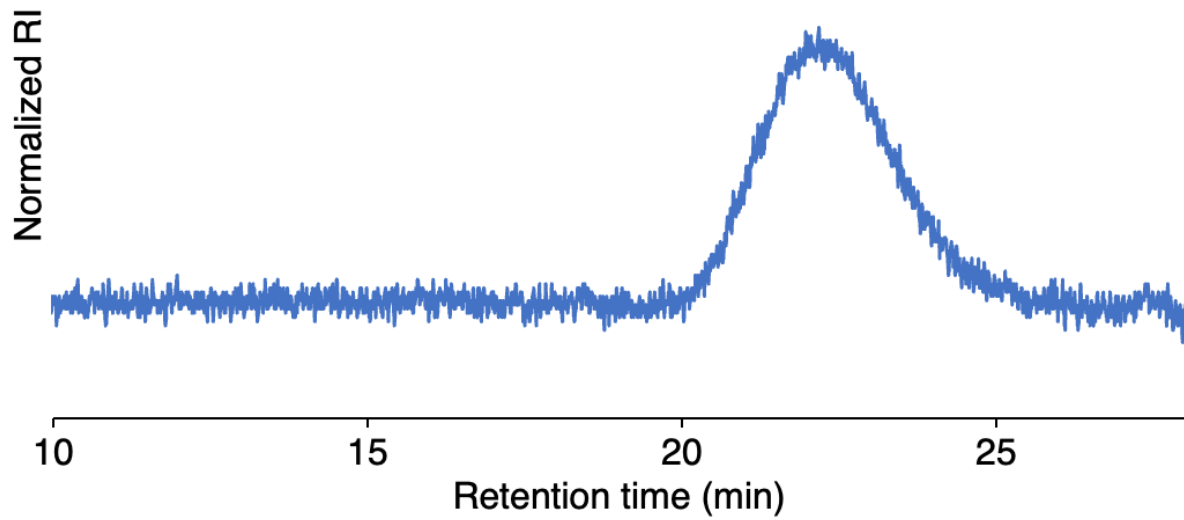


Figure 2.12.10.2. SEC trace of PC-3

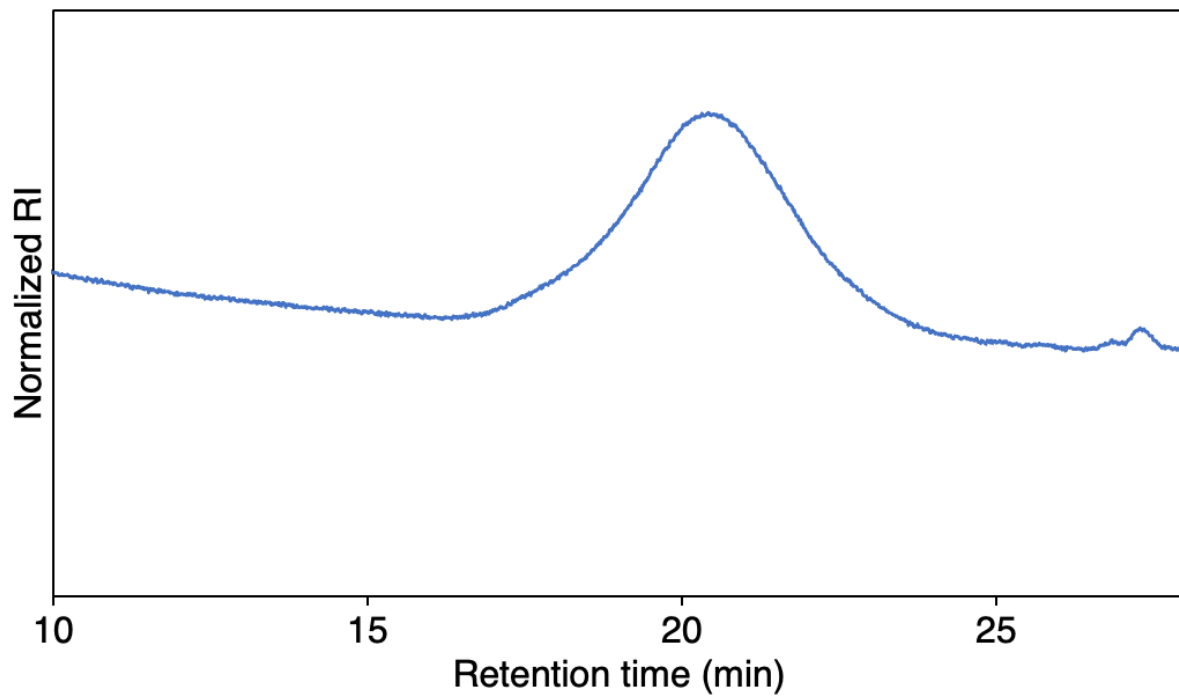


Figure 2.12.10.3. SEC trace of PE-2-3

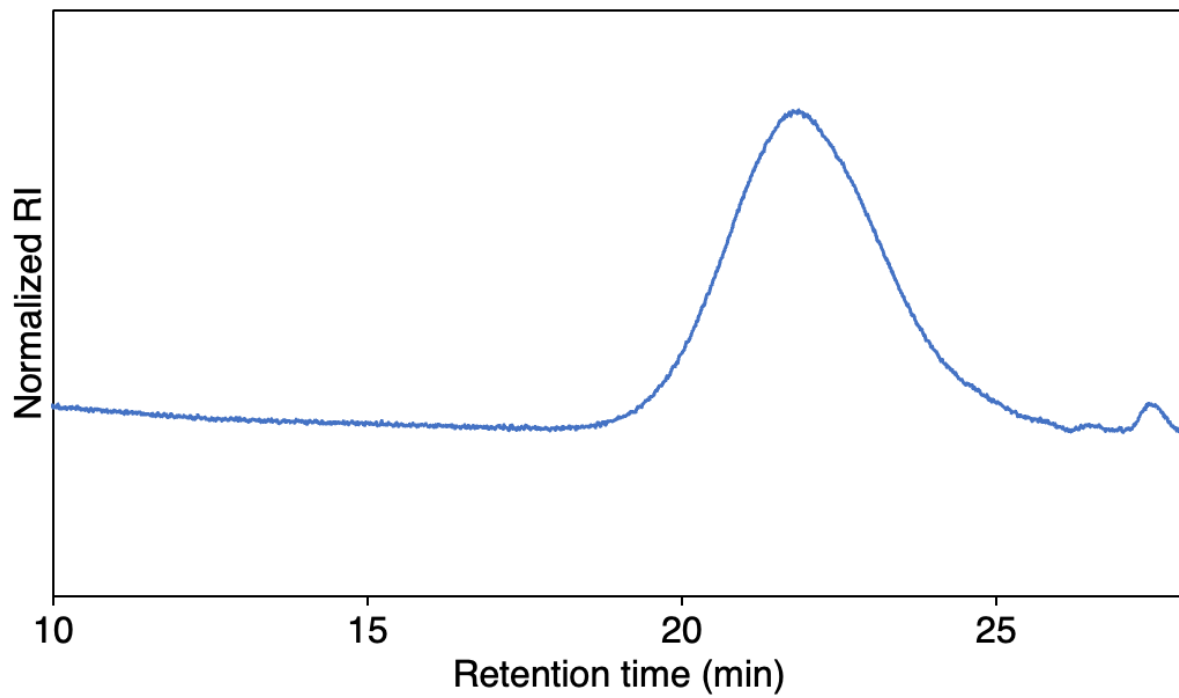


Figure 2.12.10.4. SEC trace of PE-2-C10

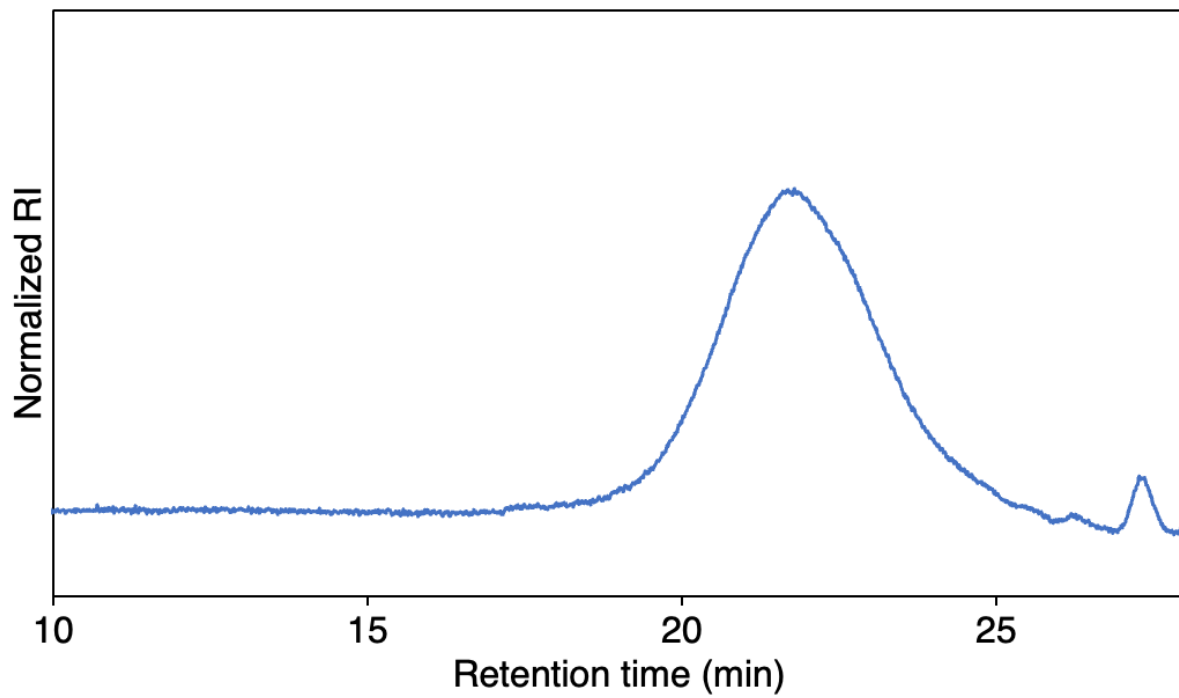


Figure 2.12.10.5. SEC trace of PE-2-C12

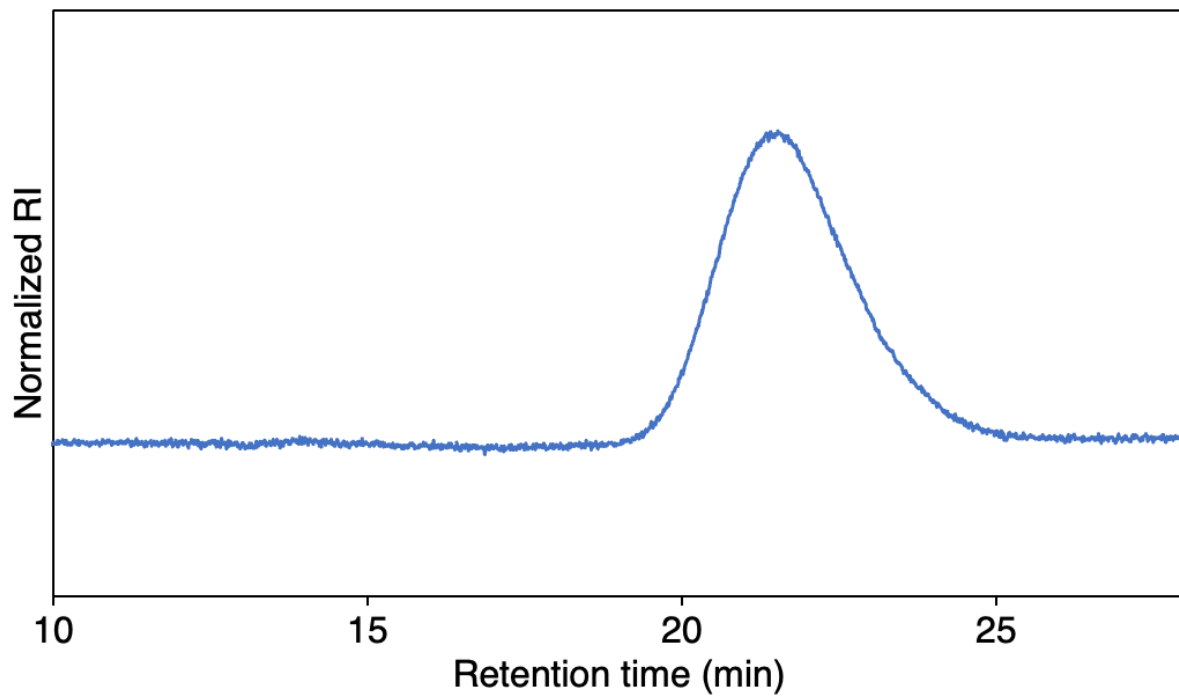


Figure 2.12.10.6. SEC trace of PE-6

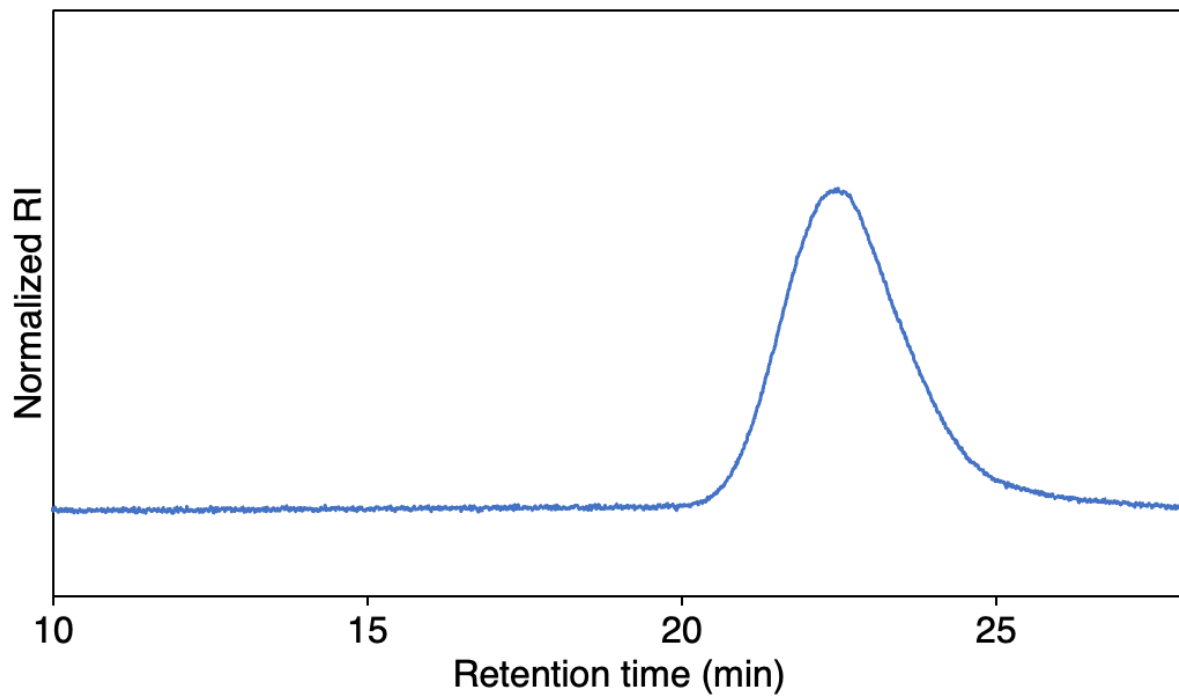


Figure 2.12.10.7. SEC trace of PLLA₁₈-PE-644-PLLA₁₈

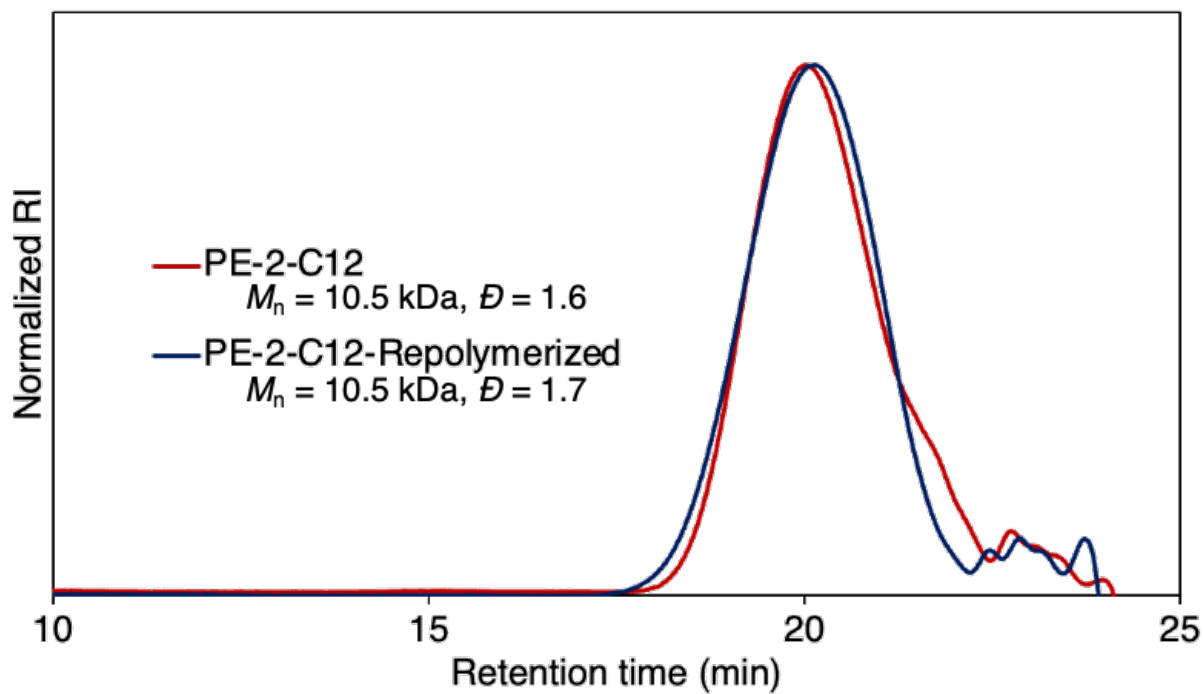


Figure 2.12.10.8. SEC traces of PE-2-C12 and repolymerized PE-2-C12

2.12.11 Procedure for tensile tests of PU-3

1. Sample preparation: Polymer films of **PU-3** ($350 \pm 50 \mu\text{m}$ thickness) were prepared by either drop casting from a solution of **PU-3** in THF or on a hot press at 120°C for 1 min to provide melts. Specifically, polymer samples between two Kapton films were pressed between steel plates at 2000 psi. Steel shims were used to control film thickness. The samples were then cooled at room temperature and cut into a dog-bone geometry using a cutting die (ASTM D-638V) to obtain samples that were 9.53 mm in length and 3.18 mm in width.

2. Experimental procedures for tensile tests: Tensile testing was conducted according to ASTM D638 on an Instron universal materials tester. Tensile stress and strain were measured at room temperature using an extension rate of 50 mm/min. Measurements were repeated for at least three samples, and average values are reported.

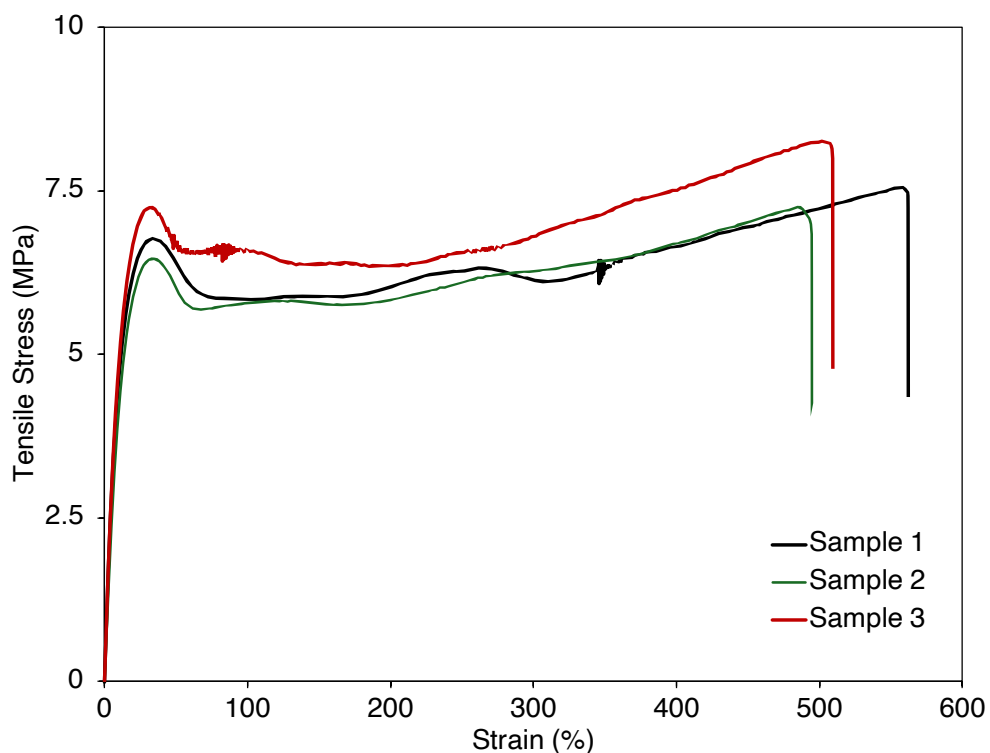


Figure 2.12.11.1. Stress-strain curves for different samples of **PU-3**

Table 2.12.11.1. Summary of results of tensile tests

Sample	Elongation at Break (%)	Young's Modulus (MPa)	Toughness (MJ/m^3)	Tensile Strength (MPa)	Yield Stress (MPa)
1	562.2	66.1	35.8	7.6	6.8
2	494.8	52.0	30.5	7.3	6.5
3	509.4	65.5	35.1	8.3	7.3

2.13 References

Chapter Three

Chemical Modification of Oxidized Polyethylene Enables Access to Functional Polyethylenes
with Greater Reuse

3.1 Introduction

Polyethylene is a ubiquitous commodity material that is used in applications that include food storage, packaging, and even medical devices.³ The favorable properties and low cost of polyethylene has led to a global production of over 150 million tons annually.³⁹ Because polyethylene is nonpolar, it is doped with additives, such as plasticizers and compatibilizers, that allow it to blend with more polar polymers to generate composite materials.^{30, 32} These additives disincentivize recycling and increase the volume of plastic waste.^{30, 38, 41, 63}

To address the shortcomings of polyethylene, functional polyolefins have been synthesized. These functional polyolefins possess enhanced properties that enable them to be more compatible with polar media.^{156, 157} Due to this increased compatibility, functional polyolefins could require fewer additives to generate consumer materials, thereby reducing the barriers to recovery and reuse.^{63, 158}

Functional polyolefins can be made by copolymerization of an α -olefin with a polar vinyl comonomer; however, catalytic copolymerizations are often plagued by poisoning of the catalysts by the polar functional group, and radical-initiated copolymerizations produce polymers with high degrees of branching.^{41, 63, 159} Furthermore, the degree of functional-group incorporation and sequence distribution is challenging to control in copolymerizations because of the difference in relative rates of polymerization of each monomer.⁶³

Functional polyolefins also can be made by installation of the functional group after the polyolefin has been prepared. By such post-polymerization functionalization, the polymer architecture can be controlled by the many polyolefin catalysts prior to functionalization, and functional groups can be installed onto this defined architecture and can be installed in a more uniform fashion.^{41, 62, 63, 160} Plasma treatment can functionalize polyolefins; however, these methods require specialized equipment, only modify the surface of the material, and are accompanied by substantial crosslinking and chain-scission.^{26, 66, 67} These drawbacks necessitate the development of more selective methods to functionalize polyolefins with bulk properties targeted for specific applications. Indeed, reactions catalyzed by transition metals or initiated by radicals have been developed to furnish functional polymers from polyethylenes of varying architecture to produce polymers with enhanced properties, increased compatibility with commercial polymers, and more facile degradation.^{41, 62, 63, 82, 83, 85, 86, 88}

However, many potentially valuable functional polymers cannot be prepared by copolymerization or current methods for C–H functionalization. The requisite monomers would poison current catalysts, and the functional groups cannot be installed because of the absence of known reactions or because the known reactions induce crosslinking or scission of polymer chains, the reagents and catalysts are poorly miscible with the nonpolar polymers, or the reactivity of the systems are low toward the types of C–H bonds in polyolefins, such as secondary C–H bonds of polyethylene, and the hindered primary or secondary C–H bonds in polypropylene or polyisobutylene.^{41, 63, 64}

To address this limitation, we envisioned that an oxidized polyethylene could be used as an intermediate to access a wide range of polyethylenes containing functional groups that, at least currently, cannot be prepared by the functionalization of C–H bonds (Figure 3.1.1).⁸³ Our group reported the oxidation of polyethylene catalyzed by a ruthenium-porphyrin complex to form *oxo*-polyethylene **1** containing an approximately equal ratio of hydroxyl groups and ketone units, and this material could serve as the foundation to prepare these materials. Moreover, interconversions of the alcohol and ketone could generate polymers with varying ratios of these functional groups or with just one of the two groups. By varying the ratios of these groups and installing additional

groups, we could modify the surface properties and the bulk mechanical properties to increase value, and we could vary the solubility to facilitate separations of polyethylenes with varying architectures or of polyethylenes from additional components of the composites for reuse.⁶⁵

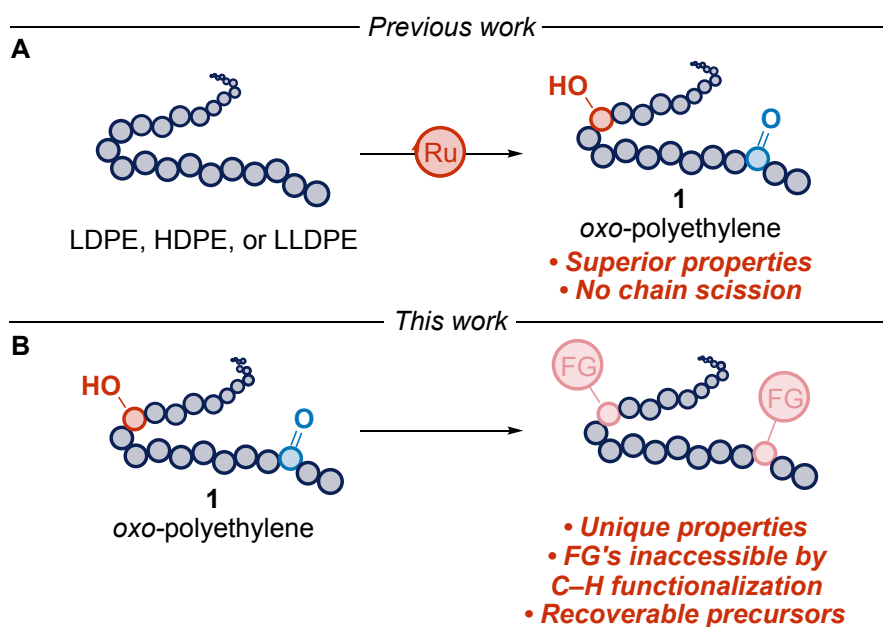


Figure 3.1.1. (A) Prior work: ruthenium-catalyzed oxidative functionalization of polyethylene. (B) This work: derivatization of *oxo*-polyethylene

Chemical transformations of alcohols and ketones are some of the most fundamental transformations of organic chemistry; however, few methods to derivatize functional groups installed on polyolefins have been reported.^{27, 63, 68, 69, 161} Methods to derivatize functionalized polyolefins commercially include ring-opening modification of grafted polyolefins containing maleimide⁶⁹, oxazoline²⁷, or glycidyl methacrylate⁶⁸ groups introduced by radical-based functionalization strategies that substantially modify the molecular weight of the polymer. Furthermore, derivatizations of these grafted-polyethylenes are limited towards reactions that tolerate high temperatures and nonpolar conditions in the polymer melt.

Consequently, we hypothesize that the dearth of strategies to derivatize functional polyolefins can be attributed to the lack of catalysts and reagents that are compatible with the nonpolar nature of polymer chains, that are tolerant of the high temperatures required to process polyolefins, and that are easily separable after functionalization. The combination of these factors renders many reactions that functionalize small molecules difficult to apply to polyolefins.

Here, we report methods to derivatize *oxo*-polyethylene **1** to access polyethylenes containing solely hydroxyl groups, solely ketone units, and a series of groups that would be challenging to install directly from unmodified polyethylene, as well as grafts initiated by these groups that can increase compatibility of polyethylenes with polar materials. In concert, we have determined the effect of these functional groups on both surface and bulk properties. Finally, we show that hydrolysis of the pendant functional groups on these polymers can be conducted to revert them to their respective *oxo* precursors for reuse. The results of these studies illustrate the challenge of translating classical transformations of small molecules to the interconversion of functional groups on polyolefins. Yet, they also show that the superior properties, relative to their unfunctionalized counterparts, capacity to be derived from waste plastics, and recoverability of these functional

polymers shows that the reaction chemistry on polyethylenes shown here charts a path to overcome the limitations in compatibility and chemical recycling of unfunctionalized material.

3.2 Synthesis of Monofunctional *keto*-Polyethylene

Our Ru-catalyzed oxidation of low density polyethylene (LDPE), high density polyethylene (HDPE), and linear-low density polyethylene (LLDPE) generates *oxo*-polyethylene **1** that possesses a ratio of hydroxyl groups to ketones that is close to 1 : 1 and molecular weights that are nearly unchanged from the starting polymer.⁸³ The alcohol and ketone units of this material were shown to provide it with enhanced wettability and adhesion. To examine the effect of each functional group and the ratio of the two functional groups on the properties of the material, we first sought to synthesize monofunctional polyethylenes containing only ketone or alcohol groups.

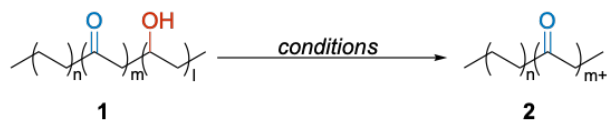
We began by investigating conditions to convert polymer **1** to *keto*-polyethylene **2**, which would contain ketones as the only *oxo* units by oxidation of the alcohols (Table 3.2.1). *Oxo*-polyethylene **1** synthesized from LDPE was selected for all transformations because it dissolves faster than HDPE and LLDPE in organic solvents, and it is commonly used in materials. Conditions that readily oxidize small molecules were tested for the oxidation of polymer **1**, but no conversion of the alcohols in polymer **1** to ketones was observed, as judged by ¹H NMR spectroscopy. These conditions included DMSO-based oxidations, such as the Pfitzner–Moffat and Albright–Goldman reactions, and sodium hypochlorite based oxidations.¹⁶² The incompatibility of oxidants, such as sodium hypochlorite, with the high temperatures and the immiscibility of DMSO in nonpolar solvents required to dissolve the polymer prevented the oxidation of polymer **1** to polymer **2** by these classical methods.^{162, 163} The inability of classical stoichiometric oxidations to furnish polymer **2** highlights the challenges of applying transformations of small molecules to polyolefins. To overcome the incompatibility of oxidizing agents at high temperatures, transfer hydrogenation reactions with catalysts tolerant of high temperatures were pursued. Reactions of *oxo*-polyethylene **1** with aluminum-based catalysts that are suitable with DCM, a solvent that dissolves polymer **1** at 80 °C, were either low-yielding or formed no product, even at superstoichiometric loadings of aluminum (Table 3.2.1, entries 1–4).

In contrast to these classical oxidations, catalytic dehydrogenations of alcohols with ruthenium and iridium complexes were examined to increase the ketone content of the polymer. These reactions were examined because they are known to occur at high temperatures in nonpolar media.¹⁶⁴⁻¹⁶⁷ Ruthenium-based catalysts used in conjunction with either acetone or *m*CPBA as oxidant either only partially oxidized polymer **1** or did not react (Table 3.2.1, entries 5–6). In contrast, oxidation of polymer **1** to *keto*-polyethylene **2** occurred with pentamethylcyclopentadienyl iridium di-chloride dimer ([Cp*IrCl₂]₂) as the catalyst and acetone as the hydrogen acceptor in toluene at 140 °C to high conversion (Table 3.2.1, entries 9–10).

The reaction mixture was homogeneous, indicating complete dissolution of the polyethylene in the toluene solvent. In the absence of acetone, complete oxidation was also observed, but a higher catalyst loading was needed (Table 3.2.1, entry 7). Most likely, this acceptorless dehydrogenation occurs because the high operating temperature facilitates the elimination of dihydrogen from the catalyst and the system, thus requiring no terminal oxidant to regenerate the active catalyst.¹⁶⁶ When the acceptorless oxidation was performed with 4 mol % [Cp*IrCl₂]₂ instead of 10 mol %, only 38% of the alcohols were converted to ketones as determined by NMR spectroscopy (Table 3.2.1, entry 8). Oxidation of polymer **1** to polymer **2** was achieved on a multigram scale with 3.75 mol % [Cp*IrCl₂]₂ per alcohol (0.05 mol % per monomer) as the catalyst

and acetone as the oxidant. No change in the molecular weight distribution was observed by high temperature size exclusion chromatography (HTSEC) when polymer **1** was oxidized in this fashion (Figure 3.3.1C). Thus, this iridium-catalyzed oxidation of *oxo*-polyethylene **1** with acetone as the oxidant is a suitable method of obtaining monofunctional *keto*-polyethylene **2** because of the availability of the oxidant, facile separation of byproducts, and amenability to scale-up.

Table 3.2.1. Investigation of Catalysts and Oxidants for the Oxidation of *oxo*-Polyethylene **1**



entry	catalyst	equiv catalyst ^b	oxidant	equiv oxidant ^b	temperature (°C)	time (h)	conversion (%) ^a
1 ^e	AlMe ₃	0.1	acetophenone	20	80	24	NR
2 ^e	AlMe ₃	0.1	benzophenone	20	80	24	NR
3 ^e	Al(O <i>i</i> Pr) ₃	2.4	acetone	10	80	24	3
4 ^e	Al(O <i>i</i> Pr) ₃	2.4	benzophenone	10	80	24	8
5 ^e	Ru(PPh) ₃ Cl ₂	0.1	acetone	660	80	24	54
6 ^e	Ru(PPh) ₃ Cl ₂	0.1	<i>m</i> CPBA	2	80	24	NR
7 ^{d,f}	(Cp*IrCl ₂) ₂	0.1	--	--	140	48	quant. ^d
8 ^{d,f}	(Cp*IrCl ₂) ₂	0.04	--	--	140	48	38
9 ^{d,f}	(Cp*IrCl ₂) ₂	0.1	acetone	660	140	48	quant. ^d
10 ^{d,f}	(Cp*IrCl ₂) ₂	0.04	acetone	20	140	48	quant. ^d

^aConversion of the alcohol groups to ketones as determined by ¹H NMR spectroscopy at room temperature in CDCl₃. ^bEquivalents with respect to the amount of alcohol groups on polymer **1**. ^cQuantitative conversion of alcohol groups into ketone groups as determined by ¹H NMR spectroscopy. ^dReaction performed with the addition of 1.0 equiv of K₂CO₃. ^eReaction performed in DCM. ^fReaction performed in PhMe.

3.3 Synthesis of Monofunctional *hydroxy*-Polyethylene

The equilibrium of transfer hydrogenations is well understood with small molecules and may be shifted selectively toward reduction in the presence of alcohols.^{168, 169} Thus, we sought to conduct the reduction of *oxo*-polyethylene **1** to furnish *hydroxy*-polyethylene **3**, a monofunctional polyethylene containing only alcohol units, by the transfer hydrogenation with isopropanol as reductant.

Attempts to reduce monofunctional polymer **2** in the presence of an excess of isopropanol and [Cp*IrCl₂]₂ led to recovery of a polyethylene containing both ketone and alcohol functional groups in a ratio of 2 : 1, as determined by ¹H NMR spectroscopy, and this ratio did not increase at longer reaction times or higher loadings of reductant. To suppress oxidation through the elimination of hydrogen gas, the reaction was performed under 1000 psig of hydrogen; however, reduction did not occur because of catalyst decomposition, as indicated by the formation of iridium black in the reaction mixture.

Thus, to conduct the ketone hydrogenation with a simple catalyst known for this transformation, we tested reactions catalyzed by ruthenium complexes ligated by diamine and phosphine ligands.¹⁶⁹ Initial attempts to reduce polymer **1** to polymer **3** in commonly used protic

solvents such as isopropanol or *tert*-butanol did not convert the ketones of polymer **1** to alcohols as determined by ^1H NMR and FTIR spectroscopy. We hypothesize that this lack of reactivity is caused by the insolubility of polymer **1** in these polar solvents. To address this lack of reactivity, we hypothesized that polymer **1** would be soluble in a less polar alcohol than isopropanol and *tert*-butanol. Indeed, when the solvent was switched to *tert*-amyl alcohol, the reduction of polymer **1** to polymer **3** with 4 mol % $[\text{Ru}(\text{PPh}_3)_3\text{Cl}_2]$ per ketone (0.06 mol % per monomer) as precatalyst with ethylene diamine (0.08% per monomer) under 750 psig of hydrogen as the reductant at 120 $^\circ\text{C}$ afforded quantitative conversion of the ketones to alcohols. A slight decrease in M_n was observed as judged by high-temperature size-exclusion chromatography (HTSEC) when polymer **1** was reduced in this manner (Figure 3.3.1C).

We also sought to prepare materials with varying ratios of alcohols to ketones along the polymer. To do so, we tested a series of reagents that would allow this ratio to be controlled by stoichiometry. Testing of aluminum and boron-based hydride agents showed that sodium borohydride and Super-Hydride[®] reduced polymer **2** to polymer **3**. A linear dependence of alcohol functionality with the loading of sodium borohydride was observed, indicating that the ratio of ketone to alcohol groups may be controlled simply by the amount of borohydride added. No change in M_n that would substantially impact the bulk properties of the material was observed by HTSEC (see Table 3.10.15.1) when polymer **3** was synthesized with sodium borohydride (Figure 3.3.1B).

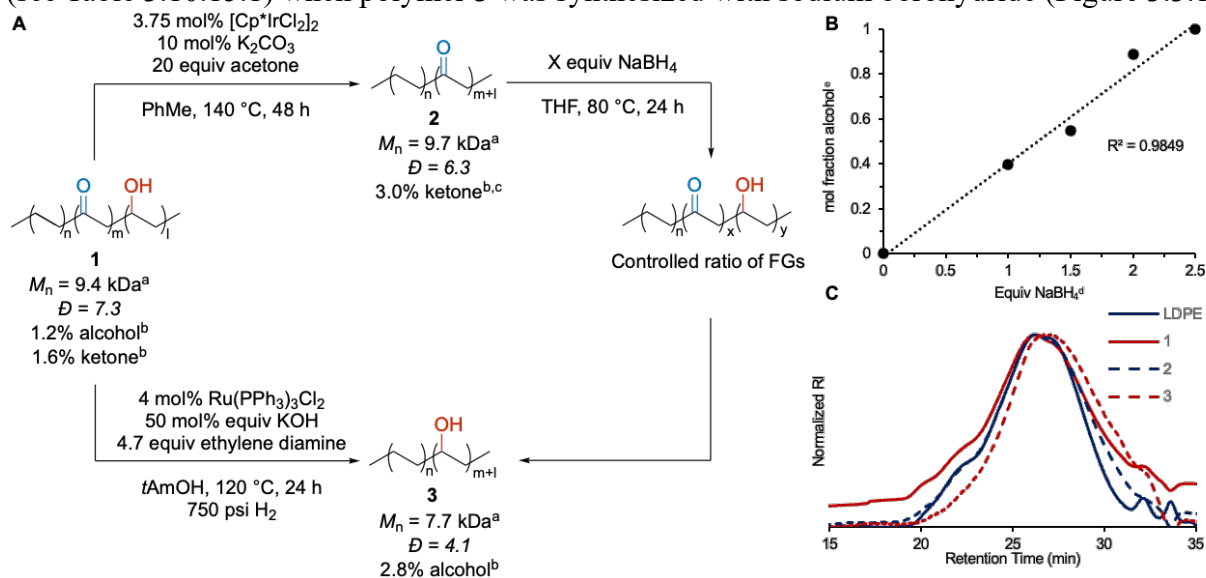


Figure 3.3.1. (A) Optimized conditions for the oxidation and reduction of polymer **1**. ^a M_n with respect to polyethylene standards. ^bDegree of functionalization with respect to monomer units as determined by ^1H NMR spectroscopy at 100 $^\circ\text{C}$. ^cThe small 0.2% discrepancy in percent functionality can likely be attributed to the inherent error of determining percent functionalization of a polymer by NMR spectroscopy. (B) Linear dependency of the amount of hydroxyl groups per equivalent of sodium borohydride. ^dEquivalents of NaBH_4 with respect to ketones. ^eRatio of number of alcohol units per sum of alcohol and ketone units. (C) HTSEC traces of polymers **1**, **2**, **3**, and LDPE.

3.4 Derivatization of Hydroxyl Groups in *hydroxy*-Polyethylene

To assess whether covalent versions of common additives in polyethylenes can be installed on the oxygens of *hydroxy*-polyethylene **3**, we first evaluated methods to functionalize the alcohol

groups in a manner that would render the polyethylene compatible with polar polymers. Polymers containing esters are prevalent in adhesives,¹⁷⁰ coatings,^{171, 172} and membranes.^{173, 174} These esters could be designed to behave as dyes, plasticizers, or stabilizers for specific applications. Furthermore, covalently bound additives could prevent the leaching of additives from polyethylene.²⁹

We attempted to acylate the alcohols of *hydroxy*-polyethylene **3** with carboxylic acids because of their widespread availability. Acid-catalyzed esterification, such as the Fischer esterification, did not furnish esters on the polymer. The polymer that was recovered from these reactions was insoluble and could not be characterized by standard analytical techniques. We postulate that under acidic conditions, the pendant alcohols of *hydroxy*-polyethylene **3** could dissociate as water to generate carbocations, which would subsequently be trapped by either another hydroxyl group or an olefin formed by elimination to crosslink the polyethylene chains. Steglich esterifications to install esters with dicyclohexylcarbodiimide (DCC), 4-(dimethylamino)pyridine (DMAP), and a carboxylic acid also did not acylate the hydroxyl group of polymer **3**. We posit that the insolubility of carboxylic acids in nonpolar solvents limited the extent of their reaction with polyethylene **3**.

Reactions to acylate polymer **3** with acid chlorides were investigated because of the increased solubility and electrophilicity of the acylating reagent. In this case, acylation of polymer **3** occurred with a classical combination of an acid chloride and 4-(dimethylamino)pyridine (DMAP) in dichloromethane at 80 °C to yield polymer **4** with pendant ester units on the polymer (Figure 3.3A). No remaining alcohols were detectable by NMR and FTIR spectroscopy after acylation, indicating quantitative conversion of the alcohols to esters. The esters installed were chosen to imbue *hydroxy*-polyethylene **3** with improved bulk properties. We hypothesized that esters with similar structures as repeat units present in tough plastics would improve the mechanical properties of the polymer because of the non-covalent interactions formed between the functional groups of the polymer chains.¹⁷⁵

To this end, reactions with benzoyl and butyryl chloride were conducted to furnish polymers **4a** and **4d**, respectively, with pendant ester groups (Figure 3.4.1A). We also aimed to install esters that mimic the additives found in commercial plastics. For example, oleamide is a lubricant that is added to polyethylene to aid processing.¹⁷⁶ Reactions of polymer **3** with oleoyl chloride afforded polymer **4b** with a pendant oleoyl group. Phosphate esters are flame retardants that are doped into plastics.¹⁷⁷ Reactions of *hydroxy* polyethylene **3** with diphenyl chlorophosphate afforded polymer **4c** with an attached phosphate ester. Butylated hydroxytoluene (BHT) is a common stabilizer in PE materials to prevent photooxidation.¹⁷⁸ Reactions of polymer **3** with 3,5-di-tert-butyl-4-hydroxybenzoyl chloride yielded polymer **4g** in which the BHT moiety is covalently bound through an ester linkage. Finally, reaction of an acid chloride containing a protected catechol furnished polymer **4f**. Polymers containing catechol are versatile materials with applications in drug delivery, adhesion, and metal-sequestration,¹⁷⁹⁻¹⁸¹ and the installation of a catechol on polyethylene could impart polyethylene with properties to be utilized in these applications. Partial desilylation to generate the free or monoprotected catechol, which we attribute to the hydrochloric acid generated over the course of the reaction, was observed by ¹H NMR spectroscopy and complete removal of the protecting silyl groups to afford polymer **4g** was achieved by simply adding triethylamine trihydrofluoride (Et₃N·3HF) to a solution of polymer **4f** in tetrahydrofuran (THF) at 80 °C.

To assess the reversibility of the polymer acylation, we identified conditions to remove the acyl group from polymer **4d**. To achieve this transformation, it was necessary to identify an appropriate solvent for a process that is typically conducted in water or polar media. We found that

polymers **4a**, **4b**, and **4d** are soluble in *tert*-amyl alcohol, and hydrolysis with excess lithium hydroxide in this solvent at 120 °C regenerated polymer **3** in 81% yield. The *hydroxy*-polyethylene **3** then can be used for additional applications after installation of a different acyl group, demonstrating one type of circularity enabled by this functionalization (Figure 3.4.1A). Acid-catalyzed hydrolysis did not regenerate polymer **3** because crosslinking of the polymer chains occurred in acidic media, as indicated by the formation of insoluble gels over the course of the reaction.

Polyolefins grafted with poly(ϵ -caprolactone) (PCL) have been reported to compatibilize polyolefins with PCL when used as an additive in polyolefin-PCL blends.^{80, 82} To synthesize polyethylene-based compatibilizers for blending PE with polar polymers, we conducted the ring-opening polymerization (ROP) of ϵ -caprolactone initiated by the hydroxyl groups of polymer **3** to furnish polyethylene **5** with grafted PCL oligomers. The degree of polymerization was assessed by ¹H NMR spectroscopy, indicating an average of approximately 100 ϵ -caprolactone monomer units per hydroxyl functionality (see Figure 3.10.11.43). Polymer **5** is distinct from the PCL-grafted PE derived from the nickel-catalyzed oxidation of PE we reported previously because it lacks the pendant ketones, chlorides, and main-chain esters that were present in the material generated by nickel-catalyzed oxidation.^{80, 82} The PCL grafted PE **5** compatibilized polyethylene and poly(ϵ -caprolactone), as determined by scanning electron microscopy (SEM) (Figure 3.4.1B).

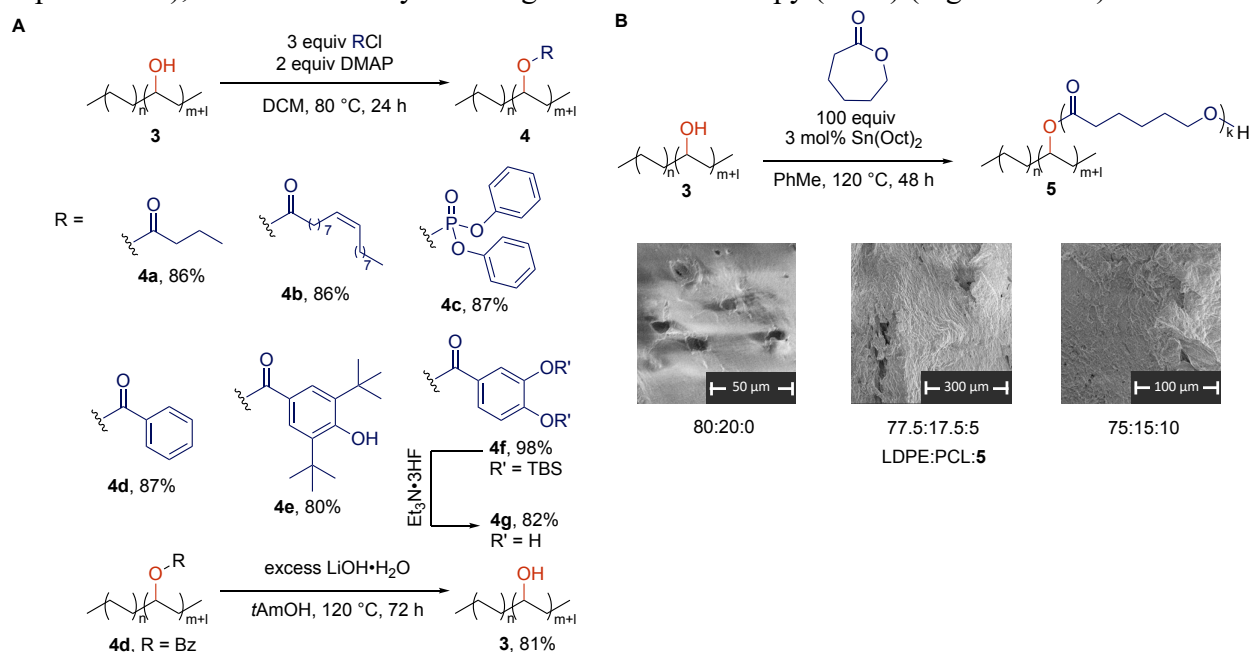


Figure 3.4.1. (A) Acylation of polymer **3** with acid chlorides. (B) Graft polymerization of ϵ -caprolactone and SEM images of LDPE, PCL, and PCL-LDPE **5** blends. Yields are reported in wt %

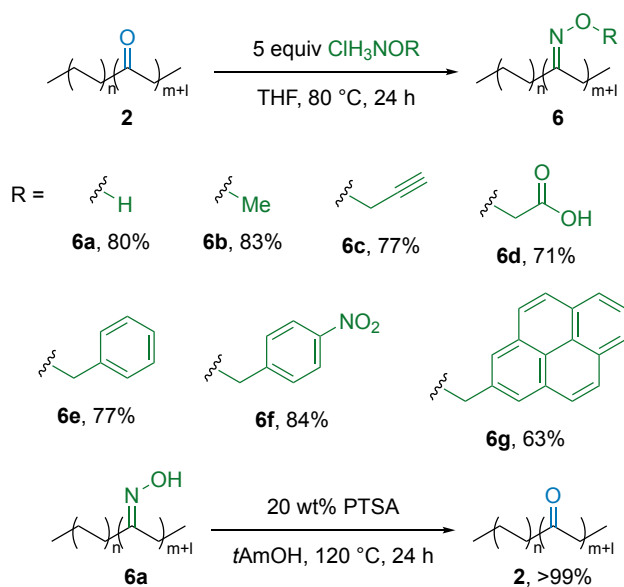
3.5 Synthesis of Monofunctional Polyethylenes Containing Oximes

The ketone units of polymer **2** are versatile handles to install a range of functional groups challenging to install by direct functionalization of C–H bonds. Oximes form readily from ketones,¹⁸²⁻¹⁸⁴ and could serve as a valuable anchor point to connect substituents to polyethylene, and oximes have been used to create dynamic and self-healing materials. Thus, functionalization of polymers with substituted hydroxylamines could provide a modular method to install functional

groups onto polyethylene that could impart new properties to the material. Furthermore, the pendant oximes of the polyethylene could be removed by hydrolysis to recover polymer **2** for reuse and enabling a second type of circularity.

Polyethylenes containing oximes with a variety of substituents at the oxygen were synthesized by treating polymer **2** with the corresponding hydroxylamine or hydroxylamine hydrochloride salt (Figure 3.5.1). No remaining ketones were detected by NMR and FTIR spectroscopy after condensation, indicating quantitative conversion of the ketones to oximes. Hydroxylamines containing unprotected functional groups were tolerated. For example, reactions of hydroxylamine hydrochloride and *O*-(carboxymethyl)hydroxylamine hemihydrochloride with *keto*-polymer **2** furnished polymers **6a** and **6d** with unprotected hydroxyl and carboxylic acid groups, respectively. We reasoned that the surface properties of polymers with hydroxyl and carboxylic acid groups would be distinct from those of unmodified polyethylene because the Lewis basicity of the heteroatoms would form stronger interactions with metal surfaces than would the hydrocarbon materials.¹⁸⁵

Hydroxylamines with alkyl substituents at the oxygen were also tolerated under the reaction conditions. Polymers **6b**, **6c**, and **6e** were synthesized by treating *keto*-polyethylene **2** with *O*-methyl, *O*-propargyl, and *O*-benzyl hydroxylammonium chloride. Electron-poor substituents, such as a nitro group, were also successfully installed onto polymer **2** to furnish polymer **6f**. Nitroarenes are reported to give rise to antimicrobial activity.^{186, 187} Finally, reactions of polymer **2** with a hydroxylamine derived from pyrene generated polyethylene **6g** with a fluorescent functional group that could be utilized in biomedical and waste sorting applications.¹⁸⁸⁻¹⁹⁰ Although qualitative, we found that this material was fluorescent when irradiated with a conventional UV-lamp for visualizing TLC plates.



Yields are reported in wt %

Figure 3.5.1. Synthesis of Oxime Containing Polyethylenes.

To identify conditions that would reverse the installation of the oxime group, we sought conditions that would hydrolyze the oxime in a non-polar environment. Treatments of oxime-containing polymers **6a** with 20 wt % *p*-toluenesulfonic acid (PTSA) in wet *tert*-amyl alcohol at 120 °C for 24 h cleaved the oximes to form the starting polymer **2** in quantitative yield. The

recovered polymer **2** was able to be dissolved, indicating no substantial crosslinking was caused by the acidic conditions during hydrolysis. This interconversion between ketones and oximes demonstrates how groups installed at the ketone units from polyolefin oxidation can impart distinct properties to the polymer in a circular fashion by a cycle of condensation and hydrolysis.

3.6 Properties of Materials

With a range of monofunctional polyethylenes in hand, we sought to evaluate the effect of the functional groups on the bulk properties of the materials. We previously reported that the mechanical properties of *oxo*-polyethylene **1** were similar to those of unmodified polyethylene but that the surface properties were distinct.⁸³ Given that polymer **1** contains both ketone and alcohol units, we sought to elucidate whether the ketones or alcohols contributed more to the adhesive properties of polymer **1** by conducting lap-shear tests with *keto*-polymer **2** and *hydroxy*-polymer **3** as the tie layer between aluminum plates. The lap-shear tests showed that polymer **3** was more adhesive to aluminum (6.16 ± 0.59 MPa) than polymer **2** (4.67 ± 0.50 MPa) (Figure 3.6.1A). We propose that polymer **3** is more adhesive because the pendant alcohols of polymer **3** interact more strongly with the oxidized surface of aluminum through hydrogen bonding than the pendant ketones of polymer **2**. Unmodified LDPE was unable to be tested in this manner for comparison because samples suitable for testing could not be constructed as assessed by the lap joints breaking during the clamping process, qualitatively supporting that the functional groups installed are vital to the observed surface adhesion.

We also investigated the adhesive characteristics of polymers **4g**, **6a**, and **6d** containing catechols, the parent oxime, and carboxylic acid-substituted oximes respectively by lap-shear tests. These materials contain hydrogen-bond donors that also can form strong interfacial interactions with metal surfaces. The adhesion of polymer **4g** to aluminum (2.60 ± 0.53 MPa) was the lowest of the six polymers we tested, indicating that catechols are less adhesive than ketones or alcohols. The adhesion of polymer **6a** (6.03 ± 1.01 MPa) to aluminum was similar to that of hydroxyl polymer **3**, and the adhesion of polymer **6d** (6.68 ± 1.10 MPa) was higher than that of polymer **6a** and the highest of all the polymers we tested. The lap shear tests indicate that the adhesive strengths of the polymers we tested to aluminum are comparable to those of commercial adhesives.¹⁹¹

In addition to adhesion to metal, we investigated the hydrophilic properties of polymers **6a** and **6d** by measuring the contact angle of water droplets on the surface of polymer films (see Table 3.10.17.3.1). Indeed, the contact angles of polyethylenes **6a** and **6d** (84.2 ± 4.3 and 86.1 ± 3.7) were lower than those of unmodified LDPE (97.0 ± 2.1), indicating that the polar functional groups on the surface increase the hydrophilicity of the material (see Figure 3.10.17.3.1). Because the functional groups can be hydrolyzed, our derivatization strategy enables selective tuning of the surface properties of functionalized polyethylenes.

We also evaluated changes in the mechanical properties that result from the installation of this suite of functional groups. We postulated that the mechanical properties of benzoyloxy polymer **4d** containing pendant esters would be distinct from those of unmodified LDPE because of the ability of the esters to create interchain interactions non-covalently.^{192, 193}

To assess this hypothesis, tensile tests of benzoyloxy polymer **4d** were conducted. The tensile strength of polymer **4d** (15.0 ± 2.2 MPa) was higher than that of unmodified LDPE (11.4 ± 1.1 MPa). In addition, the elongation at break and toughness of polymer **4d** ($991.2 \pm 167.2\%$ and 106.3 ± 27.6 MPa, respectively) were higher than the corresponding values of unmodified LDPE ($227.8 \pm 96.8\%$ and 20.9 ± 9.8 MPa, respectively) (Figure 3.6.1B). In contrast, the tensile strength, toughness, and elongation at break of *hydroxy* polymer **3** (8.5 ± 1.6 MPa, 18.0 ± 3.4 MPa, and

234.0 ± 44.7% respectively) were similar to the values for LDPE (Figure 3.6.1B). This set of data suggests that the pendant alcohol groups of monofunctional polymer **3** are not responsible for the enhanced tensile strength, toughness, and elongation at break of polymer **4d**.

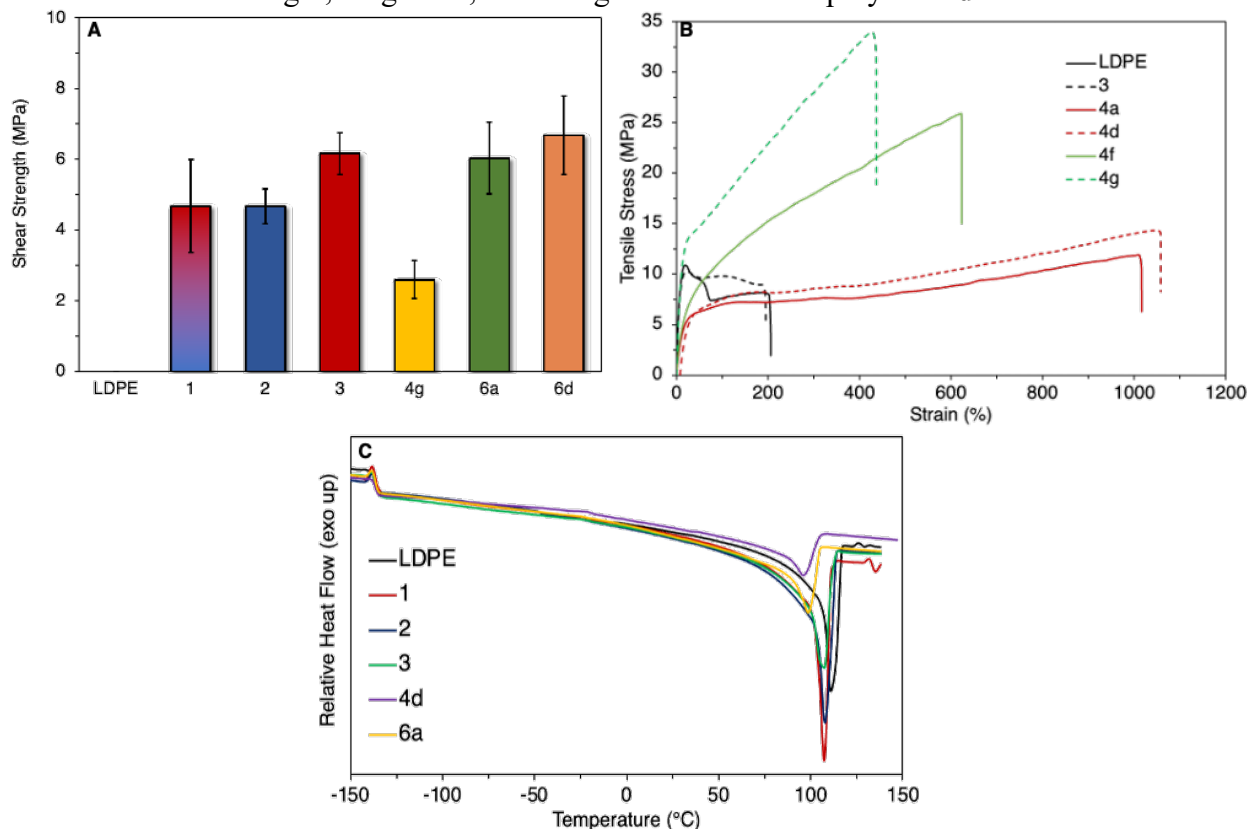


Figure 3.6.1. (A) Lap shear tests of functionalized polyethylenes with aluminum (B) Tensile tests of functionalized polyethylenes (C) DSC curves of functionalized polyethylenes.

To deduce the origins of these properties, butyryloxy polymer **4a** containing pendant esters with an aliphatic chain was subjected to tensile tests. The tensile strength of polymer **4a** (10.3 ± 1.2 MPa) was similar to that of unmodified LDPE. Likewise, the toughness and elongation at break (86.4 ± 9.2 MPa and $1006.2 \pm 89.6\%$ respectively) were more than four-fold greater than the values of unmodified LDPE and were similar to those of benzoyloxy polymer **4d**. These data suggest that the enhanced mechanical properties of these materials result from interchain interactions originating from the ester, instead of π - π stacking of the aryl substituents of polymer **4d**.

We also performed tensile tests on catechol polymer **4g** because catechol-containing polymers can form crosslinks to furnish thermosets with high strength.¹⁹⁴ Indeed, the tensile strength, toughness, and elongation of break of polymer **4g** (30.2 ± 2.6 MPa, 87.5 ± 33.7 MPa, and $360.8 \pm 124.1\%$ respectively) were higher than the values of unmodified LDPE. Specifically, the tensile strength of polymer **4g** (30.2 ± 2.6 MPa) was nearly three-fold higher than unmodified LDPE (11.4 ± 1.1 MPa) which is comparable to the tensile strengths of commercial ionomers.⁸⁸ We attribute the enhanced mechanical properties of polymer **4g** to the formation of crosslinks between pendant catechols during thermal pressing to create films. The resulting films were insoluble in 1,2,4-trichlorobenzene at 135 °C and 1,1,2,2-tetrachloroethane-*d*₄ at 120 °C, indicating formation of a thermoset. The insolubility of polymer **4g** limited its characterization by HTSEC and NMR spectroscopy.

To assess the potential formation of crosslinks in polymer **4g** further, we subjected polymer **4f**, which contains silyl-protected catechols that should not undergo crosslinking, to tensile tests. Indeed, the tensile strength and toughness of polymer **4f** (16.6 ± 5.9 MPa and 56.1 ± 41.0 MPa respectively) were lower than the values of polymer **4g** (30.2 ± 2.6 MPa and 87.5 ± 33.7 MPa respectively). Based on these material properties, we surmise that the deprotection of the silyl ethers of polymer **4f** with $\text{Et}_3\text{N}\cdot 3\text{HF}$ furnishes unprotected catechol groups that form crosslinks during thermal processing (see Figure 3.10.16.12).

We performed scanning calorimetry (DSC) to assess the changes in melting transitions of the polyethylenes resulting from the installation of pendant functional groups onto the polymer (Figure 3.6.1C). The glass transition temperatures (T_g) of nearly all the functionalized polymers were the same as that of LDPE (-137 °C and of *oxo*-PE **1** (-147 °C). The melting temperatures (T_m) of polymers **1**, **2**, and **3** (108 °C, 108 °C, and 105 °C respectively) were slightly lower than the T_m of unmodified LDPE (111 °C). This reduction in melting temperatures of *keto*- and/or *hydroxy*-functionalized polyethylenes is expected because the oxygenated functional groups cause defects within the crystalline regions of polyethylene that lower the T_m .⁸³ The T_m values of polymers **4d** and **6a**, which contain esters and oximes respectively (96 °C and 99 °C), are lower than that of polymers **1**, **2**, and **3**. We hypothesize that the larger functional groups of polymers **4d** and **6a** disrupt the crystallinity of the polymer more than the ketone and alcohol units of polymers **1**, **2**, and **3**, leading to a larger decrease in T_m .

3.7 Applications to Waste Plastic

Reactions that transform waste plastics into higher-value materials are challenging to conduct because waste plastics typically contain additives that could poison catalysts or consume the reagent. To access oxidized polymer **1** from waste plastic, we conducted ruthenium-catalyzed oxidation of a plastic bag, a shampoo bottle, a coffee container, and a food package that were pre-treated only by water to remove any residue prior to performing the reaction (Figure 3.7.1). ^1H NMR and IR spectroscopy showed that the levels of ketone and alcohol units in the resulting material were like those in oxidized polymer **1** derived from virgin polyethylene (see Table 3.10.9.1). Likewise, the oxidized waste plastics underwent derivatization at the *keto*- and *hydroxy*-functionality in a fashion similar to the oxidized virgin plastic.

For example, the treatment of *oxo*-HDPE derived from a shampoo bottle furnished monofunctional HDPEs containing only alcohol and ketone units in a total level of functionalization of 2.1% (Figure 3.7.1.E). This material then underwent iridium-catalyzed dehydrogenation of the alcohols to form the *oxo*-PE **2** in a fashion indistinguishable from the oxidized **1** from virgin PE. Likewise, it underwent Ru-catalyzed hydrogenation to form the *hydroxy*-PE **3** in a reaction indistinguishable from that of **1** from virgin PE. These results show the surprising robustness of this type of catalytic chemistry to the additives on polyolefin plastics.

3.8 Application to the Separation of Plastic Mixtures

Commercial polyethylene products are difficult to recycle chemically because it is challenging to separate the components required to manufacture them.^{28, 30} For instance, polyolefins are scrubbed with supercritical fluids to remove additives^{36, 195}; however, these methods require high pressures of fluid and are expensive.^{33, 196} We have demonstrated that additives can be attached covalently through the derivatization of the *hydroxy*- and *keto*- functionalities of polymer **1** and can be removed by simple hydrolysis in acidic or basic conditions. In this manner, we envisioned that our strategy could provide an alternative method to remove additives from polyolefins.

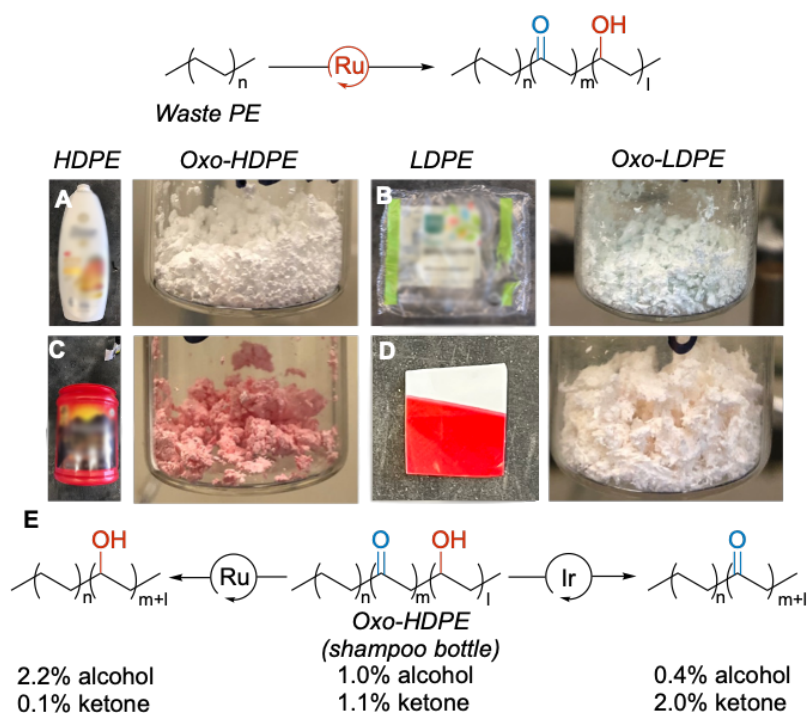


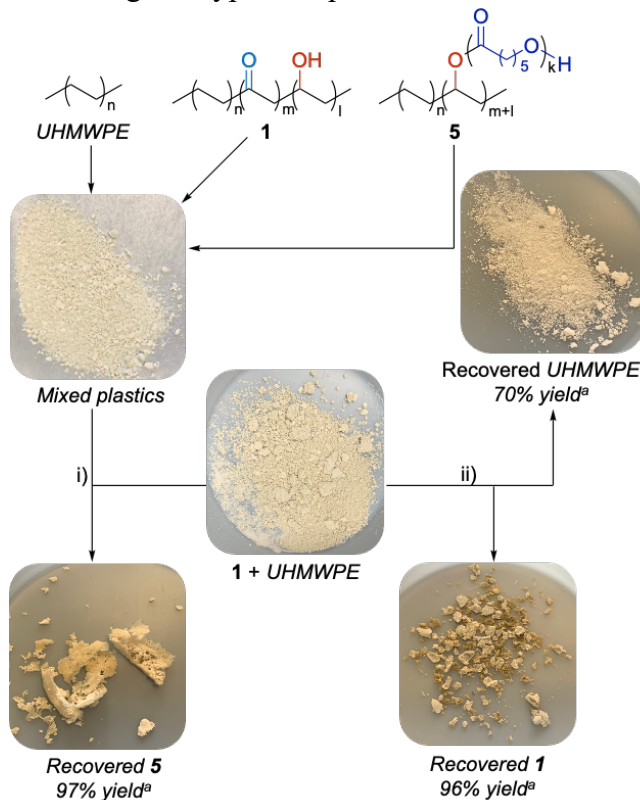
Figure 3.7.1. Oxidative functionalization of waste polyethylenes and separation of plastics from a mechanically mixed blend. (A) *Oxo*-HDPE derived from a shampoo bottle. (B) *Oxo*-LDPE derived from food packaging. (C) *Oxo*-HDPE derived from a coffee container. (D) *Oxo*-LDPE derived from a plastic bag. (E) Further catalytic derivatization of *Oxo*-HDPE derived from a shampoo bottle

In addition, we envisioned that selective dissolution of functional polyethylenes from mixtures of plastics could enable recovery of polyethylenes from waste (Figure 3.8.1). The solubility of the PCL-functionalized polyethylene **5** is distinct from that of the oxo-functionalized PE and unfunctionalized PE. For example, the side-chain PCL oligomers of polymer **5** enable its dissolution in acetone at room temperature, while oxo-functionalized PE and unfunctionalized PE are insoluble in acetone. These different solubilities enable separation of the functionalized material from other components of a mechanically mixed plastic blend.

To assess the ability to separate polymers **1** and **5** in such a blend, powders of the two materials were ground and mixed with unmodified, ultra-high molecular weight polyethylene (UHMWPE) to form a blend of mixed plastics (Figure 3.8.1). The polymers were evenly dispersed in this mix, and no substantial phase separation was observable by eye. Treatment of this blend of plastics with acetone led to the selective dissolution of PCL-functionalized-polyethylene **5**. Polymer **5** was recovered in 97% yield from the acetone by evaporating the solvent in vacuo. The solids in the remaining mixture, which comprised polymer **1** and UHMWPE, were then separated. Dissolution of polymer **1** selectively in toluene at 70 °C enabled recovering of polymer **1** in 96% yield by precipitation of the filtrate with methanol. The remaining solid was determined to be UHMWPE and collected in 70% yield.

Variable temperature ¹H NMR spectroscopy at 100 °C showed that each separated material was indistinguishable from its precursor before mixing and contained the same degree of functionality (see Section 3.10.14). These results show that separation of each material from the

blend of mixed plastics is possible, and that derivatization of the materials can create materials with specific solubilities enabling this type of separation.



^aYields are reported in mass %. Conditions: i) acetone, 50 °C, ii) toluene, 70 °C.

Figure 3.8.1. Separation of Plastics from a Mechanically Mixed Blend.

3.9 Conclusion

We have applied a series of methods that derivatize *oxo*-polyethylene **1** to install pendant functional groups that are inaccessible by existing methods for direct C–H functionalization. The resulting polymers possess properties that are distinct from those of their precursors and can be reverted to their oxidized precursors in a fashion that would allow for circularity between oxidized polymers **1-3** and the further derivatized materials. Monofunctional polyethylenes containing polar functional groups possessed mechanical and adhesive properties that are superior to those of unmodified polyethylene, and the greater solubility of these materials permitted their separation from a composite material.

Thus, our installation of functional groups shows how these groups can both increase the value of polyolefins and facilitate recycling and reuse by generating consumer plastics with fewer additives. Furthermore, the ability of waste polyethylenes to undergo catalytic oxidation expands the scope of plastic substrates that are amenable to our derivatization strategy and shows that waste plastics can serve as a feedstock and address the harmful effects caused by the accumulation of plastic waste. Future work seeks to elucidate the mechanistic differences between small molecule and polymer functionalization to facilitate the development of new methods to upcycle polyolefins.

3.10 Experimental Section

3.10.1 General Information

All air sensitive manipulations were conducted under an inert atmosphere in a nitrogen-filled or argon-filled glovebox or by standard Schlenk techniques. All reagents were purchased from commercial sources and used without further purification. Low density polyethylene (LDPE) was purchased from Sigma-Aldrich, and Ultra High Molecular Weight Polyethylene (UHMWPE) was purchased from Alfa Aesar. Solvents were degassed with nitrogen and dried in a solvent purification system with a 1 m column containing activated alumina and stored under 4Å molecular sieves. Fourier-transform infrared spectra were collected using a Bruker Vortex 80 spectrometer. Room-temperature NMR spectra were collected using 400, 500, and 600 MHz Bruker Instruments at the University of California, Berkeley. Variable-temperature NMR spectroscopic analysis was conducted on the 500 and 600 MHz instruments at University of California Berkeley. ¹H chemical shifts were reported in ppm relative to the resonance of the residual solvent (CDCl₃, 7.26 ppm; C₂D₂Cl₄, 6.00 ppm). ¹³C chemical shifts were reported in ppm relative to the resonance of the residual solvent (CDCl₃, 77.16 ppm; C₂D₂Cl₄, 73.78 ppm). High-temperature, size-exclusion chromatography (HT-SEC) was performed on a Tosoh EcoSEC-HT with three TSKgel GMHhr-H(S) HT columns in series. Runs were performed at 135 °C and 1 mL/min with 1,2,4-trichlorobenzene + 0.05% butylated hydroxytoluene (BHT) as mobile phase. Molecular weight was determined relative to polyethylene standards. Size exclusion chromatography (SEC) was performed on a Malvern OMNISEC equipped with refractive index, light scattering, and intrinsic viscosity detectors calibrated with a single poly(styrene) standard. Analysis was performed in tetrahydrofuran running at 1 mL min⁻¹ and 35 °C with two Malvern T6000M mixed bed columns in series. Differential scanning calorimetry (DSC) was performed on a Mettler Toledo DSC 1 STAR System instrument. Aluminum 6061 (Al-6061) substrates were cut at the UC Berkeley Cory Hall Machine shop from 0.160 cm thick, 10.16 cm x 121.92 cm (0.063” thick, 4”x48”) sheet stock purchased from McMaster-Carr (USA). Lap shear adhesion testing was conducted according to ASTM D1002-10 on an Instron universal materials tester equipped with a 5 kN load cell with a shear rate of 1.5 mm/min. Adhesion strength was determined by the maximum load divided by the bonded overlap area, which was measured with digital calipers prior to testing, and the apparent failure mode was assessed visually. The adhesive strengths of LDPE and functionalized polyethylenes to aluminum were assessed by single lap shear testing on rectangular aluminum 6061 (Al 6061) substrates with dimensions 0.16 cm thick x 1 cm width x 10 cm length. Compression molding was conducted on a Grizzly Industrial 10-ton benchtop shop press with heated plates (model H6231Z) or a Carver benchtop lab press with heated platens (model 4386). Tensile testing was conducted according to ASTM D638 on an Instron universal materials tester. Tensile stress and strain were measured at room temperature using an extension rate of 50 mm/min. Scanning electron microscope (SEM) imaging was conducted on a SCios 2 DualBeam with an accelerating voltage of 2 kV and a current of 12 pA. Carbon tape was used to secure samples onto holders prior to imaging. Samples were prepared by dissolving the polymers in 1,2-dichlorobenzene at 120 °C until homogeneous and removing the residual solvent at 180 °C under a stream of nitrogen. The samples were cryofractured and etched with acetone at 50 °C. Contact angles were measured using a Ramé-Hart goniometer. Thermogravimetric analysis (TGA) was performed with a TA Discovery TGA 550 instrument. *O*-(pyren-1-ylmethyl)hydroxylammonium chloride was synthesized by a literature procedure.¹⁹⁷ 3,5-di-*tert*-butyl-4-hydroxybenzoyl chloride was synthesized according to a literature procedure.¹⁹⁸ 3,4-bis(*tert*-butyldimethylsilyloxy)benzoyl chloride was synthesized according to a literature procedure.¹⁹⁹

3.10.2 Assessment of the degree of functionalization

The degree of functionalization was determined by ^1H NMR spectroscopy at $100\text{ }^\circ\text{C}$ in $\text{C}_2\text{D}_2\text{Cl}_4$. The integration of the peaks between 1.7 and 0.7 ppm was set to 400 (4 proton per monomer unit, 100 monomer units in total). The integration of the methine proton that was alpha to the esters or the methylene protons alpha to the oximes were then compared to the integration of the protons of the monomer units.

3.10.3 Calculation of the stoichiometry of catalysts and reagents

The stoichiometry for the catalysts and reagents were calculated based on the number of functional groups in the polymer.

$$\text{mmol}_{\text{alcohol or ketone}} = \frac{\text{mass}_{\text{polymer}}}{\text{MW}_{\text{repeat unit}}} * \frac{\% \text{ functionalization}}{100} * 1000$$

For example, 1 g of polymer **3** with 3.0% functionalization:

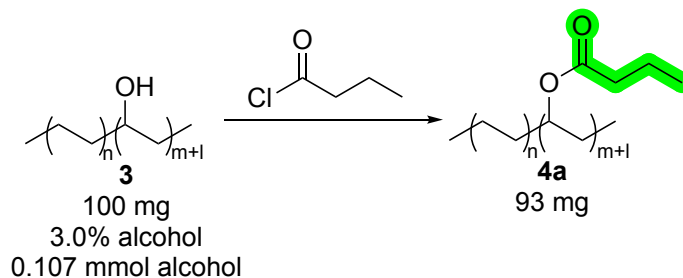
$$\text{mmol}_{\text{alcohol or ketone}} = \frac{1.0 \text{ g}}{\left(28.05 \frac{\text{g}}{\text{mol}}\right)} * \frac{3.0\%}{100} * 1000 = 1.1 \text{ mmol}_{\text{alcohol or ketone}}$$

3.10.4 Calculation of yield

The yield for each reaction was determined by the following equation where $\text{mass}_{\text{product,actual}}$ denotes the mass of the polymer obtained after the reaction, and $\text{mass}_{\text{product,theoretical}}$ denotes the mass of the polymer if all of the initial functional groups have been functionalized.

$$\% \text{ mass yield} = 100 * \left(\frac{\text{mass}_{\text{product,actual}}}{\text{mass}_{\text{product,theoretical}}} \right)$$

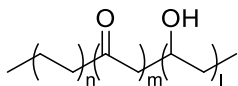
For example, for the synthesis of polymer **4a** by the acylation of polymer **3**:



$$\text{mass}_{\text{product,theoretical}} = 0.100 \text{ g} + \frac{0.107 \text{ mmol} * \text{MW}_{\text{C}_4\text{H}_6\text{O}}}{1000} = 0.107 \text{ g}$$

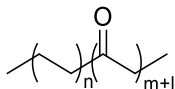
$$\% \text{ mass yield} = 100 * \left(\frac{0.093 \text{ g}}{0.107 \text{ g}} \right) = 86\%$$

3.10.5 Synthesis of polymers



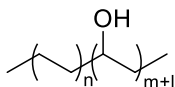
To a 250 mL pressure vessel with a stir bar, 3.00 g of LDPE (107 mmol) and 1.77 g 2,6-dichloropyridine *N*-oxide (10.7 mmol) were added. The solids were suspended in 107 mL of 1,2-dichloroethane. The vessel was heated at 120 °C until the solids dissolved. The vessel was cooled to room temperature slowly. In a separate 4 mL vial, 5.9 mg of tetrakis-pentafluorophenylporphyrin ruthenium carbonyl (0.0054 mmol) were dissolved in 5.3 mL of dichloromethane. The solution was added to the pressure vessel, and the vessel was tightly sealed and heated in a preheated oil bath at 120 °C for 1 h. The vessel was cooled slightly, opened carefully, and the contents were poured into 500 mL of chilled methanol under vigorous stirring to precipitate the polymer. The slurry was filtered to recover polymer **1** as a light green powder (2.9 g, 97%). The degree of functionalization was determined to be 2.8% total functionalization (1.6% ketone and 1.2% alcohol) by variable temperature ¹H NMR spectroscopy at 100 °C. The ¹H NMR spectrum of polymer **1** matched those published previously.⁸³ ¹H NMR (600 MHz, C₂D₂Cl₄) δ 3.62 (br, CHOH), 2.40 (t, *J* = 7.2 Hz, CH₂C(O)CH₂), 1.61 (br), 1.34 (br), 0.98 – 0.88 (m). ¹³C NMR (151 MHz, C₂D₂Cl₄) δ 71.8 (CHOH), 42.5, 39.4, 37.5, 37.4, 33.9, 33.5, 32.1, 31.6, 30.1, 29.9, 29.5, 29.4, 29.4, 29.3, 29.3, 29.2, 29.1, 29.1, 29.0, 28.9, 26.7, 26.3, 25.4, 23.8, 23.4, 23.3, 23.1, 22.9, 22.4, 13.8, 13.7.

***Keto*-LDPE (2)**



To a 500 mL Corning bottle containing a stir bar under nitrogen, 6.0 g of polymer **1** (2.8 mmol alcohol), 78 mg of pentamethylcyclopentadienyl iridium dichloride dimer (0.098 mmol), and 40 mg of potassium carbonate (0.28 mmol) were added. The solids were suspended in 250 mL of toluene, and 4 mL of acetone (54 mmol) were added. The bottle was tightly sealed and heated at 140 °C for 48 h. The bottle was cooled slightly, and the contents were poured into 1 L of chilled methanol under vigorous stirring to precipitate the polymer. The slurry was filtered to recover polymer **2** as a light-tan powder (5.5 g, 92%). The degree of functionalization was determined to be 3.0% ketone by variable temperature ¹H NMR spectroscopy at 100 °C. ¹H NMR (600 MHz, C₂D₂Cl₄) δ 2.40 (t, *J* = 7.2 Hz, CH₂C(O)CH₂), 1.61 (br), 1.34 (br), 0.98 – 0.88 (m). ¹³C NMR (151 MHz, C₂D₂Cl₄) δ 42.5, 33.9, 29.9, 29.4, 29.2, 29.1, 26.7, 23.8, 22.8, 22.4, 13.7.

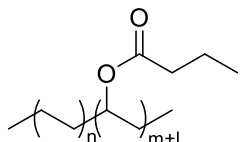
***Hydroxy*-LDPE (3)**



To a 100 mL Corning bottle with a stir bar under nitrogen, 1.8 g of polymer **1** (1.12 mmol ketone), 50 mg of tris(triphenylphosphine)ruthenium dichloride (0.052 mmol), and 30 mg of potassium hydroxide (0.53 mmol) were added. The solids were suspended in 60 mL of 2-methyl-2-butanol, and 300 μL of ethylene diamine (4.5 mmol) were added to the bottle. The bottle was placed in a

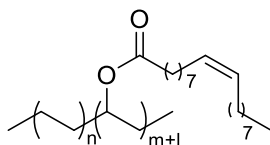
parr reactor (internal volume 450 mL) and tightly sealed. The reactor was charged with 750 psi of hydrogen and heated in an aluminum heating block at 120 °C for 24 h. The reactor was then cooled to room temperature, and the headspace vented slowly to depressurize the reactor. To the bottle were added 40 mL of toluene, and the bottle was reheated to redissolve the polymer. The contents of the bottle were poured into 300 mL of chilled methanol under vigorous stirring to precipitate the polymer. The slurry was filtered to recover polymer **3** as a light tan powder (1.5 g, 86%). The degree of functionalization was determined to be 2.8% alcohol by variable temperature ¹H NMR spectroscopy at 100 °C. ¹H NMR (600 MHz, C₂D₂Cl₄) δ 3.62 (br, CHOH), 1.61 (br), 1.34 (br), 0.98 – 0.88 (m). ¹³C NMR (151 MHz, C₂D₂Cl₄) δ 71.8 (CHOH), 37.4, 33.9, 29.5, 29.4, 26.7, 25.4, 22.8.

Butyryl LDPE (4a)



To a 20 mL vial containing a stir bar, 100 mg of polymer **3** (0.107 mmol alcohol) was suspended in 4 mL of anhydrous DCM. The vial was heated at 80 °C until the polymer dissolved. The vial was cooled to room temperature, and 26 mg of 4-(dimethylamino)pyridine (0.214 mmol) and 33 μL of butyryl chloride (0.321 mmol) were added. The headspace in the vial was quickly sparged with nitrogen before the vial was sealed tightly. The vial was heated at 80 °C for 24 h. After cooling, the contents of the vial were poured into chilled methanol under vigorous stirring to precipitate the polymer. The slurry was filtered to yield polymer **4a** as a white powder (93 mg, 86%). The degree of functionalization was determined to be 2.0% ester by variable temperature ¹H NMR spectroscopy at 100 °C. ¹H NMR (600 MHz, C₂D₂Cl₄) δ 4.90 (p, *J* = 6.2 Hz, CHOC(O)CH₂CH₂CH₃), 2.30 (t, *J* = 7.3 Hz, CHOC(O)CH₂CH₂CH₃), 1.70 (h, *J* = 7.4 Hz, CHOC(O)CH₂CH₂CH₃), 1.61 (br), 1.34 (br), 1.01 (t, *J* = 7.4 Hz, CHOC(O)CH₂CH₂CH₃), 0.98 – 0.88 (m). ¹³C NMR (151 MHz, C₂D₂Cl₄) δ 173.2 (CHOC(O)CH₂CH₂CH₃), 37.8, 36.8, 34.3, 34.2, 31.9, 30.2, 29.7, 29.6, 29.5, 29.3, 29.2, 27.0, 25.4, 23.1, 22.7, 18.6, 14.0, 13.7.

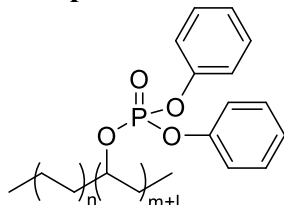
Oleoyl LDPE (4b)



To a 20 mL vial containing a stir bar, 100 mg of polymer **3** (0.107 mmol alcohol) was suspended in 4 mL of anhydrous DCM. The vial was heated at 80 °C until the polymer dissolved. The vial was cooled to room temperature, and 26 mg of 4-(dimethylamino)pyridine (0.214 mmol) and 107 μL of oleoyl chloride (0.321 mmol) were added. The headspace in the vial was quickly sparged with nitrogen before the vial was sealed tightly. The vial was heated at 80 °C for 24 h. After cooling, the contents of the vial were poured into chilled methanol under vigorous stirring to precipitate the polymer. The slurry was filtered to yield polymer **4b** as a white powder (110 mg, 86%). The degree of functionalization was determined to be 1.8% ester by variable temperature ¹H NMR spectroscopy at 100 °C. ¹H NMR (600 MHz, C₂D₂Cl₄) δ 5.45 (br, CHOC(O)(CH₂)₇CH=CH(CH₂)₇CH₃), 4.93 (br, CHOC(O)R), 2.36 (t, *J* = 7.4 Hz,

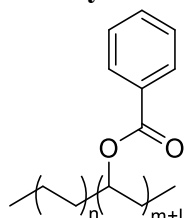
CHOC(O)CH₂(CH₂)₆CHCH(CH₂)₇CH₃), 2.12 (br), 1.72 (br), 1.62 (br), 1.34 (br), 0.98 – 0.88 (m). ¹³C NMR (151 MHz, C₂D₂Cl₄) δ 173.0 (CHOC(O)(CH₂)₇CHCH(CH₂)₇CH₃), 129.8 (CHOC(O)(CH₂)₇CHCH(CH₂)₇CH₃), 129.6 (CHOC(O)(CH₂)₇CHCH(CH₂)₇CH₃), 64.0, 38.3, 37.5, 34.5, 34.0, 33.9, 33.5, 32.1, 31.6, 29.9, 29.5, 29.4, 29.3, 29.3, 29.2, 29.1, 29.0, 29.0, 28.9, 28.9, 27.0, 27.0, 26.7, 26.3, 25.1, 24.9, 22.8, 22.3, 13.7, 13.7.

Phosphate Ester LDPE (4c)



To a 20 mL vial containing a stir bar, 100 mg of polymer **3** (0.107 mmol alcohol) were suspended in 4 mL of anhydrous DCM. The vial was heated at 80 °C until the polymer dissolved. The vial was cooled to room temperature, and 26 mg of 4-(dimethylamino)pyridine (0.214 mmol) and 67 μL of diphenyl chlorophosphate (0.321 mmol) were added. The headspace in the vial was quickly sparged with nitrogen before the vial was sealed tightly. The vial was heated at 80 °C for 24 h. After cooling, the contents of the vial were poured into chilled methanol under vigorous stirring to precipitate the polymer. The slurry was filtered to yield polymer **4c** as a light brown powder (109 mg, 87%). The degree of functionalization was determined to be 2.3% phosphate ester by variable temperature ¹H NMR spectroscopy at 100 °C. ¹H NMR (600 MHz, C₂D₂Cl₄) δ 7.37 (t, *J* = 7.5 Hz), 7.27 (d, *J* = 7.9 Hz), 7.21 (t, *J* = 7.0 Hz), 4.65 (q, *J* = 6.4 Hz, CHOP(O)(OPh)₂), 1.81 – 0.61 (m), 1.34 (br), 0.98 – 0.88 (m). ¹³C NMR (151 MHz, C₂D₂Cl₄) δ 129.3, 124.7, 120.0, 119.9, 82.4 (CHOP(O)(OPh)₂), 34.9, 33.9, 31.6, 29.9, 29.4, 29.3, 29.2, 29.2, 28.9, 26.7, 24.6, 22.8, 22.3, 13.7. ³¹P NMR (243 MHz, C₂D₂Cl₄) δ -12.9.

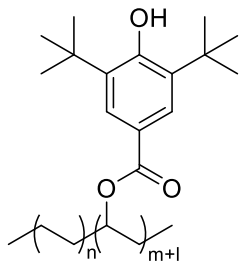
Benzoyl LDPE (4d)



To a 20 mL vial containing a stir bar, 100 mg of polymer **3** (0.107 mmol alcohol) was suspended in 4 mL of anhydrous DCM. The vial was heated at 80 °C until the polymer dissolved. The vial was cooled to room temperature, and 26 mg of 4-(dimethylamino)pyridine (0.214 mmol) and 37 μL of benzoyl chloride (0.321 mmol) were added. The headspace in the vial was quickly sparged with nitrogen before the vial was sealed tightly. The vial was heated at 80 °C for 24 h. After cooling, the contents of the vial were poured into chilled methanol under vigorous stirring to precipitate the polymer. The slurry was filtered to yield polymer **4d** as a white powder (97 mg, 87%). The degree of functionalization was determined to be 2.5% ester by variable temperature ¹H NMR spectroscopy at 100 °C. ¹H NMR (600 MHz, C₂D₂Cl₄) δ 8.07 (d, *J* = 6.9 Hz), 7.58 (t, *J* = 7.5 Hz), 7.47 (t, *J* = 7.6 Hz), 5.16 (p, *J* = 6.3 Hz, CHOC(O)Ph) 1.72 (br), 1.34 (br), 0.98 – 0.88 (m). ¹³C NMR (151 MHz, C₂D₂Cl₄) δ 166.0 (HCOC(O)Ph), 132.3, 131.2,

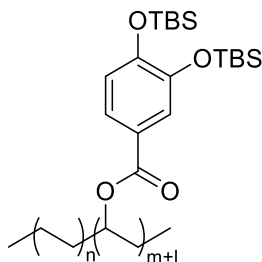
129.3, 128.0, 75.2 (HCOC(O)Ph), 37.5, 34.0, 33.9, 33.5, 32.1, 31.6, 29.9, 29.4, 29.4, 29.3, 29.2, 29.0, 26.7, 25.1, 22.9, 22.4, 13.8.

BHT LDPE (4e)



To a 20 mL vial containing a stir bar, 100 mg of polymer **3** (0.107 mmol alcohol) was suspended in 4 mL of anhydrous DCM. The vial was heated at 80 °C until the polymer dissolved. The vial was cooled to room temperature, and 26 mg (0.214 mmol) of 4-(dimethylamino)pyridine and 86 mg (0.321 mmol) of 3,5-di-tert-butyl-4-hydroxybenzoyl chloride were added. The headspace in the vial was quickly sparged with nitrogen before the vial was sealed tightly. The vial was heated at 80 °C for 24 h. After cooling, the contents of the vial were poured into chilled methanol under vigorous stirring to precipitate the polymer. The slurry was filtered to yield polymer **4e** as a white powder (100 mg, 80%). The degree of functionalization was determined to be 1.6% ester by variable temperature ¹H NMR spectroscopy at 100 °C. ¹H NMR (600 MHz, C₂D₂Cl₄) δ 7.93 (s), 5.08 (p, *J* = 6.2 Hz, CHOC(O)R), 1.57 (m), 1.53 (s, C(CH₃)₃), 1.80 – 0.80 (m). ¹³C NMR (151 MHz, C₂D₂Cl₄) δ 166.6 (HCOC(O)Ph/Bu₂OH), 157.6, 135.8, 126.7, 122.3, 74.6, 37.5, 34.1, 34.0, 33.9, 33.5, 31.6, 31.3, 30.1, 29.9, 29.4, 29.3, 29.0, 28.9, 26.7, 25.4, 25.1, 22.9, 22.4, 13.8.

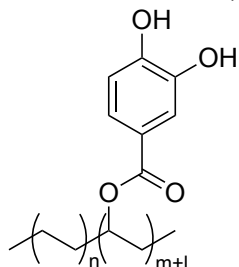
Protected Catechol LDPE (4f)



To a 500 mL pressure vessel containing a stir bar, 1.00 g of polymer **3** (1.07 mmol alcohol) was suspended in 40 mL of anhydrous DCM. The pressure vessel was heated at 80 °C until the polymer dissolved. The vessel was cooled to room temperature, and 260 mg of 4-(dimethylamino)pyridine (2.14 mmol) and 1.28 g of 3,4-bis((tert-butyldimethylsilyl)oxy)benzoyl chloride (3.19 mmol) were added. The headspace in the vessel was quickly sparged with nitrogen before the vessel was sealed tightly. The vial was heated at 80 °C for 24 h. After cooling, the contents of the vial were poured into chilled methanol under vigorous stirring to precipitate the polymer. The slurry was filtered to yield polymer **4f** as a stringy-white solid (1.36 g, 98%). Partial desilylation was observed by ¹H and ¹³C NMR spectroscopy (approximately 36% of the silyl ethers were desilylated). The degree of functionalization was determined to be 1.7% ester by variable temperature ¹H NMR spectroscopy at 100 °C. ¹H NMR (600 MHz, C₂D₂Cl₄) δ 7.70 (m), 7.58 (m), 7.23 (m), 6.97 (m), 6.89 (m), 5.13 (br, CHOC(O)R), 5.08 (br, CHOC(O)R), 1.73 (br), 1.58 – 1.17 (m), 1.08 (br), 1.00 – 0.90 (m), 0.35 – 0.15 (m, CHOC(O)PhO₂Si₂(CH₃)₄(C(CH₃)₃)₂).

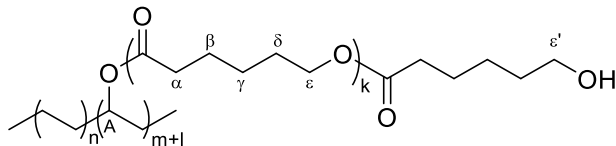
^{13}C NMR (151 MHz, $\text{C}_2\text{D}_2\text{Cl}_4$) δ 165.7, 151.1, 146.9, 146.4, 146.1, 129.4, 124.3, 124.2, 123.5, 123.2, 122.6, 122.6, 121.9, 121.5, 120.4, 120.1, 37.5, 34.0, 33.9, 33.5, 32.2, 31.7, 29.9, 29.4, 29.3, 29.0, 28.9, 26.7, 26.3, 25.8, 25.8, 25.8, 25.7, 25.7, 25.4, 25.4, 25.1, 22.9, 22.4, 18.3, 18.2, 17.8, 13.8, 13.7, -4.2, -4.2, -4.2, -4.2, -4.5, -4.6.

Catechol LDPE (4g)



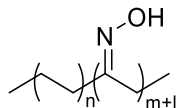
To a 100 mL Corning bottle containing a stir bar, 1.10 g of polymer **3** (1.18 mmol ester) was suspended in 40 mL of THF. The bottle was heated at 80 °C until the polymer dissolved. The bottle was cooled to room temperature, and 500 μL of triethylamine trihydrogenfluoride (3.07 mmol) were added. The bottle was heated at 80 °C for 24 h. After cooling, the contents of the vial were poured into chilled methanol under vigorous stirring to precipitate the polymer. The slurry was filtered to yield polymer **4g** as a stringy-white solid (760 mg, 82%). Polymer **4g** was insoluble in 1,1,2,2-tetrachloroethane- d_2 at 100 °C and 1,2,4-trichlorobenzene at 135 °C and was not able to be characterized by variable temperature NMR spectroscopy and HTSEC.

Poly(ϵ -Caprolactone)-graft-LDPE (5)



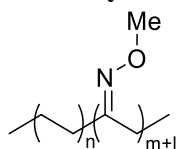
To a 20 mL vial containing a stir bar under nitrogen, 100 mg of polymer **3** (0.107 mmol alcohol) and 1.20 mL of ϵ -caprolactone (10.8 mmol) were added. The solids were suspended in 4 mL of toluene, and 1 μL of tin(II)-2-ethylhexanoate (0.003 mmol) was added to the vial. The vial was capped and heated at 120 °C for 48 h. After cooling, the contents of the vial were diluted with acetone. The slurry was poured into methanol. The methanolic solution was transferred to a centrifuge tube and placed in a centrifuge operated at 4000 rpm for 10 min. The supernatant was removed from the tube, and the remaining solid was dried under vacuum to yield a white powder (943 mg). The degree of polymerization was calculated to be approximately 100:1 ϵ -caprolactone to hydroxyl functionality by integration of the resonances of H_α and H_A (see Figure S12). ^1H NMR (600 MHz, $\text{C}_2\text{D}_2\text{Cl}_4$) δ 4.89 (m, $\text{CH}_2\text{CH}_A\text{ORCH}_2$), 4.12 (t, $J = 6.7$ Hz, $\text{CH}_2\epsilon'\text{OH}$), 3.67 (t, $J = 6.5$ Hz, $\text{CH}_2\epsilon\text{OH}$), 2.35 (t, $J = 7.4$ Hz, $\text{OC(O)CH}_2\alpha$), 1.76 – 1.66 (m, $\text{CH}_2\beta\text{CH}_2\text{CH}_2\delta$), 1.52 – 1.42 (m, $\text{CH}_2\text{CH}_2\gamma\text{CH}_2$), 1.34 (br). ^{13}C NMR (151 MHz, $\text{C}_2\text{D}_2\text{Cl}_4$) δ 172.9, 68.8 ($\text{CH}_A\text{OC(O)}$), 63.9 ($\text{CH}_2\epsilon\text{OC(O)}$), 62.4 ($\text{CH}_2\epsilon\text{OH}$), 34.4 ($\text{OC(O)CH}_2\alpha$), 34.3, 34.1, 34.1, 34.0, 33.8, 32.2, 29.9, 29.4, 28.6, 28.3 ($\text{CH}_2\delta\text{CH}_2\text{OC(O)}$), 28.2, 25.4 ($\text{CH}_2\gamma\text{CH}_2\text{CHOC(O)}$), 25.3, 25.2, 24.5 ($\text{CH}_2\beta\text{CH}_2\gamma\text{CH}_2\text{CH}_2\text{OC(O)}$), 24.4, 24.3, 22.8.

Oxime-LDPE (6a)



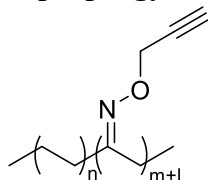
To a 100 mL round-bottom flask containing a stir bar, 1.0 g of polymer **2** (1.1 mmol ketone) and 0.38 g of hydroxylamine hydrochloride (5.4 mmol) were added. The solids were suspended in 40 mL pyridine, and the flask was heated at 100 °C for 24 h. The contents of the flask were then poured into 200 mL of chilled methanol under vigorous stirring to precipitate the polymer. The slurry was filtered to recover polymer **6a** as a light tan powder (890 mg, 80%). The degree of functionalization was determined to be 2.8% oxime by variable temperature ^1H NMR spectroscopy at 100 °C. Polymer **6a** was not able to be characterized by HTSEC because no peak was observed in the chromatogram; we posit this is caused by aggregation of the oximes in 1,2,4-trichlorobenzene at 135 °C which prevents elution of the polymer to be detected. ^1H NMR (600 MHz, $\text{C}_2\text{D}_2\text{Cl}_4$) δ 2.38 (t, $J = 7.8$ Hz, $\text{CH}_2\text{CNOHCH}_2$), 2.21 (t, $J = 7.2$ Hz, $\text{CH}_2\text{CNOHCH}_2$), 1.61 (br), 1.34 (br), 0.98 – 0.88 (m). ^{13}C NMR (151 MHz, $\text{C}_2\text{D}_2\text{Cl}_4$) δ 33.9, 33.8, 29.9, 29.6, 29.3, 29.2, 28.9, 27.3, 26.7, 26.2, 25.5, 22.8, 13.7.

***O*-methyl oxime LDPE (6b)**



To a 4 mL vial containing a stir bar, 100 mg of polymer **2** (0.107 mmol ketone) and 45 mg of *O*-benzylhydroxylamine hydrochloride (0.54 mmol) were added. The solids were suspended in 2 mL THF, and the vial was heated at 80 °C for 24 h. After cooling, the contents of the vial were poured into chilled methanol under vigorous stirring. The slurry was filtered to yield polymer **6b** as a light tan powder (86 mg, 83%). The degree of functionalization was determined to be 2.8% oxime by variable temperature ^1H NMR spectroscopy at 100 °C. ^1H NMR (600 MHz, $\text{C}_2\text{D}_2\text{Cl}_4$) δ 3.83 (s, NOCH_3), 2.32 (t, $J = 7.8$ Hz, $\text{CH}_2\text{CNOMeCH}_2$), 2.18 (t, $J = 7.8$ Hz, $\text{CH}_2\text{CNOMeCH}_2$), 1.61 (br), 1.34 (br), 0.98 – 0.88 (m). ^{13}C NMR (151 MHz, $\text{C}_2\text{D}_2\text{Cl}_4$) δ 160.9 (CNOCH_3), 60.6 (CNOCH_3), 42.5, 37.5, 33.9, 33.8, 33.5, 32.1, 31.6, 30.1, 29.9, 29.6, 29.4, 29.4, 29.3, 29.3, 29.2, 29.2, 29.1, 29.1, 29.0, 28.9, 27.9, 26.7, 26.4, 26.3, 25.7, 23.8, 23.3, 22.8, 22.3, 13.7, 13.7.

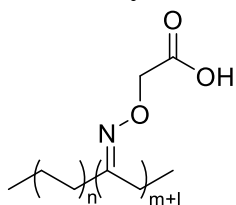
***O*-propargyl oxime LDPE (6c)**



To a 4 mL vial containing a stir bar, 100 mg of polymer **2** (0.107 mmol ketone) and 58 mg of *O*-propargylhydroxylamine hydrochloride (0.55 mmol) were added. The solids were suspended in 2 mL THF, and the vial was heated at 80 °C for 24 h. After cooling, the contents of the vial were poured into chilled methanol under vigorous stirring. The slurry was filtered to yield polymer **6c** as a light tan powder (81 mg, 77%). The degree of functionalization was determined to be 2.7% oxime by variable temperature ^1H NMR spectroscopy at 100 °C. Polymer **6c** was insoluble in

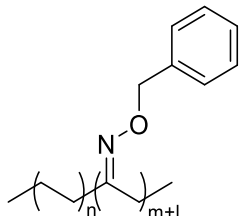
1,2,4-trichlorobenzene at 135 °C and was therefore not able to be characterized by HTSEC. ¹H NMR (600 MHz, C₂D₂Cl₄) δ 4.68 (d, *J* = 2.4 Hz, NOCH₂CCH), 2.47 (br, NOCH₂CCH), 2.39 (t, *J* = 7.8 Hz, CH₂CNOCH₂CCHCH₂), 2.25 (t, *J* = 7.5 Hz, CH₂CNOCH₂CCHCH₂), 1.61 (br), 1.34 (br), 0.98 – 0.88 (m). ¹³C NMR (151 MHz, C₂D₂Cl₄) δ 162.5 (CNOCH₂CCH), 80.8 (NOCH₂CCH), 73.3 (NOCH₂CCH), 60.5 (NOCH₂CCH), 37.5, 33.9, 33.8, 33.5, 31.6, 29.9, 29.5, 29.4, 29.4, 29.3, 29.3, 29.1, 29.1, 28.9, 28.1, 26.7, 26.2, 25.7, 22.8, 22.3, 13.7.

***O*-carboxylic acid oxime LDPE (6d)**



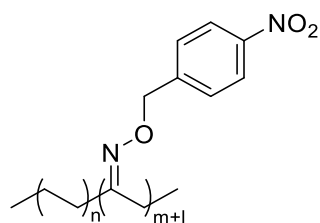
To a 4 mL vial containing a stir bar, 100 mg of polymer **2** (0.107 mmol ketone) and 60 mg of *O*-(carboxymethyl)hydroxylamine hemihydrochloride (0.55 mmol) were added. The solids were suspended in 2 mL THF, and the vial was heated at 80 °C for 24 h. After cooling, the contents of the vial were poured into chilled methanol under vigorous stirring. The slurry was filtered to yield polymer **6d** as a light tan powder (77 mg, 71%). The degree of functionalization was determined to be 1.5% oxime by variable temperature ¹H NMR spectroscopy at 100 °C. ¹H NMR (600 MHz, C₂D₂Cl₄) δ 4.58 (s), 2.41 (t, *J* = 7.4 Hz), 2.26 (t, *J* = 7.6 Hz), 1.61 (br), 1.34 (br), 0.98 – 0.88 (m). ¹³C NMR (151 MHz, C₂D₂Cl₄) δ 140.9 (CNOCH₂CO₂H), 69.9 (CNOCH₂CO₂H), 33.9, 29.9, 29.4, 29.2, 29.0, 28.9, 28.5, 26.7, 25.9, 25.6, 22.9, 22.4, 13.8.

***O*-benzyl oxime LDPE (6e)**



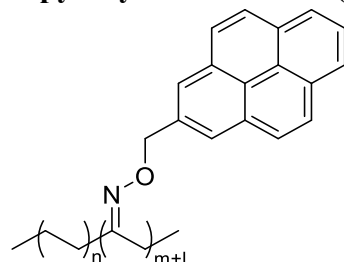
To a 4 mL vial containing a stir bar, 100 mg of polymer **2** (0.107 mmol ketone) and 85 mg of *O*-benzylhydroxylamine hydrochloride (0.53 mmol) were added. The solids were suspended in 2 mL THF, and the vial was heated at 80 °C for 24 h. After cooling, the contents of the vial were poured into chilled methanol under vigorous stirring. The slurry was filtered to yield polymer **6e** as a light tan powder (88 mg, 79%). The degree of functionalization was determined to be 2.9% oxime by variable temperature ¹H NMR spectroscopy at 100 °C. ¹H NMR (600 MHz, C₂D₂Cl₄) δ 7.41 – 7.31 (m), 7.31 – 7.27 (m), 5.10 (s, NOCH₂Ph), 2.37 (t, *J* = 7.5 Hz, CH₂CNOBnCH₂), 2.20 (t, *J* = 7.5 Hz, CH₂CNOBnCH₂), 1.61 (br), 1.34 (br), 0.98 – 0.88 (m). ¹³C NMR (151 MHz, C₂D₂Cl₄) δ 161.4 (CNOCH₂Ph), 138.9 (CNOCH₂C(C₂H₂)(C₂H₂)CH), 127.9 (CNOCH₂C(C₂H₂)(C₂H₂)CH), 127.5 (CNOCH₂C(C₂H₂)(C₂H₂)CH), 127.0 (CNOCH₂C(C₂H₂)(C₂H₂)CH), 75.0, 37.5, 33.9, 31.7, 29.9, 29.6, 29.4, 29.3, 29.1, 28.9, 28.2, 26.7, 26.3, 25.7, 22.9, 13.8.

***O*-*p*-nitrobenzyl oxime LDPE (6f)**



To a 4 mL vial containing a stir bar, 100 mg of polymer **2** (0.107 mmol ketone) and 90 mg of *O*-(4-nitrobenzyl)hydroxylamine (0.54 mmol) were added. The solids were suspended in 2 mL THF, and the vial was heated at 80 °C for 24 h. After cooling, the contents of the vial were poured into chilled methanol under vigorous stirring. The slurry was filtered to yield polymer **6f** as a light tan powder (97 mg, 84%). The degree of functionalization was determined to be 2.0% oxime by variable temperature ¹H NMR spectroscopy at 100 °C. ¹H NMR (600 MHz, C₂D₂Cl₄) δ 8.20 (d, *J* = 8.7 Hz, 1H), 7.53 (d, *J* = 8.3 Hz, 1H), 5.17 (s), 2.38 (t, *J* = 7.8 Hz, 1H), 2.20 (t, *J* = 7.5 Hz, 1H), 1.61 (br), 1.34 (br), 0.98 – 0.88 (m). ¹³C NMR (151 MHz, C₂D₂Cl₄) δ 162.3 (CNOCH₂CCH₄CNO₂), 147.4 (NOCH₂CCH₄CNO₂), 146.6 (NOCH₂CCH₄CNO₂), 127.9, 123.1, 73.7 (CNOCH₂R), 37.5, 33.9, 33.8, 33.5, 32.1, 31.6, 29.9, 29.6, 29.4, 29.4, 29.3, 29.3, 29.1, 29.1, 29.0, 28.9, 28.2, 26.7, 26.1, 25.7, 22.9, 22.4, 13.8, 13.7.

***O*-pyrenyl oxime LDPE (6g)**

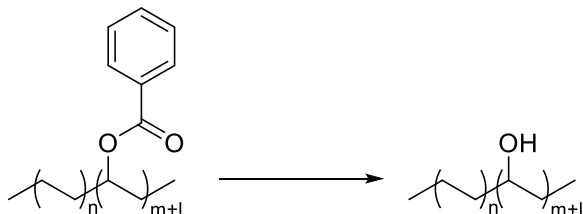


To a 4 mL vial containing a stir bar, 100 mg of polymer **2** (0.107 mmol ketone) and 150 mg of *O*-(pyren-1-ylmethyl)hydroxylammonium chloride (0.54 mmol) were added. The solids were suspended in 2 mL THF, and the vial was heated at 80 °C for 24 h. After cooling, the contents of the vial were poured into chilled methanol under vigorous stirring. The slurry was filtered to yield polymer **6g** as a light tan powder (78 mg, 63%). The degree of functionalization was determined to be 2.1% oxime by variable temperature ¹H NMR spectroscopy at 100 °C. ¹H NMR (600 MHz, C₂D₂Cl₄) δ 8.48 – 8.42 (m), 8.25 – 7.96 (m), 5.81 (s, NOCH₂R), 2.36 (t, *J* = 6.9 Hz, CH₂CNORCH₂), 2.22 (t, *J* = 7.2 Hz, CH₂CNORCH₂), 1.61 (br), 1.34 (br), 0.98 – 0.88 (m). ¹³C NMR (151 MHz, C₂D₂Cl₄) δ 161.7 (CNOCH₂R), 132.2, 131.2, 131.0, 130.8, 129.3, 127.3, 127.2, 127.1, 125.7, 124.9, 124.9, 124.7, 124.3, 123.7, 73.5 (CNOCH₂R), 37.5, 33.9, 33.9, 33.5, 32.1, 31.6, 29.9, 29.5, 29.4, 29.2, 29.1, 29.1, 29.1, 28.9, 28.3, 26.7, 26.3, 25.8, 22.9, 22.4, 13.8.

3.10.6 Procedure for the reduction polymer 1 with sodium borohydride

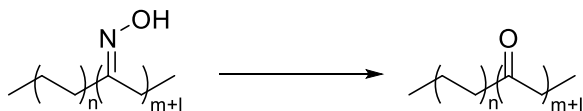
To a 20 mL vial containing a stir bar, 100 mg of polymer **1** (0.057 mmol ketone) and the corresponding amount of sodium borohydride were added. The solids were suspended in 4 mL THF, and the vial was heated at 80 °C for 24 h. After cooling, the contents of the vial were poured into chilled methanol under vigorous stirring. The slurry was filtered to yield the polymer as a tan powder.

3.10.7 Procedure for the hydrolysis of polymer 4d



To a 4 mL vial containing a stir bar were added 25 mg of polymer **4d** (0.027 mmol ester) and 37 mg of lithium hydroxide monohydrate (0.891 mmol). The solids were suspended in 1 mL of *tert*-amyl alcohol, and the vial was heated at 120 °C for 72 h. After cooling, the contents of the vial were poured into chilled methanol under vigorous stirring. The slurry was filtered to yield polymer **3** as a white powder (18 mg, 81%). The degree of functionalization was determined to be 2.7% alcohol by variable temperature ^1H NMR spectroscopy at 100 °C.

3.10.8 Procedure for the hydrolysis of polymer 6a






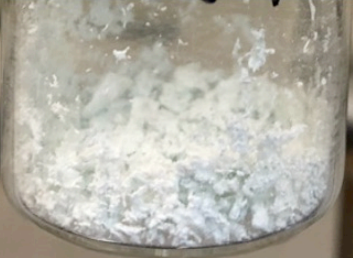




To a 4 mL vial containing a stir bar were added 25 mg of polymer **6a** (0.027 mmol oxime) and 5 mg of *p*-toluenesulfonic acid monohydrate (0.027 mmol). The solids were suspended in 1 mL of *tert*-amyl alcohol, and the vial was heated at 120 °C for 24 h. After cooling, the contents of the vial were poured into chilled methanol under vigorous stirring. The slurry was filtered to yield polymer **2** as a white powder (25 mg, 100%). The degree of functionalization was determined to be 2.6% ketone by variable temperature ^1H NMR spectroscopy at 100 °C.

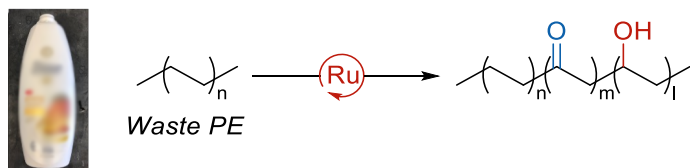
3.10.9 Procedure for the oxidation of and derivatization of waste plastics

To a 20 mL vial containing a stir bar were added 56 mg of waste plastic (2.0 mmol monomer). The solids were suspended in 2 mL of 1,2-dichloroethane and heated at 120 °C until the plastic dissolved. The vial was then cooled to room temperature, and 33 mg of 2,6-dichloropyridine *N*-oxide (0.20 mmol) were added. A solution of Ru(TPFPP)CO in dichloromethane (1 mM) was prepared, and 100 μL of this solution was added to the vial. The vial was heated at 120 °C for 30 min. The contents of the vial were cooled and poured into chilled methanol under vigorous stirring. The slurry was filtered to yield oxidized waste polyethylenes. The ¹H NMR and FTIR spectra of the oxidized products were similar to those of oxidized polyethylenes derived from virgin polyethylene.

Table 3.10.9.1. Oxidation of various waste plastics.

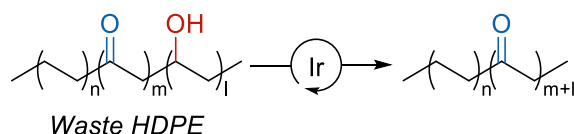
Waste PE Source	Type of PE	Oxidation Product	Degree of Functionalization
 Shampoo bottle	HDPE		1.0% alcohol 1.1% ketone
 Coffee container	HDPE		1.8% alcohol 1.8% ketone
 Food packaging	LDPE		1.6% alcohol 2.7% ketone
 Plastic bag	LDPE		1.5% alcohol 2.7% ketone

3.10.9.1 Ruthenium catalyzed oxidation of a shampoo bottle



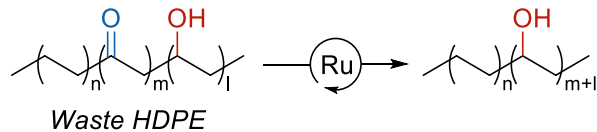
To a 20 mL vial with stir bar were added 158 mg (5.6 mmol monomer) of a shampoo bottle that was cut in pieces with scissors. The solids were suspended in 5.6 mL of 1,2-dichloroethane and heated at 120 °C until the plastic dissolved. The vial was then cooled to room temperature, and 92 mg of 2,6-dichloropyridine *N*-oxide (0.56 mmol) were added. A solution of Ru(TPFPP)CO in dichloromethane (1 mM) was prepared, and 282 μ L of this solution was added to the vial. The vial was heated at 120 °C for 30 min. The contents of the vial were cooled and poured into chilled methanol under vigorous stirring. The slurry was filtered to yield a white powder (84 mg, 53%). The degree of functionalization was determined to be 2.1% total functionalization (1.1% ketone and 1.0% alcohol) by variable temperature ^1H NMR spectroscopy at 100 °C.

3.10.9.2 Oxidation of the functionalized shampoo bottle



To a 20 mL vial with stir bar were added 25 mg of oxo-waste HDPE (0.009 mmol alcohol), 0.35 mg of $[\text{Cp}^*\text{IrCl}_2]_2$ (0.05 mmol), and 1 mg of potassium carbonate (0.007 mmol). The solids were suspended in 1 mL of toluene, and 100 μ L of acetone (1.35 mmol) were added to the vial. The vial was heated at 140 °C for 48 h. The contents of the vial were cooled and poured into chilled methanol under vigorous stirring. The slurry was filtered to yield a white powder (20 mg, 80%). The degree of functionalization was determined to be 2.5% total functionalization (2.0% ketone and 0.5% alcohol) by variable temperature ^1H NMR spectroscopy at 100 °C.

3.10.9.3 Reduction of the functionalized shampoo bottle



To a 18 mL test tube with stir bar under nitrogen were added 25 mg of oxo-waste HDPE (0.010 mmol ketone), 0.7 mg of $\text{Ru}(\text{PPh}_3)_3\text{Cl}_2$ (0.0007 mmol), and 1 mg of potassium hydroxide (0.018 mmol). The solids were suspended in 1 mL of *tert*-amyl alcohol, and 100 μ L of ethylene diamine (1.50 mmol) were added to the tube. The tube was placed inside a Parr reactor (450 L internal volume) and sealed. The reactor was charged with 750 psi of hydrogen and heated at 120 °C for 24 h. After the reactor was cooled to room temperature, the pressure was released slowly. The contents of the tube were then poured into chilled methanol under vigorous stirring. The slurry was filtered to yield a brown powder (12 mg, 50%). The degree of functionalization was determined to be 2.2% total functionalization (0.1% ketone and 2.1% alcohol) by variable temperature ^1H NMR spectroscopy at 100 °C.

3.10.9.4 Reduction of the functionalized shampoo bottle with NaBH₄

To a 4 mL vial containing a stir bar were added 25 mg of oxo-waste HDPE (0.010 mmol ketone) and 5 mg of sodium borohydride (0.13 mmol) were added. The solids were suspended in 1 mL THF, and the vial was heated at 80 °C for 24 h. After cooling, the contents of the vial were poured into chilled methanol under vigorous stirring. The slurry was filtered to yield the polymer as a white powder. The conversion of ketones to alcohols was assessed to be 92% by ¹H NMR spectroscopy.

3.10.10 Procedure for the separation of polymers

To a mortar were added 200 mg of UHMWPE, 250 mg of polyethylene **1**, and 250 mg of polymer **5**. The polymers were mixed with a pestle until a uniform powder was obtained. The powder was then transferred to a glass fritted funnel and washed with boiling acetone (3 x 50 mL). The filtrate was concentrated to yield polymer **5** (242 mg, 97%). The powder that remained in the frit was then transferred to a glass fritted funnel equipped with a heating jacket. Water heated at 70 °C was circulated through the jacket to keep it at a constant temperature. The powder was washed with toluene at 70 °C (3 x 20 mL). The filtrate was then concentrated to afford polymer **1** (240 mg, 96%). The solid that remained was UHMWPE which was collected (140 mg, 70%).

3.10.11 Characterization of synthesized polymers

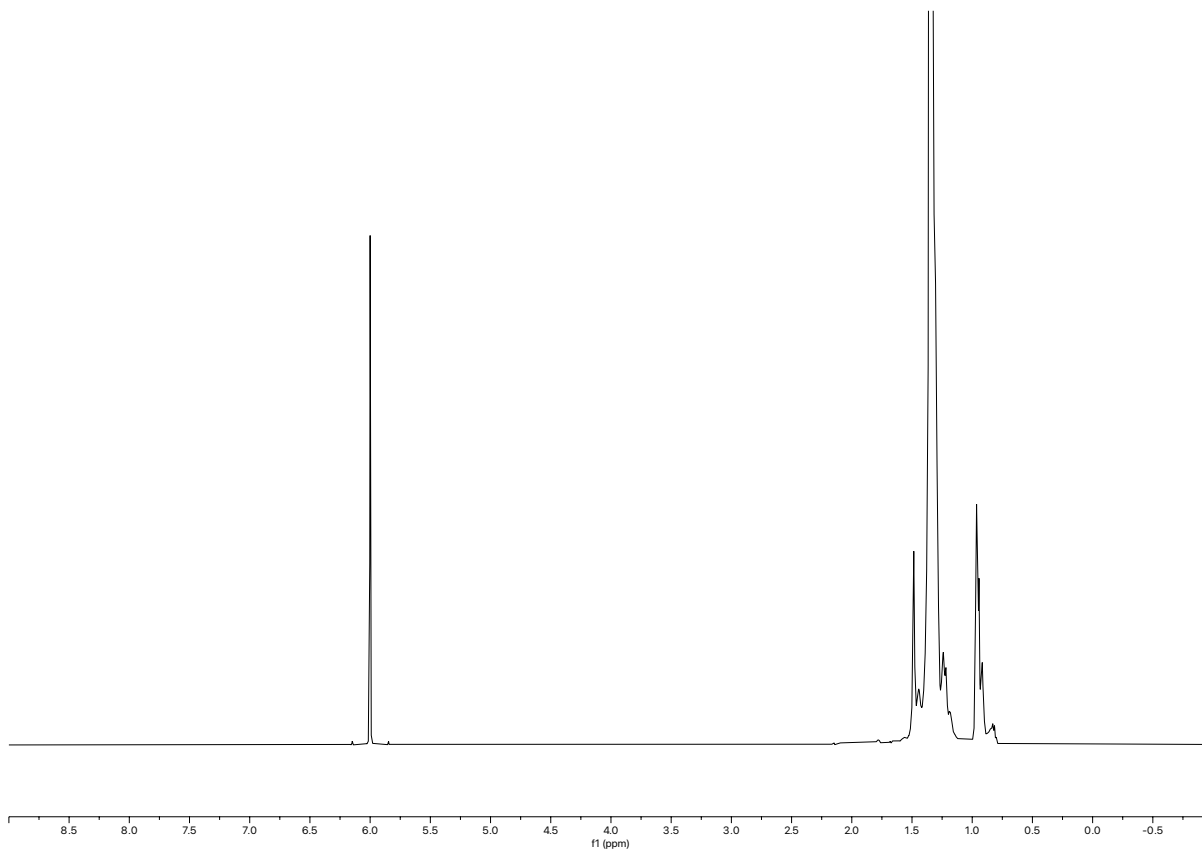
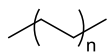


Figure 3.10.11.1. ^1H NMR spectrum of unmodified LDPE

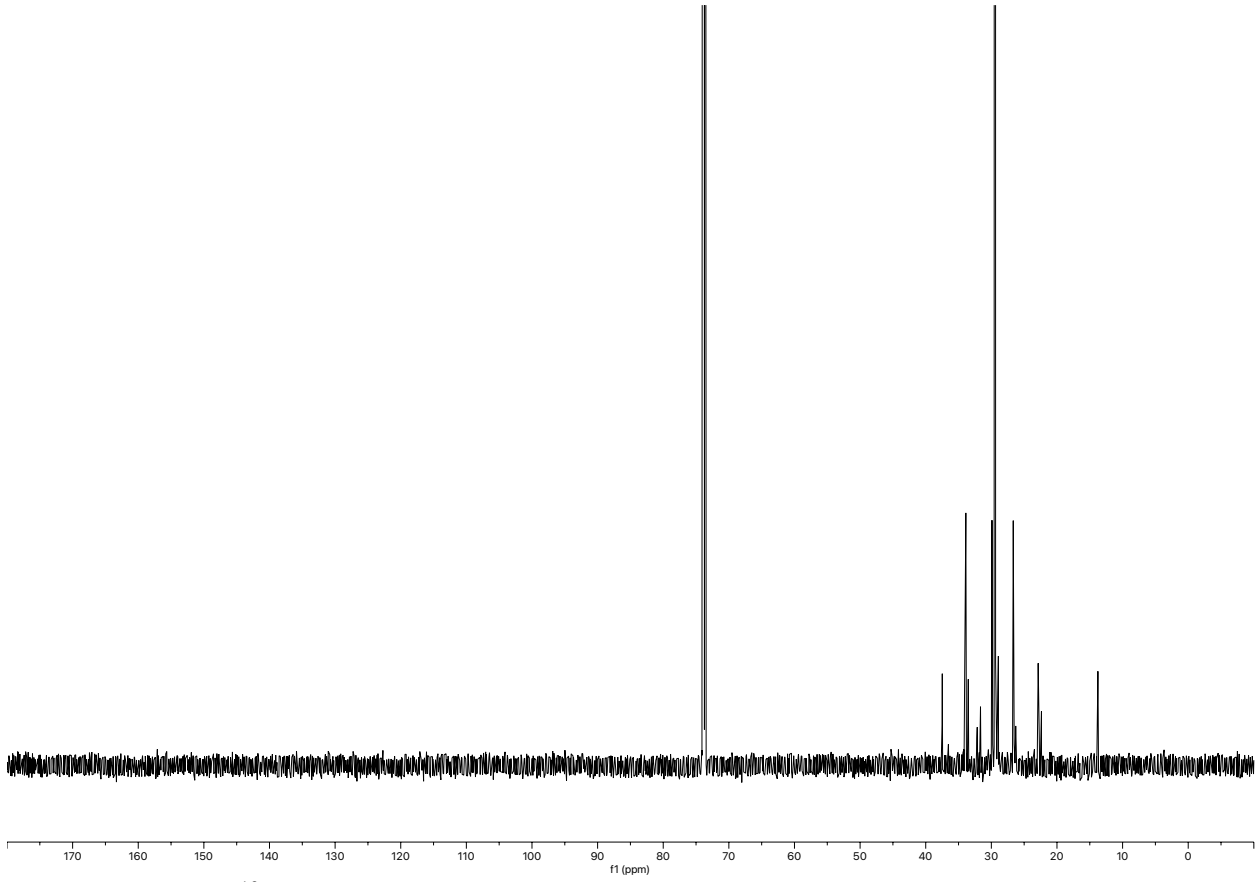
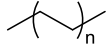


Figure 3.10.11.2. ^{13}C NMR spectrum of unmodified LDPE

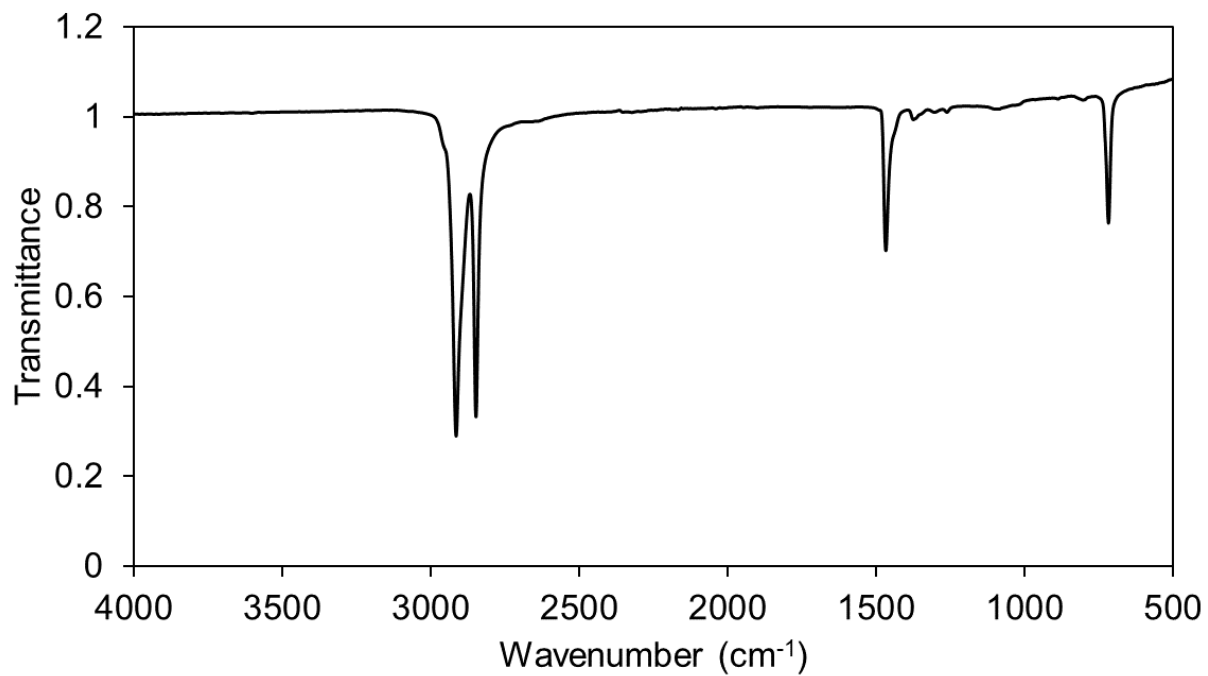


Figure 3.10.11.3. FTIR spectra of unmodified LDPE. Major peaks ν (cm⁻¹): 2915, 2848, 1468, 1375, 718

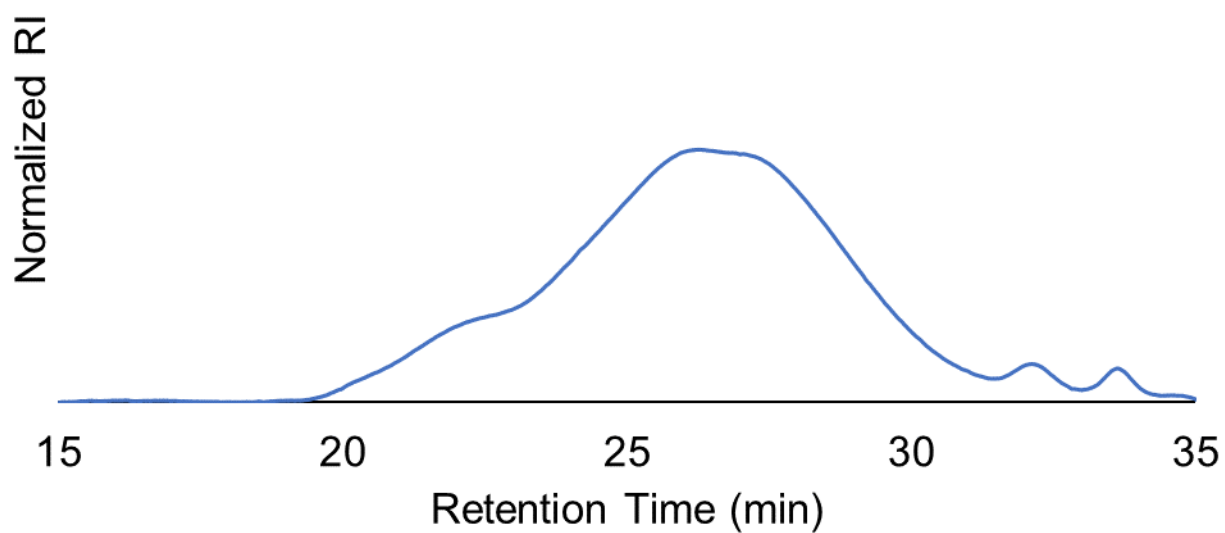


Figure 3.10.11.4. Gel permeation chromatogram of unmodified LDPE. $M_n = 9.6$ kDa, $D = 6.7$. Molecular weight was determined relative to polyethylene standards.

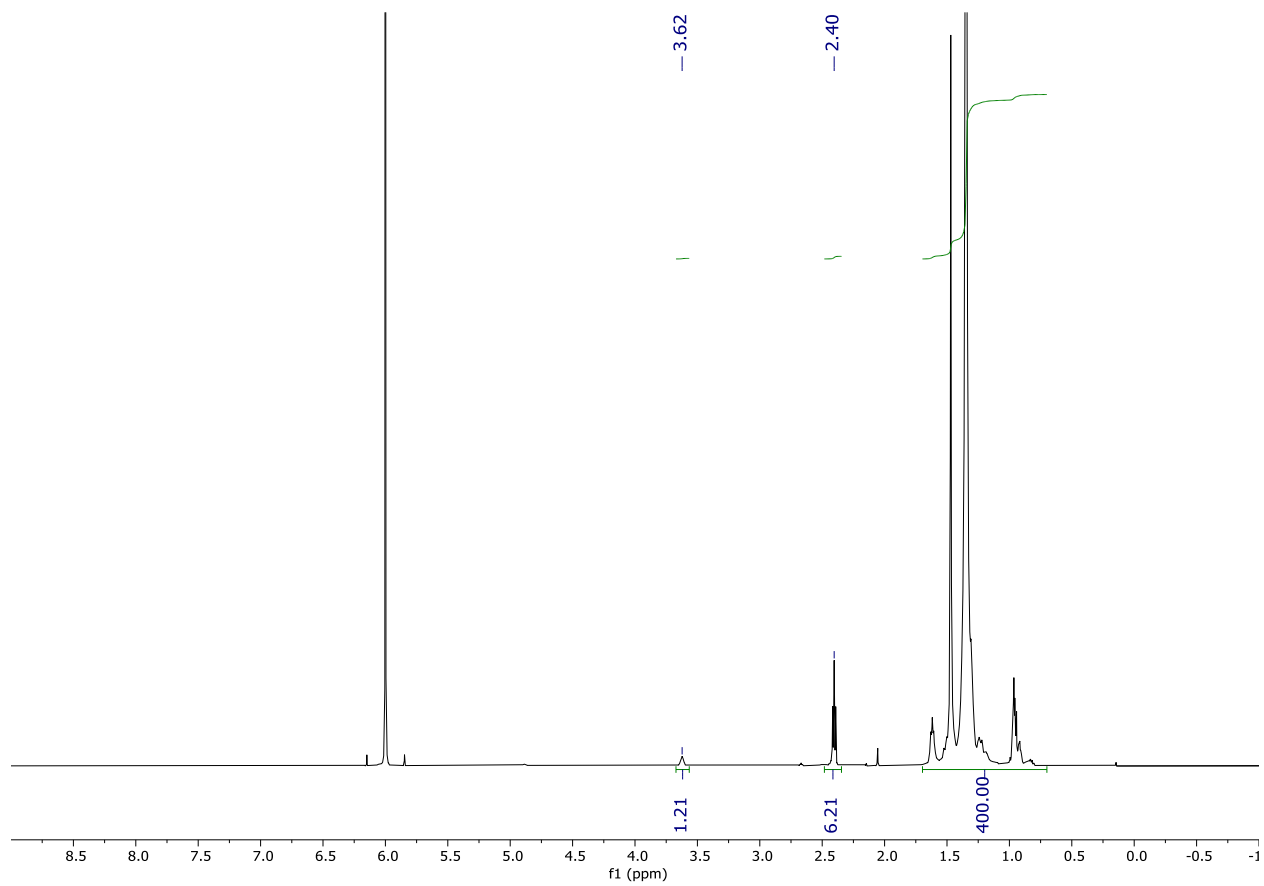
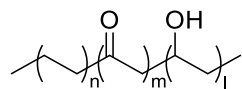


Figure 3.10.11.5. ^1H NMR spectrum of polymer 1

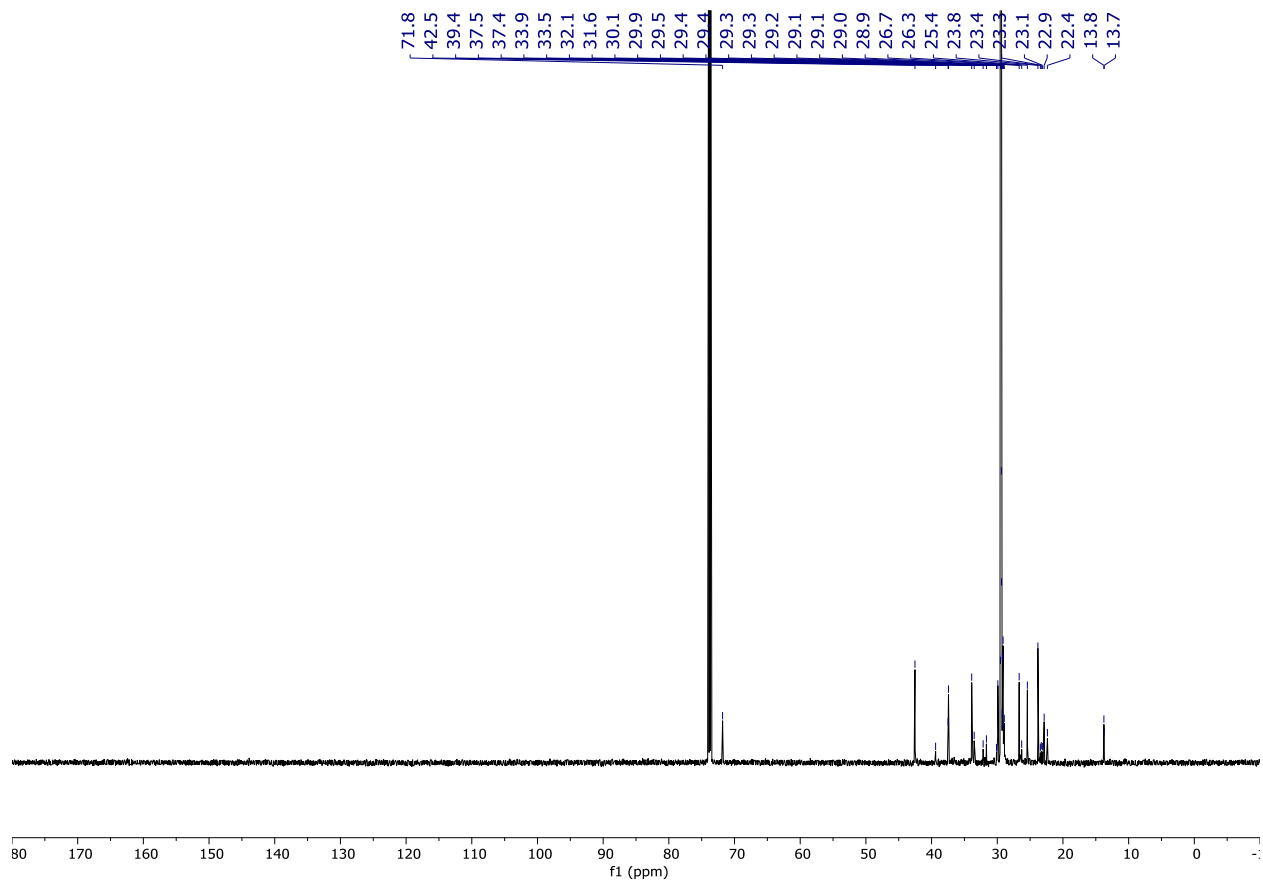
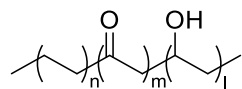


Figure 3.10.11.6. ^{13}C NMR spectrum of polymer 1

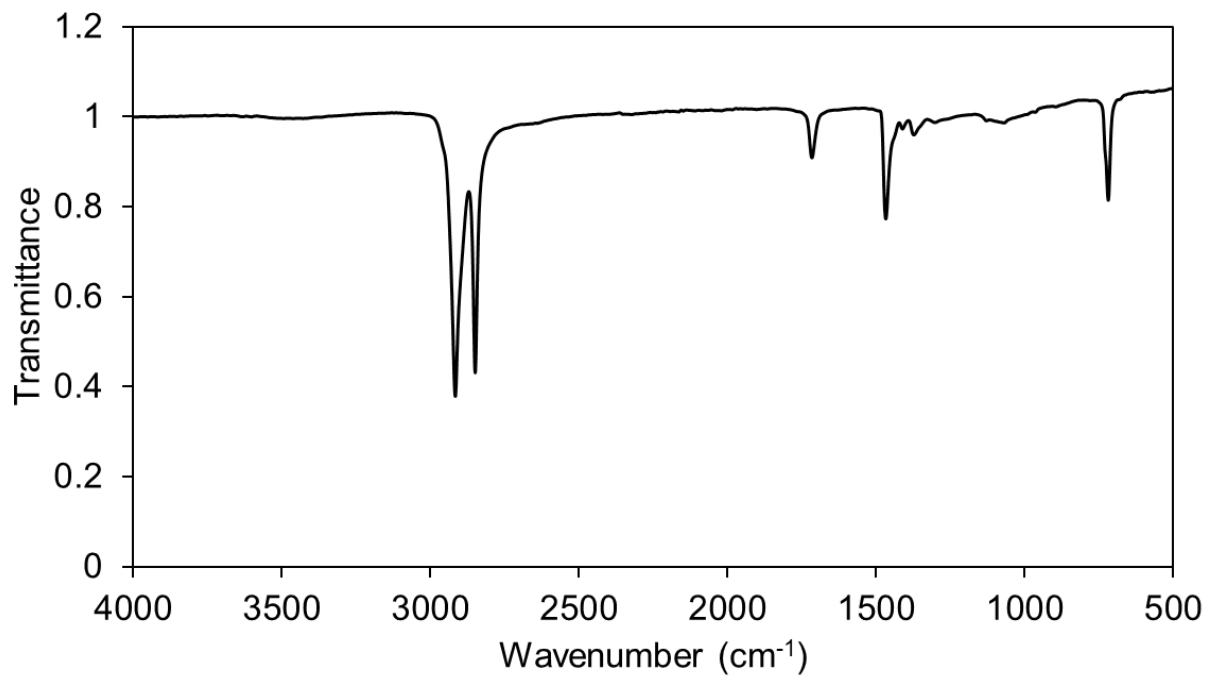


Figure 3.10.11.7. FTIR spectra of polymer **1**. Major peaks ν (cm⁻¹): 3461, 2916, 2849, 1716, 1467, 1411, 1373, 1302, 1070, 719

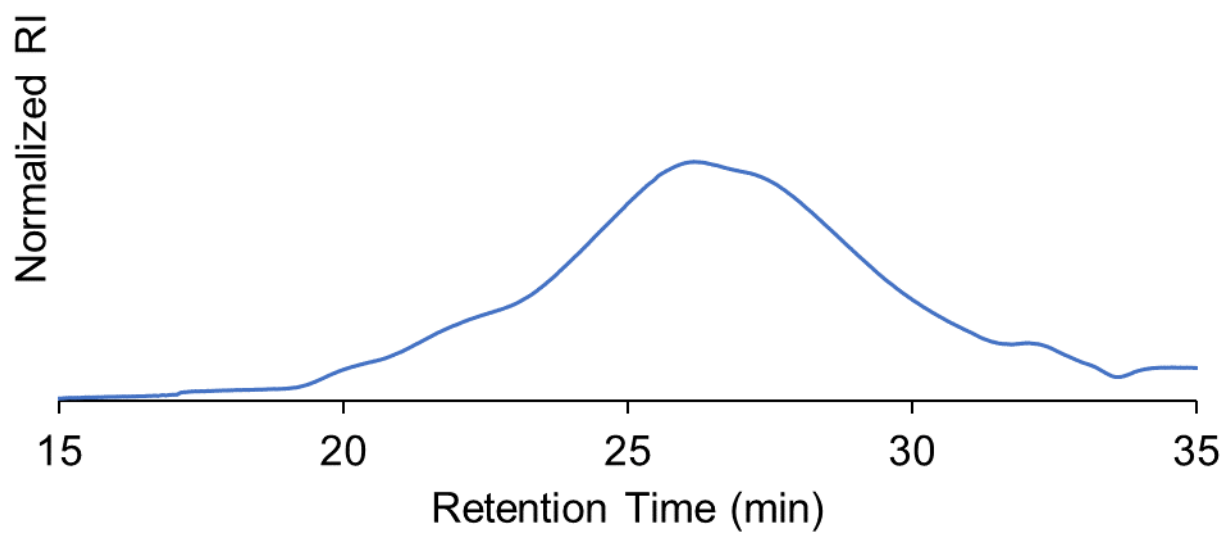


Figure 3.10.11.8. Gel permeation chromatogram of polymer **1**. $M_n = 9.4$ kDa, $D = 7.3$. Molecular weight was determined relative to polyethylene standards.

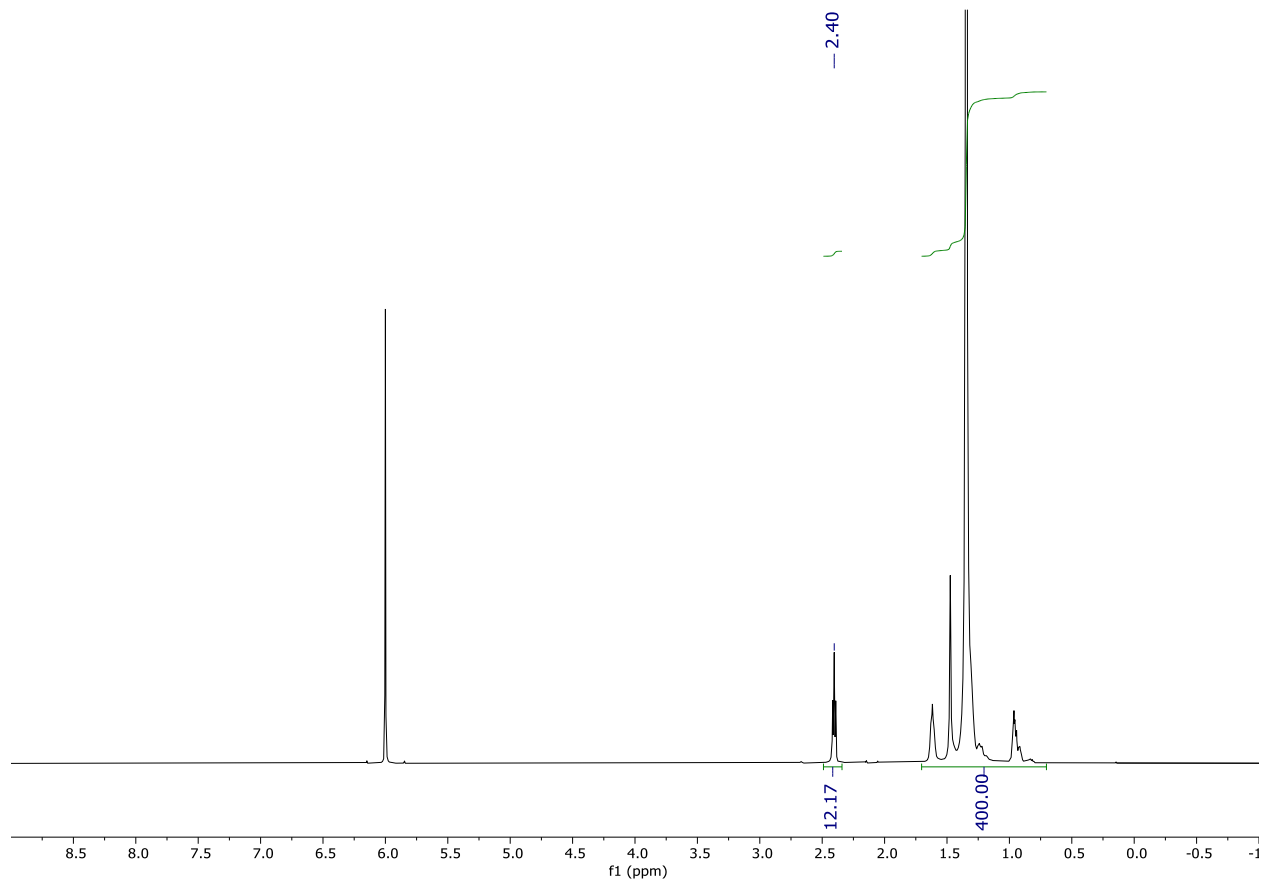
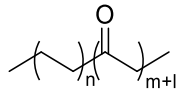


Figure 3.10.11.9. ^1H NMR spectrum of polymer 2

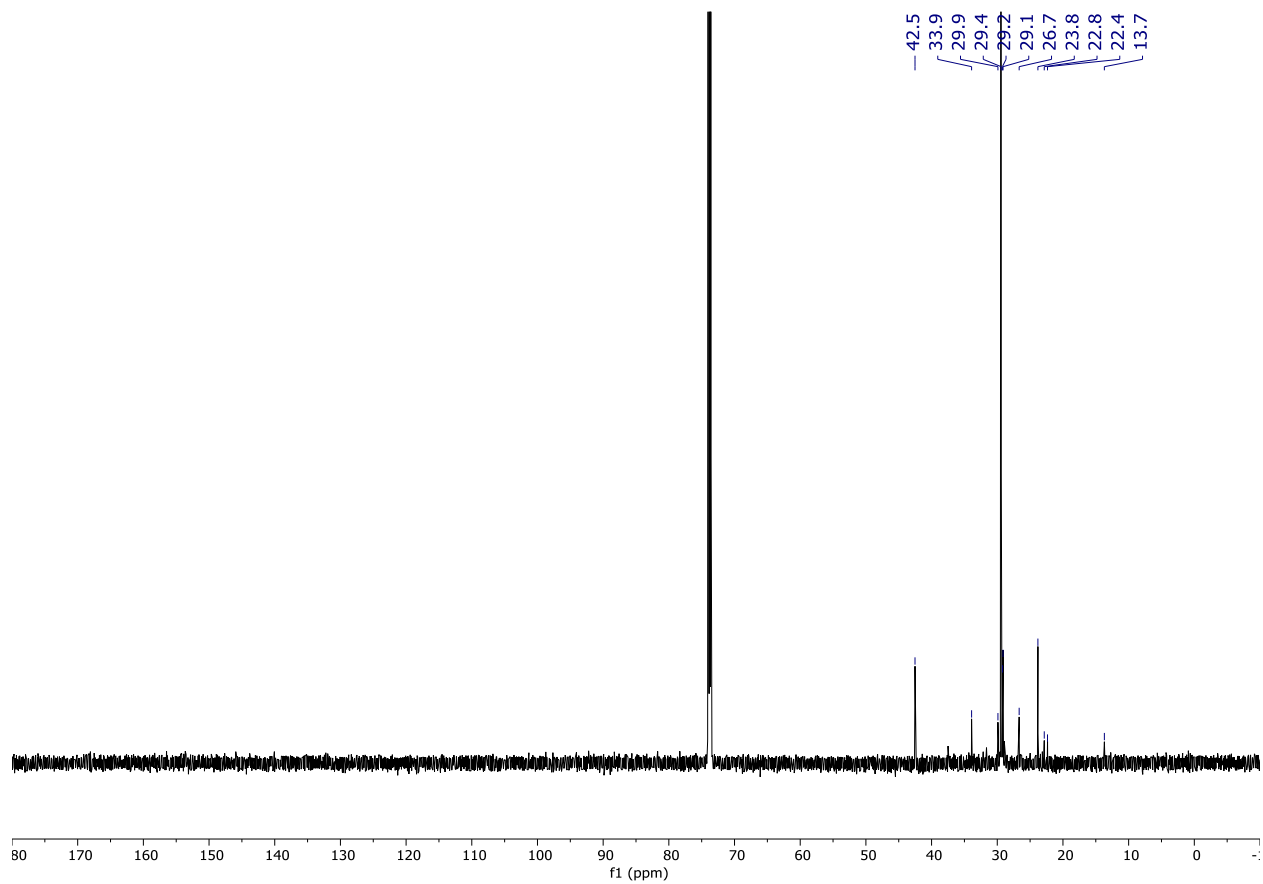
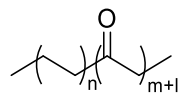


Figure 3.10.11.10. ^{13}C NMR spectrum of polymer 2

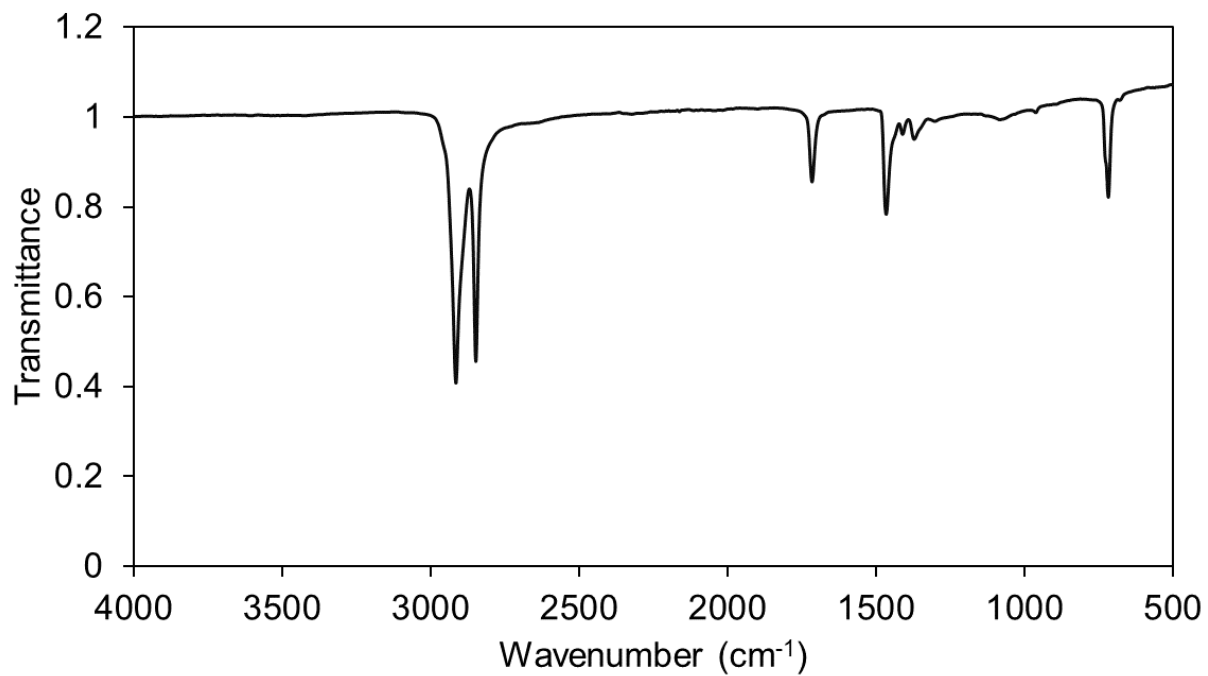


Figure 3.10.11.11. FTIR spectra of polymer **2**. Major peaks ν (cm⁻¹): 2916, 2849, 1717, 1467, 1412, 1373, 1084, 719

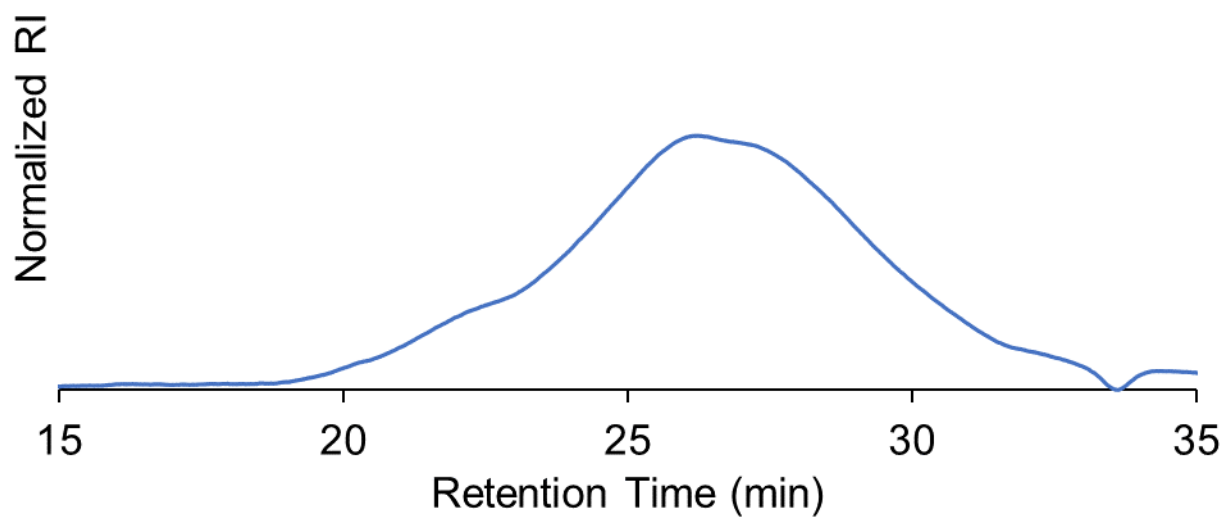


Figure 3.10.11.12. Gel permeation chromatogram of polymer **2**. $M_n = 9.7$ kDa, $D = 6.3$. Molecular weight was determined relative to polyethylene standards.

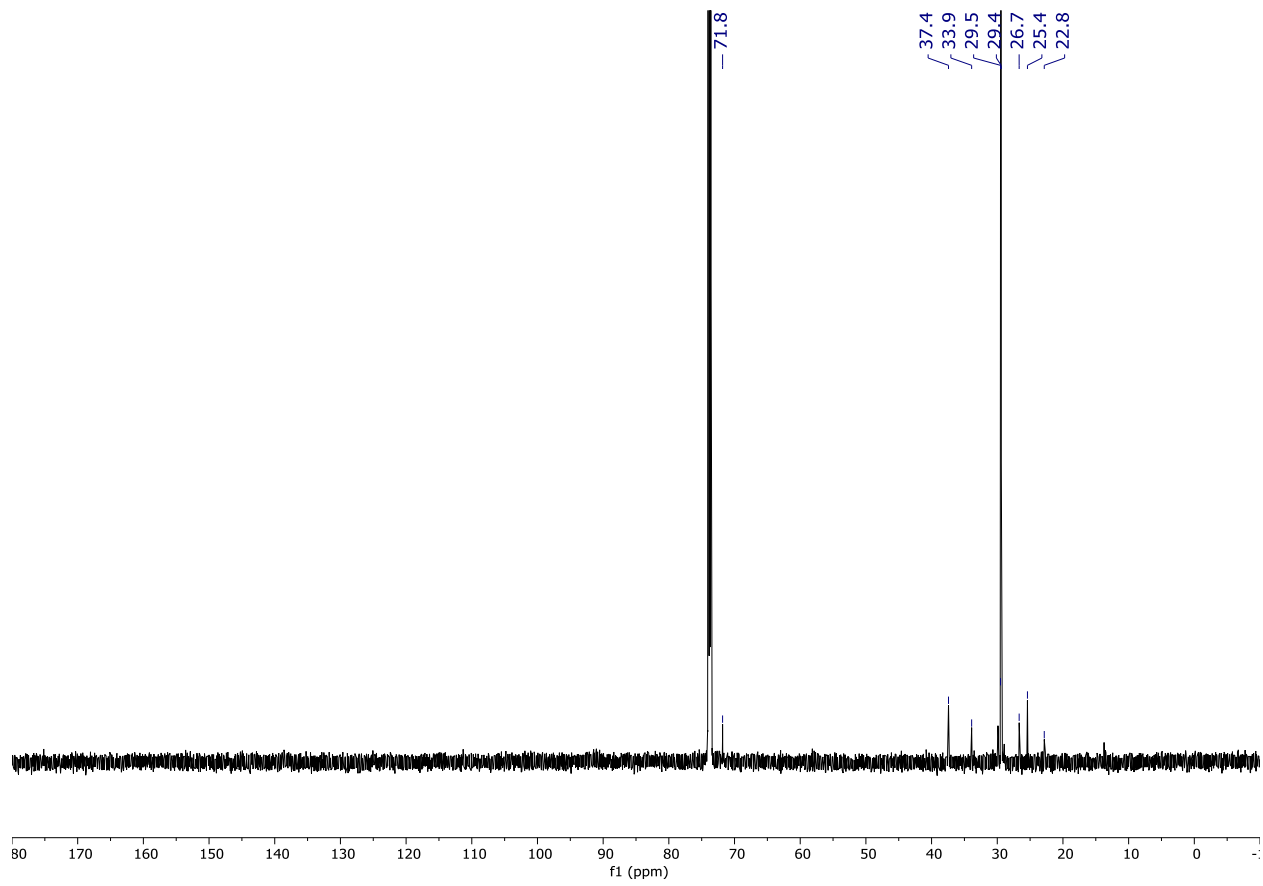
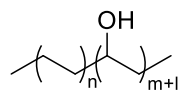


Figure 3.10.11.14. ^{13}C NMR spectrum of polymer 3

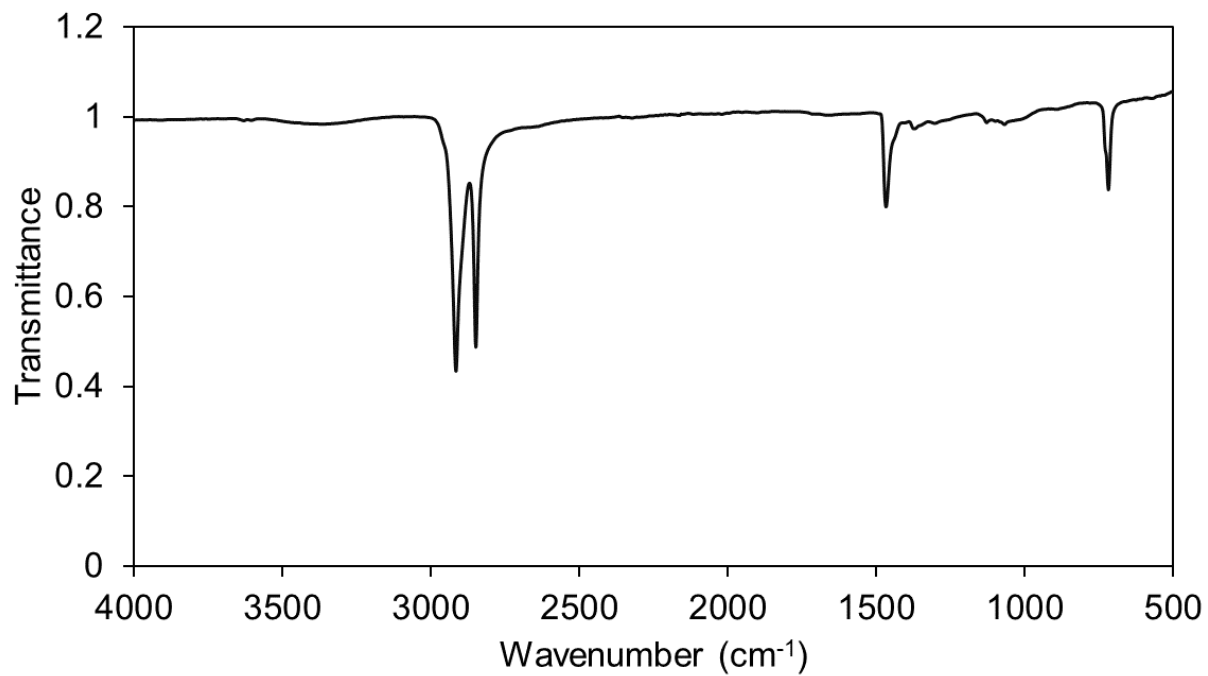


Figure 3.10.11.15. FTIR spectra of polymer **3**. Major peaks ν (cm⁻¹): 3365, 2916, 2849, 1468, 1373, 1129, 1068, 719

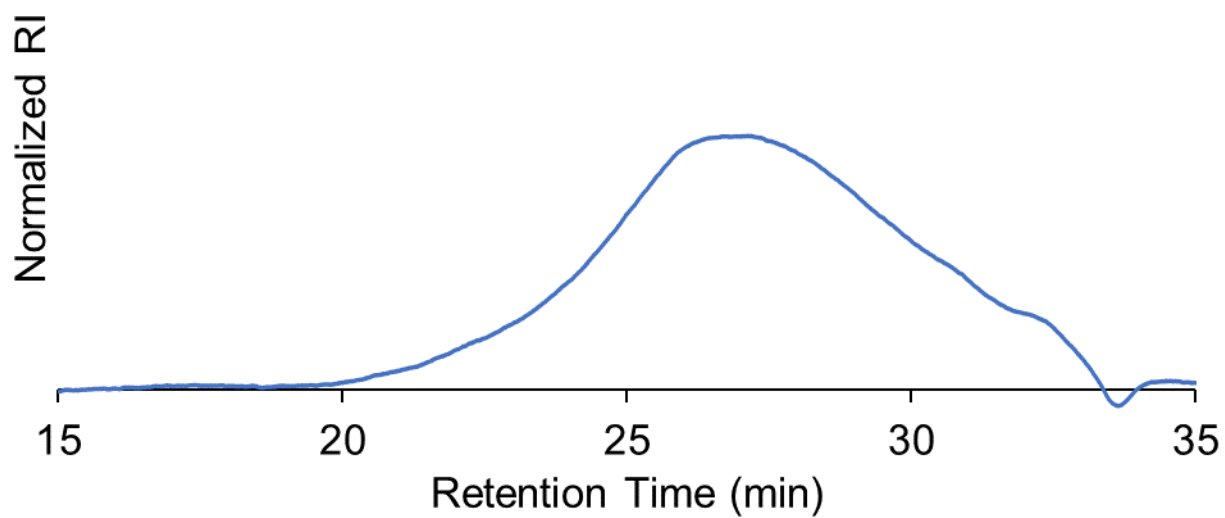


Figure 3.10.11.16. Gel permeation chromatogram of polymer **3**. $M_n = 7.7$ kDa, $D = 4.1$. Molecular weight was determined relative to polyethylene standards.

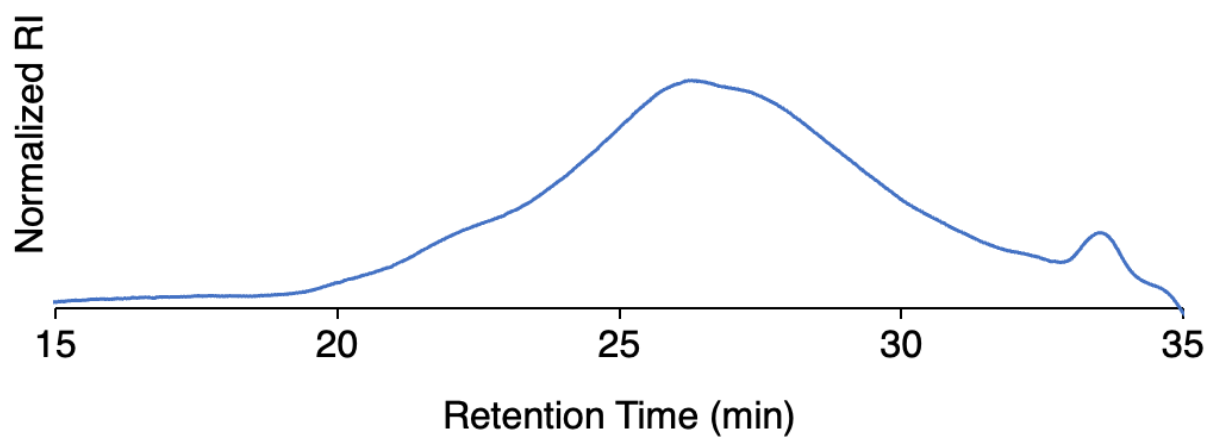


Figure 3.10.11.17. Gel permeation chromatogram of polymer **3** synthesized by reduction with sodium borohydride. $M_n = 9.8$ kDa, $D = 6.1$. Molecular weight was determined relative to polyethylene standards.

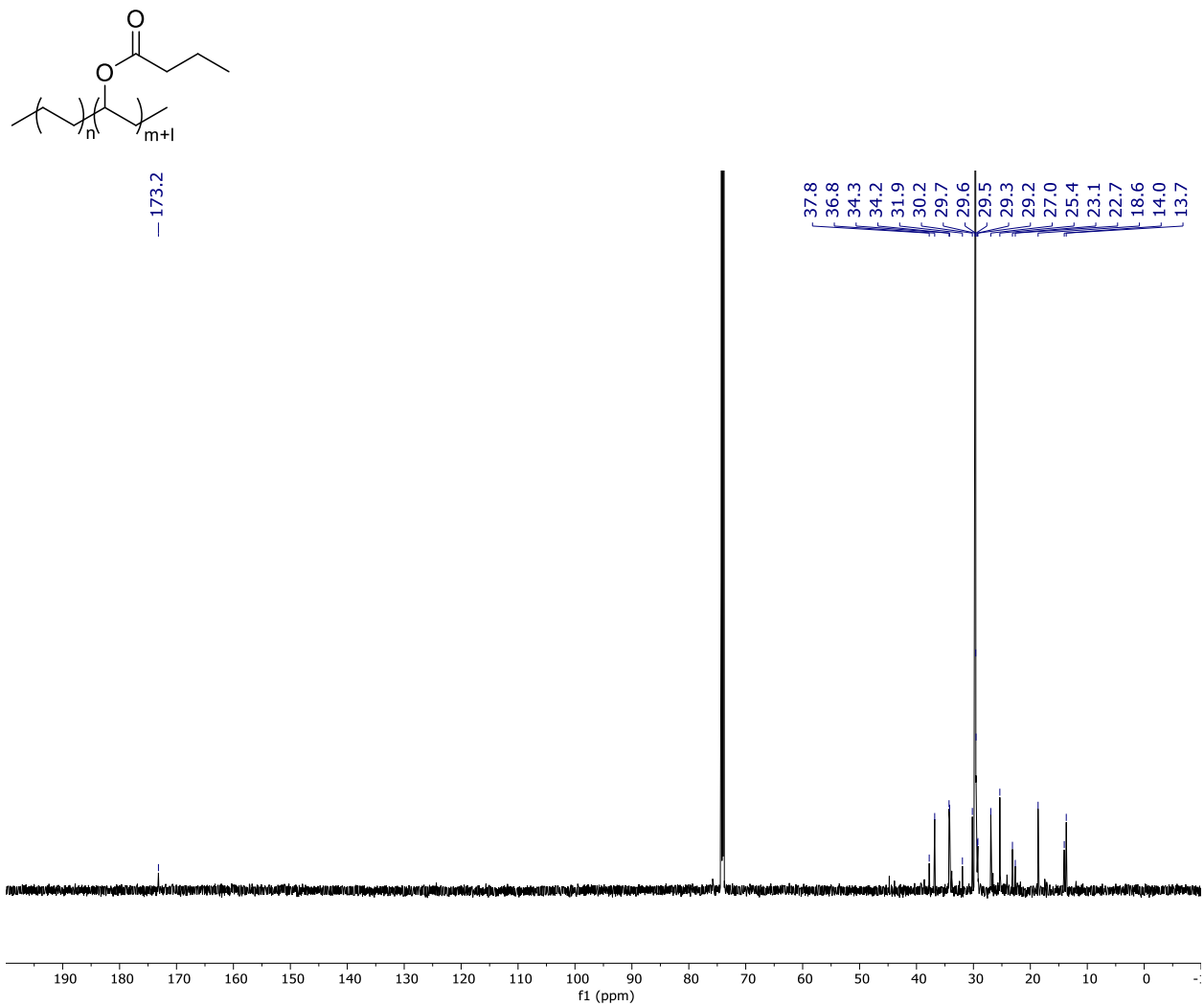


Figure 3.10.11.19. ^{13}C NMR spectrum of polymer **4a**

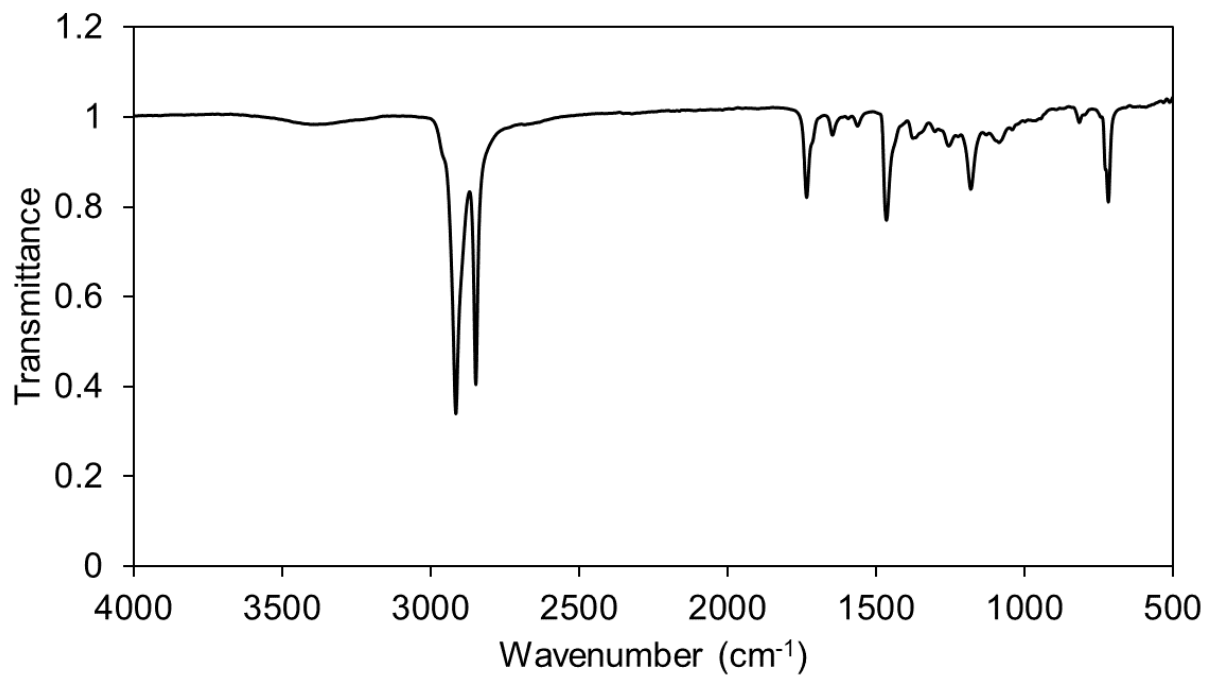


Figure 3.10.11.20. FTIR spectra of polymer **4a**. Major peaks ν (cm⁻¹): 2915, 2849, 1735, 1648, 1563, 1466, 1377, 1303, 1256, 1182, 1087, 817, 719

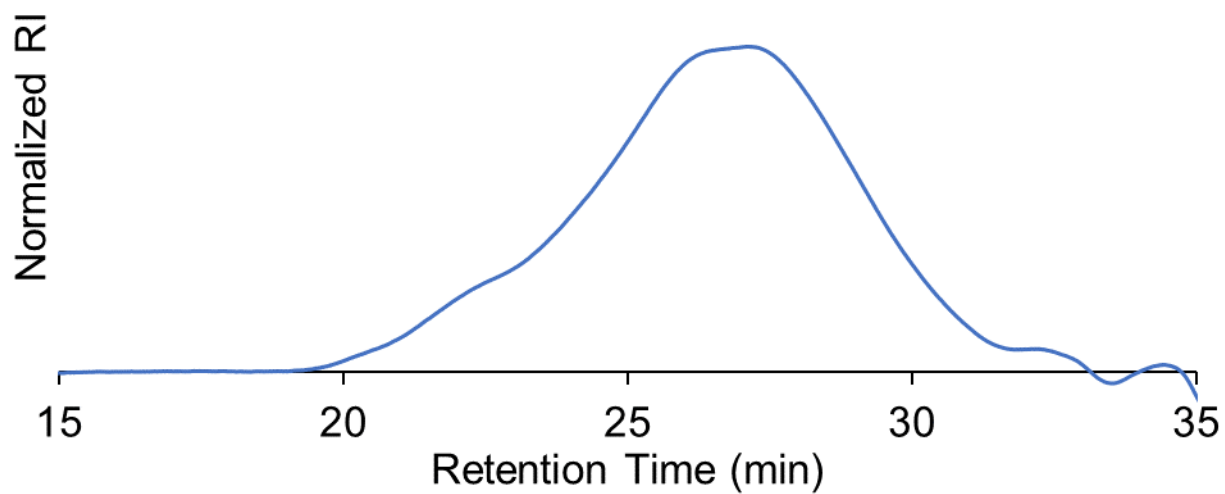


Figure 3.10.11.21. Gel permeation chromatogram of polymer **4a**. $M_n = 7.8$ kDa, $D = 6.4$. Molecular weight was determined relative to polyethylene standards.

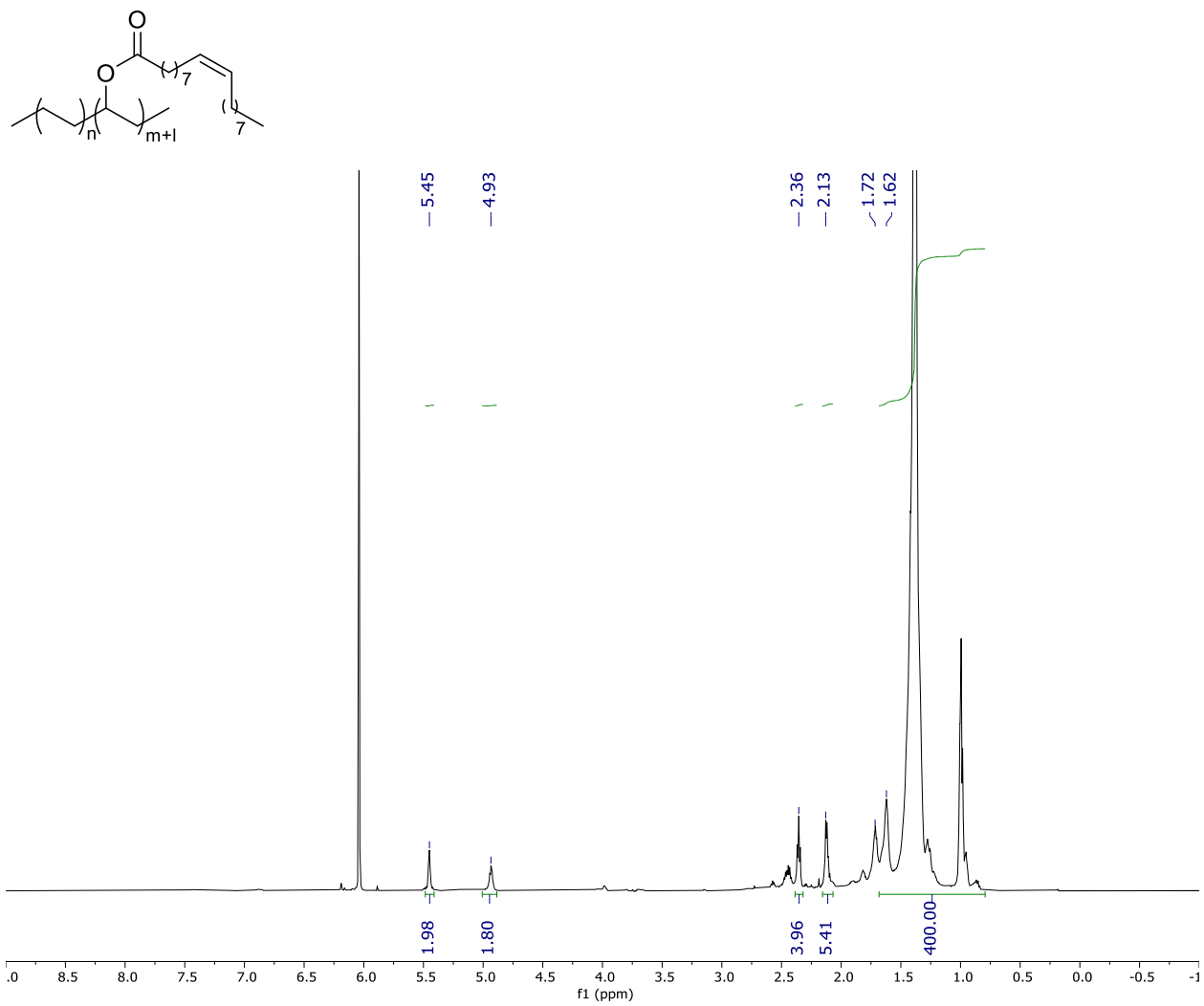


Figure 3.10.11.22. ¹H NMR spectrum of polymer **4b**

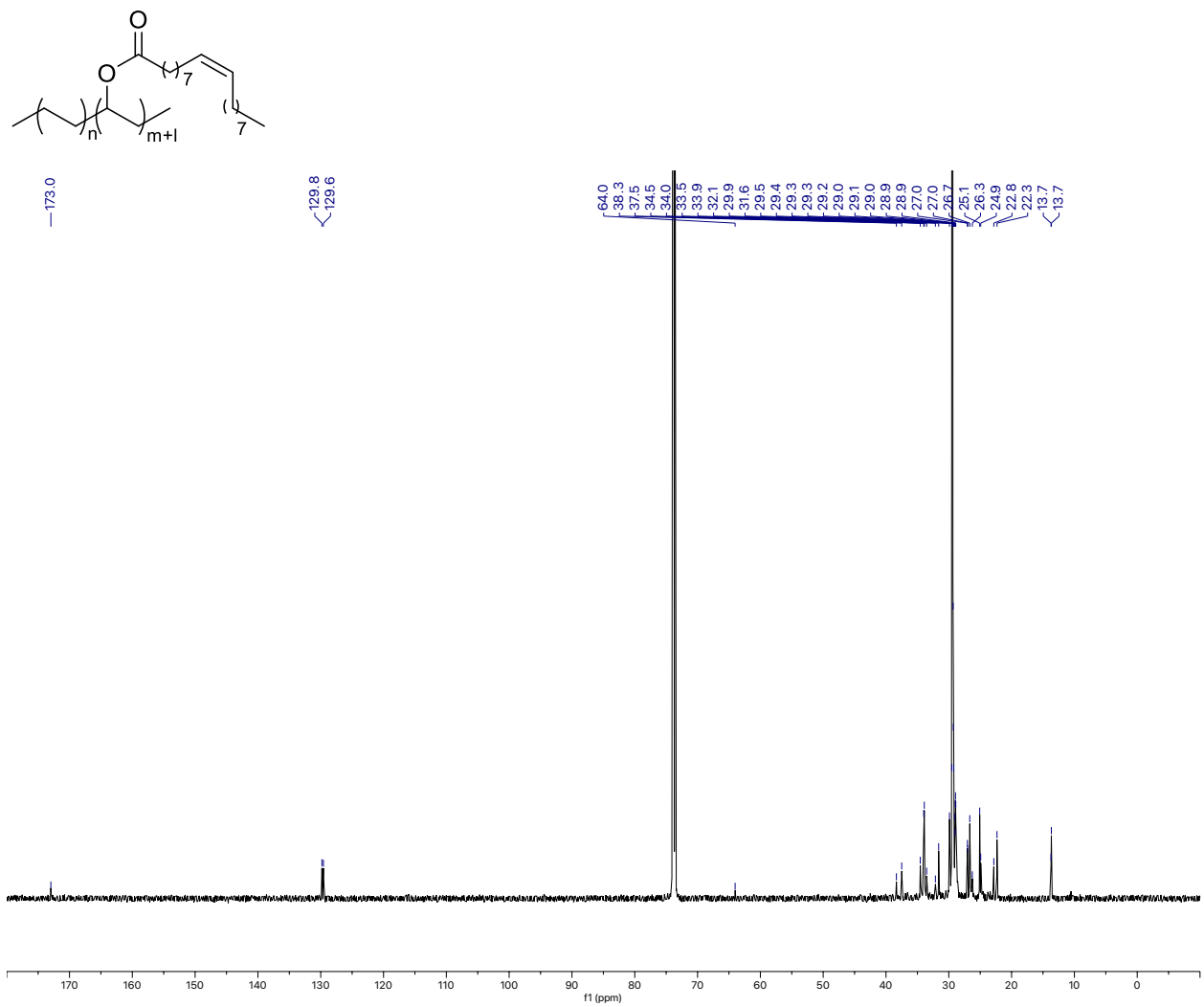


Figure 3.10.11.23. ¹³C NMR spectrum of polymer 4b

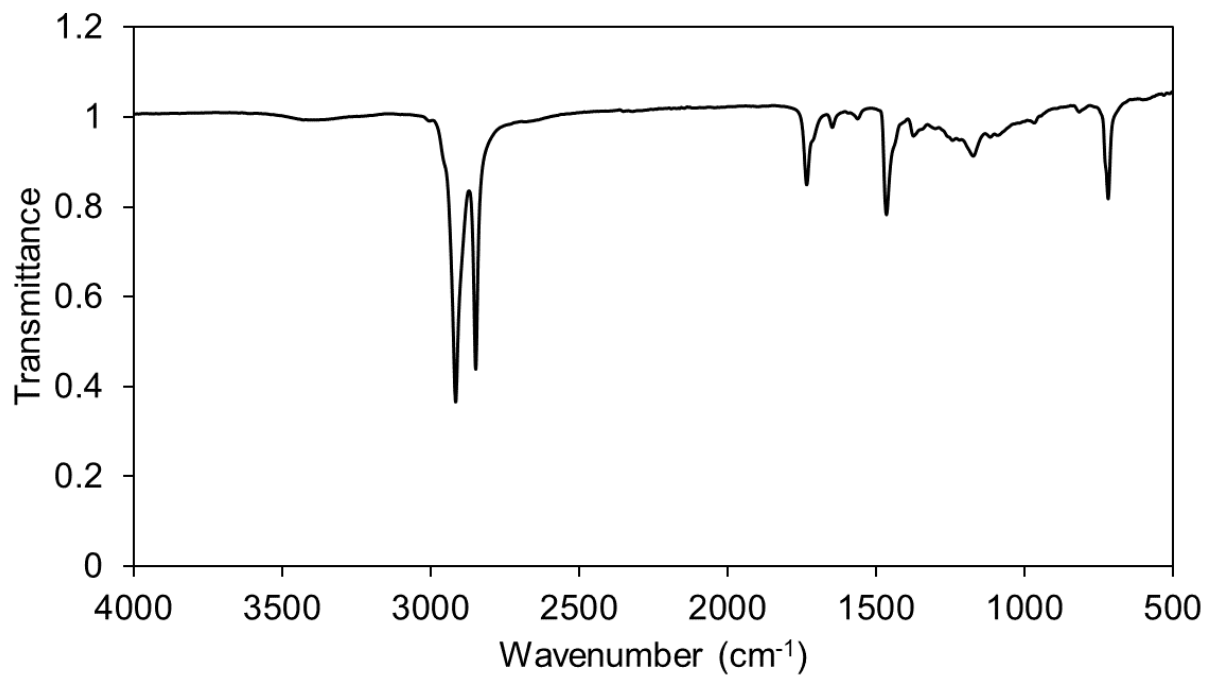


Figure 3.10.11.24. FTIR spectra of polymer **4b**. Major peaks ν (cm⁻¹): 2917, 2849, 1734, 1648, 1563, 1466, 1375, 1174, 1117, 968, 719

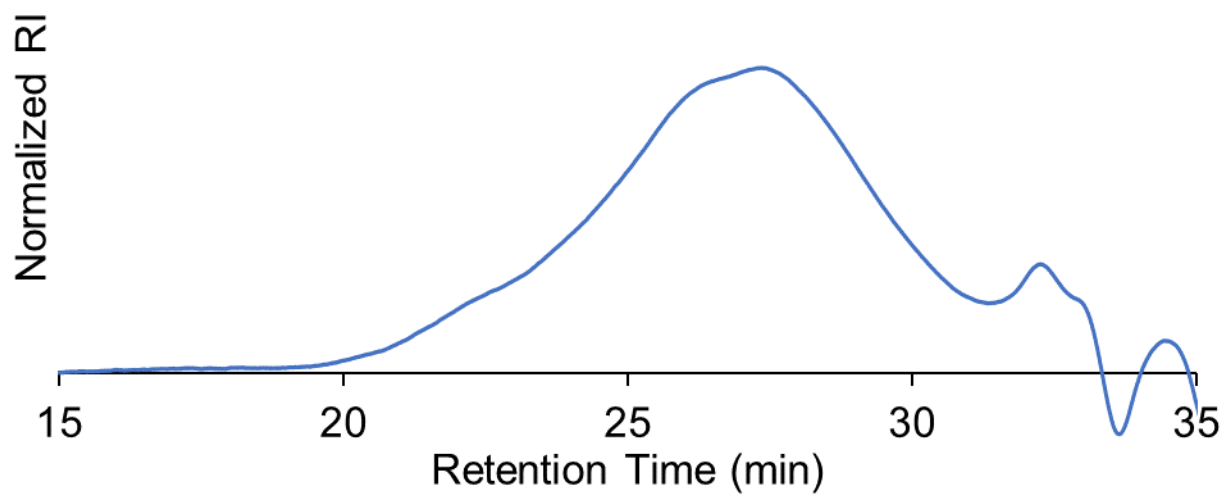


Figure 3.10.11.25. Gel permeation chromatogram of polymer **4b**. $M_n = 8.8$ kDa, $D = 4.8$. Molecular weight was determined relative to polyethylene standards.

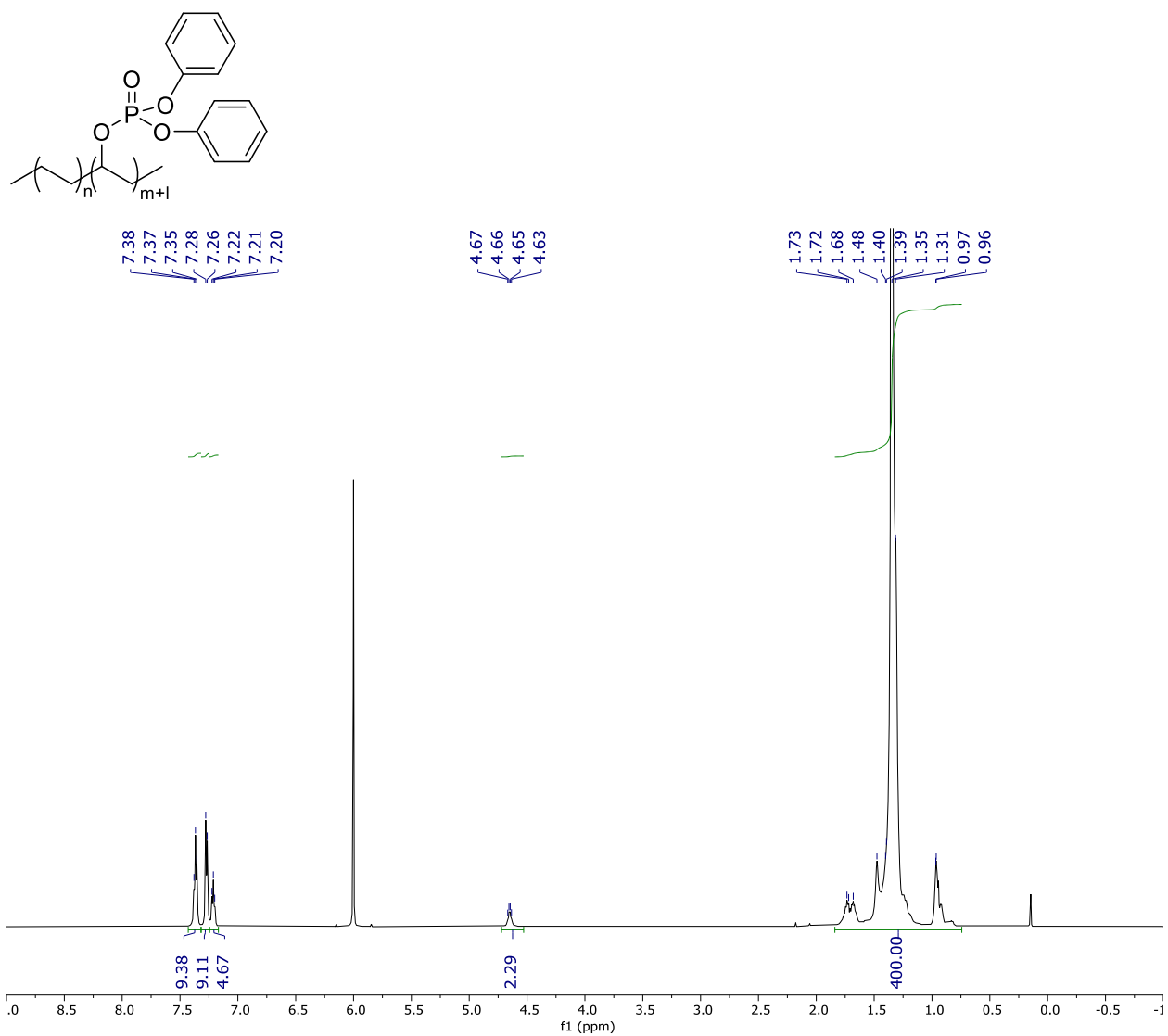


Figure 3.10.11.26. ¹H NMR spectrum of polymer 4c

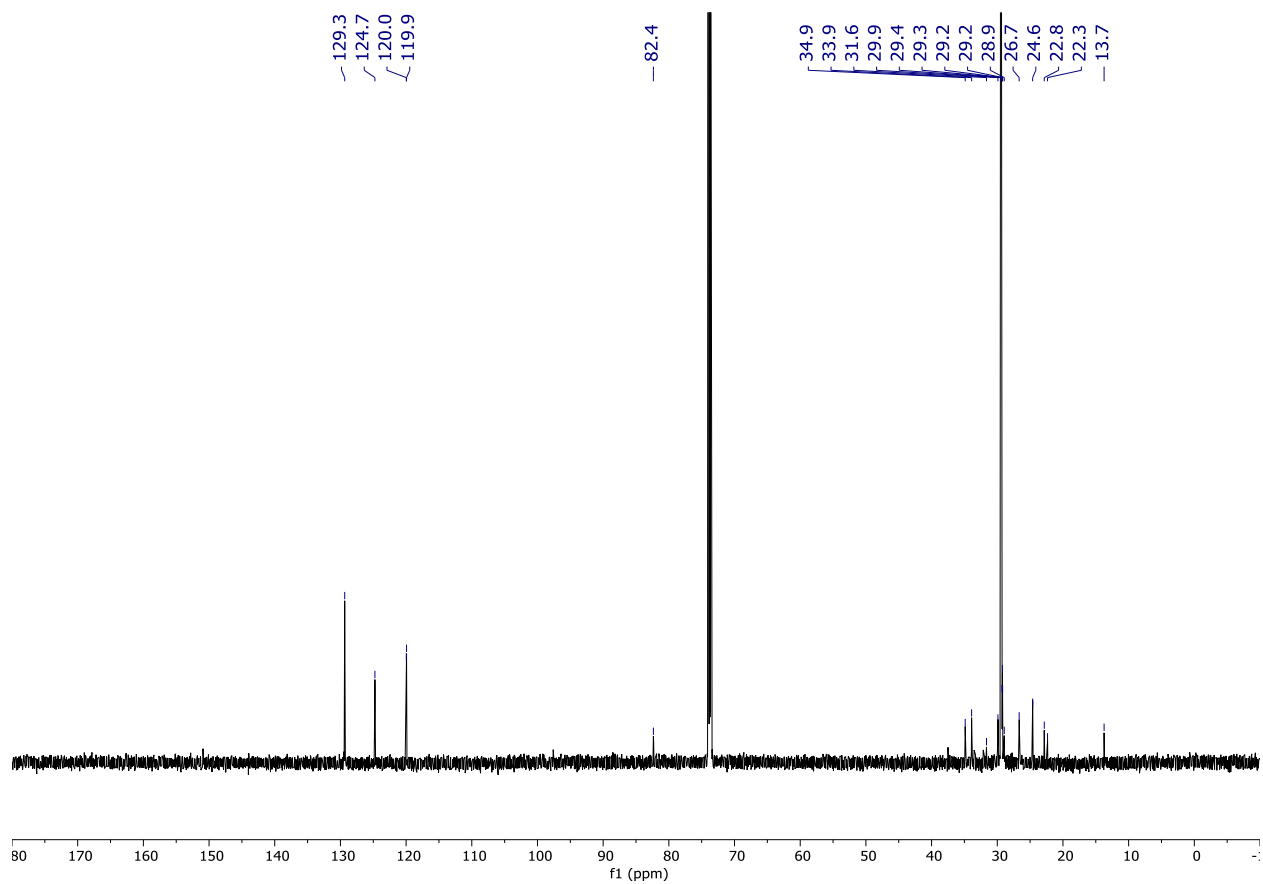
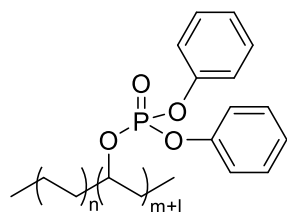


Figure 3.10.11.27. ^{13}C NMR spectrum of polymer 4c

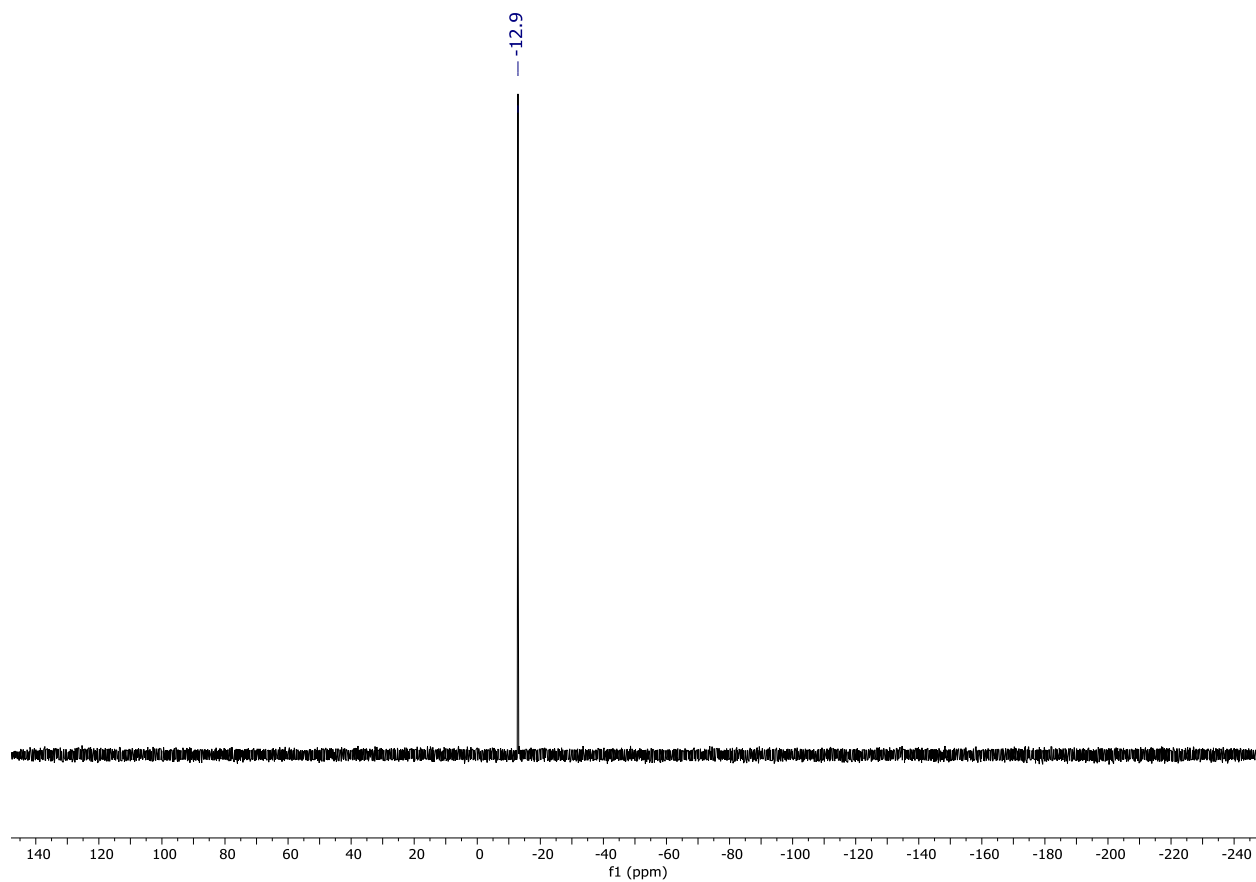
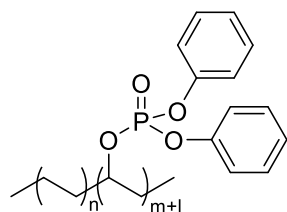


Figure 3.10.11.28. ^{31}P NMR spectrum of polymer 4c

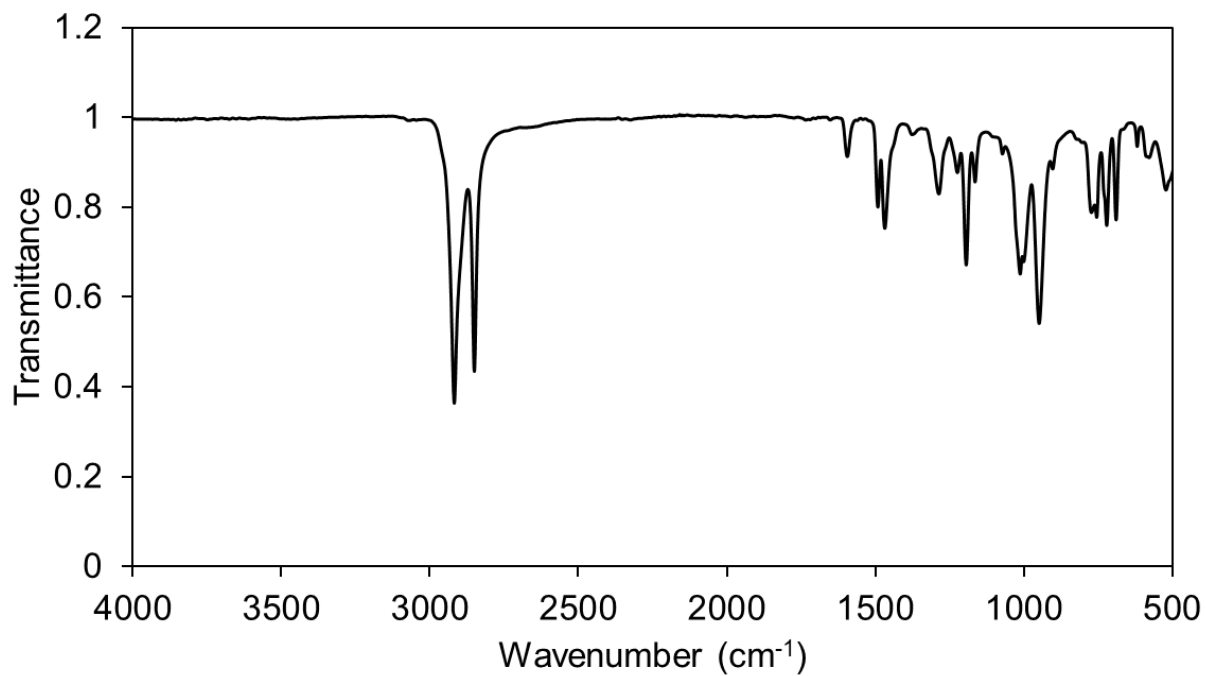


Figure 3.10.11.29. FTIR spectra of polymer **4c**. Major peaks ν (cm⁻¹): 2916, 2849, 1593, 1490, 1467, 1285, 1222, 1193, 1163, 1071, 1011, 999, 947, 901, 771, 753, 719, 688, 577, 520

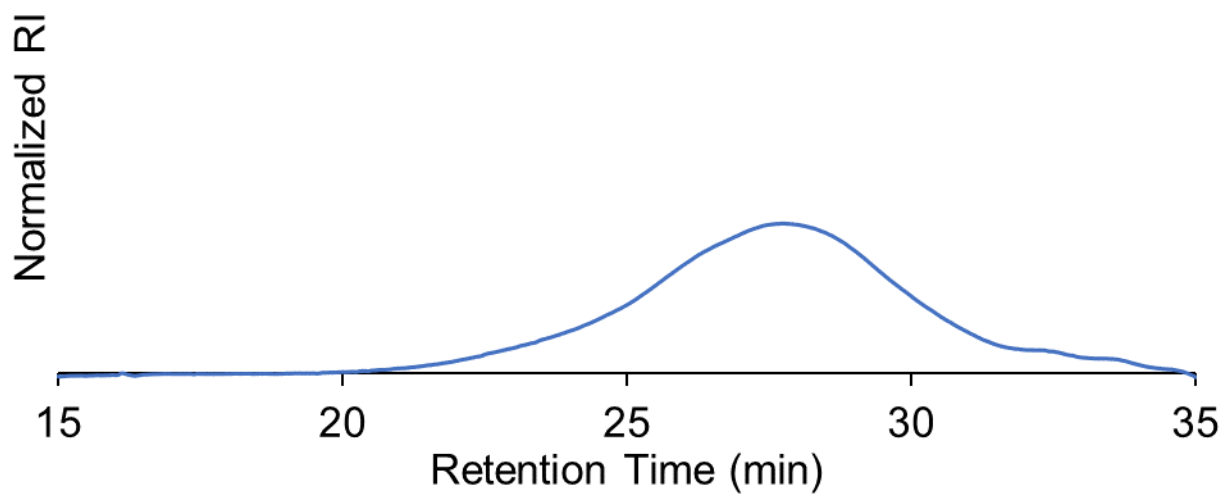


Figure 3.10.11.30. Gel permeation chromatogram of polymer **4c**. $M_n = 5.3$ kDa, $D = 4.2$. Molecular weight was determined relative to polyethylene standards. We attribute the decrease in M_n to the change in conformation of the polymer because of the interchain interactions caused by the polar functional group.

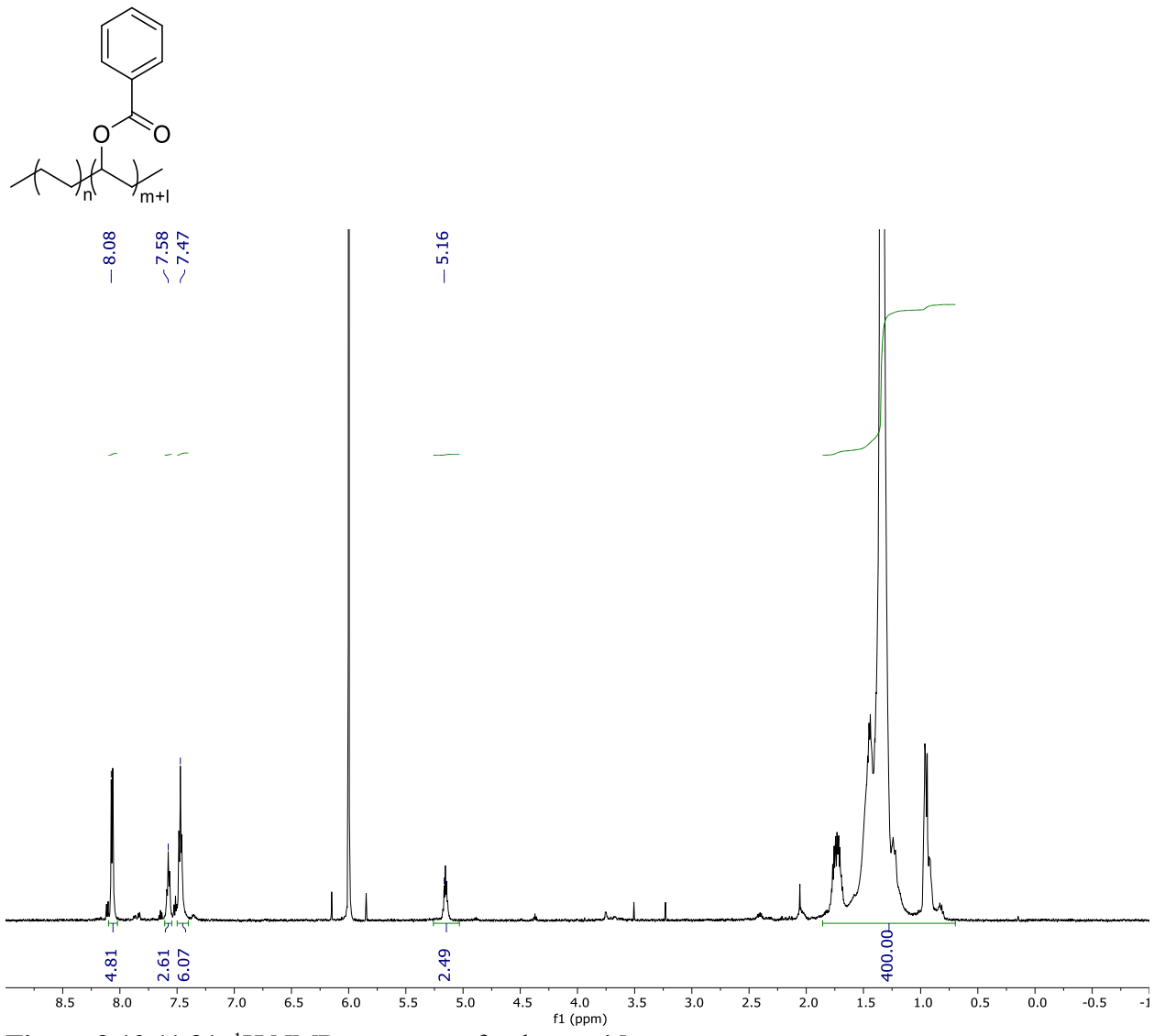


Figure 3.10.11.31. ^1H NMR spectrum of polymer 4d

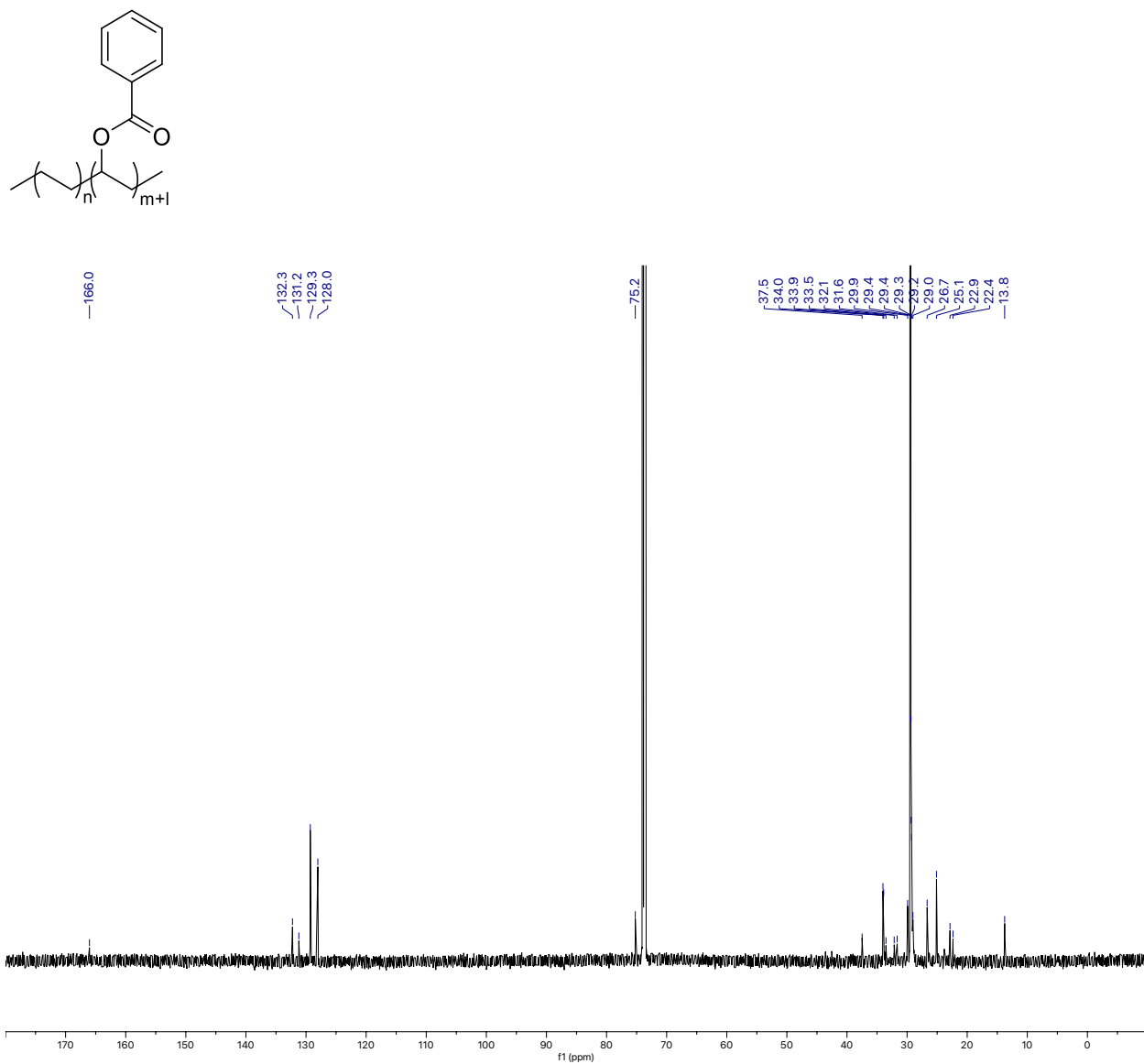


Figure 3.10.11.32. ^{13}C NMR spectrum of polymer 4d

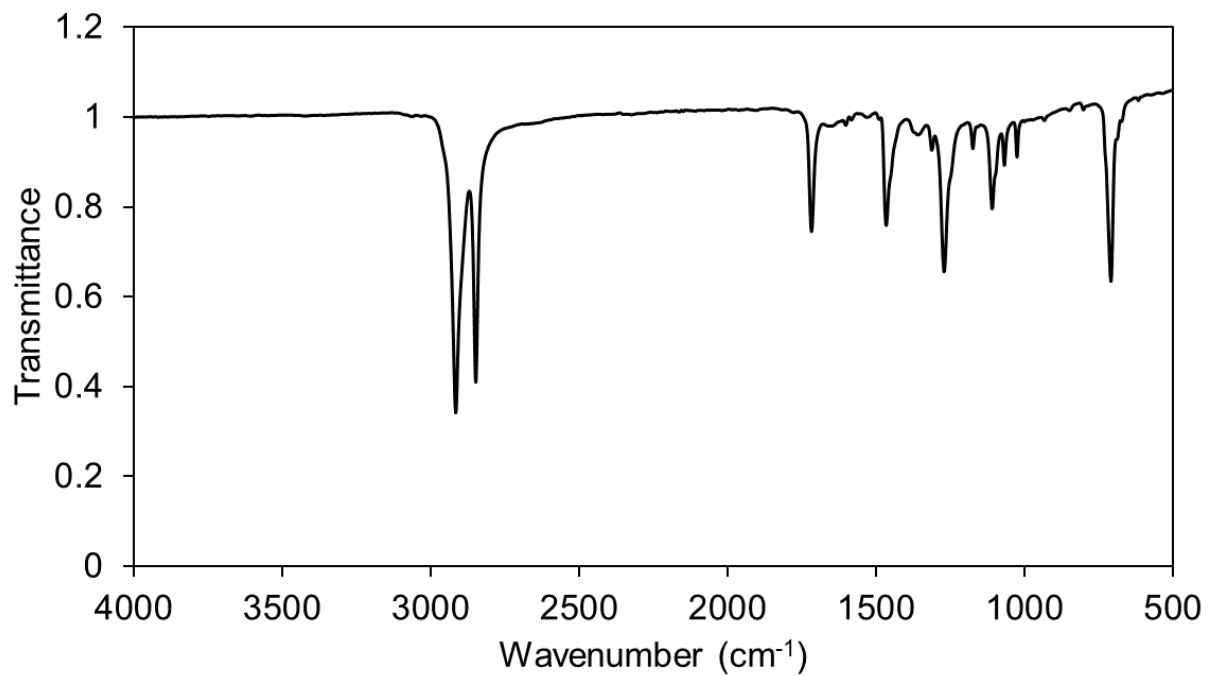


Figure 3.10.11.33. FTIR spectra of polymer **4d**. Major peaks ν (cm⁻¹): 2916, 2849, 1718, 1467, 1359, 1313, 1272, 1175, 1110, 1069, 1026, 710

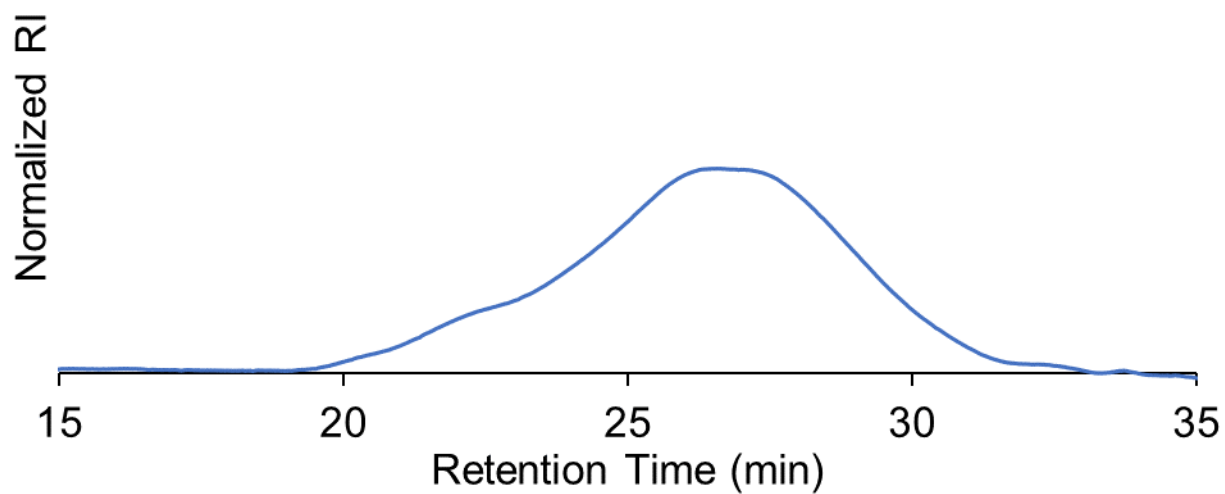


Figure 3.10.11.34. Gel permeation chromatogram of polymer **4d**. $M_n = 8.1$ kDa, $D = 7.1$. Molecular weight was determined relative to polyethylene standards.

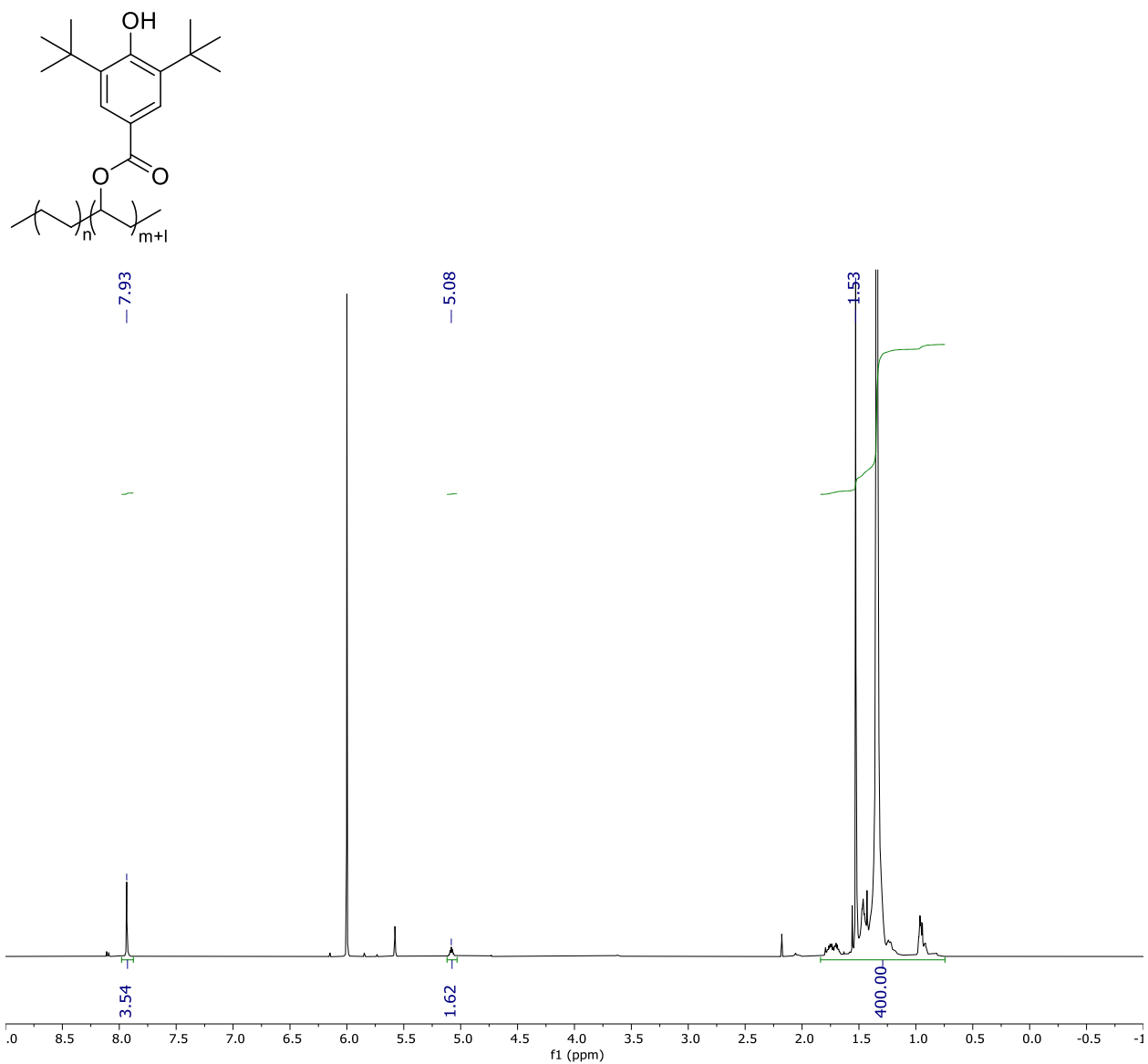


Figure 3.10.11.35. ¹H NMR spectrum of polymer 4e

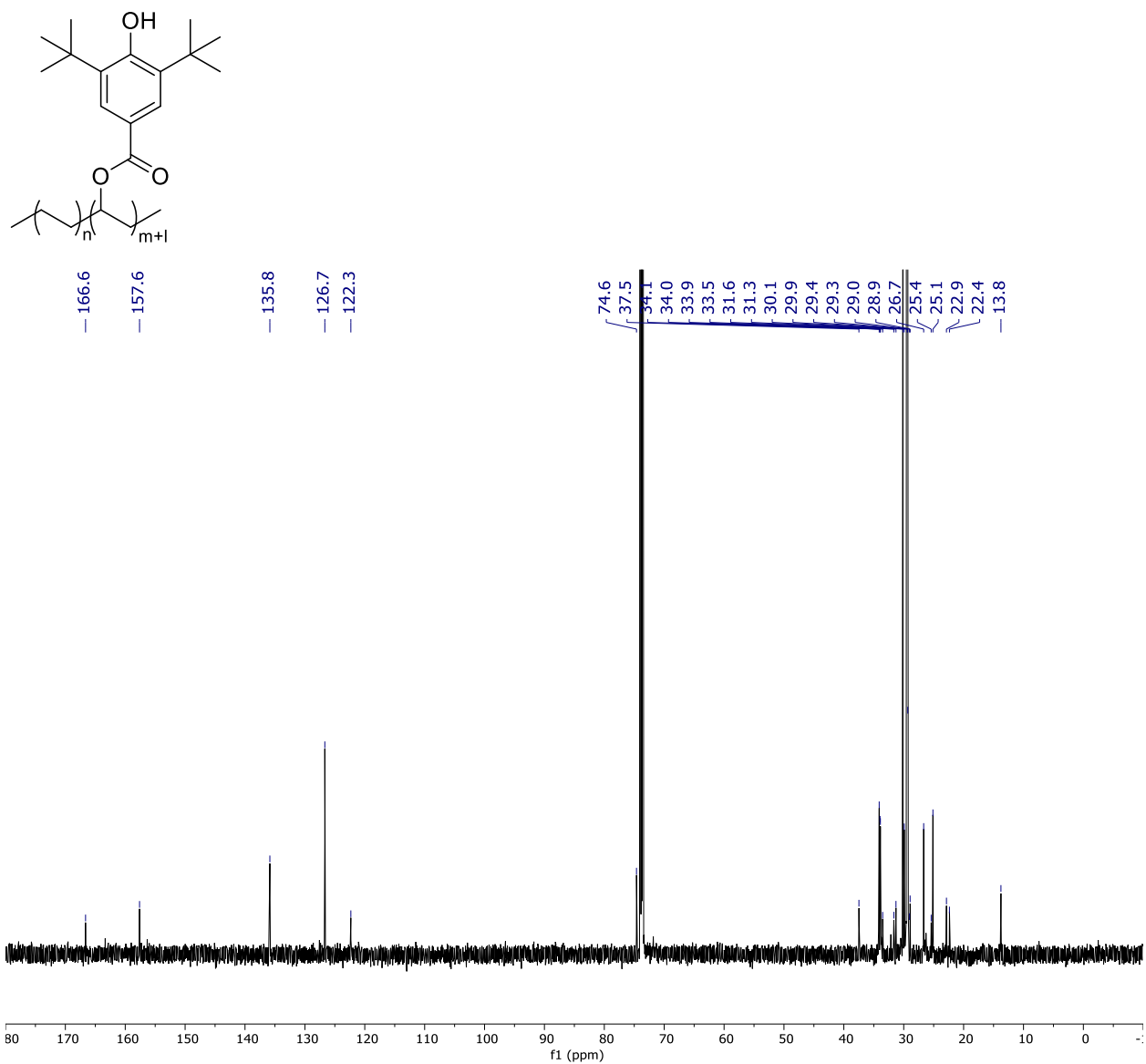


Figure 3.10.11.36. ¹³C NMR spectrum of polymer 4e

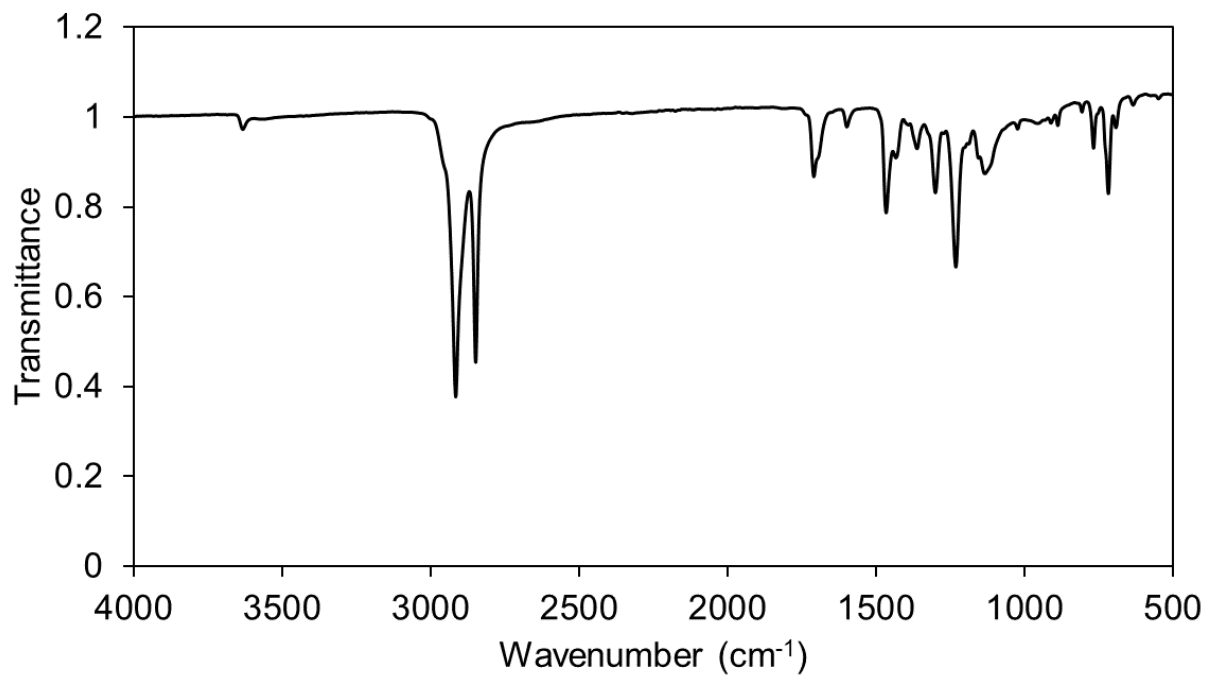


Figure 3.10.11.37. FTIR spectra of polymer **4e**. Major peaks ν (cm⁻¹): 3633, 2916, 2849, 1710, 1599, 1467, 1434, 1363, 1301, 1232, 1135, 1024, 955, 912, 889, 769, 719, 693

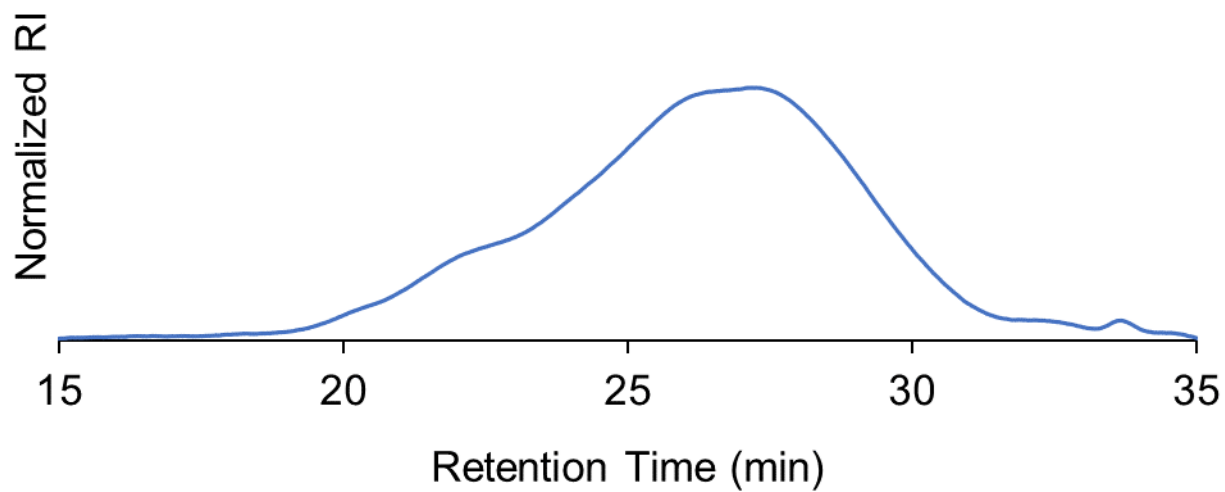


Figure 3.10.11.38. Gel permeation chromatogram of polymer **4e**. $M_n = 8.4$ kDa, $D = 7.8$. Molecular weight was determined relative to polyethylene standards.

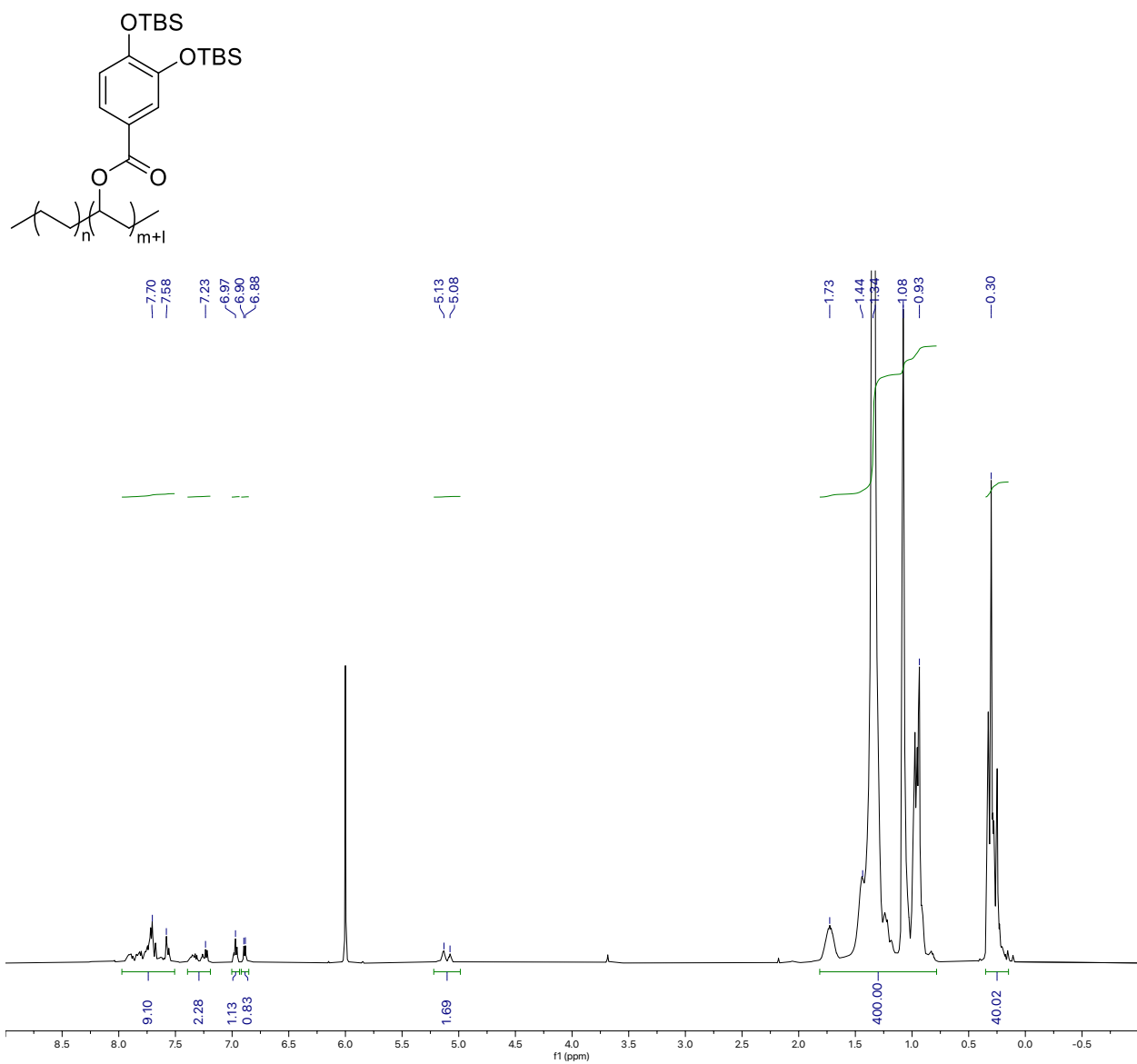


Figure 3.10.11.39. ¹H NMR spectrum of polymer 4f

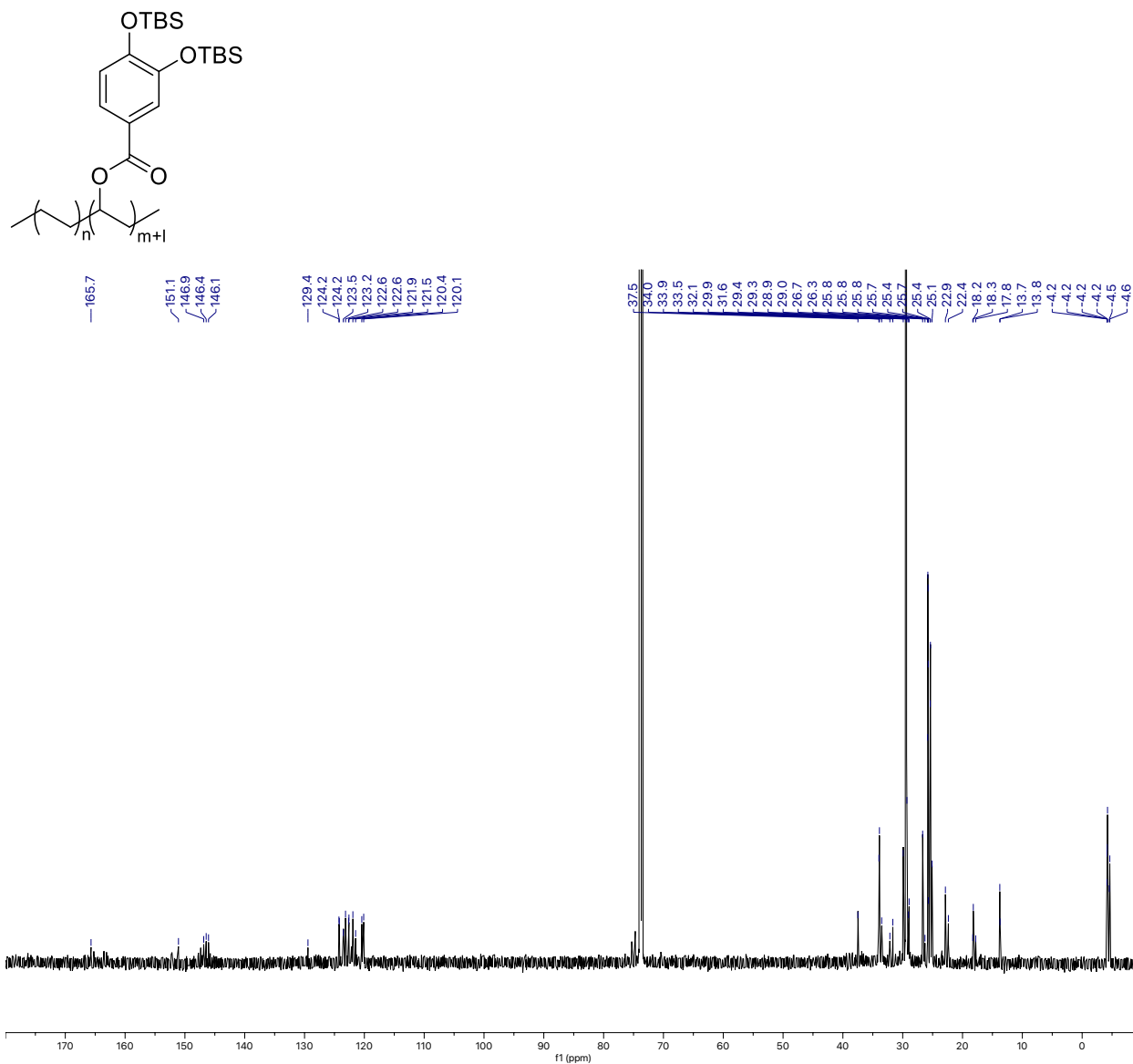


Figure 3.10.11.40. ¹³C NMR spectrum of polymer 4f

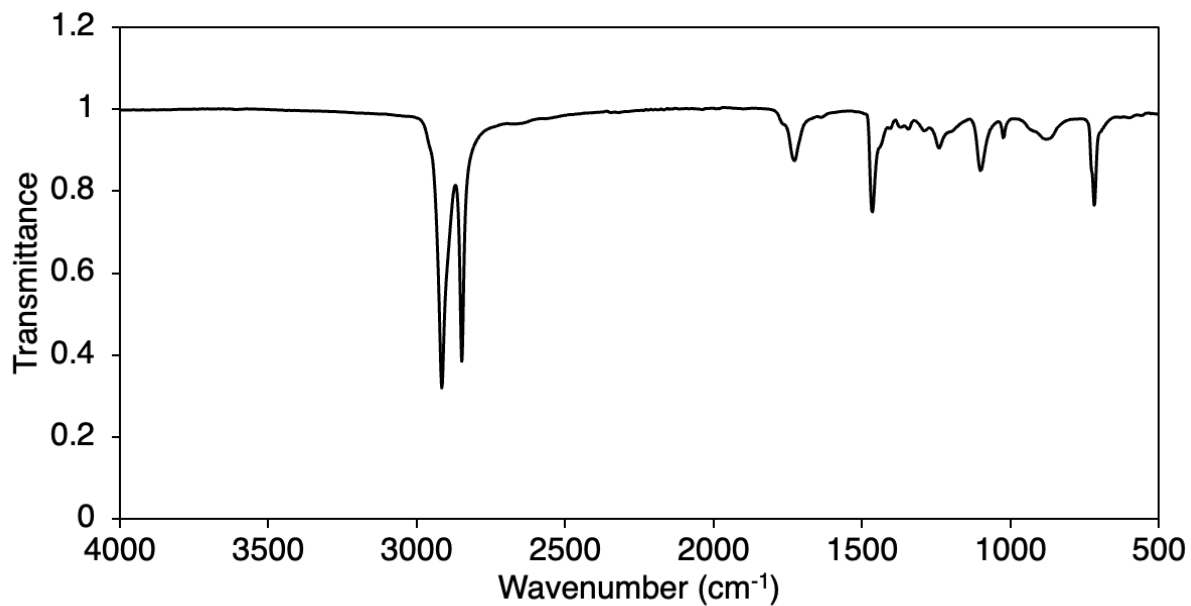


Figure 3.10.11.41. FTIR spectra of polymer **4f**. Major peaks ν (cm⁻¹): 2917, 2849, 1746, 1717, 1599, 1508, 1468, 1421, 1362, 1296, 1256, 1203, 1175, 1115, 1055, 1006, 964, 898, 838, 806, 782, 760, 719, 675

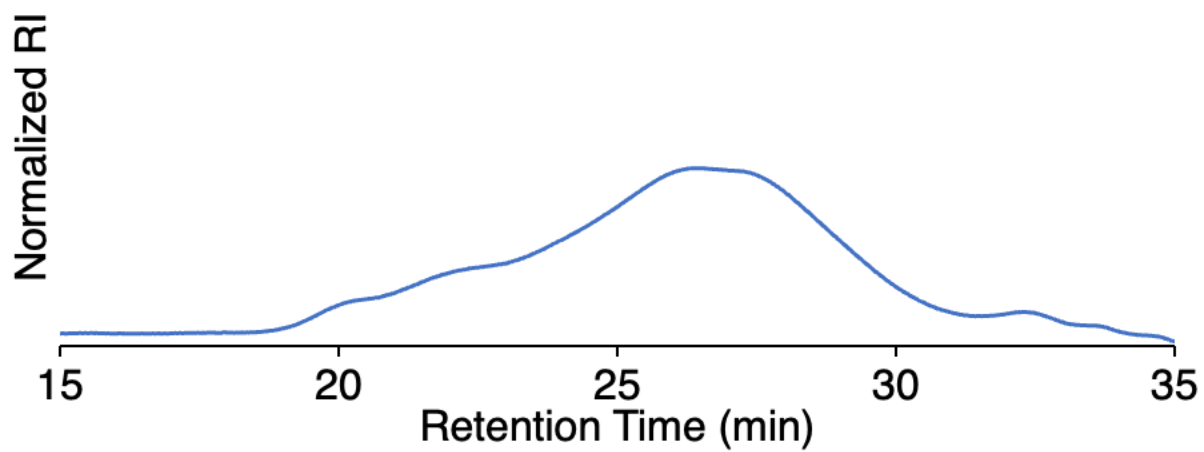


Figure 3.10.11.42. Gel permeation chromatogram of polymer **4f**. $M_n = 10.4$ kDa, $\mathcal{D} = 9.7$. Molecular weight was determined relative to polyethylene standards.

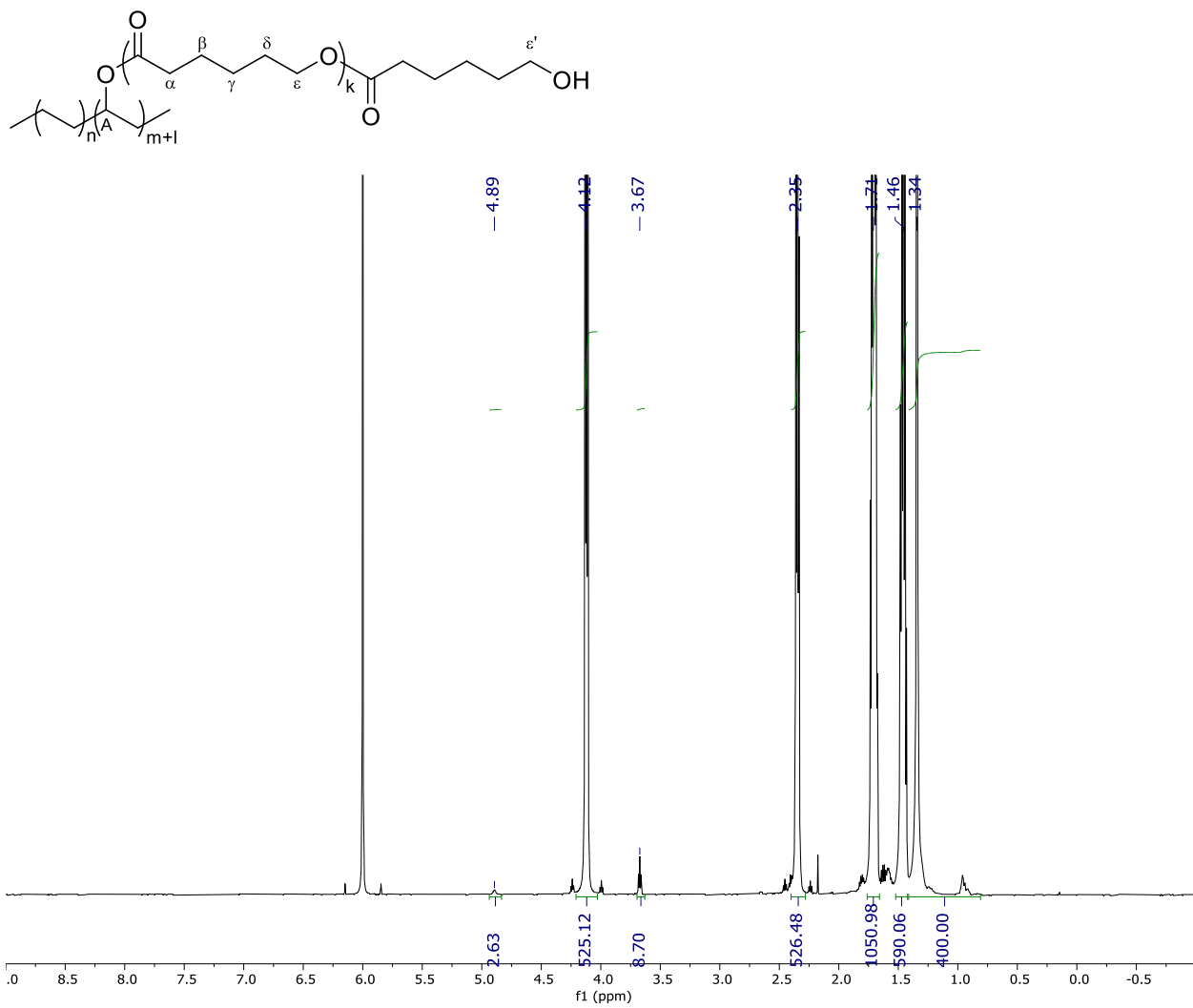


Figure 3.10.11.43. ¹H NMR spectrum of polymer 5

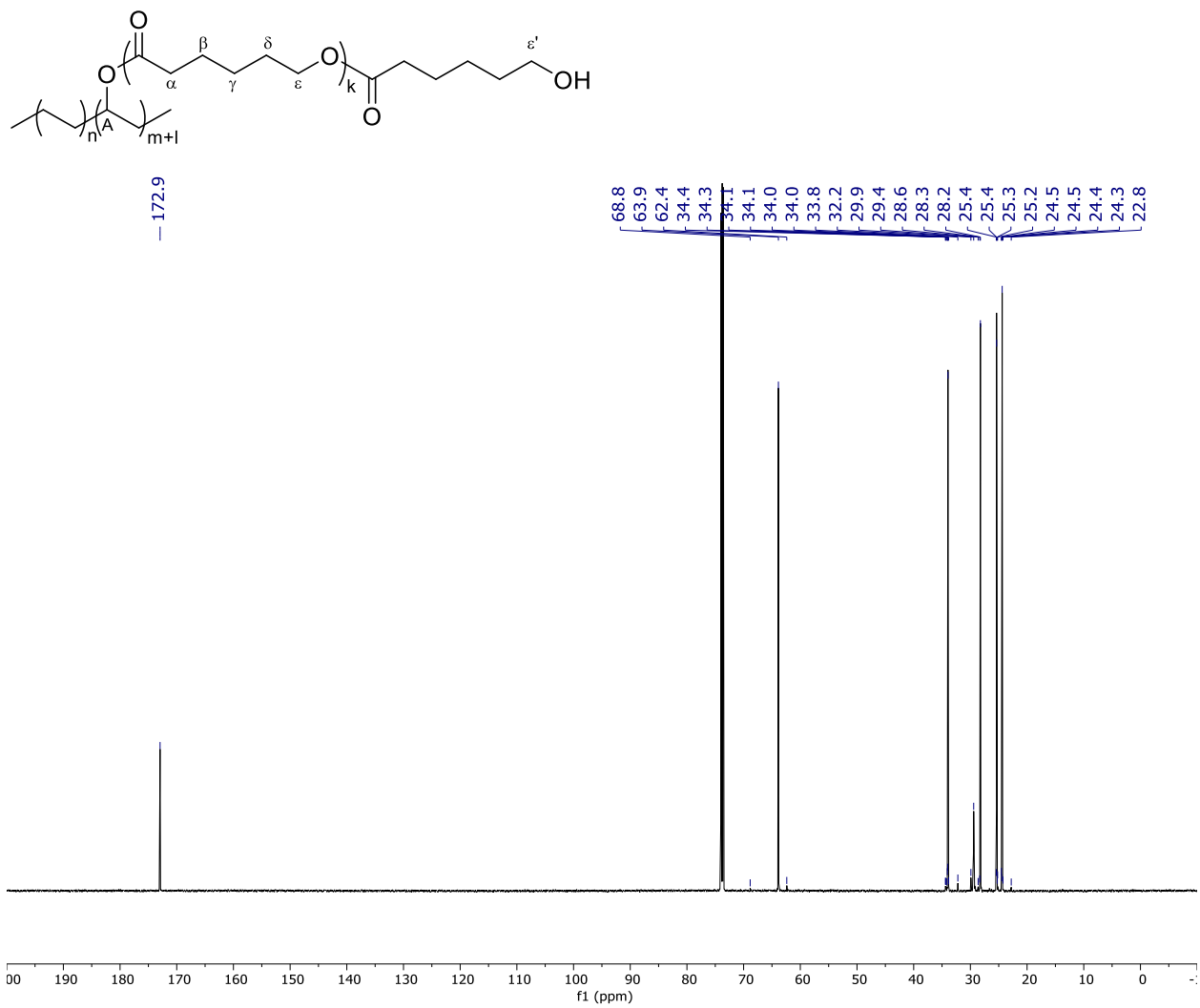


Figure 3.10.11.44. ¹³C NMR spectrum of polymer 5

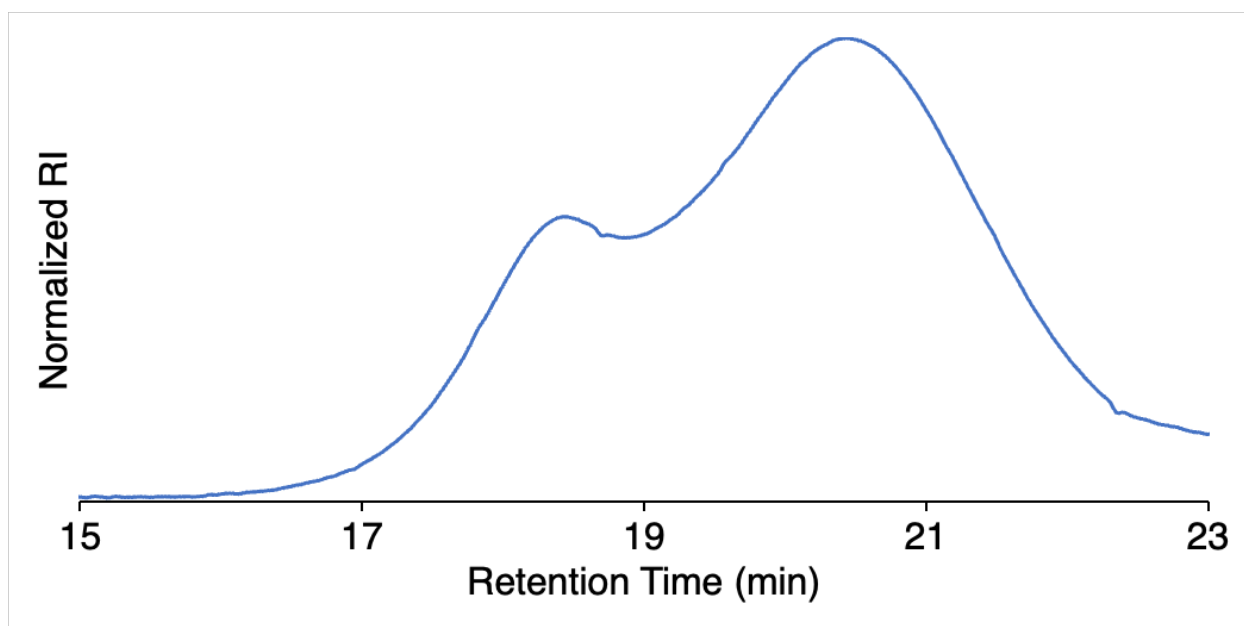


Figure 3.10.11.45. Gel permeation chromatogram of polymer **5**. $M_n = 150$ kDa, $D = 1.5$. Molecular weight was determined relative to polyethylene standards.

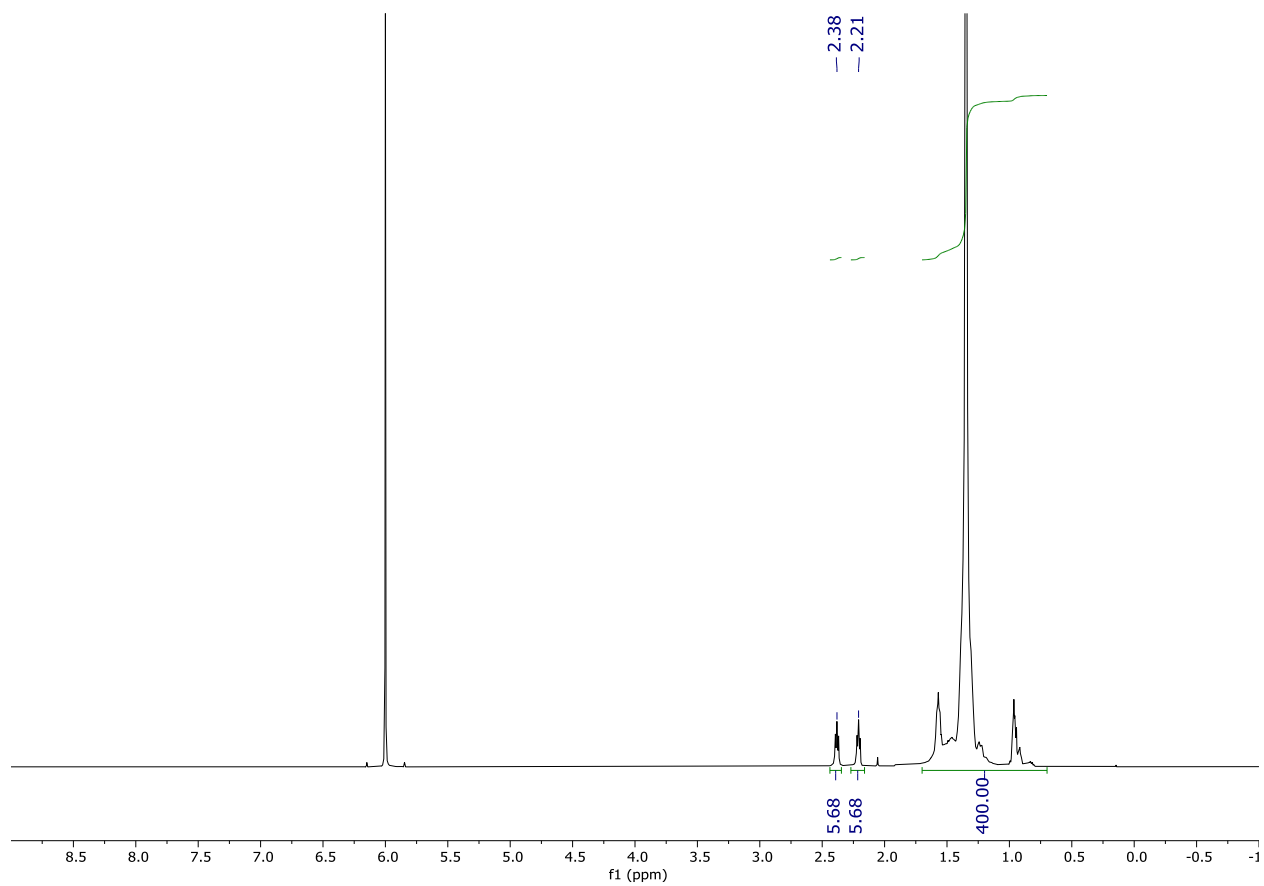
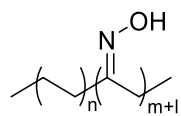


Figure 3.10.11.46. ^1H NMR spectrum of polymer 6a

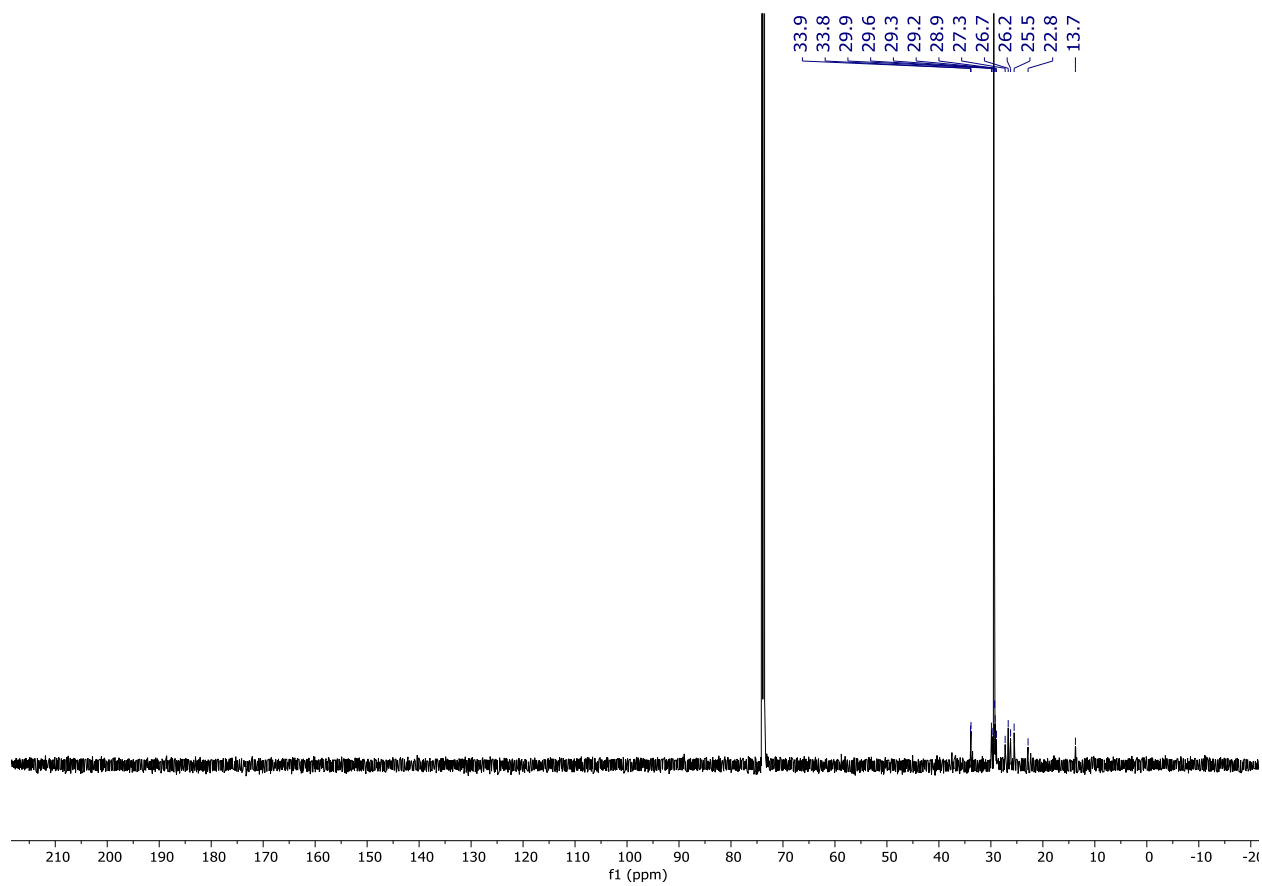
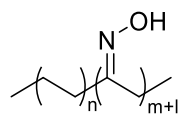


Figure 3.10.11.47. ^{13}C NMR spectrum of polymer 6a

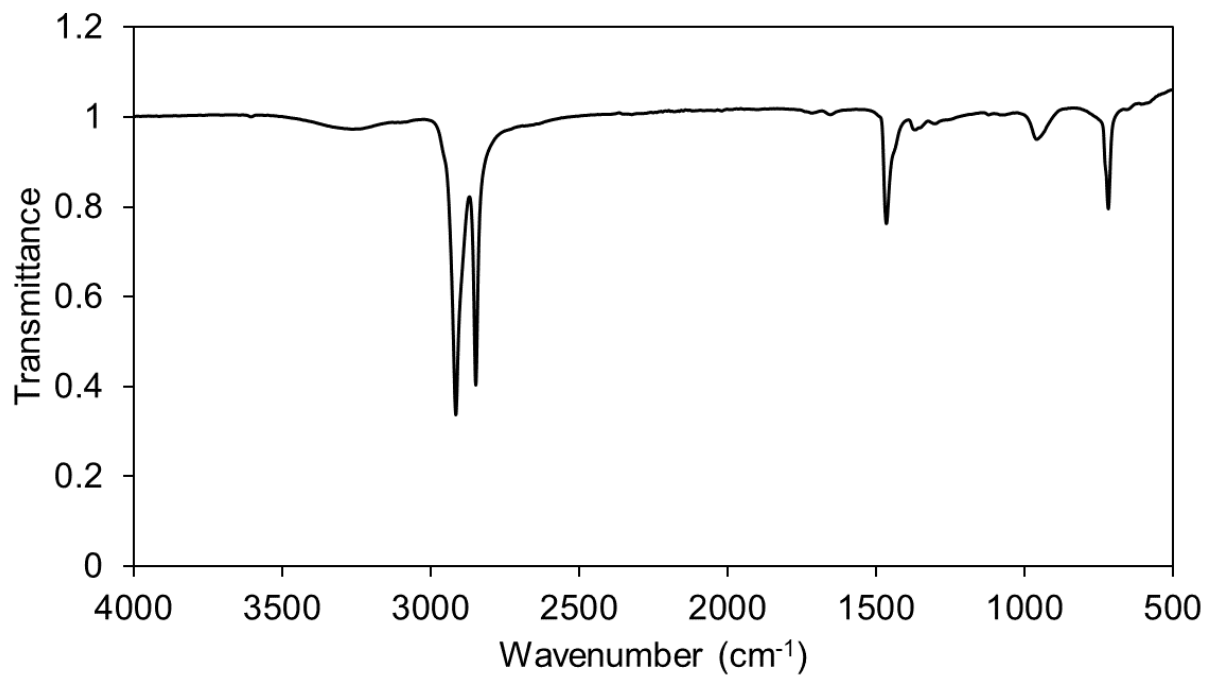


Figure 3.10.11.48. FTIR spectra of polymer **6a**. Major peaks ν (cm⁻¹): 3263, 2916, 2849, 1655, 1466, 1369, 960, 719

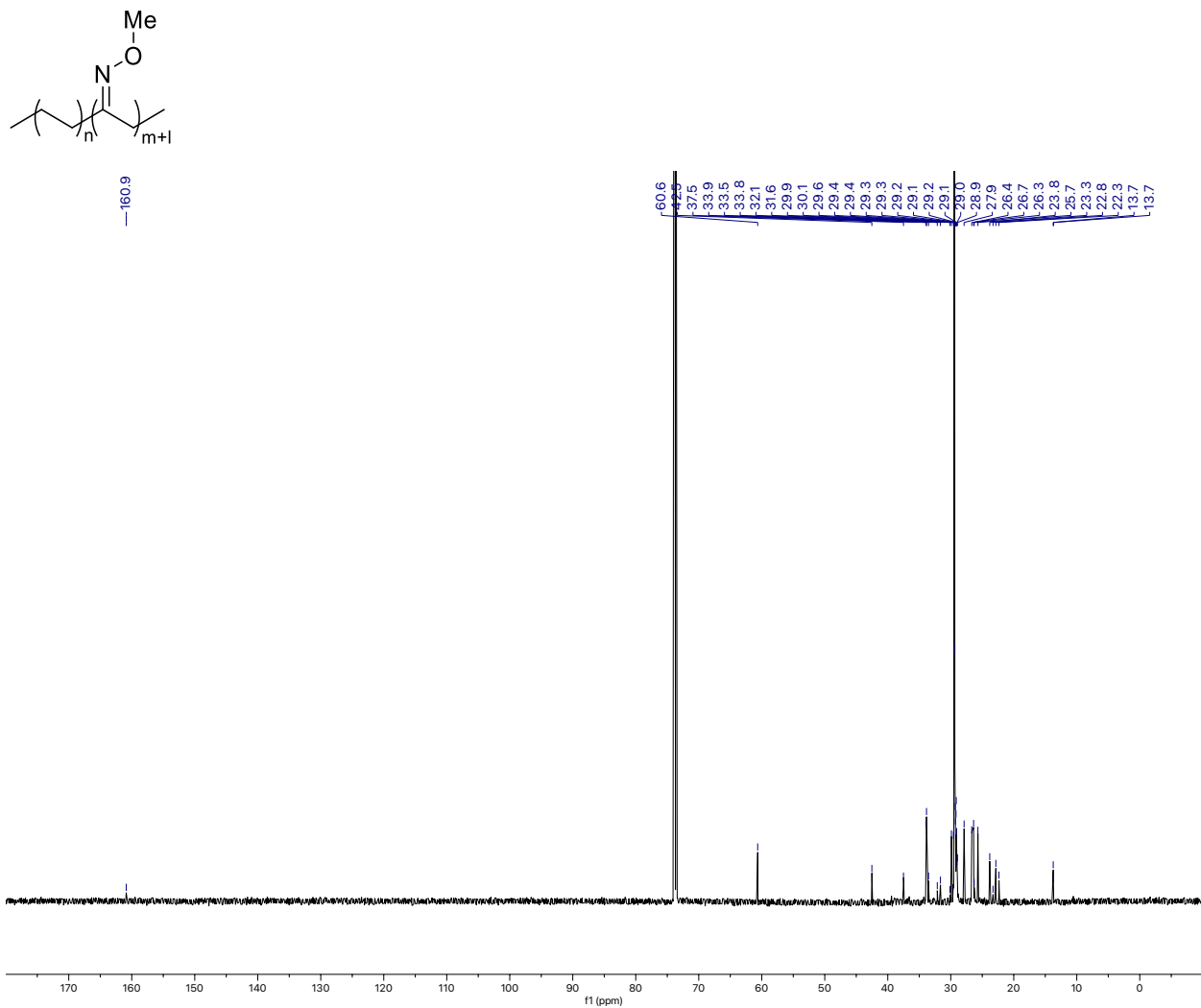


Figure 3.10.11.50. ¹³C NMR spectrum of polymer 6b

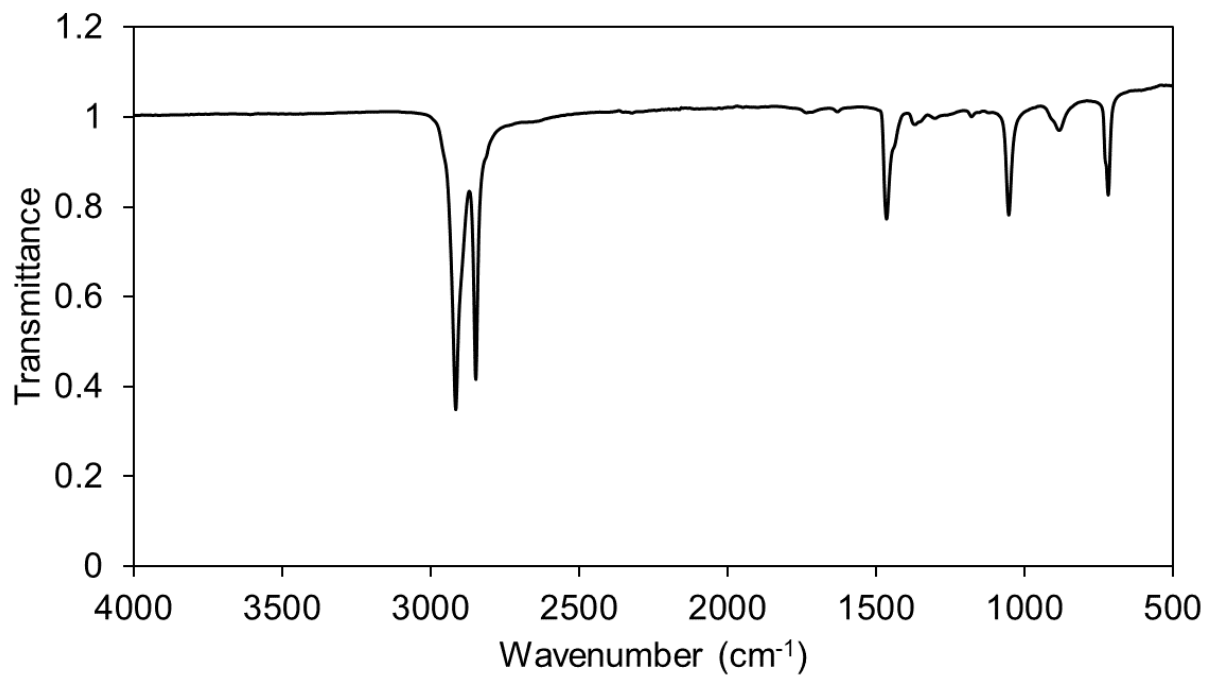


Figure 3.10.11.51. FTIR spectra of polymer **6b**. Major peaks ν (cm⁻¹): 2916, 2849, 1735, 1631, 1466, 1370, 1179, 1054, 884, 719

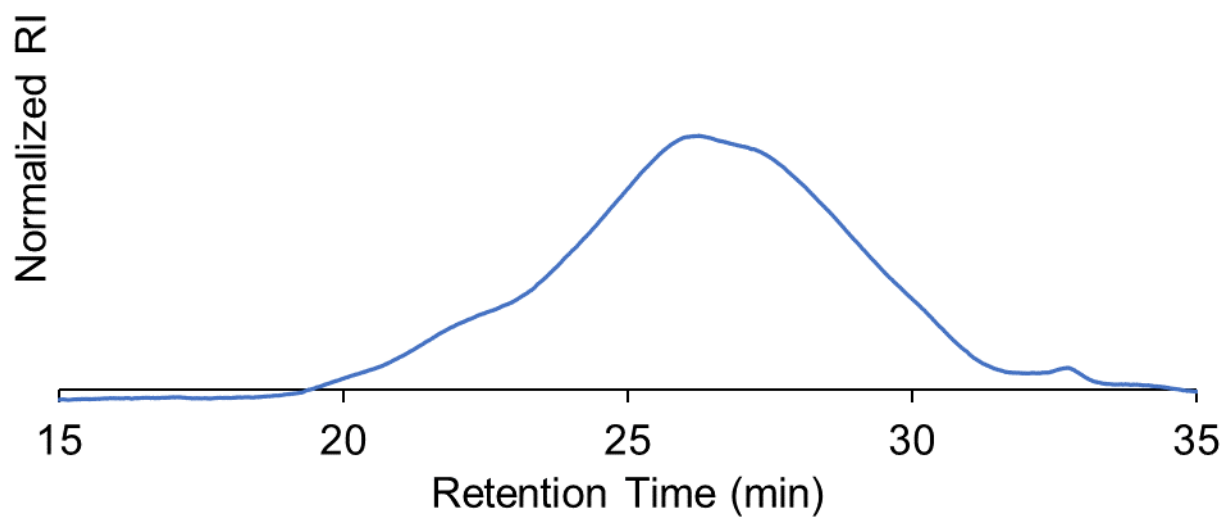


Figure 3.10.11.52. Gel permeation chromatogram of polymer **6b**. $M_n = 9.3$ kDa, $D = 7.0$. Molecular weight was determined relative to polyethylene standards.

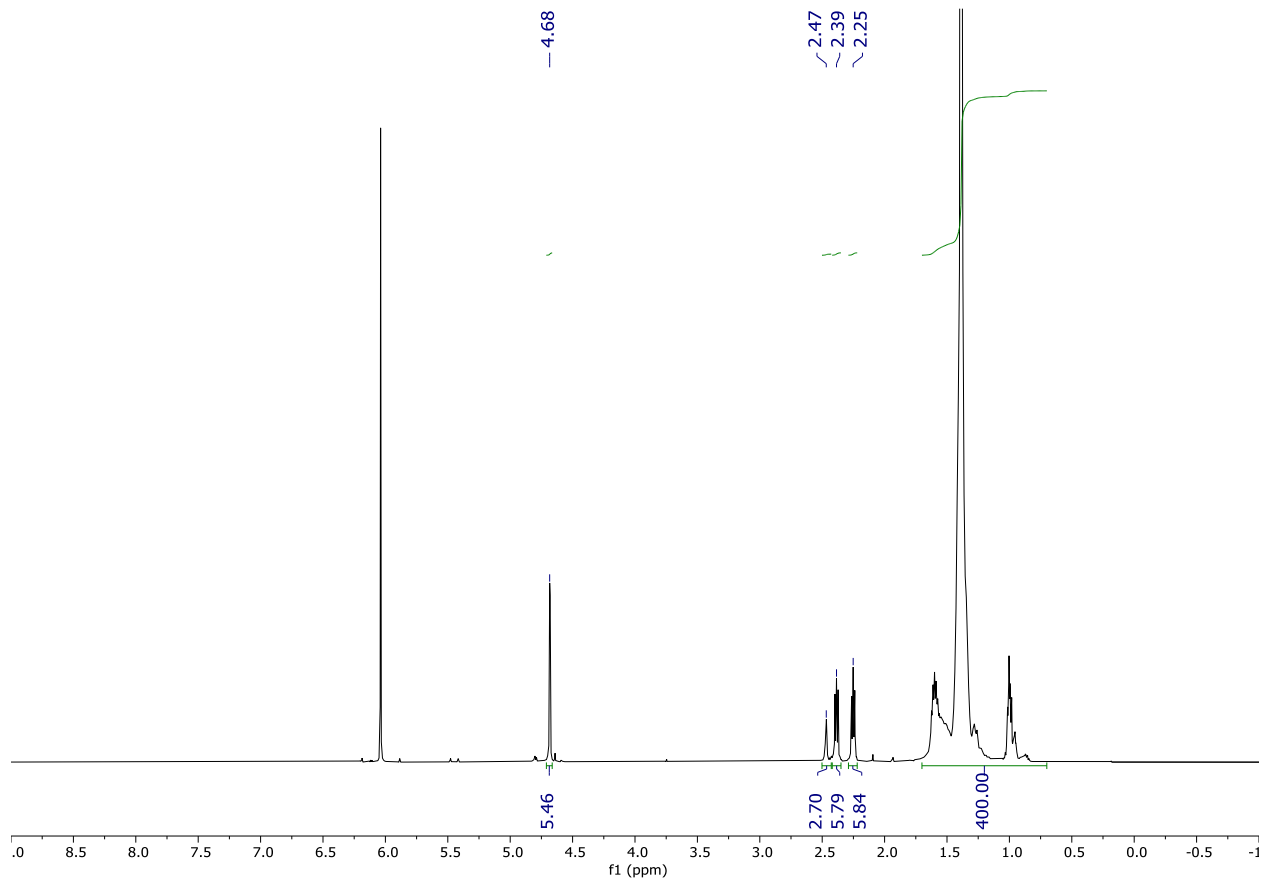
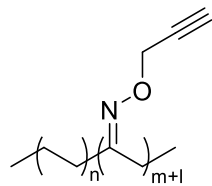


Figure 3.10.11.53. ^1H NMR spectrum of polymer 6c

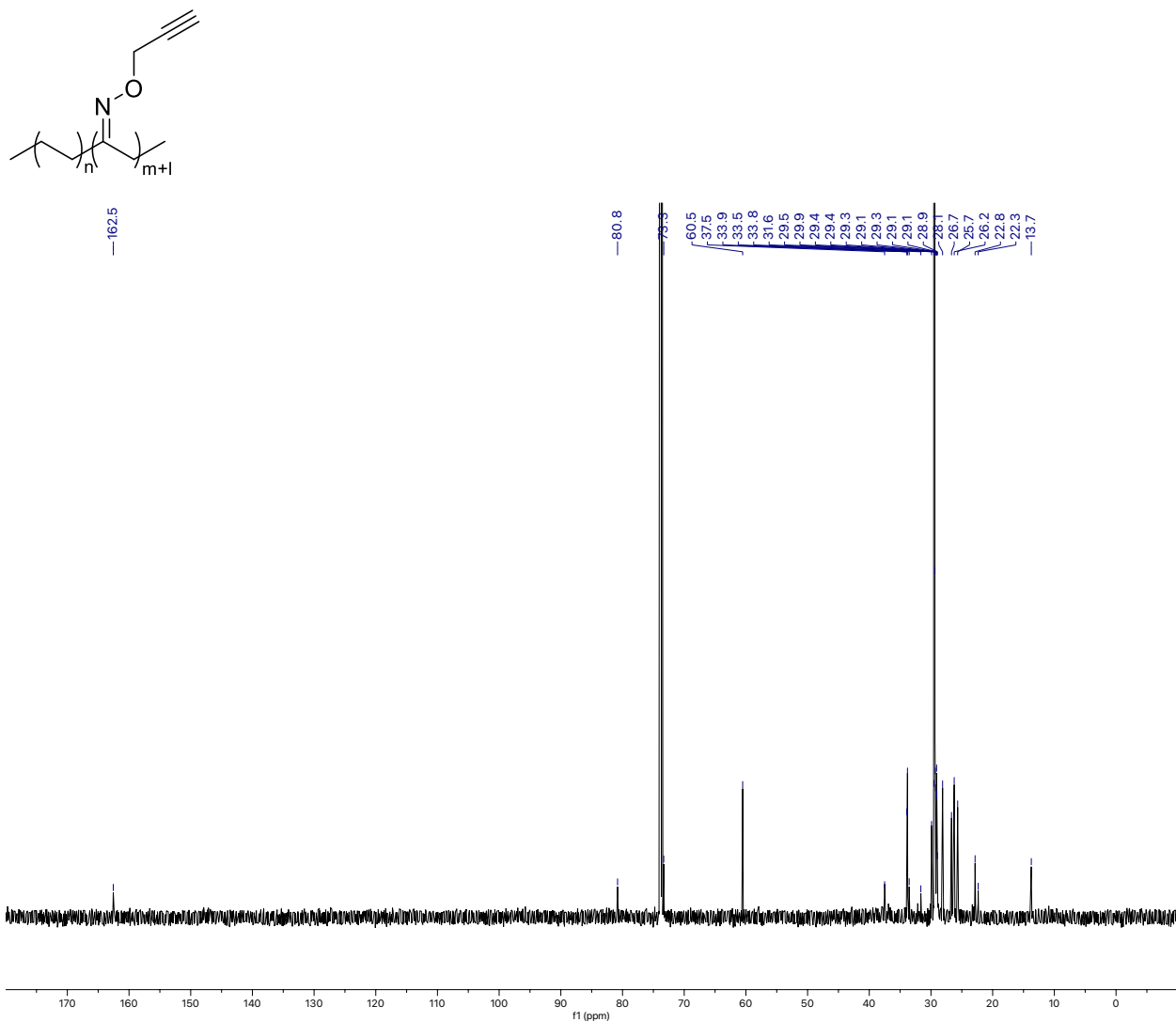


Figure 3.10.11.54. ¹³C NMR spectrum of polymer 6c

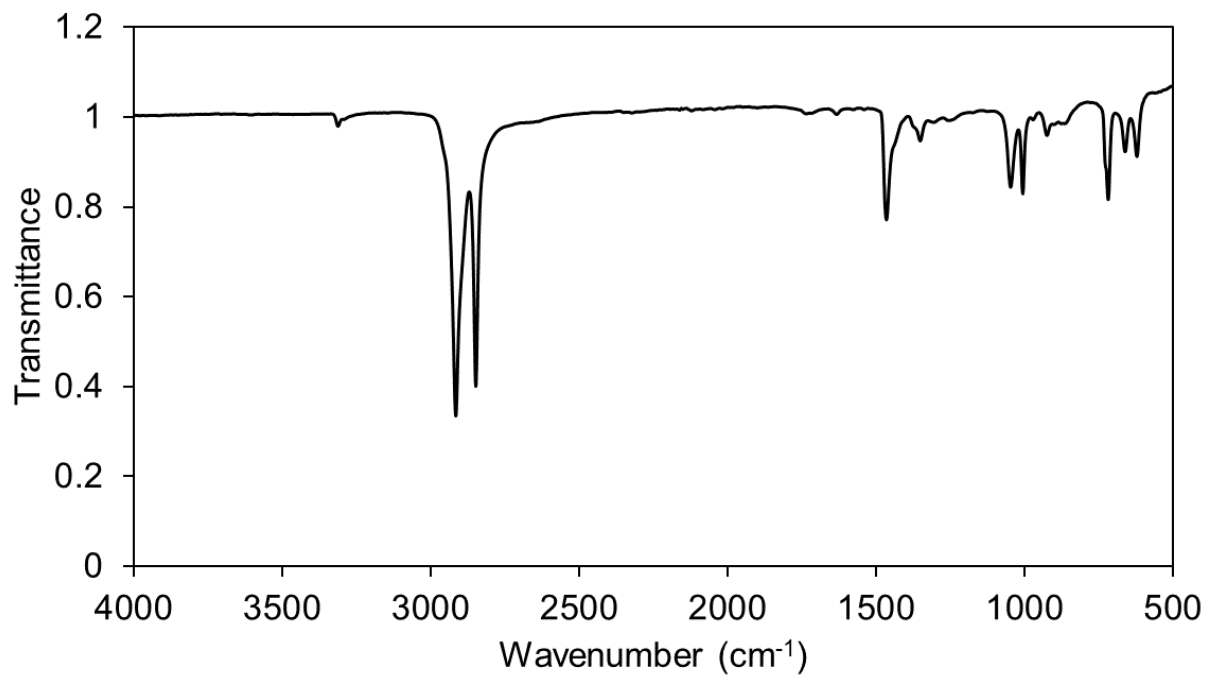


Figure 3.10.11.55. FTIR spectra of polymer **6c**. Major peaks ν (cm⁻¹): 3313, 2916, 2849, 1735, 1634, 1466, 1352, 1256, 1048, 1007, 925, 719, 662, 623

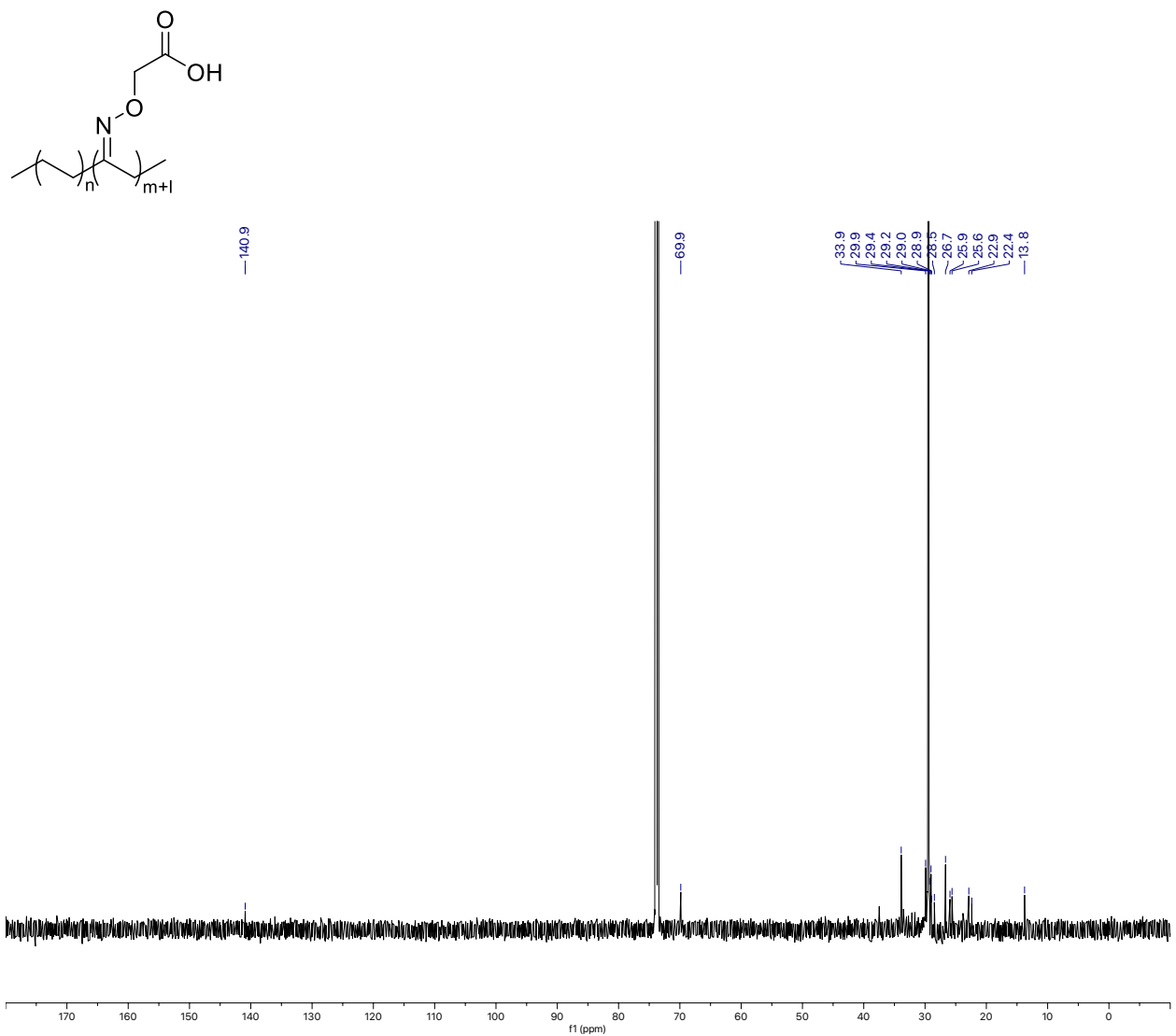


Figure 3.10.11.57. ¹³C NMR spectrum of polymer 6d

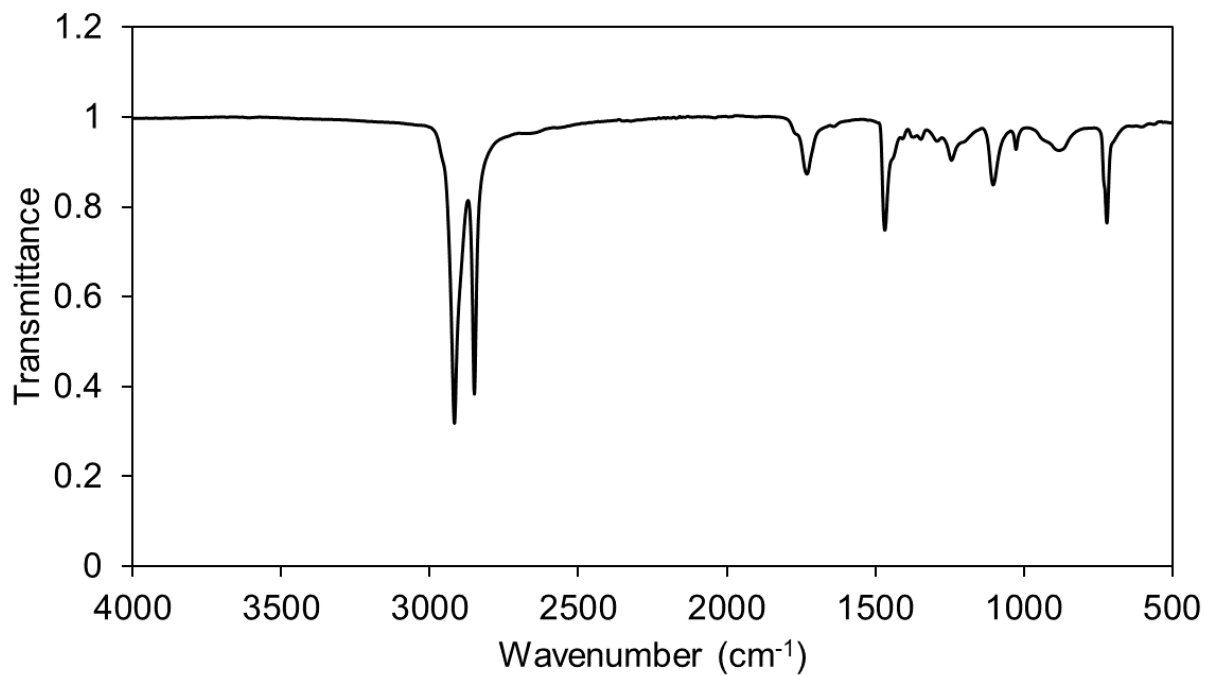


Figure 3.10.11.58. FTIR spectra of polymer **6d**. Major peaks ν (cm⁻¹): 2916, 2849, 1606, 1525, 1466, 1344, 1109, 1064, 1014, 918, 856, 800, 719

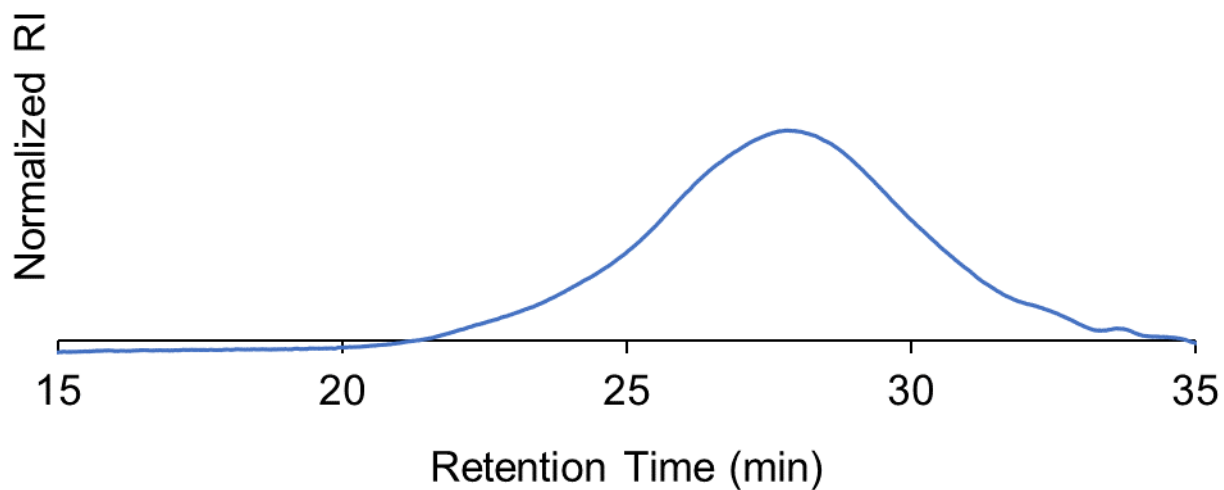


Figure 3.10.11.59. Gel permeation chromatogram of polymer **6d**. $M_n = 4.7$ kDa, $D = 4.6$. Molecular weight was determined relative to polyethylene standards. We attribute the decrease in M_n to the change in conformation of the polymer because of the interchain interactions caused by the polar functional group.

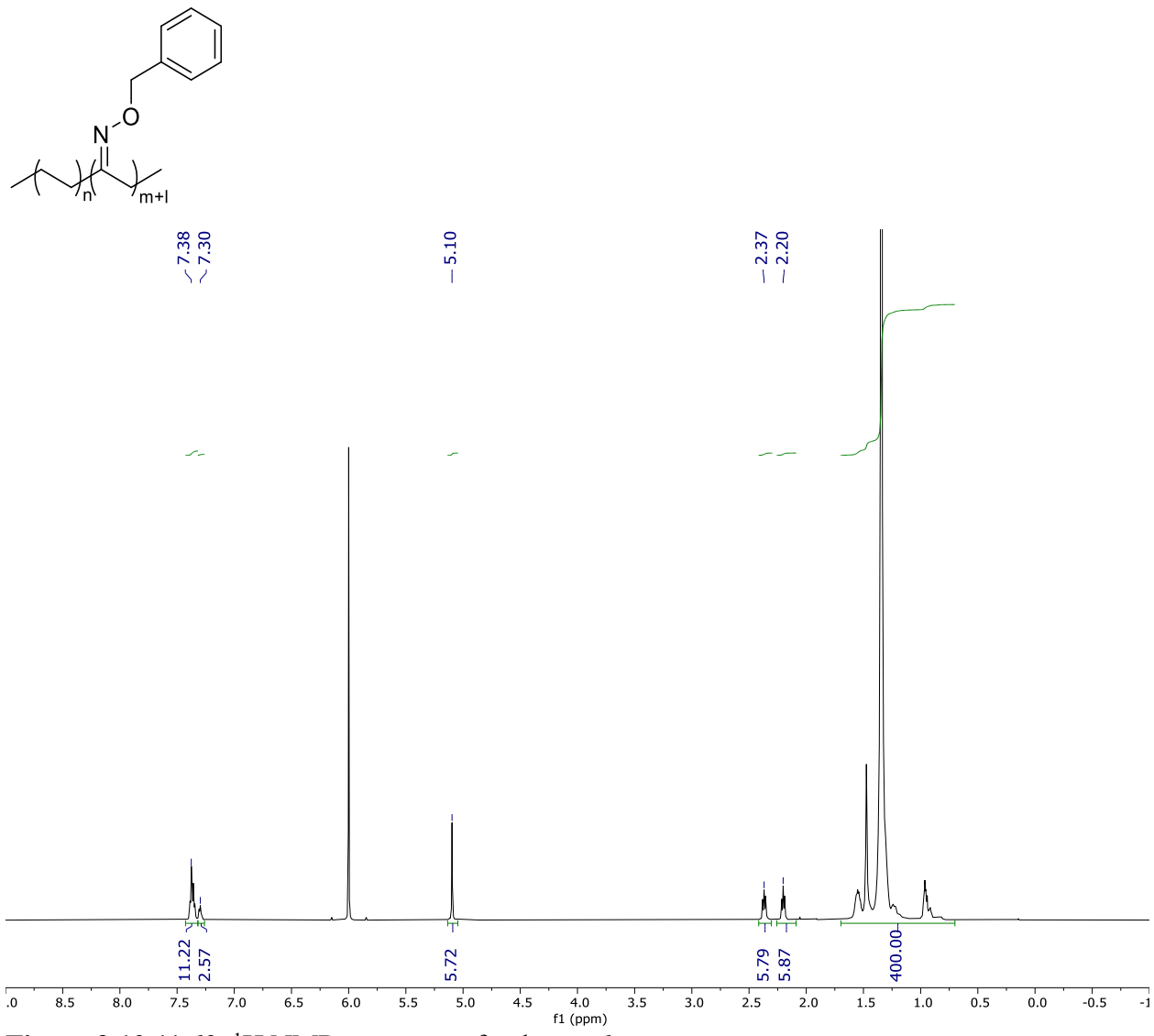


Figure 3.10.11.60. ¹H NMR spectrum of polymer 6e

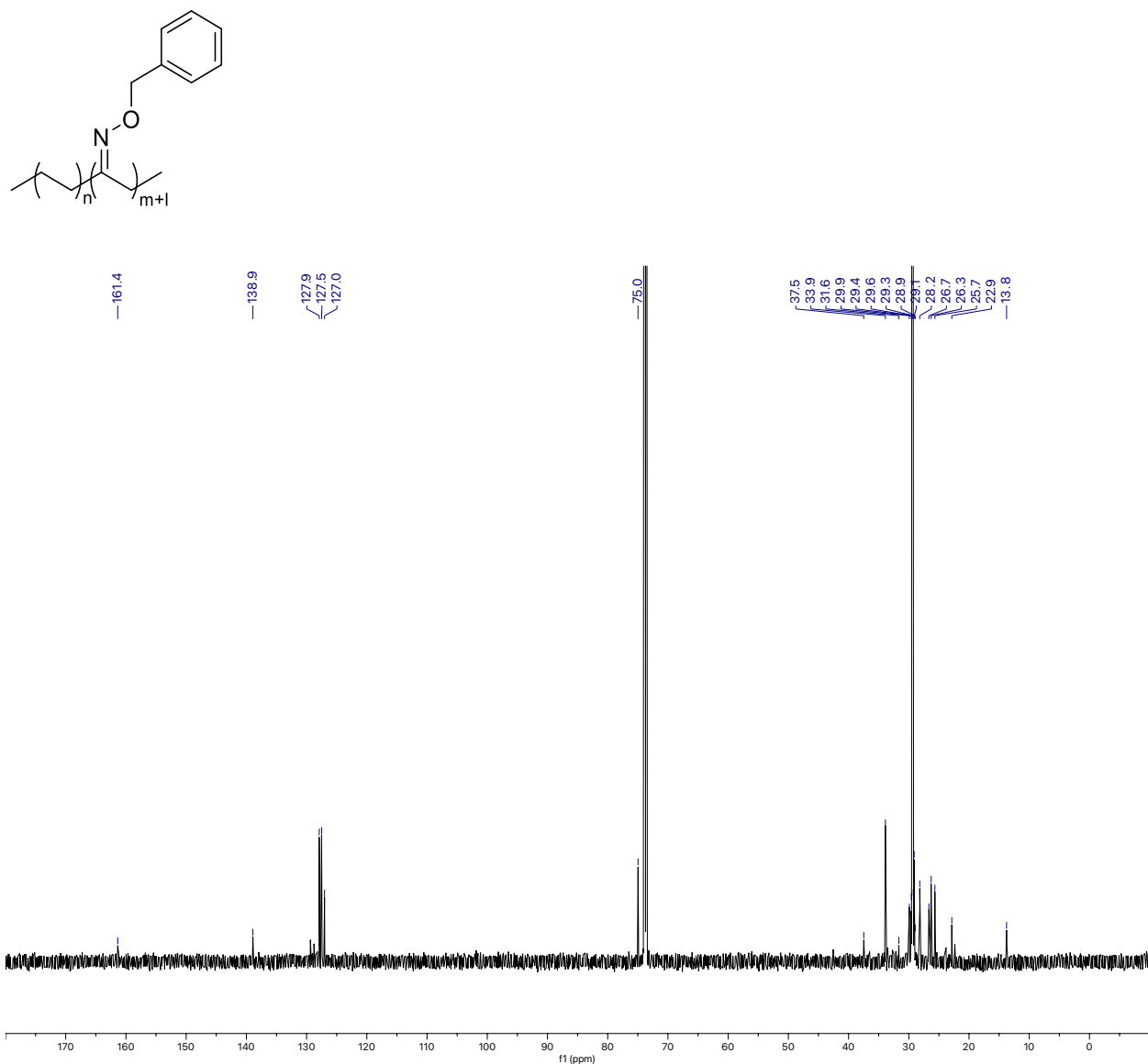


Figure 3.10.11.61. ¹³C NMR spectrum of polymer 6e

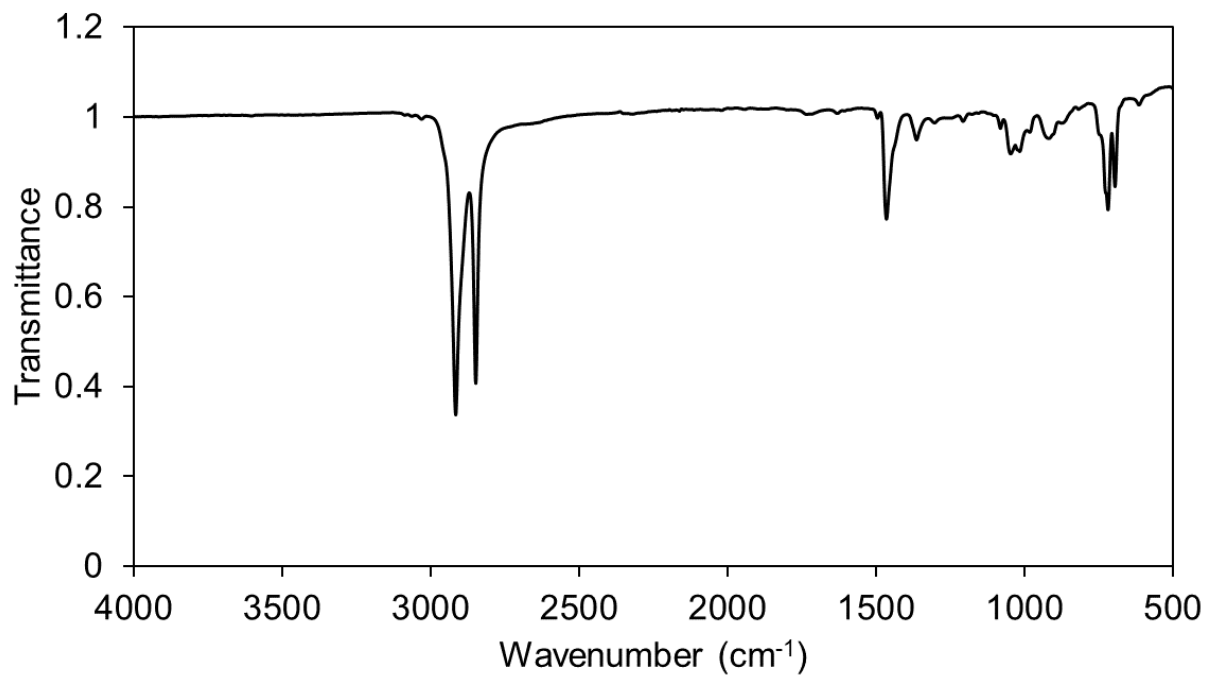


Figure 3.10.11.62. FTIR spectra of polymer **6e**. Major peaks ν (cm⁻¹): 2916, 2849, 1734, 1496, 1466, 1365, 1304, 1208, 1082, 1048, 1017, 920, 720, 696

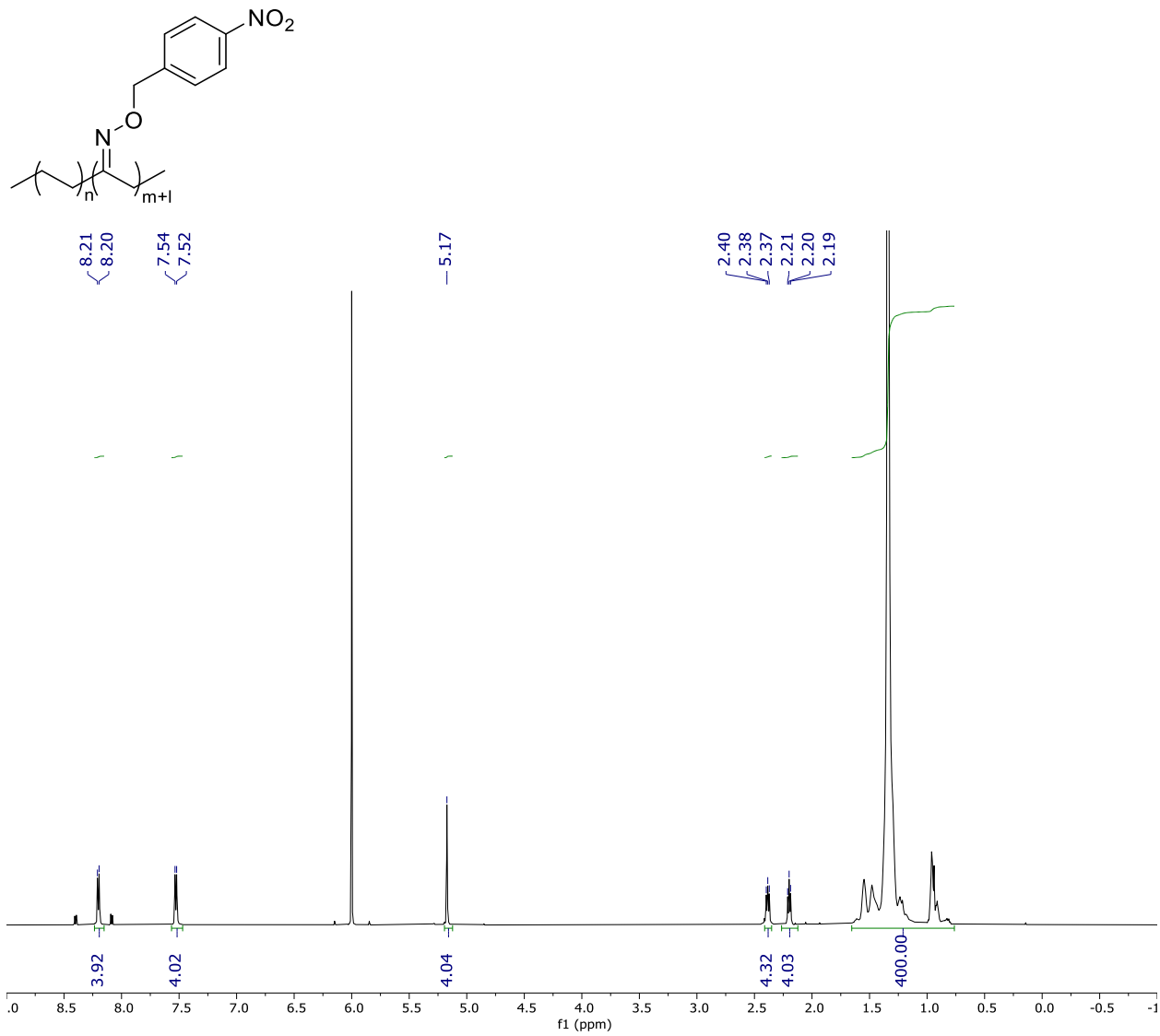


Figure 3.10.11.63. ¹H NMR spectrum of polymer **6f**

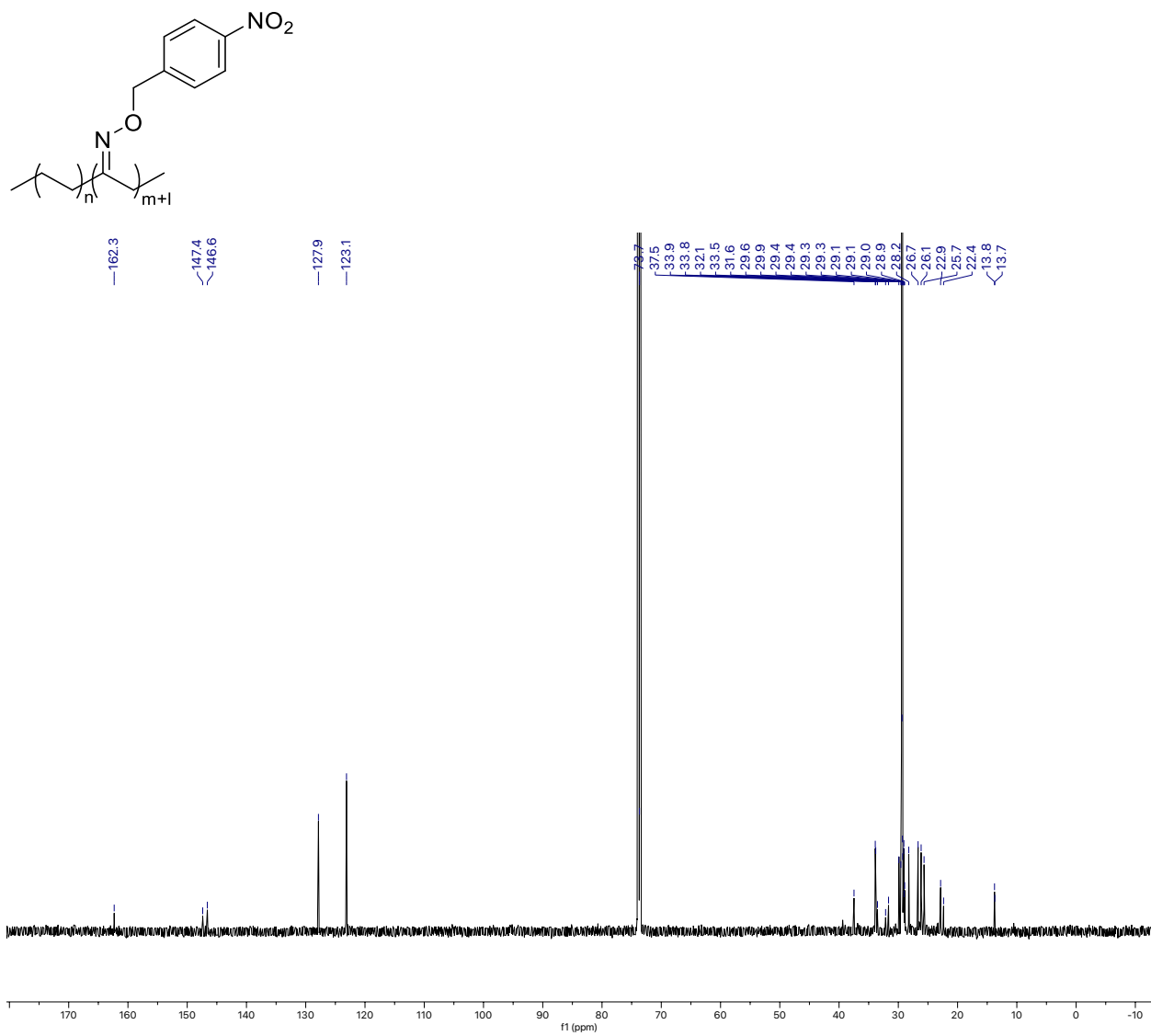


Figure 3.10.11.64. ^{13}C NMR spectrum of polymer 6f

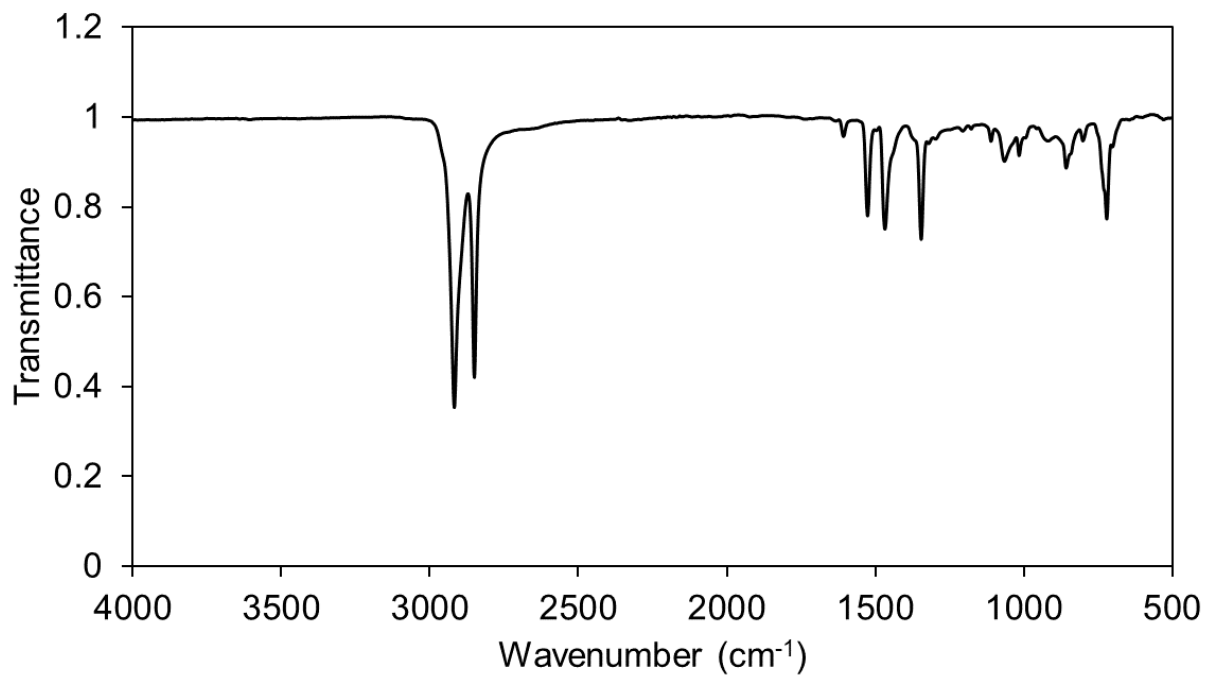


Figure 3.10.11.65. FTIR spectra of polymer **6f**. Major peaks ν (cm⁻¹): 2916, 2849, 1606, 1525, 1466, 1344, 1109, 1064, 1014, 918, 856, 800, 719

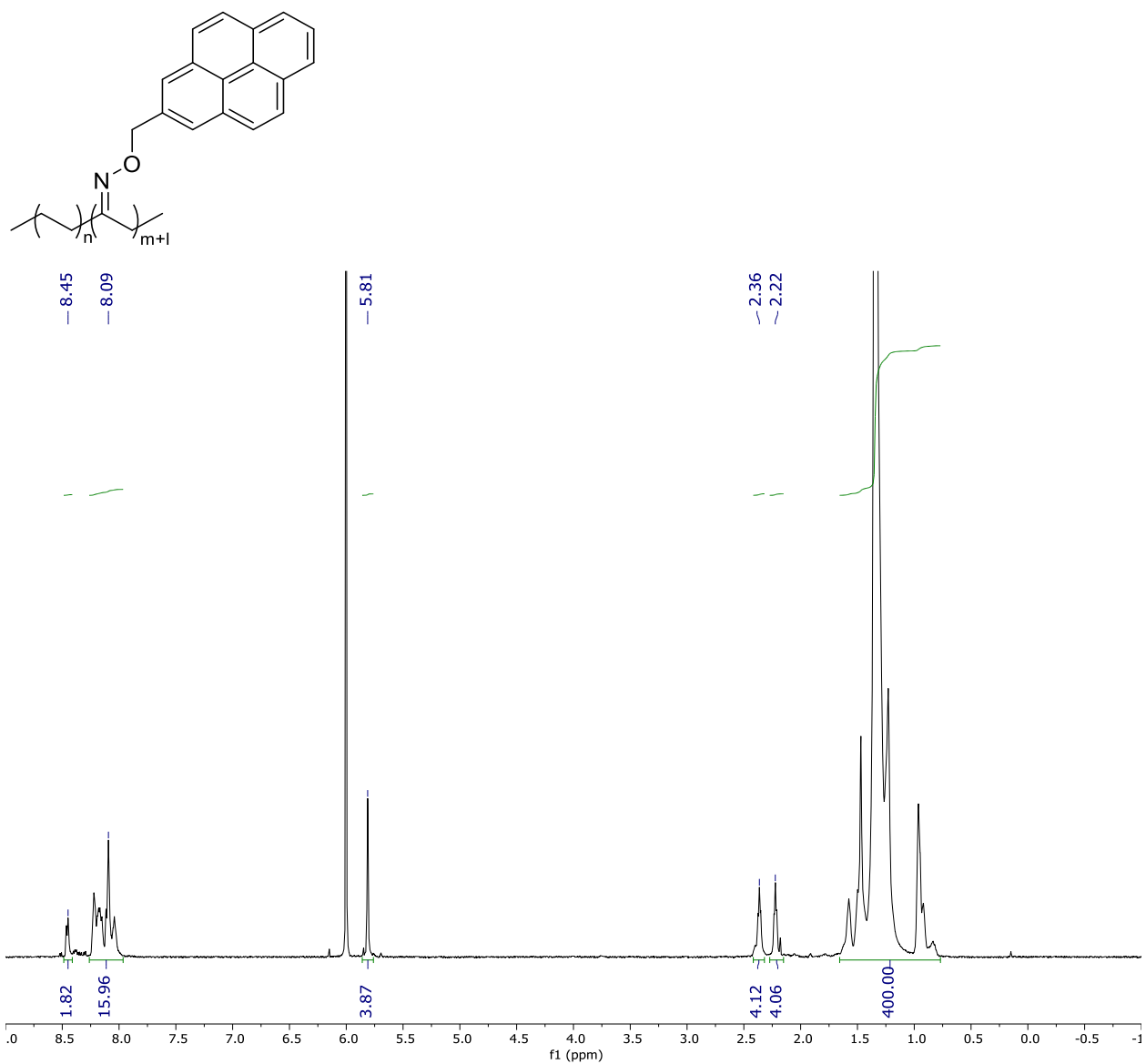


Figure 3.10.11.66. ¹H NMR spectrum of polymer **6g**

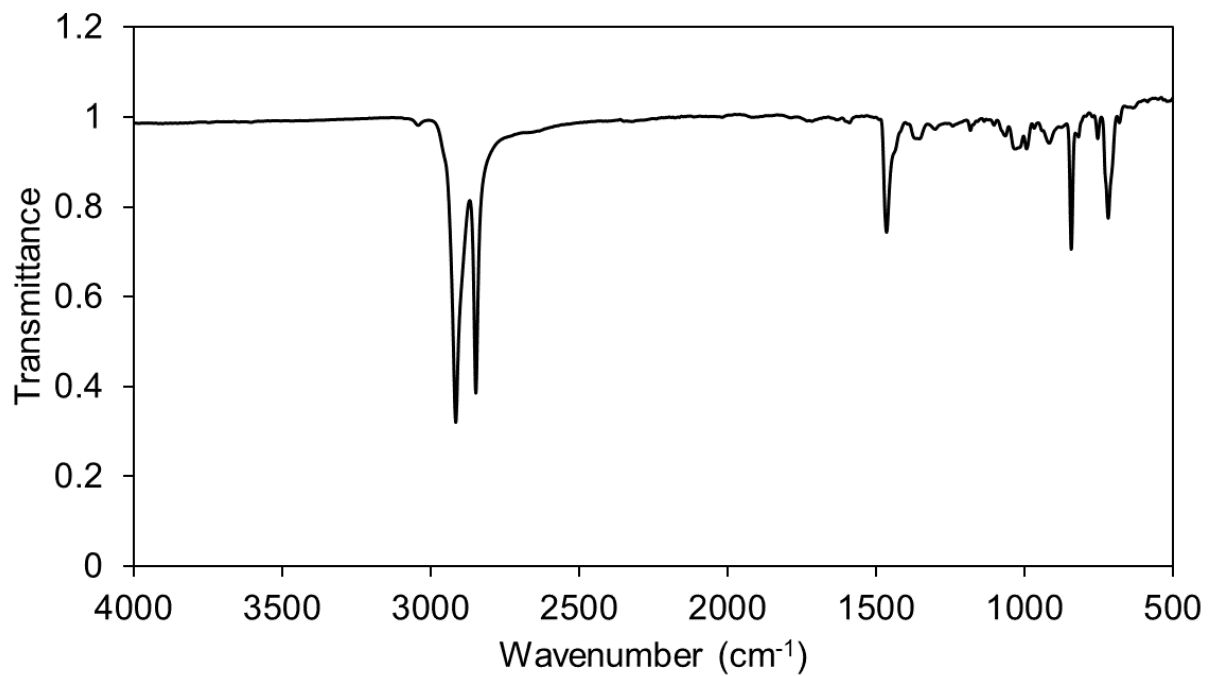


Figure 3.10.11.68. FTIR spectra of polymer **6g**. Major peaks ν (cm⁻¹): 2916, 2849, 1466, 1355, 1033, 994, 918, 843, 755, 719

3.10.12 Characterization of the functionalization of waste plastics

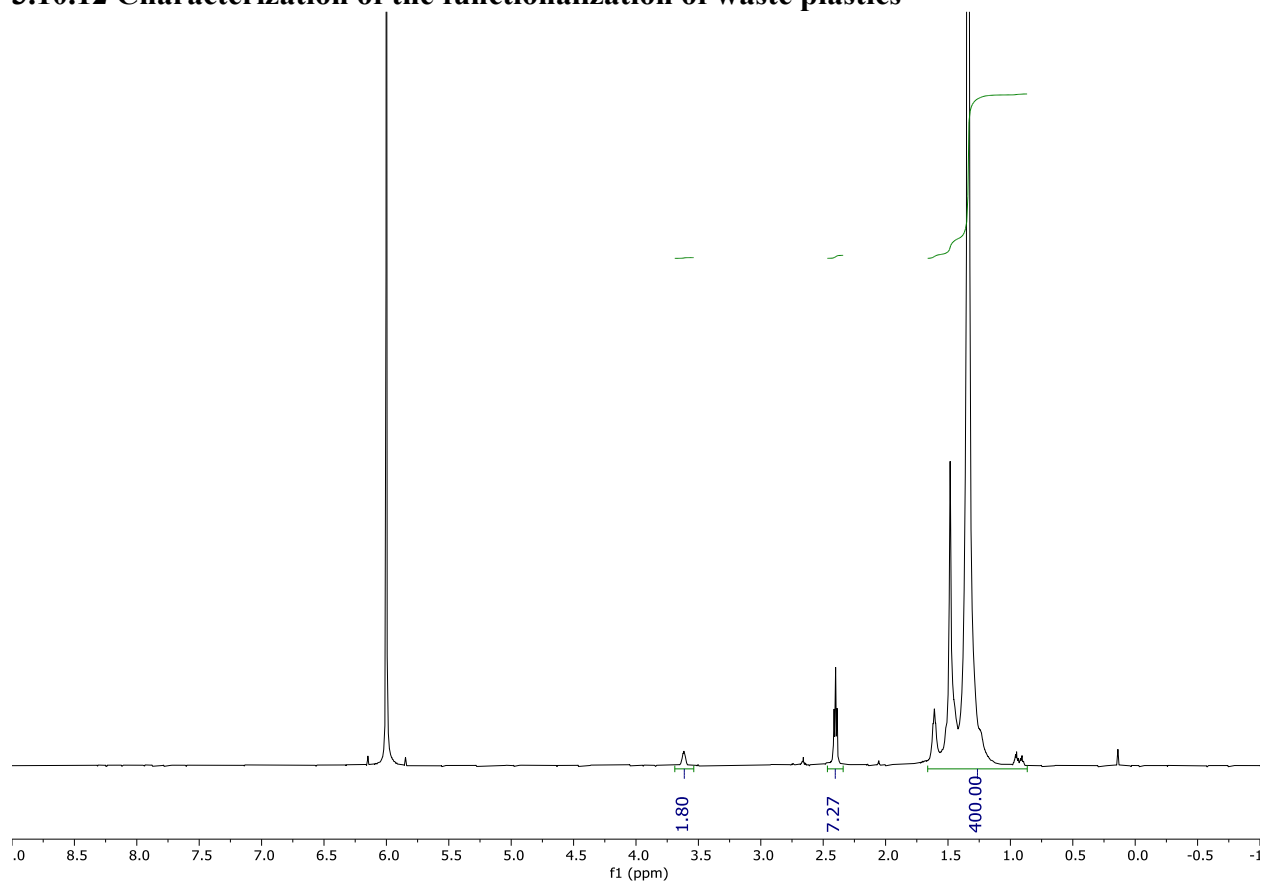


Figure 3.10.12.1. ^1H NMR spectrum of oxo polyethylene derived from a coffee container

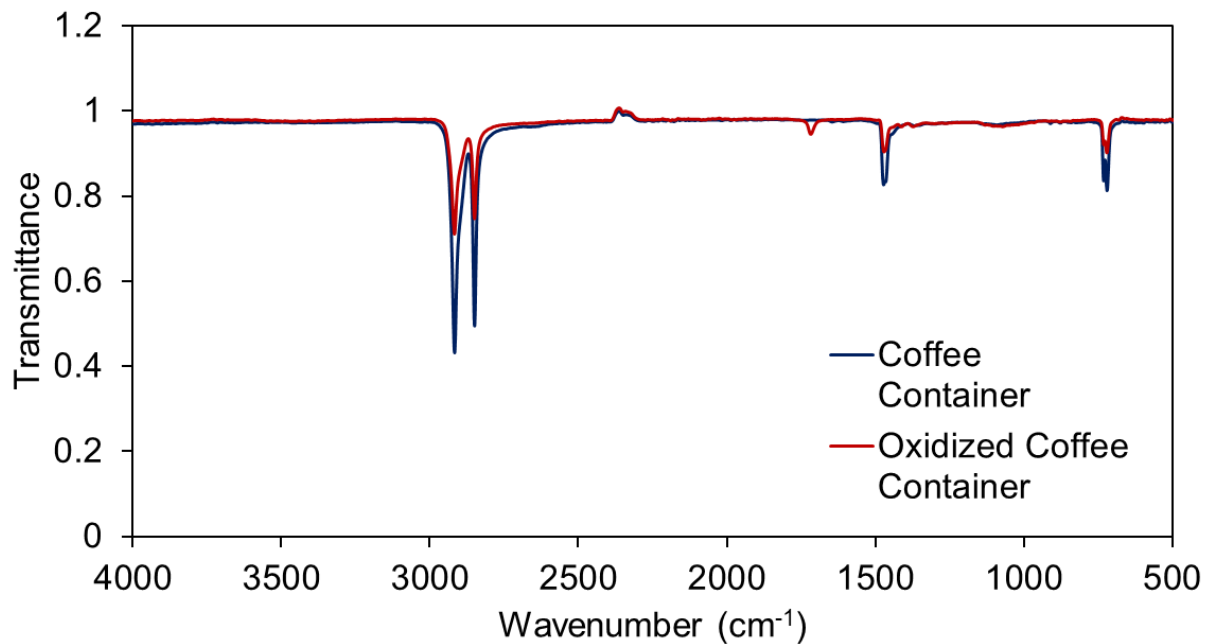


Figure 3.10.12.2. FTIR spectra of a coffee container before and after oxidation. Major peaks ν (cm⁻¹): 3428 and 1716 indicate installation of hydroxy and keto functional groups.

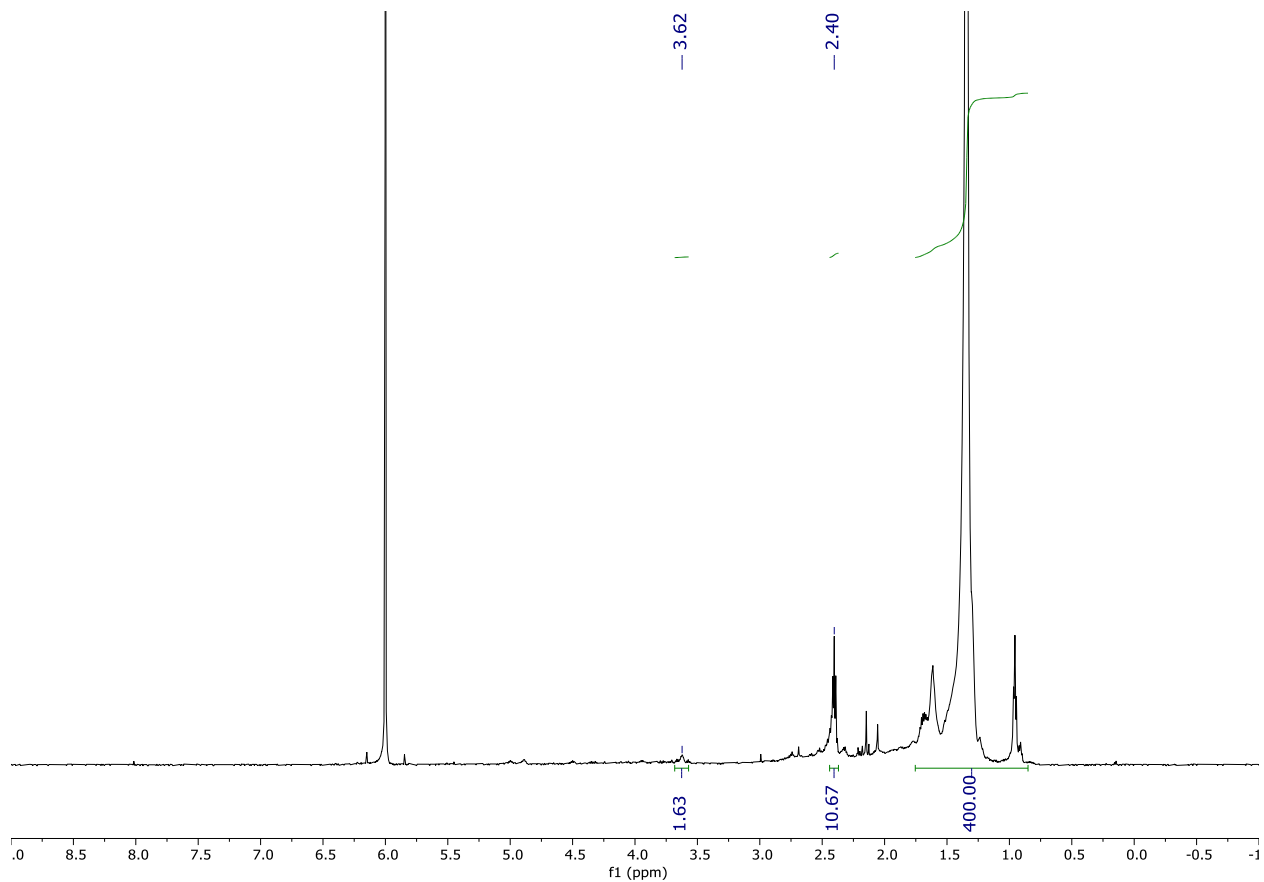


Figure 3.10.12.3. ^1H NMR spectrum of oxo polyethylene derived from food packaging.

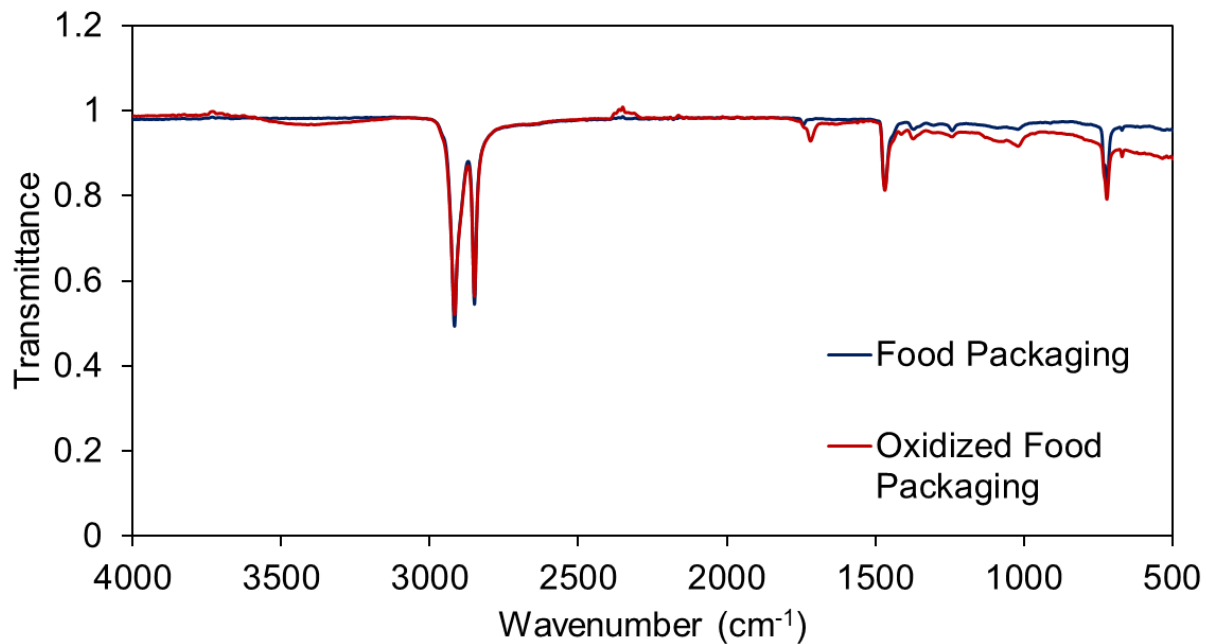


Figure 3.10.12.4. FTIR spectra of food packaging before and after oxidation. Major peaks ν (cm⁻¹): 3387 and 1717 indicate installation of hydroxy and keto functional groups.

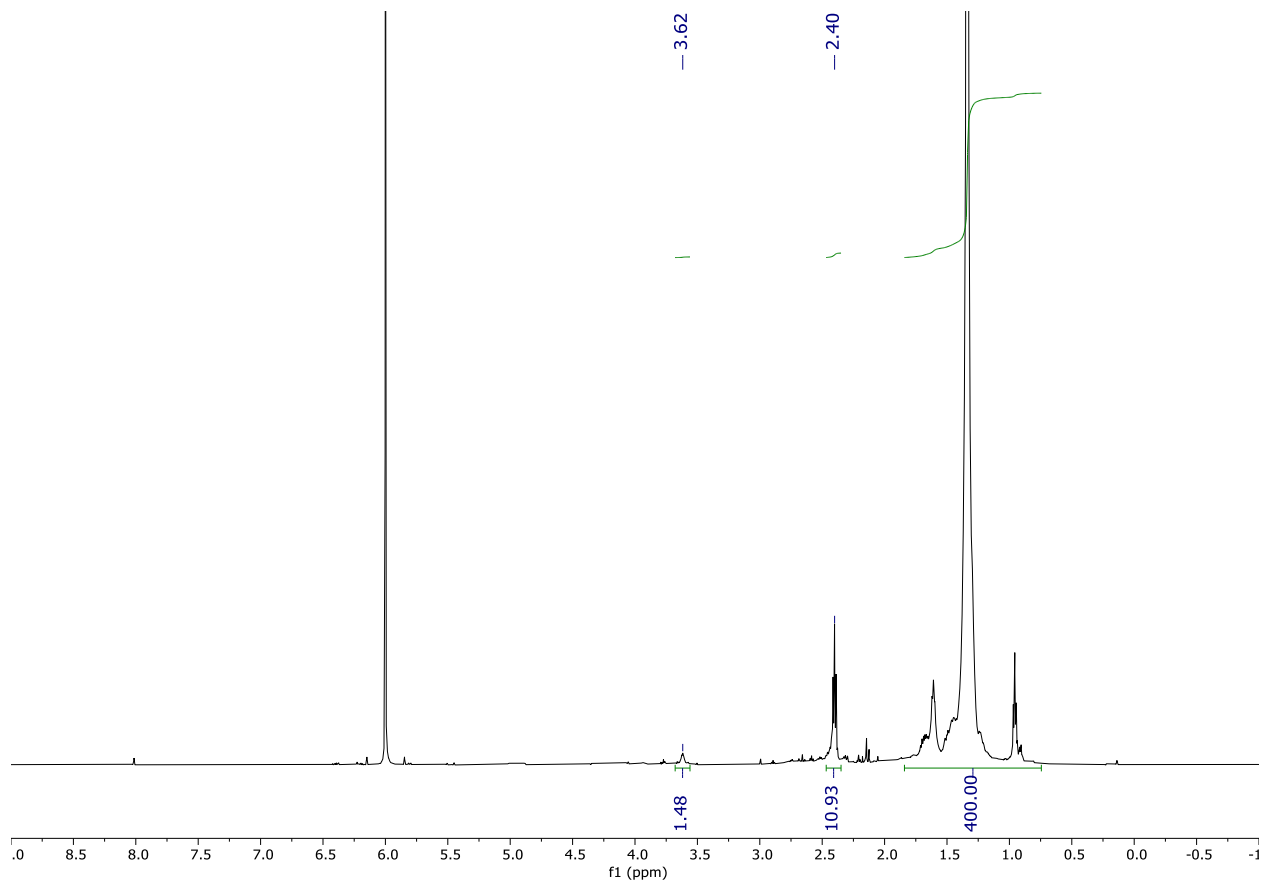


Figure 3.10.12.5. ^1H NMR spectrum of *oxo*-polyethylene derived from a plastic bag

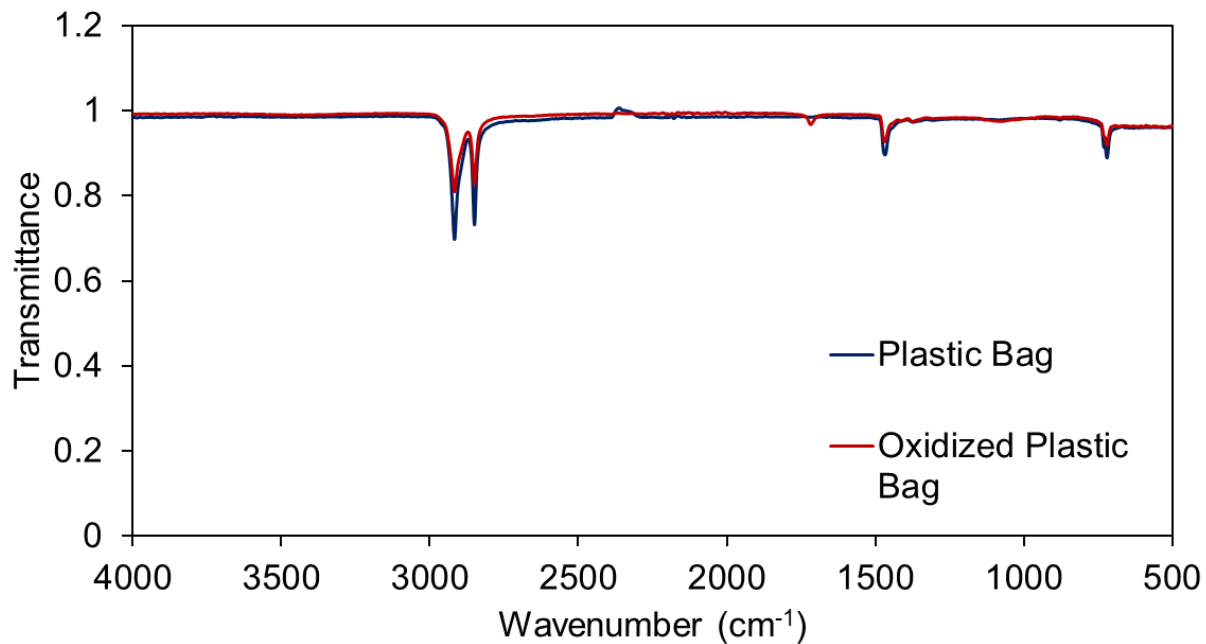


Figure 3.10.12.6. FTIR spectra of a plastic bag before and after oxidation. Major peaks ν (cm⁻¹): 3465 and 1716 indicate installation of hydroxy and keto functional groups.

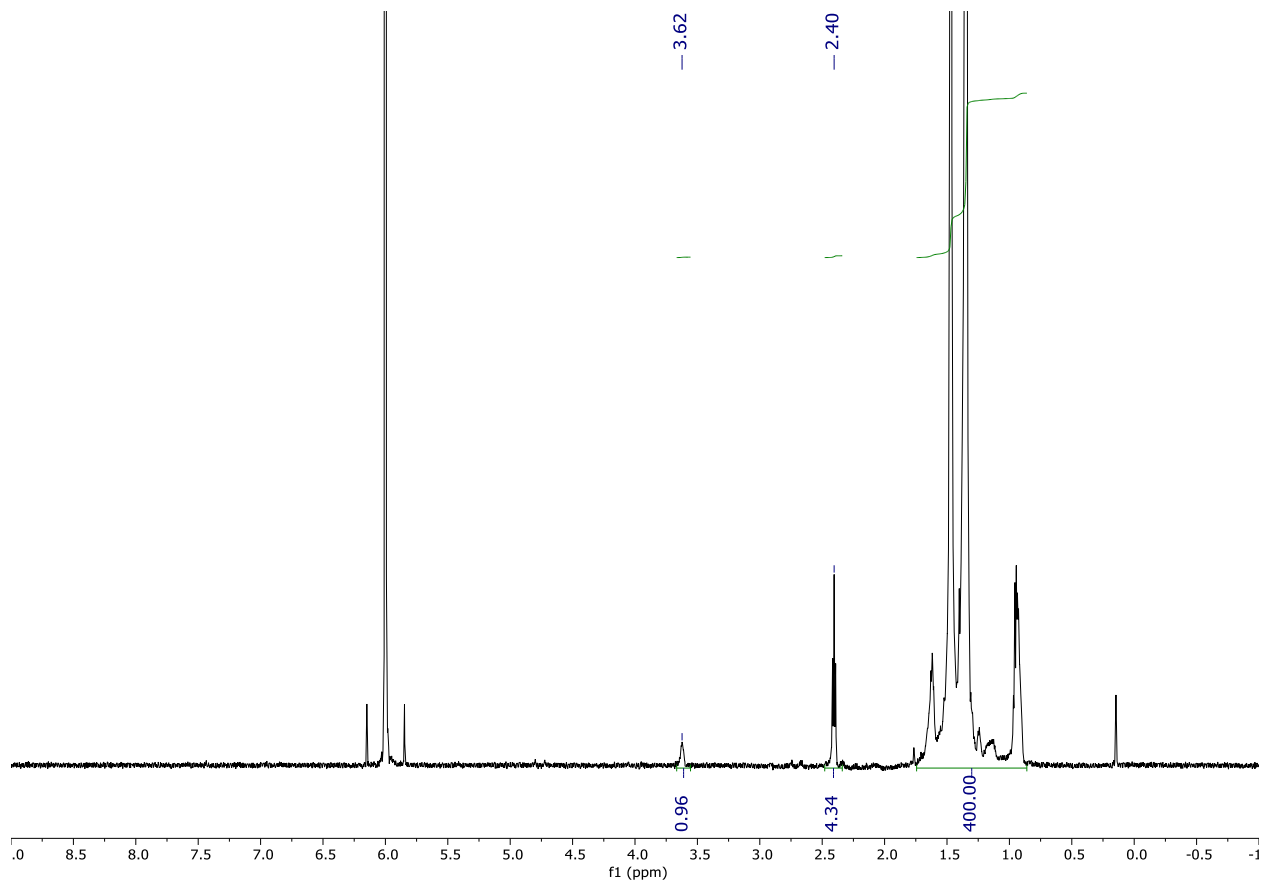


Figure 3.10.12.7. ^1H NMR spectrum of *oxo*-polyethylene derived from a shampoo bottle

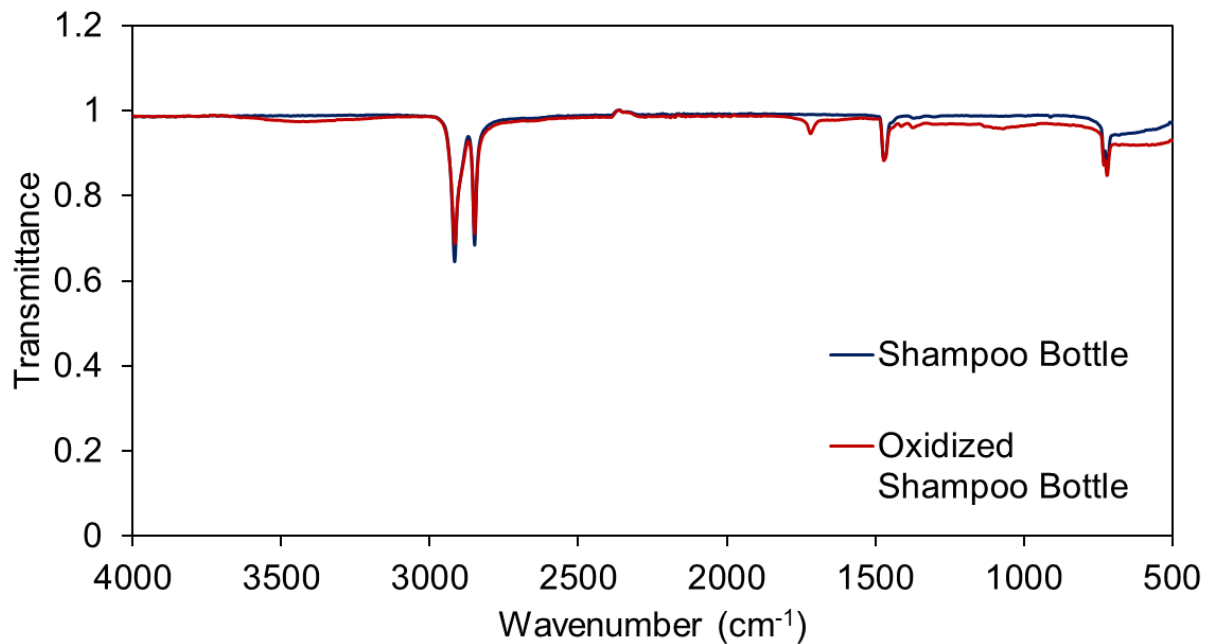


Figure 3.10.12.8. FTIR spectra of a shampoo bottle before and after oxidation. Major peaks ν (cm⁻¹): 3435 and 1717 indicate installation of hydroxy and keto functional groups.

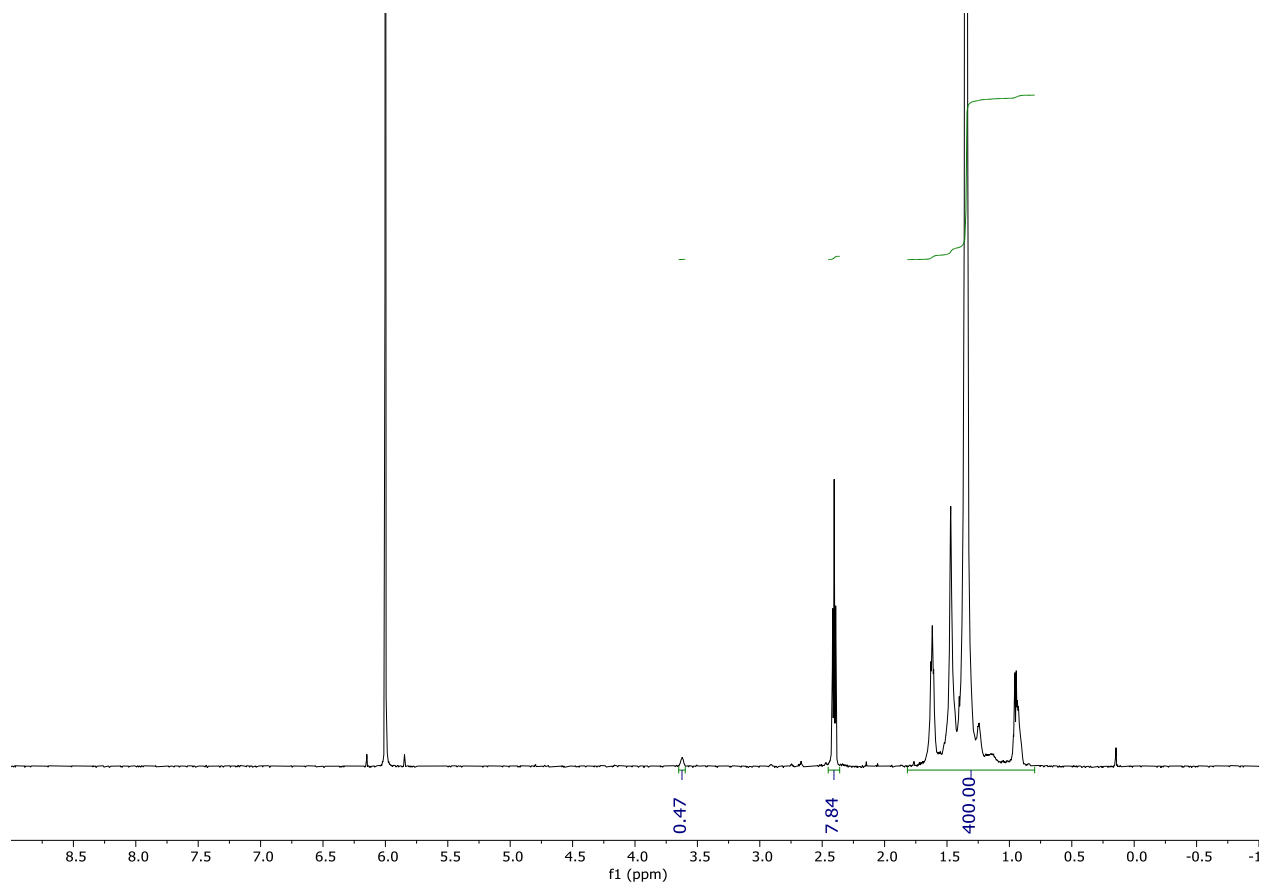


Figure 3.10.12.9. ^1H NMR spectrum of the oxidation of *oxo*-polyethylene derived from a shampoo bottle.

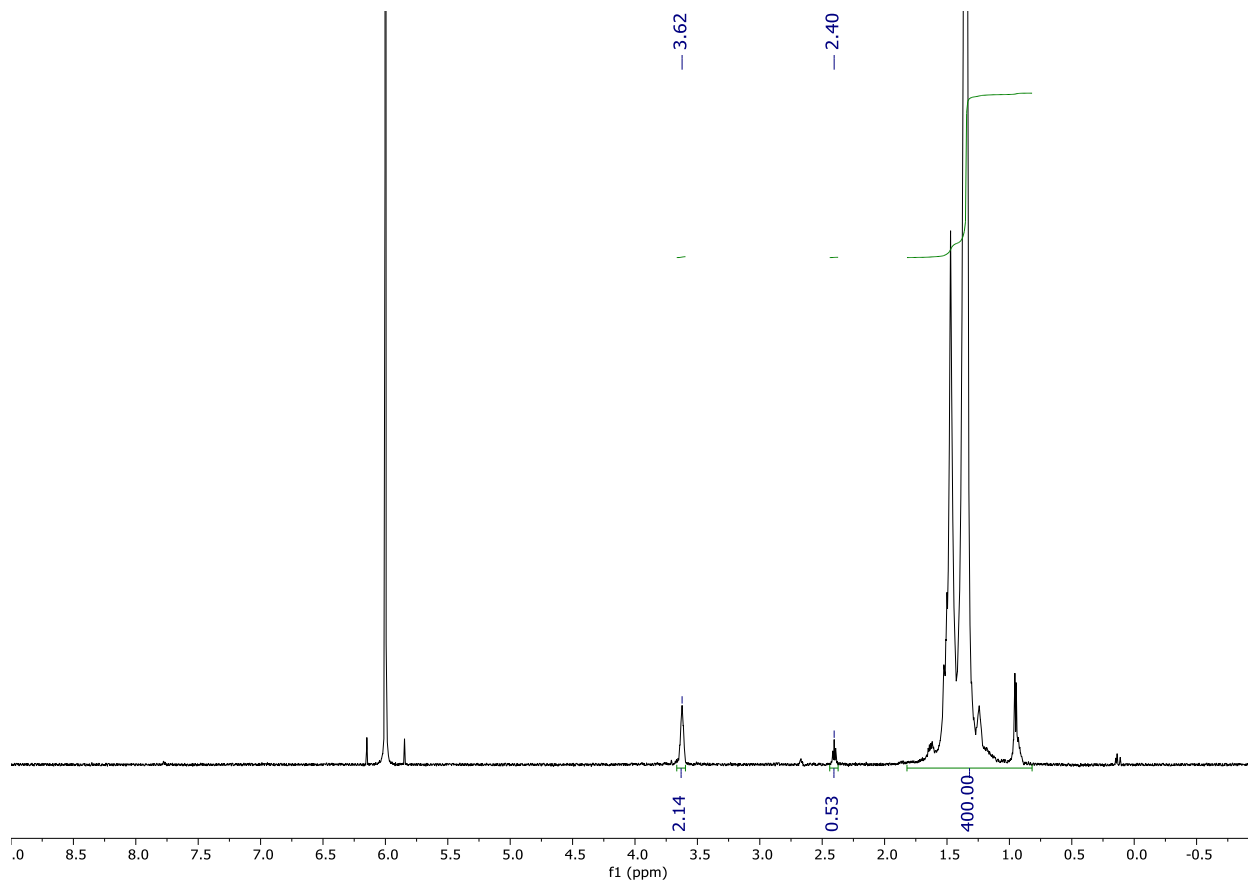


Figure 3.10.12.10. ^1H NMR spectrum of the reduction of *oxo*-polyethylene derived from a shampoo bottle.

3.10.13 Characterization of the hydrolysis of functional groups

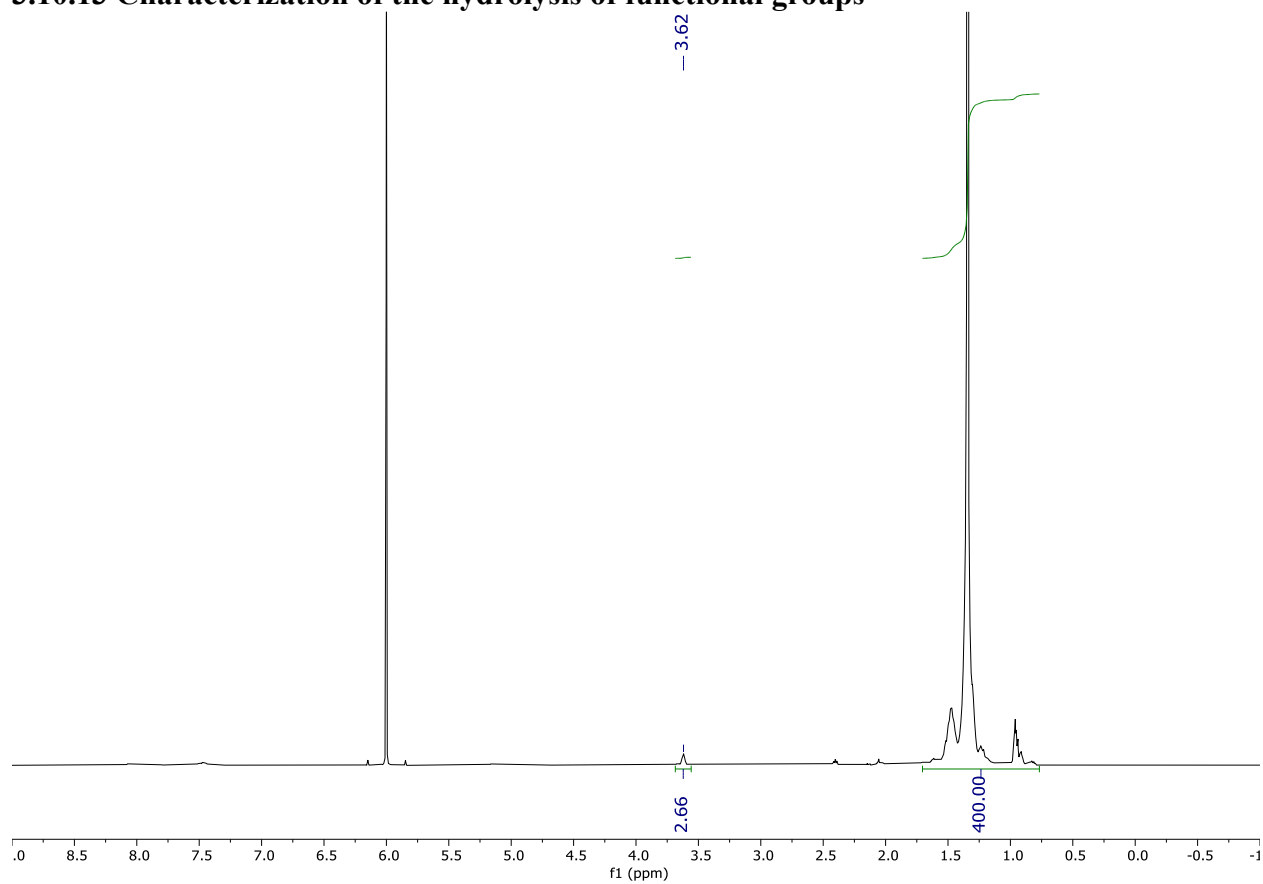


Figure 3.10.13.1. ^1H NMR spectrum of the hydrolysis of polymer 4d.

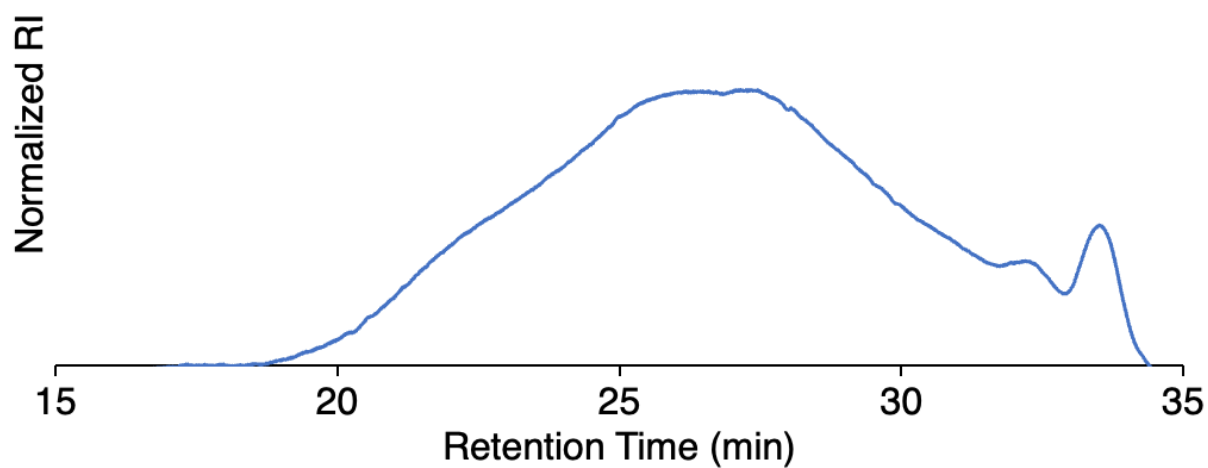


Figure 3.10.13.2. Gel permeation chromatogram of polymer **3** obtained by the hydrolysis of polymer **4d**. $M_n = 7.7$ kDa, $D = 6.3$. Molecular weight was determined relative to polyethylene standards.

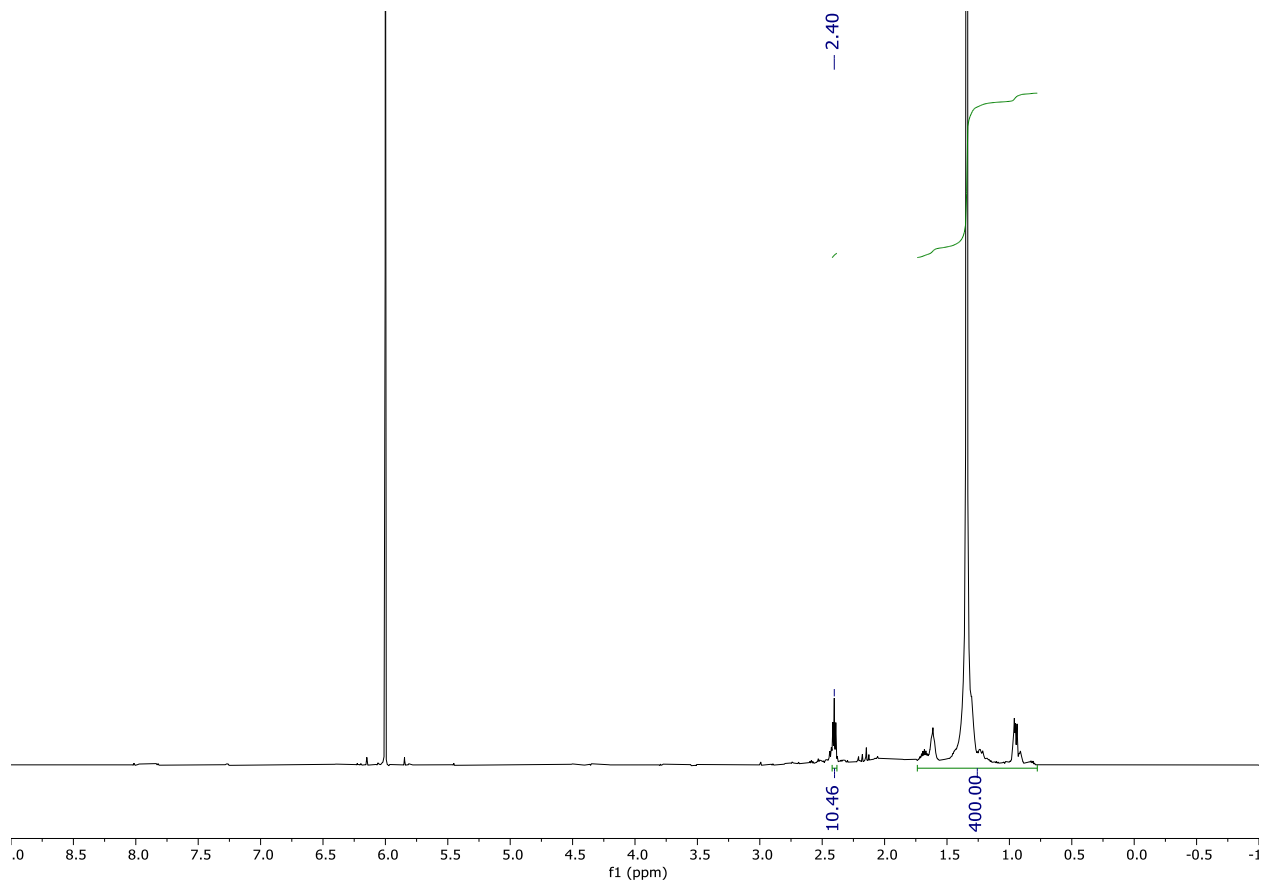


Figure 3.10.13.3. ^1H NMR spectrum of the hydrolysis of polymer **6a**.

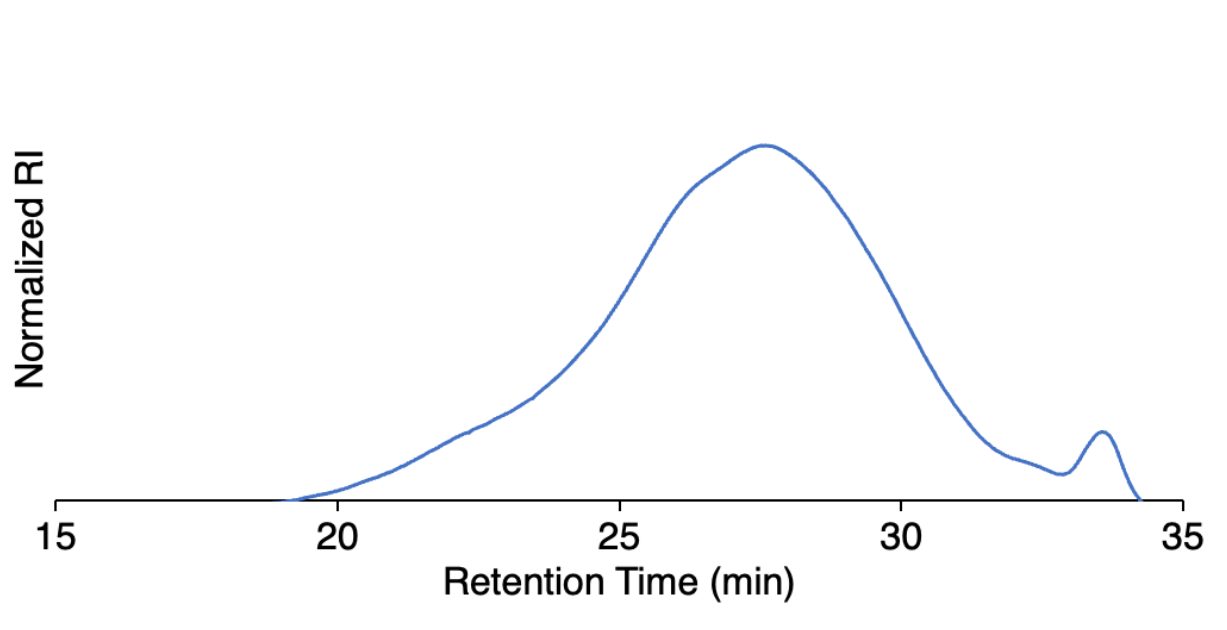


Figure 3.10.13.4. Gel permeation chromatogram of polymer **2** obtained by the hydrolysis of polymer **6a**. $M_n = 6.7$ kDa, $D = 5.9$. Molecular weight was determined relative to polyethylene standards.

3.10.14 Characterization for the separation of plastics from a mechanically mixed blend

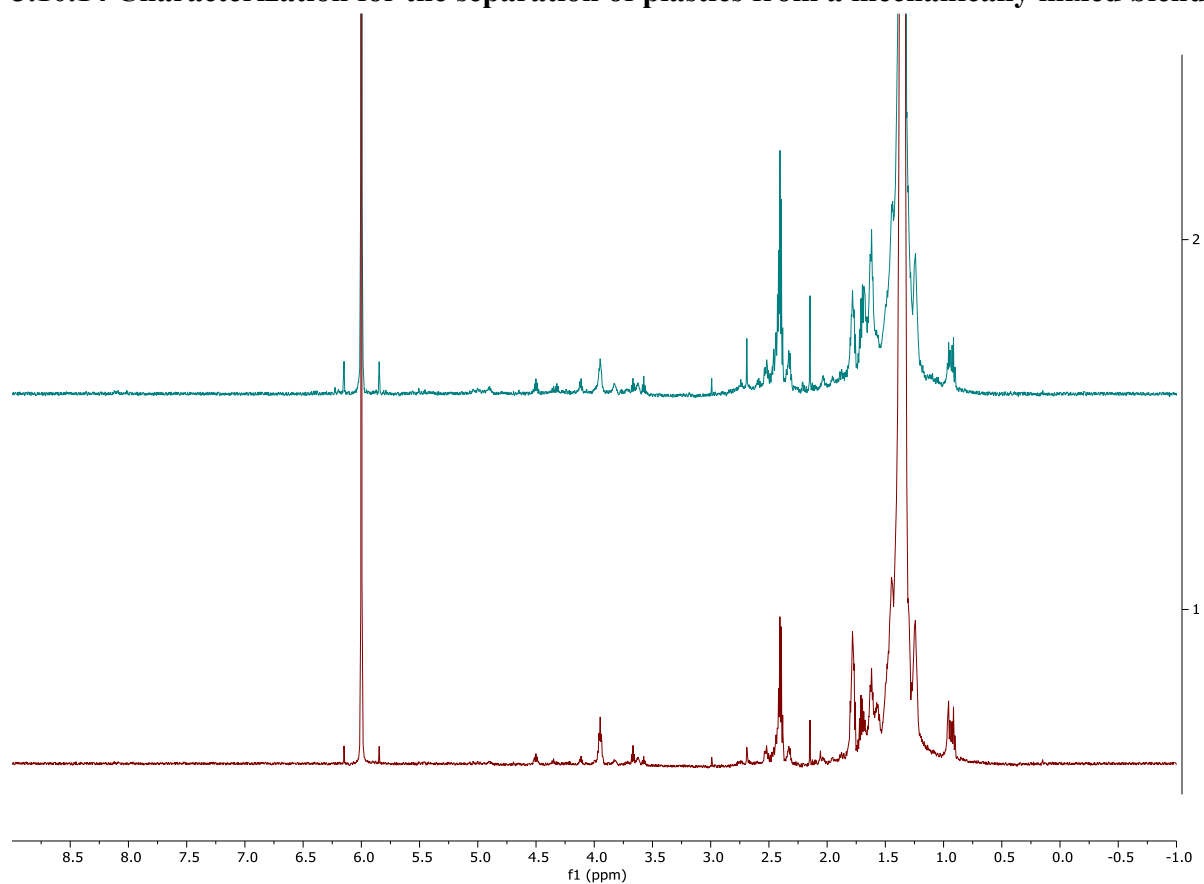


Figure 3.10.13.5. ¹H NMR spectrum of UHMWPE before (above) and after (below) separation

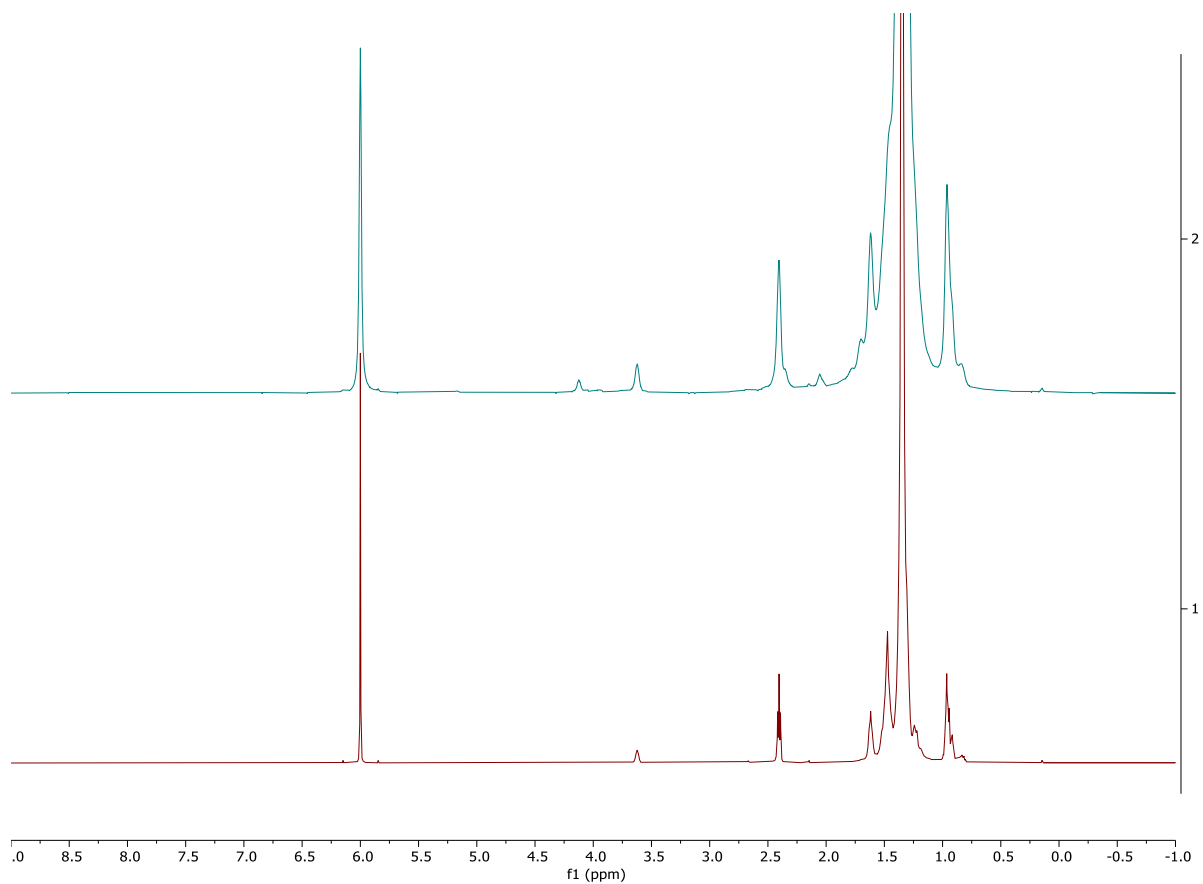


Figure 3.10.13.6. ¹H NMR spectrum of polymer **1** before (below) and after (above) separation
Before separation: 1.4% ketone and 1.4% alcohol
After separation: 1.4% ketone and 1.3% alcohol

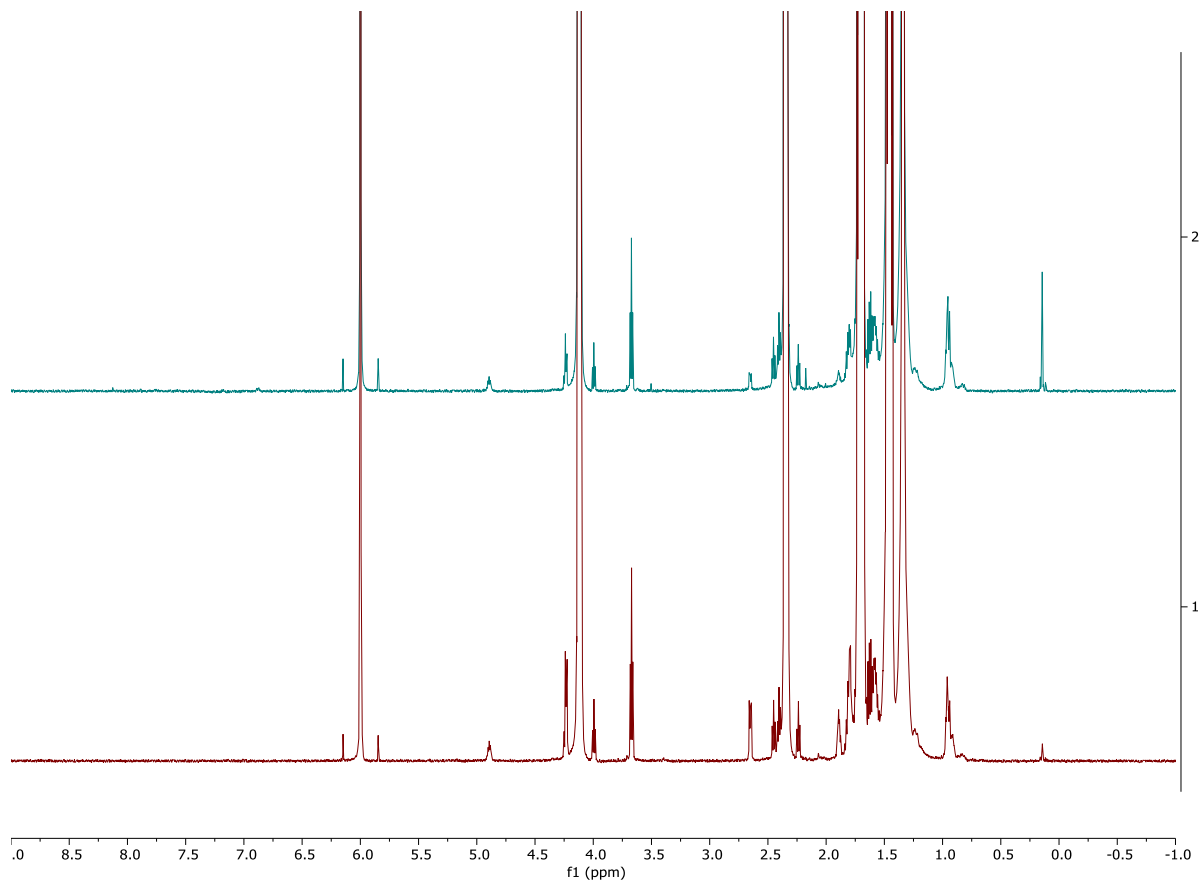


Figure 3.10.13.7. ¹H NMR spectrum of polymer **5** before (below) and after (above) separation

3.10.15 Table of Molecular Weights

Table 3.10.15.1. Summary of SEC data. Molecular weights are reported against polyethylene standards unless stated otherwise.

Polymer	M_n (kDa)	\bar{D}
LDPE	9.6	6.7
1	9.4	7.3
2	9.7	6.3
2^a	6.7	5.9
3	7.7	4.1
3^b	7.7	6.3
3^c	9.8	6.1
4a	7.8	6.4
4b	8.8	4.8
4c	5.3	4.2
4d	8.1	7.1
4e	8.4	7.8
4f	10.4	9.7
5^d	150	1.5
6b	9.3	7.0
6d	4.7	4.6
6e	9.4	7.3
6f	7.7	6.4
6g	8.7	6.4

^aSynthesized by the hydrolysis of polymer 6a. ^bSynthesized by the hydrolysis of polymer 4d. ^cSynthesized by the reduction of polymer 1 with sodium borohydride. ^dMolecular weight determined with refractive index, light scattering, and intrinsic viscosity detectors calibrated with a single poly(styrene) standard.

3.10.16 Differential Scanning Calorimetry (DSC) Data

DSC was performed on a TA Q200 instrument. Each sample (ca. 5 mg) was placed in a hermetic aluminum pan, sealed, and scanned at a rate of 10 °C/min from -150 °C to 150 °C. Data were plotted from the 2nd heating cycle. Glass transition temperatures (T_g) and peak melting temperatures (T_m) were recorded at the second scan (Table S3).

X_c , % crystallinity was calculated using the following equation:

$$X_c = 100 * \frac{\Delta H_m}{\Delta H_{100}}$$

ΔH_m is the enthalpy absorbed during heating, and ΔH_{100} is the enthalpy absorbed during heating of a sample that is 100% crystalline. For polyethylene, $\Delta H_{100} = 293 \text{ J/g}$.²⁰⁰

Table 3.10.16.1. Summary of glass transition (T_g) and melting (T_m) temperatures and X_c for all polymers.

Polymer	T_g (°C)	T_m (°C)	X_c (%)
LDPE	-136.5	110.7	45
1	-146.5	107.5	37
2	-136.5	107.6	39
3	-136.5	104.7	37
4a	-136.5	98.8	33
4b	-136.5	92.9	25
4c	-136.5	95.9	30
4d	-136.5	95.9	35
4e	-136.5	95.8	31
4f	-16.5	92.9	22
4g	-136.5	98.9	16
5	-136.5	56.6	23
6a	-136.5	98.8	30
6b	-136.5	98.8	30
6c	-136.5	95.8	31
6d	-136.5	98.8	40
6e	-136.5	98.8	26
6f	-136.5	98.8	40
6g	-136.5	98.8	36

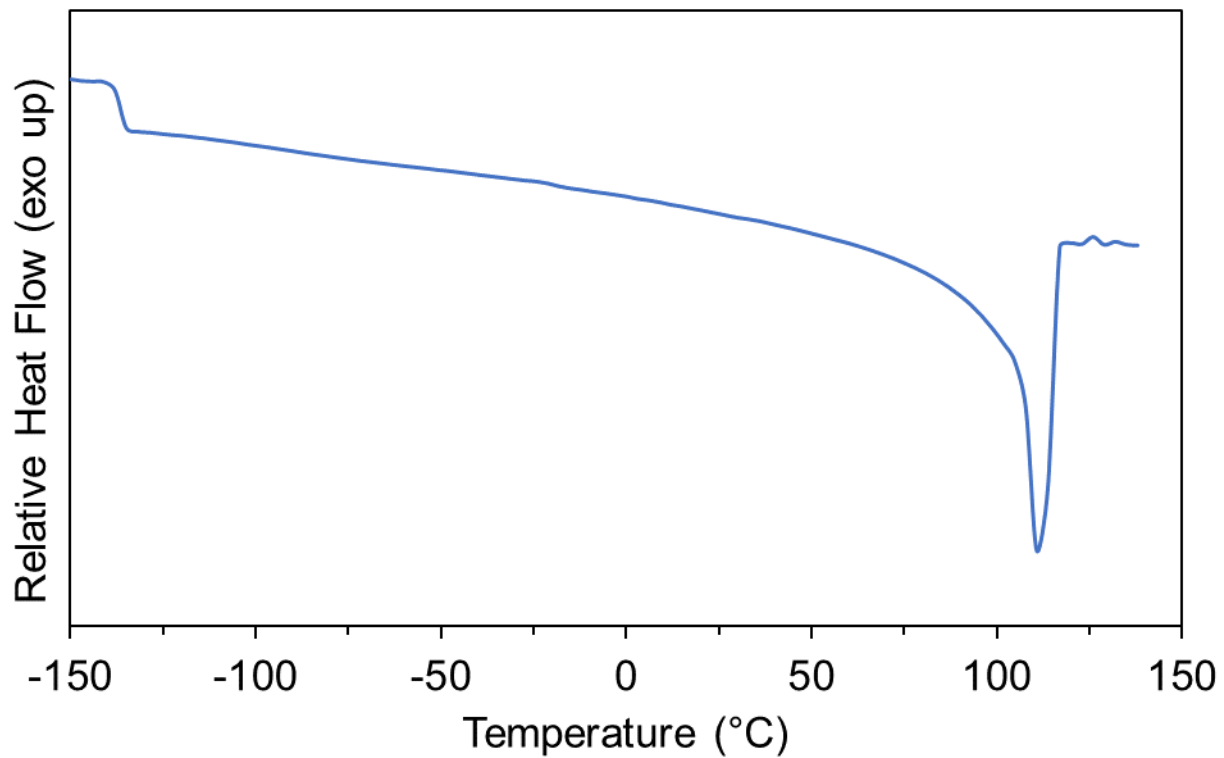


Figure 3.10.16.1. Differential scanning calorimetry (DSC) curve of unmodified polyethylene. $T_g = -136.5\text{ }^\circ\text{C}$, $T_m = 110.7\text{ }^\circ\text{C}$.

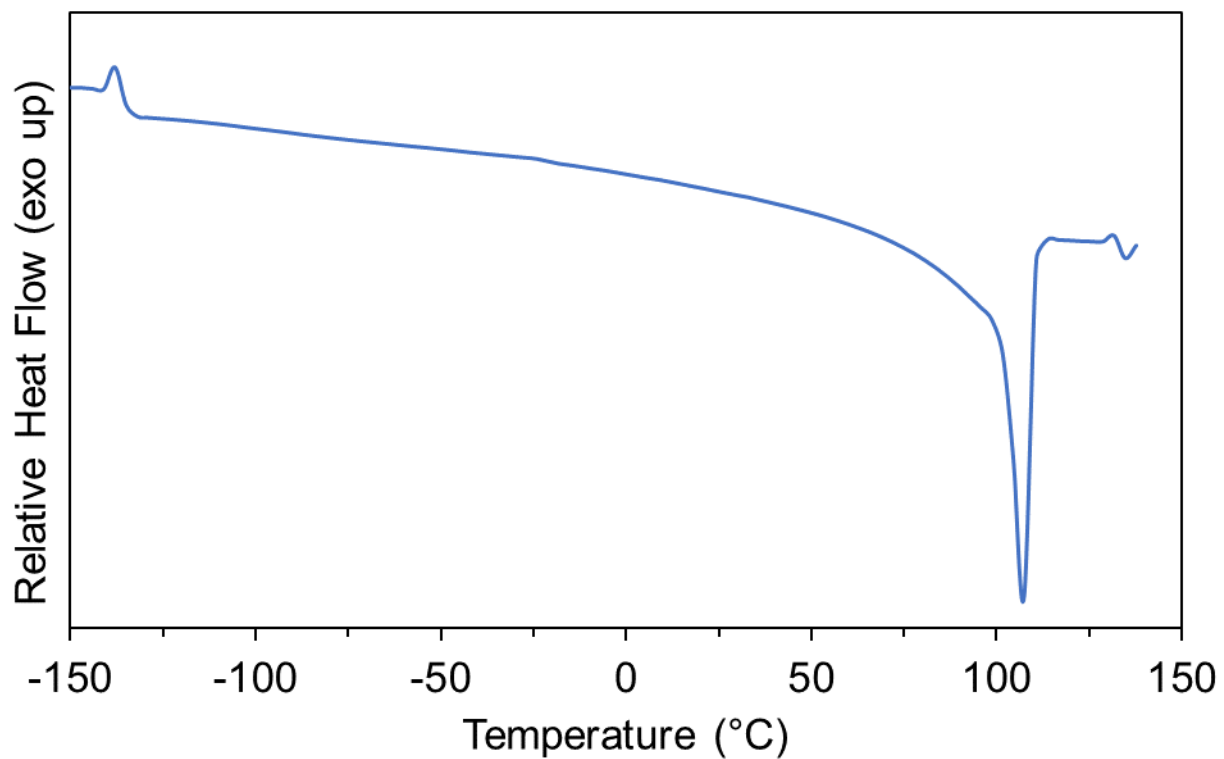


Figure 3.10.16.2. Differential scanning calorimetry (DSC) curve of polymer **1**. $T_g = -146.5$ °C, $T_m = 107.5$ °C.

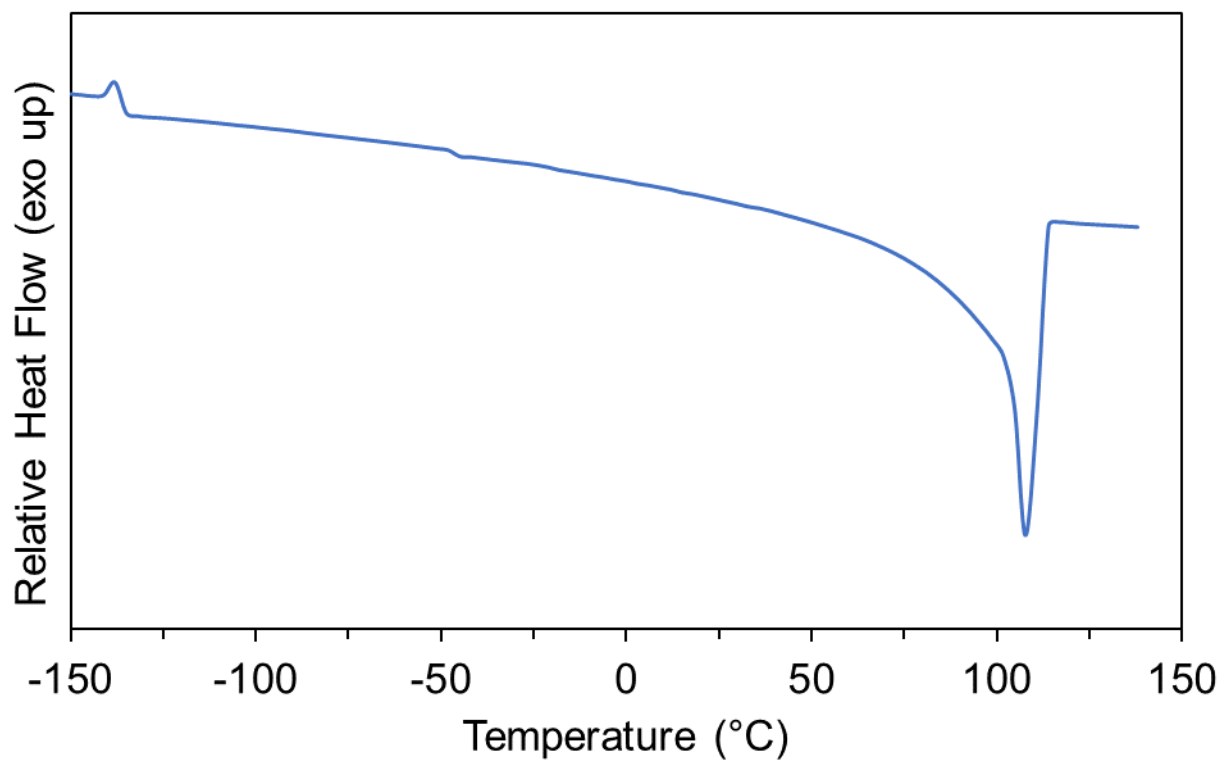


Figure 3.10.16.3. Differential scanning calorimetry (DSC) curve of polymer **2**. $T_g = -136.5\text{ }^\circ\text{C}$, $T_m = 107.6\text{ }^\circ\text{C}$.

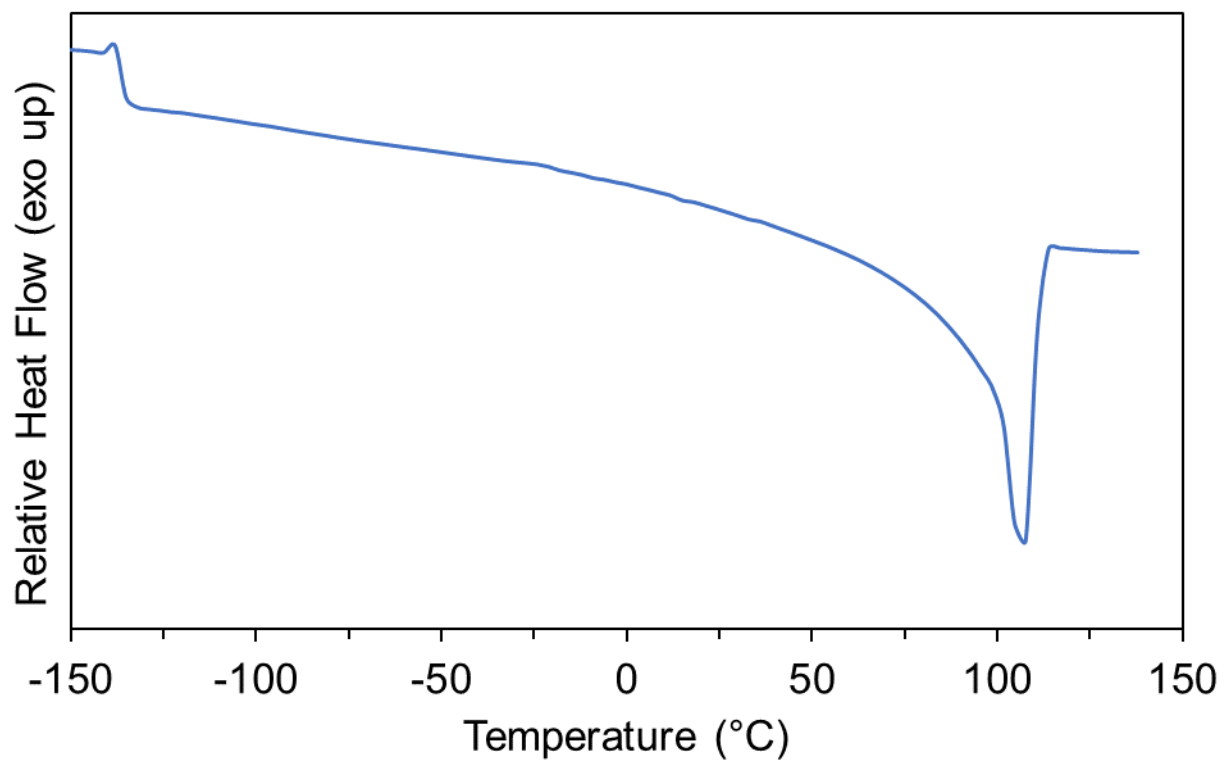


Figure 3.10.16.4. Differential scanning calorimetry (DSC) curve of polymer **3**. $T_g = -136.5$ °C, $T_m = 104.7$ °C.

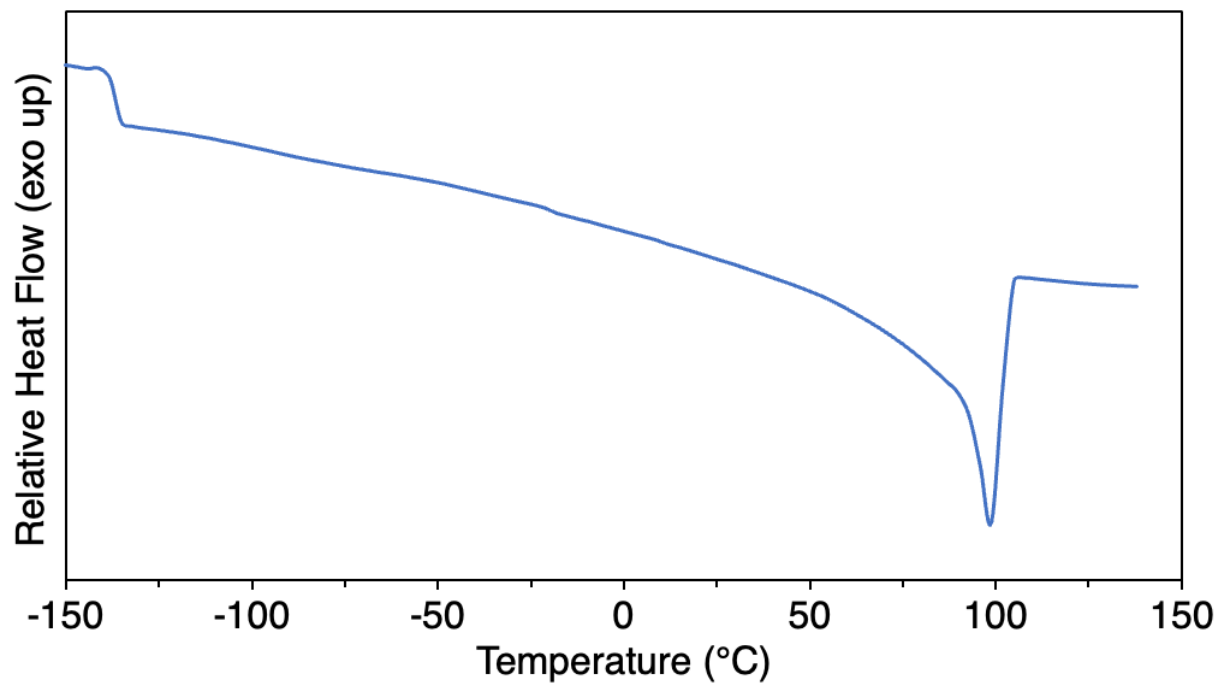


Figure 3.10.16.5. Differential scanning calorimetry (DSC) curve of polymer **4a**. $T_g = -136.5\text{ }^\circ\text{C}$, $T_m = 98.8\text{ }^\circ\text{C}$.

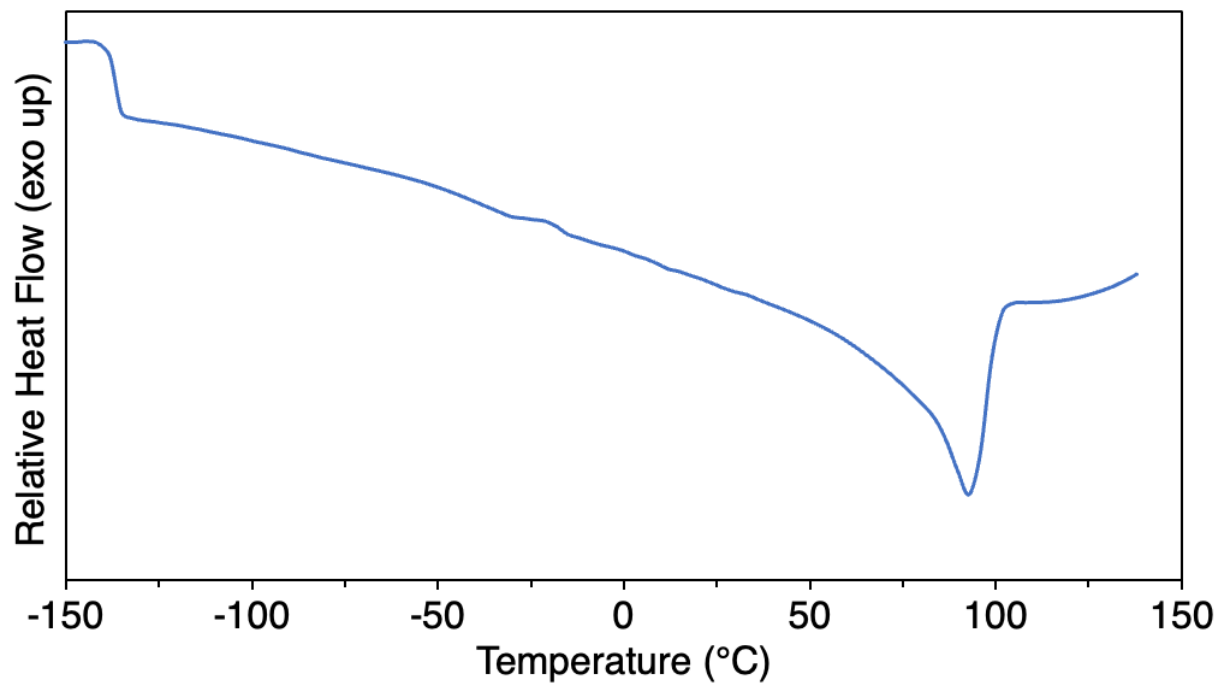


Figure 3.10.16.6. Differential scanning calorimetry (DSC) curve of polymer **4b**. $T_g = -136.5\text{ }^\circ\text{C}$, $T_m = 92.9\text{ }^\circ\text{C}$.

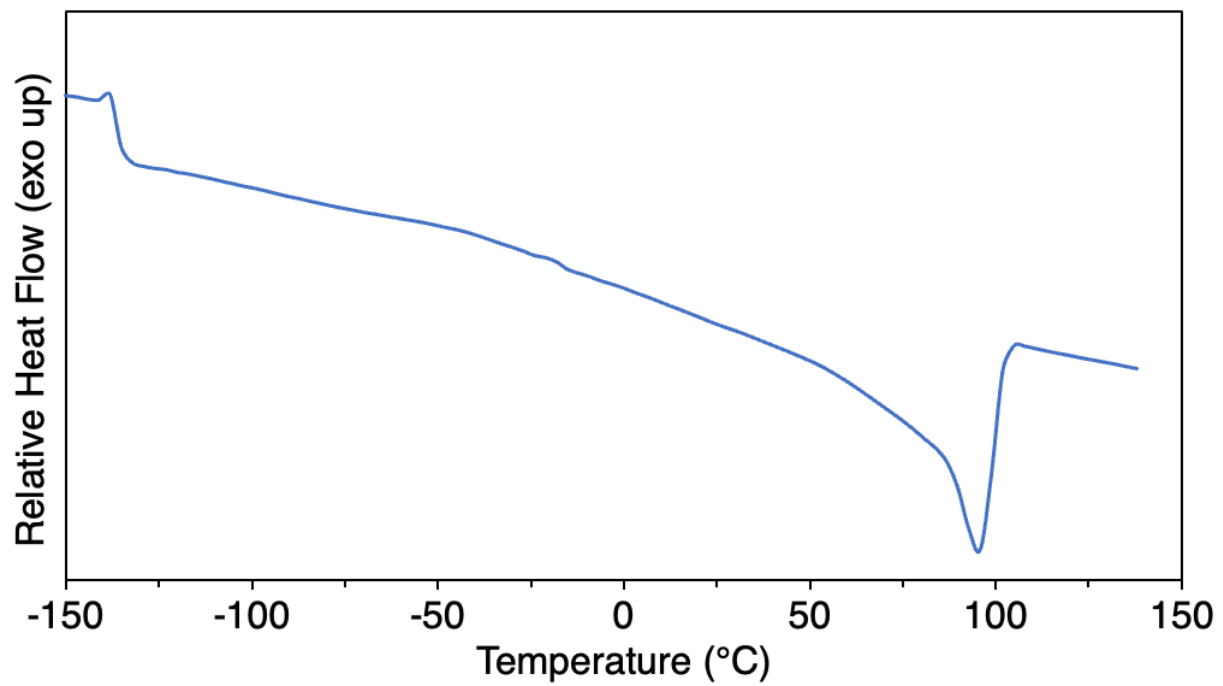


Figure 3.10.16.7. Differential scanning calorimetry (DSC) curve of polymer **4c**. $T_g = -136.5\text{ }^\circ\text{C}$, $T_m = 95.9\text{ }^\circ\text{C}$.

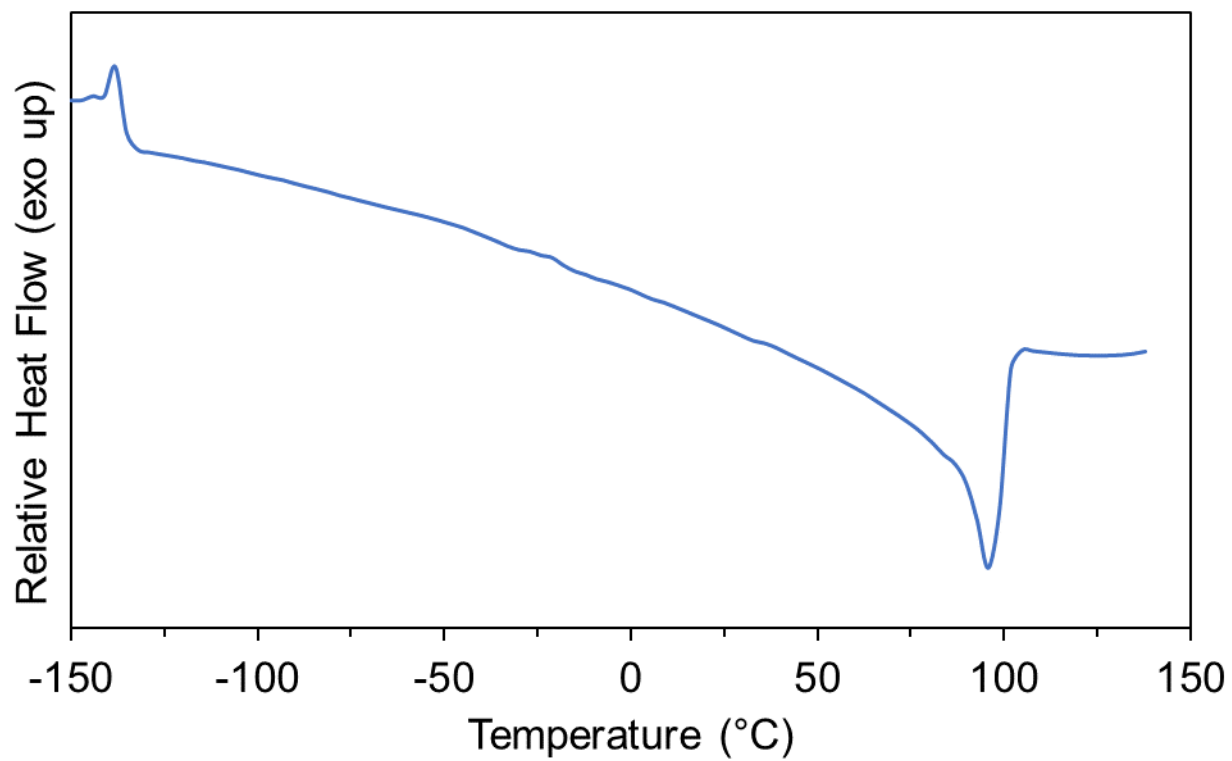


Figure 3.10.16.8. Differential scanning calorimetry (DSC) curve of polymer **4d**. $T_g = -136.5$ °C, $T_m = 95.9$ °C.

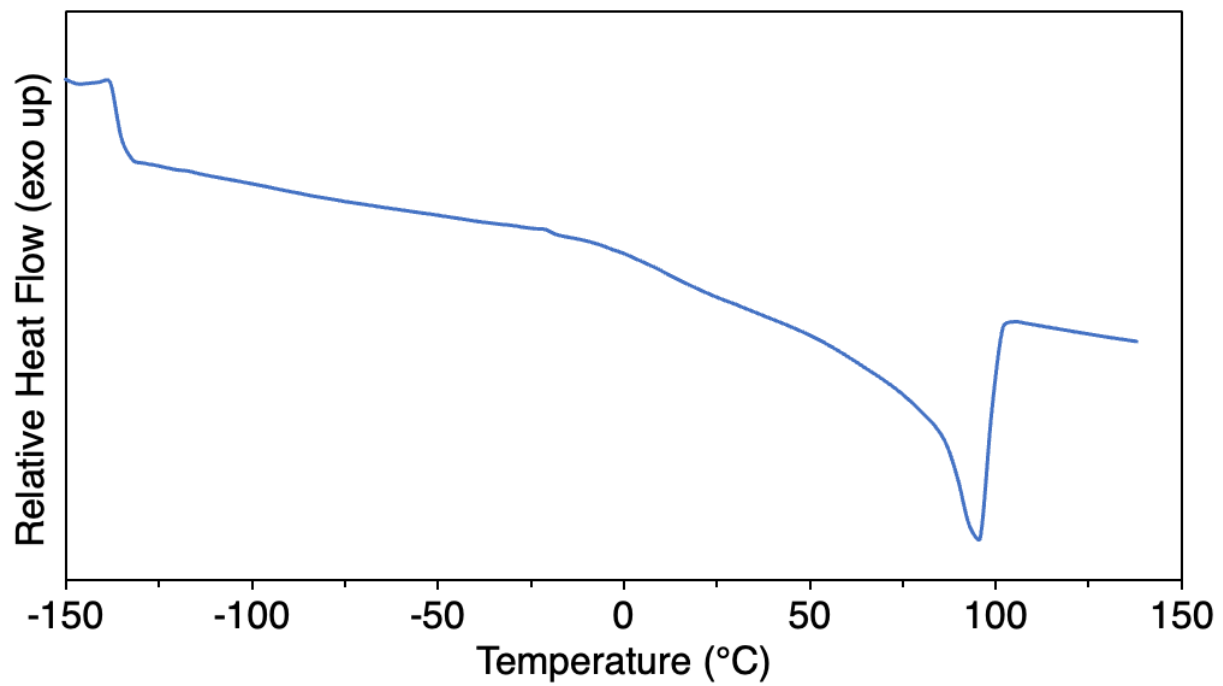


Figure 3.10.16.9. Differential scanning calorimetry (DSC) curve of polymer **4e**. $T_g = -136.5\text{ }^\circ\text{C}$, $T_m = 95.8\text{ }^\circ\text{C}$.

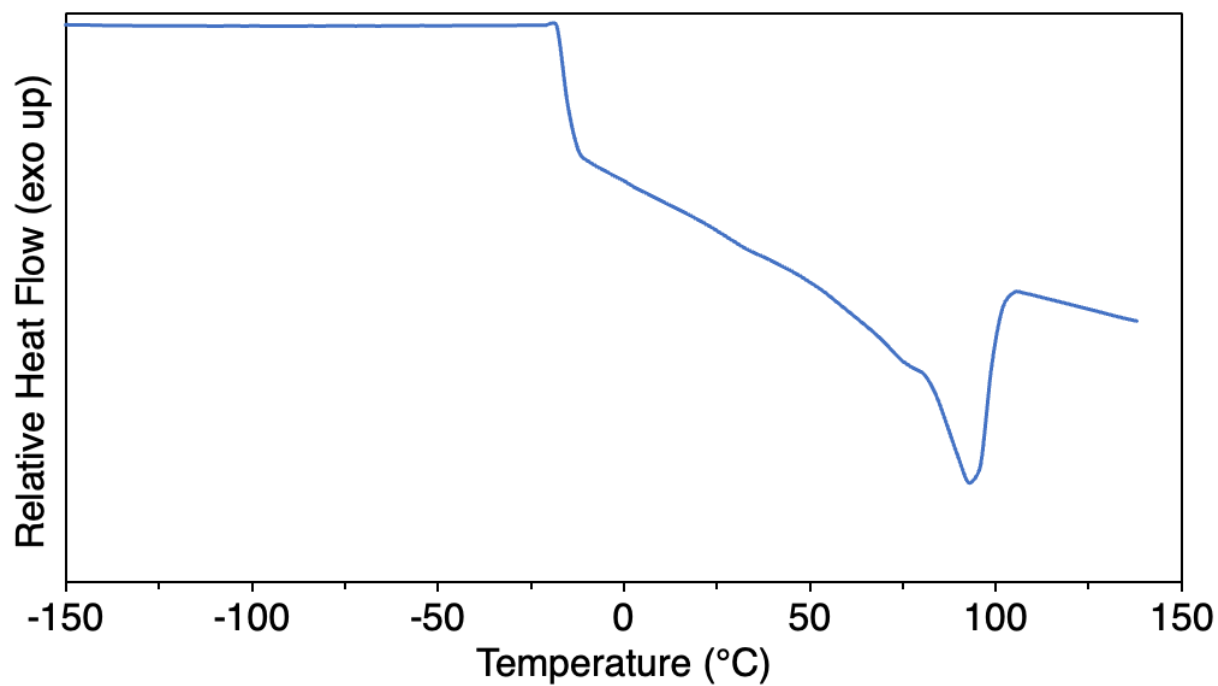


Figure 3.10.16.10. Differential scanning calorimetry (DSC) curve of polymer **4f**. $T_g = -16.5\text{ }^\circ\text{C}$, $T_m = 92.9\text{ }^\circ\text{C}$.

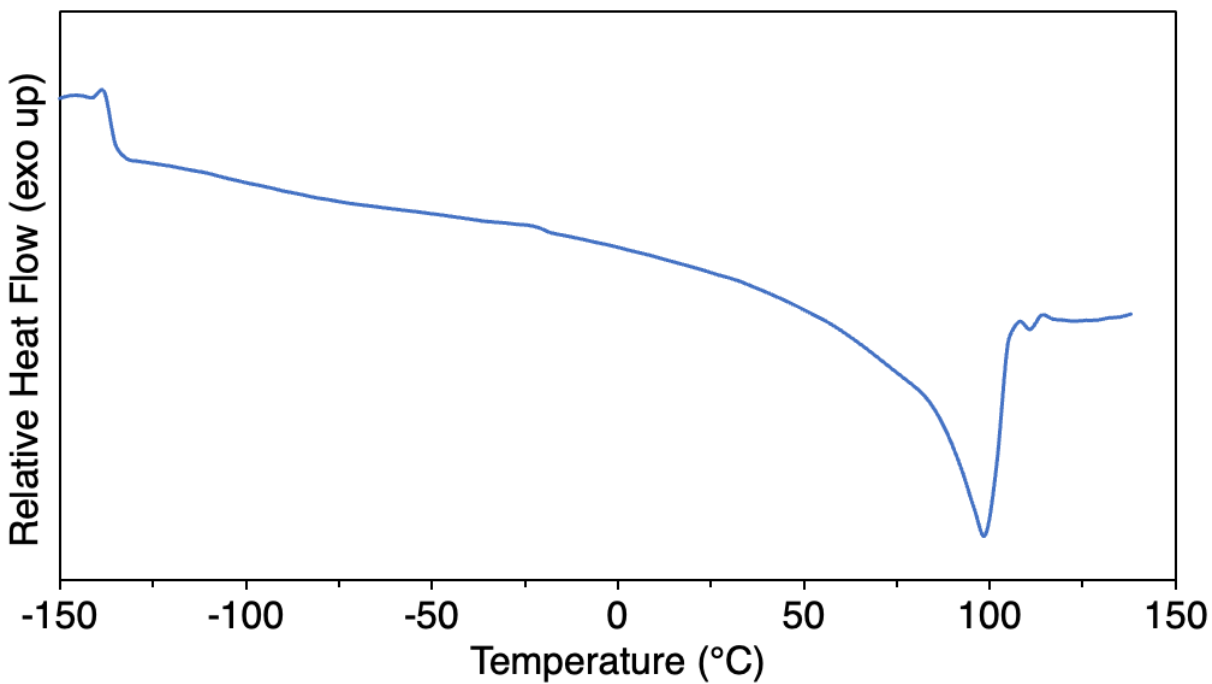


Figure 3.10.16.11. Differential scanning calorimetry (DSC) curve of polymer **4g**. $T_g = -136.5\text{ }^\circ\text{C}$, $T_m = 98.9\text{ }^\circ\text{C}$.

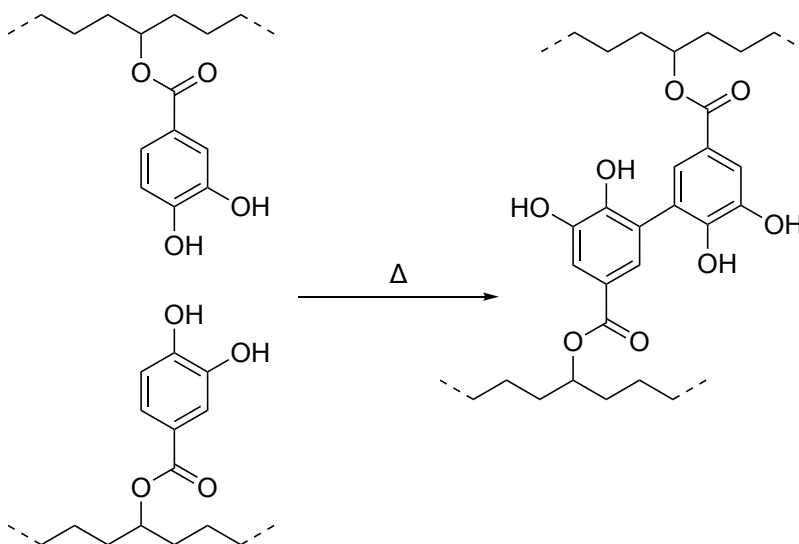


Figure 3.10.16.12. Putative structure for the crosslinks formed by the catechols of polymer **4g**

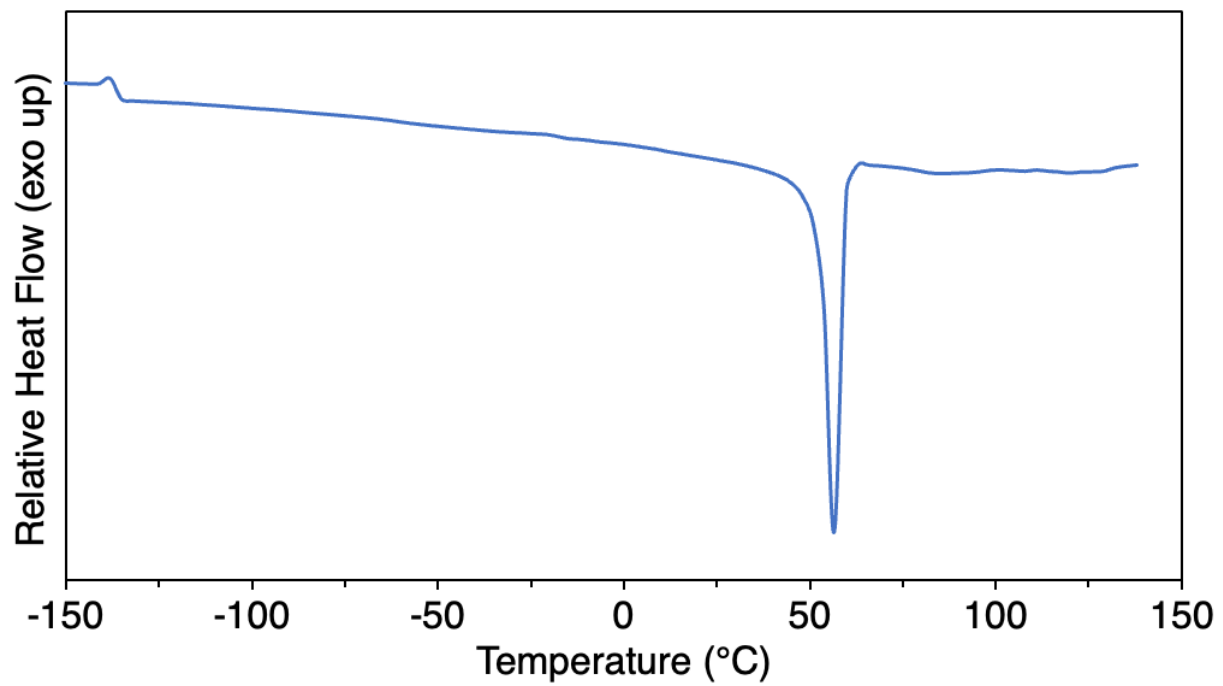


Figure 3.10.16.13. Differential scanning calorimetry (DSC) curve of polymer **5**. $T_g = -136.5$ °C, $T_m = 56.6$ °C.

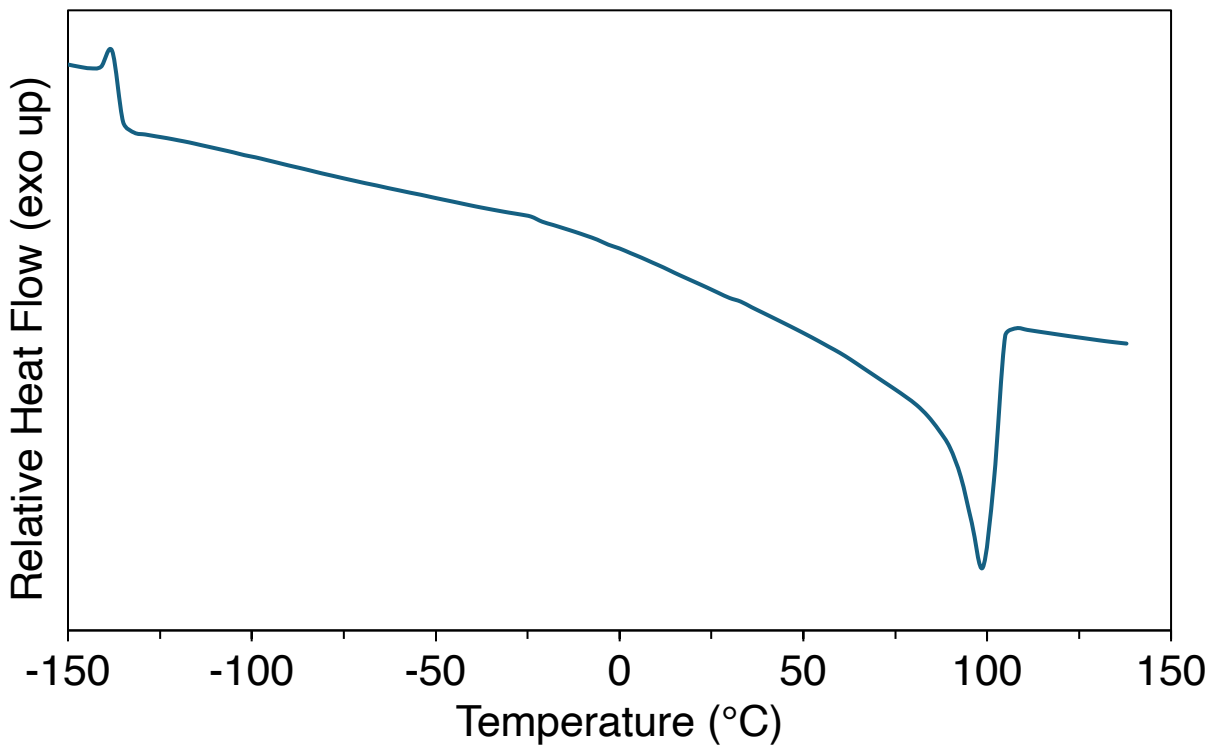


Figure 3.10.16.14. Differential scanning calorimetry (DSC) curve of polymer **6a**. $T_g = -136.5\text{ }^\circ\text{C}$, $T_m = 98.8\text{ }^\circ\text{C}$.

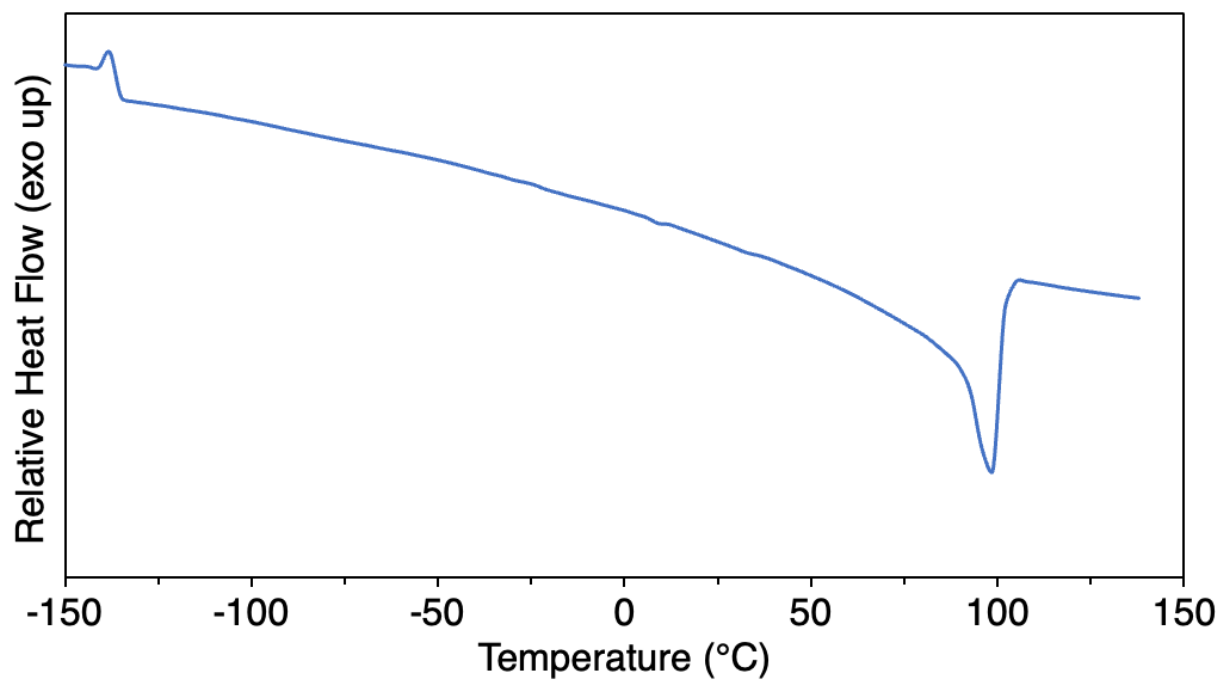


Figure 3.10.16.15. Differential scanning calorimetry (DSC) curve of polymer **6b**. $T_g = -136.5$ °C, $T_m = 98.8$ °C.

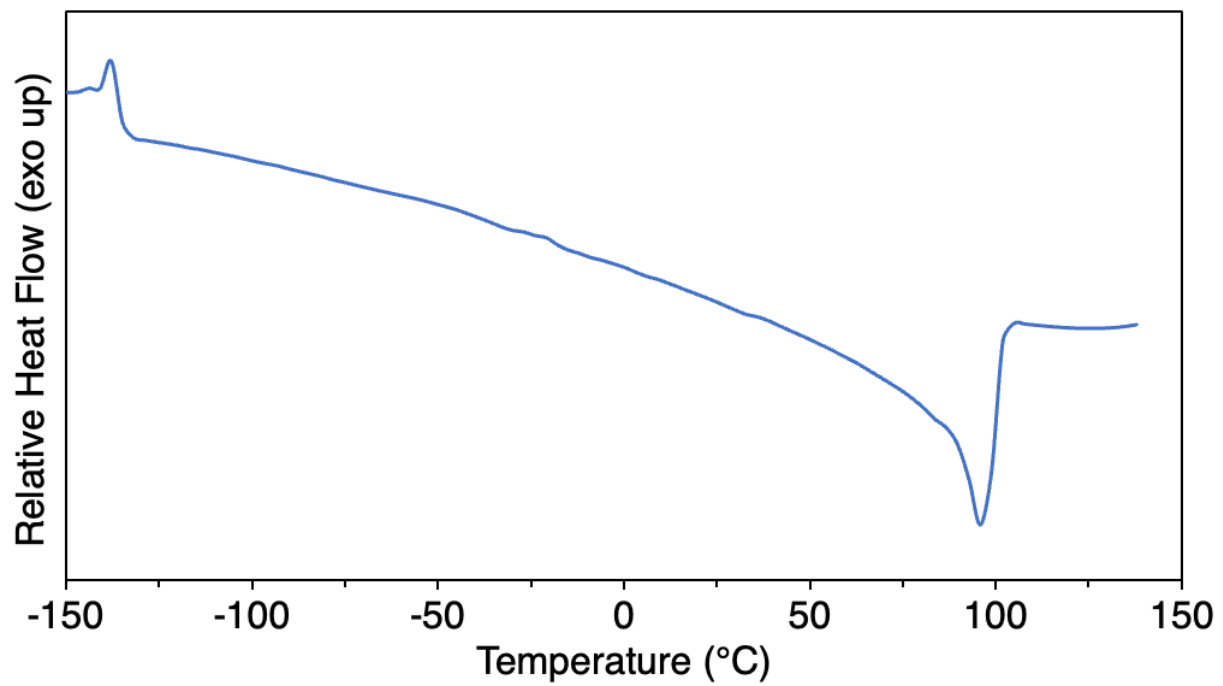


Figure 3.10.16.16. Differential scanning calorimetry (DSC) curve of polymer **6c**. $T_g = -136.5\text{ }^\circ\text{C}$, $T_m = 95.8\text{ }^\circ\text{C}$.

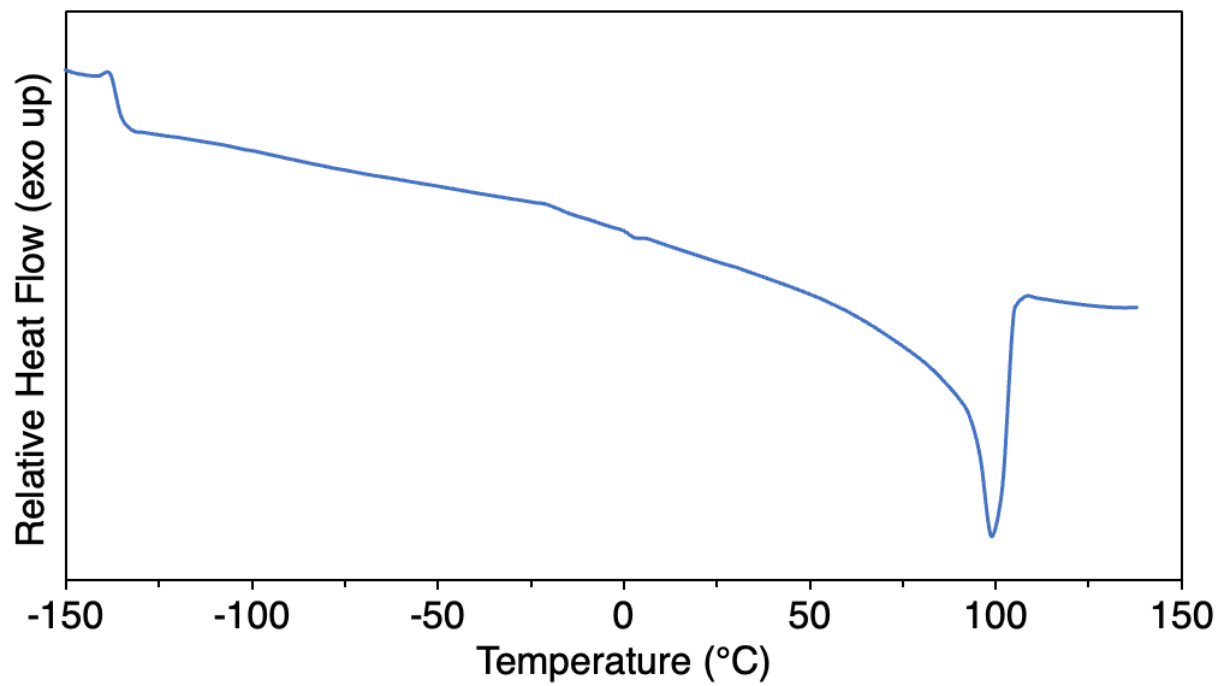


Figure 3.10.16.17. Differential scanning calorimetry (DSC) curve of polymer **6d**. $T_g = -136.5\text{ }^\circ\text{C}$, $T_m = 98.8\text{ }^\circ\text{C}$.

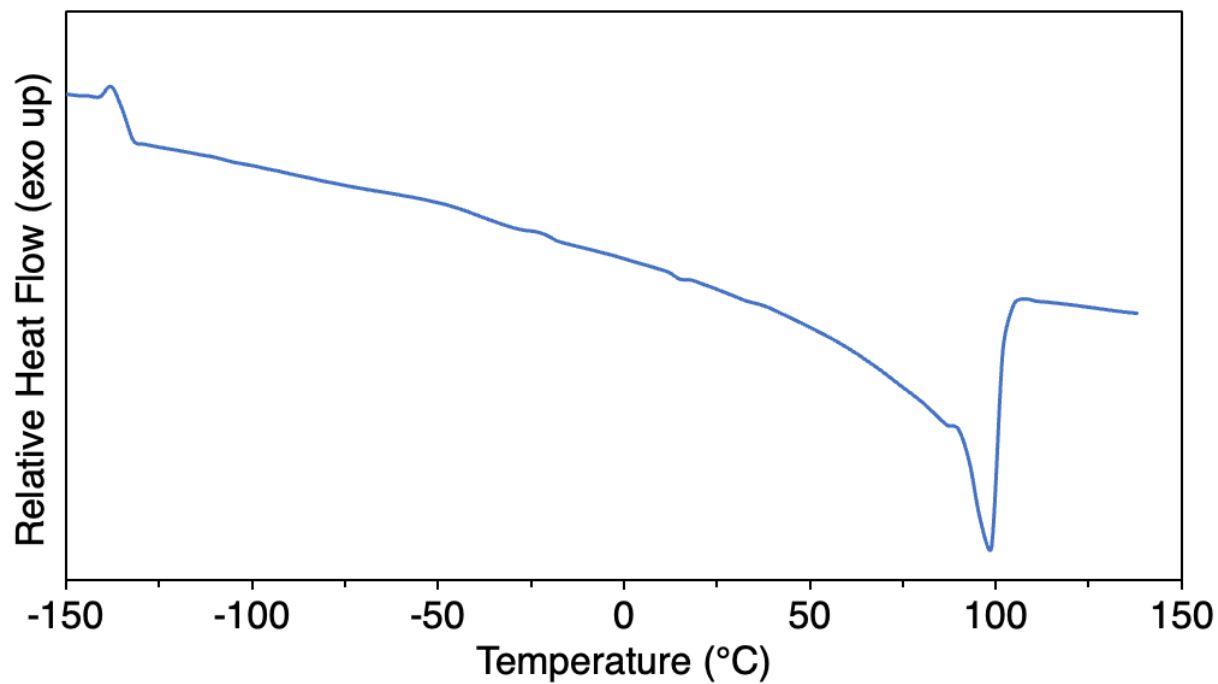


Figure 3.10.16.18. Differential scanning calorimetry (DSC) curve of polymer **6e**. $T_g = -136.5\text{ °C}$, $T_m = 98.8\text{ °C}$.

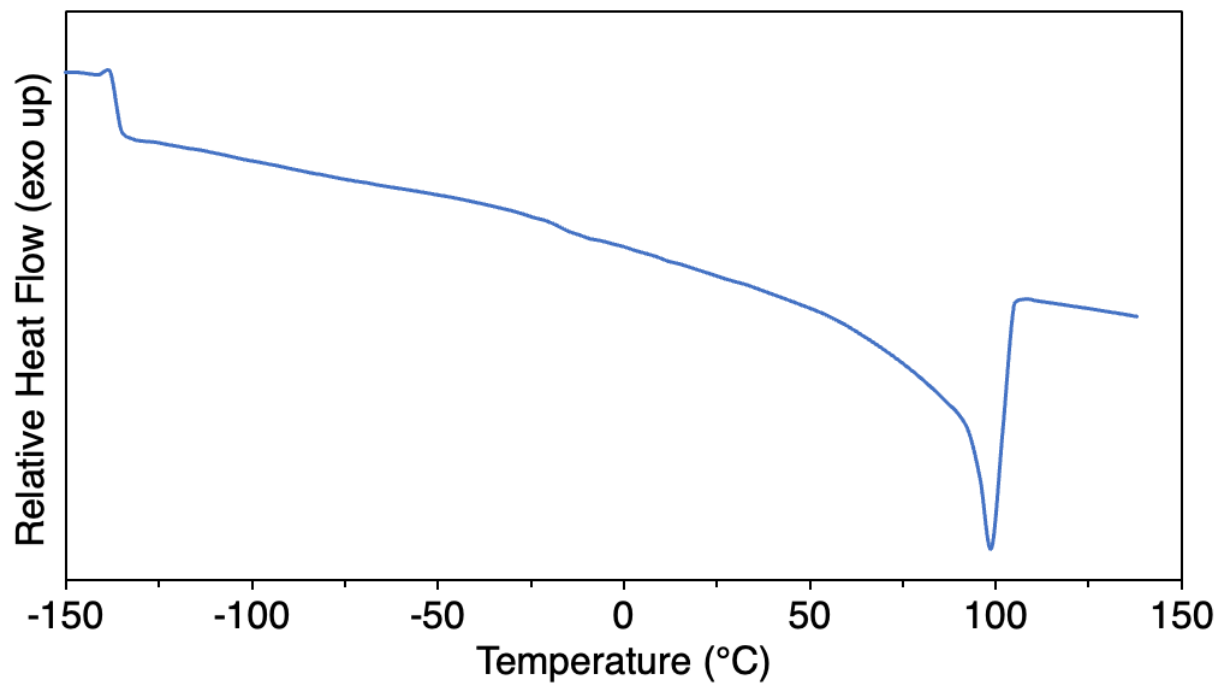


Figure 3.10.16.19. Differential scanning calorimetry (DSC) curve of polymer **6f**. $T_g = -136.5\text{ }^\circ\text{C}$, $T_m = 98.8\text{ }^\circ\text{C}$.

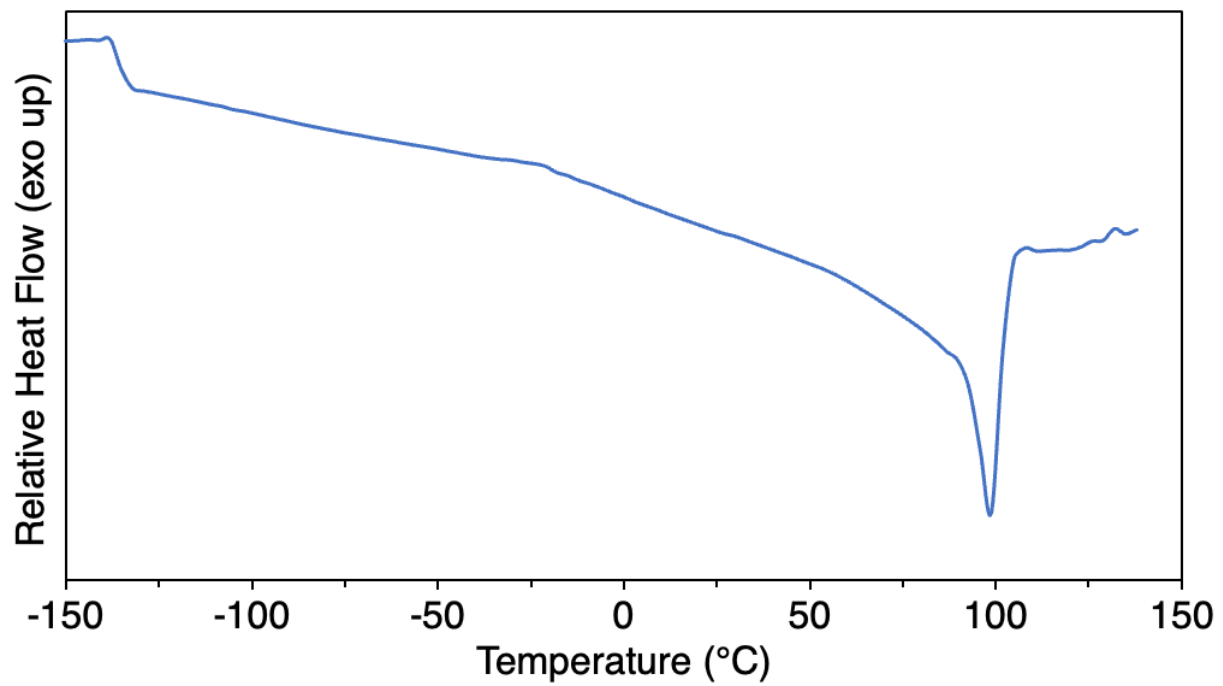


Figure 3.10.16.20. Differential scanning calorimetry (DSC) curve of polymer **6g**. $T_g = -136.5\text{ }^\circ\text{C}$, $T_m = 98.8\text{ }^\circ\text{C}$.

3.10.17 Material testing

3.10.17.1 Procedure for lap shear tests

Lap shear tests were conducted according to ASTM D1002-10 on an Instron universal materials tester equipped with a 5 kN load cell with a shear rate of 1.5 mm/min. Adhesion strength was determined by the maximum load divided by the bonded overlap area, which was measured with digital calipers prior to testing, and the apparent failure mode was assessed visually.

Substrate and Lap Joint Preparation

1. **Degreased Substrates:** To prepare the aluminum substrates for adhesive bonding, they were degreased. Substrates were wiped with a fresh Kimwipe soaked in acetone, followed by a second Kimwipe soaked in ethyl acetate. Substrates were air-dried, and a 1 cm x 1 cm area was isolated with vinyl electrical tape.
2. **Lap joint preparation:** Polymer films of LDPE and functionalized LDPEs (0.1 – 0.3 mm) were prepared on a hot press at 80 °C for 45 seconds to provide melts. Specifically, polymer samples between two Teflon films were pressed between steel plates at 1000 psi. Steel shims were used to control film thickness. The samples were cooled at room temperature, and a 1 cm x 1 cm piece of the polymer film was cut. The cut films were placed at the end of a clean Al 6061 adherend, and vinyl masking tape was removed. The substrates were overlapped in an antiparallel arrangement, clamped with two small binder clips, and subsequently transferred to a pre-heated oven. Samples were heated at 120 °C for 5 minutes. All samples were allowed to cool slowly to room temperature. Excess polyethylene adhesive was carefully removed from the edges with a razor. Shims were applied to lap joint ends to help align the grip of the mechanical tester. Multiple attempts to prepare lap joints with LDPE failed, as indicated by breaking of the lap joint during the clamping process. Thus, the adhesion strengths of LDPE were unmeasurable by this method. All measurable samples were loaded at 1.5 mm/min in shear until failure, whereas the dimensions of the bonded area were measured with calipers. Finally, the adhesive strength was determined by the peak load divided by the overlap area. Lap shear measurements were repeated for at least four specimens, and the values reported are averages of the measurements of these sets of specimens.

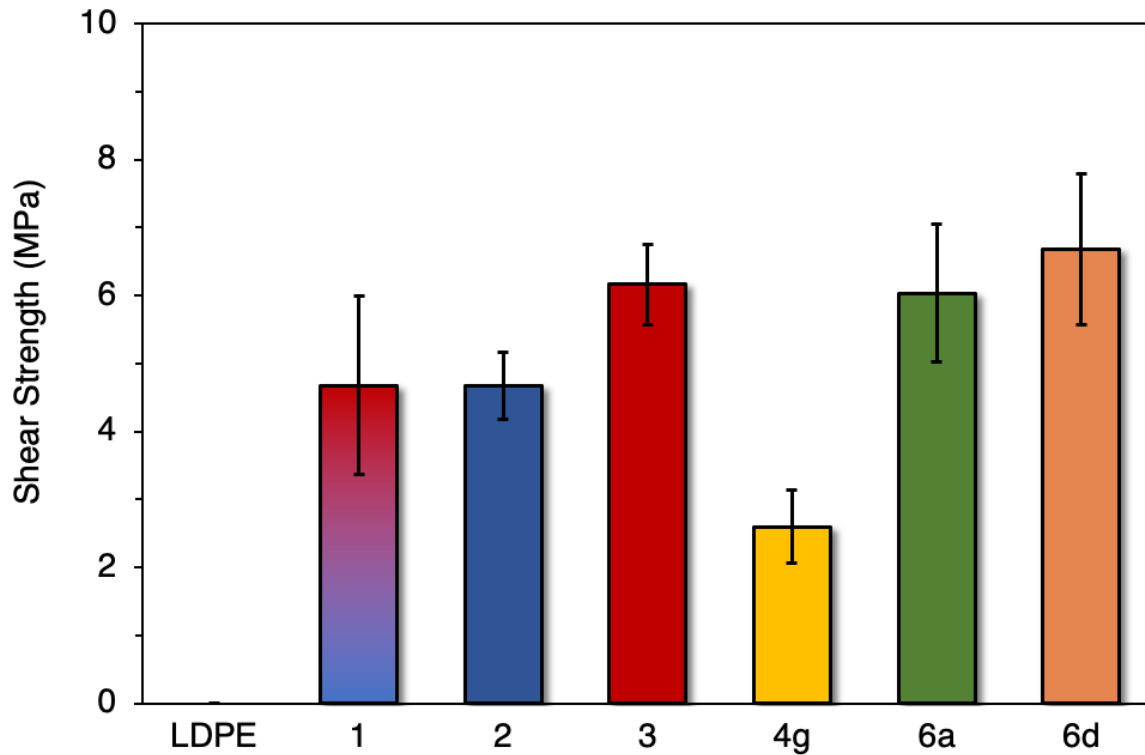


Figure 3.10.17.1.1. Lap shear strength of joints Al-LDPE-Al, Al-1-Al, Al-2-Al, Al-3-Al, Al-4g-Al, Al-6a-Al, Al-6d-Al. Error bars represent standard deviations.

Table 3.10.17.1.1. Summary of results of adhesion strength in lap shear tests

Entry	Interface	Shear Strength (MPa)	Mode of Failure
1 ^a	Al-LDPE-Al	--	--
2	Al-1-Al	4.7 ± 1.3	Cohesive
3	Al-2-Al	4.7 ± 0.5	Cohesive
4	Al-3-Al	6.2 ± 0.6	Adhesive
5	Al-4g-Al	2.6 ± 0.5	Adhesive
6	Al-6a-Al	6.0 ± 1.0	Cohesive
7	Al-6d-Al	6.7 ± 1.1	Cohesive

^aShear strength not measurable because of lap joint failure during the clamping process.

3.10.17.2 Procedure for tensile tests

1. **Sample preparation:** Polymer films of LDPE and functionalized LDPEs ($350 \pm 50\mu\text{m}$ thickness) were prepared on a hot press at $80\text{ }^\circ\text{C}$ for 45 seconds to provide melts. Specifically, polymer samples between two Teflon films were pressed between steel plates at 2000 psi. Steel shims were used to control film thickness. The samples were then cooled at room temperature and cut into a dog-bone geometry using a cutting die (ASTM D-638-V) to obtain samples that were 9.53 mm in length and 3.18 mm in width.
2. **Experimental procedures for tensile tests:** Tensile testing was conducted according to ASTM D638 on an Instron universal materials tester. Tensile stress and strain were measured at room temperature using an extension rate of 50 mm/min. Measurements were repeated for at least three samples, and average values are reported.

Table 3.10.17.2.1. Summary of results of tensile tests

Polymer	tensile stress at max load (MPa)	Young's Modulus (MPa)	tensile strain (extension) at break (%)	toughness (MJ/m ³)	yield stress (MPa)
LDPE	11.4 ± 1.1	148.5 ± 16.8	227.8 ± 96.8	19.5 ± 9.8	11.4 ± 1.1
3	8.5 ± 1.6	122.3 ± 14.9	234.0 ± 44.7	18.0 ± 3.8	8.5 ± 1.6
4a	10.3 ± 1.2	39.1 ± 5.3	1006.2 ± 89.6	86.4 ± 9.2	5.4 ± 0.4
4d	15.0 ± 2.2	39.9 ± 6.3	991.2 ± 167.2	106.3 ± 27.6	7.1 ± 0.6
4f	26.0 ± 3.5	32.1 ± 4.8	651.3 ± 71.6	115.6 ± 22.2	9.0 ± 1.7
4g	33.6 ± 1.9	133.8 ± 14.6	360.8 ± 124.1	87.5 ± 33.7	16.9 ± 2.3

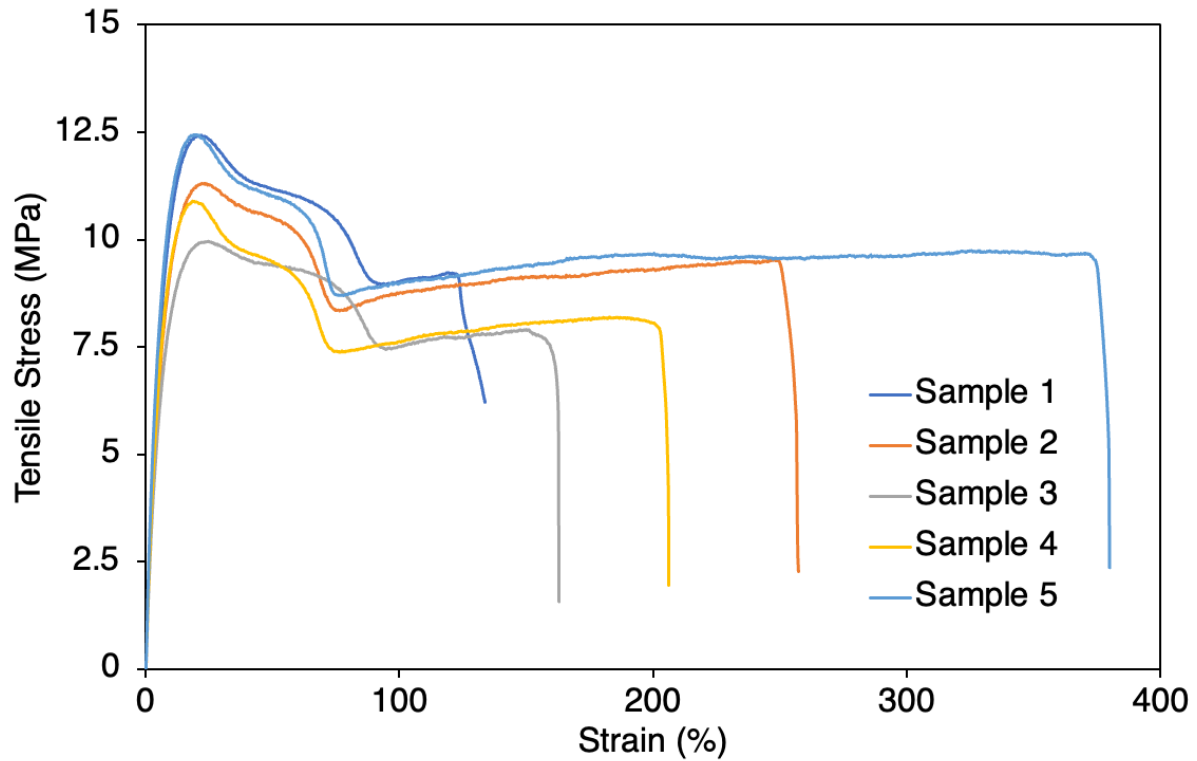


Figure 3.10.17.2.1. Tensile test curves for unmodified LDPE

Table 3.10.17.2.2. Summary of results of tensile tests for unmodified LDPE

Sample	tensile stress at max load (MPa)	Young's Modulus (MPa)	tensile strain (extension) at break (%)	toughness (MJ/m ³)	yield stress (MPa)
1	12.4	160.4	133.7	13.4	12.4
2	11.3	142.4	256.7	13.5	11.3
3	10.0	125.8	162.8	17.1	10.0
4	10.9	144.9	206.1	36.7	10.9
5	12.5	169.0	379.8	16.9	12.5

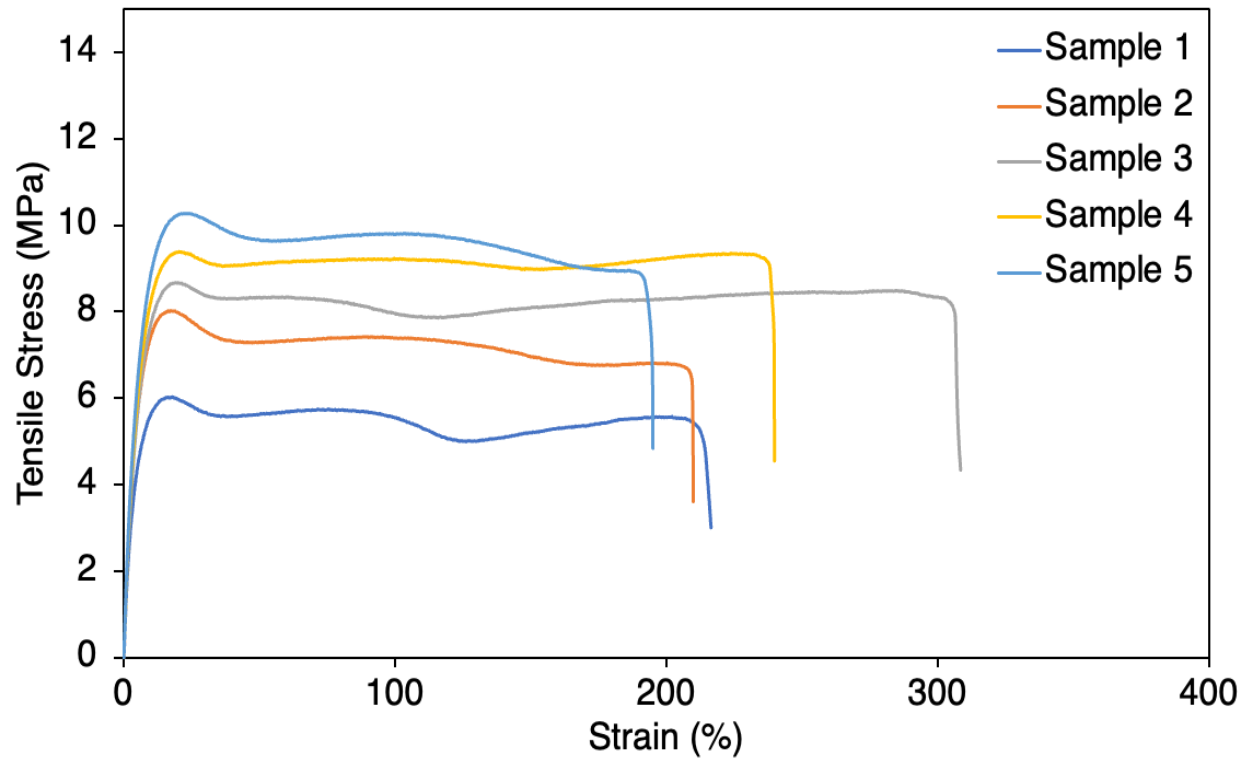


Figure 3.10.17.2.2. Tensile test curves for polymer 3

Table 3.10.17.2.3. Summary of results of tensile tests for polymer 3

Sample	tensile stress at max load (MPa)	Young's Modulus (MPa)	tensile strain (extension) at break (%)	toughness (MJ/m ³)	yield stress (MPa)
1	6.0	98.0	216.6	11.7	6.0
2	8.0	124.0	210.0	18.7	8.0
3	8.7	122.0	308.5	18.0	8.7
4	9.4	130.0	239.9	20.4	9.4
5	10.3	137.5	195.1	21.3	10.3

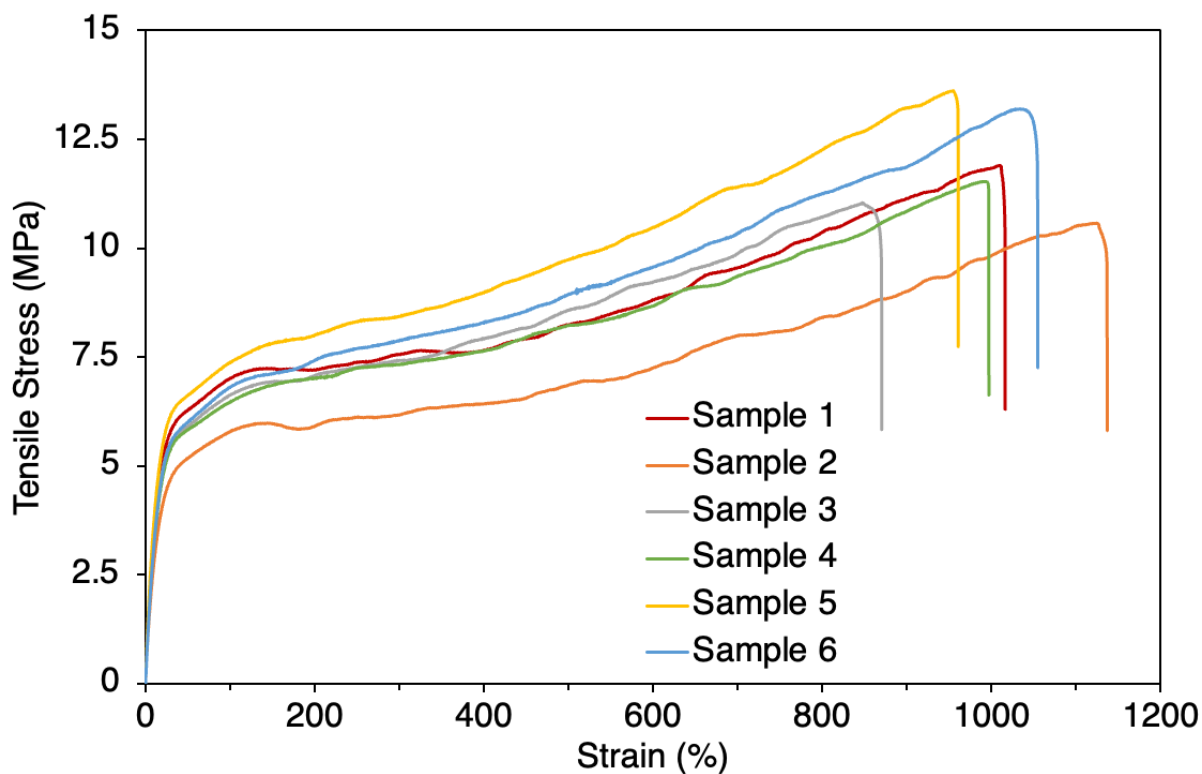


Figure 3.10.17.2.3. Tensile test curves for polymer 4a

Table 3.10.17.2.4. Summary of results of tensile tests for polymer 4a

Sample	tensile stress at max load (MPa)	Young's Modulus (MPa)	tensile strain (extension) at break (%)	toughness (MJ/m ³)	yield stress (MPa)
1	11.9	48.2	1016.4	87.7	5.5
2	10.6	36.4	1137.1	84.6	5.0
3	11.0	38.7	870.4	71.8	5.2
4	8.5	35.4	997.2	82.3	5.3
5	10.3	42.1	960.9	93.8	6.2
6	9.3	34.1	1054.9	98.1	5.0

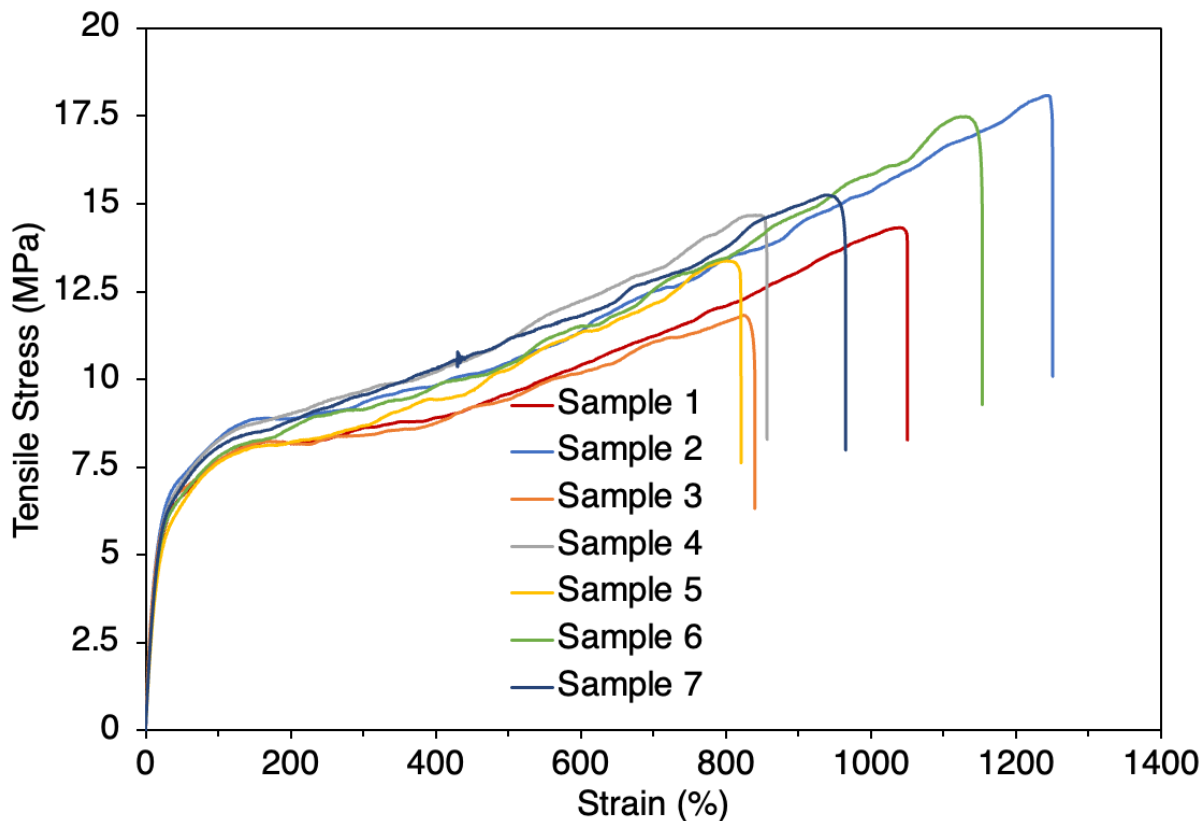


Figure 3.10.17.2.4. Tensile test curves for polymer 4d

Table 3.10.17.2.5. Summary of results of tensile tests for polymer 4d

Sample	tensile stress at max load (MPa)	Young's Modulus (MPa)	tensile strain (extension) at break (%)	toughness (MJ/m ³)	yield stress (MPa)
1	14.3	45.1	1050.5	106.3	6.6
2	18.1	40.4	1250.6	150.8	6.6
3	11.8	51.4	840.1	76.7	6.8
4	14.7	36.8	856.9	91.5	7.8
5	13.4	34.0	821.0	79.3	16.5
6	17.5	34.9	1153.7	133.8	7.7
7	15.3	36.5	965.4	105.9	7.8

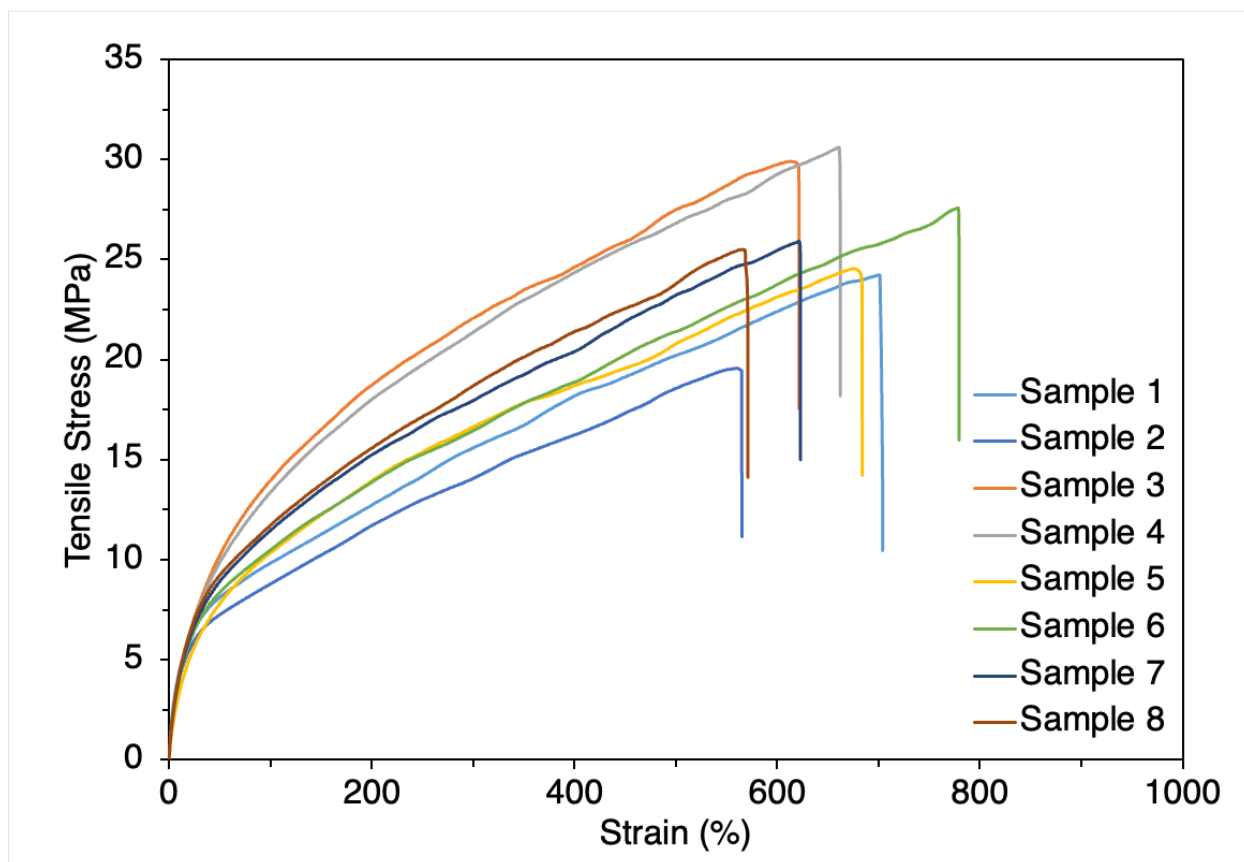


Figure 3.10.17.2.5. Tensile test curves for polymer 4f

Table 3.10.17.2.6. Summary of results of tensile tests for polymer 4f

Sample	tensile stress at max load (MPa)	Young's Modulus (MPa)	tensile strain (extension) at break (%)	toughness (MJ/m ³)	yield stress (MPa)
1	24.2	36.8	704.0	114.4	8.0
2	19.6	39.1	565.1	75.0	7.9
3	29.9	30.2	621.6	130.8	11.6
4	30.6	29.2	662.2	140.0	11.2
5	24.6	24.1	683.8	114.1	8.9
6	27.6	29.4	779.4	141.6	7.3
7	25.9	32.7	622.9	109.6	9.6
8	25.5	35.1	571.1	99.6	7.5

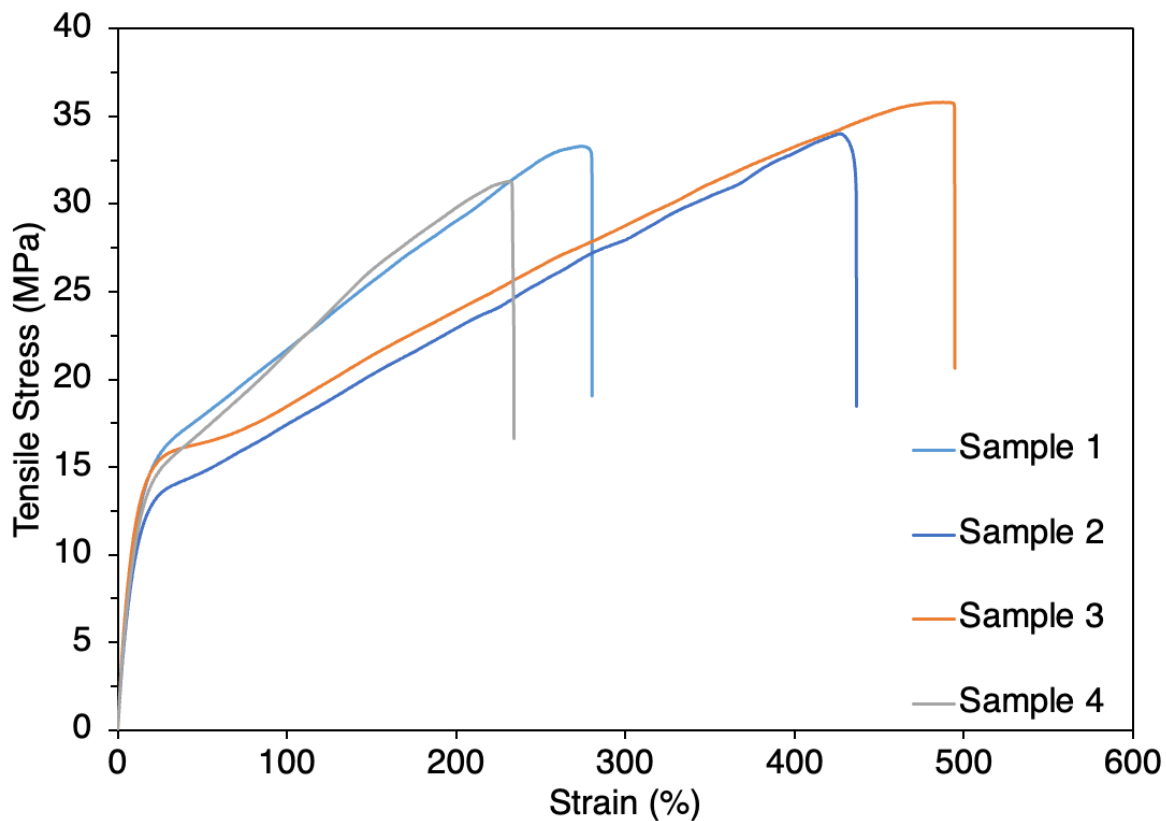


Figure 3.10.17.2.7. Tensile test curves for polymer 4g

Table 3.10.17.2.7. Summary of results of tensile tests for polymer 4g

Sample	tensile stress at max load (MPa)	Young's Modulus (MPa)	tensile strain (extension) at break (%)	toughness (MJ/m ³)	yield stress (MPa)
1	33.3	142.4	280.4	67.8	18.6
2	34.0	116.0	436.7	102.4	13.8
3	35.8	148.5	494.8	127.2	16.4
4	31.3	128.3	234.2	52.62	18.7

3.10.17.3 Procedure for contact angle measurements

Polymer films from LDPE and functionalized LDPEs were prepared by hot pressing. Static water contact angles were with deionized water (Milli-Q, 10 μ L) in three repetitive tests using the Sessile Drop Technique, and the average of these values of contact angles was calculated. The decrease in the contact angle after oxidation can be attributed to the pendant polar functional groups on the surface of polymer films that render the sample more hydrophilic.

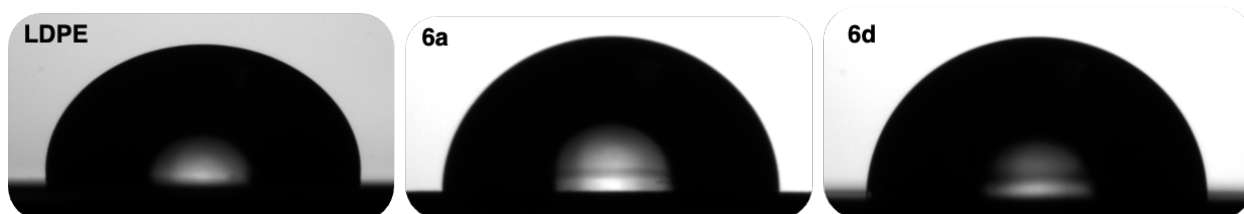


Figure 3.10.17.3.1. Selected pictures of water droplets on films made from LDPE and functionalized LDPEs

Table 3.10.17.3.1. Summary of results of contact angle measurements

Polymer	Contact Angle
LDPE	97.0 ± 2.1
6a	84.2 ± 4.3
6d	86.1 ± 3.7

3.10.18 Thermogravimetric Analysis (TGA)

Each sample (ca. 5 mg) was heated from 40 °C to 600 °C under N₂ at a scan rate of 20 °C/min. Decomposition onset temperatures (T_d) were measured at 5 % mass loss (Table S13)

Table 3.10.18.1. Summary of decomposition temperature (T_d) for the polymers

Polymer	T_d (°C)
LDPE	360.8
1	419.3
2	405.1
3	414.1
4a	322.6
4b	250.9
4c	253.0
4d	333.8
4e	328.1
4f	331.0
4g	380.7
5	288.0
6a	300.8
6b	372.3
6c	395.0
6d	236.5
6e	267.8
6f	296.7
6g	281.0

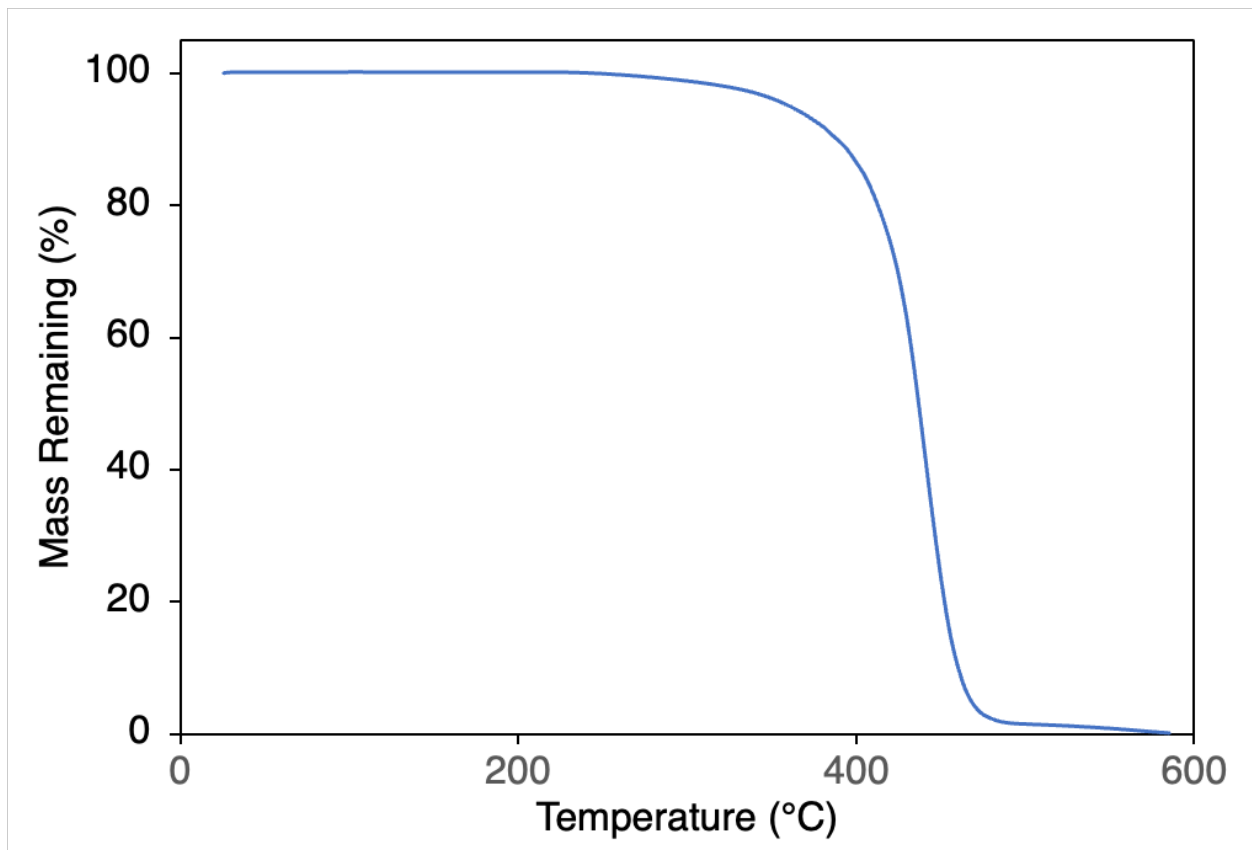


Figure 3.10.18.1. TGA plot of unmodified LDPE, $T_d = 360.8$ °C

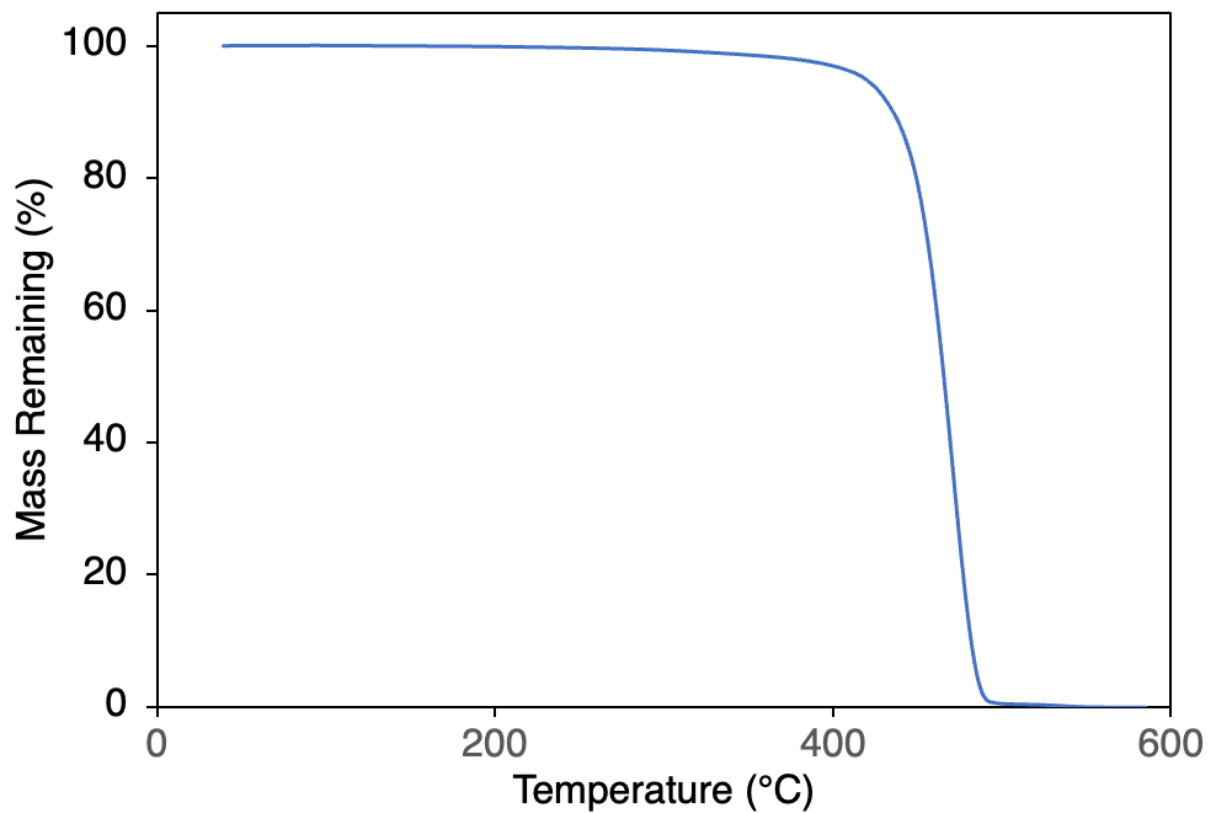


Figure 3.10.18.2. TGA plot of polymer **1**, $T_d = 419.3$ °C

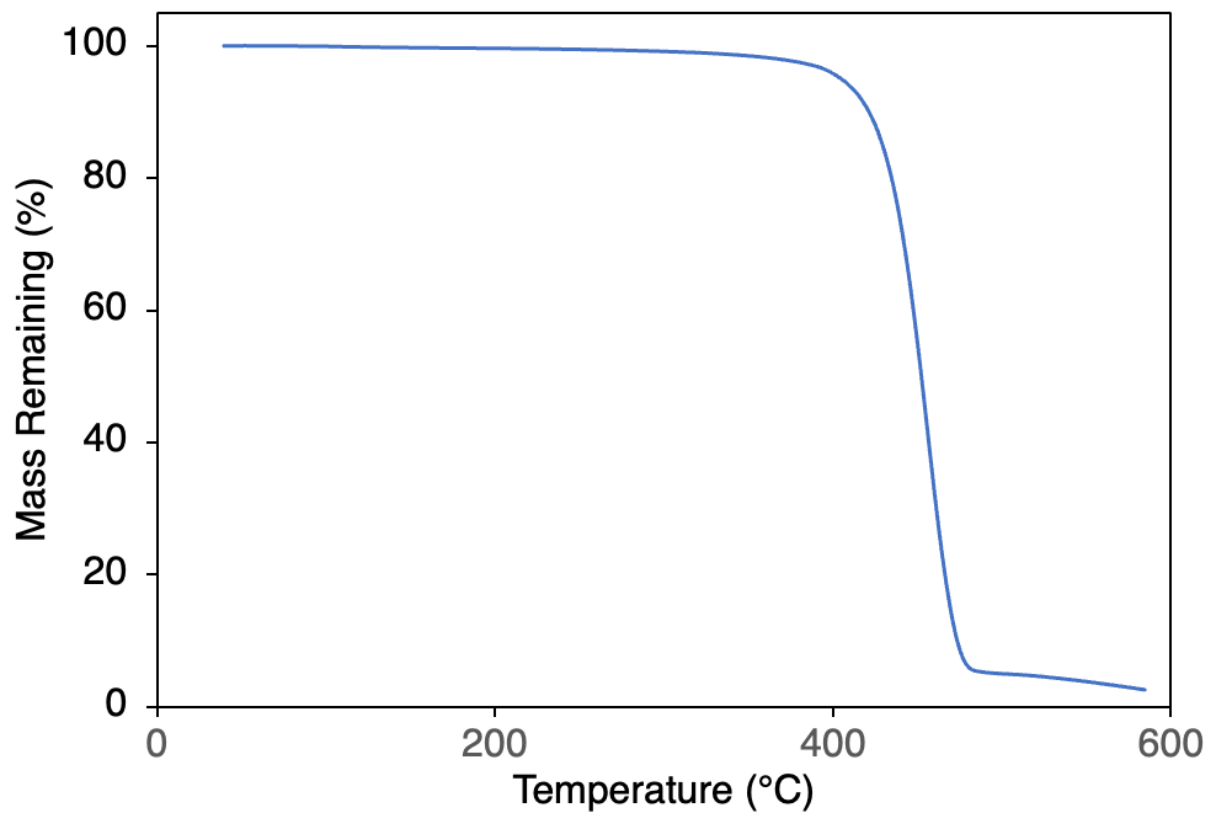


Figure 3.10.18.3. TGA plot of polymer 2, $T_d = 405.1\text{ }^\circ\text{C}$

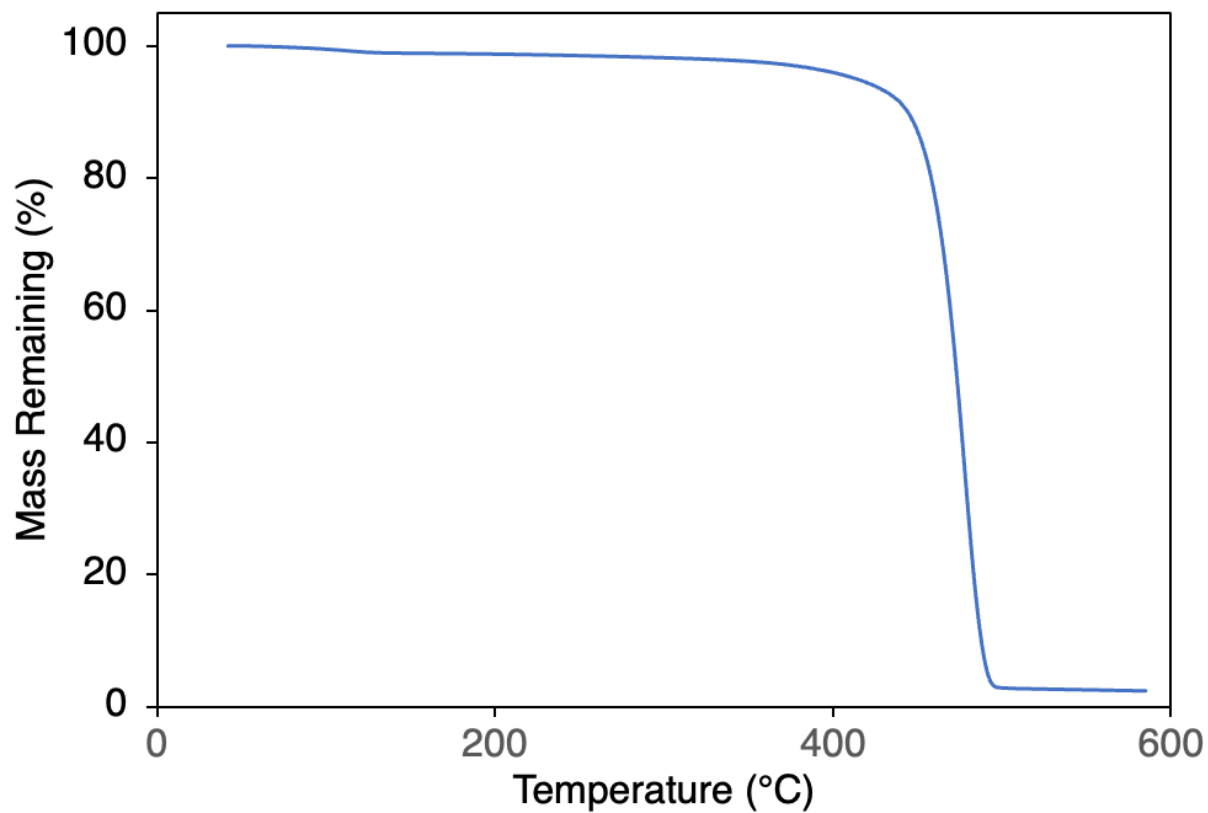


Figure 3.10.18.4. TGA plot of polymer **3**, $T_d = 414.1$ °C

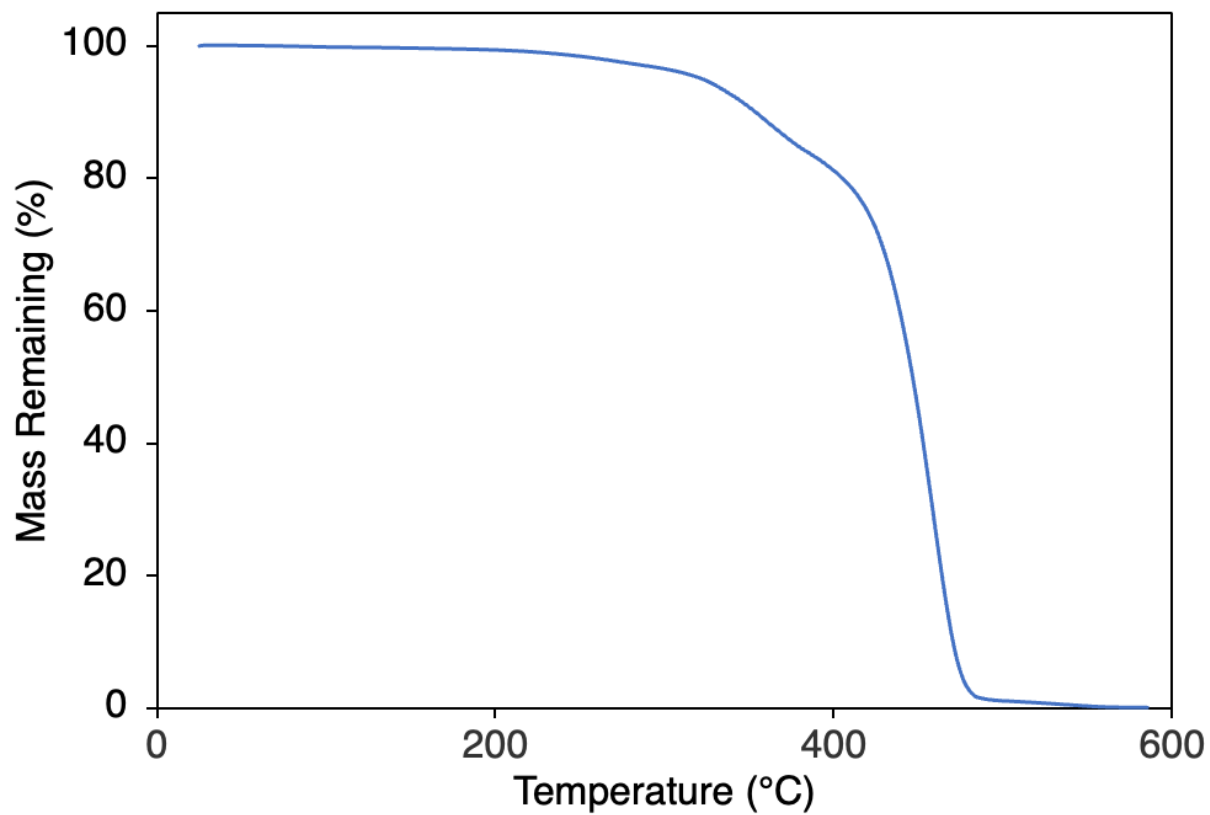


Figure 3.10.18.5. TGA plot of polymer **4a**, $T_d = 322.6$ °C

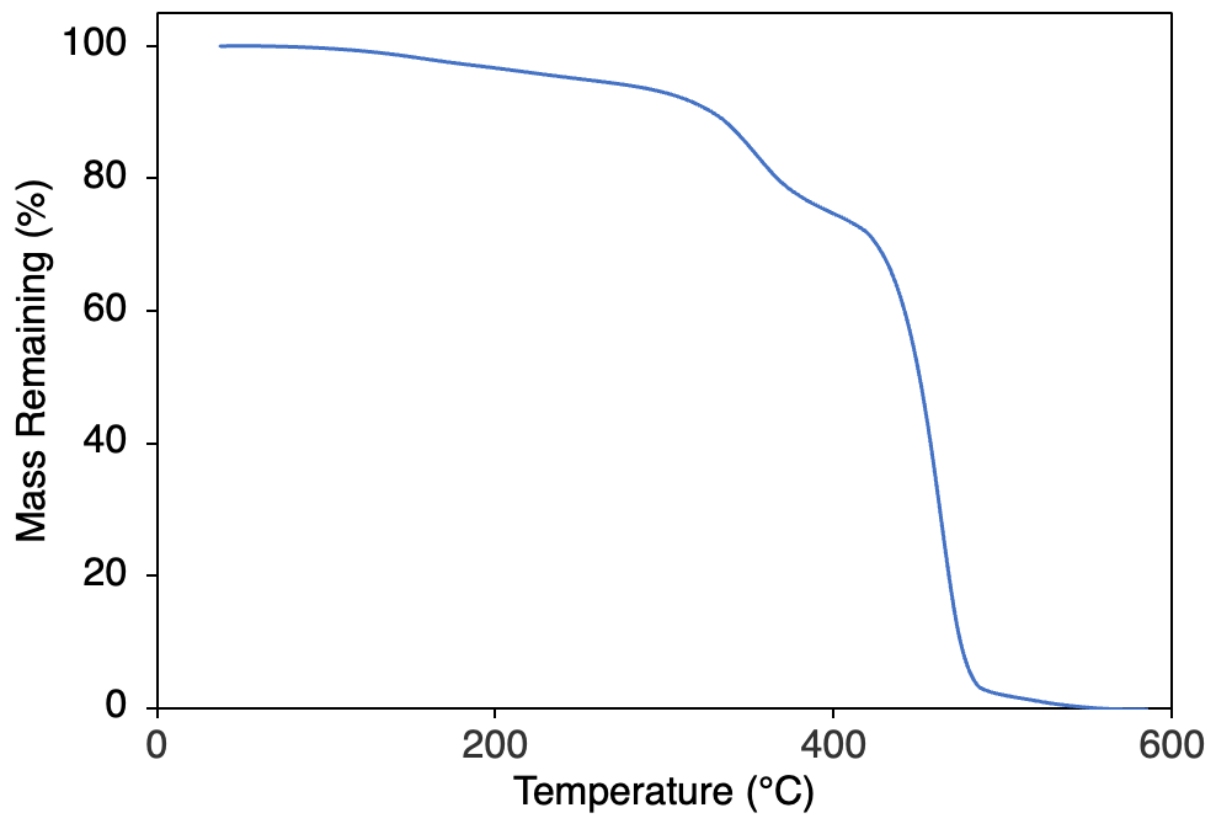


Figure 3.10.18.6. TGA plot of polymer **4b**, $T_d = 250.9$ °C

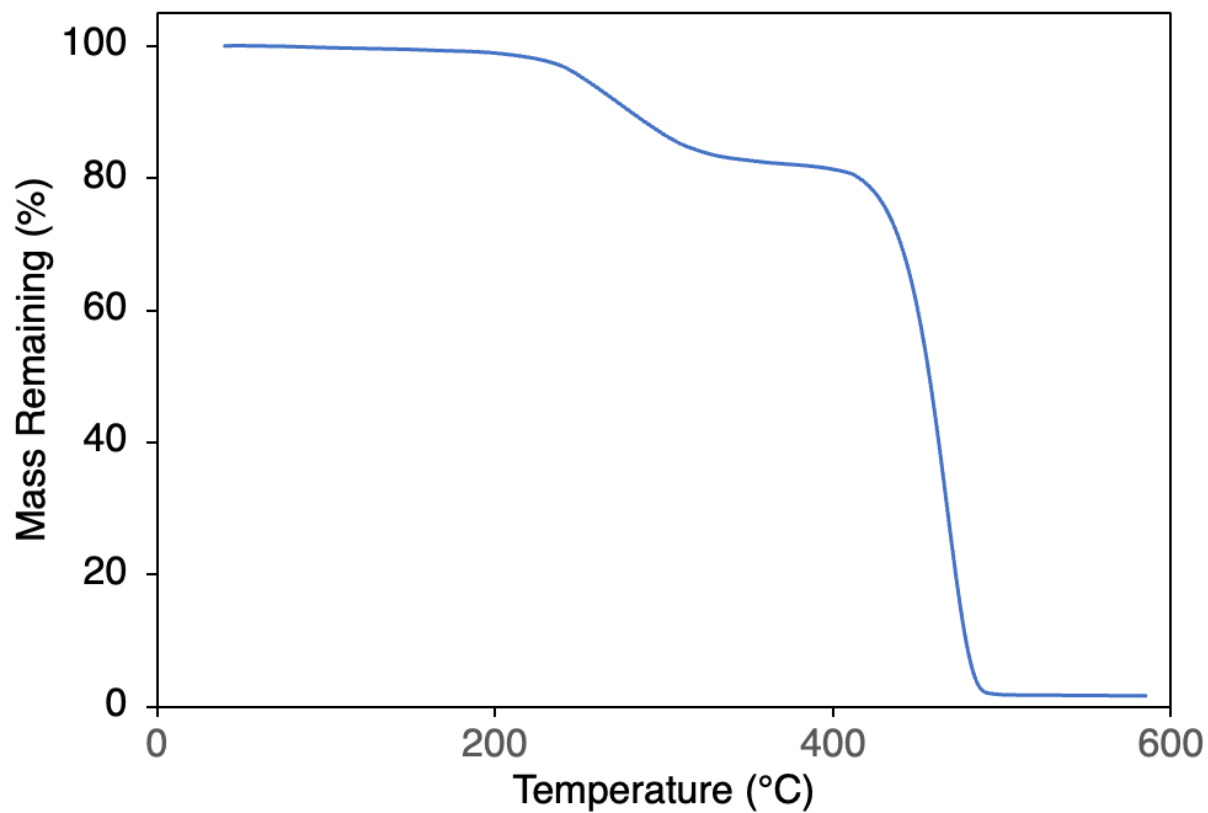


Figure 3.10.18.7. TGA plot of polymer **4c**, $T_d = 253.0$ °C

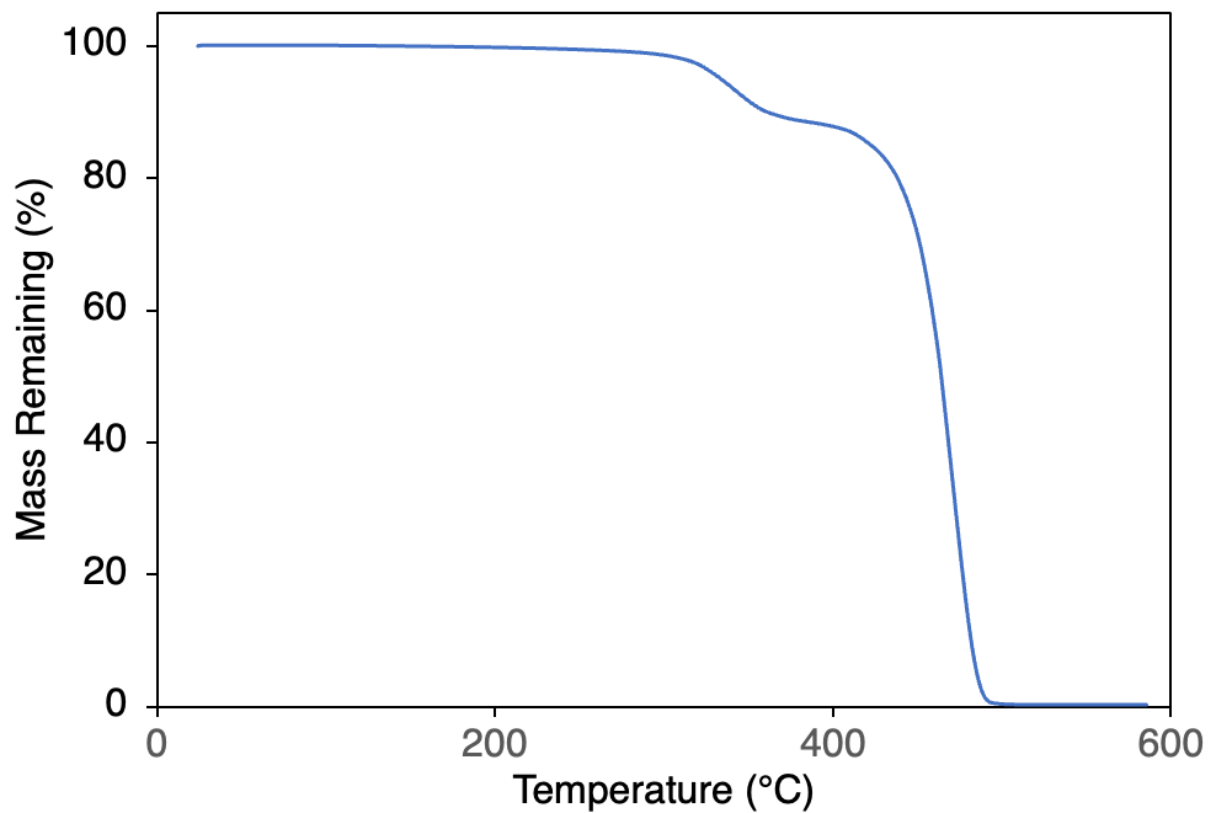


Figure 3.10.18.8. TGA plot of polymer **4d**, $T_d = 333.8$ °C

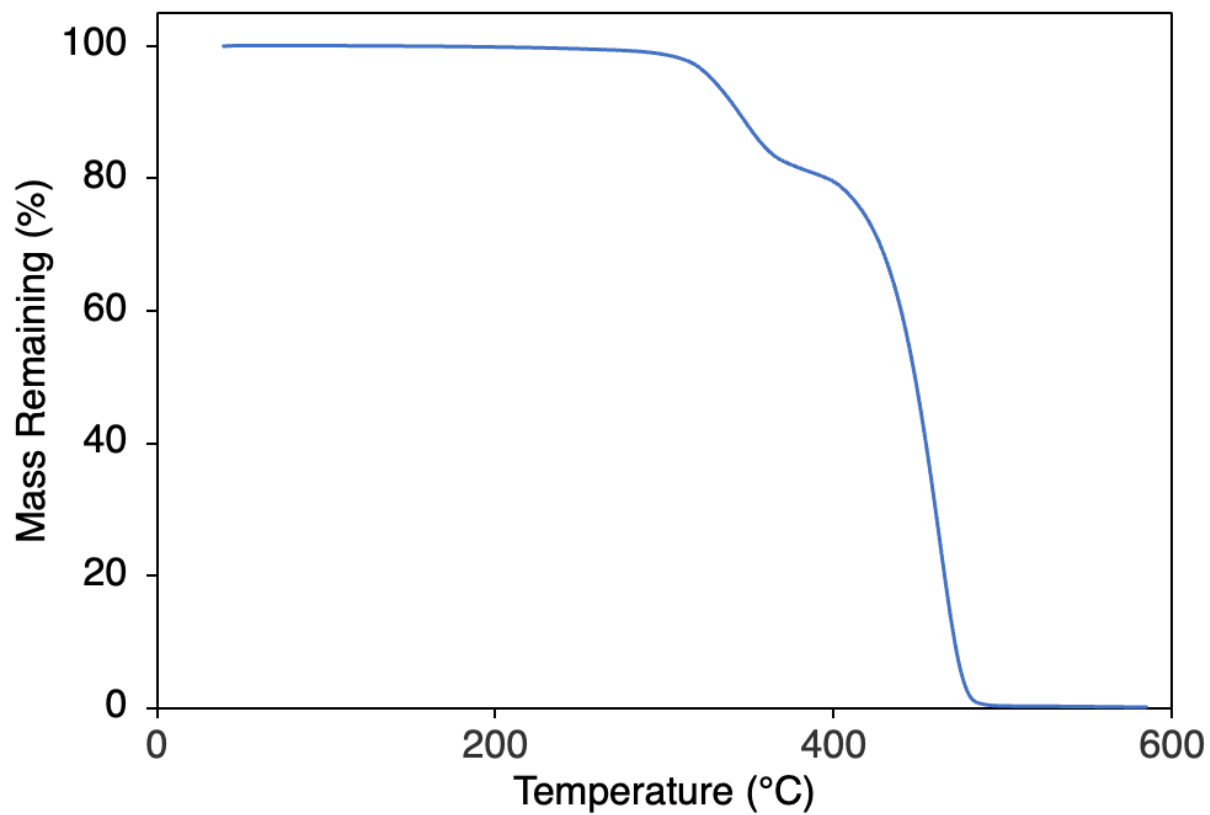


Figure 3.10.18.9. TGA plot of polymer **4e**, $T_d = 328.1$ °C

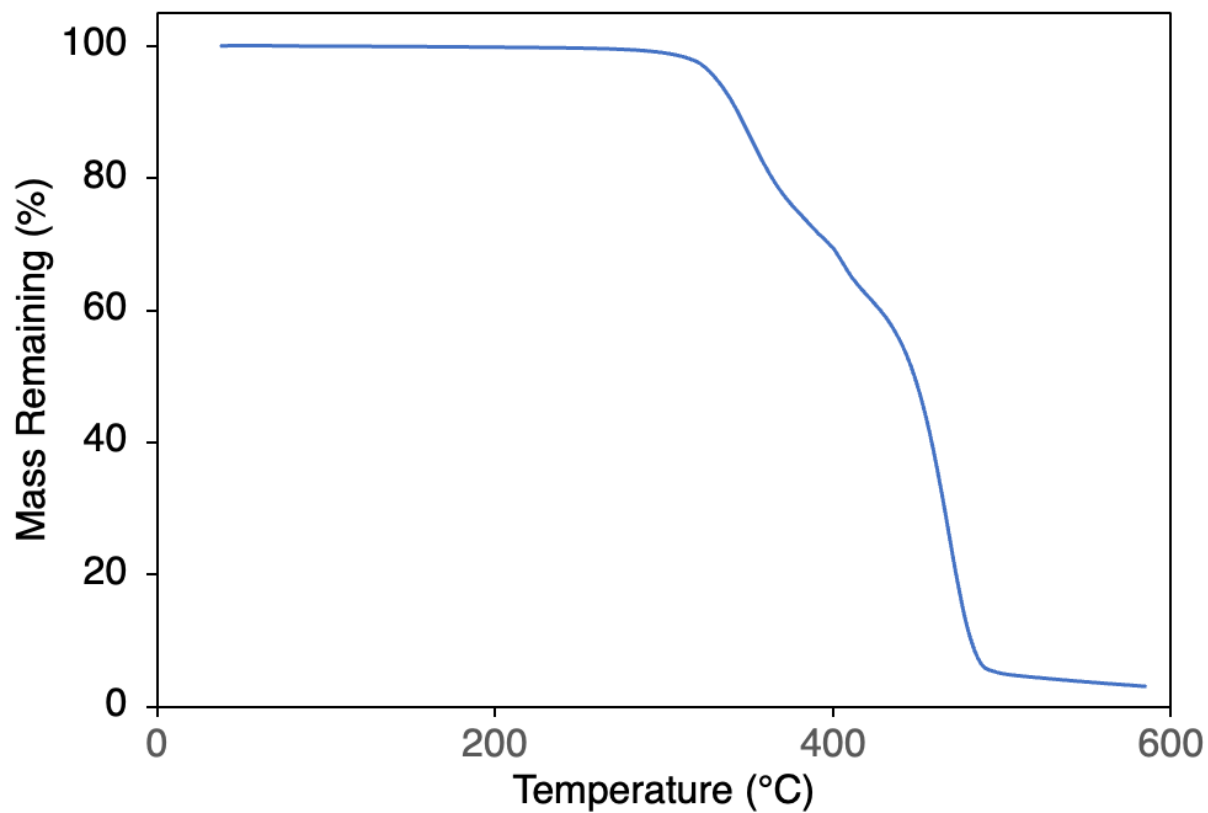


Figure 3.10.18.10. TGA plot of polymer **4f**, $T_d = 331.0$ °C

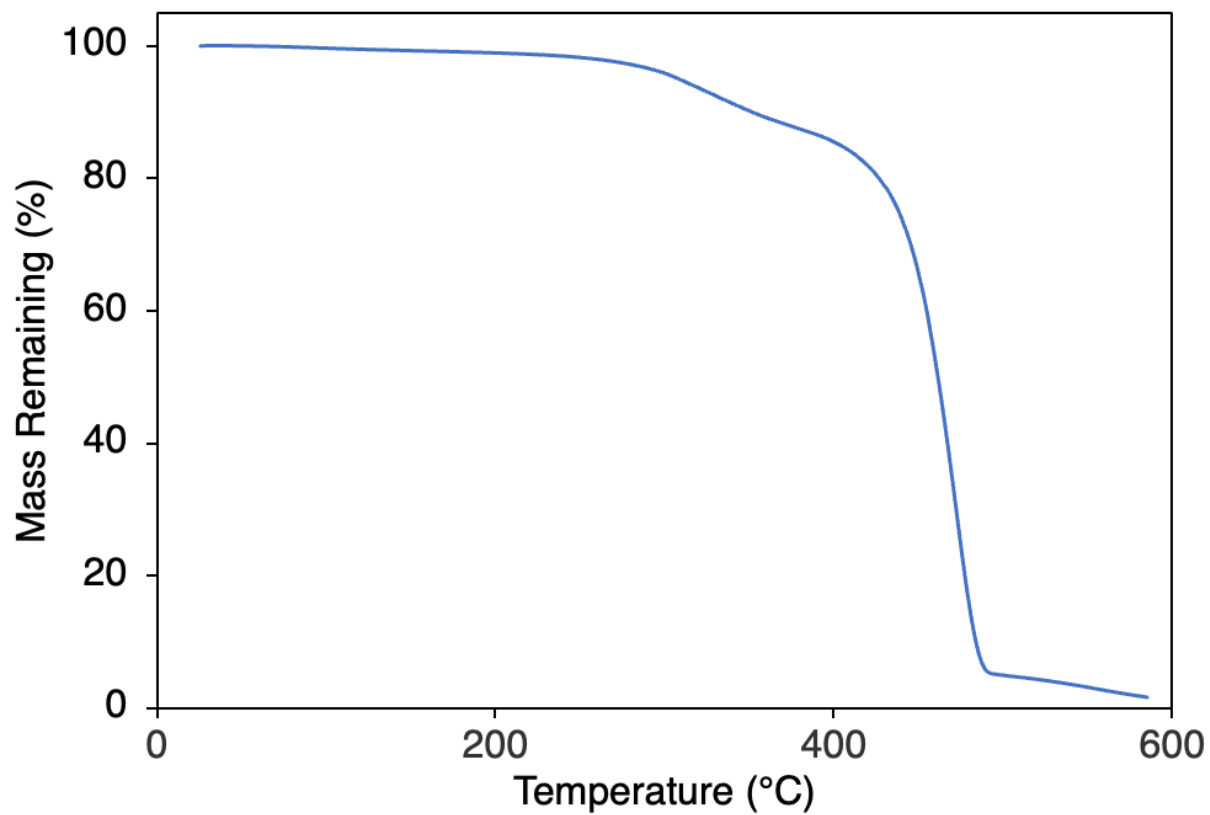


Figure 3.10.18.11. TGA plot of polymer **4g**, $T_d = 308.7$ °C

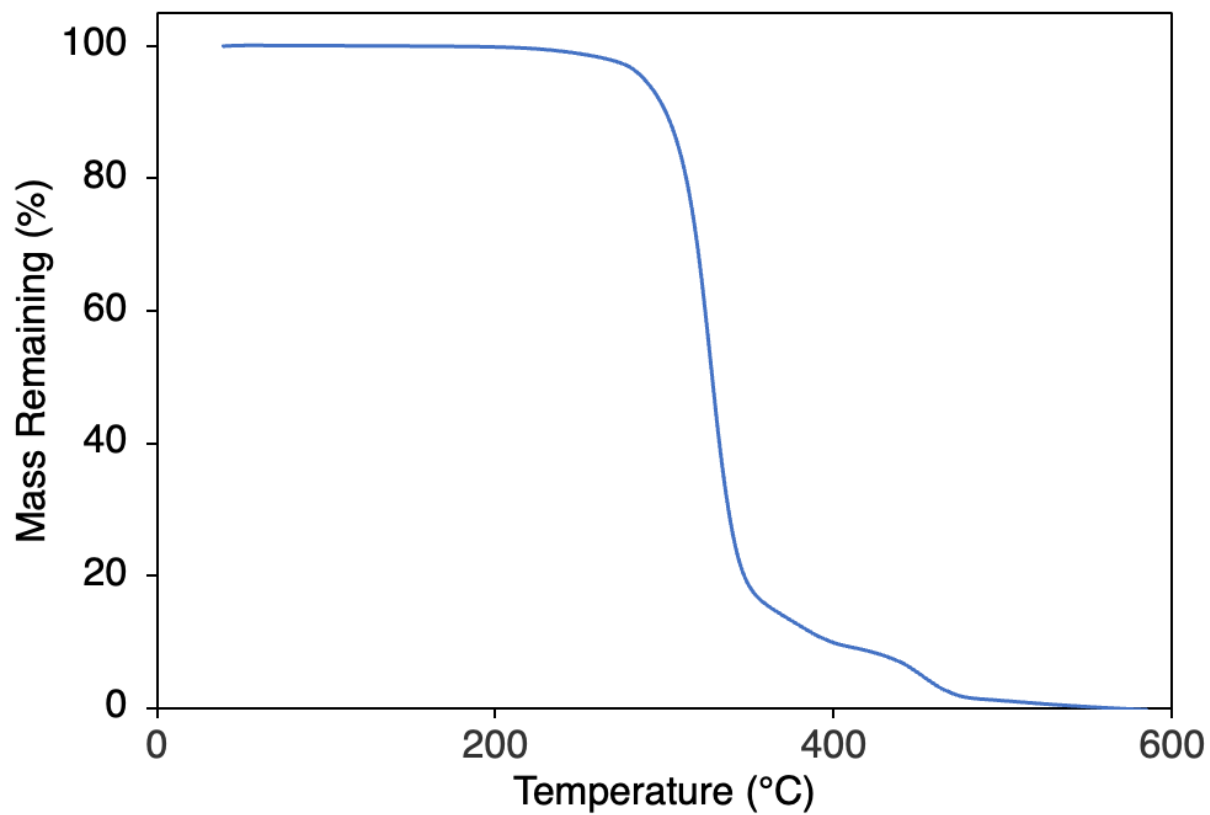


Figure 3.10.18.12. TGA plot of polymer **5**, $T_d = 288.0$ °C

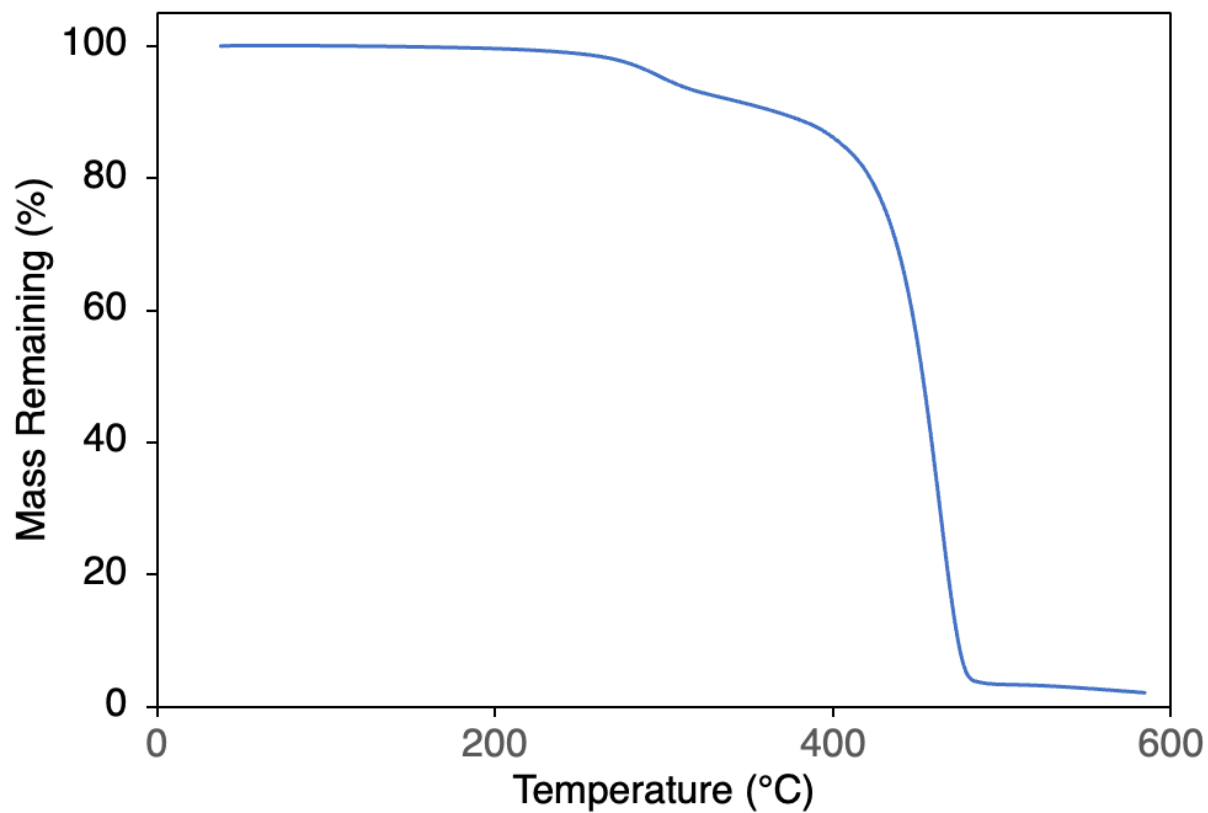


Figure 3.10.18.13. TGA plot of polymer 6a, $T_d = 300.8$ °C

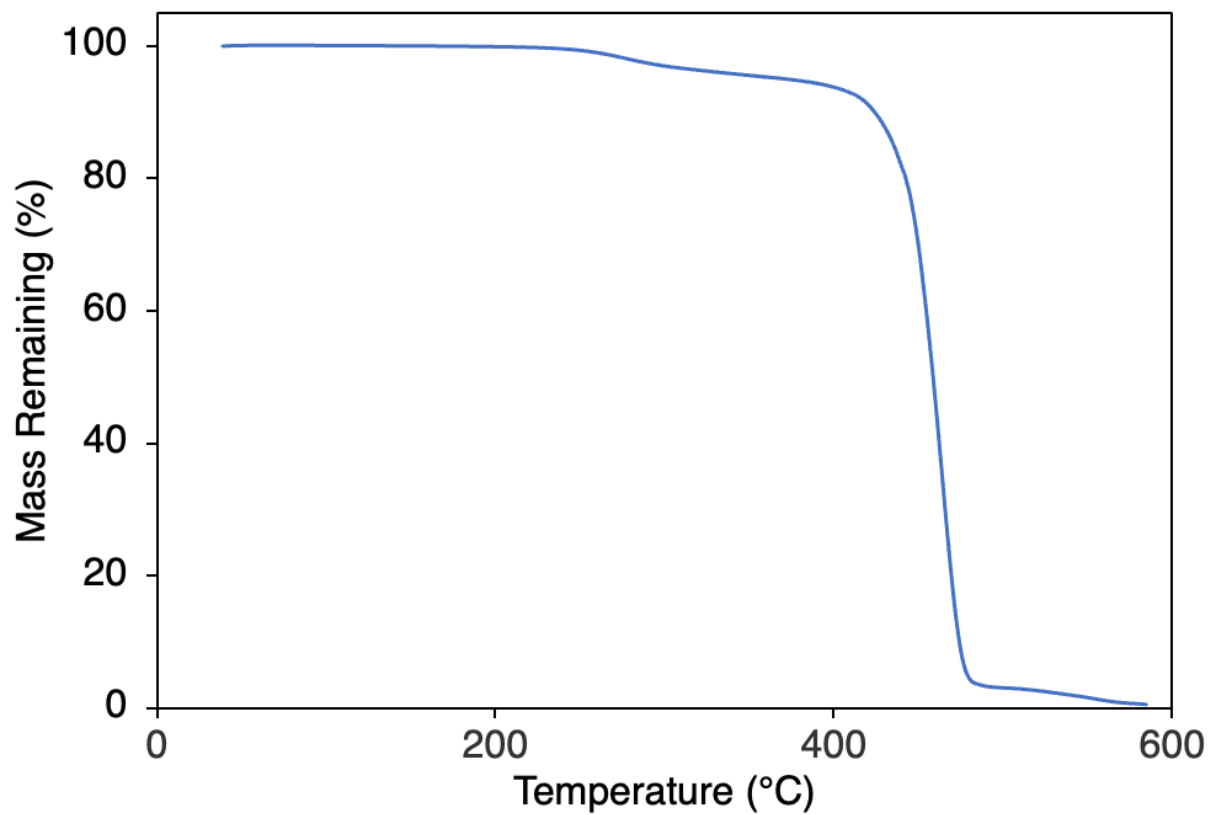


Figure 3.10.18.14. TGA plot of polymer **6b**, $T_d = 372.3\text{ }^\circ\text{C}$

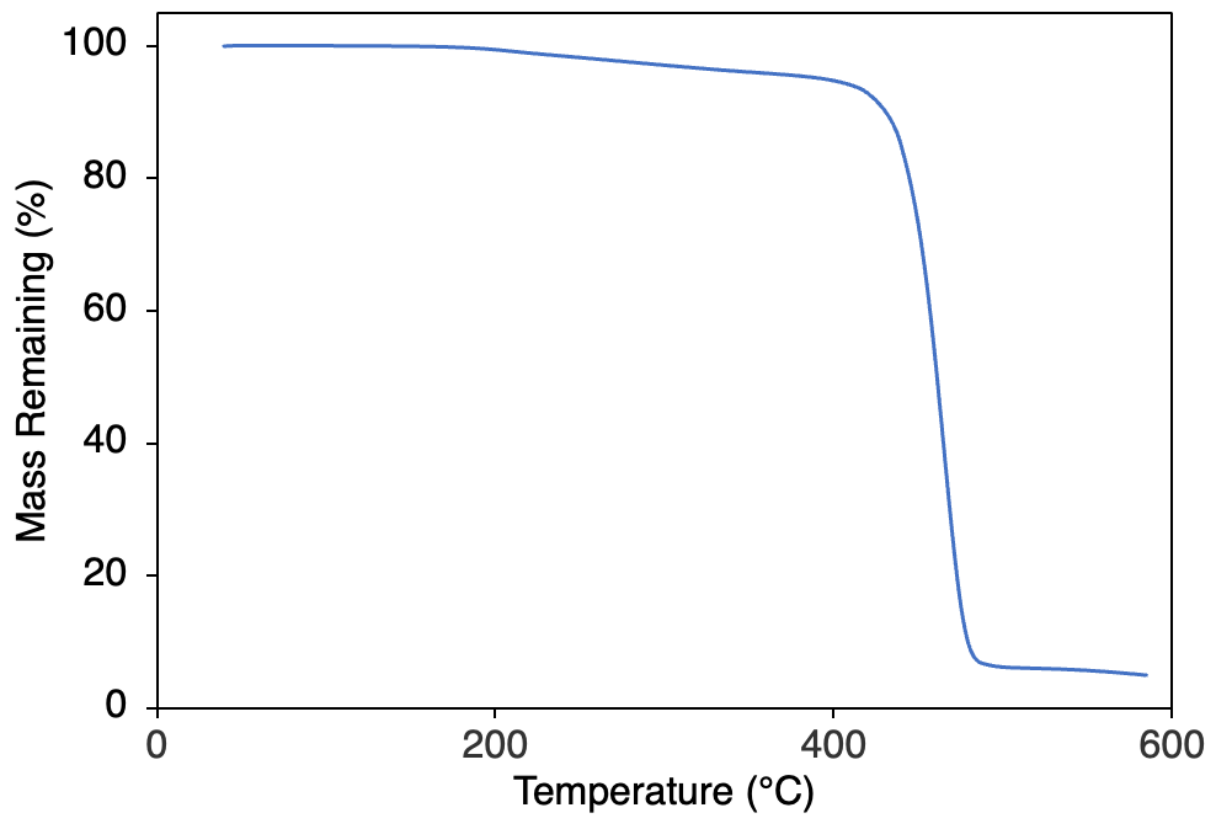


Figure 3.10.18.15. TGA plot of polymer **6c**, $T_d = 395.0$ °C

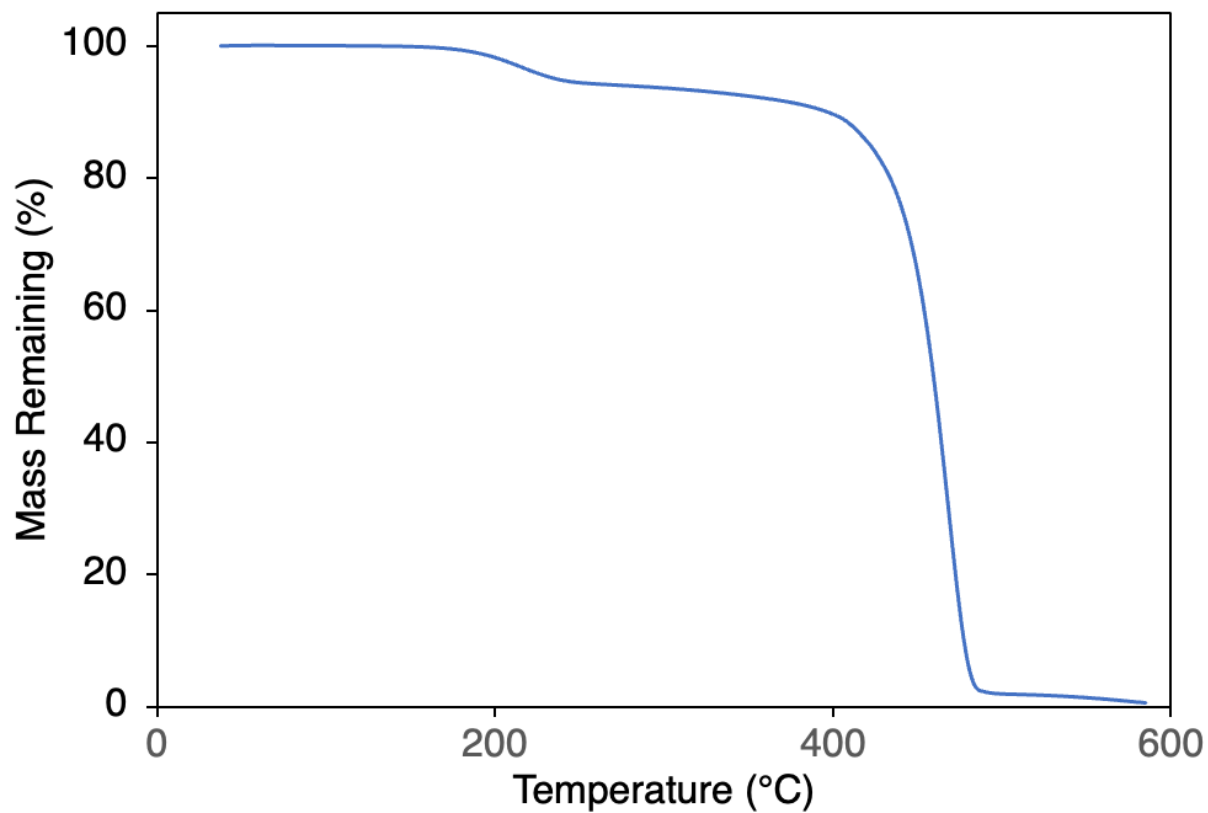


Figure 3.10.18.16. TGA plot of polymer 6d, $T_d = 236.5\text{ }^\circ\text{C}$

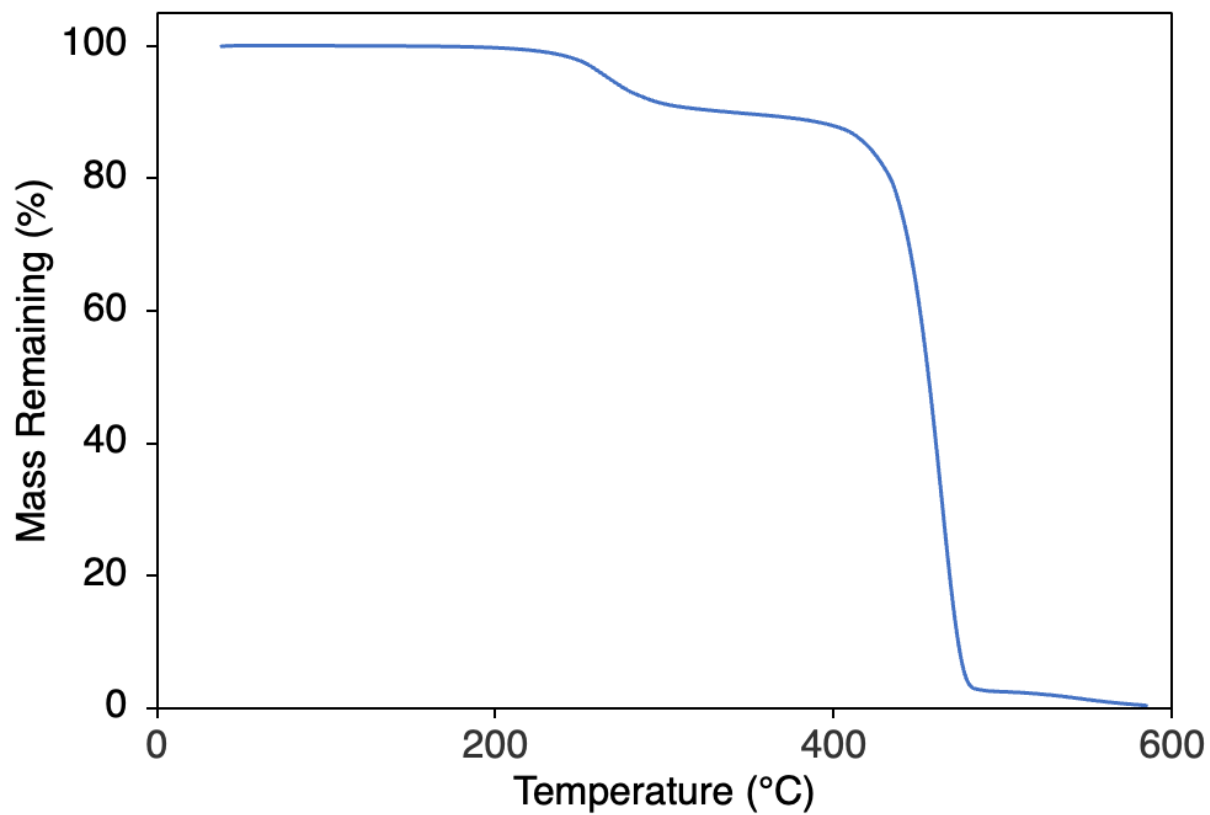


Figure 3.10.18.17. TGA plot of polymer **6e**, $T_d = 267.8$ °C

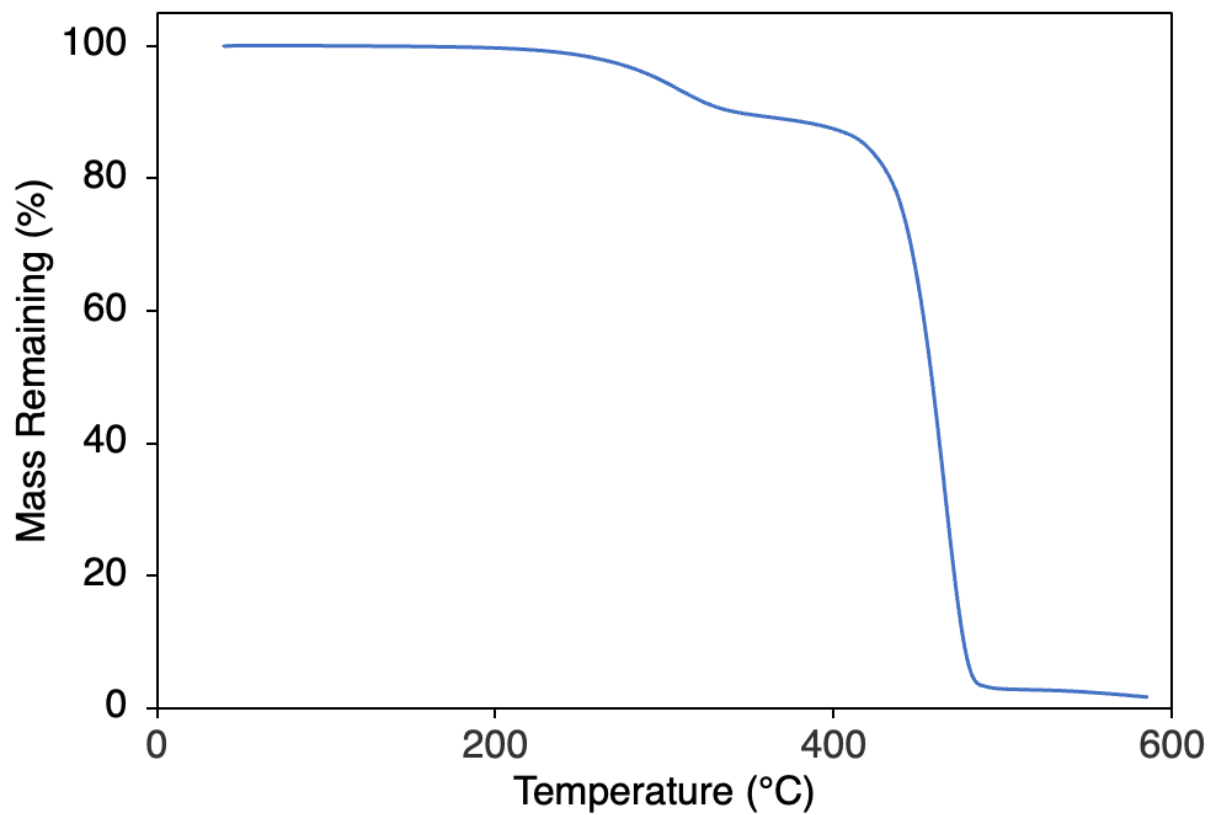


Figure 3.10.18.18. TGA plot of polymer **6f**, $T_d = 296.7$ °C

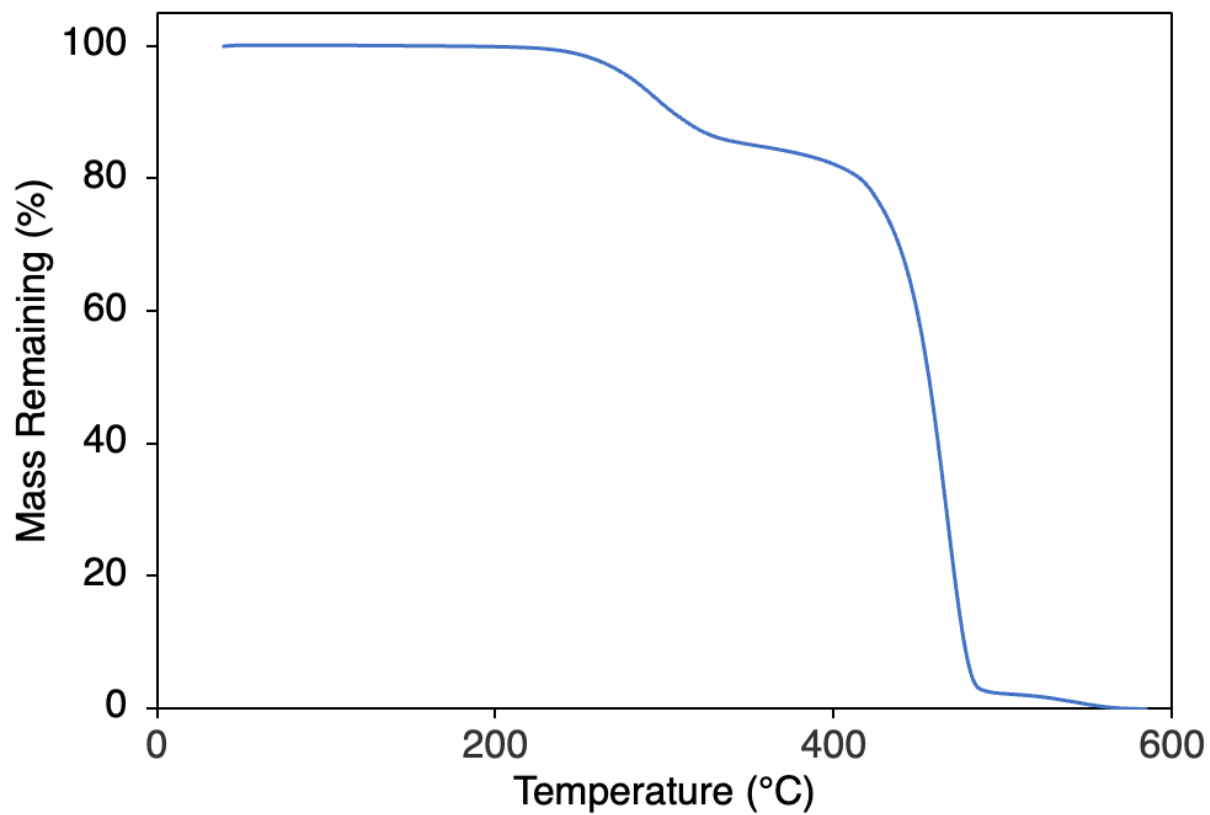


Figure 3.10.18.19. TGA plot of polymer **6g**, $T_d = 281.0$ °C

3.11 References

- (1) Kim, Y. K. The use of polyolefins in industrial and medical applications. In *Polyolefin Fibres*, Elsevier, 2017; pp 135–155.
- (2) Geyer, R.; Jambeck, J. R.; Law, K. L. Production, use, and fate of all plastics ever made. *Sci. Adv.* **2017**, *3*, e1700782
- (3) Hahladakis, J. N.; Velis, C. A.; Weber, R.; Iacovidou, E.; Purnell, P. An overview of chemical additives present in plastics: Migration, release, fate and environmental impact during their use, disposal and recycling. *Journal of Hazardous Materials* **2018**, *344*, 179–199
- (4) Ragaert, K.; Delva, L.; Van Greem, K. Mechanical and chemical recycling of solid plastic waste. *Waste Management* **2017**, *69*, 24–58
- (5) Ellen MacArthur Foundation and McKinsey & Company. <http://www.ellenmacarthurfoundation.org/publications>. (accessed 2021-08-15). The New Plastics Economy — Rethinking the future of plastics
- (6) Boanen, N. K.; Hillmyer, M. A. Post-polymerization functionalization of polyolefins. *Chem. Soc. Rev.* **2005**, *34*, 267
- (7) Plummer, C. M.; Li, L.; Chen, Y. The post-modification of polyolefins with emerging synthetic methods. *Polym. Chem.* **2020**, *11*, 6862–6872
- (8) Tan, C.; Zou, C.; Chen, C. Material Properties of Functional Polyethylenes from Transition-Metal-Catalyzed Ethylene–Polar Monomer Copolymerization. *Macromolecules* **2022**, *55*, 1910–1922
- (9) Balzade, Z.; Sharif, F.; Reza Ghaffarian Anbaran, S. Tailor-Made Functional Polyolefins of Complex Architectures: Recent Advances, Applications, and Prospects. *Macromolecules* **2022**, *55*, 1910–1922
- (10) Franssen, N. M. G.; Reek, J. N. H.; De Bruin, B. Synthesis of functional ‘polyolefins’: state of the art and remaining challenges. *Chem. Soc. Rev.* **2013**, *42*, 5809
- (11) Boffa, L. S.; Novak, B. M. Copolymerization of Polar Monomers with Olefins Using Transition-Metal Complexes. *Chem. Rev.* **2000**, *100*, 1479–1494
- (12) Williamson, J. B.; Lewis, S. E.; Johnson, R. R.; Manning, I. M.; Leibfarth, F. A. C–H Functionalization of Commodity Polymers. *Angew. Chem. Int. Ed.* **2019**, *58*, 8654–8668
- (13) Jehanno, C.; Alty, J. W.; Roosen, M.; De Meester, S.; Dove, A. P.; Chen, E. Y.-X.; Leibfarth, F. A.; Sardon, H. Critical advances and future opportunities in upcycling commodity polymers. *Nature* **2022**, *603*, 803–814
- (14) Popelka, E.; Khanam, P. N.; AlMaadeed, M. A. Surface modification of polyethylene/graphene composite using corona discharge. *Journal of Physics D: Applied Physics* **2018**, *51*, 105302
- (15) Sanchis, M. R.; Blanes, V.; Blanes, M.; Garcia, D.; Balart, R. Surface modification of low density polyethylene (LDPE) film by low pressure O₂ plasma treatment. *Eur. Polym. J.* **2006**, *42*, 1558–1568
- (16) Wu, D. Y.; Gutowski, W. S.; Li, S.; Griesser, H. J. Ammonia plasma treatment of polyolefins for adhesive bonding with a cyanoacrylate adhesive. *Journal of Adhesion Science and Technology* **2012**, *9*, 501–525
- (17) Bunescu, A.; Lee, S.; Li, Q.; Hartwig, J. F. Catalytic Hydroxylation of Polyethylenes. *ACS Central Science* **2017**, *3*, 895–903
- (18) Chen, L.; Malollari, K. G.; Uliana, A.; Sanchez, D.; Messersmith, P. B.; Hartwig, J. F. Selective, Catalytic Oxidations of C–H Bonds in Polyethylenes Produce Functional Materials with Enhanced Adhesion. *Chem* **2021**, *7*, 137–145

- (19) Fazekas, T. J.; Alty, J. W.; Neidhart, E. K.; Miller, A. S.; Leibfarth, F. A.; Alexanian, E. J. Diversification of aliphatic C-H bonds in small molecules and polyolefins through radical chain transfer. *Science* **2022**, *375*, 545–550
- (20) Williamson, J. B.; Czaplowski, W. L.; Alexanian, E. J.; Leibfarth, F. A. Regioselective C-H Xanthylation as a Platform for Polyolefin Functionalization. *Angew. Chem. Int. Ed.* **2018**, *57*, 6261–6265
- (21) Chen, L.; Malollari, K. G.; Uliana, A.; Hartwig, J. F. Ruthenium-Catalyzed, Chemoselective and Regioselective Oxidation of Polyisobutene. *J. Am. Chem. Soc.* **2021**, *143*, 4531–4535
- (22) Menendez Rodriguez, G.; Díaz-Requejo, M. M.; Pérez, P. J. Metal-Catalyzed Postpolymerization Strategies for Polar Group Incorporation into Polyolefins Containing C–C, C=C, and Aromatic Rings. *Macromolecules* **2021**, *54*, 4971–4985
- (23) Walker, T. W.; Frelka, N.; Shen, Z.; Chew, A. K.; Banick, J.; Grey, S.; Kim, M. S.; Dumesic, J. A.; Van Lehn, R. C.; Huber, G. W. Recycling of multilayer plastic packaging materials by solvent-targeted recovery and precipitation. *Sci. Adv.* **2020**, *6*, aba7599
- (24) Zhang, Y.; Wang, T.; Bai, J.; You, W. Repurposing Mitsunobu Reactions as a Generic Approach toward Polyethylene Derivatives. *ACS Macro Lett.* **2022**, *11*, 33–38
- (25) Samay, G.; Nagy, T.; White, J. L. Grafting maleic anhydride and comonomers onto polyethylene. *J. Appl. Polym. Sci.* **1995**, *56*, 1423–1433
- (26) Vocke, C.; Anttila, U.; Heino, M.; Hietaoja, P.; Seppälä, J. Use of oxazoline functionalized polyolefins and elastomers as compatibilizers for thermoplastic blends. *J. Appl. Polym. Sci.* **1998**, *70*, 1923–1930
- (27) Seko, N.; Ninh, N. T. Y.; Tamada, M. Emulsion grafting of glycidyl methacrylate onto polyethylene fiber. *Radiation Physics and Chemistry* **2010**, *79*, 22–26
- (28) Hirashita, T.; Sugihara, Y.; Ishikawa, S.; Naito, Y.; Matsukawa, Y.; Araki, S. Revisiting Sodium Hypochlorite Pentahydrate (NaOCl·5H₂O) for the Oxidation of Alcohols in Acetonitrile without Nitroxyl Radicals. *Synlett* **2018**, *29*, 2404–2407
- (29) Kimura, Y.; Okada, T.; Asawa, T.; Sugiyama, Y.; Kirihara, M.; Iwai, T. Sodium Hypochlorite Pentahydrate (NaOCl·5H₂O) Crystals as an Extra-ordinary Oxidant for Primary and Secondary Alcohols. *Synlett* **2014**, *25*, 596–598
- (30) Almeida, M. L. S.; Beller, M.; Wang, G.-Z.; Bäckvall, J.-E. Ruthenium(II)-Catalyzed Oppenauer-Type Oxidation of Secondary Alcohols. *Chemistry - A European Journal* **1996**, *2*, 1533–1536
- (31) Fujita, K.-I.; Yoshida, T.; Imori, Y.; Yamaguchi, R. Dehydrogenative Oxidation of Primary and Secondary Alcohols Catalyzed by a Cp*Ir Complex Having a Functional C,N-Chelate Ligand. *Org. Lett.* **2011**, *13*, 2278–2281
- (32) Fujita, K.-I.; Tanino, N.; Yamaguchi, R. Ligand-Promoted Dehydrogenation of Alcohols Catalyzed by Cp*Ir Complexes. A New Catalytic System for Oxidant-Free Oxidation of Alcohols. *Org. Lett.* **2007**, *9*, 109–111
- (33) Murahashi, S.-I.; Naota, T.; Oda, Y.; Hirai, N. Ruthenium-Catalyzed Oxidation of Alcohols with Peracids. *Synlett* **1995**, *1995*, 733–734
- (34) Ikariya, T.; Blacker, A. J. Asymmetric Transfer Hydrogenation of Ketones with Bifunctional Transition Metal-Based Molecular Catalysts†. *Acc. Chem. Res.* **2007**, *40*, 1300–1308
- (35) Ohkuma, T.; Ooka, H.; Yamakawa, M.; Ikariya, T.; Noyori, R. Stereoselective Hydrogenation of Simple Ketones Catalyzed by Ruthenium(II) Complexes. *The Journal of Organic Chemistry* **1996**, *61*, 4872–4873

- (36) Burdurlu, E.; Kiliç, Y.; Eli'Bol, G. C.; Kiliç, M. Shear strength of calabrian pine (*Pinus brutia* Ten.) bonded with polyurethane and polyvinyl acetate adhesives. *J. Appl. Polym. Sci.* **2006**, *100*, 4856–4867
- (37) Hagenmaier, R. D.; Grohmann, K. Polyvinyl Acetate as a High-gloss Edible Coating. *Journal of Food Science* **1999**, *64*, 1064–1067
- (38) Kramár, S.; Trcala, M.; Chitbanyong, K.; Král, P.; Puangsin, B. Basalt-Fiber-Reinforced Polyvinyl Acetate Resin: A Coating for Ductile Plywood Panels. *Materials* **2019**, *13*, 49
- (39) Kamiya, Y.; Mizoguchi, K.; Naito, Y.; Hirose, T. Gas sorption in poly(vinyl benzoate). *J. Polym. Sci., Part B: Polym. Phys.* **1986**, *24*, 535–547
- (40) Hirose, T.; Mizoguchi, K.; Kamiya, Y. Gas transport in poly(vinyl benzoate). *J. Appl. Polym. Sci.* **1985**, *30*, 401–410
- (41) Chen, W.; Gong, Y.; Mckie, M.; Almuhtaram, H.; Sun, J.; Barrett, H.; Yang, D.; Wu, M.; Andrews, R. C.; Peng, H. Defining the Chemical Additives Driving *In Vitro* Toxicities of Plastics. *Environ. Sci. Technol.* **2022**, *56*, 14627–14639
- (42) Dezern, J. F. Synthesis and characterization of BTDA-based polyamide-imides. *J. Polym. Sci., Part A: Polym. Chem.* **1988**, *26*, 2157–2169
- (43) Naumoska, K.; Jug, U.; Metličar, V.; Vovk, I. Oleamide, a Bioactive Compound, Unwittingly Introduced into the Human Body through Some Plastic Food/Beverages and Medicine Containers. *Foods* **2020**, *9*, 549
- (44) Saillenfait, A.-M.; Ndaw, S.; Robert, A.; Sabaté, J.-P. Recent biomonitoring reports on phosphate ester flame retardants: a short review. *Archives of Toxicology* **2018**, *92*, 2749–2778
- (45) Till, D. E.; Ehntholt, D. J.; Reid, R. C.; Schwartz, P. S.; Sidman, K. R.; Schwoppe, A. D.; Whelan, R. H. Migration of BHT antioxidant from high density polyethylene to foods and food simulants. *Industrial & Engineering Chemistry Product Research and Development* **1982**, *21*, 106–113
- (46) Su, J.; Chen, F.; Cryns, V. L.; Messersmith, P. B. Catechol Polymers for pH-Responsive, Targeted Drug Delivery to Cancer Cells. *J. Am. Chem. Soc.* **2011**, *133*, 11850–11853
- (47) Putnam, A. A.; Wilker, J. J. Changing polymer catechol content to generate adhesives for high versus low energy surfaces. *Soft Matter* **2021**, *17*, 1999–2009
- (48) Zhang, Q.; Nurumbetov, G.; Simula, A.; Zhu, C.; Li, M.; Wilson, P.; Kempe, K.; Yang, B.; Tao, L.; Haddleton, D. M. Synthesis of well-defined catechol polymers for surface functionalization of magnetic nanoparticles. *Polym. Chem.* **2016**, *7*, 7002–7010
- (49) Bae, C.; Hartwig, J. F.; Boen Harris, N. K.; Long, R. O.; Anderson, K. S.; Hillmyer, M. A. Catalytic Hydroxylation of Polypropylenes. *J. Am. Chem. Soc.* **2005**, *127*, 767–776
- (50) Hill, M. R.; Mukherjee, S.; Costanzo, P. J.; Sumerlin, B. S. Modular oxime functionalization of well-defined alkoxyamine-containing polymers. *Polym. Chem.* **2012**, *3*, 1758–1762
- (51) Binder, W. H.; Sachsenhofer, R. 'Click' Chemistry in Polymer and Material Science: An Update. *Macromolecular Rapid Communications* **2008**, *29*, 952–981
- (52) Collins, J.; Nadgorny, M.; Xiao, Z.; Connal, L. A. Doubly Dynamic Self-Healing Materials Based on Oxime Click Chemistry and Boronic Acids. *Macromolecular Rapid Communications* **2017**, *38*, 1600760
- (53) Calatayud, M.; Ruppert, A. M.; Weckhuysen, B. M. Theoretical Study on the Role of Surface Basicity and Lewis Acidity on the Etherification of Glycerol over Alkaline Earth Metal Oxides. *Chemistry - A European Journal* **2009**, *15*, 10864–10870
- (54) Andrade, J. T.; Alves, S. L. G.; Lima, W. G.; Sousa, C. D. F.; Carmo, L. F.; De Sá, N. P.; Morais, F. B.; Johann, S.; Villar, J. A. F. P.; Ferreira, J. M. S. Pharmacologic potential of new nitro-

compounds as antimicrobial agents against nosocomial pathogens: design, synthesis, and in vitro effectiveness. *Folia Microbiologica* **2020**, *65*, 393–405

(55) Clark, N. G.; Croshaw, B.; Leggetter, B. E.; Spooner, D. F. Synthesis and antimicrobial activity of aliphatic nitro compounds. *Journal of Medicinal Chemistry* **1974**, *17*, 977–981

(56) Yan, Z.; Liu, J.; Miao, C.; Su, P.; Zheng, G.; Cui, B.; Geng, T.; Fan, J.; Yu, Z.; Bu, N.; Yuan, Y.; Xia, L. Pyrene-Based Fluorescent Porous Organic Polymers for Recognition and Detection of Pesticides. *Molecules* **2021**, *27*, 126

(57) Zhao, Y.; Long, J.; Zhuang, P.; Ji, Y.; He, C.; Wang, H. Transforming polyethylene and polypropylene into nontraditional fluorescent polymers by thermal oxidation. *Journal of Materials Chemistry C* **2022**, *10*, 1010–1016

(58) Yin, S.; Duvigneau, J.; Vancso, G. J. Fluorescent Polyethylene by In Situ Facile Synthesis of Carbon Quantum Dots Facilitated by Silica Nanoparticle Agglomerates. *ACS Applied Polymer Materials* **2021**, *3*, 5517–5526

(59) Rahman, M. A.; Bowland, C.; Ge, S.; Acharya, S. R.; Kim, S.; Cooper, V. R.; Chen, X. C.; Irle, S.; Sokolov, A. P.; Savara, A.; Saito, T. Design of tough adhesive from commodity thermoplastics through dynamic crosslinking. *Sci. Adv.* **2021**, *7*, eabk2451

(60) Lallemand, M.; Yu, L.; Cai, W.; Rischka, K.; Hartwig, A.; Haag, R.; Hugel, T.; Balzer, B. N. Multivalent non-covalent interactions lead to strongest polymer adhesion. *Nanoscale* **2022**, *14*, 3768–3776

(61) Buaksuntear, K.; Limarun, P.; Suethao, S.; Smitthipong, W. Non-Covalent Interaction on the Self-Healing of Mechanical Properties in Supramolecular Polymers. *International Journal of Molecular Sciences* **2022**, *23*, 6902

(62) Yang, J.; Bos, I.; Pranger, W.; Stuijver, A.; Velders, A. H.; Cohen Stuart, M. A.; Kamperman, M. A clear coat from a water soluble precursor: a bioinspired paint concept. *Journal of Materials Chemistry A* **2016**, *4*, 6868–6877

(63) Wiesinger, H.; Wang, Z.; Hellweg, S. Deep Dive into Plastic Monomers, Additives, and Processing Aids. *Environ. Sci. Technol.* **2021**, *55*, 9339–9351

(64) Anouar, B. S.; Guinot, C.; Ruiz, J.-C.; Carton, F.; Dole, P.; Joly, C.; Yvan, C. Purification of post-consumer polyolefins via supercritical CO₂ extraction for the recycling in food contact applications. *The Journal of Supercritical Fluids* **2015**, *98*, 25–32

(65) Vollmer, I.; Jenks, M. J. F.; Roelands, M. C. P.; White, R. J.; Harmelen, T.; Wild, P.; Laan, G. P.; Meirer, F.; Keurentjes, J. T. F.; Weckhuysen, B. M. Beyond Mechanical Recycling: Giving New Life to Plastic Waste. *Angew. Chem. Int. Ed.* **2020**, *59*, 15402–15423

(66) Zhao, Y.-B.; Lv, X.-D.; Ni, H.-G. Solvent-based separation and recycling of waste plastics: A review. *Chemosphere* **2018**, *209*, 707–720

(67) Knez, Ž.; Markočič, E.; Leitgeb, M.; Primožič, M.; Hrnčič, M. K.; Škerget, M. Industrial applications of supercritical fluids: A review. *Energy* **2014**, *77*, 235–243

(68) Tian, H.-Z.; Wu, S.-F.; Lin, G.-Q.; Sun, X.-W. Asymmetric synthesis of pyrrolo[2,3-b]indole scaffolds by organocatalytic [3 + 2] dearomative annulation. *Tetrahedron Letters* **2022**, *103*, 153969

(69) Han, L.; Geng, J.; Wang, Z.; Hua, J. Balancing anti-migration and anti-aging behavior of binary antioxidants for high-performance 1,2-polybutadiene rubber. *Polymers for Advanced Technologies* **2022**, *33*, 3619–3627

(70) Ruiz-Avila, L. B.; Huecas, S.; Artola, M.; Vergoñós, A.; Ramírez-Aportela, E.; Cercenado, E.; Barasoain, I.; Vázquez-Villa, H.; Martín-Fontecha, M.; Chacón, P.; López-Rodríguez, M. L.;

Andreu, J. M. Synthetic Inhibitors of Bacterial Cell Division Targeting the GTP-Binding Site of FtsZ. *ACS Chemical Biology* **2013**, *8*, 2072–2083

(71) Li, D.; Zhou, L.; Wang, X.; He, L.; Yang, X. Effect of Crystallinity of Polyethylene with Different Densities on Breakdown Strength and Conductance Property. *Materials* **2019**, *12*, 1746

Chapter Four

Backbone Editing of Polyethylene to Nylon by Beckmann Rearrangement

4.1 Introduction

Polyethylene is the commodity plastic formed in the largest quantity, with global production currently exceeding 110 million metric tons annually.¹ Its durability and inertness render it useful over a variety of applications, from packaging to construction; however, its resistance to chemical transformations necessitate that it be blended or layered with polar polymers to broaden the range of properties that polyethylene can possess.^{2,3} The resulting polymer composites, the formation of which typically requires compatibilizers and other additives, cannot readily be separated into their components after use, and are, therefore, challenging to recycle.³⁻⁶ For this reason, many polyethylene products are produced for single-use applications and are major contributors to the accumulation of plastic waste.^{1,3}

Functionalized polyethylenes could serve as a more sustainable alternative to these polyethylene composites. They can be tailored to possess enhanced properties, such as increased adhesion and solubility in polar solvents over their unmodified counterparts, whereas such properties from polyethylene would require polymer blending. The functionalized polymers also could be more amenable to deconstruction and recycling than composite materials.⁷⁻⁹ Typically, these functionalized polyolefins are synthesized by copolymerization of ethylene and polar comonomers. However, copolymerization methods are limited; free-radical copolymerization does not allow for a significant degree of control over monomer ratios or polymer architecture, and copolymerization catalyzed by transition-metal systems is prone to catalyst deactivation by polar functional groups.^{8,9} Therefore, these processes can generate only a limited range of functional materials.

Post-polymerization functionalization can circumvent some of these disadvantages by enabling the structure of the polymer to be established prior to the introduction of polar groups.^{8,9} In addition, post-polymerization functionalization can occur with existing polyolefins as feedstock to upcycling post-consumer polyolefins directly into functional materials suitable for a range of applications.¹⁰⁻¹³

Our group reported a ruthenium-catalyzed oxidation of the C–H bonds in polyethylenes of varying architectures and in waste polyethylenes to generate *oxo*-polyethylenes containing a mixture of pendant alcohol and ketone units.¹⁴ These *oxo*-polyethylenes display enhanced bulk properties and are amenable to further modification by conversion of all installed polar moieties to either the alcohols or the ketones, followed by grafting of other functional handles. One such transformation generated oxime-containing polyethylenes by reaction of ketone-functionalized polyethylene with a variety of *O*-substituted hydroxylammonium chloride salts. The resulting *oxime*-polyethylenes display enhanced adhesion over the unmodified polyethylene and can be reverted to their ketone-containing precursors by simple hydrolysis. Because most previously reported functionalizations of polyolefins modify only the pendent C–H bonds, methods for in-chain modification that could further broaden the range of polymer structures and properties accessible by post-polymerization functionalization are needed.¹⁵

We envisioned that further derivatization of *oxime*-polyethylenes could generate polymers with in-chain amide linkages by a Beckmann rearrangement and that the resulting polymers could have properties different from those of polyethylene or that they could be cleaved to form telechelic units to create new materials with greater circularity, or both (Figure 4.1.1). During the preparation of this manuscript, Nozaki and coworkers published the formation of polyamides from linear polyketones generated from palladium-catalyzed copolymerization of ethylene and diiron nonacarbonyl, by sequential oxime formation and Beckmann rearrangement using a large excess of diethylamino sulfur trifluoride (DAST) and assessed the thermal and mechanical profiles of the

polyamides.¹⁶ Here, we report the synthesis of nylon-like polyamides from multiple forms of *oxo*-polyethylene from commercial and waste polyethylenes, testing of thermal, tensile and surface properties of the materials, and the cleavage of the amide linkages to form telechelic macromonomers that serve as chain extenders for the synthesis of polyurea urethanes.

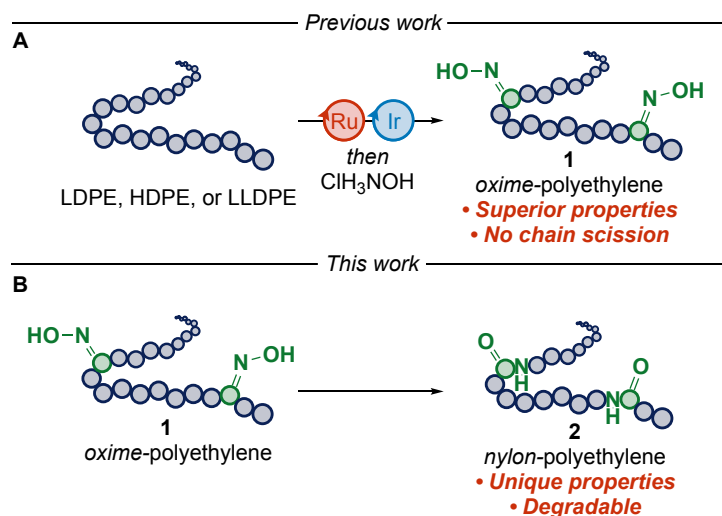


Figure 4.1.1. (A) Prior work: synthesis of *oxime*-polyethylene (B) This work: Beckmann rearrangement of *oxime*-polyethylene to form in-chain amide linkages

4.2 Beckmann Rearrangement of Oxime-Polyethylene

The conversion of polyketones to polyamides can be achieved in one step by a Schmidt reaction.^{17, 18} Our group has previously reported a method to access polyketones directly from polyethylene by sequential C–H functionalization and oxidation.¹⁹ However, because *keto*-polyethylenes derived from our strategy require higher temperatures to dissolve than polyketones synthesized by radical polymerization, the high operating temperatures required to dissolve *keto*-polyethylene discourages the use of hydrazoic acid for this transformation.²⁰

To this end, we started from oxime-containing low-density polyethylene (LDPE) **1a** derived from oxidation and condensation of LDPE to furnish in-chain amide linkages through Beckmann rearrangement. Conditions that readily convert small-molecule oximes to amides were investigated (Table 4.2.1).²¹ Organocatalysts, such as cyanuric chloride (CNC) and the combination of triphenylphosphine with carbon tetrabromide,^{22, 23} did not to catalyze the formation of amides from the oximes (Table 4.2.1 entries 1–2). Furthermore, strong acids, such as *p*-toluenesulfonic acid (PTSA) and trifluoroacetic acid (TFA), formed the amides in trace amounts (Table 4.2.1 entries 3–4). Low conversions of the oxime occurred from reactions with trifluoroacetic anhydride (TFAA) (Table 1 entry 5). The low conversions of the reactions with these reagents highlight the challenges of applying transformations of small molecules to polyethylene.

Reactions conducted with *para*-toluenesulfonyl chloride (TsCl) and propylphosphonic anhydride (T3P) converted the oximes quantitatively, as assessed by ¹H NMR spectroscopy (Table 4.2.1 entries 6–7); however, hydrolysis of the oxime to the ketone was also observed after reactions with TsCl (presumably catalyzed by the HCl that is formed as a byproduct). In addition, a substantial decrease in *M_n* from unmodified LDPE to *nylon*-LDPE **2a** was observed after reactions with TsCl, presumably caused by competing Beckmann fragmentation (Table 4.2.1 entry 6).²⁴ A

lower extent of hydrolysis of the oxime to the ketone was observed after reactions with T3P, and less chain scission was observed from reactions with T3P than from reactions with TsCl (Table 4.2.1, entry 7).

Based on these results, we reasoned that T3P could be a safer and cheaper reagent than DAST for the synthesis of *nylon*-polyethylenes from other polyethylenes. To this end, we applied the reaction conditions to *oxime*-polyethylenes derived from high-density polyethylene (HDPE) and post-consumer HDPE from a milk jug (Figure 4.2.1). The conversion of oximes to amides in all these polymers was quantitative, as judged by ¹H NMR spectroscopy, indicating installation of amide linkages into the polyethylene main chains (see Section 4.7.8).

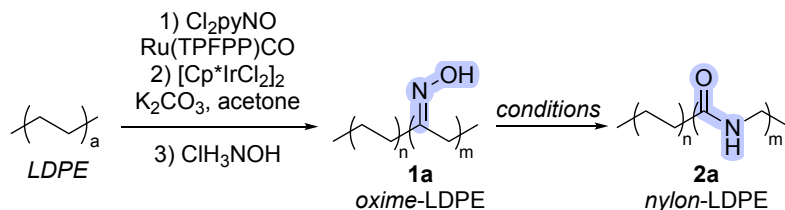


Table 4.2.1. Optimization of the Beckmann rearrangement of *oxime*-LDPE **1a** to *nylon*-LDPE **2a**.

entry ^a	conditions	conversion ^h	M_n (kDa) ^{i,j}	D
1 ^b	1 equiv PPh ₃ , 1 equiv CBr ₄	n.r.	--	--
2 ^b	1 equiv CNC	n.r.	--	--
3 ^b	5 equiv PTSA	trace	--	--
4 ^c	50 equiv TFA	trace	--	--
5 ^c	30 equiv TFAA	15%	--	--
6 ^b	5 equiv TsCl	>99%	2.7	2.3
7 ^d	3 equiv T3P	>99%	8.1	2.4

^aAll reactions run for 24 h. ^bReaction run in PhMe. ^cReaction run in DCM. ^dReaction run in THF. ^eReaction run at 80 °C. ^fReaction run at 120 °C. ^gEquivalents with respect to the number of oximes. ^hConversion of oximes as determined by ¹H NMR spectroscopy in CDCl₃ at room temperature. ⁱMolecular weight with respect to polyethylene standards. ^j $M_{n,LDPE} = 9.6$ kDa and $D_{LDPE} = 6.7$.

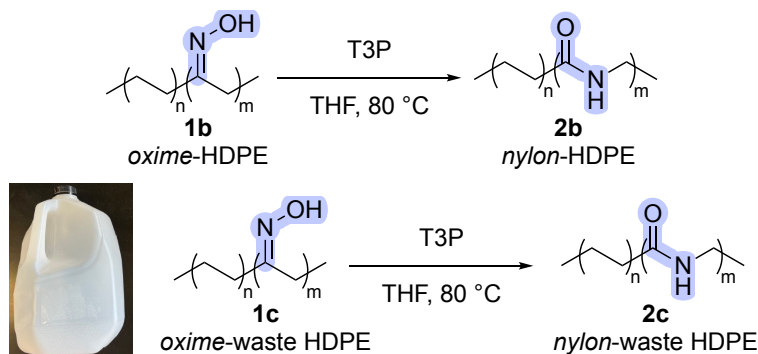
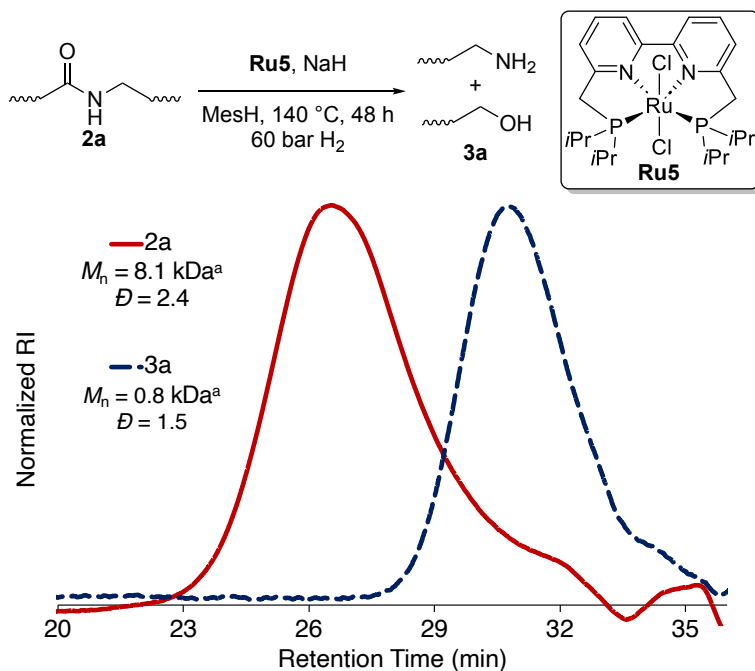


Figure 4.2.1. Beckmann rearrangement of other *oxime*-polyethylenes.

4.3 Hydrogenolysis of Amide Linkages

To cleave *nylon*-LDPE **2a** into end-functionalized fragments, we sought to develop methods for hydrogenolysis of this material at the amide linkages. Because *nylon*-LDPE **2a** ($M_n = 8.1$ kDa) contains about 2% of amide linkages (average of six amides per chain), cleavage at these linkages would generate an average of five telechelic segments for every two monofunctional oligomers.

We tested the ability of several ruthenium complexes that have been reported to catalyze the hydrogenolysis of aliphatic amides to catalyze hydrogenolysis of the amide units in polymer **2a**.²⁵⁻²⁹ Preliminary testing of catalyst activity was conducted with *nylon*-LDPE **2a** (see Table 4.7.2.6.1). We found that air-stable catalyst **Ru5**, which contains a tetradentate bipyridyl bisphosphine ligand, converted the amide linkages in polymer **2a** quantitatively to alcohol- and amine-terminated oligomers, as assessed by ¹H NMR spectroscopy. A decrease in M_n was also observed by high-temperature size-exclusion chromatograph (HTSEC), indicating that polymer **2a** was cleaved at the amide linkages (Figure 4.3.1). We hypothesized that the activity of catalyst **Ru5** for hydrogenolysis of polymer **2a** can be attributed to the resistance of the tetradentate bipyridyl bisphosphine ligand to dissociate from the ruthenium because of its high binding affinity. Application of the optimized conditions to *nylon*-polyethylenes **2b** and **2c** afforded complete hydrogenolysis of the amide linkages, as assessed by ¹H NMR spectroscopy (see Section 4.7.8). These results show that this system for catalytic hydrogenolysis operates on polyamides with various architectures and tolerates additives that may remain in *nylon*-polythene **2c** derived from post-consumer waste HDPE.



^aMolecular weight with respect to polyethylene standards.

Figure 4.3.1. Hydrogenolysis of Amide Linkages in *nylon*-LDPE.

4.4 Polymerization of Alcohol- and Amine-Terminated Fragments

The oligomers resulting from the hydrogenolysis of polymer **2a** at the amide linkages could serve as precursors to new materials. For example, these long-chain alcohol- and amine-terminated

segments could be used as chain extenders for the synthesis of polyurea-urethane (PUU) elastomers derived from waste polyethylene. PUUs are valuable materials that are durable, self-healable, and reprocessable.^{30, 31} To this end, the alcohol- and amine-terminated segments **3a** were polymerized with methylene diphenyl diisocyanate (MDI) and poly(tetrahydrofuran) (*p*THF, $M_n = 1000$ Da) as the soft segment catalyzed by tin(II) 2-ethylhexanoate ($\text{Sn}(\text{oct})_2$) to form PUU **4** (Figure 4.4.1). ^1H NMR spectroscopy at 100 °C showed that polymerization of the soft and hard segments occurred with MDI (see Figure 4.7.8.25).

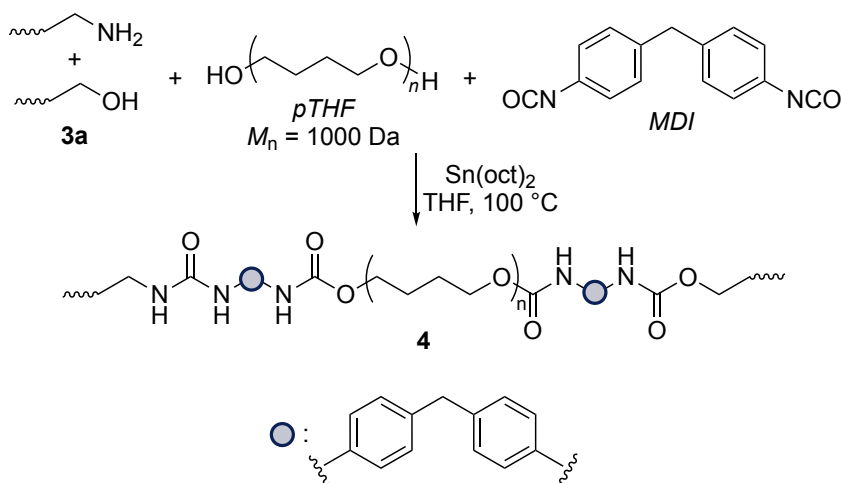


Figure 4.4.1. Synthesis of PUUs through polymerization of alcohol- and amine-terminated LDPE with MDI and *p*THF.

4.5 Materials Testing

With these polymers in hand, we investigated their properties. To gauge the thermal properties of polyamide **2a** and PUU **4**, we performed thermal gravimetric analysis (TGA) and differential scanning calorimetry (DSC). TGA revealed that the decomposition temperature (T_d) of *nylon*-LDPE **2a** (368.5 °C) was comparable to the T_d of unmodified LDPE (360.8 °C), indicating that the thermal stability of the polymer does not change appreciably by the transformations to form the polyamide (Figure 4.5.1A). TGA revealed a two-stage decomposition of PUU **4**, with the first stage occurring at 290 °C, corresponding to the degradation of the THF segment, and the second stage occurring at 371 °C, corresponding to the degradation of the polyolefin segment, and indicating that PUU **4** is thermally robust.³² DSC showed that the melting temperature (T_m) of unmodified LDPE is 111 °C, whereas the T_m of *nylon*-LDPE **2a** was a lower 98.1 °C (Figure 4.5.1B). This difference in melting temperature is consistent with a decrease in crystallinity caused by the installation of amides into the polymer backbone. The T_m of PUU **4** was determined to be 91.5 °C by DSC, indicating that it could be melt processed.

Because polymer **2a** contains amide linkages, we envisioned that it would be adhesive to nylon-6,6. To this end, we analyzed the adhesion of *nylon*-PE **2a** to nylon-6,6 by lap-shear tests (Figure 4.5.1C). The lap-shear tests indicated that polymer **2a** was more adhesive to nylon-6,6 (2.62 ± 0.15 MPa) than was unmodified LDPE (0.31 ± 0.04 MPa). We also measured the adhesion of *nylon*-LDPE **2a** to aluminum and glass. When used as an interlayer between aluminum or glass substrates, unmodified LDPE was not sufficiently adhesive to create a testable sample, whereas polymer **2a** adhered to both aluminum and glass (5.87 ± 0.33 MPa and 10.9 ± 0.90 MPa

respectively). The adhesion of polymer **2a** to glass is stronger than the adhesion of some epoxy resins.^{33, 34} These adhesion data suggest that the installation of amide linkages into the backbone of polyethylene can create polymers with surface properties that are enhanced over those of unmodified LDPE. PUU **4** was moderately adhesive to nylon-6,6, aluminum, and glass (1.17 ± 0.22 MPa, 0.76 ± 0.05 MPa, 0.65 ± 0.01 and MPa respectively), indicating that the surface properties of materials derived from LDPE can be more favorable than those of unmodified LDPE.

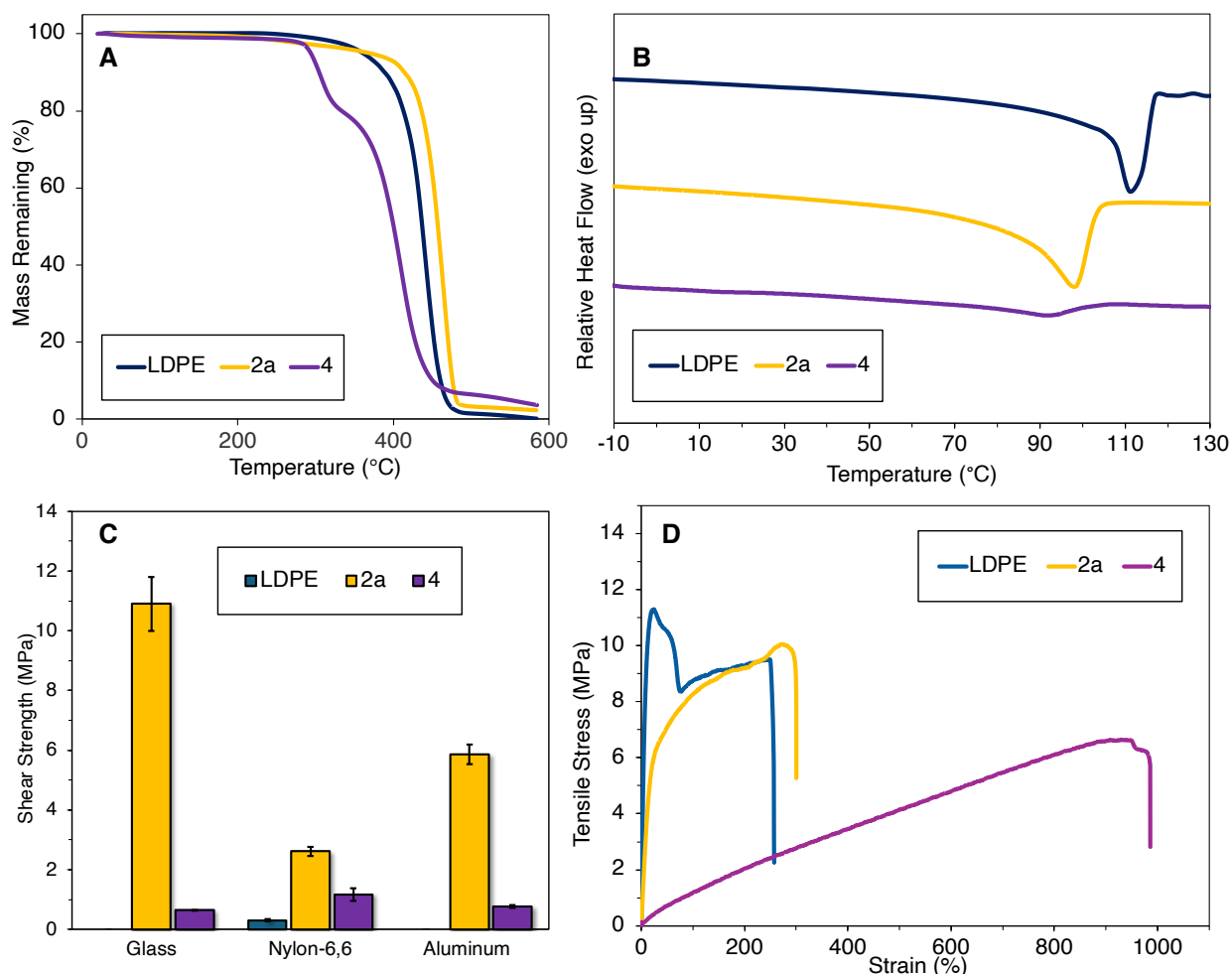


Figure 4.5.1. (A) TGA curves of unmodified LDPE, polymer **2a**, and PUU **4**. (B) DSC traces of unmodified LDPE, polymer **2a**, and PUU **4**. (C) Lap-shear tests of unmodified LDPE, polymer **2a**, and PUU **4** as interlayers with aluminum, nylon-6,6, and glass substrates. (D) Stress-strain curves of unmodified LDPE, polymer **2a**, and PUU **4**.

We also investigated the mechanical properties of *nylon-PE 2a* and PUU **4** by tensile tests (Figure 4.5.1D). The elongation at break (ϵ_B), tensile strength (σ_B), toughness (U_T), and Young's modulus (E) of **2a** were $303.9 \pm 75.0\%$, 11.2 ± 1.4 MPa, 27.2 ± 7.2 MJ m⁻³, 57.0 ± 10.2 MPa respectively. These values for ϵ_B , U_T , and σ_B are similar to the values of unmodified LDPE ($227.8 \pm 96.8\%$, 20.9 ± 9.8 MJ m⁻³, 11.4 ± 1.1 MPa respectively). However, the E of polymer **2a** (57.0 ± 10.2 MPa) was significantly lower than that of unmodified LDPE (148.5 ± 16.8 MPa), presumably because of the defects in the crystalline regions caused by the amide linkages in **2a**. Overall, the bulk properties of the polymer are largely retained after incorporation of an in-chain amide linkage. However, when PUU **4** was subjected to tensile testing, the E and σ_B of PUU **4** (0.9 ± 0.2 MPa and

5.5 ± 0.9 MPa respectively) were found to be significantly different from the values of unmodified LDPE (148.5 ± 16.8 MPa and 11.4 ± 1.1 MPa respectively) and polymer **2a** (57.0 ± 10.2 MPa and 11.2 ± 1.4 MPa respectively). The ϵ_B of PUU **4** ($939.2 \pm 89.9\%$) was found to be much greater than the ϵ_B of LDPE ($227.8 \pm 96.8\%$) and polymer **2a** ($303.9 \pm 75.0\%$), while the U_T of PUU **4** (29.9 ± 6.6 MJ m⁻³) was similar to the U_T of LDPE (20.9 ± 9.8 MJ m⁻³) and of polymer **2a** (27.2 ± 7.2 MJ m⁻³). Elastic hysteresis curves of PUU **4** verified the elastic nature of this material containing the harder polyamide and softer polyether units (see Figure 4.7.9.2.4). This wide range of bulk and surface properties possessed by these polymers highlight the ability to create valuable materials by selective chemical transformations of polyolefins.

4.6 Conclusion

In conclusion, we have demonstrated a strategy to integrate the pendent functional groups installed onto polyethylene by C–H functionalization into the backbone C–C bonds of the polymer to furnish cleavable linkages. We developed routes to polyamides from oxidized polyethylenes by Beckmann rearrangement of the intermediate oximes. These polyamides have enhanced surface properties, relative to unmodified polyethylene, while maintaining similar mechanical properties, and they underwent reductive cleavage at the amide linkages to afford telechelic fragments by ruthenium-catalyzed hydrogenolysis. The resulting telechelic units were then polymerized to form PUU elastomers. This work points to strategies that could lower the barriers to reuse of polyethylene and increase the sustainability of hydrocarbon-based plastics.

4.7 Experimental Section

4.7.1 General Information

All air sensitive manipulations were conducted under an inert atmosphere in a nitrogen-filled or argon-filled glovebox or by standard Schlenk techniques. All reagents were purchased from commercial sources and used without further purification. Low density polyethylene (LDPE) and -high density polyethylene (HDPE), were purchased from Sigma-Aldrich. Solvents were degassed with nitrogen and dried in a solvent purification system with a 1 m column containing activated alumina and stored under 4Å molecular sieves. Fourier-transform infrared spectra were collected using a Bruker Vortex 80 spectrometer. Room-temperature NMR spectra were collected using 400, 500, and 600 MHz Bruker Instruments at the University of California, Berkeley. Variable-temperature NMR spectroscopic analysis was conducted on the 500 and 600 MHz instruments at University of California Berkeley. ¹H chemical shifts were reported in ppm, relative to the resonance of the residual solvent (CDCl₃, 7.26 ppm; C₂D₂Cl₄, 6.00 ppm). ¹³C chemical shifts were reported in ppm, relative to the resonance of the residual solvent (CDCl₃, 77.16 ppm; C₂D₂Cl₄, 73.78 ppm). High-temperature, size-exclusion chromatography (HT-SEC) was performed on a Tosoh EcoSEC-HT with three TSKgel GMHhr-H(S) HT columns in series. Runs were performed at 135 °C and 1 mL/min with 1,2,4-trichlorobenzene + 0.05% butylated hydroxytoluene (BHT) as mobile phase. Molecular weight was determined relative to polyethylene standards. Differential scanning calorimetry (DSC) was performed on a TA Discovery DSC 25 instrument. Aluminum 6061 (Al-6061) and nylon-6,6 (ASTM D5989) substrates were cut at the UC Berkeley Cory Hall Machine shop from 0.160 cm thick, 10.16 cm x 121.92 cm (0.063" thick, 4"x48") and from 0.635 cm thick, 15.24 cm x 121.92 cm (0.25" thick, 6"x48") sheet stocks, respectively, purchased from McMaster-Carr (USA). Lap shear adhesion testing was conducted according to ASTM D1002-10 on an Instron universal materials tester equipped with a 5 kN load cell with a shear rate of 1.5 mm/min. Adhesion strength was determined by the maximum load divided by the bonded overlap area, which was measured with digital calipers prior to testing, and the apparent failure mode was assessed visually. The adhesive strengths of LDPE and functionalized polyethylenes to aluminum were assessed by single lap shear testing on rectangular aluminum 6061 (Al 6061) substrates with dimensions 0.16 cm thick x 1 cm width x 10 cm length. The adhesive strengths of LDPE and functionalized polyethylenes to nylon-6,6 was assessed by single lap shear testing on rectangular nylon-6,6 (ASTM D5989) substrates with dimensions 0.16 cm thick x 1 cm width x 10 cm length. Compression molding was conducted on a Carver benchtop lab press with heated plates (model 4386). Tensile testing was conducted according to ASTM D638 on an Instron universal materials tester. Tensile stress and strain were measured at room temperature using an extension rate of 50 mm/min. Thermogravimetric analysis (TGA) was performed with a TA Discovery TGA 550 instrument.

4.7.2 Assessment of the Degree of Functionalization

The degree of functionalization was determined by ^1H NMR spectroscopy at $100\text{ }^\circ\text{C}$ in $\text{C}_2\text{D}_2\text{Cl}_4$. The integration of the peaks between 1.7 and 0.7 ppm was set to 400 (4 proton per monomer unit, 100 monomer units in total). The integration of the protons that are alpha to the functional groups of interest were then compared to the integration of the protons of the monomer units.

4.7.3 Calculation of the Stoichiometry of Catalysts and Reagents

The stoichiometry for the catalysts and reagents were calculated based on the number of functional groups in the polymer.

$$\text{mmol}_{\text{amide}} = \frac{\text{mass}_{\text{polymer}}}{\text{MW}_{\text{repeat unit}}} * \frac{\% \text{ functionalization}}{100} * 1000$$

For example, 1 g of polymer **2a** with 3.0% functionalization:

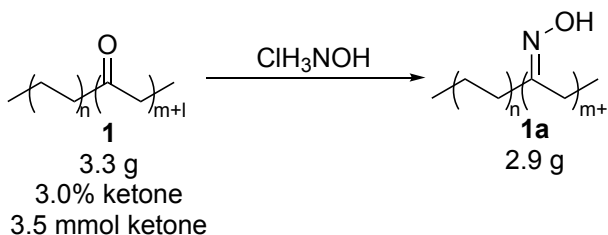
$$\text{mmol}_{\text{amide}} = \frac{1.0 \text{ g}}{\left(28.05 \frac{\text{g}}{\text{mol}}\right)} * \frac{3.0\%}{100} * 1000 = 1.1 \text{ mmol}_{\text{amide}}$$

4.7.4 Calculation of Yield

The yield for each reaction was determined by the following equation in which $\text{mass}_{\text{product,actual}}$ denotes the mass of the polymer obtained after the reaction, and $\text{mass}_{\text{product,theoretical}}$ denotes the mass of the polymer if all of the initial functional groups have been functionalized.

$$\% \text{ mass yield} = 100 * \left(\frac{\text{mass}_{\text{product,actual}}}{\text{mass}_{\text{product,theoretical}}} \right)$$

For example, for the synthesis of polymer **1a** by the condensation of polymer **1** with hydroxylamine hydrochloride:

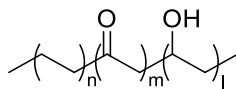


$$\text{mass}_{\text{product,theoretical}} = 3.3 \text{ g} + \frac{3.5 \text{ mmol} * \text{MW}_{\text{NH}}}{1000} = 3.4 \text{ g}$$

$$\% \text{ mass yield} = 100 * \left(\frac{2.9 \text{ g}}{3.4 \text{ g}} \right) = 85\%$$

4.7.5 Synthesis of polymers

Oxo-PE



The synthesis of *oxo*-PE was adapted from a literature procedure.¹⁴

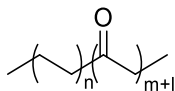
To a 250 mL round-bottom flask with a stir bar, 3.00 g of PE (LDPE, HDPE, or waste HDPE (milk jug), 107 mmol) were added. The solids were suspended in 107 mL of 1,2-dichlorobenzene. The flask was heated at 120 °C until the polymer dissolved. Then, 1.77 g of 2,6-dichloropyridine-*N*-oxide (10.7 mmol) were added to the flask. In a separate 4 mL vial, 5.9 mg of tetrakis(pentafluorophenyl)porphyrin ruthenium carbonyl (0.0054 mmol) were dissolved in 5.3 mL of dichloromethane. To the flask heated at 120 °C, the solution containing the catalyst was added with a pipette in a portion wise manner (CAUTION: dichloromethane evaporates vigorously when the solution is added). The flask was heated at 120 °C for 1 h. The flask was cooled slightly, and the contents were poured in 300 mL of methanol under vigorous stirring to precipitate the polymer. The slurry was filtered, and the powder was washed with copious amounts of methanol to afford *oxo*-PE as a light tan powder. Mass recovery: LDPE: 2.9 g, 97%; HDPE: 3.0 g, >99%; Waste HDPE: 2.9 g, 97%. Molar yield with respect to 2,6-dichloropyridine-*N*-oxide: LDPE: 33%; HDPE: 38%; Waste HDPE: 27%.

LDPE: The degree of functionalization was determined to be 3.3% total functionalization (2.4% ketone and 0.9% alcohol) by ¹H NMR spectroscopy at 100 °C. ¹H NMR (600 MHz, C₂D₂Cl₄) δ 3.62 (br, CHOH), 2.40 (t, *J* = 7.2 Hz, CH₂C(O)CH₂), 1.62 (br), 1.35 (br), 0.98 – 0.88 (m).

HDPE: The degree of functionalization was determined to be 3.8% total functionalization (2.5% ketone and 1.3% alcohol) by ¹H NMR spectroscopy at 100 °C. ¹H NMR (600 MHz, C₂D₂Cl₄) δ 3.62 (br, CHOH), 2.40 (t, *J* = 7.2 Hz, CH₂C(O)CH₂), 1.61 (br), 1.34 (br), 0.98 – 0.88 (m).

Waste HDPE (milk jug): The degree of functionalization was determined to be 2.7% total functionalization (1.9% ketone and 0.8% alcohol) by ¹H NMR spectroscopy at 100 °C. ¹H NMR (600 MHz, C₂D₂Cl₄) δ 3.62 (br, CHOH), 2.40 (t, *J* = 7.2 Hz, CH₂C(O)CH₂), 1.62 (br), 1.35 (br), 0.98 – 0.92 (m).

Keto-PE



The synthesis of *keto-PE* was adapted from a literature procedure.¹⁹

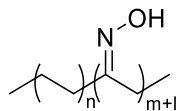
To a 250 mL Corning bottle containing a stir bar under nitrogen, 3.0 g of *Oxo-PE* (LDPE, HDPE, or waste HDPE (milk jug), 1.3% alcohol, 1.4 mmol alcohol), 42 mg of pentamethylcyclopentadienyl iridium dichloride dimer (0.052 mmol), and 19 mg of potassium carbonate (0.14 mmol) were added. The solids were suspended in 120 mL of toluene, and 2 mL of acetone (27 mmol) were added. The bottle was tightly sealed and heated at 140 °C for 48 h. The bottle was cooled slightly, and the contents were poured in 300 mL of methanol under vigorous stirring to precipitate the polymer. The slurry was filtered, and the powder was washed with copious amounts of methanol to afford *keto-PE* as a light tan powder. Mass recovery: LDPE: 2.8 g, 93%; HDPE: 2.7 g, 90%; Waste HDPE: 2.6 g, 87%.

LDPE: The degree of functionalization was determined to be 3.1% ketone by ¹H NMR spectroscopy at 100 °C. ¹H NMR (600 MHz, C₂D₂Cl₄) δ 2.40 (t, *J* = 7.2 Hz, CH₂C(O)CH₂), 1.62 (br), 1.35 (br), 0.98 – 0.88 (m).

HDPE: The degree of functionalization was determined to be 3.8% ketone by ¹H NMR spectroscopy at 100 °C. ¹H NMR (600 MHz, C₂D₂Cl₄) δ 2.40 (t, *J* = 7.2 Hz, CH₂C(O)CH₂), 1.62 (br), 1.34 (br), 0.98 – 0.92 (m).

Waste HDPE (milk jug): The degree of functionalization was determined to be 2.8% ketone by ¹H NMR spectroscopy at 100 °C. ¹H NMR (600 MHz, C₂D₂Cl₄) δ 2.40 (t, *J* = 7.2 Hz, CH₂C(O)CH₂), 1.62 (br), 1.35 (br), 0.98 – 0.92 (m).

Oxime-PE



The synthesis of *oxime-PE* was adapted from a literature procedure.¹⁹

For LDPE: To a 250 mL Corning bottle with a stir bar, 3.28 g of *keto-LDPE* (3% ketone, 3.51 mmol ketone) and 1.22 g of hydroxylamine hydrochloride (17.6 mmol) were added. The solids were suspended in 110 mL of pyridine. The bottle was heated at 100 °C for 12 h. The bottle was cooled slightly, and the contents were poured in 300 mL of methanol under vigorous stirring to precipitate the polymer. The slurry was filtered, and the powder was washed with copious amounts of methanol to afford *oxime-LDPE* as a light tan powder (2.85 g, 86%)

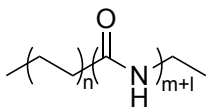
For HDPE and waste-HDPE: To a 4 mL vial with a stir bar, 25 mg of *keto-HDPE* (3% ketone, 0.027 mmol ketone) and 10 mg of hydroxylamine hydrochloride (0.14 mmol) were added. The solids were suspended in 1 mL of pyridine. The vial was heated at 120 °C for 3 h and 30 min. The vial was cooled slightly, and 3 mL of methanol were added to the vial under vigorous stirring to precipitate the polymer. The slurry was filtered, and the powder was washed with copious amounts of methanol to afford *oxime-HDPE* as a light tan powder. Mass recovery: HDPE: 21 mg, 84%; Waste HDPE: 23 g, 92%.

LDPE: The degree of functionalization was determined to be 3.1% oxime by ¹H NMR spectroscopy at 100 °C. ¹H NMR (600 MHz, C₂D₂Cl₄) δ 2.38 (t, *J* = 7.8 Hz, CH₂CNOHCH₂), 2.21 (t, *J* = 7.2 Hz, CH₂CNOHCH₂), 1.57 (br), 1.34 (br), 0.98 – 0.88 (m).

HDPE: The degree of functionalization was determined to be 3.5% oxime by ¹H NMR spectroscopy at 100 °C. ¹H NMR (600 MHz, C₂D₂Cl₄) δ 2.38 (t, *J* = 7.8 Hz, CH₂CNOHCH₂), 2.21 (t, *J* = 7.2 Hz, CH₂CNOHCH₂), 1.57 (br), 1.35 (br), 0.98 – 0.88 (m).

Waste HDPE (milk jug): The degree of functionalization was determined to be 2.4% oxime by ¹H NMR spectroscopy at 100 °C. ¹H NMR (600 MHz, C₂D₂Cl₄) δ 2.38 (t, *J* = 7.8 Hz, CH₂CNOHCH₂), 2.21 (t, *J* = 7.2 Hz, CH₂CNOHCH₂), 1.57 (br), 1.34 (br), 0.98 – 0.92 (m).

Nylon-PE



For LDPE: To a 250 mL Corning bottle with a stir bar, 1.00 g of *oxime*-LDPE (3% oxime, 3.2 mmol oxime) were added. The solids were suspended in 100 mL of THF. The flask was heated at 80 °C until the polymer dissolved. The bottle was cooled to room temperature, and 5.7 mL of a propanephosphonic acid anhydride in ethyl acetate (1.7 M, 9.6 mmol) solution were added to the bottle. The bottle was tightly sealed and heated at 80 °C for 24 h. The bottle was cooled slightly, and the contents were poured in 300 mL of methanol under vigorous stirring to precipitate the polymer. The slurry was filtered, and the powder was washed with copious amounts of methanol to afford *nylon*-LDPE as a light tan powder (830 mg, 83%).

For HDPE and waste-HDPE: To a 20 mL vial with a stir bar, 75 mg of *oxime*-HDPE (3% oxime, 0.081 mmol oxime) were added. The solids were suspended in 3 mL of THF. The vial was heated at 80 °C until the polymer dissolved. The vial was cooled to room temperature, and 144 μ L of a propanephosphonic acid anhydride in ethyl acetate (1.7 M, 0.24 mmol) solution were added to the vial. The vial was tightly sealed and heated at 120 °C for 5 min and then at 80 °C for 24 h. The vial was cooled slightly, and 16 mL of methanol was added to the vial under vigorous stirring to precipitate the polymer. The slurry was filtered, and the powder was washed with copious amounts of methanol to afford *nylon*-HDPE as a light tan powder. Mass recovery: HDPE: 60 mg, 80%; Waste HDPE: 54 mg, 72%.

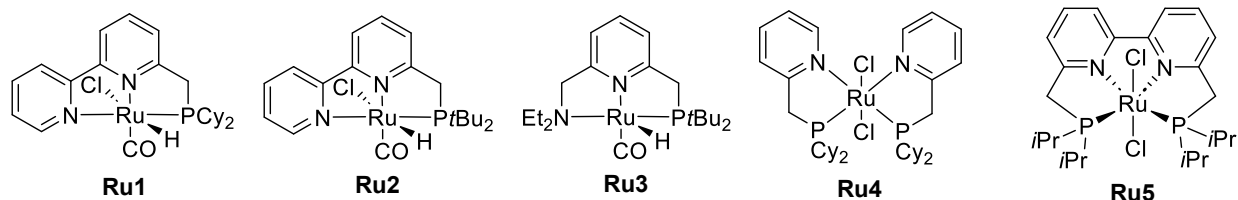
LDPE: The degree of functionalization was determined to be 2.2% amide by ^1H NMR spectroscopy at 100 °C. ^1H NMR (600 MHz, $\text{C}_2\text{D}_2\text{Cl}_4$) δ 5.28 (br, $\text{CH}_2\text{C}(\text{O})\text{NHCH}_2$), 3.30 – 3.20 (m, $\text{CH}_2\text{C}(\text{O})\text{NHCH}_2$), 2.17 (t, $J = 7.5$ Hz, $\text{CH}_2\text{C}(\text{O})\text{NHCH}_2$), 1.66 (m), 1.54 (br), 1.35 (br), 0.98 – 0.88 (m). ^{13}C NMR (151 MHz, $\text{C}_2\text{D}_2\text{Cl}_4$) δ 172.4 ($\text{CH}_2\text{C}(\text{O})\text{NHCH}_2$), 42.5, 39.4, 37.5, 36.6, 35.1, 33.9, 33.5, 32.1, 31.6, 30.1, 29.9, 29.6, 29.4, 29.4, 29.3, 29.3, 29.2, 29.1, 29.1, 29.0, 28.9, 28.5, 26.7, 26.7, 26.3, 25.5, 23.8, 23.4, 23.3, 22.8, 22.3, 13.7, 13.7.

HDPE: The degree of functionalization was determined to be 3.0% amide by ^1H NMR spectroscopy at 100 °C. ^1H NMR (600 MHz, $\text{C}_2\text{D}_2\text{Cl}_4$) δ 5.29 (br, $\text{CH}_2\text{C}(\text{O})\text{NHCH}_2$), 3.30 – 3.20 (m, $\text{CH}_2\text{C}(\text{O})\text{NHCH}_2$), 2.17 (t, $J = 7.5$ Hz, $\text{CH}_2\text{C}(\text{O})\text{NHCH}_2$), 1.66 (m), 1.54 (br), 1.35 (br), 1.09 (m), 0.98 – 0.88 (m).

Waste HDPE (milk jug): The degree of functionalization was determined to be 2.5% amide by ^1H NMR spectroscopy at 100 °C. ^1H NMR (600 MHz, $\text{C}_2\text{D}_2\text{Cl}_4$) δ 5.26 (br, $\text{CH}_2\text{C}(\text{O})\text{NHCH}_2$), 3.30 – 3.20 (m, $\text{CH}_2\text{C}(\text{O})\text{NHCH}_2$), 2.17 (t, $J = 7.5$ Hz, $\text{CH}_2\text{C}(\text{O})\text{NHCH}_2$), 1.66 (m), 1.54 (br), 1.35 (br), 1.24 (m), 1.10 (m), 0.98 – 0.88 (m).

4.7.6 Hydrogenolysis of Polymers

4.7.6.1 Synthesis of Catalysts



Complex **Ru1** was synthesized according to literature procedure.²⁹ Complex **Ru2** was synthesized according to literature procedure.²⁶ Complex **Ru3** was synthesized according to literature procedure.³⁵ Complex **Ru4** was synthesized according to literature procedure.²⁸ Complex **Ru5** was synthesized according to literature procedure.²⁷

4.7.6.2 Hydrogenolysis of Nylon-PE with Ruthenium Catalysts

To a 20 mL glass liner with a stir bar were added 50 mg of *nylon*-PE (2.0% amide, 0.036 mmol), a corresponding amount of ruthenium catalyst, and a corresponding amount of base. The solids were suspended in 2 mL of solvent. The glass liner was placed in a Parr reactor (25 mL internal volume), and the reactor was sealed under nitrogen. The reactor was charged with hydrogen and heated for an allotted time. The reactor was then cooled to room temperature, and the reactor was depressurized slowly and opened. The liner was reheated to dissolve the polymer, and methanol was added to precipitate the polymer. The slurry was filtered to afford the product. The extent of hydrogenolysis of the amide linkages was assessed by ¹H NMR spectroscopy. The conditions and result for each reaction performed are summarized in Table 4.7.6.2.1.

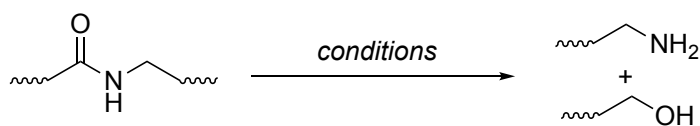
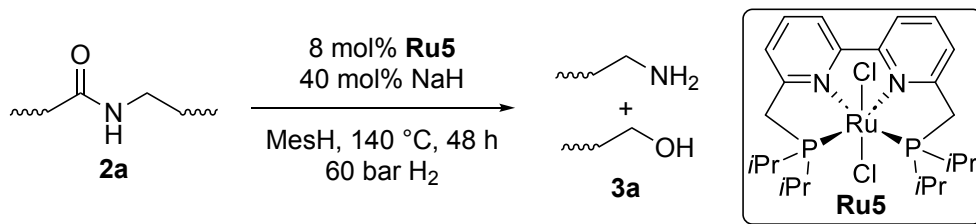


Table 4.7.6.2.1. Conditions for the hydrogenolysis of nylon-LDPE with ruthenium catalysts.

Entry	Catalyst ^a	P _{H2} (bar)	Temp (°C)	Base	Conversion (%) ^f
1 ^{b,d}	4 mol% Ru1	50	120	20 mol% KOtBu	52
2 ^{b,d}	4 mol% Ru2	50	120	20 mol% KOtBu	n.r.
3 ^{b,d}	4 mol% Ru3	50	120	20 mol% KOtBu	86
4 ^{c,e}	5 mol% Ru4	80	150	20 mol% 2-methyl-2-adamantanol, 20 mol% NaH	14
5 ^{c,d}	5 mol% Ru5	40	130	20 mol% NaH	15
6 ^{c,e}	5 mol% Ru5	40	130	20 mol% NaH	>99

^aCatalyst loading with respect to equivalents of amide. ^bReaction run in THF. ^cReaction run in PhMe. ^dReaction run for 24 h. ^eReaction run for 48 h. ^fConversion of amides as determined by ¹H NMR spectroscopy in CDCl₃ at room temperature.



4.7.6.3 Procedure for the Large Scale Hydrogenolysis of Nylon-LDPE with Ru5

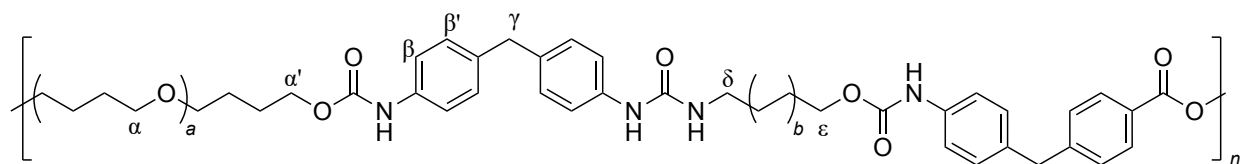
To a 300 mL glass liner with a stir bar were added 1.5 g of *nylon*-LDPE (2% amide, 1.1 mmol), 48 mg of **Ru5** (0.082 mmol), and 9.0 mg of sodium hydride (0.38 mmol). The solids were suspended in 40 mL of mesitylene. The bottle was placed in a Parr reactor (300 mL internal volume), and the reactor was sealed under nitrogen. The reactor was charged with 60 bar of hydrogen and heated at 140 °C for 48 h. The reactor was then cooled to room temperature, and the reactor was depressurized slowly and opened. The liner was reheated to dissolve the polymer, and methanol was added to precipitate the polymer. The slurry was filtered to afford the product as a brown powder. The extent of hydrogenolysis of the amide linkages was quantitative as assessed by ^1H NMR spectroscopy at 100 °C.

Hydrogenolysis of *nylon*-LDPE: The degree of functionalization was determined to be 2.6% total functionalization (1.6% alcohol and 1.1% amine) by ^1H NMR spectroscopy at 100 °C. ^1H NMR (600 MHz, $\text{C}_2\text{D}_2\text{Cl}_4$) δ 3.66 (t, $J = 6.6$ Hz, CH_2OH), 3.05 (br, CH_2NH_2), 1.62 (br), 1.35 (br), 1.00 – 0.89 (m). ^{13}C NMR (151 MHz, $\text{C}_2\text{D}_2\text{Cl}_4$) δ 42.5, 33.9, 29.9, 29.4, 29.2, 29.1, 26.7, 23.8, 22.8, 22.4, 13.7. ^{13}C NMR (151 MHz, $\text{C}_2\text{D}_2\text{Cl}_4$) δ 62.8 (CH_2OH), 39.8 (CH_2NH_2), 37.5, 33.9, 33.5, 32.7, 32.1, 31.6, 29.9, 29.5, 29.4, 29.3, 29.2, 29.2, 29.0, 28.9, 28.8, 27.5, 26.7, 26.4, 25.6, 25.4, 22.8, 22.3, 13.7, 13.7.

Hydrogenolysis of *nylon*-HDPE: The degree of functionalization was determined to be 4.1% total functionalization (2.3% alcohol and 1.8% amine) by ^1H NMR spectroscopy at 100 °C. ^1H NMR (600 MHz, $\text{C}_2\text{D}_2\text{Cl}_4$) δ 3.66 (t, $J = 6.6$ Hz, CH_2OH), 3.03 (br, CH_2NH_2), 1.62 (br), 1.35 (br), 1.00 – 0.92 (m).

Hydrogenolysis of *nylon*-Waste HDPE (milk jug): The degree of functionalization was determined to be 2.1% total functionalization (1.4% alcohol and 0.7% amine) by ^1H NMR spectroscopy at 100 °C. ^1H NMR (600 MHz, $\text{C}_2\text{D}_2\text{Cl}_4$) δ 3.67 (t, $J = 6.6$ Hz, CH_2OH), 3.06 (br, CH_2NH_2), 1.62 (br), 1.35 (br), 1.00 – 0.91 (m).

4.7.7 Synthesis of Polyurea-Urethane 4



To a 20 mL vial with a stir bar under nitrogen were added 535 mg of poly(tetrahydrofuran) ($M_n = 1000$ Da, 0.54 mmol) and 161 mg of methylene diphenyldiisocyanate (0.64 mmol). The solids were suspended in 4 mL of THF, and the vial was heated at 80 °C for 3 h. The vial was cooled to room temperature. Then 75 mg of alcohol-amine-LDPE (0.11 mmol amine and alcohol) and 12.5 mg of tin(II) 2-ethylhexanoate (0.03 mmol) were added to the vial under nitrogen. The solids were further diluted with the addition of 4 mL of THF, and the vial was heated at 100 °C overnight. The viscous reaction mixture was poured into 200 mL of methanol under rigorous stirring to precipitate the polymer. The resulting solid was filtered and washed with copious amounts of methanol and dried under high vacuum at 80 °C overnight. The polymer was collected as a stringy yellow solid (664 mg). The polymer was unable to be characterized by SEC because of its insolubility in THF at 35 °C, DMF at 55 °C, or 1,2,4-trichlorobenzene at 135 °C.

^1H NMR (600 MHz, $\text{C}_2\text{D}_2\text{Cl}_4$) δ 7.32 (d, $J = 8.0$ Hz, H_β), 7.16 (d, $J = 8.0$ Hz, $\text{H}_{\beta'}$), 6.56 (s, H_γ), 4.22 (t, $J = 6.8$ Hz, H_ϵ), 3.94 (br, $\text{H}_{\alpha'}$), 3.46 (br, H_α), 1.80 (br, H_δ), 1.72 – 1.58 (m), 1.50 (br), 1.43 – 1.24 (m), 0.96 (br).

^{13}C NMR (151 MHz, $\text{C}_2\text{D}_2\text{Cl}_4$) δ 154.7, 153.5, 136.2, 136.1, 129.2, 119.2, 70.5, 70.4, 69.9, 65.1, 40.4, 29.4, 26.5, 26.2, 25.9.

4.7.8 Characterization of Compounds

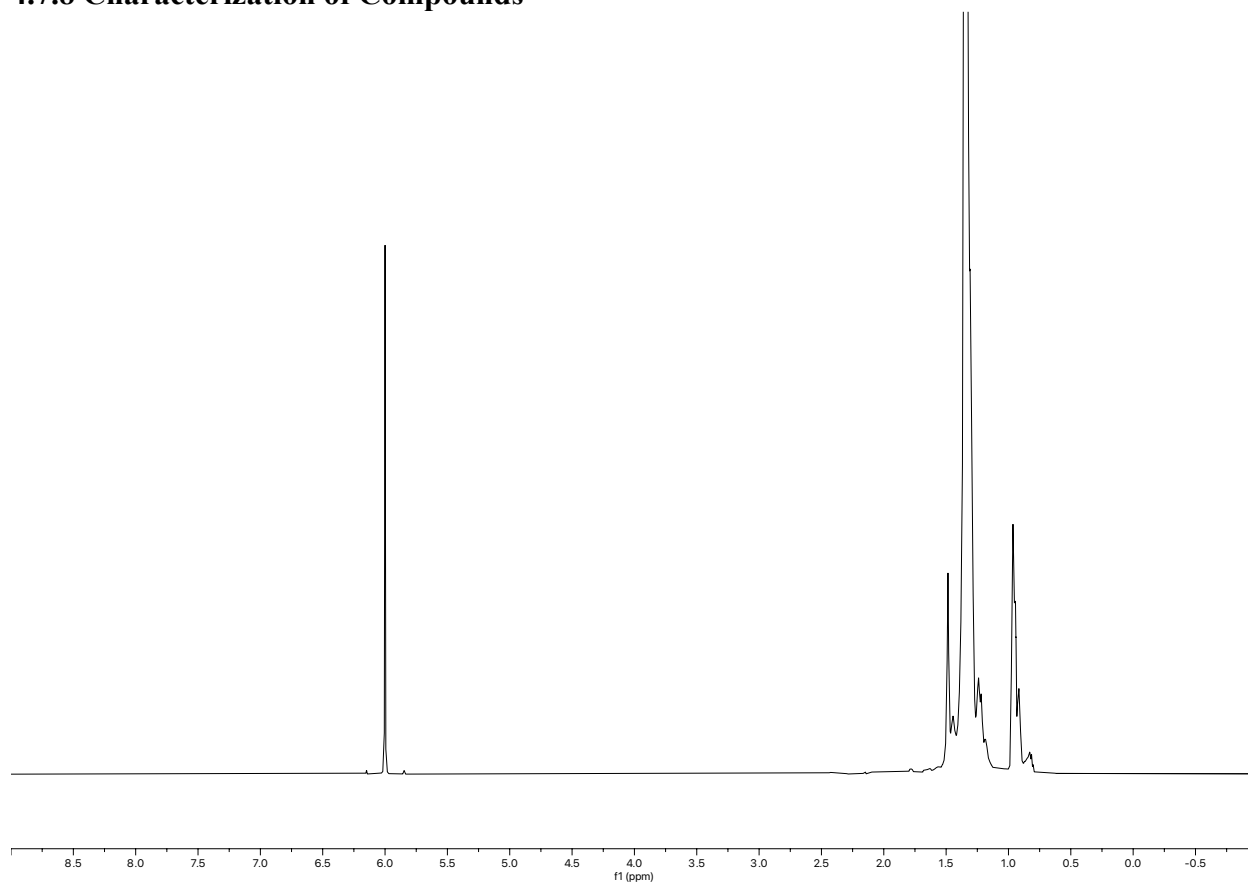


Figure 4.7.8.1. ¹H NMR spectra of unmodified LDPE.

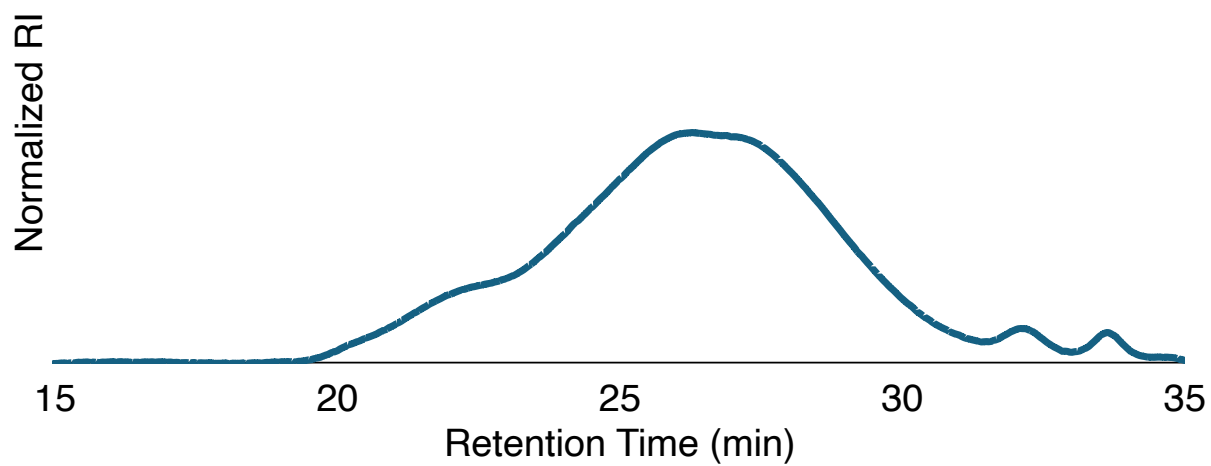


Figure 4.7.8.2. Size exclusion chromatogram of unmodified LDPE. $M_n = 9.6$ kDa, $\mathcal{D} = 6.7$. Molecular weight was determined relative to polyethylene standards.

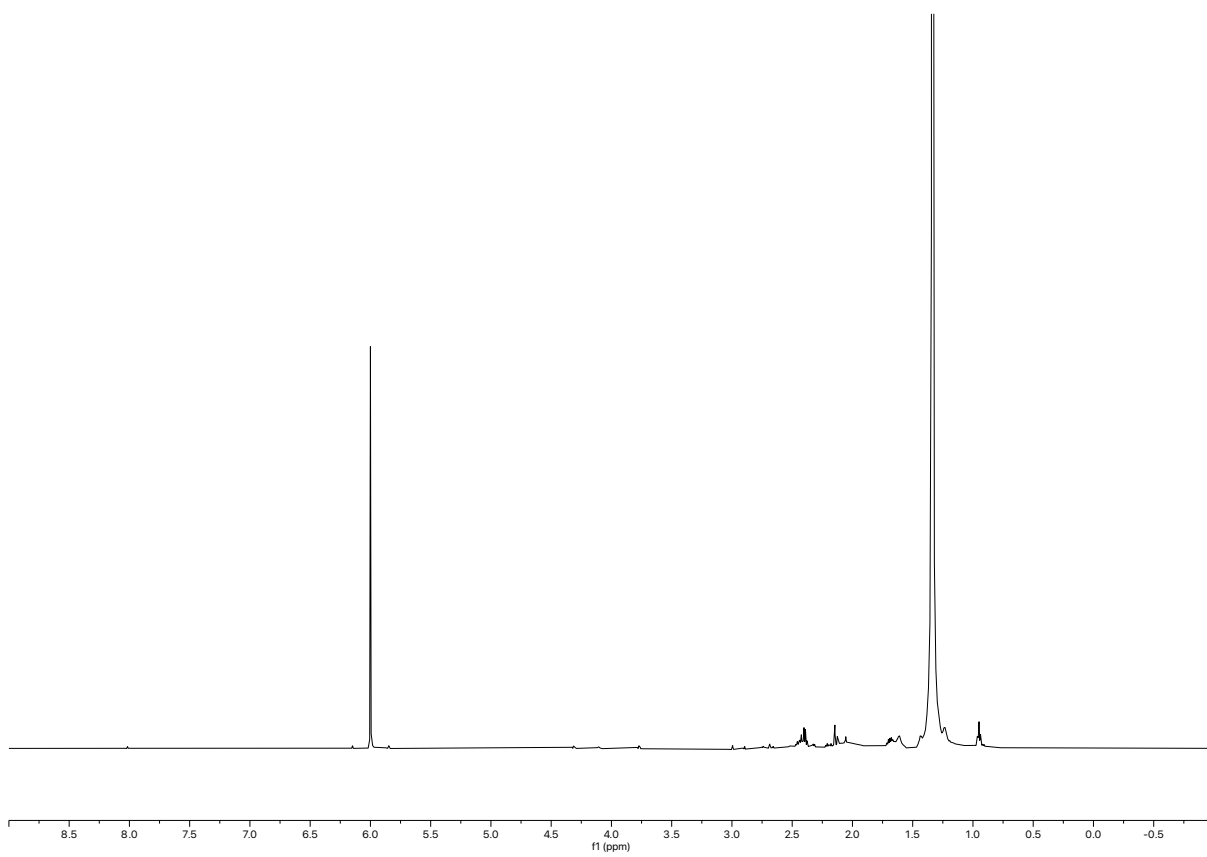


Figure 4.7.8.3. ^1H NMR spectra of unmodified HDPE.

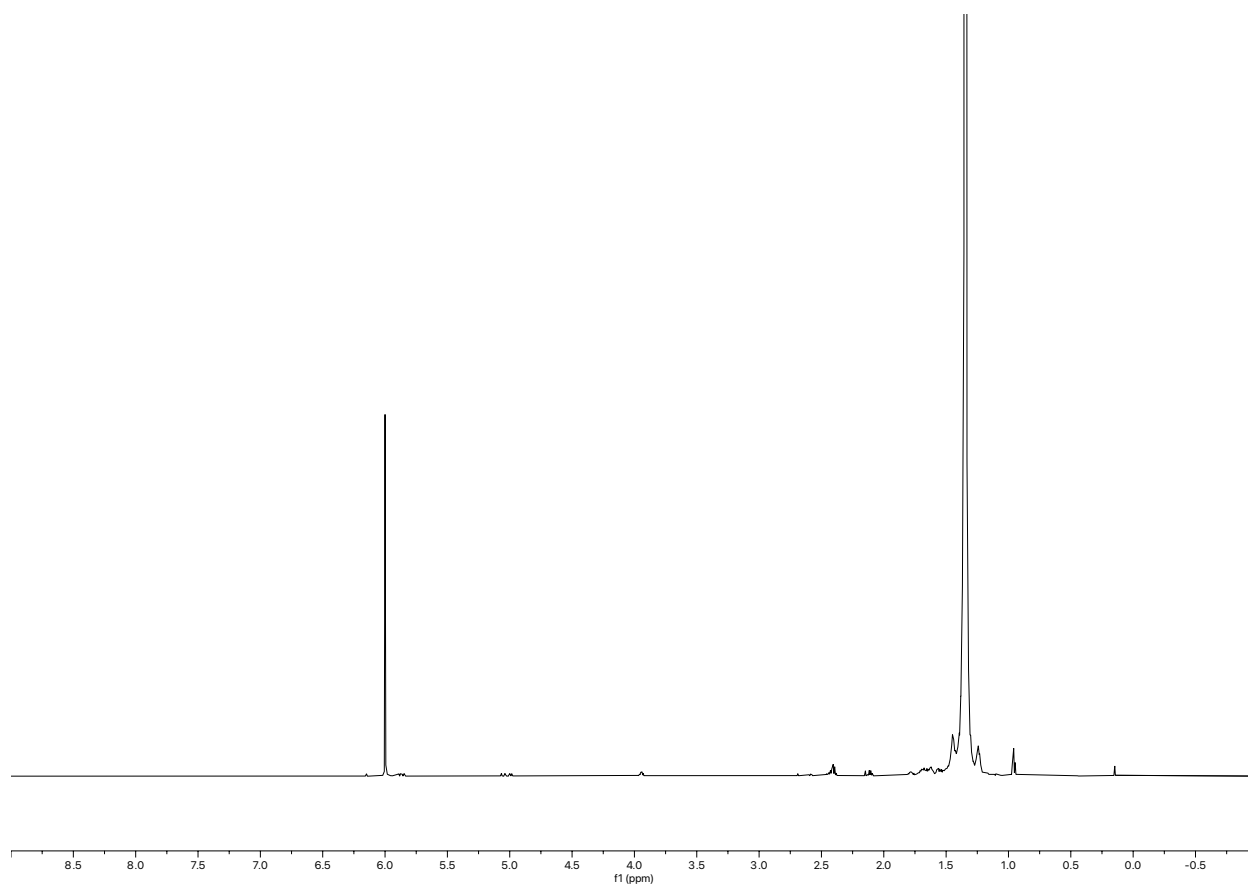


Figure 4.7.8.4. ^1H NMR spectra of unmodified waste-HDPE (milk jug).

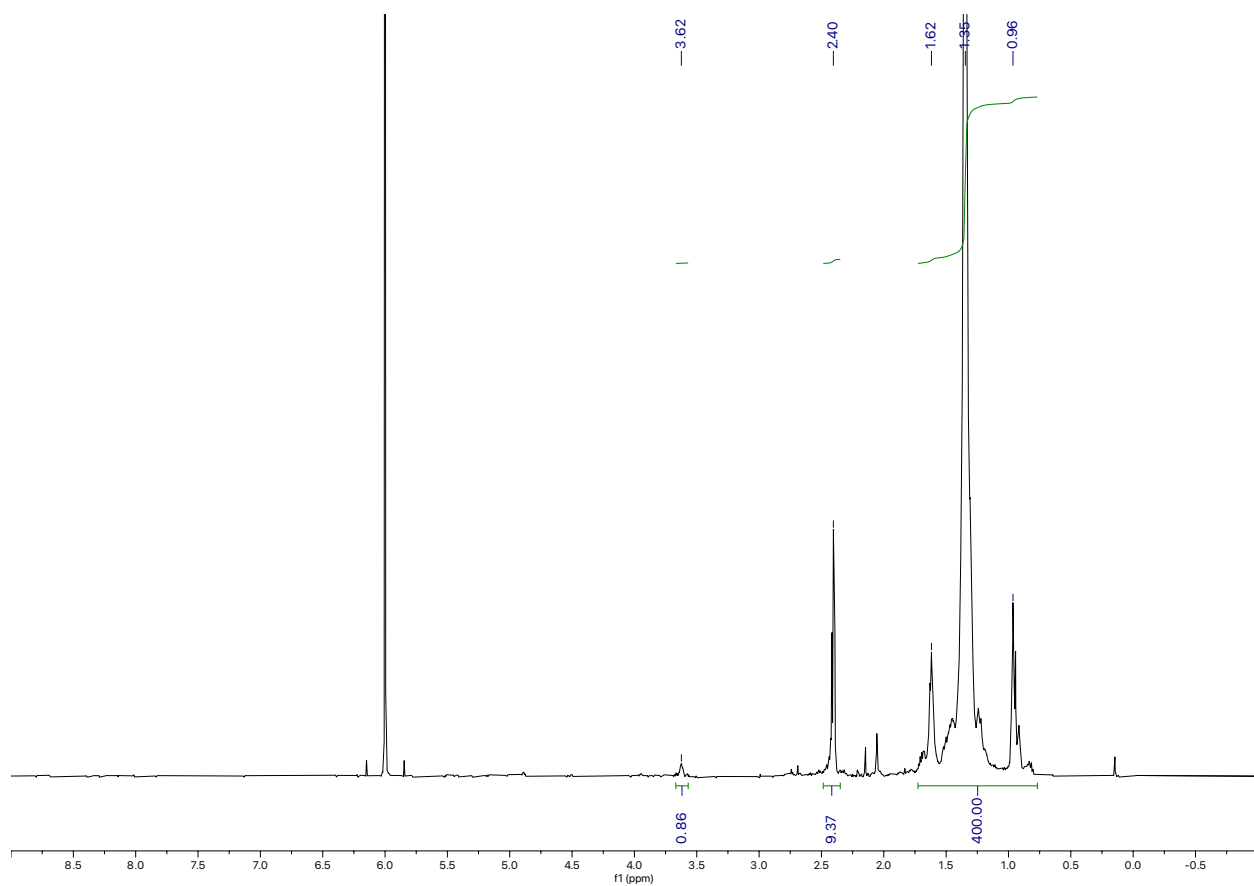


Figure 4.7.8.5. ^1H NMR spectra of *oxo*-LDPE.

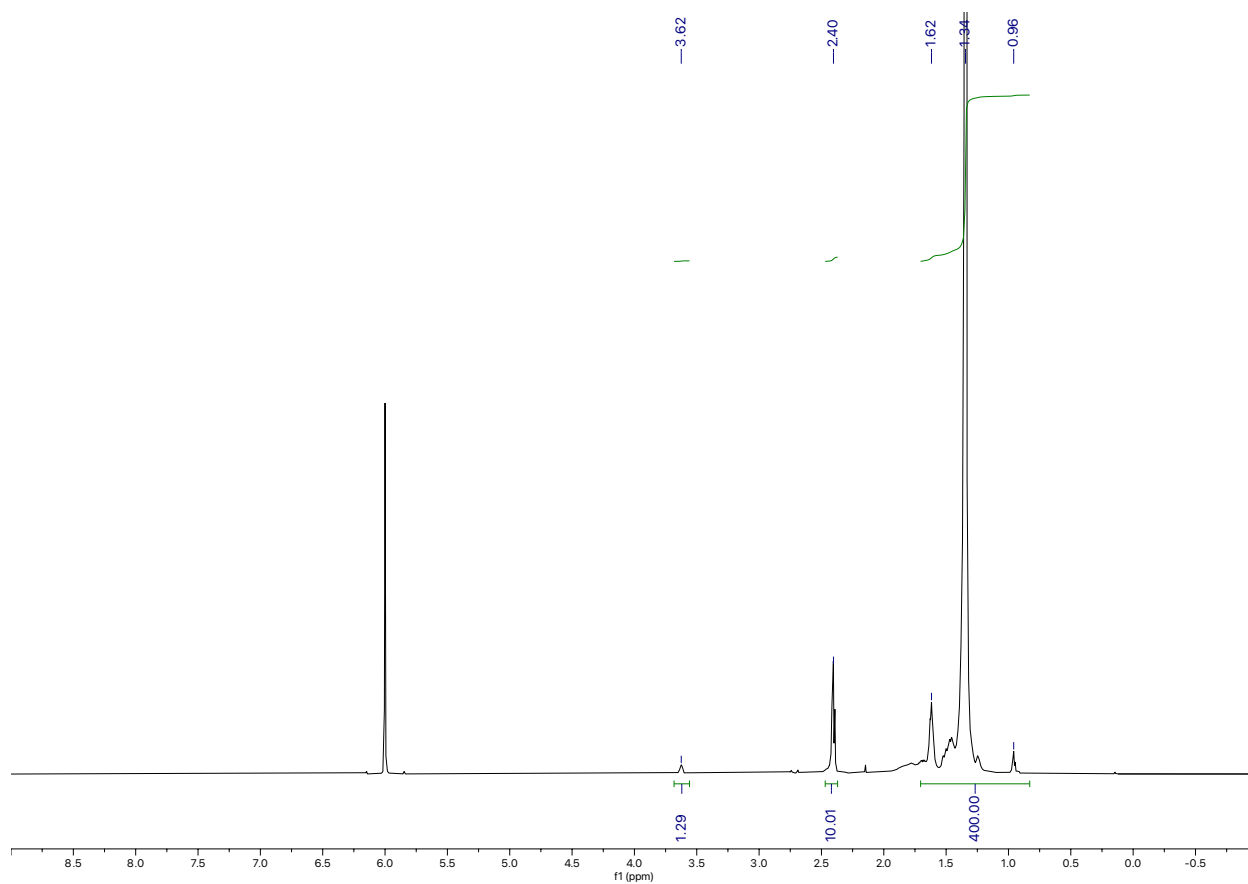


Figure 4.7.8.6. ^1H NMR spectra of *oxo*-HDPE.

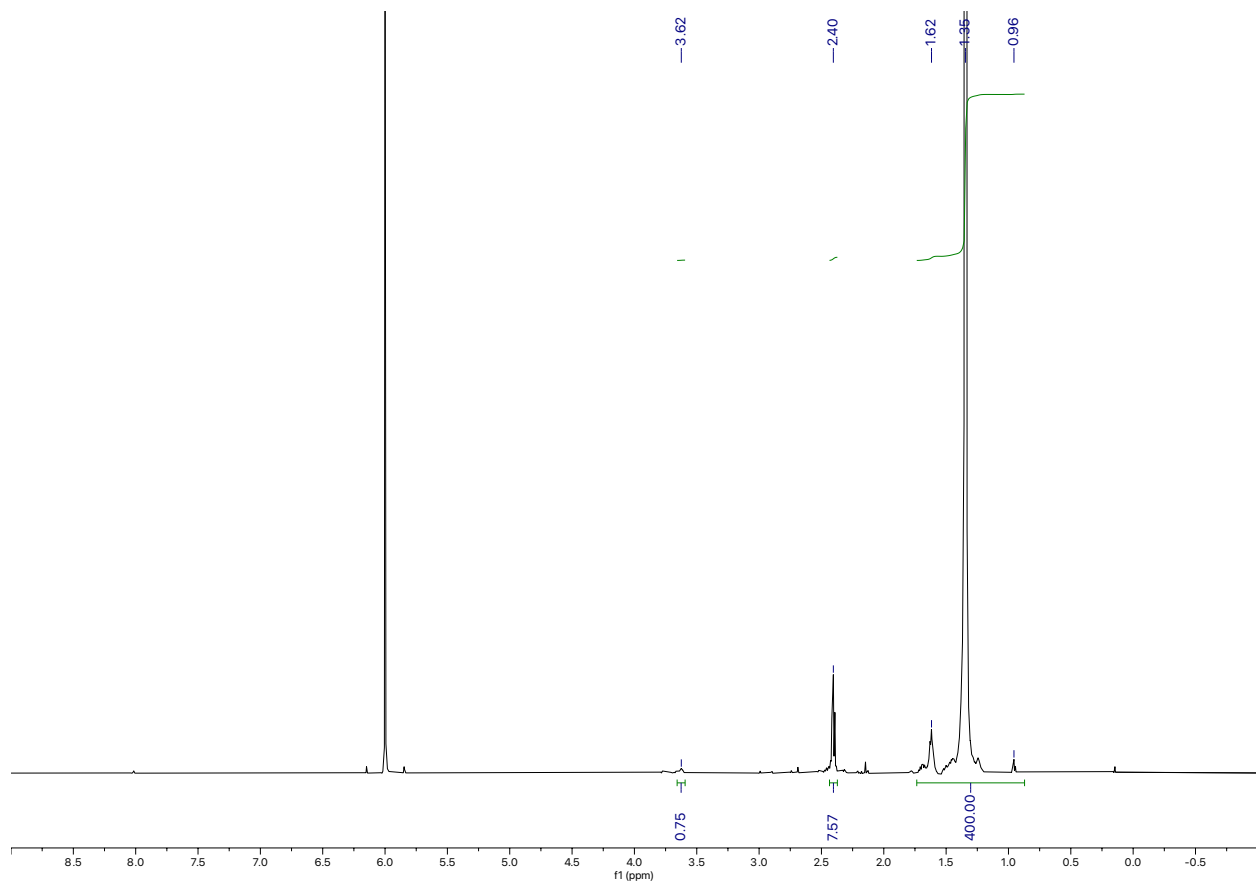


Figure 4.7.8.7. ¹H NMR spectra of *oxo*-waste-HDPE (milk jug).

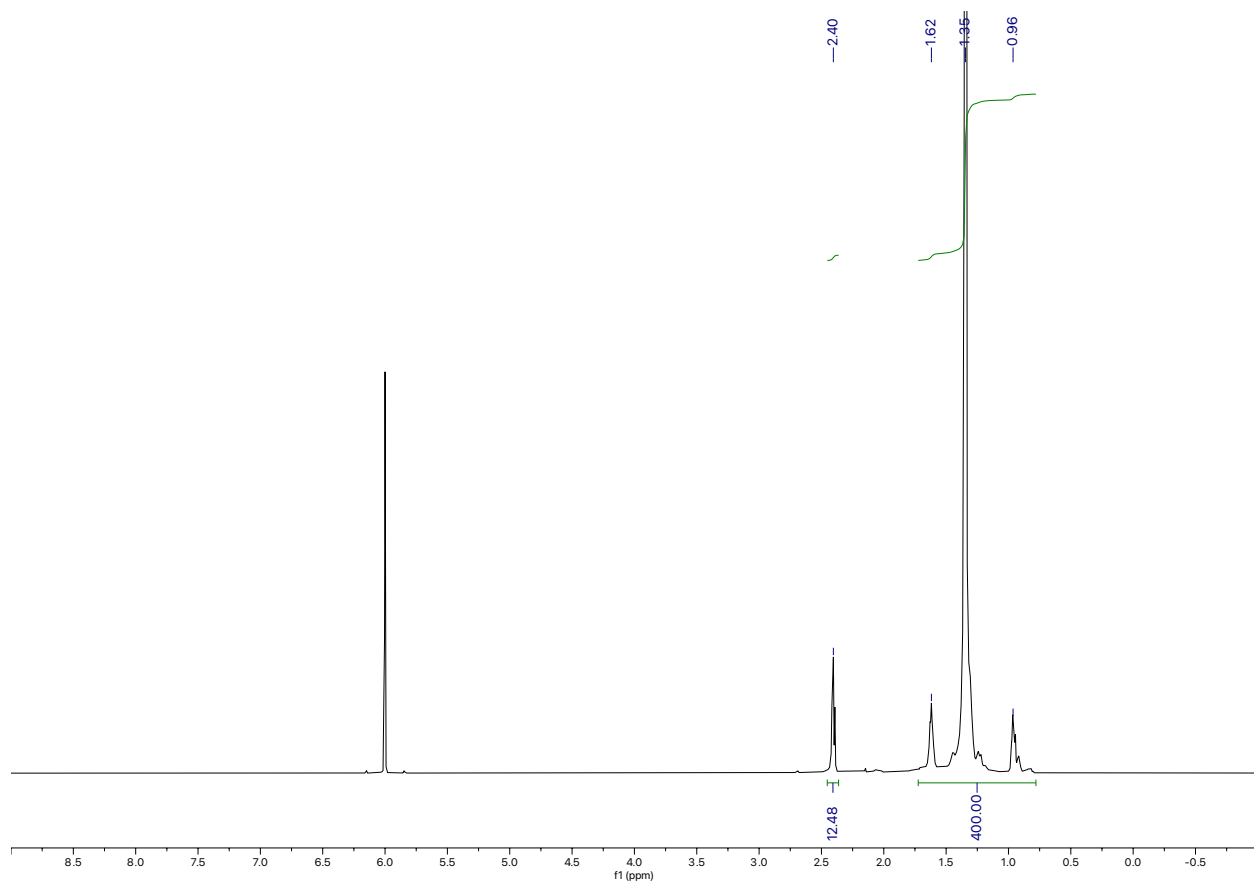


Figure 4.7.8.8. ^1H NMR spectra of *keto*-LDPE.

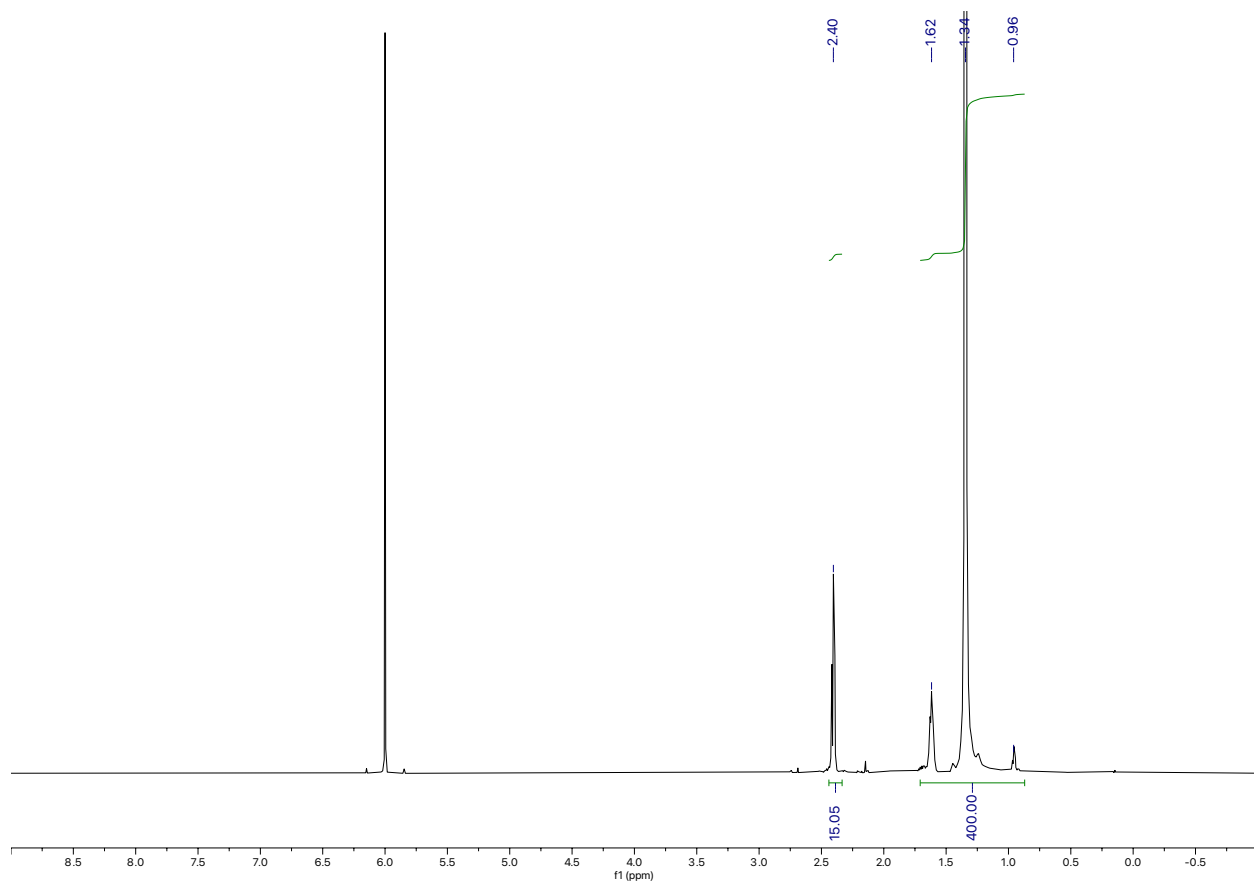


Figure 4.7.8.9. ¹H NMR spectra of *keto*-HDPE.

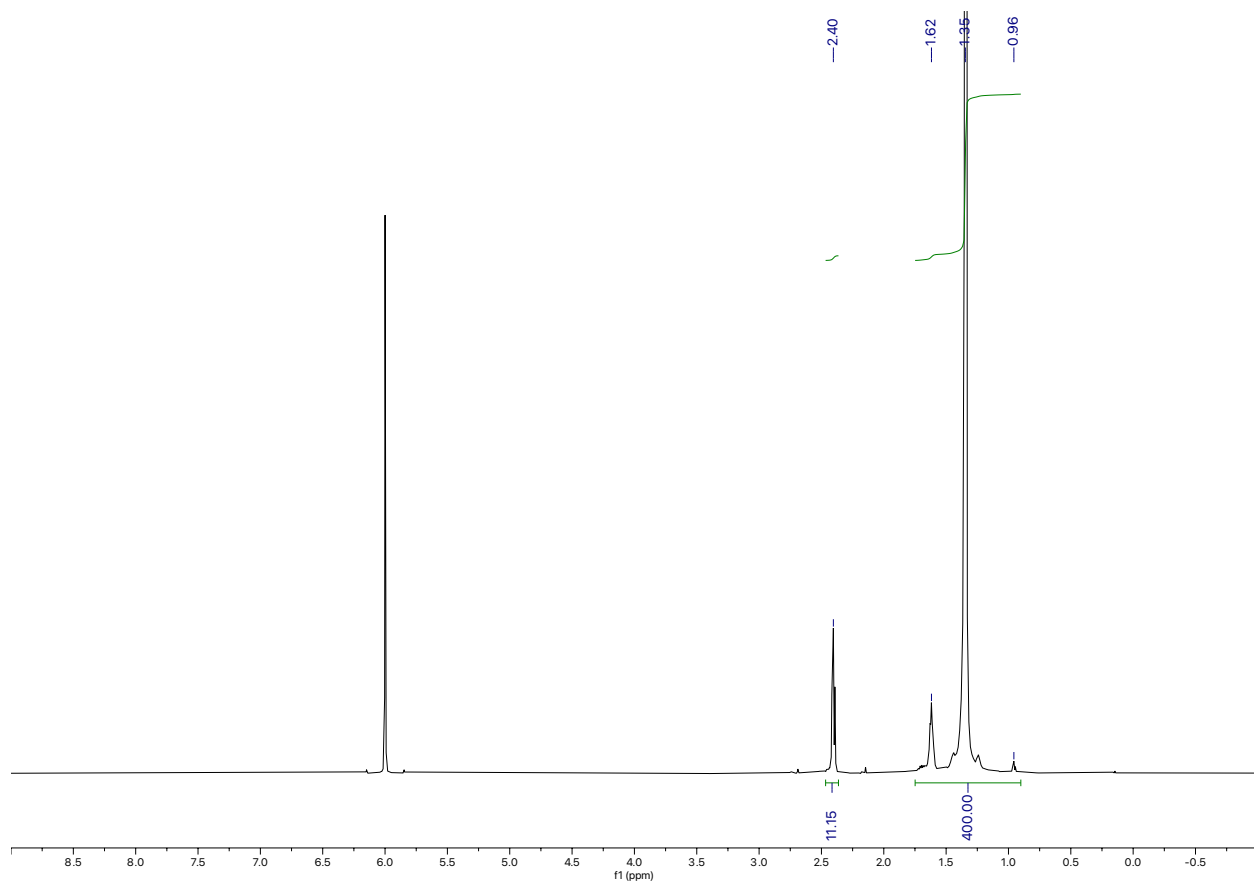


Figure 4.7.8.10. ¹H NMR spectra of *keto-waste*-HDPE (milk jug).

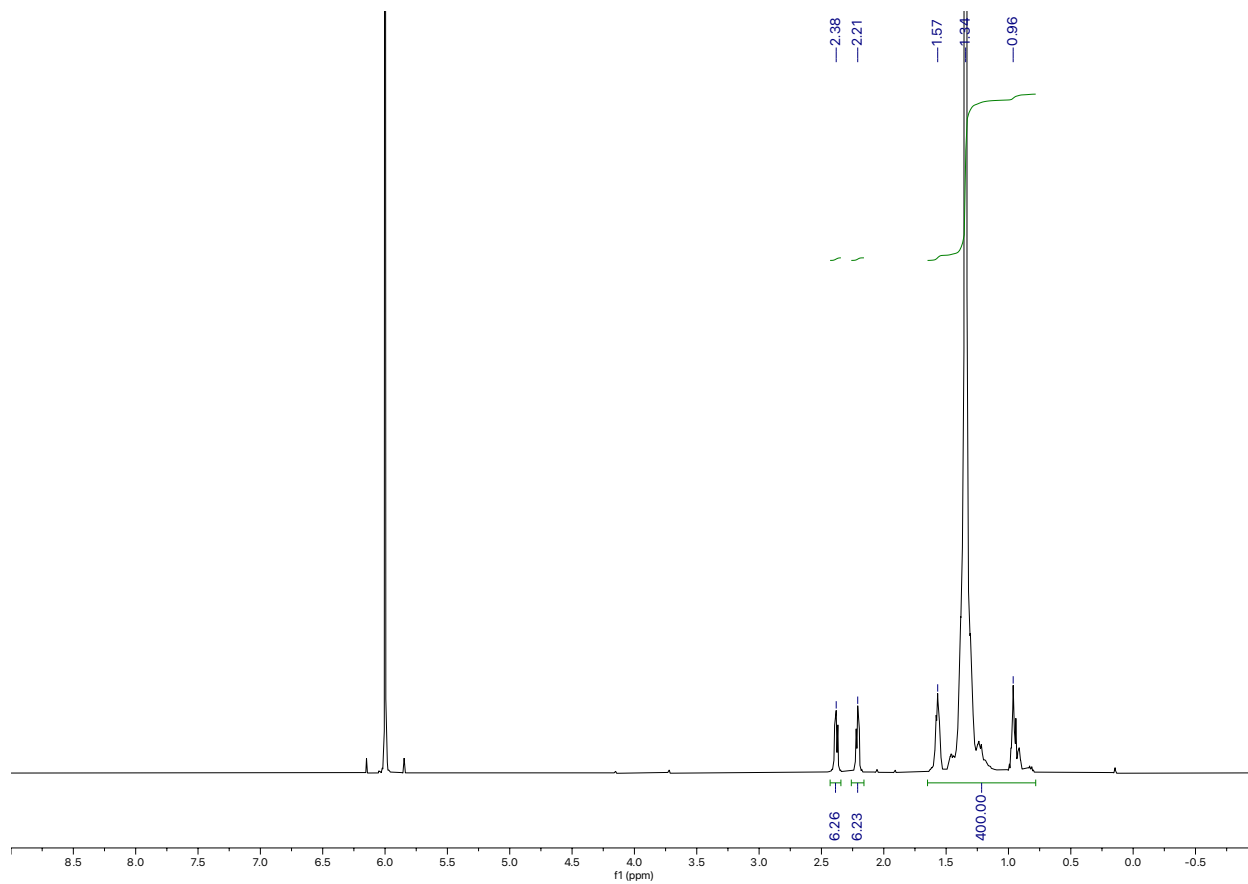


Figure 4.7.8.11. ¹H NMR spectra of *oxime*-LDPE.

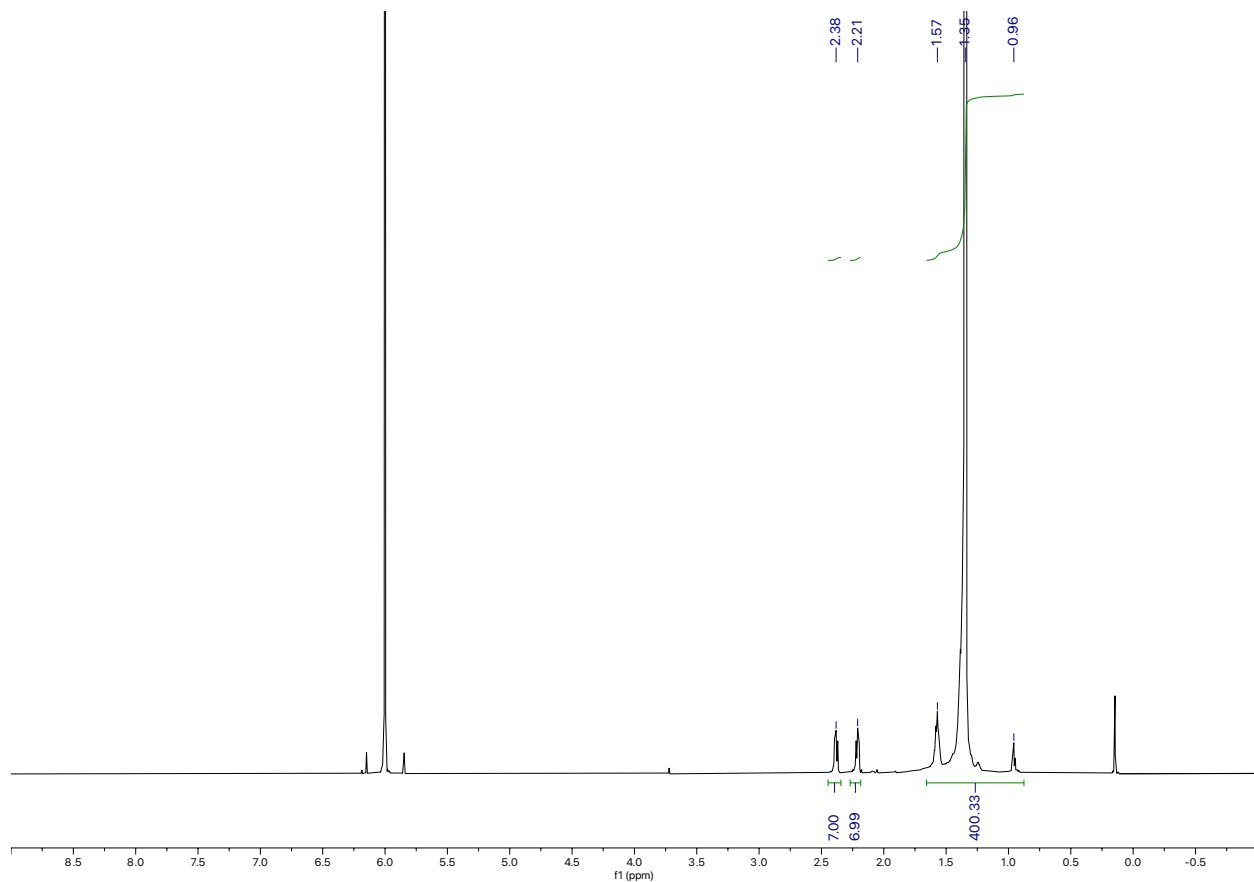


Figure 4.7.8.12. ¹H NMR spectra of *oxime*-HDPE.

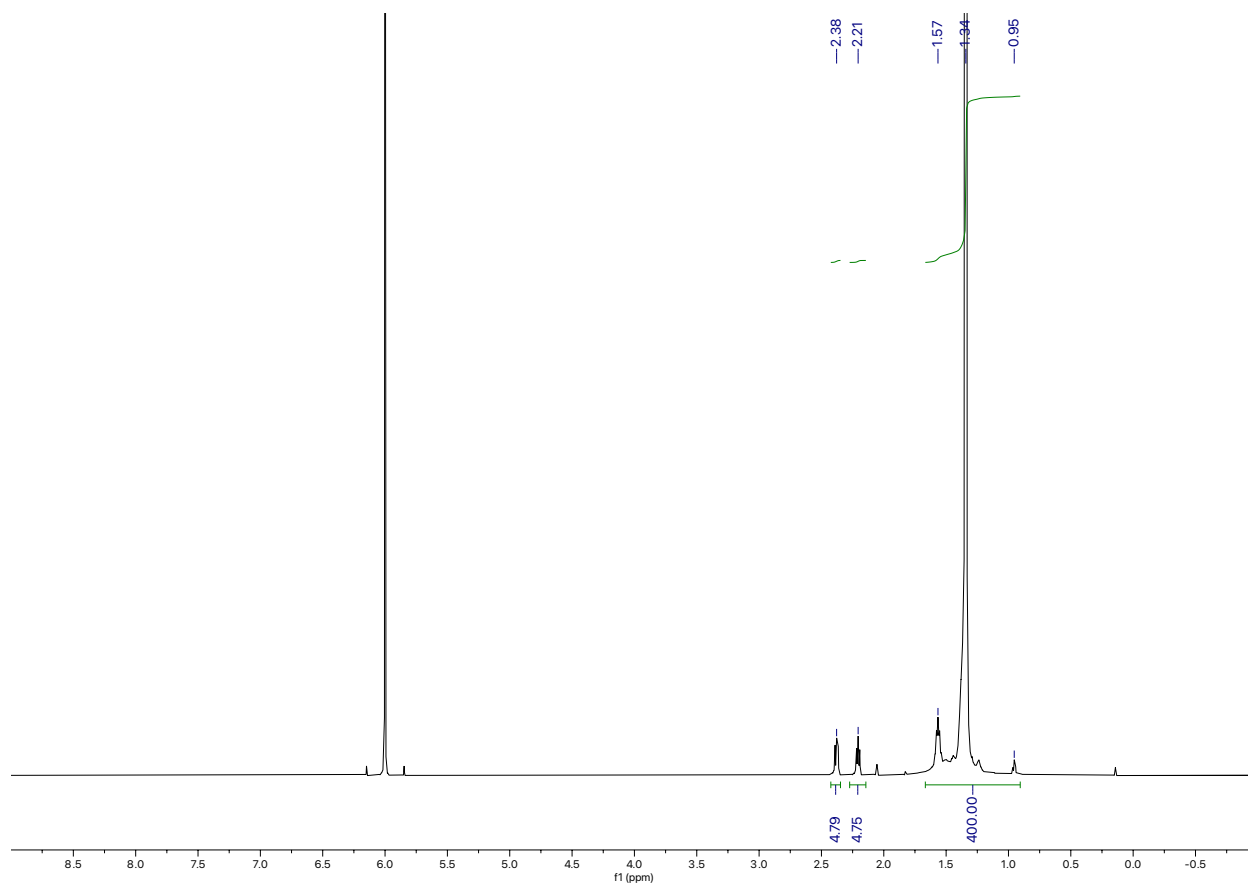


Figure 4.7.8.13. ^1H NMR spectra of *oxime-waste*-HDPE (milk jug).

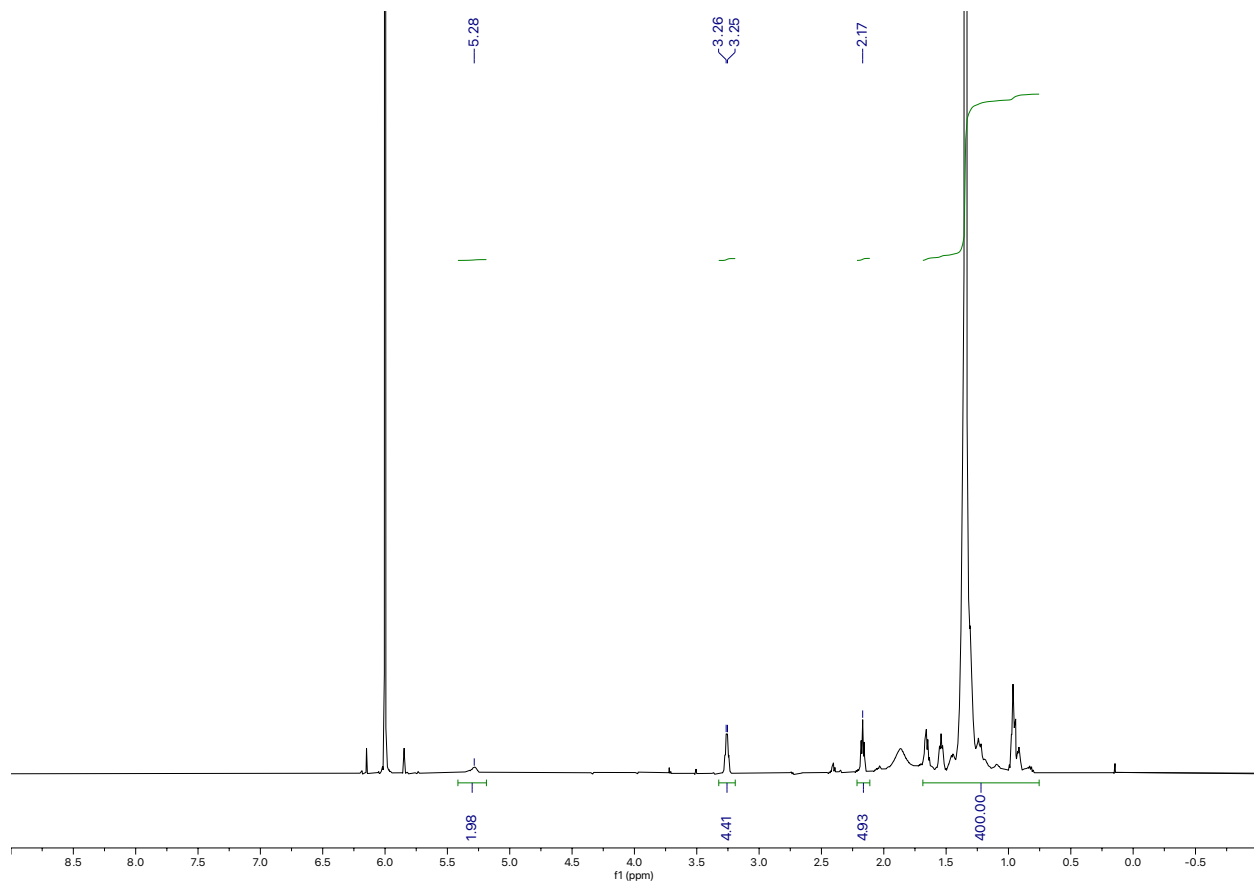


Figure 4.7.8.14. ^1H NMR spectra of *nylon-LDPE 2a*.

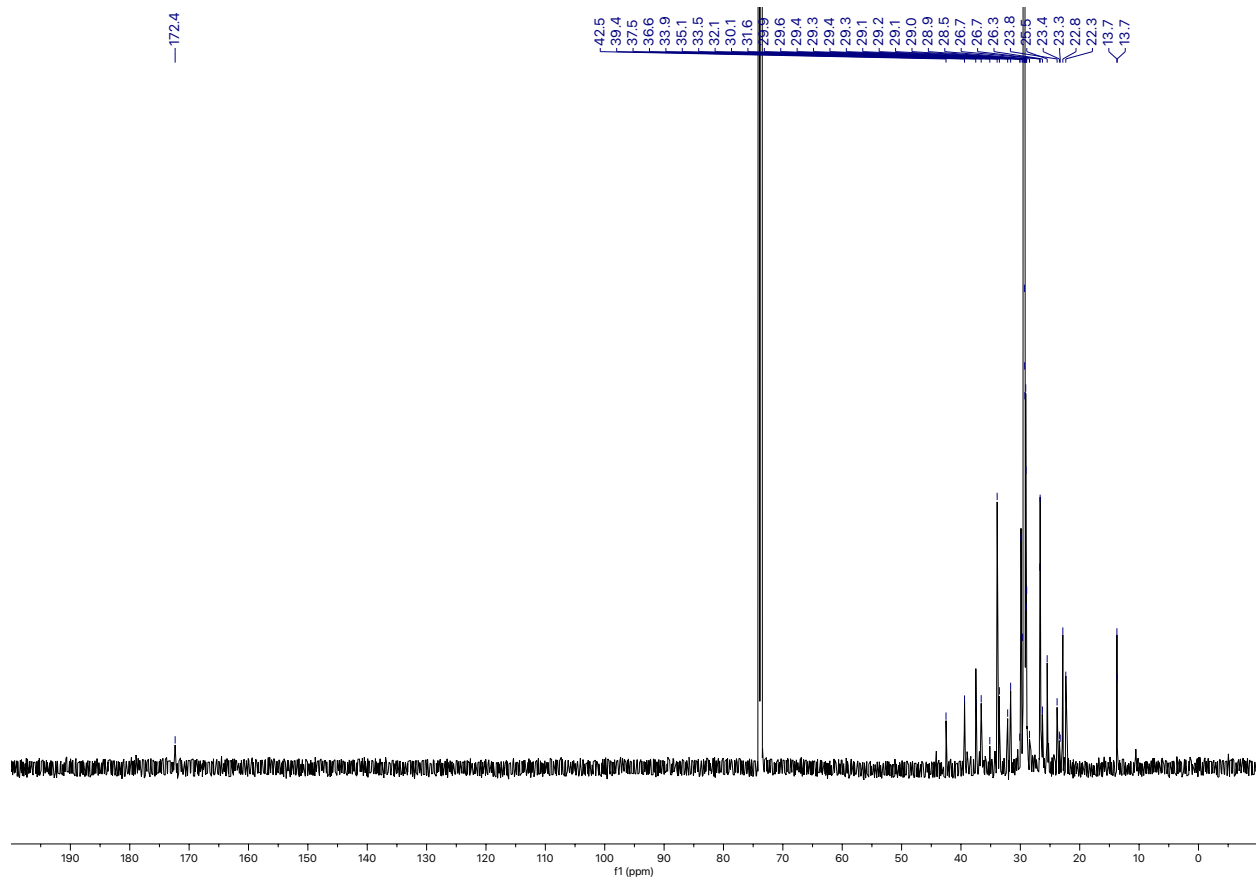


Figure 4.7.8.15. ^{13}C NMR spectra of *nylon*-LDPE 2a.

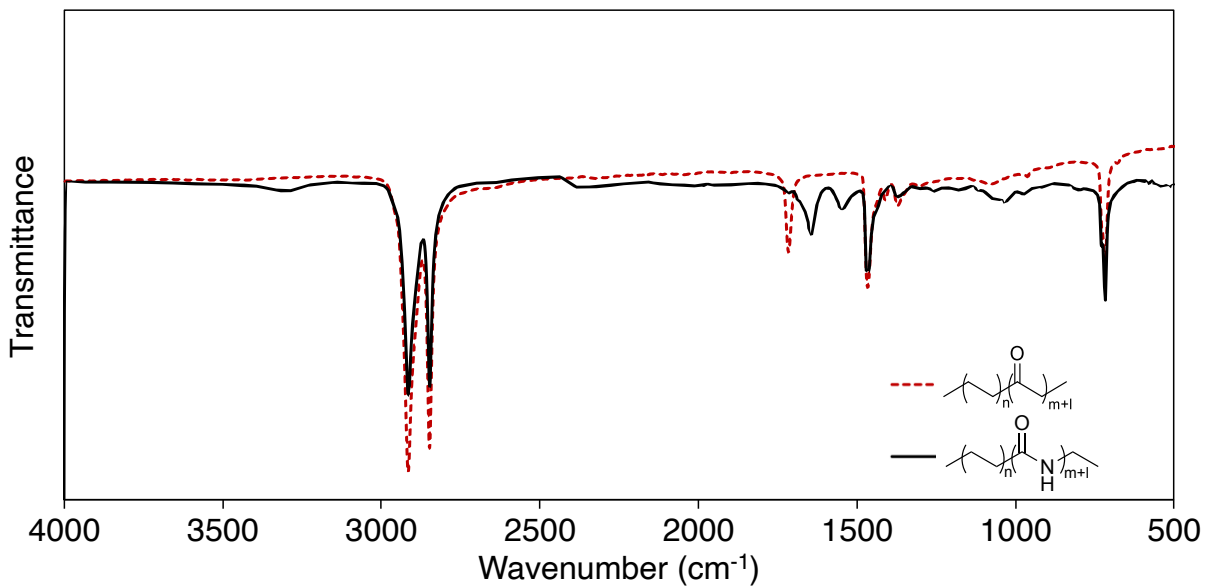


Figure 4.7.8.16. Overlay of the FTIR spectra of *nylon*-LDPE **2a**, major peaks ν (cm⁻¹): 3305, 2915, 2848, 1645, 1548, 1464, 1370, 1261, 1035, 729, 718, and the FTIR spectra of *keto*-LDPE, major peaks ν (cm⁻¹): 2916, 2849, 1717, 1467, 1412, 1373, 1084, 719.

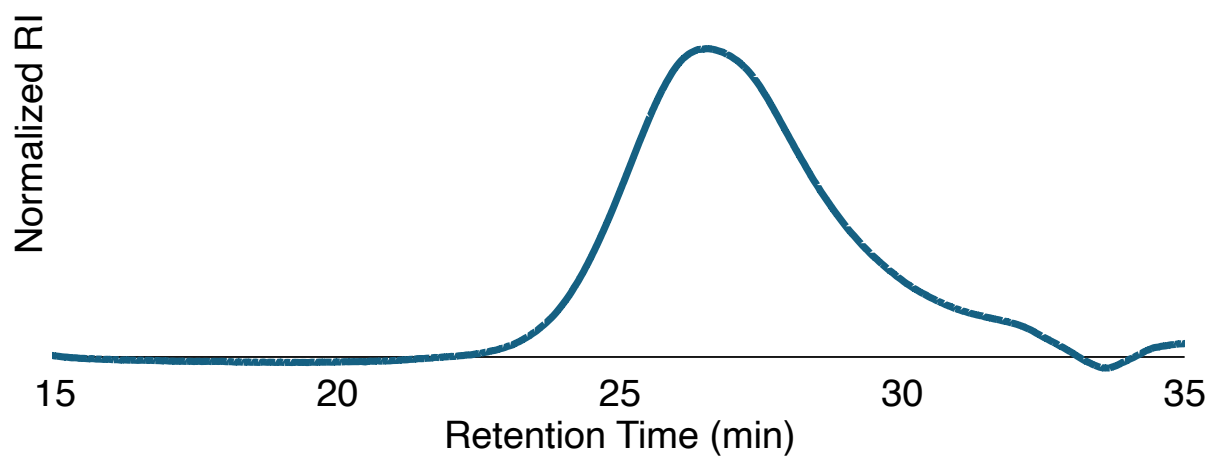


Figure 4.7.8.17. Size exclusion chromatogram of *nylon-LDPE 2a*. $M_n = 8.1$ kDa, $D = 2.4$. Molecular weight was determined relative to polyethylene standards.

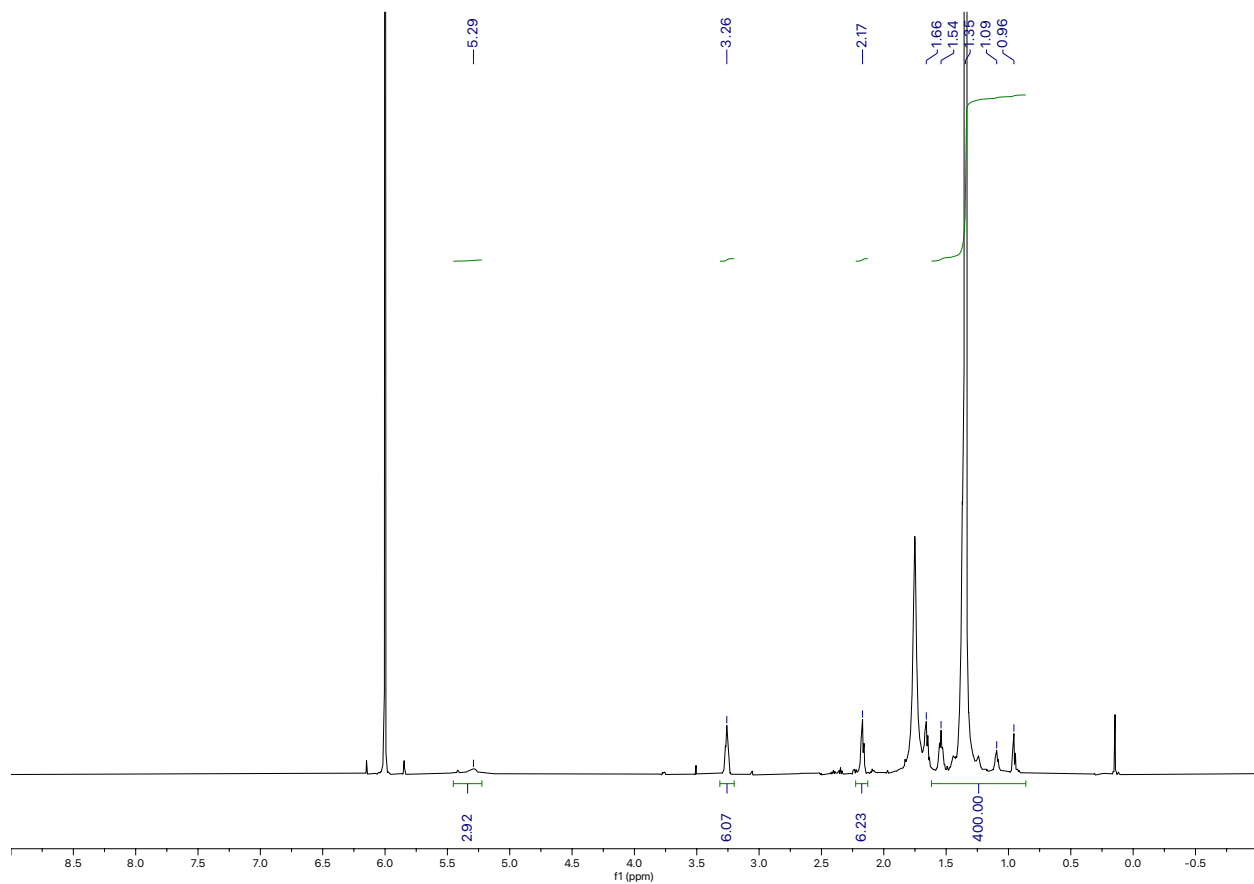


Figure 4.7.8.18. ^1H NMR spectra of *nylon*-HDPE **2b**.

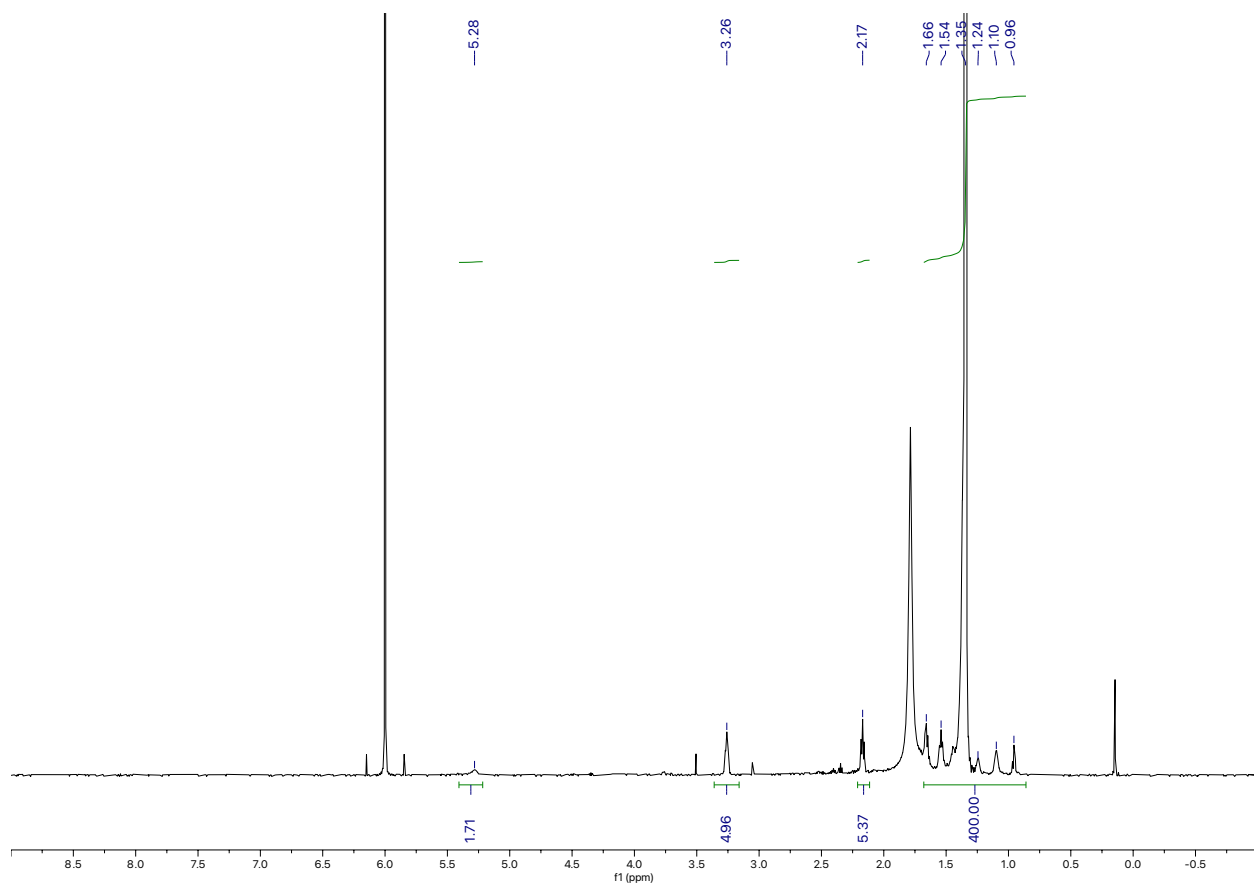


Figure 4.7.8.19. ^1H NMR spectra of *nylon-waste*-HDPE (milk jug) **2c**.

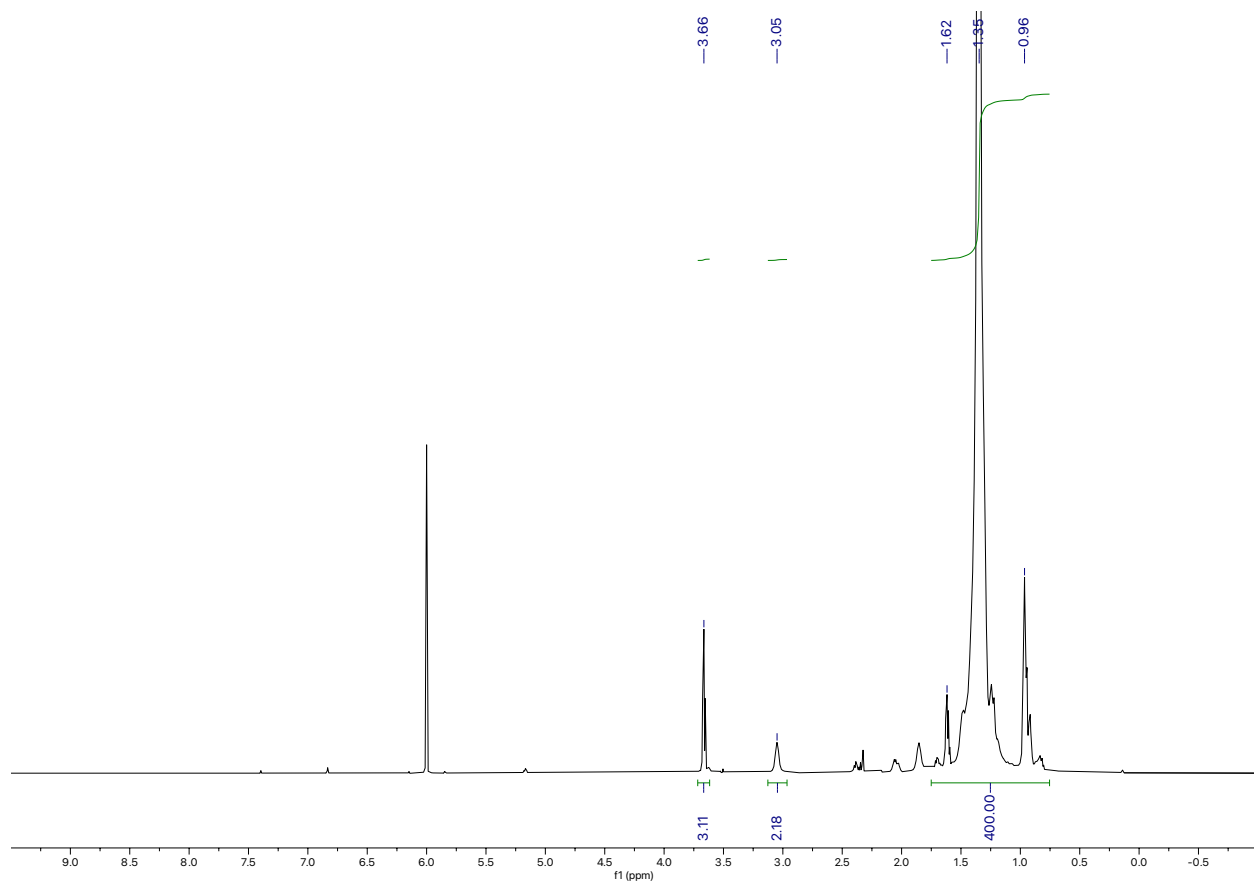


Figure 4.7.8.20. ^1H NMR spectra of the hydrogenolysis of *nylon-LDPE 2a*.

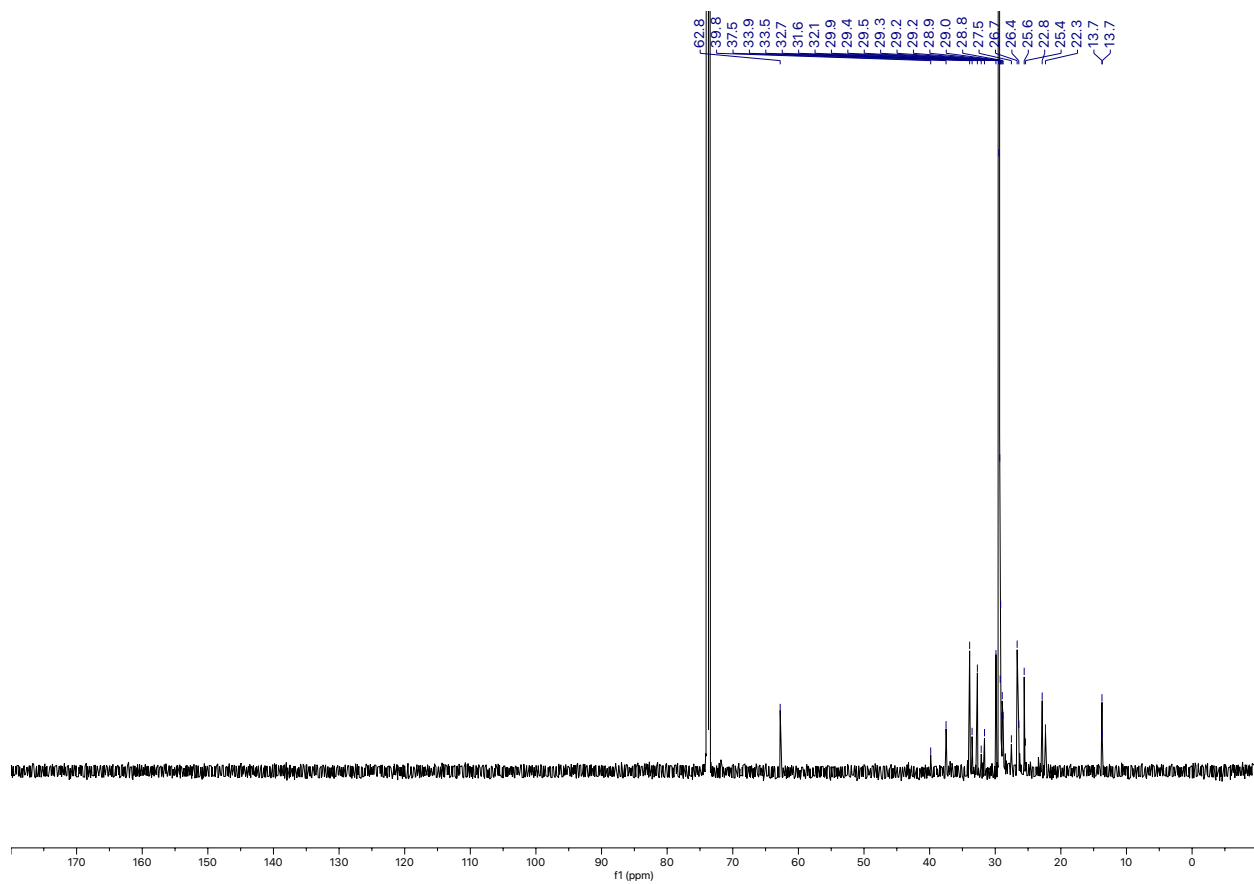


Figure 4.7.8.21. ^{13}C NMR spectra of the hydrogenolysis of *nylon-LDPE 2a*.

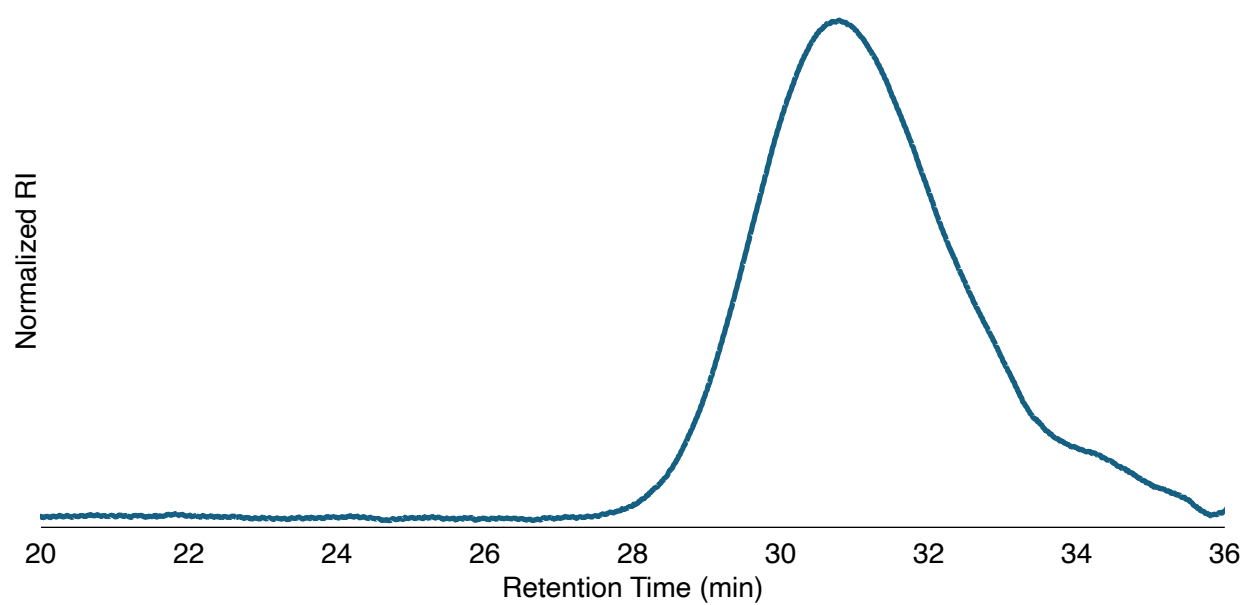


Figure 4.7.8.22. Size exclusion chromatogram of the hydrogenolysis product of *nylon*-LDPE **2a**. $M_n = 803$ Da, $D = 1.5$. Molecular weight was determined relative to polyethylene standards.

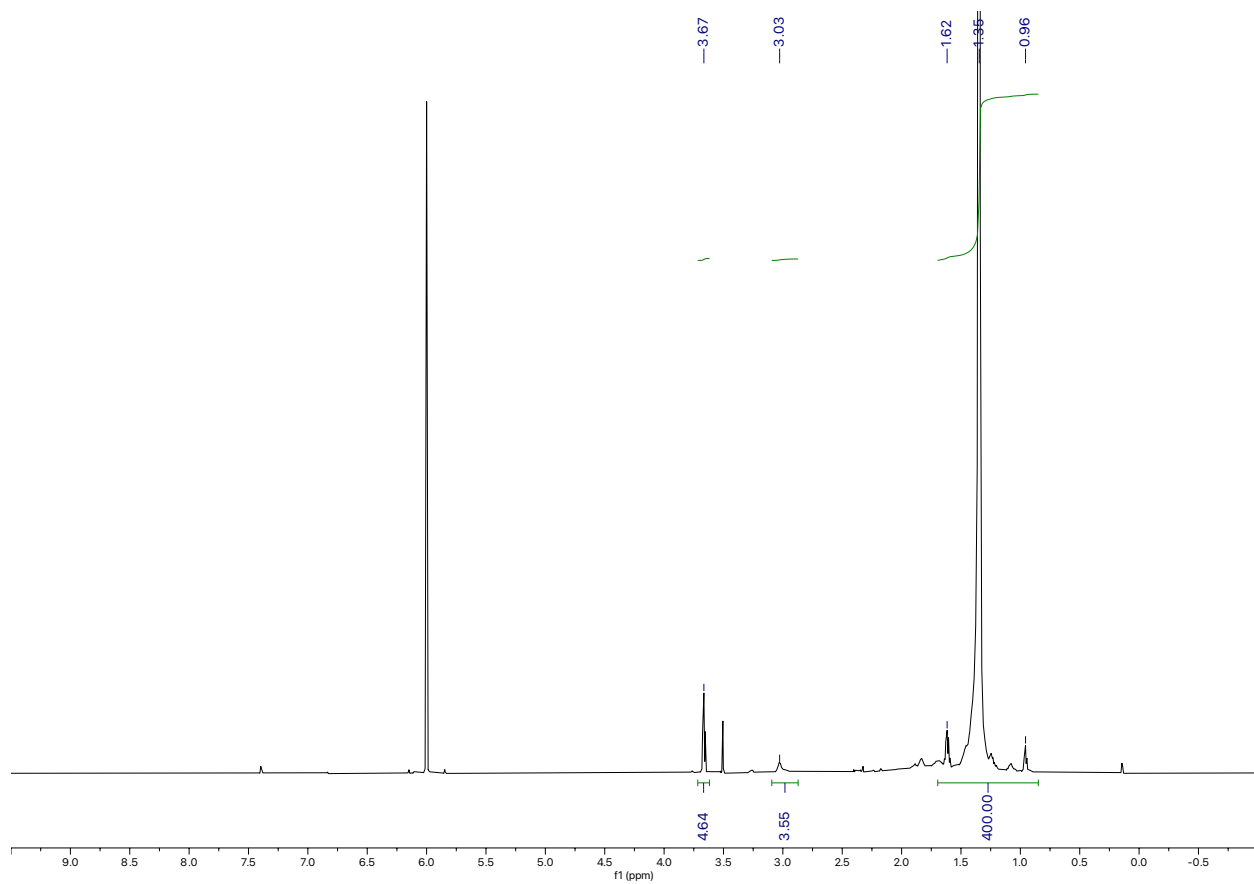


Figure 4.7.8.23. ^1H NMR spectra of the hydrogenolysis of *nylon*-HDPE **2b**.

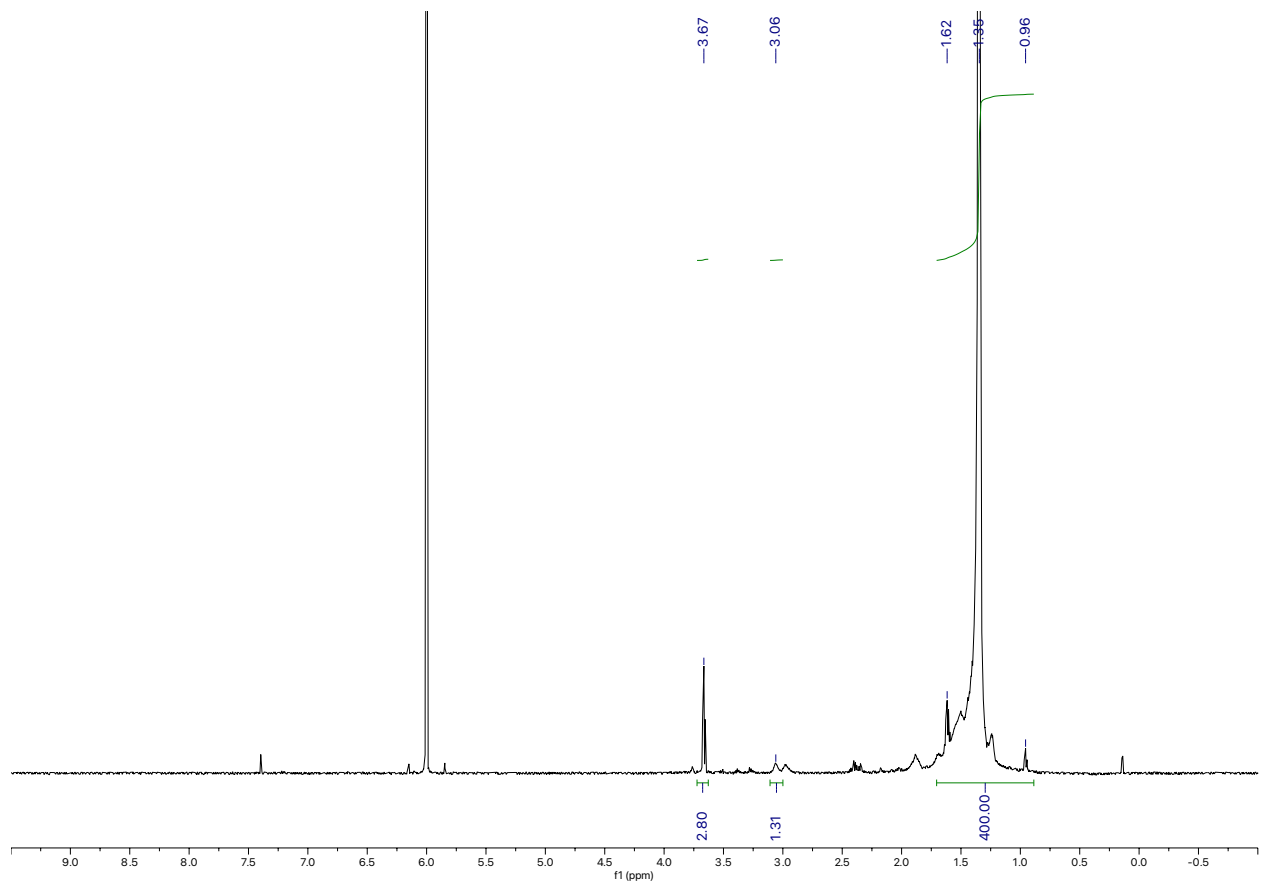


Figure 4.7.8.24. ^1H NMR spectra of the hydrogenolysis of *nylon-waste-HDPE* (milk jug) **2c**.

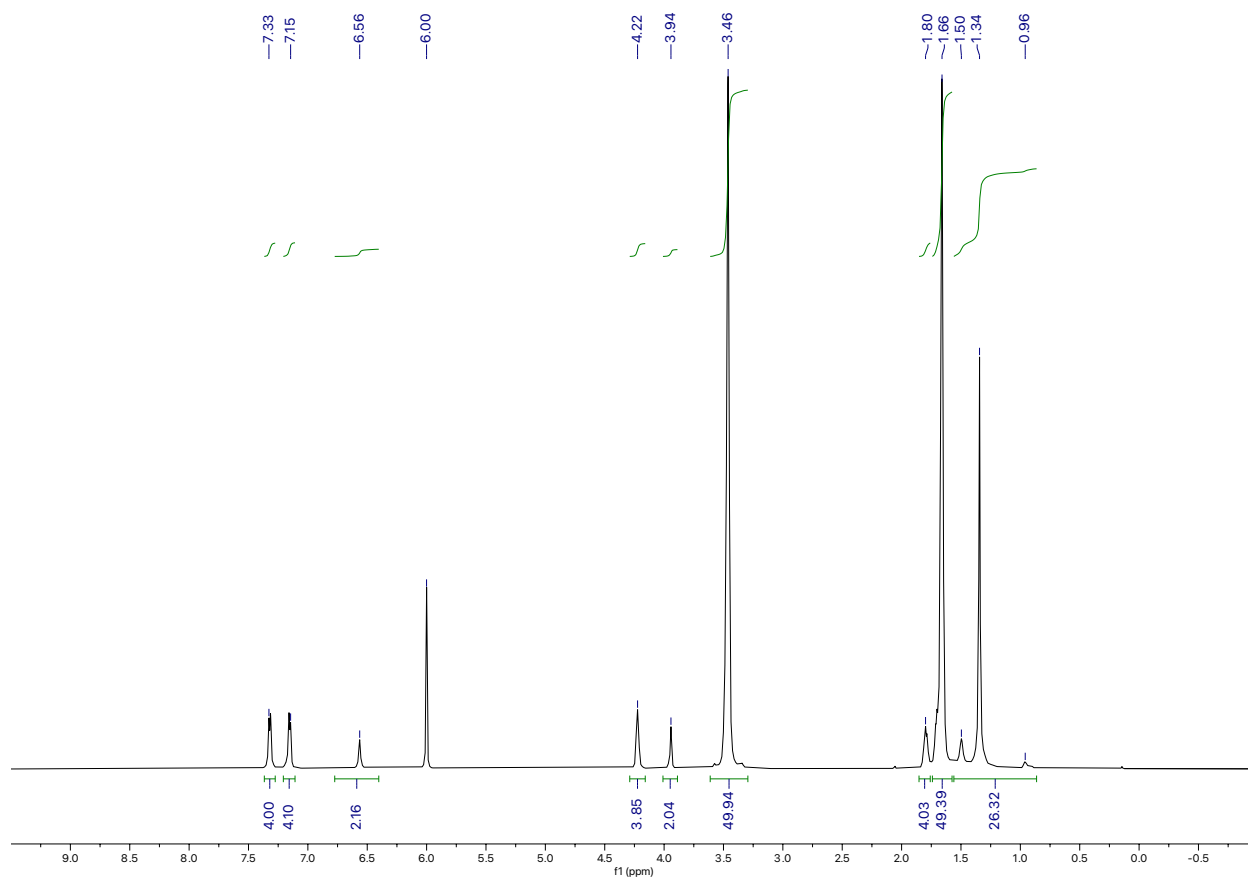


Figure 4.7.8.25. ^1H NMR spectra of PUU 4.

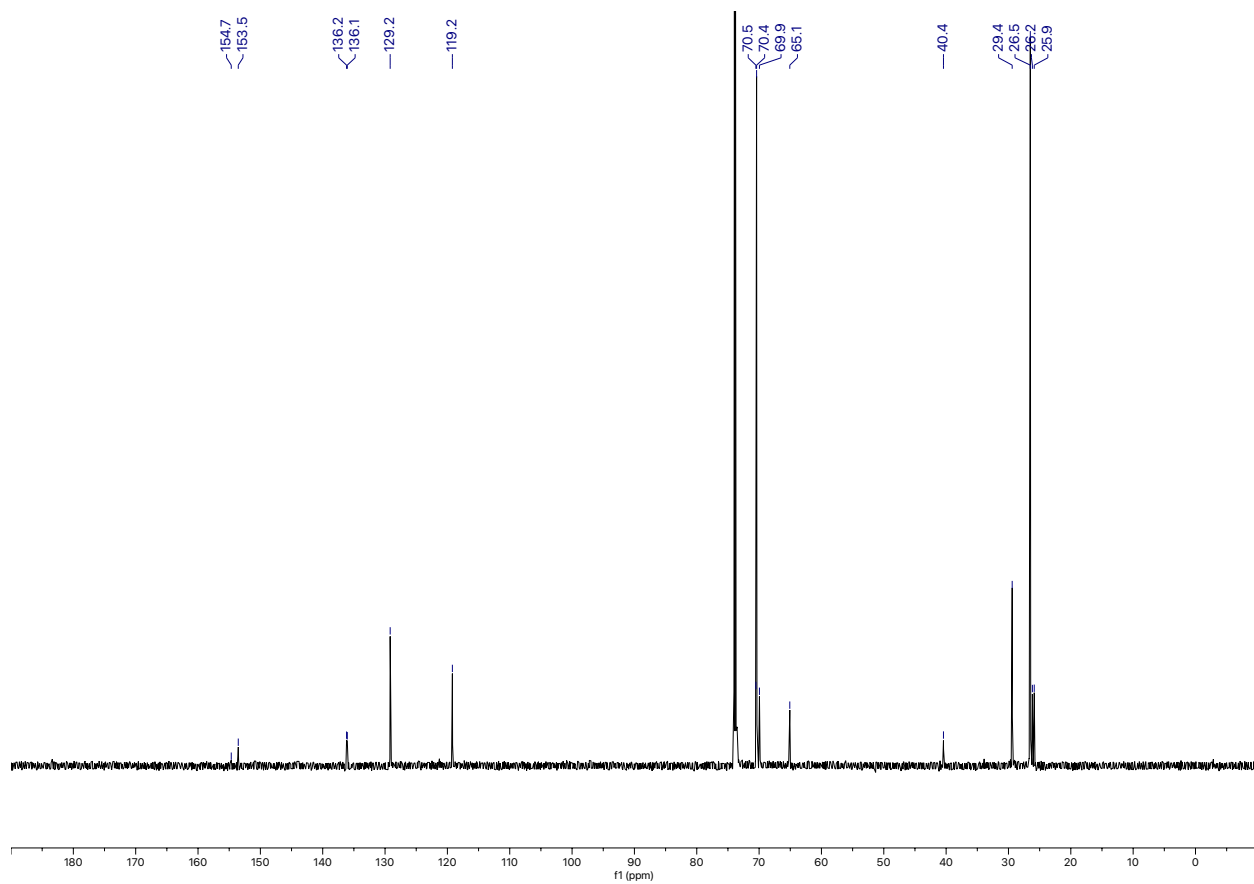


Figure 4.7.8.26. ^{13}C NMR spectra of PUU 4.

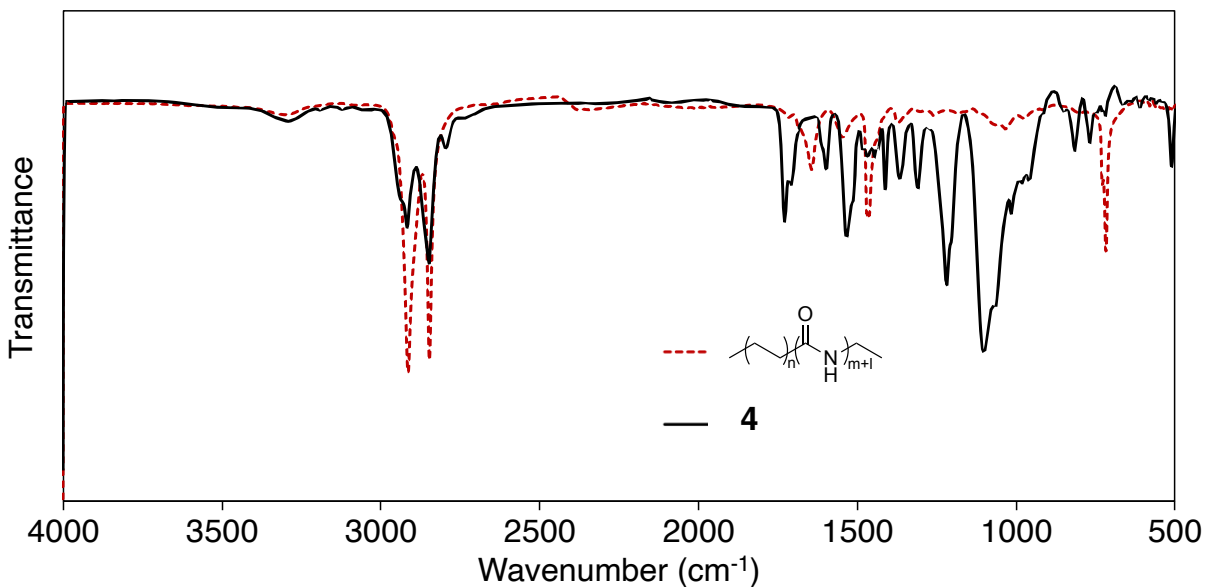


Figure 4.7.8.27. Overlay of the FTIR spectra of PUU **4**, major peaks ν (cm⁻¹): 3292, 2918, 2849, 2796, 1730, 1710, 1599, 1534, 1467, 1447, 1413, 1367, 1310, 1220, 1103, 1017, 982, 960, 816, 767, 720, 611, 511, and the FTIR spectra of *nylon*-LDPE **2a**, major peaks ν (cm⁻¹): 3305, 2915, 2848, 1645, 1548, 1464, 1370, 1261, 1035, 729, 718.

4.7.9 Materials Testing

4.7.9.1 Procedure for Lap Shear Tests

Lap shear tests were conducted according to ASTM D1002-10 on an Instron universal materials tester equipped with a 5 kN load cell with a shear rate of 1.5 mm/min. Adhesion strength was determined by the maximum load divided by the bonded overlap area, which was measured with digital calipers prior to testing, and the apparent failure mode was assessed visually.

Substrate and Lap Joint Preparation

1. **Degreased Substrates:** To prepare the aluminum and glass substrates for adhesive bonding, they were degreased. Substrates were wiped with a fresh Kimwipe soaked in acetone, followed by a second Kimwipe soaked in ethyl acetate. Substrates were air-dried, and a 1 cm x 1 cm area was isolated with vinyl electrical tape.
2. **Lap joint preparation:** Polymer films of LDPE, polymer **2a**, and PUU **4** (0.1 – 0.3 mm) were prepared on a hot press at 120 °C for 45 seconds to provide melts. Specifically, polymer samples between two Kapton films were pressed between steel plates at 2000 psig. Teflon shims were used to control film thickness. The samples were cooled at room temperature, and a 1 cm x 1 cm piece of the polymer film was cut. The cut films were placed at the end of a clean Al 6061 adherend or glass, and vinyl masking tape was removed. The substrates were overlapped in an antiparallel arrangement, clamped with two small binder clips, and subsequently transferred to a pre-heated oven. Samples were heated at 140 °C for 5 minutes. All samples were allowed to cool slowly to room temperature. Excess polyethylene adhesive was carefully removed from the edges with a razor. Shims were applied to lap joint ends to help align the grip of the mechanical tester. Multiple attempts to prepare lap joints with LDPE failed, as indicated by breaking of the lap joint during the clamping process. Thus, the adhesion strengths of LDPE were unmeasurable by this method. All measurable samples were loaded at 1.5 mm/min in shear until failure, whereas the dimensions of the bonded area were measured with calipers. Finally, the adhesive strength was determined by the peak load divided by the overlap area. Lap shear measurements were repeated for at least four specimens, and the values reported are averages of the measurements of these sets of specimens.

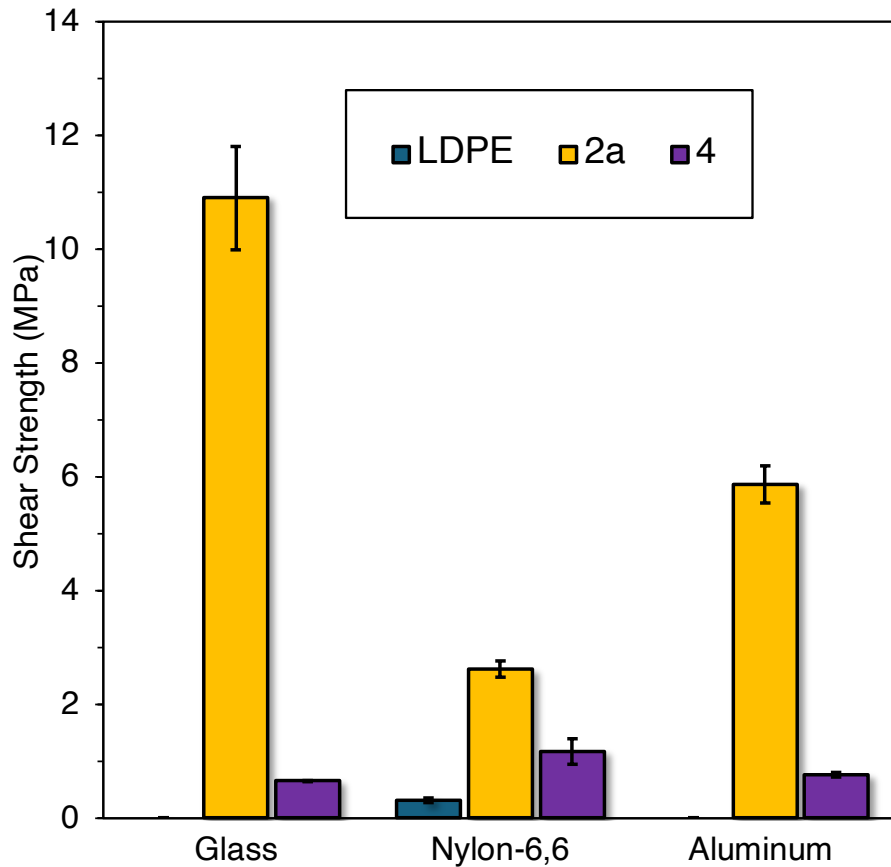


Figure 4.7.9.1.1. Lap shear strength of joints Al-LDPE-Al, nylon-6,6-LDPE-nylon-6,6, glass-LDPE-glass, Al-**2a**-Al, nylon-6,6-**2a**-nylon-6,6, glass-**2a**-glass, Al-**4**-Al, nylon-6,6-**4**-nylon-6,6, glass-**4**-glass. Error bars represent standard deviations.

Table 4.7.9.1.1. Summary of results of adhesion strength in lap shear tests

Entry	Interface	Shear Strength (MPa)	Mode of Failure
1 ^a	Al-LDPE-Al	--	--
2	nylon-6,6-LDPE-nylon-6,6	0.3 ± 0.04	Adhesive
3 ^a	glass-LDPE-glass	--	--
4	Al- 2a -Al	5.9 ± 0.3	Adhesive
5	nylon-6,6- 2a -nylon-6,6	2.6 ± 0.1	Adhesive
6	glass- 2a -glass	10.9 ± 0.9	Adhesive
7	Al- 4 -Al	0.8 ± 0.05	Adhesive
8	nylon-6,6- 4 -nylon-6,6	1.2 ± 0.2	Adhesive
9	glass- 4 -glass	0.7 ± 0.01	Adhesive

^aShear strength not measurable because of lap joint failure during the clamping process.

4.7.9.2 Procedure for Tensile Tests

- 1. Sample preparation:** Polymer films of LDPE, polymer **2a**, and PUU **4** were prepared on a hot press at 120 °C for 45 seconds to provide melts ($350 \pm 50\mu\text{m}$ thickness). Specifically, polymer samples between two Kapton films were pressed between steel plates at 2000 psig. Teflon shims were used to control film thickness. The samples were then cooled at room temperature and cut into a dog-bone geometry using a cutting die (ASTM D-638V) to obtain samples that were 9.53 mm in length and 3.18 mm in width.
- 2. Experimental procedures for tensile tests:** Tensile testing was conducted according to ASTM D638 on an Instron universal materials tester. Tensile stress and strain were measured at room temperature using an extension rate of 50 mm/min. Measurements were repeated for at least three samples, and average values are reported.
- 3. Experimental procedures for elastic hysteresis tests:** Elastic hysteresis testing was conducted according to ASTM D638 on an Instron universal materials tester. Tensile stress and strain were measured at room temperature using an extension rate of 50 mm/min until the dog-bone was stretched to 60 mm in length and then backwards at a rate of 50 mm/min until the force returned to zero.

Table 4.7.9.2.1. Summary of results of tensile tests

Polymer	tensile stress at max load (MPa)	Young's Modulus (MPa)	tensile strain (extension) at break (%)	toughness (MJ/m ³)
LDPE	11.4 ± 1.1	148.5 ± 16.8	227.8 ± 96.8	19.5 ± 9.8
2a	8.5 ± 1.6	122.3 ± 14.9	234.0 ± 44.7	18.0 ± 3.8
4	5.5 ± 0.9	0.9 ± 0.2	939.2 ± 89.9	29.9 ± 6.6

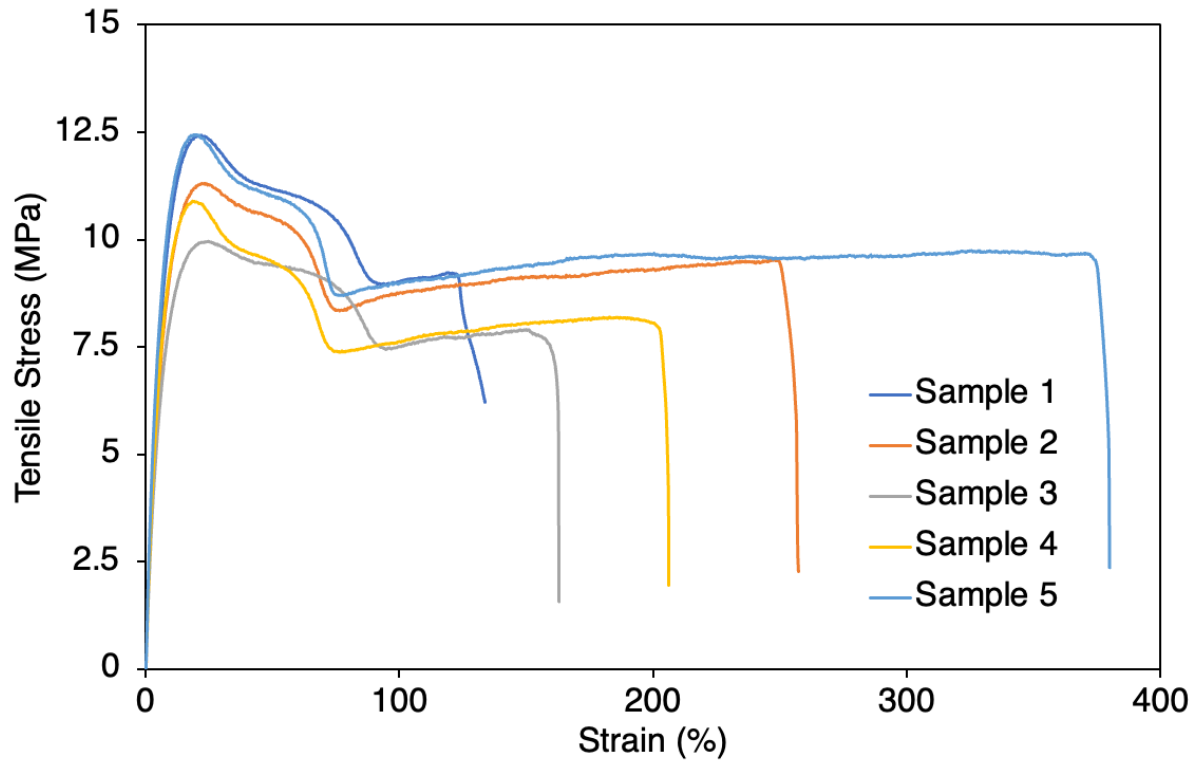


Figure 4.7.9.2.1. Stress-strain curves for unmodified LDPE

Table 4.7.9.2.2. Summary of results of tensile tests for unmodified LDPE

Sample	tensile stress at max load (MPa)	Young's Modulus (MPa)	tensile strain (extension) at break (%)	toughness (MJ/m ³)
1	12.4	160.4	133.7	13.4
2	11.3	142.4	256.7	13.5
3	10.0	125.8	162.8	17.1
4	10.9	144.9	206.1	36.7
5	12.5	169.0	379.8	16.9

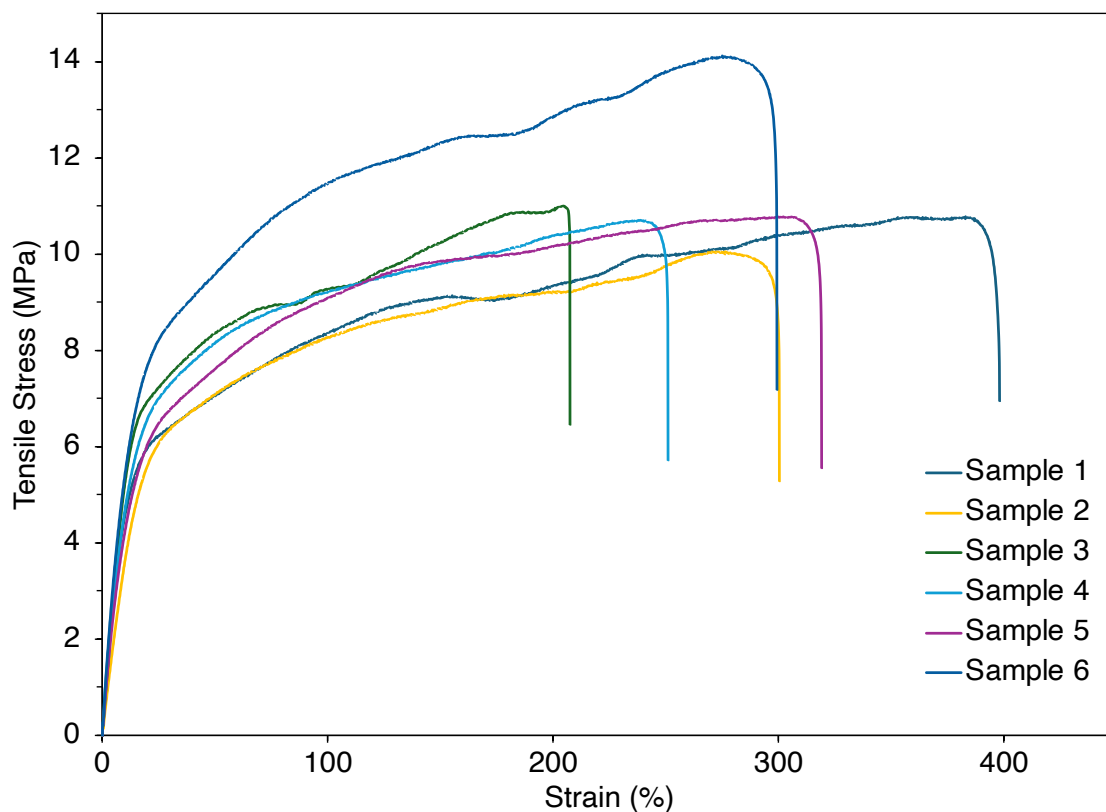


Figure 4.7.9.2.2. Stress-strain curves for polymer **2a**

Table 4.7.9.2.3. Summary of results of tensile tests for polymer **2a**

Sample	tensile stress at max load (MPa)	Young's Modulus (MPa)	tensile strain (extension) at break (%)	toughness (MJ/m ³)
1	10.8	65.9	429.0	35.1
2	10.1	39.1	317.8	24.8
3	11.0	57.3	207.4	16.7
4	10.7	60.1	250.9	22.6
5	10.6	52.8	319.1	29.4
6	13.9	66.9	299.2	34.6

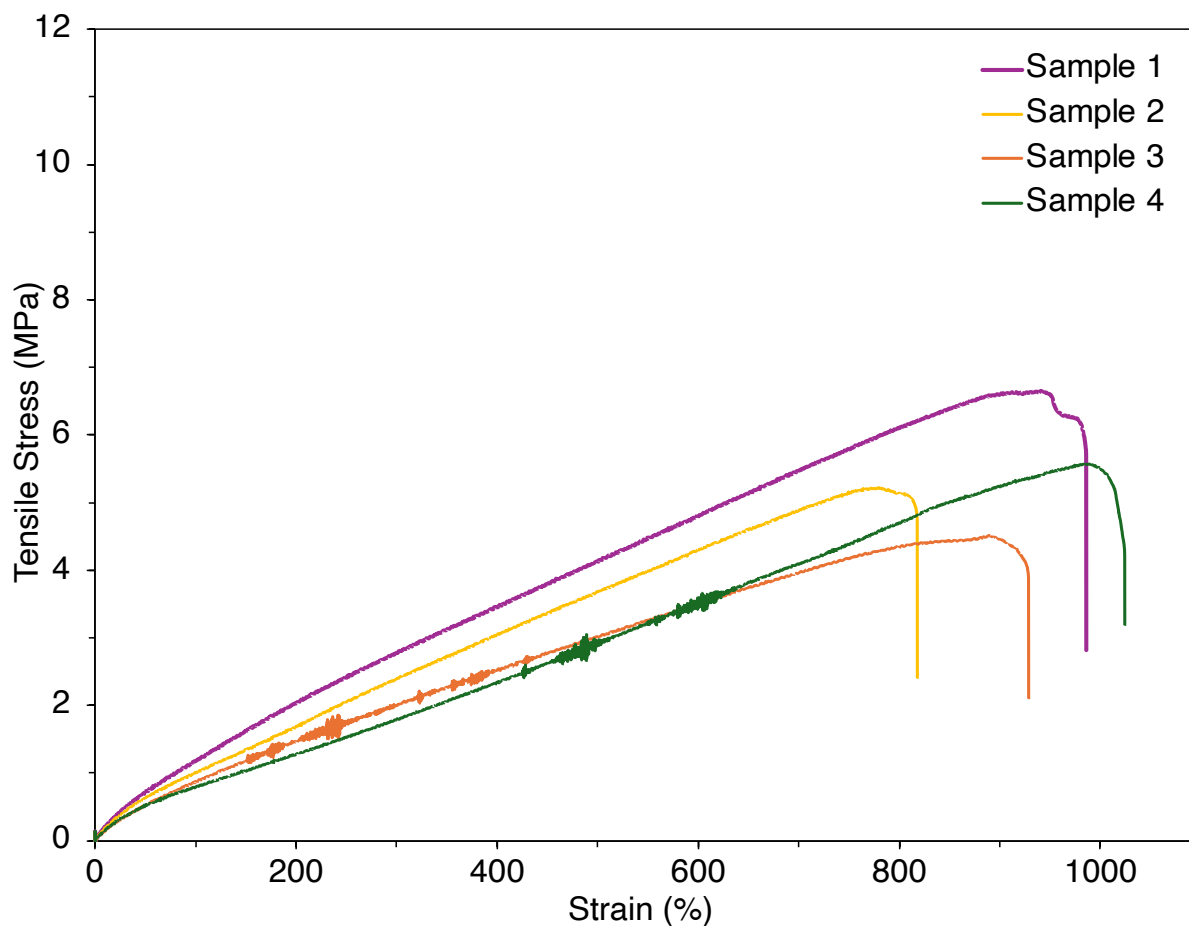


Figure 4.7.9.2.3. Stress-strain curves for polymer 4

Table 4.7.9.2.4. Summary of results of tensile tests for polymer 4

Sample	tensile stress at max load (MPa)	Young's Modulus (MPa)	tensile strain (extension) at break (%)	toughness (MJ/m ³)
1	6.7	1.1	986.0	39.0
2	5.2	1.0	818.0	24.6
3	4.5	0.8	928.7	25.3
4	5.6	0.6	1024.3	30.8

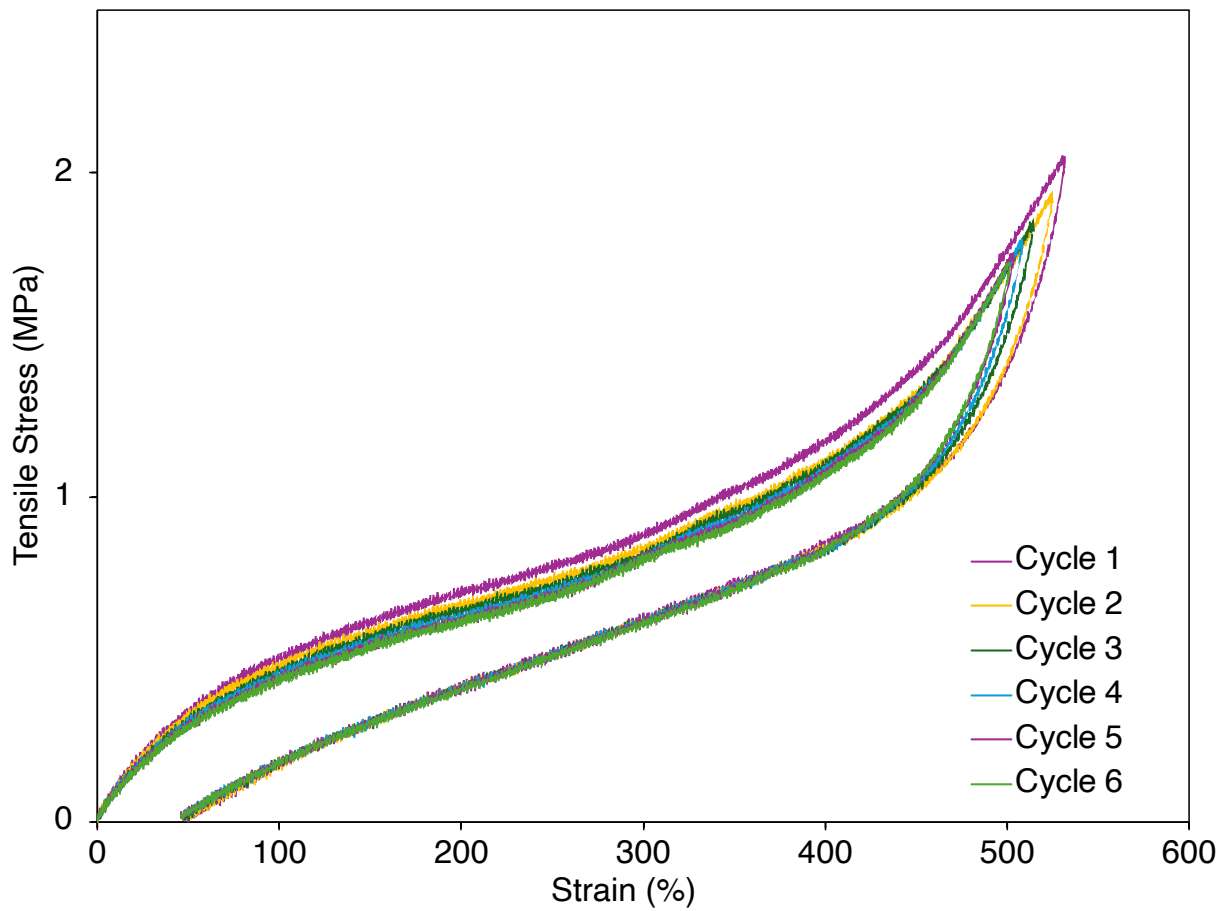


Figure 4.7.9.2.4. Elastic hysteresis curves of polymer 4

4.8 References

- (1) Geyer, R.; Jambeck, J. R.; Law, K. L. Production, use, and fate of all plastics ever made. *Sci. Adv.* **2017**, *3*, e1700782
- (2) Yao, Z.; Seong, H. J.; Jang, Y.-S. Environmental toxicity and decomposition of polyethylene. *Ecotoxicol. Environ. Saf.* **2022**, *242*, 113933
- (3) Hahladakis, J. N.; Velis, C. A.; Weber, R.; Iacovidou, E.; Purnell, P. An overview of chemical additives present in plastics: Migration, release, fate and environmental impact during their use, disposal and recycling. *J. Hazard. Mater.* **2018**, *344*, 179–199
- (4) Wiesinger, H.; Wang, Z.; Hellweg, S. Deep Dive into Plastic Monomers, Additives, and Processing Aids. *Environ. Sci. Technol.* **2021**, *55*, 9339–9351
- (5) Spell, H. L.; Eddy, R. D. Determination of additives in polyethylene by absorption spectroscopy. *Anal. Chem.* **1960**, *32*, 1811–1814
- (6) Chen, W.; Gong, Y.; Mckie, M.; Almuhtaram, H.; Sun, J.; Barrett, H.; Yang, D.; Wu, M.; Andrews, R. C.; Peng, H. Defining the Chemical Additives Driving *In Vitro* Toxicities of Plastics. *Environ. Sci. Technol.* **2022**, *56*, 14627–14639
- (7) Balzade, Z.; Sharif, F.; Reza Ghaffarian Anbaran, S. Tailor-Made Functional Polyolefins of Complex Architectures: Recent Advances, Applications, and Prospects. *Macromolecules* **2022**, *55*, 1910–1922
- (8) Plummer, C. M.; Li, L.; Chen, Y. The post-modification of polyolefins with emerging synthetic methods. *Polym. Chem.* **2020**, *11*, 6862–6872
- (9) Boen, N. K.; Hillmyer, M. A. Post-polymerization functionalization of polyolefins. *Chem. Soc. Rev.* **2005**, *34*, 267
- (10) Williamson, J. B.; Lewis, S. E.; Johnson, R. R.; Manning, I. M.; Leibfarth, F. A. C–H Functionalization of Commodity Polymers. *Angew. Chem. Int. Ed.* **2019**, *58*, 8654–8668
- (11) Williamson, J. B.; Czaplowski, W. L.; Alexanian, E. J.; Leibfarth, F. A. Regioselective C–H Xanthylation as a Platform for Polyolefin Functionalization. *Angew. Chem. Int. Ed.* **2018**, *57*, 6261–6265
- (12) Jehanno, C.; Alty, J. W.; Roosen, M.; De Meester, S.; Dove, A. P.; Chen, E. Y.-X.; Leibfarth, F. A.; Sardon, H. Critical advances and future opportunities in upcycling commodity polymers. *Nature* **2022**, *603*, 803–814
- (13) Fazekas, T. J.; Alty, J. W.; Neidhart, E. K.; Miller, A. S.; Leibfarth, F. A.; Alexanian, E. J. Diversification of aliphatic C–H bonds in small molecules and polyolefins through radical chain transfer. *Science* **2022**, *375*, 545–550
- (14) Chen, L.; Malollari, K. G.; Uliana, A.; Sanchez, D.; Messersmith, P. B.; Hartwig, J. F. Selective, Catalytic Oxidations of C–H Bonds in Polyethylenes Produce Functional Materials with Enhanced Adhesion. *Chem* **2021**, *7*, 137–145
- (15) Ditzler, R. A. J.; King, A. J.; Towell, S. E.; Ratushnyy, M.; Zhukhovitskiy, A. V. Editing of polymer backbones. *Nat. Rev. Chem.* **2023**,
- (16) Lu, Y.; Takahashi, K.; Zhou, J.; Nontarin, R.; Nakagawa, S.; Yoshie, N.; Nozaki, K. Synthesis of Long-Chain Polyamides via Main-Chain Modification of Polyethyleneketones. *Angew. Chem. Int. Ed.* **2024**, e202410849
- (17) Iwakura, Y.; Uno, K.; Takiguchi, T. Syntheses of aromatic polyketones and aromatic polyamide. *J. Polym. Sci. A Polym. Chem.* **1968**, *6*, 3345–3355
- (18) Michel, R. H.; Murphey, W. A. Intramolecular rearrangements of polyketones. *J. Polym. Sci.* **1961**, *55*, 741–751

- (19) Shi, J. X.; Ciccina, N. R.; Pal, S.; Kim, D. D.; Brunn, J. N.; Lizandara-Pueyo, C.; Ernst, M.; Haydl, A. M.; Messersmith, P. B.; Helms, B. A.; Hartwig, J. F. Chemical Modification of Oxidized Polyethylene Enables Access to Functional Polyethylenes with Greater Reuse. *J. Am. Chem. Soc.* **2023**, *145*, 21527–21537
- (20) Treitler, D. S.; Leung, S. How Dangerous Is Too Dangerous? A Perspective on Azide Chemistry. *J. Org. Chem.* **2022**, *87*, 11293–11295
- (21) Kaur, K.; Srivastava, S. Beckmann rearrangement catalysis: a review of recent advances. *New J. Chem.* **2020**, *44*, 18530–18572
- (22) Hashimoto, M.; Obora, Y.; Ishii, Y. An Efficient Catalytic Method for the Beckmann Rearrangement of Ketoximes to Lactams by Cyanuric Chloride and Phosphazene Catalysts. *Org. Process Res. Dev.* **2009**, *13*, 411–414
- (23) Gao, P.; Bai, Z. Carbon Tetrabromide/Triphenylphosphine-Activated Beckmann Rearrangement of Ketoximes for Synthesis of Amides. *Chin. J. Chem.* **2017**, *35*, 1673–1677
- (24) Hill, R. K.; Conley, R. T.; Chortyk, O. T. A Fragmentation-Recombination Mechanism for the Beckmann Rearrangement in Strong Acid. *J. Am. Chem. Soc.* **1965**, *87*, 5646–5651
- (25) Kumar, A.; Von Wolff, N.; Rauch, M.; Zou, Y.-Q.; Shmul, G.; Ben-David, Y.; Leitun, G.; Avram, L.; Milstein, D. Hydrogenative Depolymerization of Nylons. *J. Am. Chem. Soc.* **2020**, *142*, 14267–14275
- (26) Balaraman, E.; Gnanaprakasam, B.; Shimon, L. J. W.; Milstein, D. Direct Hydrogenation of Amides to Alcohols and Amines under Mild Conditions. *J. Am. Chem. Soc.* **2010**, *132*, 16756–16758
- (27) Miura, T.; Naruto, M.; Toda, K.; Shimomura, T.; Saito, S. Multifaceted catalytic hydrogenation of amides via diverse activation of a sterically confined bipyridine–ruthenium framework. *Sci. Rep.* **2017**, *7*, <https://doi.org/10.1038/s41598-41017-01645-z>
- (28) Miura, T.; Held, I. E.; Oishi, S.; Naruto, M.; Saito, S. Catalytic hydrogenation of unactivated amides enabled by hydrogenation of catalyst precursor. *Tetrahedron Lett.* **2013**, *54*, 2674–2678
- (29) Zhou, W.; Neumann, P.; Al Batal, M.; Rominger, F.; Hashmi, A. S. K.; Schaub, T. Depolymerization of Technical-Grade Polyamide 66 and Polyurethane Materials through Hydrogenation. *ChemSusChem* **2021**, *14*, 4176–4180
- (30) Wang, H.-H.; Lin, M.-S. Poly(urea-urethane) polymers with multi-functional properties. *J. Polym. Res.* **2000**, *7*, 81–90
- (31) Xiang, X.; Zhang, L.; Sheng, D.; Yang, X.; Qi, X.; Wei, S.; Dai, H. Healable and Recyclable Polyurea-Urethane Elastomer with High Mechanical Robustness, Superhigh Elastic Restorability, and Exceptional Crack Tolerance. *Adv. Funct. Mater.* **2024**, *34*, 2312571
- (32) Costa, L.; Luda, M. P.; Cameron, G. G.; Qureshi, M. Y. The thermal and thermo-oxidative degradation of poly(tetrahydrofuran) and its complexes with LiBr and LiI. *Polym. Degrad. Stab.* **2000**, *67*, 527–533
- (33) Machalická, K.; Eliášová, M. Adhesive joints in glass structures: effects of various materials in the connection, thickness of the adhesive layer, and ageing. *Int. J. Adhes. Adhes.* **2017**, *72*, 10–22
- (34) Marchione, F.; Munafò, P. Experimental strength evaluation of glass/aluminum double-lap adhesive joints. *J. Build. Eng.* **2020**, *30*, 101284
- (35) Zhang, J.; Leitun, G.; Ben-David, Y.; Milstein, D. Facile Conversion of Alcohols into Esters and Dihydrogen Catalyzed by New Ruthenium Complexes. *J. Am. Chem. Soc.* **2005**, *127*, 10840–10841

- (1) Geyer, R.; Jambeck, J. R.; Law, K. L. Production, use, and fate of all plastics ever made. *Sci. Adv.* **2017**, *3*, e1700782
- (2) Yao, Z.; Seong, H. J.; Jang, Y.-S. Environmental toxicity and decomposition of polyethylene. *Ecotoxicol. Environ. Saf.* **2022**, *242*, 113933
- (3) Hahladakis, J. N.; Velis, C. A.; Weber, R.; Iacovidou, E.; Purnell, P. An overview of chemical additives present in plastics: Migration, release, fate and environmental impact during their use, disposal and recycling. *J. Hazard. Mater.* **2018**, *344*, 179–199
- (4) Wiesinger, H.; Wang, Z.; Hellweg, S. Deep Dive into Plastic Monomers, Additives, and Processing Aids. *Environ. Sci. Technol.* **2021**, *55*, 9339–9351
- (5) Spell, H. L.; Eddy, R. D. Determination of additives in polyethylene by absorption spectroscopy. *Anal. Chem.* **1960**, *32*, 1811–1814
- (6) Chen, W.; Gong, Y.; Mckie, M.; Almuhtaram, H.; Sun, J.; Barrett, H.; Yang, D.; Wu, M.; Andrews, R. C.; Peng, H. Defining the Chemical Additives Driving *In Vitro* Toxicities of Plastics. *Environ. Sci. Technol.* **2022**, *56*, 14627–14639
- (7) Balzade, Z.; Sharif, F.; Reza Ghaffarian Anbaran, S. Tailor-Made Functional Polyolefins of Complex Architectures: Recent Advances, Applications, and Prospects. *Macromolecules* **2022**, *55*, 1910–1922
- (8) Plummer, C. M.; Li, L.; Chen, Y. The post-modification of polyolefins with emerging synthetic methods. *Polym. Chem.* **2020**, *11*, 6862–6872
- (9) Boen, N. K.; Hillmyer, M. A. Post-polymerization functionalization of polyolefins. *Chem. Soc. Rev.* **2005**, *34*, 267
- (10) Williamson, J. B.; Lewis, S. E.; Johnson, R. R.; Manning, I. M.; Leibfarth, F. A. C–H Functionalization of Commodity Polymers. *Angew. Chem. Int. Ed.* **2019**, *58*, 8654–8668
- (11) Williamson, J. B.; Czaplowski, W. L.; Alexanian, E. J.; Leibfarth, F. A. Regioselective C–H Xanthylation as a Platform for Polyolefin Functionalization. *Angew. Chem. Int. Ed.* **2018**, *57*, 6261–6265
- (12) Jehanno, C.; Alty, J. W.; Roosen, M.; De Meester, S.; Dove, A. P.; Chen, E. Y.-X.; Leibfarth, F. A.; Sardon, H. Critical advances and future opportunities in upcycling commodity polymers. *Nature* **2022**, *603*, 803–814
- (13) Fazekas, T. J.; Alty, J. W.; Neidhart, E. K.; Miller, A. S.; Leibfarth, F. A.; Alexanian, E. J. Diversification of aliphatic C–H bonds in small molecules and polyolefins through radical chain transfer. *Science* **2022**, *375*, 545–550
- (14) Chen, L.; Malollari, K. G.; Uliana, A.; Sanchez, D.; Messersmith, P. B.; Hartwig, J. F. Selective, Catalytic Oxidations of C–H Bonds in Polyethylenes Produce Functional Materials with Enhanced Adhesion. *Chem* **2021**, *7*, 137–145
- (15) Ditzler, R. A. J.; King, A. J.; Towell, S. E.; Ratushnyy, M.; Zhukhovitskiy, A. V. Editing of polymer backbones. *Nat. Rev. Chem.* **2023**,
- (16) Lu, Y.; Takahashi, K.; Zhou, J.; Nontarin, R.; Nakagawa, S.; Yoshie, N.; Nozaki, K. Synthesis of Long-Chain Polyamides via Main-Chain Modification of Polyethyleneketones. *Angew. Chem. Int. Ed.* **2024**, e202410849
- (17) Iwakura, Y.; Uno, K.; Takiguchi, T. Syntheses of aromatic polyketones and aromatic polyamide. *J. Polym. Sci. A Polym. Chem.* **1968**, *6*, 3345–3355
- (18) Michel, R. H.; Murphey, W. A. Intramolecular rearrangements of polyketones. *J. Polym. Sci.* **1961**, *55*, 741–751

- (19) Shi, J. X.; Ciccina, N. R.; Pal, S.; Kim, D. D.; Brunn, J. N.; Lizandara-Pueyo, C.; Ernst, M.; Haydl, A. M.; Messersmith, P. B.; Helms, B. A.; Hartwig, J. F. Chemical Modification of Oxidized Polyethylene Enables Access to Functional Polyethylenes with Greater Reuse. *J. Am. Chem. Soc.* **2023**, *145*, 21527–21537
- (20) Treitler, D. S.; Leung, S. How Dangerous Is Too Dangerous? A Perspective on Azide Chemistry. *J. Org. Chem.* **2022**, *87*, 11293–11295
- (21) Kaur, K.; Srivastava, S. Beckmann rearrangement catalysis: a review of recent advances. *New J. Chem.* **2020**, *44*, 18530–18572
- (22) Hashimoto, M.; Obora, Y.; Ishii, Y. An Efficient Catalytic Method for the Beckmann Rearrangement of Ketoximes to Lactams by Cyanuric Chloride and Phosphazene Catalysts. *Org. Process Res. Dev.* **2009**, *13*, 411–414
- (23) Gao, P.; Bai, Z. Carbon Tetrabromide/Triphenylphosphine-Activated Beckmann Rearrangement of Ketoximes for Synthesis of Amides. *Chin. J. Chem.* **2017**, *35*, 1673–1677
- (24) Hill, R. K.; Conley, R. T.; Chortyk, O. T. A Fragmentation-Recombination Mechanism for the Beckmann Rearrangement in Strong Acid. *J. Am. Chem. Soc.* **1965**, *87*, 5646–5651
- (25) Kumar, A.; Von Wolff, N.; Rauch, M.; Zou, Y.-Q.; Shmul, G.; Ben-David, Y.; Leitun, G.; Avram, L.; Milstein, D. Hydrogenative Depolymerization of Nylons. *J. Am. Chem. Soc.* **2020**, *142*, 14267–14275
- (26) Balaraman, E.; Gnanaprakasam, B.; Shimon, L. J. W.; Milstein, D. Direct Hydrogenation of Amides to Alcohols and Amines under Mild Conditions. *J. Am. Chem. Soc.* **2010**, *132*, 16756–16758
- (27) Miura, T.; Naruto, M.; Toda, K.; Shimomura, T.; Saito, S. Multifaceted catalytic hydrogenation of amides via diverse activation of a sterically confined bipyridine–ruthenium framework. *Sci. Rep.* **2017**, *7*, <https://doi.org/10.1038/s41598-41017-01645-z>
- (28) Miura, T.; Held, I. E.; Oishi, S.; Naruto, M.; Saito, S. Catalytic hydrogenation of unactivated amides enabled by hydrogenation of catalyst precursor. *Tetrahedron Lett.* **2013**, *54*, 2674–2678
- (29) Zhou, W.; Neumann, P.; Al Batal, M.; Rominger, F.; Hashmi, A. S. K.; Schaub, T. Depolymerization of Technical-Grade Polyamide 66 and Polyurethane Materials through Hydrogenation. *ChemSusChem* **2021**, *14*, 4176–4180
- (30) Wang, H.-H.; Lin, M.-S. Poly(urea-urethane) polymers with multi-functional properties. *J. Polym. Res.* **2000**, *7*, 81–90
- (31) Xiang, X.; Zhang, L.; Sheng, D.; Yang, X.; Qi, X.; Wei, S.; Dai, H. Healable and Recyclable Polyurea-Urethane Elastomer with High Mechanical Robustness, Superhigh Elastic Restorability, and Exceptional Crack Tolerance. *Adv. Funct. Mater.* **2024**, *34*, 2312571
- (32) Costa, L.; Luda, M. P.; Cameron, G. G.; Qureshi, M. Y. The thermal and thermo-oxidative degradation of poly(tetrahydrofuran) and its complexes with LiBr and LiI. *Polym. Degrad. Stab.* **2000**, *67*, 527–533
- (33) Machalická, K.; Eliášová, M. Adhesive joints in glass structures: effects of various materials in the connection, thickness of the adhesive layer, and ageing. *Int. J. Adhes. Adhes.* **2017**, *72*, 10–22
- (34) Marchione, F.; Munafò, P. Experimental strength evaluation of glass/aluminum double-lap adhesive joints. *J. Build. Eng.* **2020**, *30*, 101284
- (35) Zhang, J.; Leitun, G.; Ben-David, Y.; Milstein, D. Facile Conversion of Alcohols into Esters and Dihydrogen Catalyzed by New Ruthenium Complexes. *J. Am. Chem. Soc.* **2005**, *127*, 10840–10841

Chapter Five

Nickel-Catalyzed Acyloxylation of C–H Bonds in Polyethylene

5.1 Introduction

Polyolefins are the most widely manufactured plastics for packaging, insulation, and surgical implants because of their chemical inertness and mechanical durability.^{1, 2} However, because of this inertness and their incompatibility with polar media, polyolefins are difficult to recycle chemically. Current methods to recycle polyolefins chemically are inefficient, and processes for diversifying the properties of polyolefin-based materials frequently involve the generation of complex composites that prove challenging to recycle or lead to substantial changes in molecular weight.^{3, 4} As a result, most polyolefins are made as single-use plastics, leading to the accumulation of 400 million metric tons of plastics waste in 2015. The accumulation of plastic waste is expected to increase exponentially in the future.⁵

The development of functional polyolefins is one approach to broadening the range of valuable properties that plastics can possess without the need to synthesize composites. This approach could lower the barriers confronting the recovery of these materials at their end of life.⁶⁻¹⁰ Pendent polar functionalities bound to polyolefin chains also improve the adhesion properties of these materials, rendering them potential coatings, compatibilizers, drug delivery modalities, and adhesives.^{9, 10} However, methods to create functional polyolefins by copolymerization with transition-metal catalysts are limited to classes of functional groups that do not poison these catalysts, and those by copolymerization with radical initiators lead to undesired branching in the polymer.^{6, 11}

Post-polymerization functionalization, which enables the structure of the polyolefin backbone to be established prior to the addition of polar functionalities, could circumvent some of the aforementioned challenges associated with copolymerization and broaden the scope of polyolefins containing polar functional groups that can be accessed.^{6, 11, 12} Previously reported catalytic methods to form C–O, C–X (X = CN, Cl, F, I), or C–N bonds to the polymer chain have been shown to yield various functional polyolefins, while minimizing undesired chain scission or crosslinking.¹³⁻¹⁷

Previously, our group reported a ruthenium-catalyzed oxidation of polyethylenes to install pendent ketone and hydroxyl groups without significant changes in molecular weight.¹⁸ These oxidized materials possessed improved adhesion and processability, even at low levels of functionalization. In addition, we showed they could be further derivatized into ester- and oxime-functionalized polyethylenes that have tunable properties, depending on the structure of the pendent group, such as increased adhesion to metal surfaces and tensile strength. In particular, the ester-containing polyethylenes had mechanical properties that were similar to those of ethylene-vinyl acetate (EVA), but with much lower glass transition temperatures because the levels of ester incorporation were lower than those in EVA synthesized by copolymerization.^{19, 20} Commercial EVA is highly branched because it is synthesized by free radical copolymerization; thus linear EVA is difficult to access through copolymerization.²¹ Post-polymerization functionalization of high-density polyethylene could provide a method to access linear EVA.

However, the methods used to synthesize these functional materials involved multiple synthetic steps following the initial C–H oxidation reaction (Figure 5.1.1A). To this end, strategies to furnish these polymers in fewer steps with inexpensive catalysts are needed. Here, we report a nickel-catalyzed acyloxylation of polyethylene to afford ester-functionalized polyethylenes in one chemical step (Figure 5.1.1B). Oxidation of the C–H bonds of polyethylene with cyclic diacyl peroxides installed pendent esters carrying alkyl or aryl substituents, and the surface and bulk properties of these functional polyethylenes are enhanced over those of unmodified polyethylene. These efforts, in concert, demonstrate the potential for the acyloxylation of C–H bonds of polyolefins to furnish functional polyolefins with greater reuse than traditional polyolefins.

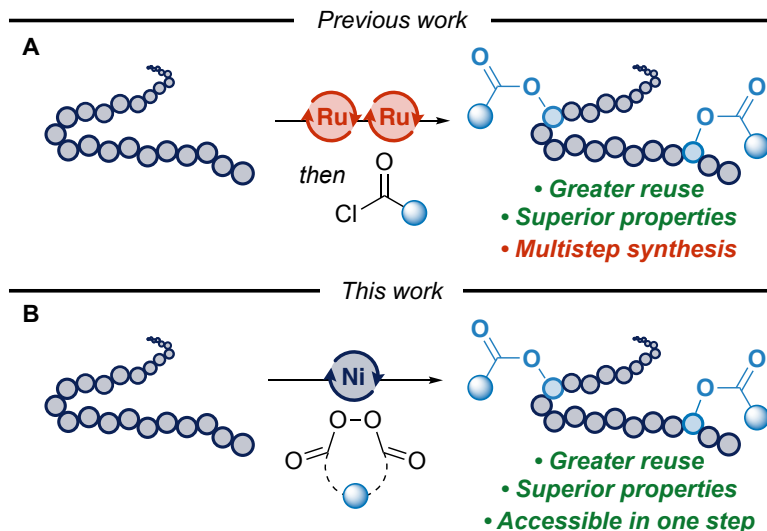


Figure 5.1.1. (A) Prior work: multistep synthesis of ester-functionalized polyethylenes. (B) This work: one-step synthesis of ester-functionalized polyethylenes.

5.2 Identification of Conditions for the Acyloxylation of C–H bonds

The acyloxylation of alkyl C–H bonds has been challenging because of the propensity of O-centered carboxy radicals to undergo decarboxylation or scission to generate C-centered radicals before they abstract a hydrogen atom.²² The functionalization of activated alkyl C–H bonds has been demonstrated to install esters efficiently;^{23–25} However, the acyloxylation of unactivated alkyl C–H bonds is underdeveloped. In addition, the nonpolar nature of polyolefins requires reagents and catalyst to be compatible with nonpolar media and high temperatures to functionalize the backbone of the polymer. These limitations lead to the difficulty in applying reactions that functionalize small molecules to polyolefins. To this end, we envisioned that the nickel-catalyzed acyloxylation of light alkanes with diacyl peroxides at 120 °C reported by Terent’ev, Alabugin and coworkers could be applied to the functionalization of polyethylene.²⁶ The mechanism of the acyloxylation of alkanes is proposed to start from a nickel(II) dicarboxylate, which undergoes oxidation to a nickel(III) carboxy radical by the diacyl peroxide (Figure 5.2.1). This radical, then, can abstract a hydrogen atom from the alkane to generate an alkyl radical, which recombines with the nickel center to furnish the C–O bond after reductive elimination.²⁷ Decarboxylation of the β -carboxy acid produces the product. Given that diacyl peroxide **1** contains a cyclopropane, fragmentation of the O-centered radical to generate a cyclopropyl C-centered radical is disfavored.²⁸

We began our studies by treating low density polyethylene (LDPE, $M_n = 9.4$ kDa, $D = 6.7$) with 4 mol % (with respect to monomer) diacyl peroxide **1** and 0.1 mol % (with respect to the monomer) nickel(II) acetate ($\text{Ni}(\text{OAc})_2$) at 120 °C in 1,2-dichlorobenzene (1,2-DCB), which enabled dissolution of the polymer (Table 5.2.1 entry 2). Swelling of the polymer was observed within an hour, and the precipitated polymer was not soluble in toluene or 1,1,2,2-tetrachloroethane, indicating formation of a crosslinked network. In addition, trace amounts of functionalization were observed in the soluble fraction by variable temperature ^1H NMR spectroscopy at 100 °C.

We reasoned that thermal decomposition of diacyl peroxide **1** initiates the crosslinking of polymer chains. To probe this, polyethylene was heated with diacyl peroxide **1** at 120 °C in the

absence of any nickel species, and swelling of the polymer was observed. These results support the proposal that diacyl peroxide **1** crosslinks the polymer (Table 5.2.1 entry 1). We hypothesized that the incompatibility of Ni(OAc)₂ with the nonpolar polymer chains resulted in little productive oxidation of the polymer over the course of the reaction because of the inability of generated alkyl radicals to recombine with the nickel center to furnish the product.²⁷

We performed the reaction with nickel catalysts containing substituents that rendered them more soluble in the polymer solution than Ni(OAc)₂. Swelling of the polymer was observed with reactions conducted with nickel(II) bis(acetylacetonate) (Ni(acac)₂) as a catalyst (Table 5.2.1 entry 3). However, when reactions were conducted with nickel(II) laurate (Ni(laurate)₂) as catalyst, approximately 0.8% of the monomer units were functionalized, as assessed by ¹H NMR spectroscopy at 100 °C (Table 5.2.1 entry 4). We presume that the longer alkyl substituents on nickel(II) carboxylates enables the catalyst to diffuse more readily within polymer domains. However, at higher loadings of diacyl peroxide **1**, crosslinking of the polymer resulted from reactions with Ni(laurate)₂, as determined by the insolubility of the recovered polymers in those reactions.

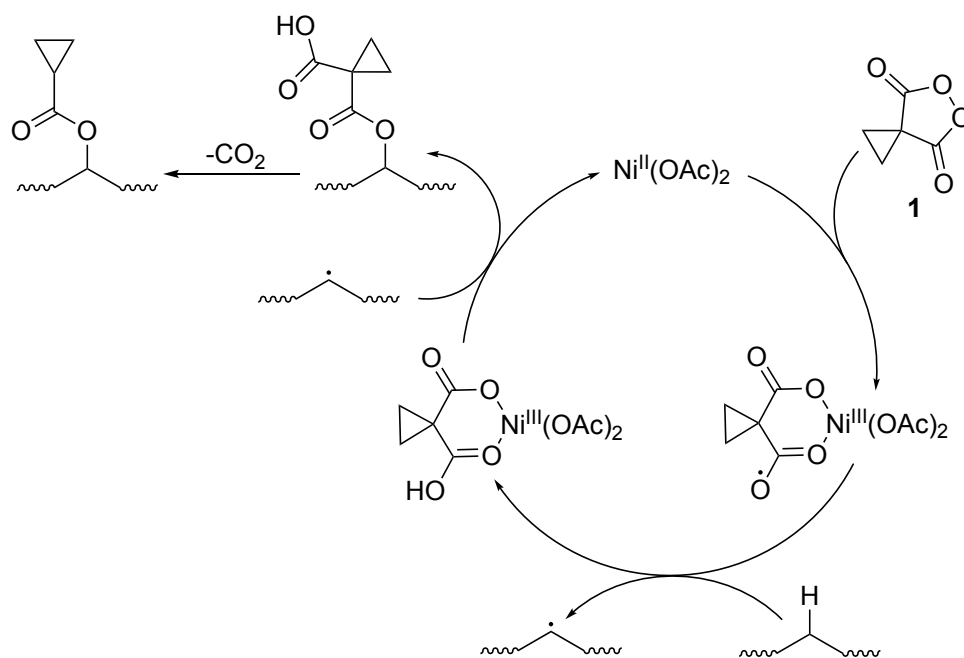
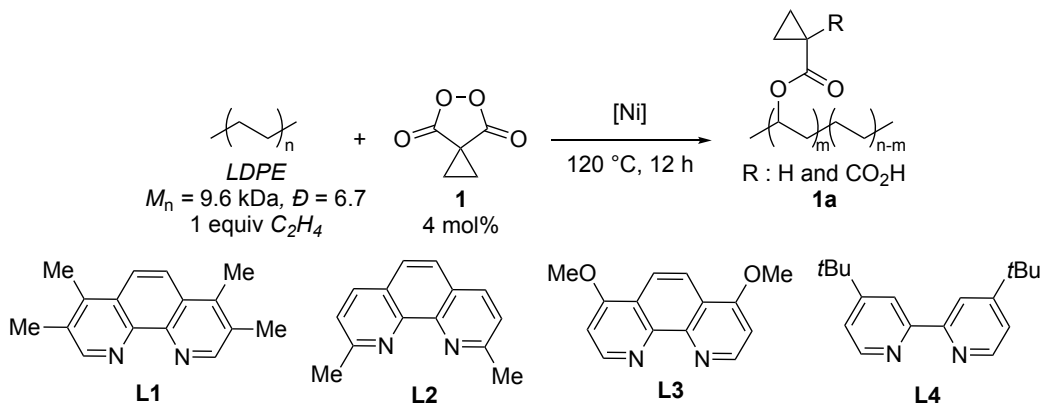


Figure 5.2.1. Proposed mechanism for the acyloxylation of alkanes with diacyl peroxides.

To increase the extent of functionalization and to minimize the degree of crosslinking of the polymer, we conducted reactions with nickel(II) complexes ligated by phenanthroline ligands ([Ni(L)₃](BPh₄)₂) because of their activity for the oxidation of polyethylenes to furnish pendent ketones and alcohols with peracids as the oxidant (Table 5.2.1 entries 5–8).¹³ Because reactions with [Ni(L)₃](BPh₄)₂ are proposed to operate through a radical-chain mechanism, chlorination of the polymer was also observed from the chlorinated solvent.²⁹ Instead of using *meta*-chloroperoxybenzoic acid as the oxidant, we used diacyl peroxide **1**. When [Ni(L1)₃](BPh₄)₂ was used as the catalyst, 1.0% of the monomer units were functionalized. Reactions with [Ni(L2)₃](BPh₄)₂ produced polyethylene with the highest extent of functionalization (1.2%). The yields of reactions with [Ni(L3)₃](BPh₄)₂ were similar to those of reactions catalyzed by

$[\text{Ni}(\mathbf{L1})_3](\text{BPh}_4)_2$, and the yields of reactions with $[\text{Ni}(\mathbf{L4})_3](\text{BPh}_4)_2$ were lower than those catalyzed by nickel ligated by phenanthroline ligands, indicating that bipyridine ligands are the least effective ligand for this transformation. Because reactions catalyzed by $[\text{Ni}(\mathbf{L3})_3](\text{BPh}_4)_2$ occurred in the highest yield, future reactions were conducted with $[\text{Ni}(\mathbf{L3})_3](\text{BPh}_4)_2$. Across all of the reactions conducted with $[\text{Ni}(\mathbf{L})_3](\text{BPh}_4)_2$ catalysts, swelling of the polymer was not observed over the course of the reaction. In addition, little chlorination was observed in all reactions run with $[\text{Ni}(\mathbf{L})_3](\text{BPh}_4)_2$ catalysts.

Table 5.2.1. Investigation of different nickel catalysts for the acyloxylation of polyethylene



entry	$[\text{Ni}]$	solvent	ester incorporation (%) ^a	yield (%) ^b
1 ^{c,e}	none	1,2-dichlorobenzene	--	--
2 ^{c,e}	$\text{Ni}(\text{OAc})_2$	1,2-dichlorobenzene	--	--
3 ^{c,e}	$\text{Ni}(\text{acac})_2$	1,2-dichlorobenzene	--	--
4 ^{c,f}	$\text{Ni}(\text{laurate})_2$	1,2-dichlorobenzene	0.8	20
5 ^{d,f}	$[\text{Ni}(\mathbf{L1})_3](\text{BPh}_4)_2$	1,2-dichloroethane	1.0	25
6 ^{d,f}	$[\text{Ni}(\mathbf{L2})_3](\text{BPh}_4)_2$	1,2-dichloroethane	1.2	30
7 ^{d,f}	$[\text{Ni}(\mathbf{L3})_3](\text{BPh}_4)_2$	1,2-dichloroethane	1.0	25
8 ^{d,f}	$[\text{Ni}(\mathbf{L4})_3](\text{BPh}_4)_2$	1,2-dichloroethane	0.7	18

^aAmount of monomer that is functionalized as determined by ¹H NMR spectroscopy at 100 °C.

^bYield with respect to the loading of peroxide. ^cReaction performed with 0.1 mol% catalyst.

^dReaction performed with 0.015 mol% catalyst. ^eReaction performed with 400 mg PE per mL of solvent. ^fReaction performed with 160 mg PE per mL of solvent.

5.3 Investigation of the Scope of Peroxides

With conditions that functionalize polyethylene in hand, we investigated the scope of esters that could be appended to polyethylene. In this fashion, one set of conditions could be applied to the transformations of polyethylenes to install multiple functional groups to modulate properties to the polymer by varying the oxidant. Treatment of a dicarboxylic acid with a solution of urea hydrogen peroxide in methanesulfonic acid furnished select diacyl peroxides with aryl and alkyl substituents (see Section 5.6.4).

With these peroxides in hand, we investigated their reactivity in the acyloxylation of polyethylene catalyzed by $[\text{Ni}(\text{L3})_3](\text{BPh}_4)_2$ (Figure 5.3.1). Diacyl peroxides with geminal methyl and ethyl groups did not undergo acyloxylation of polyethylene. Peroxide **2** did not react under the conditions, and reactions with peroxide **3** produced *keto*-polyethylenes with approximately 0.9% of the monomers functionalized. Spirocyclic peroxide **4**, which contains a cyclobutane, also did not react appreciably under these conditions. We propose that the lack of reactivity with peroxide **4** results from the rapid fragmentation of the O-centered radical. Reactions performed with phthaloyl peroxide **5** as the oxidant produced ester-functionalized polyethylene with 1.2% benzoyloxy groups. These results highlight the ability of ester-functionalized polyethylenes to be synthesized in one step by nickel catalysts.

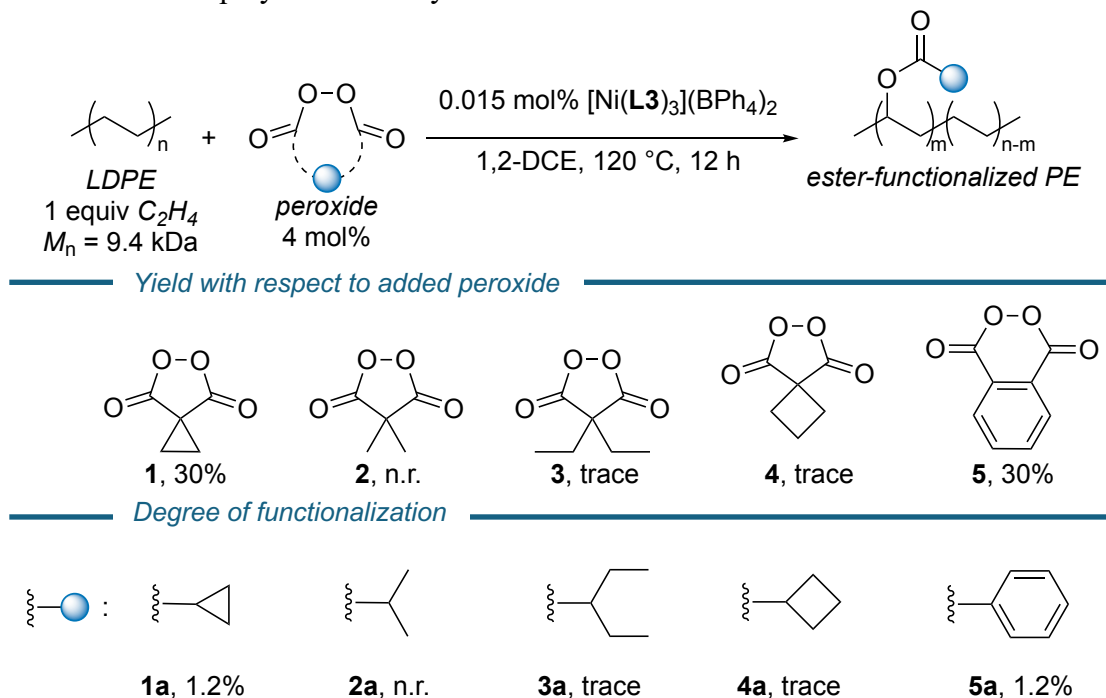


Figure 5.3.1. Scope of functional polyethylenes synthesized.

5.4 Material Testing

Because the toughness and elongation at break of polyethylenes containing pendent esters have been shown to be greater than those of the unfunctionalized material, we sought to gauge the bulk properties of the polyethylenes containing pendent ester groups by tensile tests.³⁰ To this end, we performed tensile tests on polymer **1a**, which was synthesized with $\text{Ni}(\text{laurate})_2$ as catalyst and contains 0.7% of functionalized monomer units (Figure 5.4.1A). The elongation at break (ϵ_B) and toughness (U_T) of polymer **1a** ($520.2 \pm 76.6\%$ and $54.2 \pm 13.9\text{ MJ m}^{-3}$ respectively) were higher than those of unmodified LDPE ($\epsilon_B = 227.8 \pm 96.8\%$ and $U_T = 19.5 \pm 9.8\text{ MJ m}^{-3}$), indicating the effect of the esters on the polymer backbone on these properties. The acyloxylation of polyethylene did not change the strength of the polymer significantly; the tensile strength (σ_B) of polymer **1a** ($12.1 \pm 1.3\text{ MPa}$) was similar to that of unmodified LDPE ($11.4 \pm 1.1\text{ MPa}$). Finally, the Young's Modulus (E) of polymer **1a** ($90.3 \pm 7.8\text{ MPa}$) was lower than that of the unmodified LDPE ($148.5 \pm 16.8\text{ MPa}$) because the ester moieties disrupt the overall crystallinity of the material.¹⁸ The results of the tensile tests reveal that the acyloxylation of polyethylene in one step can produce oxygen-

functionalized polymers with properties akin to those of polyolefins generated in multiple steps or EVA copolymers containing low levels of vinyl acetate monomers.²⁰

We envisioned that the installed esters would modify the surface properties of the polymer, such as adhesion. To probe this hypothesis, we subjected polymer **1a** to lap-shear tests with aluminum substrates (Figure 5.4.1B). Unmodified LDPE was not adhesive enough to create a testable sample. Indeed, polymer **1a** was more adhesive to aluminum (1.6 ± 0.4 MPa) than was unmodified LDPE. We propose that the pendent esters form attractive interactions with the oxidized surface of the aluminum. The lap shear tests show that although the installation of ester groups enhances the adhesion of polyethylene. The adhesion of polymer **1a** to aluminum is less than that of *hydroxy*-polyethylene synthesized through the direct oxidation of polyethylene (6.0 ± 0.9 MPa).¹⁸ Although both alcohols and esters are able to form hydrogen-bonding interactions with the metal oxide surface, the alcohols on *hydroxy*-polyethylene could form covalent bonds with the aluminum by displacement of water, leading to higher adhesion.³¹

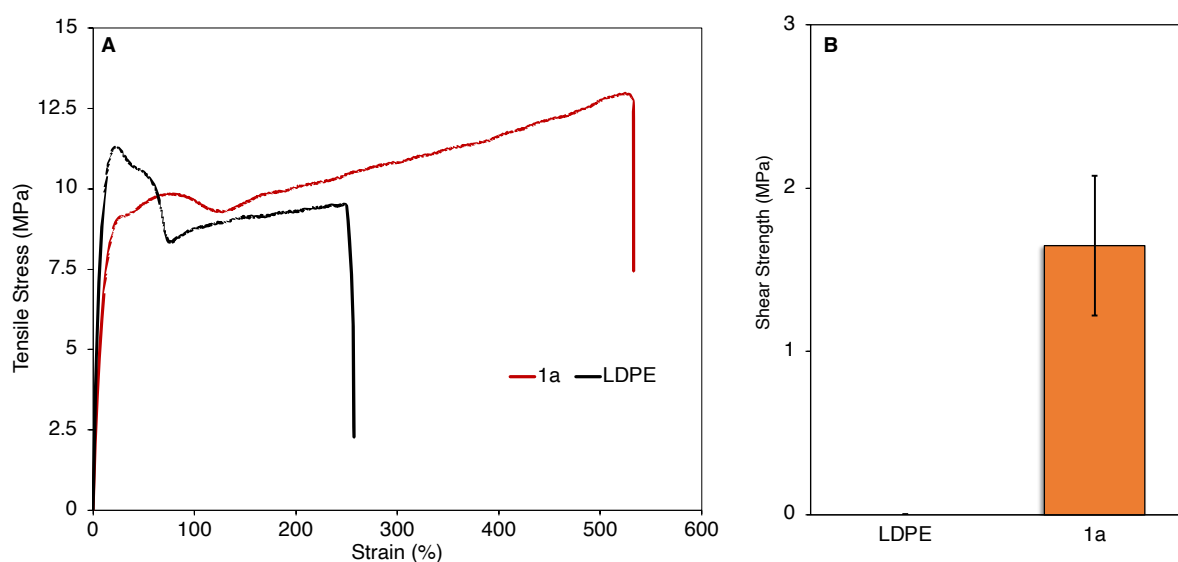


Figure 5.4.1. (A) Tensile tests of unmodified LDPE and polymer **1a**. (B) Lap-shear tests of unmodified LDPE and polymer **1a** with aluminum substrates

5.5 Conclusions and Future Directions

In conclusion, this work reveals a method to install esters onto polyethylene with nickel-based catalysts. The oxidants used were cyclic diacyl peroxides containing small or aromatic rings, which can be synthesized readily from the corresponding dicarboxylic acid with urea hydrogen peroxide. Preliminary materials testing of the ester-containing polyethylenes showed that the toughness, ductility, and adhesion to aluminum increase after functionalization. These efforts show that the development of strategies for the functionalization of C–H bonds in polyolefins could engender materials of higher value efficiently from the starting polyolefins.

Future work seeks to apply the nickel-catalyzed acyloxylation to other polyethylenes such as high-density polyethylene (HDPE), linear low-density polyethylene (LLDPE), and even polyethylene waste. Bifunctional polyethylenes containing two types of pendent esters also could be furnished by this strategy upon the addition of two peroxides to the reaction. The pendent functional groups could be hydrolyzed to cleave the ester and generate *hydroxy*-polyethylenes,

conferring an element of circularity to these polymers by enabling them to be subsequently re-functionalized.³⁰

5.6 Experimental Section

5.6.1 General Information

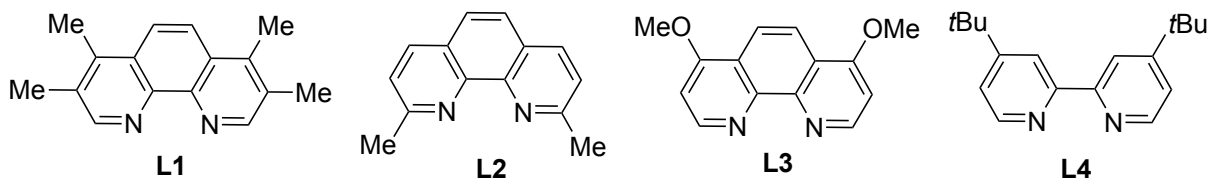
All air sensitive manipulations were conducted under an inert atmosphere in a nitrogen-filled or argon-filled glovebox or by standard Schlenk techniques. All reagents were purchased from commercial sources and used without further purification. Low density polyethylene (LDPE) was purchased from Sigma-Aldrich. Solvents were degassed with nitrogen and dried in a solvent purification system with a 1 m column containing activated alumina and stored under 4 Å molecular sieves. Fourier-transform infrared spectra were collected using a Bruker Vortex 80 spectrometer. Room-temperature NMR spectra were collected using 500 and 600 MHz Bruker Instruments at the University of California, Berkeley. Variable-temperature NMR spectroscopic analysis was conducted on the 600 MHz instruments at University of California Berkeley. ^1H chemical shifts were reported in ppm relative to the resonance of the residual solvent (CDCl_3 , 7.26 ppm; $\text{C}_2\text{D}_2\text{Cl}_4$, 6.00 ppm). ^{13}C chemical shifts were reported in ppm relative to the resonance of the residual solvent (CDCl_3 , 77.16 ppm; $\text{C}_2\text{D}_2\text{Cl}_4$, 73.78 ppm). Aluminum 6061 (Al-6061) substrates were cut at the UC Berkeley Cory Hall Machine shop from 0.160 cm thick, 10.16 cm x 121.92 cm (0.063" thick, 4"x48") sheet stocks purchased from McMaster-Carr (USA). Lap shear adhesion testing was conducted according to ASTM D1002-10 on an Instron universal materials tester equipped with a 5 kN load cell with a shear rate of 1.5 mm/min. Adhesion strength was determined by the maximum load divided by the bonded overlap area, which was measured with digital calipers prior to testing, and the apparent failure mode was assessed visually. The adhesive strengths of LDPE and functionalized polyethylenes to aluminum were assessed by single lap shear testing on rectangular aluminum 6061 (Al 6061) substrates with dimensions 0.16 cm thick x 1 cm width x 10 cm length. Compression molding was conducted on a Carver benchtop lab press with heated plates (model 4386). Tensile testing was conducted according to ASTM D638 on an Instron universal materials tester. Tensile stress and strain were measured at room temperature using an extension rate of 50 mm/min.

5.6.2 Calculation of Yield and Degree of Functionalization

The degree of functionalization was determined by ^1H NMR spectroscopy at 100°C in $\text{C}_2\text{D}_2\text{Cl}_4$. The integration of the peaks between 1.0–1.7 ppm was set to 400 (4 proton per monomer unit, 100 monomer units in total). The integration of the methine proton that was alpha to the esters was then compared to the integration of the protons of the monomer units. Yield was calculated by the degree of functionalization divided by the initial loading of peroxide in the reaction mixture.

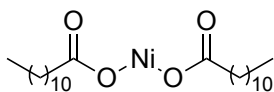
5.6.3 Synthesis of Nickel Catalysts

Synthesis of $[\text{Ni}(\text{L}_n)_3](\text{BPh}_4)_2$ complexes:



The general procedure for the synthesis of $[\text{Ni}(\text{L})_3](\text{BPh}_4)_2$ complexes was adapted from a literature procedure.¹³ To a 20 mL vial, $\text{Ni}(\text{OAc})_2 \cdot 4\text{H}_2\text{O}$ (1.0 equiv) and the corresponding ligand (3.0 equiv) were dissolved in methanol. The reaction mixture was stirred at room temperature for 2 h. Then, NaBPh_4 was added to the reaction mixture, and the vial was stirred at room temperature for 12 h. A precipitate formed, which was filtered and washed with copious amounts of water, ethanol, and hexane. The solid was then dissolved in DCM, and the solution was dried over sodium sulfate. The DCM was concentrated *in vacuo*, and the resulting solid was recrystallized from acetone and filtered to yield the product.

Synthesis of $\text{Ni}(\text{laurate})_2$:

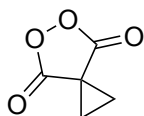


To a 40 mL vial equipped with a stir bar were added 1.0 g (4.5 mmol, 1.0 equiv) sodium laurate. The solids were suspended in H_2O (20 mL). The mixture was heated at 70°C until the sodium laurate dissolved. A solution of 291 mg NiCl_2 (2.2 mmol, 0.5 equiv) dissolved in 5 mL H_2O was then added dropwise to the vial while stirring. The resulting mixture was heated at 70°C for 4 h. After cooling to room temperature, the mixture was decanted into two 50 mL centrifuge tubes and spun at 7500 rpm for 12 min. The supernatant was discarded, and the remaining pellets were redispersed in 25 mL H_2O and sonicated for 5 min. The redispersed pellets were spun at 7500 rpm for 12 min. The sonication and centrifugation steps were then repeated a total of five times. For the final wash, the pellets were dispersed in 20 mL methanol prior to centrifugation. The pellets were air-dried overnight, then transferred to a 20 mL vial and dried under vacuum at 80°C .

5.6.4 Synthesis of Peroxides

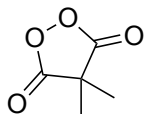
CAUTION: Organic peroxides are potentially explosive compounds. Proper safety precautions should be taken while following the procedures listed herein. Avoid excess heat or shock when working with any organic peroxide.

5,6-dioxaspiro[2.4]heptane-4,7-dione (1)



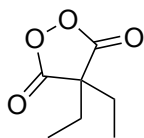
The synthesis of the title compound was adapted from a literature procedure.³² To a 100 mL round-bottom flask equipped with a stir bar were added 15 mL of methanesulfonic acid. Then, urea hydrogen peroxide (4.8 g, 51 mmol) was added to the flask. The flask was stirred in a water bath at room temperature until the peroxide dissolved. Cyclopropane-1,1-dicarboxylic acid (2.2 g, 17 mmol) was then added to the flask, and the flask was stirred in the water bath at room temperature for 24 h. Then the reaction mixture was diluted with ice and ethyl acetate, and the layers were separated. The aqueous portion was washed with ethyl acetate (2 x 20 mL). The combined organic layers were washed with a saturated solution of sodium bicarbonate (2 x 20 mL) and aqueous brine (2 x 20 mL). The organic layer was dried over magnesium sulfate and concentrated to yield the product as a white solid (1.6 g, 74%). The ¹H NMR and ¹³C NMR spectra matched the literature report. ¹H NMR (500 MHz, CDCl₃) δ 2.10 (s, 4H). ¹³C NMR (125 MHz, CDCl₃) δ 172.2, 23.7, 19.9.

4,4-dimethyl-1,2-dioxolane-3,5-dione (2)



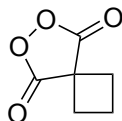
The synthesis of the title compound was adapted from a literature procedure.³³ To a 40 mL glass vial flask equipped with a stir bar were added 5 mL of methanesulfonic acid. Then, urea hydrogen peroxide (1.1 g, 12 mmol) was added to the vial. The vial was stirred in a water bath at room temperature until the peroxide dissolved. Dimethylmalonic acid (500 mg, 3.8 mmol) was then added to the vial, and the vial was stirred in the water bath at room temperature for 24 h. Then, the reaction mixture was diluted with ice and ethyl acetate, and the layers were separated. The aqueous portion was washed with ethyl acetate (2 x 20 mL). The combined organic layers were washed with a saturated solution of sodium bicarbonate (2 x 20 mL) and aqueous brine (2 x 20 mL). The product was collected as a crystalline white solid (111 mg, 23%). The ¹H NMR and ¹³C NMR spectra matched the literature report. ¹H NMR (500 MHz, CDCl₃) δ 1.58 (s, 6H). ¹³C NMR (125 MHz, CDCl₃) δ 174.8, 39.0, 21.7.

4,4-diethyl-1,2-dioxolane-3,5-dione (3)



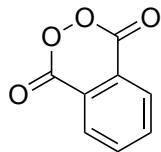
The synthesis of the title compound was adapted from a literature procedure.³³ To a 40 mL glass vial flask equipped with a stir bar were added 5 mL of methanesulfonic acid. Then, urea hydrogen peroxide (700 mg, 7.4 mmol) was added to the vial. The vial was stirred in a water bath at room temperature until the peroxide dissolved. Diethylmalonic acid (500 mg, 3.1 mmol) was then added to the vial, and the vial was stirred in the water bath at room temperature for 24 h. Then, the reaction mixture was diluted with ice and ethyl acetate, and the layers were separated. The aqueous portion was washed with ethyl acetate (2 x 20 mL). The combined organic layers were washed with a saturated solution of sodium bicarbonate (2 x 20 mL) and aqueous brine (2 x 20 mL). The product was collected as a colorless oil (255 mg, 52%). ¹H NMR (500 MHz, CDCl₃) δ 1.96 (q, *J* = 7.5 Hz, 4H), 1.01 (t, *J* = 7.5 Hz, 6H). ¹³C NMR (125 MHz, CDCl₃) δ 174.1, 51.1, 28.8, 9.0.

6,7-dioxaspiro[3.4]octane-5,8-dione (4)



The synthesis of the title compound was adapted from a literature procedure.³² To a 40 mL glass vial flask equipped with a stir bar were added 5 mL of methanesulfonic acid. Then, urea hydrogen peroxide (1.0 g, 11 mmol) was added to the vial. The vial was stirred in a water bath at room temperature until the peroxide dissolved. Cyclobutane-1,1-dicarboxylic acid (2.2 g, 17 mmol) was then added to the vial, and the vial was stirred in the water bath at room temperature for 24 h. Then, the reaction mixture was diluted with ice and ethyl acetate, and the layers were separated. The aqueous portion was washed with ethyl acetate (2 x 20 mL). The combined organic layers were washed with a saturated solution of sodium bicarbonate (2 x 20 mL) and aqueous brine (2 x 20 mL). The organic layer was dried over magnesium sulfate and concentrated to yield the product as a white solid (420 mg, 85%). The ¹H NMR and ¹³C NMR spectra matched the literature report. ¹H NMR (500 MHz, CDCl₃) δ 2.71 (t, *J* = 8.2 Hz, 4H), 2.37 (m, 2H). ¹³C NMR (125 MHz, CDCl₃) δ 174.0, 40.5, 29.0, 16.4.

benzo[*d*][1,2]dioxine-1,4-dione (5)



The synthesis of the title compound was adapted from a literature procedure.³³ To a 40 mL glass vial flask equipped with a stir bar were added 20 mL of anhydrous dichloromethane. Then, phthaloyl dichloride (560 mg, 2.7 mmol) was added to the vial. The vial was stirred in a water bath at room temperature, and sodium percarbonate (380 mg, 2.5 mmol) was added in one portion. The vial was stirred rigorously in the water bath at room temperature for 24 h. Then, the reaction mixture was filtered, and solvent was removed *in vacuo* to yield the product as a white solid (340 mg, 95%). The ¹H NMR and ¹³C NMR spectra matched the literature report. ¹H NMR (500 MHz, CDCl₃) δ 8.29 (m, 2H), 8.04 (m, 2H). ¹³C NMR (125 MHz, CDCl₃) δ 162.0, 136.5, 130.2, 123.7.

5.6.5 Synthesis of Functionalized Polyethylenes

CAUTION: Organic peroxides are potentially explosive compounds. Proper safety precautions should be taken while following the procedures listed herein. Avoid excess heat or shock when working with any organic peroxide.

CAUTION: CO₂ can be released, leading to a buildup of pressure! Do not fill reaction vessels over one third of the total volume of the vessel.

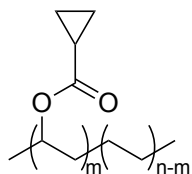
5.6.5.1 Synthesis of Functionalized Polyethylenes with [Ni(Ln)₃](BPh₄)₂ complexes

The general procedure for the synthesis of functionalized polyethylenes was adapted from a literature procedure.¹³ To a 20 mL vial equipped with a stir bar, low-density polyethylene (325 mg, 11.6 mmol monomer) was added, and the polymer was suspended in 2 mL of 1,2-dichloroethane under nitrogen. The vial was heated at 120 °C until the polymer dissolved. Then the vial was cooled to room temperature, and the corresponding peroxide (0.46 mmol) and nickel catalyst (0.0017 mmol) were added under nitrogen. The vial was heated at 120 °C for 12 h. Then, 10 mL of methanol were added to precipitate the polymer. The slurry was filtered, and the polymer was collected and dried. The polymer was dissolved in toluene and precipitated with methanol to purify it. The slurry was filtered, and the polymer was dried under vacuum overnight.

5.6.5.2 Synthesis of Functionalized Polyethylenes with Ni(laurate)₂

To a 24 mL vial equipped with a stir bar, low-density polyethylene (150 mg, 5.3 mmol monomer) and Ni(laurate)₂ (3.4 mg, 0.0074 mmol) were added, and the polymer was suspended in 1 mL of 1,2-dichlorobenzene under nitrogen. The vial was heated at 120 °C until the polymer dissolved. Then, the vial was cooled to room temperature, and the corresponding peroxide (0.21 mmol) was added under nitrogen. The vial was heated at 120 °C for 12 h. Then, 10 mL of methanol were added to precipitate the polymer. The slurry was filtered, and the polymer was collected and dried. The polymer was dissolved in toluene and precipitated with methanol to purify it. The slurry was filtered, and the polymer was dried under vacuum overnight.

5.6.6 Characterization of Polymers Cyclopropoyloxy LDPE (1a)



^1H NMR (600 MHz, $\text{C}_2\text{D}_2\text{Cl}_4$) δ 4.89 (p, $J = 6.2$ Hz, $\text{CHOC}(\text{O})\text{CO}_2\text{H}$), 1.58 (br), 1.35 (br), 1.01 (br), 0.98 – 0.88 (m), 0.84 (br).

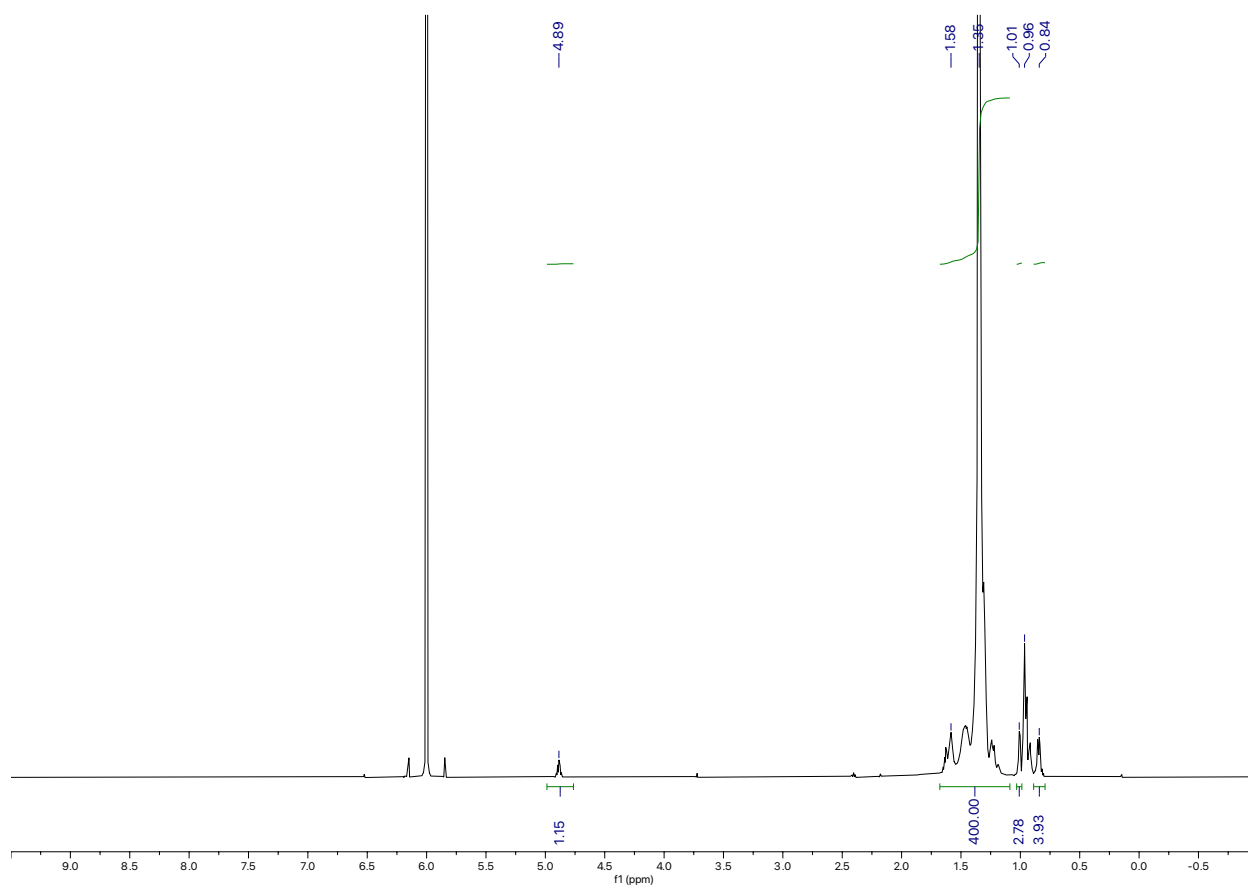
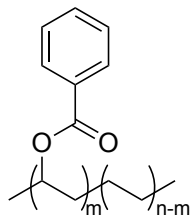


Figure 5.6.6.1. ^1H NMR spectrum of polymer 1a.

Benzoyloxy LDPE (5a)



$^1\text{H NMR}$ (600 MHz, $\text{C}_2\text{D}_2\text{Cl}_4$) δ 8.07 (d, $J = 6.9$ Hz), 7.58 (t, $J = 7.3$ Hz), 7.47 (t, $J = 7.6$ Hz), 5.16 (p, $J = 6.7$ Hz, CHOC(O)Ph), 1.73 (br), 1.35 (br), 0.98 – 0.88 (m).

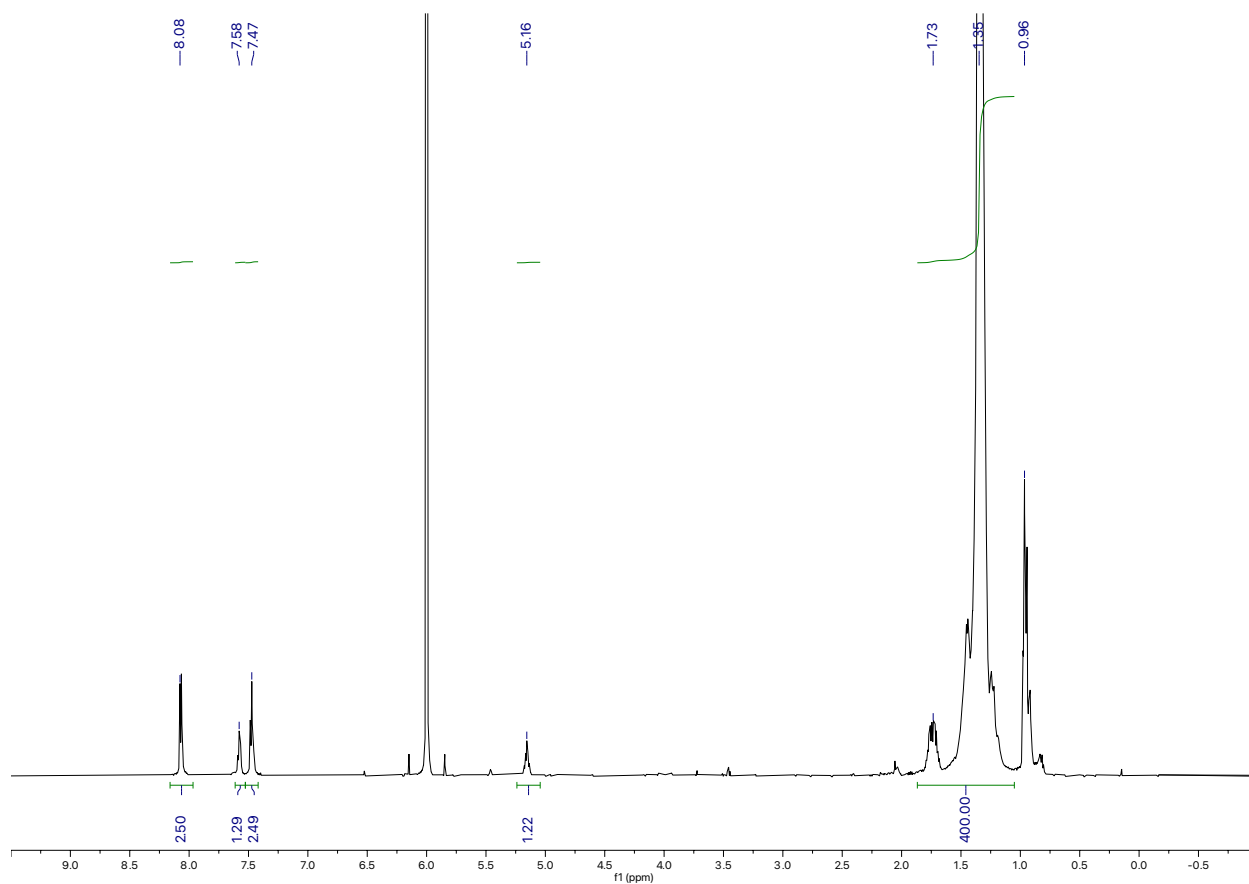


Figure 5.6.6.2. $^1\text{H NMR}$ spectrum of polymer 5a.

5.6.7 Materials Testing

5.6.7.1 Procedure for Lap Shear Tests

Lap shear tests were conducted according to ASTM D1002-10 on an Instron universal materials tester equipped with a 5 kN load cell with a shear rate of 1.5 mm/min. Adhesion strength was determined by the maximum load divided by the bonded overlap area, which was measured with digital calipers prior to testing, and the apparent failure mode was assessed visually.

Substrate and Lap Joint Preparation

- 3. Degreased Substrates:** To prepare the aluminum and glass substrates for adhesive bonding, they were degreased. Substrates were wiped with a fresh Kimwipe soaked in acetone, followed by a second Kimwipe soaked in ethyl acetate. Substrates were air-dried, and a 1 cm x 1 cm area was isolated with vinyl electrical tape.
- 4. Lap joint preparation:** Polymer films of LDPE and functionalized polyethylenes (0.1 – 0.3 mm) were prepared on a hot press at 120 °C for 45 seconds to provide melts. Specifically, polymer samples between two Kapton films were pressed between steel plates at 2000 psig. Teflon shims were used to control film thickness. The samples were cooled at room temperature, and a 1 cm x 1 cm piece of the polymer film was cut. The cut films were placed at the end of a clean Al 6061 adherend or glass, and vinyl masking tape was removed. The substrates were overlapped in an antiparallel arrangement, clamped with two small binder clips, and subsequently transferred to a pre-heated oven. Samples were heated at 140 °C for 5 minutes. All samples were allowed to cool slowly to room temperature. Excess polyethylene adhesive was carefully removed from the edges with a razor. Shims were applied to lap joint ends to help align the grip of the mechanical tester. Multiple attempts to prepare lap joints with LDPE failed, as indicated by breaking of the lap joint during the clamping process. Thus, the adhesion strengths of LDPE were unmeasurable by this method. All measurable samples were loaded at 1.5 mm/min in shear until failure, whereas the dimensions of the bonded area were measured with calipers. Finally, the adhesive strength was determined by the peak load divided by the overlap area. Lap shear measurements were repeated for at least four specimens, and the values reported are averages of the measurements of these sets of specimens.

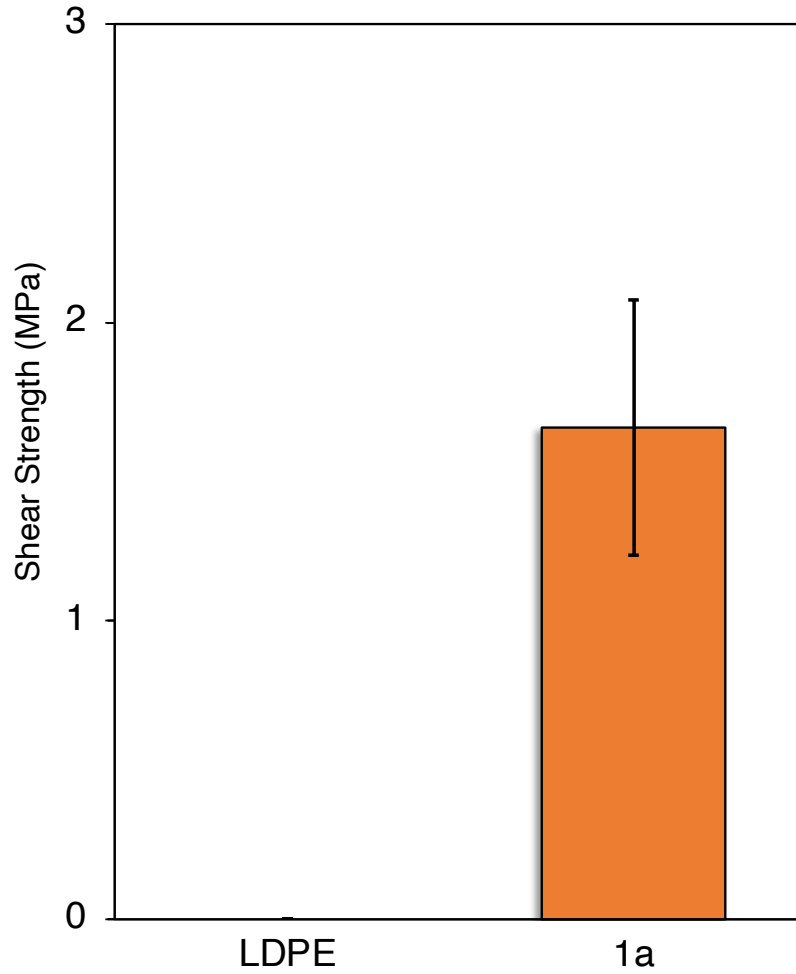


Figure 5.6.7.1.1. Lap shear strength of joints Al-LDPE-Al and Al-1a-Al

Table 5.6.7.1.1. Summary of results of adhesion strength in lap shear tests

Entry	Interface	Shear Strength (MPa)	Mode of Failure
1 ^a	Al-LDPE-Al	--	--
2	Al-1a-Al	1.6 ± 0.4	Adhesive

^aShear strength not measurable because of lap joint failure during the clamping process.

5.6.7.2 Procedure for Tensile Tests

- 4. Sample preparation:** Polymer films of LDPE, polymer **2a**, and PUU **4** were prepared on a hot press at 120 °C for 45 seconds to provide melts ($350 \pm 50 \mu\text{m}$ thickness). Specifically, polymer samples between two Kapton films were pressed between steel plates at 2000 psig. Teflon shims were used to control film thickness. The samples were then cooled at room temperature and cut into a dog-bone geometry using a cutting die (ASTM D-638V) to obtain samples that were 9.53 mm in length and 3.18 mm in width.
- 5. Experimental procedures for tensile tests:** Tensile testing was conducted according to ASTM D638 on an Instron universal materials tester. Tensile stress and strain were measured at room temperature using an extension rate of 50 mm/min. Measurements were repeated for at least three samples, and average values are reported.

Table 5.6.7.2.1. Summary of results of tensile tests

Polymer	tensile stress at max load (MPa)	Young's Modulus (MPa)	tensile strain (extension) at break (%)	toughness (MJ/m ³)
LDPE	11.4 ± 1.1	148.5 ± 16.8	227.8 ± 96.8	19.5 ± 9.8
1a	12.1 ± 1.3	90.3 ± 7.8	520.2 ± 76.6	54.2 ± 13.9

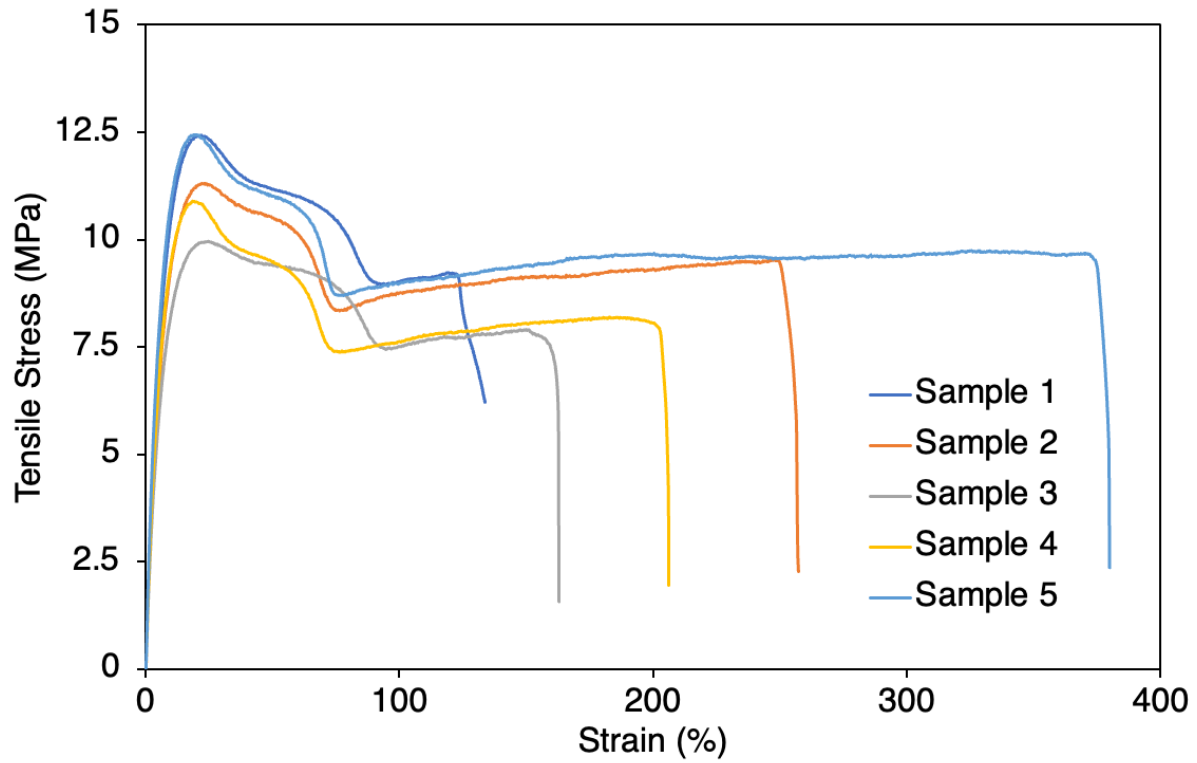


Figure 5.6.7.2.1. Stress-strain curves for unmodified LDPE

Table 5.6.7.2.3. Summary of results of tensile tests for unmodified LDPE

Sample	tensile stress at max load (MPa)	Young's Modulus (MPa)	tensile strain (extension) at break (%)	toughness (MJ/m ³)
1	12.4	160.4	133.7	13.4
2	11.3	142.4	256.7	13.5
3	10.0	125.8	162.8	17.1
4	10.9	144.9	206.1	36.7
5	12.5	169.0	379.8	16.9

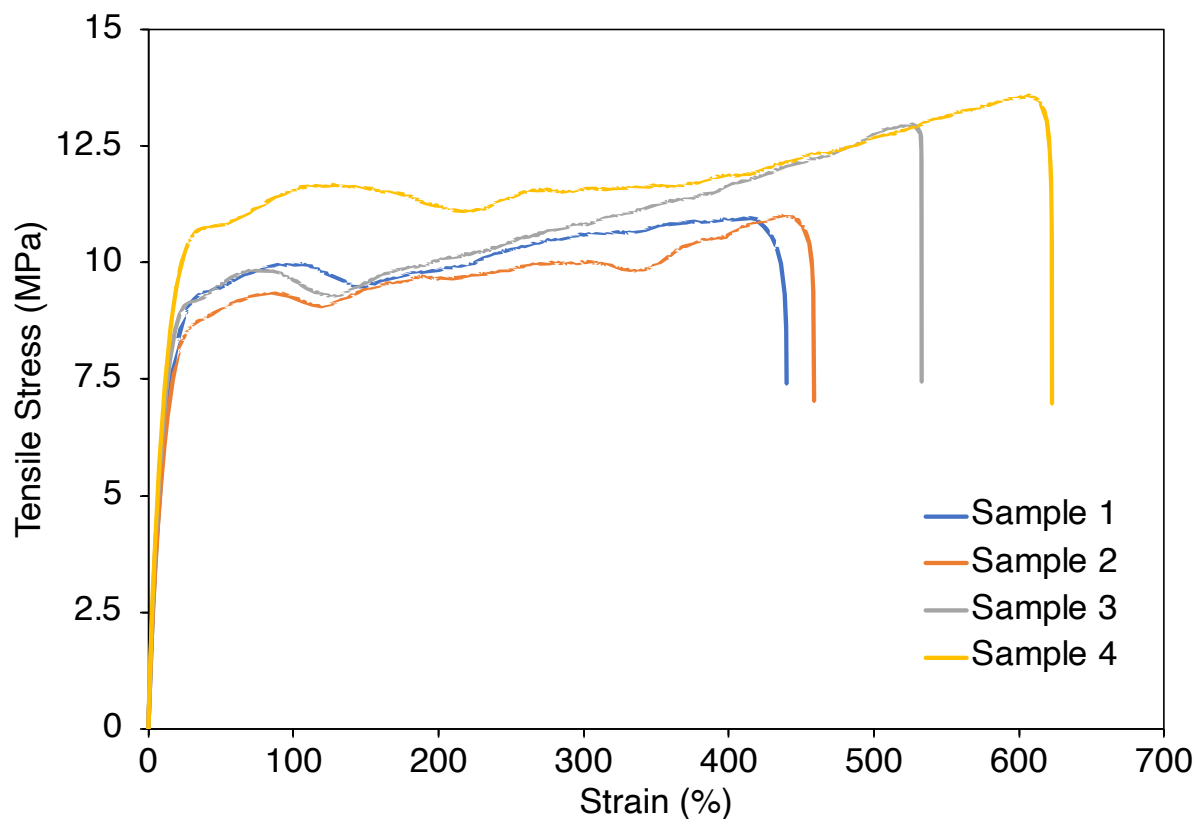


Figure 5.6.7.2.2. Stress-strain curves for polymer **1a**

Table 5.6.7.2.4. Summary of results of tensile tests for polymer **1a**

Sample	tensile stress at max load (MPa)	Young's Modulus (MPa)	tensile strain (extension) at break (%)	toughness (MJ/m ³)
1	11.0	84.5	450.4	43.6
2	11.0	82.8	474.9	43.9
3	13.0	95.5	532.9	56.5
4	13.6	98.4	622.8	72.9

5.7 References

- (1) Shorten, D. W. Polyolefins for food packaging. *Food Chem.* **1982**, *8*, 109–119
- (2) Kim, Y. K. The use of polyolefins in industrial and medical applications. In *Polyolefin Fibres*, Elsevier, 2017; pp 135–155.
- (3) Wu, D. Y.; Gutowski, W. S.; Li, S.; Griesser, H. J. Ammonia plasma treatment of polyolefins for adhesive bonding with a cyanoacrylate adhesive. *J. Adhes. Sci. Technol.* **2012**, *9*, 501–525
- (4) Sanchis, M. R.; Blanes, V.; Blanes, M.; Garcia, D.; Balart, R. Surface modification of low density polyethylene (LDPE) film by low pressure O₂ plasma treatment. *Eur. Polym. J.* **2006**, *42*, 1558–1568
- (5) Geyer, R.; Jambeck, J. R.; Law, K. L. Production, use, and fate of all plastics ever made. *Sci. Adv.* **2017**, *3*, e1700782
- (6) Boen, N. K.; Hillmyer, M. A. Post-polymerization functionalization of polyolefins. *Chem. Soc. Rev.* **2005**, *34*, 267
- (7) Gauthier, M. A.; Gibson, M. I.; Klok, H.-A. Synthesis of Functional Polymers by Post-Polymerization Modification. *Angew. Chem. Int. Ed.* **2009**, *48*, 48–58
- (8) Passaglia, E.; Coiai, S.; Cicogna, F.; Ciardelli, F. Some recent advances in polyolefin functionalization. *Polym. Int.* **2014**, *63*, 12–21
- (9) Franssen, N. M. G.; Reek, J. N. H.; De Bruin, B. Synthesis of functional ‘polyolefins’: state of the art and remaining challenges. *Chem. Soc. Rev.* **2013**, *42*, 5809
- (10) Jasinska-Walc, L.; Bouyahyi, M.; Duchateau, R. Potential of Functionalized Polyolefins in a Sustainable Polymer Economy: Synthtic Strategies and Applications. *Acc. Chem. Res.* **2022**, *55*, 1985–1996
- (11) Plummer, C. M.; Li, L.; Chen, Y. The post-modification of polyolefins with emerging synthetic methods. *Polym. Chem.* **2020**, *11*, 6862–6872
- (12) Williamson, J. B.; Lewis, S. E.; Johnson, R. R.; Manning, I. M.; Leibfarth, F. A. C–H Functionalization of Commodity Polymers. *Angew. Chem. Int. Ed.* **2019**, *58*, 8654–8668
- (13) Bunescu, A.; Lee, S.; Li, Q.; Hartwig, J. F. Catalytic Hydroxylation of Polyethylenes. *ACS Cent. Sci.* **2017**, *3*, 895–903
- (14) Williamson, J. B.; Czaplowski, W. L.; Alexanian, E. J.; Leibfarth, F. A. Regioselective C–H Xanthylation as a Platform for Polyolefin Functionalization. *Angew. Chem. Int. Ed.* **2018**, *57*, 6261–6265
- (15) Fazekas, T. J.; Alty, J. W.; Neidhart, E. K.; Miller, A. S.; Leibfarth, F. A.; Alexanian, E. J. Diversification of aliphatic C–H bonds in small molecules and polyolefins through radical chain transfer. *Science* **2022**, *375*, 545–550
- (16) Ciccina, N. R.; Shi, J. X.; Pal, S.; Hua, M.; Malollari, K. G.; Lizandara-Pueyo, C.; Risto, E.; Ernst, M.; Helms, B. A.; Messersmith, P. B.; Hartwig, J. F. Diverse functional polyethylenes by catalytic amination. *Science* **2023**, *381*, 1433–1440
- (17) Bae, C.; Hartwig, J. F.; Boen Harris, N. K.; Long, R. O.; Anderson, K. S.; Hillmyer, M. A. Catalytic Hydroxylation of Polypropylenes. *J. Am. Chem. Soc.* **2005**, *127*, 767–776
- (18) Chen, L.; Malollari, K. G.; Uliana, A.; Sanchez, D.; Messersmith, P. B.; Hartwig, J. F. Selective, Catalytic Oxidations of C–H Bonds in Polyethylenes Produce Functional Materials with Enhanced Adhesion. *Chem* **2021**, *7*, 137–145
- (19) Cerrada, M. L.; Pereña, J. M.; Benavente, R.; Pérez, E. Mechanical properties of vinyl aclohol–ethylene copolymers. *Polym. Eng. Sci.* **2004**, *40*, 1036–1045
- (20) Salyer, I. O.; Kenyon, A. S. Structure and property relationships in ethylene–vinyl acetate copolymers. *Polym. Chem.* **1971**, *9*, 3083–3103

- (21) Zarrouki, A.; Espinosa, E.; Boisson, C.; Monteil, V. Free Radical Copolymerization of Ethylene with Vinyl Acetate under Mild Conditions. *Macromolecules* **2017**, *50*, 3516–3523
- (22) Li, L.; Yao, Y.; Fu, N. Free Carboxylic Acids: The Trend of Radical Decarboxylative Functionalization. *Eur. J. Org. Chem.* **2023**, *26*, e202300166
- (23) Lu, B.; Zhu, F.; Sun, H.-M.; Shen, Q. Esterification of the Primary Benzylic C–H Bonds with Carboxylic Acids Catalyzed by Ionic Iron(III) Complexes Containing an Imidazolium Cation. *Org. Lett.* **2017**, *19*, 1132–1135
- (24) Kharasch, M. S.; Sosnovsky, G. THE REACTIONS OF t-BUTYL PERBENZOATE AND OLEFINS—A STEREOSPECIFIC REACTION¹. *J. Am. Chem. Soc.* **1958**, *80*, 756
- (25) Tran, B. L.; Driess, M.; Hartwig, J. F. Copper-Catalyzed Oxidative Dehydrogenative Carboxylation of Unactivated Alkanes to Allylic Esters via Alkenes. *J. Am. Chem. Soc.* **2014**, *136*, 17292–17301
- (26) Vil', V. A.; Barsegyan, Y. A.; Kuhn, L.; Terent'ev, A. O.; Alabugin, I. V. Creating, Preserving, and Directing Carboxylate Radicals in Ni-Catalyzed C(sp³)–H Acyloxylation of Ethers, Ketones, and Alkanes with Diacyl Peroxides. *Organometallics* **2023**, *42*, 2598–2612
- (27) Kuhn, L.; Vil', V. A.; Barsegyan, Y. A.; Terent'ev, A. O.; Alabugin, I. V. Carboxylate as a Non-innocent L-Ligand: Computational and Experimental Search for Metal-Bound Carboxylate Radicals. *Org. Lett.* **2022**, *24*, 3817–3822
- (28) Alabugin, I. V.; Bresch, S.; dos Passos Gomes, G. Orbital hybridization: a key electronic factor in control of structure and reactivity. *J. Phys. Org. Chem.* **2014**, *28*, 147–162
- (29) Qiu, Y.; Hartwig, J. F. Mechanism of Ni-Catalyzed Oxidations of Unactivated C(sp³)–H Bonds. *J. Am. Chem. Soc.* **2020**, *142*, 19239–19248
- (30) Shi, J. X.; Ciccina, N. R.; Pal, S.; Kim, D. D.; Brunn, J. N.; Lizandara-Pueyo, C.; Ernst, M.; Haydl, A. M.; Messersmith, P. B.; Helms, B. A.; Hartwig, J. F. Chemical Modification of Oxidized Polyethylene Enables Access to Functional Polyethylenes with Greater Reuse. *J. Am. Chem. Soc.* **2023**, *145*, 21527–21537
- (31) T., H.; Lakso, J.-E. Functional group efficiency in adhesion between polyethylene and aluminum. *J. Appl. Polym. Sci.* **1989**, *37*, 1287–1297
- (32) Terent'ev, A. O.; Vil', V. A.; Mulina, O. M.; Pivnitsky, K. K.; Nikishin, G. I. A convenient synthesis of cyclopropane malonyl peroxide. *Mendeleev Commun.* **2014**, *24*, 345
- (33) Pilevar, A.; Hosseini, A.; Becker, J.; Schreiner, P. R. Syn-Dihydroxylation of Alkenes Using a Sterically Demanding Cyclic Diacyl Peroxide. *J. Org. Chem.* **2019**, *84*, 12377–12386